DOT/FAA/ND-98/3

General Aviation and Vertical Flight
Program Office
Washington, DC 20591

VFR Heliport Operations in an Obstacle-Rich Environment (ORE)

Brian M. Sawyer and Eric H. Bolz

Science Applications
International Corporation (SAIC)
Arlington, Virginia

James M. Daum, James F. Grenell, Paul R. Wilkinson, and Leon A. Zmroczek

Boeing Defense & Space Group
Helicopter Division
Philadelphia, Pennsylvania

Arthur F. Kramer, Ph.D. and Timothy A. Weber

Beckman Institute, University of Illinois
Urbana, Illinois

May 1999

Final Report

U.S. Department of Transportation

Federal Aviation Administration

NOTICE

This document is disseminated under the sponsorship of the United States Department of Transportation in the interest of information exchange. The United States Government assumes no liability for the contents or use thereof.

The United States Government does not endorse products or manufacturers. Trade or manufacturer's names appear in this document solely because they are considered essential to the object of this report.

U.S. Department
of Transportation
**Federal Aviation
Administration**

800 Independence Ave., S.W.
Washington, D.C. 20591

May 17, 1999

Dear Colleague:

Enclosed is a copy of an FAA technical report entitled **VFR Heliport Operations in an Obstacle-Rich Environment (ORE)**. This investigation studied pilot performance and perception at a downtown heliport using a single-rotor, multi-engine helicopter simulation. Simulation was used in order to control and vary the height and density of obstacles in a way that could never have been achieved in actual flight. The test subjects were all high-time EMS line pilots.

This effort was motivated by concerns raised by Industry about visual flight rules (VFR) operations at a downtown urban heliport. We expect that this report will contribute to FAA/Industry discussions about VFR heliport design requirements.

Sincerely,

Steve Fisher
Manager, General Aviation and Vertical Flight
Program Office

Technical Report Documentation Page

1. Report No.	2. Government Accession No.	3. Recipient's Catalog No.
DOT/FAA/ND-98/3		

4. Title and Subtitle	5. Report Date
VFR Heliport Operations in an Obstacle-Rich Environment (ORE)	May 1999
	6. Performing Organization No.

7. Author (s)	8. Performing Organization Report No.
Brian M. Sawyer and Eric H. Bolz (SAIC); James M. Daum, James F. Grenell, Paul R. Wilkinson, Leon A. Zmroczek (Boeing); Arthur F. Kramer and Timothy A. Weber (University of Illinois)	ATSO-97R-2

9. Performing Organization Name and Address	10. Work Unit No. (TRAIS)
Science Applications International Corporation (SAIC) 1213 Jefferson Davis Highway, Suite 1500 Arlington, VA 22202	
	11. Contract or Grant No. DTFA01-93-C-00030, Task Order G7

12. Sponsoring Agency Name and Address	13. Type Report and Period Covered
Federal Aviation Administration General Aviation and Vertical Flight Program Office, AND-710 800 Independence Avenue, S. W. Washington, D. C. 20591	Final Report
	14. Sponsoring Agency Code AND-710

15. Supplementary Notes

16. Abstract

This evaluation of pilot perception and performance in a visual flight rules (VFR) heliport obstacle-rich environment (ORE) was conducted using a single-rotor, multi-engine helicopter simulator. The investigation was structured to evaluate the effects on operational safety of numerous obstacles in a VFR heliport terminal environment. An urban visual scene containing multiple obstacle types, with variable height/density, was developed specifically for the experiment. Nine pilots flew a total of 504 simulated VFR Approach and Approach operations under a variety of ambient lighting conditions. Aircraft state data, pilot physiological data, video, and pilot comment data were collected and analyzed. The results provide insight into obstacle and visibility effects on pilot workload, performance, and risk perception. They also provide a basis for discussing heliport design and development issues related to the VFR approach/departure surfaces that define the unobstructed airspace needed for safe operations.

These experiments were performed in September and October 1996, at Boeing Defense & Space Group, Helicopter Division's Flight Simulation Laboratory, under contract to Science Applications International Corporation (SAIC). SAIC is the ORE Project support contractor for the Federal Aviation Administration (FAA). The Beckman Institute of the University of Illinois provided expertise in experiment design, physiological data acquisition, and data reduction. Keystone Helicopters of West Chester, Pennsylvania and Corporate Jets, Inc. of West Mifflin, Pennsylvania provided pilot support. Infinite Computer Technologies, Inc. supported pilot questionnaire design and air traffic control (ATC) communications modeling.

17. Key Words		18. Distribution Statement
Obstacle-Rich Environment	Flight Simulation	This document is available to the Public through the National Technical Information Service, 5258 Port Royal Road, Springfield, Virginia 22161.
Obstacle Height/Density	Risk Assessment	
Single Pilot	Pilot Performance	
Multi-engine Helicopter	Pilot Perception	
Emergency Medical Services	Heliport	
Workload		

19. Security Classif. (of this report)	20. Security Classif. (of this page)	21. No. of Pages	22. Price
Unclassified	Unclassified	280	

Form DOT F 1700.7 (8-72) Reproduction of this document is authorized

Acknowledgements

The ORE team wishes to recognize the participation of Mr. John M. McCarthy of Corporate Jets, Inc. Corporate Jets supported the ORE project on their own initiative, highlighting the importance of this investigation of helicopter operators.

The team also wishes to recognize Donna N. Allen, Duncan F. Hughes, Berton Reynolds, Carl C. Robinson, James E. Taylor, and Richard M. Watson of Boeing Helicopters; Roger March of the University of Illinois; Henry Waples, Harry Eberlin, and David Nay of Infinite Computer Technologies, Inc.; and Steve Grey of Keystone Helicopters, Inc. Their dedicated efforts insured the success of the ORE simulation experiment.

In closing, the team wishes to recognize the Boeing Audio Visual Arts Department, Susann Philbrook (editor), and Jean Briner (graphic artist), whose dedicated professional efforts were critical to producing this document

TABLE OF CONTENTS

LIST OF APPENDICES

TABLE OF TABLES

TABLE OF FIGURES

Summary

Background – This investigation studied helicopter pilot performance and perception in a visual flight rule (VFR) heliport terminal obstacle-rich environment (ORE). Simulations were conducted in September and October 1996 as part of a larger effort focused on examining operational safety at U.S. heliports. Concerns raised by pilots operating at a city-center heliport motivated the study. Although none of the obstacles at this heliport protruded into the minimum recommended approach/departure airspace, pilots and their management complained of safety concerns when operating there. The ORE program was sponsored by the General Aviation and Vertical flight Program Office (AND-710) of the Federal Aviation Administration (FAA). As the primary support contractor to AND-710, Science Applications International Corporation's (SAIC) Air Transportation Systems Operation (ATSO) assembled a research team. Boeing Defense & Space Group, Helicopters Division, as simulation support subcontractor, lead the team conducting the simulation experiment. Team members and responsibilities are summarized in table 1.

This simulation investigation lays the foundation for examining the adequacy of the current VFR surfaces. It represents the first step toward understanding the effects of multiple obstacles on pilot performance and perception in OREs, and offers insight into concerns for helicopter operations in geometrically constrained city-centers.

Objectives – The ORE program was established with the intent of evaluating pilot performance and perception in a VFR ORE. While the long-term goal of the overall program is the assessment and possible redesign of VFR heliport surfaces, the simulation investigation described in this document pursued more focused objectives:

- Determine the effect of visibility, specifically time of day (TOD), on pilot ability to detect and recognize obstacles and use them for navigation within the heliport environment.
- Evaluate the effect of heliport environment obstacles on pilot ability to establish and maintain control of the helicopter and its flight path.
- Establish the effect of obstacles in heliport terminal areas on pilot performance and perceived risk.

Investigations – The ORE experiment was conducted in Boeing Helicopters' simulation facility. The simulation replicated light multi-engine helicopter flight operations in a generic, alterable urban heliport visual scene. The effects of several variables were investigated in a full-factorial experiment design:

- Obstacle height/density (OH/D) – Although obstacle height and obstacle density are separate concepts, they were varied concurrently in the simulation experiment. Four levels of OH/D were defined.
- Visibility (TOD) – The influence of TOD was investigated, with operations conducted in simulated day, dusk, and night conditions. Atmospheric visibility was held constant at two miles throughout the ORE experiment.

- Heliport lighting – Two lighting configurations were evaluated for the heliport.
- Flightpath – Two flight corridors (each with unique terrain, obstacles, and landmarks) were defined within the terminal area. Approaches and departures were conducted on both corridors.

Several emergency conditions, ranging in severity from reduced visibility (inadvertent instrument meteorological conditions (IMC)) to engine failure on takeoff, were also presented to each pilot.

TABLE 1 ORE TEAM MEMBERS

Organization	Responsibility
Federal Aviation Administration (FAA)	Program manager and technical review
Science Applications International Corporation (SAIC), Air Transportation Systems Operation	Program development, technical and criteria requirements, and data analysis
Boeing Defense & Space Group, Helicopters Division	Technical development, simulation, piloted evaluation, and data analysis
University of Illinois Beckman Institute	Technical development, physiological data acquisition, and data reduction and analysis
Keystone Helicopters, Inc.	Pilot support
Corporate Jets, Inc.	Pilot support
Infinite Computer Technologies, Inc.	Questionnaire development and air traffic communications models

3080-156

Four types of data were collected during the simulation to evaluate pilot performance, workload, and risk perception:

- Primary task measures – Flightpath accuracy and obstacle clearances.
- Secondary task measures – ATC communications, and emergency responses.
- Subjective measures – Pilot responses to questions on workload, performance, risk, and hazards.
- Physiological measures – Pilot heart rate and eye blink rate.

In addition to these measures, video and audio recordings were made of each run. Video was recorded in a quadscreen format providing full-face and over-the-shoulder views of the pilot, simulation run information, and a forward view of the external visual scene.

The experiment was designed around the participation of 12 pilots, however, only nine pilots completed the experiment. The remaining pilots discontinued the experiment after succumbing to simulator sickness, a condition traced to a simulator hardware problem.

TABLE 2 SIMULATION RESULTS

Objective	Results
Visibility (TOD) effects on obstacle recognition and navigation	• Pilots follow prescribed approach paths with greater precision (less lateral and vertical deviation) and fly more slowly as visibility declines (dusk/night). • Departure flight path lateral and vertical accuracy declines as visibility declines. • Perceived workload on approach and departure (based on subjective responses) increases as visibility declines. • On approach, obstacles generally influence flight performance less in low visibility situations. • Enhanced heliport lighting improves lateral and vertical accuracy on approach.
Obstacle effects on maneuvering and control	• Pilots land with less precision in high obstacle density conditions particularly when mobile obstacles are near the landing zone. • In high obstacle density situations, pilots adjust flight paths to increase obstacle clearance (even when obstacles do not penetrate VFR protected surfaces), potentially increasing the risk associated with greater penetration of the height-velocity avoid region). • Certain obstacles and terrain features are better than others for navigation –linear landmarks (e.g., railroads) aligned with the flight path and point landmarks along the flight path reduce lateral deviation. Area landmarks (e.g., a mall) result in less accurate navigation. • Heart rate and blink rate data indicate gradually increasing workload along the approach path (from downwind to final), but for independent variations of obstacle height/density, no significant trends were observed.
Obstacle effects on pilot performance and risk perception	• Pilots intuitively attempt to maintain obstacle clearance margins greater than the current FAA recommendations for the minimum VFR approach/departure airspace. This indicates that the current FAA recommendations do not adequately reflect pilot concerns about obstacles and pilot operating practices in the vicinity of obstacles. • High obstacle height/density increased workload on approach, but no overload situations were encountered during these experiments. • Obstacle height/density had very little effect on departure workload. • Perceived risk was highly correlated with obstacle height/density, regardless of time of day, even though almost all of the obstacles were outside of the VFR protected surfaces. • In high obstacle height/density conditions approaches were rated more risky than departures. • Night operations were rated as only slightly more risky than day operations. • Power lines are considered the most hazardous obstacle.

3080-157

Simulation Findings – The basic findings of the ORE simulation experiment are presented in table 2. Findings are grouped by objective.

Conclusions – Conclusions were developed to address three areas: test setup and simulator configuration, experiment conduct and data acquisition, and analysis of ORE data. Conclusion from the first two areas are in section 7 and are not summarized here. Based on analysis of ORE simulation data, the following conclusions on pilot performance and perception are drawn:

- On approach, obstacles elicit the greatest effects on pilot performance during high visibility conditions. As visibility declines (at dusk and night), responses to discrete obstacles are generally superseded by more conservative and cautious flight patterns.

- Pilots intuitively attempt to maintain obstacle clearance margins greater than current FAA recommendations on minimum VFR heliport approach/departure airspace. Coupled with previous analysis, this indicates that the current FAA recommendations do not adequately reflect pilot concerns about obstacles and pilot operating practices in the vicinity of obstacles. [The subject pilots' helicopter flight time averaged over 4,500 hours and their EMS experience averaged over 600 hours. This EMS experience level implies that they probably have more experience flying in an obstacle-rich heliport environment than typical industry pilots have.]

- Marking and lighting modifications that provided visual flight path guidance or enhanced the visibility of the heliport landing area improved VFR final approach navigation. Further investigation is warranted to determine which elements of enhanced heliport lighting provide the greatest benefits, and to determine their effects in other visibility conditions. Tests should be included in the research to evaluate whether these lighting configurations enable pilots to stay within the minimum airspace (VFR or IFR visual segment) associated with the configuration's operational use.

- Use of carefully selected landmarks can increase situational awareness, reduce pilot workload, and improve VFR operational safety by increasing navigational accuracy.

- High-fidelity simulation is a useful tool for conducting controlled investigations of pilot performance in challenging operational environments.

- During this program, the vertical profiles flown by the pilots in most, if not all, of the approaches and departures carried the aircraft through some portion of the H/V "avoid" region. Such deviations from flight manual recommendations do not represent safe helicopter operating procedures[44]. While pilots may choose to do this during operations at unimproved landing sites, where there is risk of encountering an unseen obstacle, the airspace in the vicinity of a heliport should permit approach and departure operations that do not require helicopters to fly through this region. There is a body of research on airspace requirements that relate to approach and departure operations that eliminate flight through the H/V "avoid" region[40,41,42,43]. This research should be used by the FAA and the helicopter industry as a basis for establishing VFR heliport airspace criteria.

1.0 INTRODUCTION

Over the last several years, the Federal Aviation Administration (FAA) and the rotorcraft industry have maintained a dialogue regarding minimum airspace requirements at visual flight rule (VFR) heliports. The industry is anxious to locate heliports in strategic downtown city-center areas, and wants to size heliport airspace to fit these constrained geometries. The FAA and industry are both concerned that sufficient airspace is provided at VFR heliports and vertiports to ensure safe operations.

At many heliports, the available airspace exceeds the minimum requirements. However, as heliports and vertiports are located in city-center areas and as the number of obstacles around them continues to increase, nearby obstacles will be a growing concern. Pilot reaction to several city-center facilities raised an FAA concern that a certain level of obstacles might make a heliport or vertiport unacceptable to user pilots, even if none of the obstacles were considered obstructions from an airspace regulatory standpoint.

Prior FAA studies and testing on this issue have been concerned with a very limited number of obstacles in the immediate vicinity of a specific heliport. No consideration has been given to the psychological effect that a large number of obstacles, or an obstacle-rich environment (ORE), in the heliport/vertiport vicinity would have on pilot performance. As shown in figure 1.0-1, this research experiment was designed to explore and investigate what part obstacles may play in pilot performance and perception when flying in and out of different heliport environments. The FAA felt there was a need to collect definitive data for operations in OREs to determine their effect on pilot performance and perception, and to clarify airspace requirement issues for vertical flight facilities. As the primary support contractor to the FAA's General Aviation and Vertical Flight Program Office (AND-710), Science Applications International Corporation's (SAIC) Air Transportation Systems Operation (ATSO) was given the task to develop and execute a test plan to address these operational concerns.

Both the FAA and SAIC concluded that the most effective means for collecting this data was to use a well-instrumented, piloted visual simulator. Simulation technology has evolved in recent years, enhancing the investigative tools available for aviation research and development (R&D) projects. A modern simulation facility provides the platform needed to vary the visual scene, presenting a variety of obstacle densities to challenge individual pilot skills, while collecting data on performance and perception. The results of this simulation experiment provide a baseline for assessing VFR heliport airspace.

The primary purpose of this project was to assess pilot performance and perception in an urban heliport terminal environment. The simulation visual scene was designed to test pilot performance at an increasingly obstacle-rich, urban heliport. Pilot performance was examined on flight segments (e.g., arrival, departure, and emergency) throughout a transition of the modeled ORE. The differences in pilot reaction to various environmental changes were evaluated. The data gathered will be used to assess performance and safety within each segment. Final simulation results on performance and perception are provided in this report.

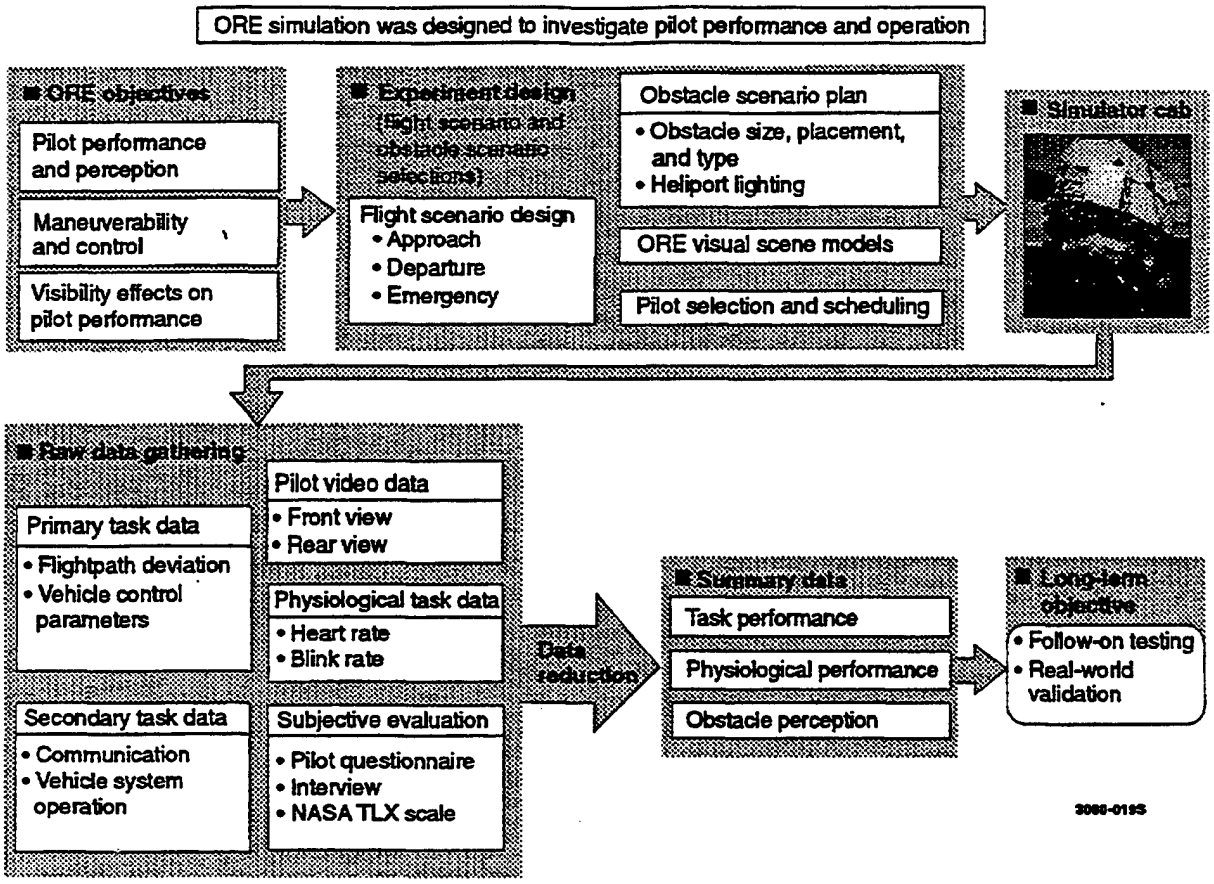

Figure 1.0-1. ORE Experiment Design

2.0 PROJECT BACKGROUND

A number of heliport development and operation issues motivated and influenced the ORE simulation program. The original test plan was developed in 1991 to support the FAA's investigation of VFR heliport airspace requirements for single-engine helicopters (SEHs). The test plan was redirected and broadened to reflect the growing interest in multi-engine rotorcraft applications and advanced vertical flight (AVF) aircraft (e.g., tiltrotor) to operate scheduled service to city-center heliports or vertiports. This project addresses only VFR airspace issues.

Specialized hardware, software, and engineering capabilities were considered essential to develop and control the anticipated range of ORE test parameters. Only a high-level R&D facility, similar to the one at the National Aeronautics and Space Administration's (NASA) research facility at Ames or a major helicopter manufacturer was expected to fulfill the requirements. After the release of a detailed request for proposal (RFP)[1] to the four major helicopter manufacturers, a rigorous evaluation process ensued. The ORE simulation support subcontract was awarded to Boeing Defense & Space Group, Helicopters Division, in Philadelphia, Pennsylvania.

As the development of the ORE program proceeded, the FAA was also investigating the use of a global positioning system (GPS) to support terminal instrument procedures (TERPS) for rotorcraft. The program focused primarily on emergency medical service (EMS) helicopters at a variety of hospital heliports. EMS is one of the most demanding environments for vertical flight operations outside of the military. EMS operations occur under a variety of meteorological conditions, both visual and instrument, with single-pilot (SP) multi-engine aircraft. The GPS project lead to the publication of vertical flight nonprecision TERPS criteria[2] in February 1996. Based on these TERPS criteria, more instrument procedures, which include both instrument and visual segments, will be developed for heliports in the near future.

Based on the success of the GPS project, the FAA felt it was valuable to focus the ORE program on the EMS, SP, multi-engine helicopter (MEH) scenario rather than base the program on a variety of aircraft types and crew complements. Consequently, the test plan was modified to examine only SP-MEH operations in an urban environment typical of EMS operations at this time. This project addresses only VFR airspace issues.

2.1 OVERALL PROGRAM OBJECTIVES

The ORE program was designed to investigate some basic pilot performance issues regarding the number, type, and placement of obstacles found "below and off to the side" of the VFR approach/departure surfaces by examining and evaluating the pilot-to-obstacle relationship. Figure 2.1-1 shows the current minimum VFR approach/departure surfaces recommended by the FAA[3] to provide the unobstructed airspace required for safe VFR operations. At a minimum, the program was designed to obtain data in the following areas:

- Pilot response and performance.
- Risk assessment for pilot decisions.
- Obstacle perception factors.
- Obstacle qualification criteria (OQC) for heliports.

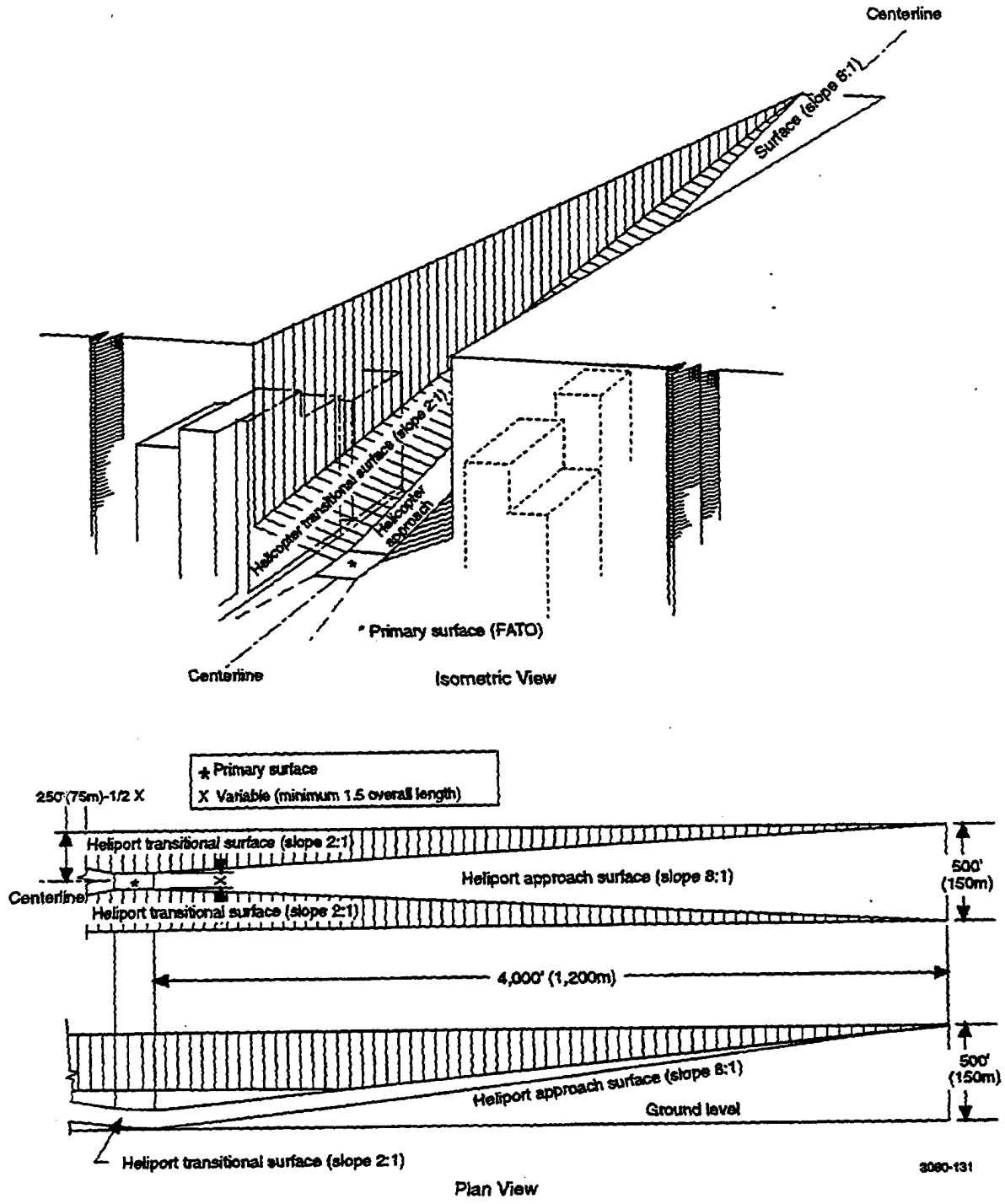

Figure 2.1-1. VFR Approach/Departure Surfaces

2.1.1 Pilot Response and Performance

Obstacles and prominent structures can simultaneously assist and threaten a pilot operating within VFR heliport terminal airspace. Obstacles provide reference for navigation and control of

the helicopter, but their presence near a flight corridor presents a threat to safe operations, particularly as visibility declines. The ORE program sought to determine if a threshold existed between desirable visual cueing and undesirable threat. Specifically, answers to the following questions were sought:

- Does obstacle density create a psychological consequence outweighing the desirability of a heliport location?
- What happens to a pilot flying to a heliport environment that has significant obstacles below or to the side of the VFR approach/departure airspace?

2.1.2 Risk-Assessment for Pilot Decisions

Flight in heliport vicinities presents a level of risk of striking obstacles. Each pilot mentally assesses this risk prior to making a decision. The ORE program examined whether a risk-assessment factor could be assigned to a pilot's decision, yielding a numerical weight value for analysis. Using pilot reactions to various obstacles (based on type and location), a risk assessment factor might be developed.

2.1.3 Obstacle Perception Factor

Helicopter approach and departure complexity varies dramatically based on the number and type of obstacles present. Pilots mentally allocate an intimidation level to the potential hazard each obstacle presents. Some obstacles are perceived as more dangerous than others, regardless of the true damage a collision would cause. Consequently, there is a supplemental factor to be considered when rating obstacle effects on pilot perception. Obstacles can be categorized on a perceived threat basis by carefully constructing questions established largely on the pilot's knowledge and experience regarding the potential threat of each obstacle. Collectively, these assessments add to the ability to evaluate obstacles found in a heliport/vertiport environment.

2.1.4 Obstacle Qualification Criteria (OQC)

Safety is of paramount importance to the FAA and the rotorcraft industry in general. Rotorcraft accident rates are comparable to those of general aviation fixed-wing aircraft for similar missions. Still, a significant portion of the public perceives rotorcraft and AVF aircraft as unsafe. If these aircraft are to be accepted by the public, operators need to continue improving their safety record. This introduces the need for analytical quantification of obstacles affecting pilot performance to generate a OQC. A heliport OQC would provide an objective way to measure and manage obstacle safety. Defining minimum airspace requirements associated with VFR heliport approach and departure corridors is fundamental to the OQC concept.

2.2 SIMULATION OBJECTIVES

The previous section summarized the objectives for the overall ORE program. The broad nature of these objectives could potentially culminate with the publication of new VFR heliport design recommendations and 14 CFR Part 77 airspace regulations. The simulation program discussed in this report was intended to accomplish the following objectives:

- Determine the effect of visibility on pilot ability to detect and recognize obstacles in the heliport environment and use them for navigation. VFR navigation relies on reference to obstacles and terrain, and pilots must see, recognize, and avoid obstacles and air traffic. This objective emphasizes factors, such as time of day (TOD), obstacle features, and heliport lighting affecting obstacle visibility and navigational accuracy.
- Evaluate the effect of heliport environment obstacles on pilot ability to establish and maintain control of the helicopter and its flightpath. VFR pilots derive speed, altitude, and attitude information from objects in the visual environment. Thus, the visibility and characteristics of objects in the visual field play a role in controlling the helicopter. Furthermore, an understanding of flightpath accuracy is needed to establish adequate airspace dimensions.
- Establish the effect of obstacles on pilot performance and on perceived risk of heliport terminal operations. Both pilot performance and risk assessment were expected to be affected by visibility and obstacle characteristics. Understanding the relationship of workload and risk assessment in an obstacle-rich heliport environment is a prerequisite to establishing an OQC.

2.3 ORIGINAL EXPERIMENT DESIGN

The original experiment design was the result of a report[4] "VFR Heliport Obstacle-Rich Environment: Draft Test Plan" dealing with flight in an ORE provided by SAIC (formerly Systems Control Technology, Inc. (SCT)) to the FAA in 1991. As part of the design process, a formal industry/government briefing was held in May of 1991. This briefing, conducted by the FAA, provided a public review of the overall problem and the experimental concepts already developed. The program evolved based on industry comments. To further define the simulation requirements and specifications, several candidate simulation facilities were visited by SAIC during 1993 to brief personnel on the program, and to assess the facilities' capabilities.

The industry/government briefing and facility visits established a baseline for the test methodology, data collection, and analysis requirements. Separate reports were provided to the FAA on the subjects of "ORE Test and Evaluation[5]," "ORE Simulation Requirements and Facilities[6]," and "ORE Pilot Briefing Materials[7]." It is from these efforts that the formal ORE Test Plan and subsequent RFP documents were finalized and distributed in late 1994. The current investigation, while narrower in scope, adheres closely to the intent of the original test plan.

3.0 SIMULATOR FACILITY

A capable R&D simulation facility was required to conduct the ORE program. This type of simulation facility is regularly used by aircraft manufacturers to evaluate flight vehicle characteristics prior to flight test, and to conduct safe, repeatable evaluations of high-risk flight regimes. The ORE program required a simulator with the capability to model a virtual urban environment for helicopter operations. Controlled variations of obstacle height, obstacle density, obstacle placement relative to flight corridors, and ambient lighting and visibility were required to successfully execute the program. Simulation allowed a structured investigation of these variables that would have been impossible in a flight environment. The Boeing simulation facility, shown in figure 3.0-1, provided the physical capabilities needed to execute the ORE program.

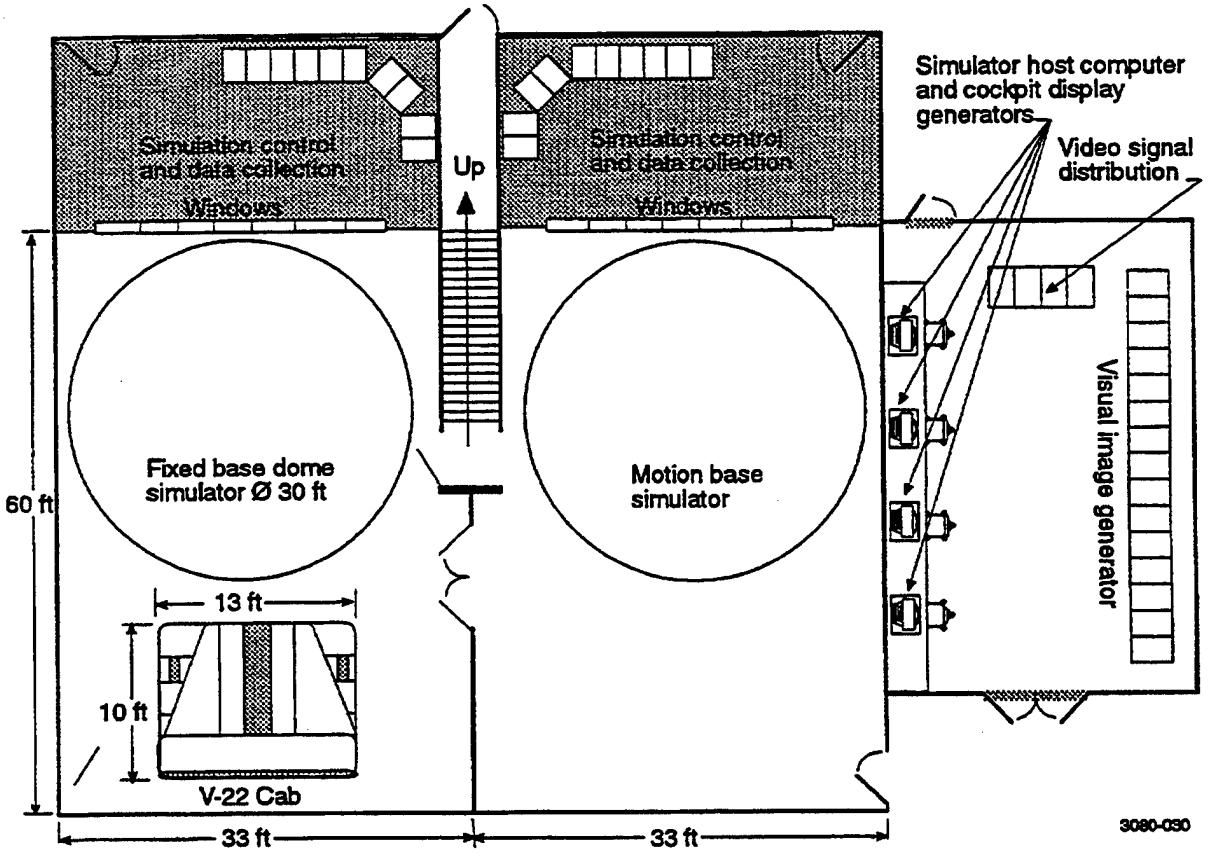

Note: Shaded area is on second level

Figure 3.0-1. Simulation Lab Facility

This facility is dedicated to rotorcraft R&D. Figure 3.0-2 shows the integrated simulation system architecture which includes high-fidelity math models, visual scene generation capabilities, and

data collection facilities. The following sections describe the hardware and software used for the ORE simulations. Specifically, the following features will be discussed:

- Helicopter math model.
- Atmospheric disturbance models.
- Cockpit controls and displays.
- Visual systems.
- Aural cueing.
- Communications.

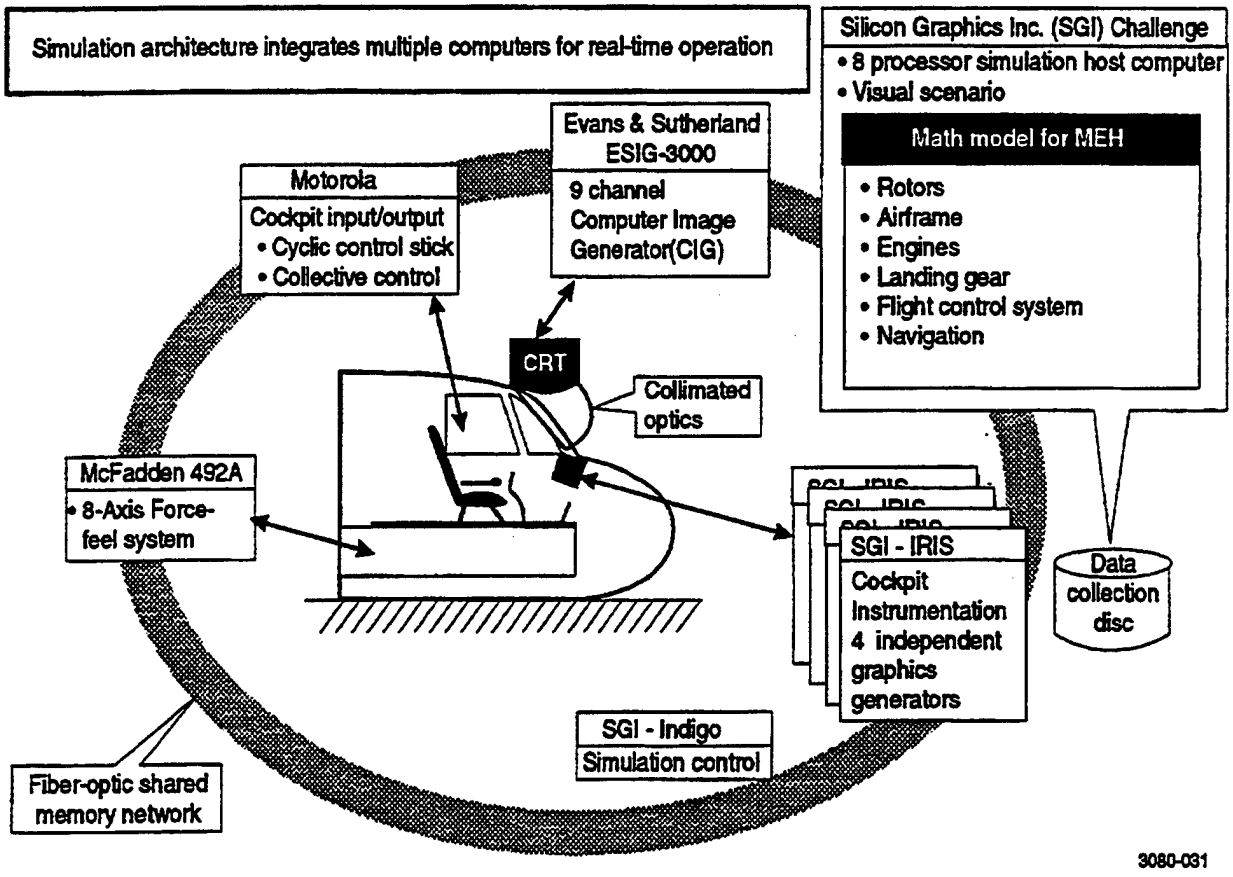

Figure 3.0-2. High-Fidelity, Multifunction, Simulation Architecture

3.1 HELICOPTER MATH MODEL

The single-rotor, multi-engine, helicopter model required for ORE testing was based on an existing, full-envelope, single-rotor model. This high-fidelity rotorcraft model is the basis for the UH-60, A-109, and RAH-66 Comanche models and is suitable for all flight regimes. An extended classical rotor model accurately represents interactional aerodynamics and ground effects. Specific helicopter characteristics used for the ORE test are summarized in table 3.1-1. The math model was executed on an eight-processor, Silicon Graphics Iris (SGI) Challenge computer. A simulation executive program ensured a fixed computation cycle of 10 msec for real-time operation.

TABLE 3.1-1. ORE HELICOPTER CHARACTERISTICS

Rotor diameter	36.1 ft.
Rotor solidity	0.078
Rotor rotation speed	385 rpm
Rotor tip speed	728 ft./sec
Tail rotor diameter	6.66 ft.
Tail rotor moment arm	21 ft.
Gross weight	5,727 lb.
Overall length	43 ft.
Number of engines	2
Maximum engine power	371 hp
Maximum torque	4,182 ft.-lb.
Longitudinal cyclic range	+/-12 deg
Lateral cyclic range	+/-6.3 deg
Collective range	+21 /-7 deg
Longitudinal stick travel	12.6 in.
Lateral stick travel	10.6 in.
Pedal travel	+/-2.8 in.
Collective lever travel	10.5 in.

3080-124

Previous comparison of flight test and simulator data confirmed that the aircraft math model and the flight control system represent single-rotor helicopter functions and characteristics. Validation of the ORE simulation's math model was limited to subjective pilot evaluation, confirming that the model was representative of single-rotor helicopters.

3.2 ATMOSPHERIC DISTURBANCE MODELS

The problems normally associated with winds and turbulence increase in an ORE. Turbulence and wind flow around obstacles have the potential to induce flightpath changes, driving the aircraft toward surrounding obstacles, and increasing pilot workload. Some of these disturbances could be anticipated by an alert pilot (e.g., turbulence around a building), provided the pilot knows local wind conditions; others are random in nature. The simulation incorporated models for both steady wind and turbulence (Dryden spectral model)[8].

Steady winds of 15 knots and turbulence of 5-knots root mean square (RMS) were included in all ORE approaches and departures. The pilots received wind information from both air traffic control (ATC) and a simulated wind sock at the ORE heliport. Wind effects involving major buildings were included to add realism. Building wakes were attached to major structures in the visual database. Wakes were modeled as a wind velocity deficit downwind of a structure. The wind deficit was greatest immediately downwind of a structure, becoming smaller and more diffuse as downwind distance increased. The wakes extended approximately 2,000 feet downwind. Wake effects of adjacent structures were additive. No effects were modeled between or upwind of structures.

3.3 CONTROLS AND DISPLAYS

The V-22 side-by-side simulator cab used for these experiments has controls for both pilot and copilot. A conventional cyclic stick and pedals were provided. Thrust control was configured as a standard collective control. Control forces were simulated using a McFadden reconfigurable hydraulic control loading system. The McFadden system is programmable to model force gradients, free play, friction, and dead band. Force characteristics were modeled for each axis providing representative forces versus displacement and velocity. Trim and magnetic brake functions were also implemented.

Three displays provided flight and performance information to the pilot. Existing 6 x 6-inch color CRTs displayed graphic representations of conventional electromechanical instruments as shown in figure 3.3-1. These displays represented the look, location, operation, and feel of a single-rotor helicopter. SGI computers generated the display graphics. The displays in front of the pilot provided all basic flight instrumentation (as well as cautions, warnings, and advisories) in a standard "T" configuration. Engine instrumentation, communication data, and ORE-specific information were all displayed on the center console to the pilot's left, as shown in figure 3.3-2. Altitude, airspeed, distance, and scenario information on the center console were provided for test director use and not displayed to the pilot.

3.4 VISUAL SYSTEM DESCRIPTION

Visual system characteristics were critical to success of the ORE program. The visual system was expected to comply with the requirements for a level C training simulator described in Advisory Circular (AC) 120-63[9]. Table 3.4-1 compares the specifications of Boeing's simulator to the Level C requirements. The facility possesses a combination of visual scene attributes (resolution, brightness, field of view, etc.) that meet the requirements for development of rotorcraft flight control laws and evaluation of aircraft handling qualities. The simulator provides a Level 1 usable cue environment (UCE), a rating of the simulator's capability to perform high-fidelity simulations, as defined in ADS-33[10]. Level 1 is the best possible rating for the UCE. As with the math model, piloted evaluations provided final confirmation that visual system performance was acceptable.

An Evans & Sutherland ESIG-3000 image generator (IG) was used to produce the out-the-window visual scene. This dual-eyepoint, nine-channel system is capable of displaying full-color imagery on up to five display devices simultaneously. The visual scene is well suited for low-speed, low-altitude, nap-of-the-earth flight near obstacles. Textured areas of grass, fields, buildings, and roads are standard features; as are effects such as fog, haze, night, and runway and tower lights. The visual scene was displayed by five 25-inch color CRTs which were collimated (focused at infinity) by folded-optic windows. Figure 3.4-1 indicates the extent of the simulator cockpit viewing angles. The cab provided 132 x 35 degrees of continuous horizontal field-of-view (FOV), plus a left window of 30 degrees interrupted only by canopy structure and the copilot's optics. The maximum FOV was 210 degrees horizontally and 80 degrees vertically. The opaque obstructions in the simulator cab were representative of the V-22 aircraft. The chin window provided look-down capability, useful for landings.

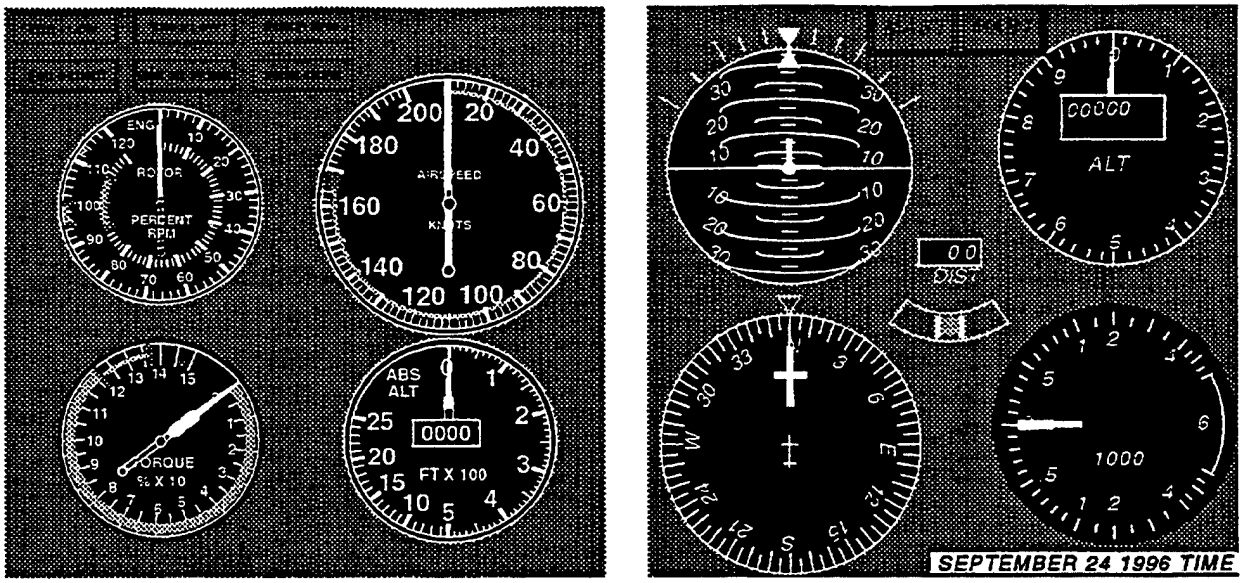

3080-011

Left Hand MFD

Right Hand MFD

Figure 3.3-1. Control Panel Multifunction Display Layouts

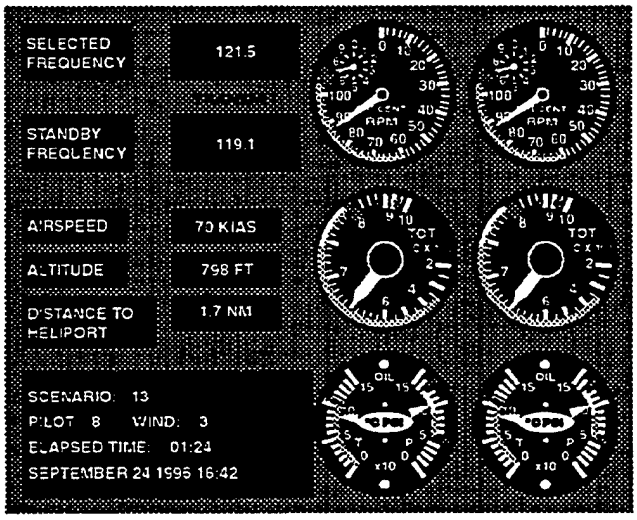

3080-010

Figure 3.3-2. Control Panel Center Console

TABLE 3.4-1. COMPARISON OF BOEING IMAGE GENERATOR CAPABILITIES AND REQUIREMENTS OF FAA AC120-63.

Helicopter simulator requirement	FAA AC120-63 Level 'C'	Boeing simulator capability	Comments
Visual system transport delay	100 millisec	100 millisec	In compliance - see section 5.5 for mid-experiment modification
Field of view-horizontal	150° continuous, collimated centered on 0° azimuth	210°	Our horizontal FOV is not continuous; this is for right seat only
Field of view-vertical	40°	80° with gaps	Functional chin window provides nearly 60° down angle
Scene content	Level 'D' requirement	Level 'D'	Level 'D' requirement
Object density	2,000 polygons	3,000 polygons/ channels 6 channels	In compliance - see section 5.5 for mid-experiment modification
Brightness	6 ft-Lamberts highlight brightness	>6 ft-Lamberts	In compliance
Contrast ratio (A/B)	5:1	>5:1	In compliance
Resolution (method is not specified)	3 arc-minutes	<3 arc-minutes per pixel	In compliance
Lightpoint size	6 arc-minutes	6 arc-minutes (=2 pixels)	In compliance

3080-029

Boeing's V-22 simulator cab meets FAA level 'C' pilot's FOV requirements.

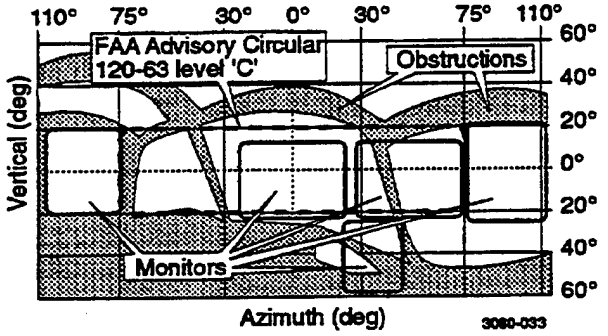

Figure 3.4-1. Boeing's V-22 Simulator Cab Pilot's Field-of-View

3.5 AURAL CUEING ENVIRONMENT

A variety of aural cues were generated to enhance pilot situational awareness and simulation reality. Rotor and engine sound cues were produced by an eight-channel Ensoniq-16+ sound-effects generator, amplified through studio amplifiers, and played through speakers located in the cab. Volumes and frequencies were tuned to be representative of an actual aircraft. Caution and

warning tones were driven by sound commands from a SGI workstation and generated into the pilot's headset.

3.6 COMMUNICATIONS NETWORK

The simulator intercom system was modified and specific communications protocols were observed for the ORE evaluations. Normally, an open-microphone intercom system is used for handing qualities simulation evaluations, allowing unencumbered communication between the simulator cab pilot and the simulation control room personnel. In operational helicopters, however, radio transmission is activated via a push-to-talk button on the cyclic stick.

For the ORE evaluations, the freedom of open-microphone communication was required between runs. However, during runs, push-to-talk protocols were enforced to more accurately reflect actual flight operations. Furthermore, continuous recording of pilot comments was required during the evaluation.

The conflicting requirements of push-to-talk protocols and continuous recording of pilot comments were satisfied using the communications network shown in figure 3.6-1. A push-to-talk switch mounted on the cyclic grip activated a light in the control room. The ATC player in the control room responded to pilot requests only if the push-to-talk light was illuminated during the transmission, and the pilot had selected the appropriate radio frequency on a simulated radio panel. Audio was recorded on a continuously running video cassette recorder (VCR). The test director and simulation operator monitored all test operations. They communicated with the pilot between runs, but maintained silence during the runs.

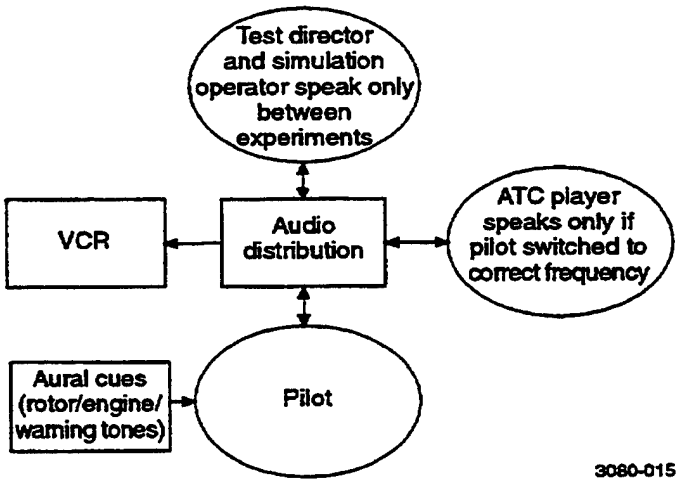

Figure 3.6-1. ORE Communications Network

4.0 EXPERIMENTAL METHOD AND DESIGN

Development of the ORE experiment continued from the time of its inception in 1991 through the actual conduct of the simulations in September and October of 1996. This section of the report describes the experiment as it was conducted, and explains some of the decisions that shaped the experiment design. The following major areas are discussed:

- Visual scene development.
- Experiment design.
- Subject pilot selection.
- Data acquisition.
- Performance assessment methodology.

Visual database development and experiment design are inextricably linked by the nature of the ORE experiments, and they were conducted as parallel efforts. For clarity in this report, however, they are described separately.

4.1 VISUAL SCENE DEVELOPMENT

Fundamental to the ORE experiment was the ability to simulate helicopter flight within a variety of obstacle environments and ambient conditions, such as time of day (TOD) and visibility. The approach taken to develop the visual database used for the ORE simulation program was the subject of much analysis and refinement during the course of the study. Two basic opposing constraints existed:

1. The need for a set of scenes presenting progressively more challenging obstacle environments, combined with TOD, visibility, and heliport design variations.
2. The limitations of the computer image generation system, and the associated need for model simplicity.

Furthermore, a generic urban visual model was preferred for the ORE experiments to avoid two potential difficulties associated with modeling a real-world site:

1. The risk of pilot familiarization – subject pilots participating in the experiment may have different levels of familiarity with the site, biasing the data obtained from the experiments.
2. Lack of flexibility – a real-world site brings with it real-world constraints on the placement and variation of obstacles.

Given the constraints, a single, generic urban environment was conceived to provide the underlying terrain and basic natural and man-made features needed for the experiments. During the early phase of visual scene development, hand-drawn maps and sketches were used. A basic terrain model was conceptualized with a gentle "V" shape. From the central point where the heliport would be located, terrain rose slowly to the north and south. A valley ran roughly east-west through the middle of the area. The valley contained a river to provide a setting for highway

bridges and waterway traffic. An area of an existing visual database was identified that possessed many of the needed terrain features. This area was used as a foundation for constructing an ORE-specific visual scene.

Various man-made features were introduced into the visual scene by developing the urban area shown in figure 4.1-1. A downtown area was placed on the river's north side, with an industrial area adjacent to the river banks which extended to the south side. A suburban area was placed to the west, and downtown congestion was extended to the east. The heliport was located on the river's north side near a group of large buildings. The actual landing site was a hospital heliport in the immediate vicinity of the hospital and adjacent office buildings. The arrival and departure corridors were designed to extend north and south of the heliport. To the north, the corridor was framed by office buildings on all sides of the VFR protected surfaces, including a pair of office towers just beyond the end of the VFR protected surfaces. To the south, the corridor passed over the river and various urban structures, including an industrial area with an assortment of smokestacks, a bridge, and a power plant.

The database provided a foundation for varying obstacle height/density (OH/D) in a systematic manner. The following parameters were manipulated to create four levels of OH/D:

- The height of buildings located beneath, immediately beyond, and adjacent to the VFR protected surfaces.
- The percentage of open or unoccupied space.
- The number, type, and placement of close-in and perimeter obstacles.

Variations in these parameters were integral to the ORE experiment design. They are described in detail in section 4.2.1.3.

The urban layout provided two flight corridors for the heliport, designated Valley and Metro, each with distinctly different characteristics. The Valley approach initiates at 900 feet mean sea level (MSL) along a ridgeline to the north and west of the city-center area, passes over a residential area, and into the city-center environment. In terms of visual landmarks, the flight corridor starts with a modified downwind leg that follows a set of railroad tracks, and then turns on a base leg to the east at a prominent microwave tower. The next leg is an extended final that heads south over a drive-in theater located directly north of the heliport. The drive-in theater helps the pilot establish a proper ground track into the city-center heliport area. The final approach path passes directly over a pair of tall buildings (twin towers), which are located immediately beyond the north end of the VFR protected surface.

The Metro approach corridor initiates (at 900 feet MSL) over rolling hills, slightly north of an arboretum. The downwind leg of the Metro approach corridor passes over the arboretum and a residential area, which includes a shopping mall. The base leg runs west over the shopping mall, and turns to the north along the west side of a power plant in an industrial area. A step down from 900 feet MSL to 700 feet MSL was permitted on the base leg. The final approach passes over an industrial area that includes high-tension lines associated with the power plant. The Metro approach flightpath also includes two passes over a river cutting through the prototype urban area.

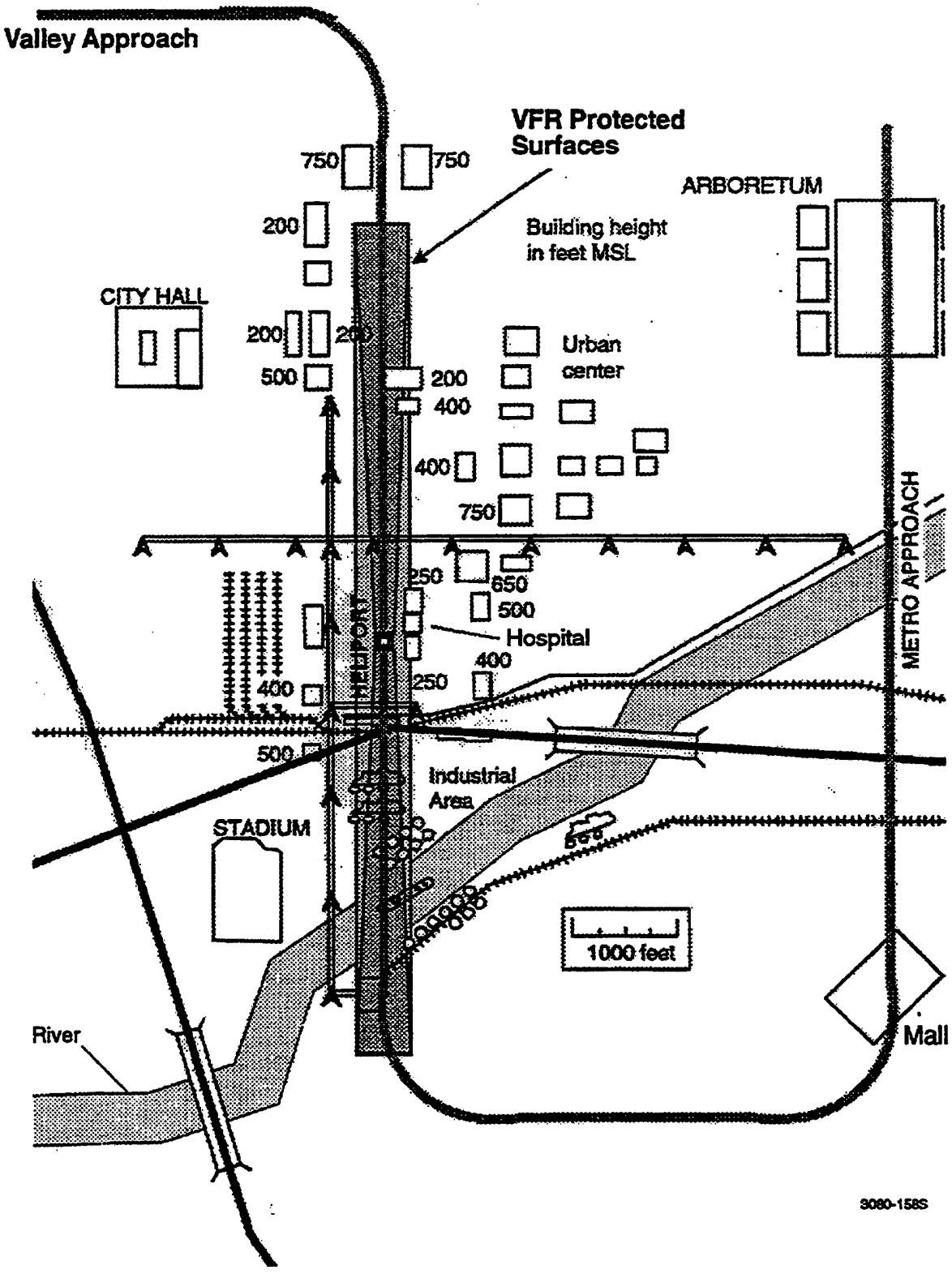

Figure 4.1-1. Conceptual ORE Urban Area With VFR Surface Overlaid

Departures initiated at the heliport and were flown outbound along the same flight corridors used in the approach cases. The departure runs were terminated when the aircraft cleared the obstacle environment.

4.1.1 Baseline Lighting Configuration

Two heliport lighting options were modeled. The baseline lighting configuration includes a combination of yellow lights outlining the final approach/takeoff area (FATO), an illuminated wind sock, and a taxiway marked with green centerline lights and blue-edge lights. The baseline lighting configuration was based on the "Heliport Design Guide," AC 150/5390-2A[3], as illustrated in figure 4.1-2. Other sources included 'Taxiway Centerline Lighting System," AC 150/5340-19[11]; "Runway and Taxiway Edge Lighting System," AC 150/5340-24[12]; and "Specification for Runway and Taxiway Light Fixtures," AC 150/5345-46[13] which contain additional information concerning these lighting systems.

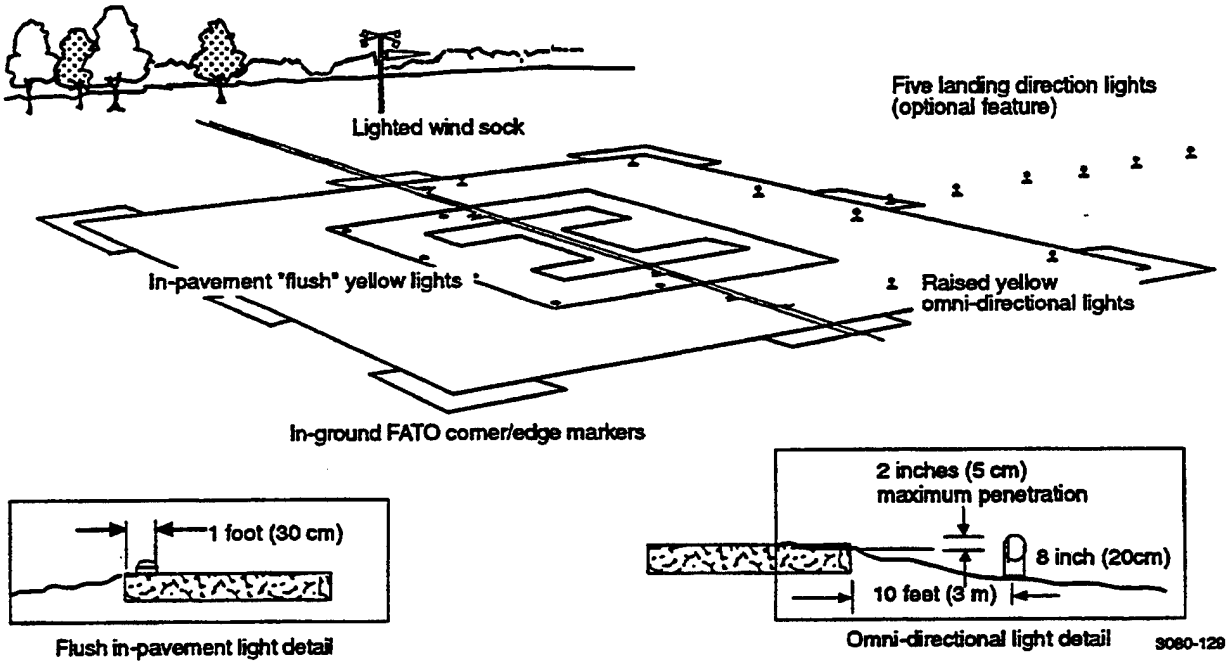

Figure 4.1-2. Lighting System for Night Operations, as Defined in AC 150/5390-2A, Heliport Design Guide

4.1.2 Enhanced Lighting Configuration

The enhanced lighting configuration contains additional orientation-enhancing features. These included landing direction lights, a heliport identification beacon, and apron floodlights illuminating the heliport landing area. A precision approach path indicator (PAPI) provided the pilots with visual guidance and descent cues. "Precision Approach Indicator Systems," AC 150/5345-28, provides additional information concerning these systems[14].

4.1.3 Examples of the Visual Scene

Figures 4.1-3 and 4.1-4 show the fully populated visual scene presented to the pilots, as viewed from the north (Valley Approach) and south (Metro Approach), respectively. Both represent the highest level of OH/D. In both figures, the heliport is exactly in the center. A detailed summary of the simulation visual scene database is provided in appendix A.

4.2 EXPERIMENT DESIGN

The ORE simulation scenarios included both approaches and departures. Each subject pilot conducted an equal number of approaches and departures over the course of the experiment. The same basic experiment design was utilized for data collection and analysis of the approach and departure cases. The same independent variables were manipulated for the approach and departure cases, but the number of manipulations made to each variable was different.

For the approach cases, a 2 x 3 x 4 factorial design was used resulting in a total of 24 approach runs per pilot. The independent variables were the flight corridor used for the approach (two levels), OH/D (three levels), and TOD/lighting (four levels). A graphical depiction of the experiment design matrix for approach cases is shown in figure 4.2-1.

Similarly for the departures, a 2 x 4 x 3 factorial design was utilized, resulting in a total of 24 departure runs per pilot. As in the approach cases, subject variables included the flight corridor used for the departure (two levels), OH/D (four levels), and TOD/lighting (three levels). A graph depiction of the experiment design matrix for the departure cases is shown in figure 4.2-2. As noted, the number of OH/D levels and lighting variables differed between approach and departure to provide an equal number of approach cases and departure cases. The enhanced heliport lighting was not applicable to the departure scenarios. Thus for the departure cases, the number of TOD lighting levels was reduced from four to three, and the number of OH/D levels was increased from three to four.

In addition to the 24 approaches and 24 departures, eight emergency condition runs were added to the experiment. The emergency scenarios were presented within the context of the other experimental conditions, such that each emergency condition was presented under the same conditions for each subject (i.e., for all subjects, a given emergency condition was presented on the same flight corridor, under the same TOD/lighting condition, and with the same OH/D condition). Emergency condition runs are not included in the graphical experiment matrices shown in figure 4.2-1 and figure 4.2-2, nor were they included in the data reduction and analysis of approach and departure cases.

A syllabus of the approach and departure cases is presented in table 4.2-1. The syllabus lists each experiment scenario or combination of variables in the ORE experiment, including emergency conditions. The simulation runs are listed in strictly numerical order. The order of the scenarios was counterbalanced across subjects to eliminate the potential influence of learning, familiarization, and fatigue on the experimental data.

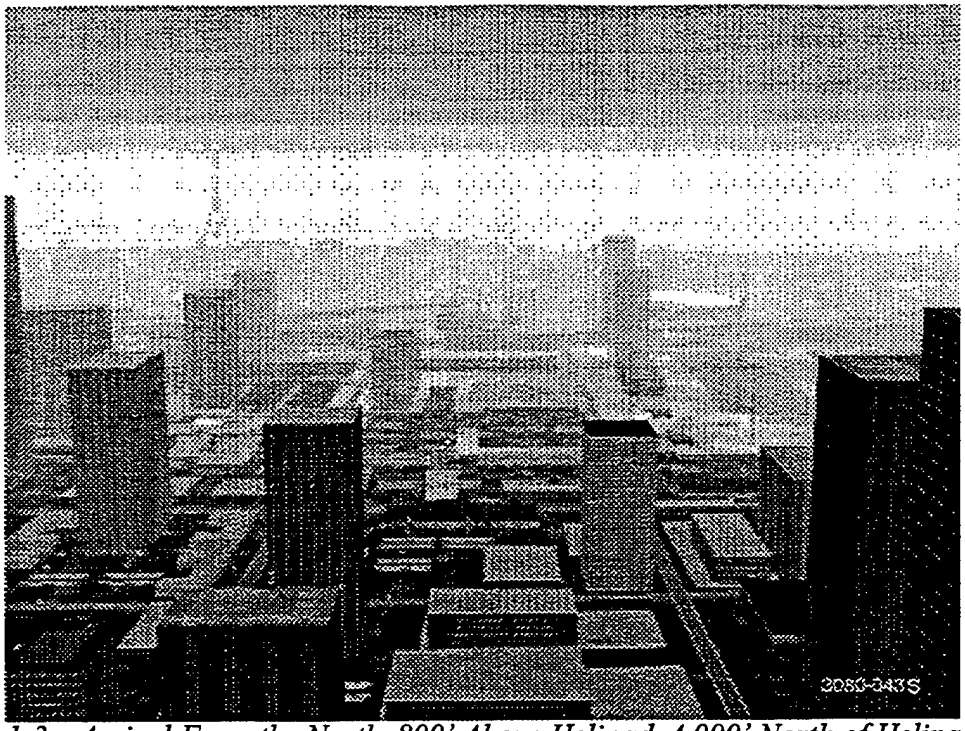

Figure 4.1-3. Arrival From the North, 800' Above Helipad, 4,000' North of Helipad, High Obstacle Density (Valley Approach)

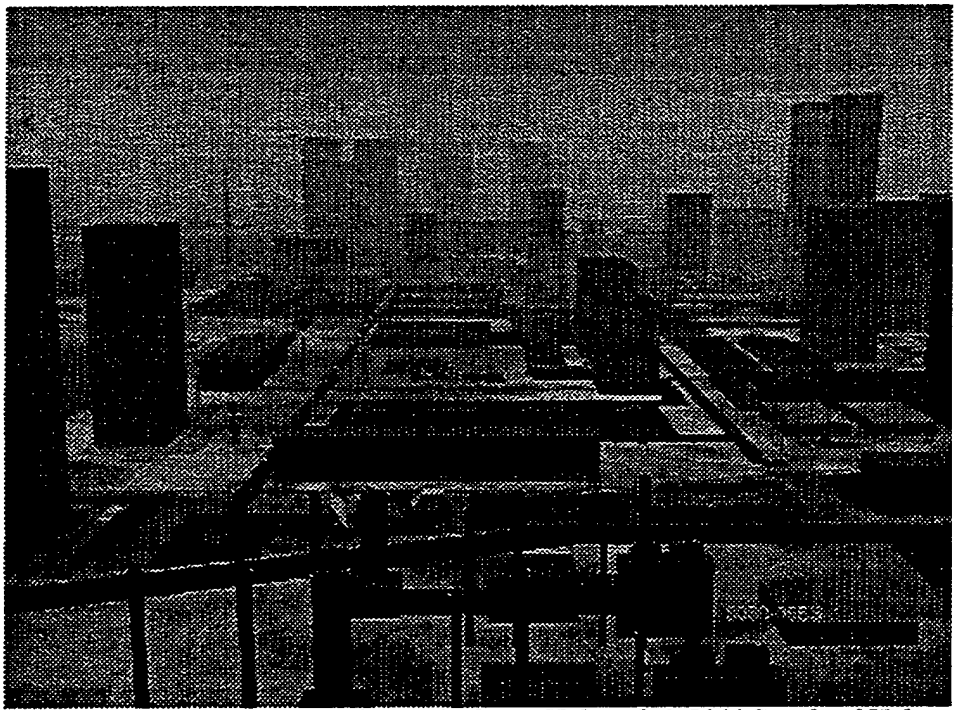

Figure 4.1-4. Arrival From the South, 500' Above Helipad, 2,500' South of Helipad, High Obstacle Density (Metro Approach)

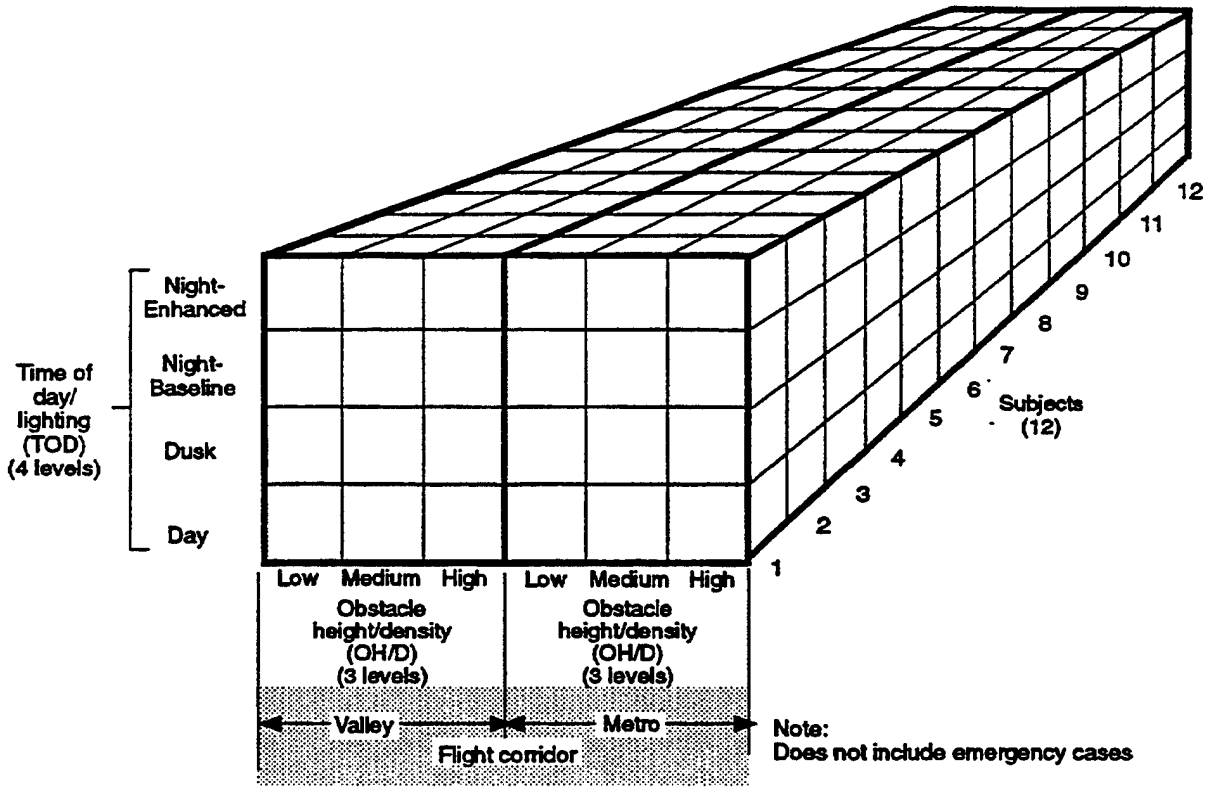

Figure 4.2-1. ORE Experiment Design – Approaches

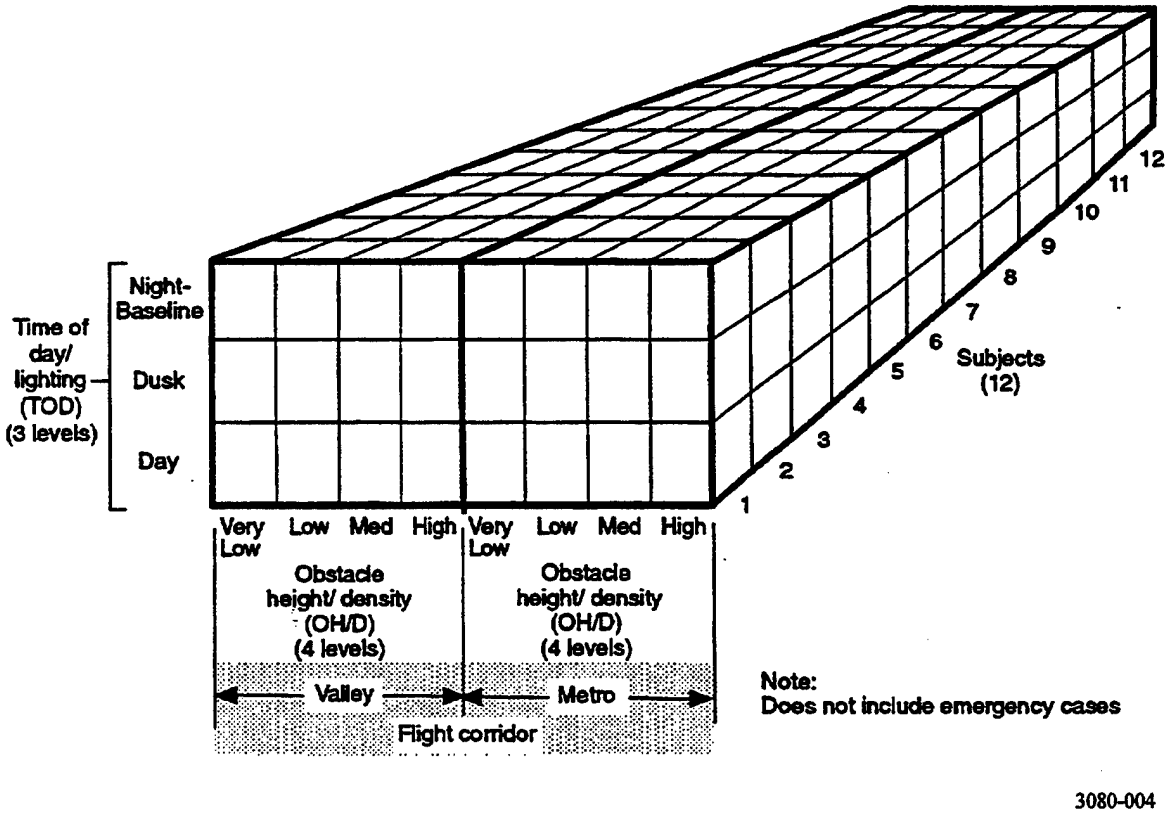

Figure 4.2-2. ORE Experiment Design - Departures

TABLE 4.2-1. SIMULATION SCENARIO SYLLABUS: APPROACHES AND DEPARTURES

Approaches

Scenario No.	Flight Corridor	Obstacle height/ Density (OH/D)	Time of day/lighting (TOD)	Emergency
A1	Valley	Low	Day	None
A2	Valley	Low	Dusk	None
A3	Valley	Low	Night-baseline	None
A4	Valley	Low	Night-enhanced	None
A5	Valley	Med	Day	None
A6	Valley	Med	Dusk	None
A7	Valley	Med	Night-baseline	None
A8	Valley	Med	Night-enhanced	None
A9	Valley	High	Day	None
A10	Valley	High	Dusk	None
A11	Valley	High	Night-baseline	None
A12	Valley	High	Night-enhanced	None
A13	Metro	Low	Day	None
A14	Metro	Low	Dusk	None
A15	Metro	Low	Night-baseline	None
A16	Metro	Low	Night-enhanced	None
A17	Metro	Med	Day	None
A18	Metro	Med	Dusk	None
A19	Metro	Med	Night-baseline	None
A20	Metro	Med	Night-enhanced	None
A21	Metro	High	Day	None
A22	Metro	High	Dusk	None
A23	Metro	High	Night-baseline	None
A24	Metro	High	Night-enhanced	None
A25	Valley	Med	Night-enhanced	Traffic incursion
A26	Valley	Low	Dusk	Fuel tach/gen failure
A27	Metro	High	Day	Eng oil press, low
A28	Metro	Med	Night-baseline	Inadvertent IMC

Departures

Scenario No.	Flight Corridor	Obstacle height/ density (OH/D)	Time of day/lighting (TOD)	Emergency
D1	Valley	Very Low	Day	None
D2	Valley	Very Low	Dusk	None
D3	Valley	Very Low	Night-baseline	None
D4	Valley	Low	Day	None
D5	Valley	Low	Dusk	None
D6	Valley	Low	Night-baseline	None
D7	Valley	Med	Day	None
D8	Valley	Med	Dusk	None
D9	Valley	Med	Night-baseline	None
D10	Valley	High	Day	None
D11	Valley	High	Dusk	None
D12	Valley	High	Night-baseline	None
D13	Metro	Very Low	Day	None
D14	Metro	Very Low	Dusk	None
D15	Metro	Very Low	Night-baseline	None
D16	Metro	Low	Day	None
D17	Metro	Low	Dusk	None
D18	Metro	Low	Night-baseline	None
D19	Metro	Med	Day	None
D20	Metro	Med	Dusk	None
D21	Metro	Med	Night-baseline	None
D22	Metro	High	Day	None
D23	Metro	High	Dusk	None
D24	Metro	High	Night-baseline	None
D25	Valley	Very Low	Day high	Engine oil temp
D26	Valley	High	Dusk	Inadvertent IMC
D27	Metro	Low	Night-Baseline	XMSN chip
D28	Metro	Med	Day	Single engine failure

Each pilot experienced every experimental condition outlined on the syllabus. Thus, each pilot completed 56 simulation runs, consisting of 28 approach scenarios and 28 departure scenarios, including the emergency conditions. The overall ORE experiment design was based on the participation of 12 subject pilots and contained a total of 672 simulation runs. However, due to pilot attrition, the experiment design was modified during the conduct of the experiment. A total of nine subjects actually completed the experiment, for a total of 504 simulation runs. The specific modifications made to the experiment, and the rationale behind these changes are detailed in section 5 of this report.

It must be mentioned at this point that a key element in designing the simulation scenarios is to address the objective of assessing VFR heliport airspace surfaces. The developmental structure of the experiments design and the use of variations in obstacle density, both the approach and departure, provide a baseline to examine the airspace issue. A detailed assessment is contained in appendix H.

4.2.1 Experiment Variables

The independent variables included in the ORE experiment design are briefly described below. Differences in the presentation of these variables (between approach and departure cases) are discussed where applicable.

4.2.1.1 Flight Corridor

The Metro and Valley flight corridors were used for both the approach and departure cases. Each path offered a unique presentation of terrain and obstacle type. A helicopter route chart of the two flight corridors is presented in figure 4.2.1.1-1. This chart includes a notional layout of the obstacles placed along each of the flight corridors. The route chart is conceptual in nature and does not represent any specific experimental condition.

4.2.1.2 Time of Day/Lighting

For the approach cases, four variations in TOD and heliport lighting were utilized: day, dusk, night with a baseline heliport lighting configuration (night-baseline), and night with an enhanced heliport lighting configuration (night-enhanced). For the departure cases, three variations in TOD and heliport lighting were presented: day, dusk, and night with baseline heliport lighting. The enhanced heliport lighting configuration was not used for the departure runs since the approach lighting aids have no applicability to the departure cases.

4.2.1.3 Obstacle Height/Density

As shown in table 4.2.1.3-1, four different levels of the OH/D factor were created by manipulating several related parameters including:

- The height of buildings located beneath, immediately beyond, or adjacent to the VFR protected surfaces.
- The percentage of "open" versus "occupied" ground space.
- The number, type, and placement of close-in and perimeter obstacles.

Thus, this variable represents the "level of threat" present in the flight environment, as influenced by a variety of factors. For the approach cases, three levels of OH/D were presented for each approach corridor. These OH/D conditions were designated as low, medium, and high. For the departure cases, four levels of OH/D were presented within each departure corridor. The four levels of OH/D for the departure cases were termed very low, low, medium, and high. Each parameter of the OH/D factor is described in the following paragraphs.

The variation in building height was accomplished by manipulating the height of 13 major structures located in the prototype city-center area. This subset of buildings included the twin office towers located directly north of the heliport and several other buildings located immediately beyond, beneath, or adjacent to the VFR corridor. This parameter was manipulated in terms of percentage of the maximum building height of the 13 major structures. For example,

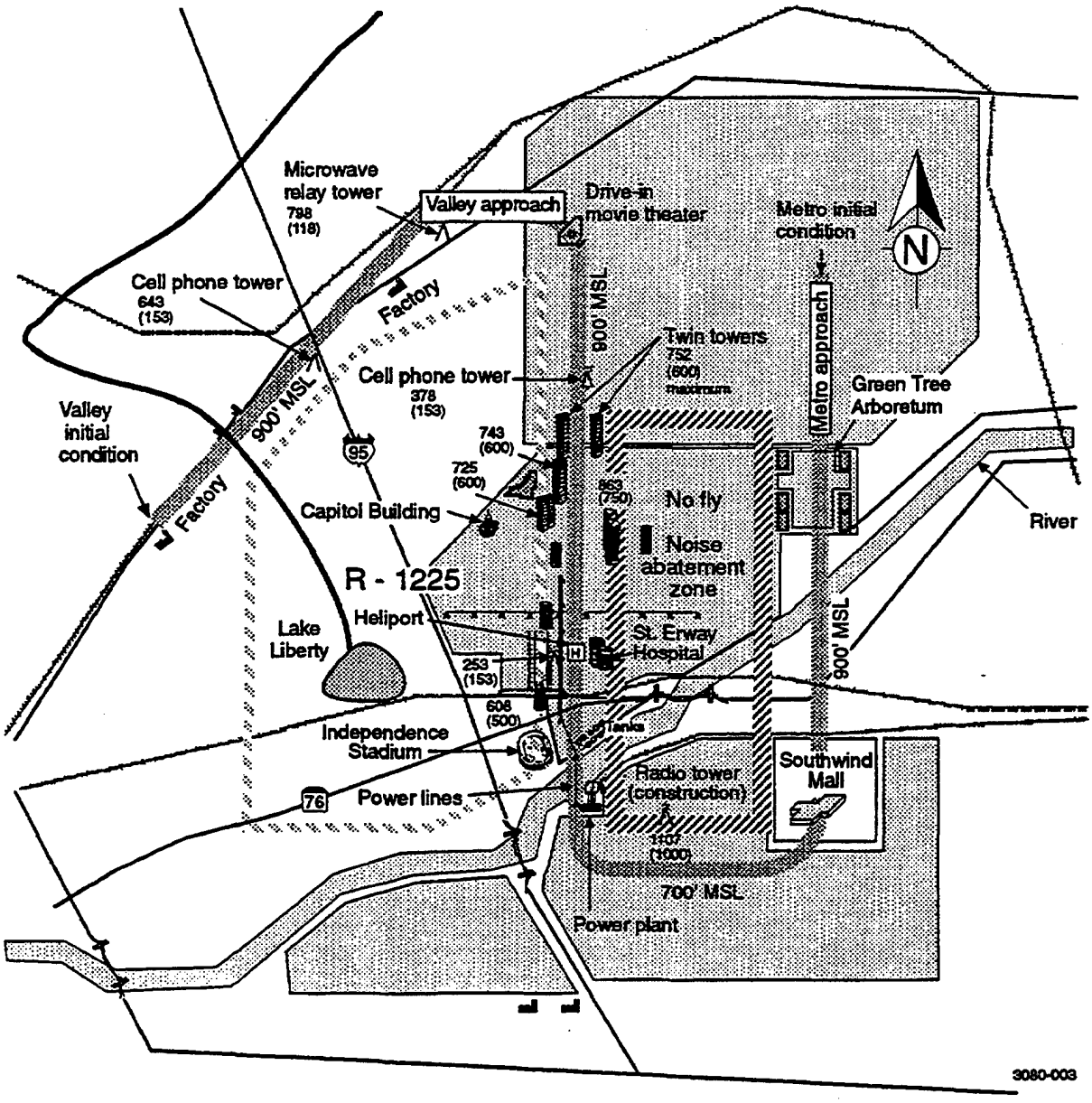

Figure 4.2.1.1-1. Helicopter Route Chart Showing Valley and Metro Flight Corridors

the twin towers had a maximum building height of 750 feet. This was considered 100 percent of their building height. For both the low and very low OH/D conditions, the major buildings were reduced to 60 percent of their maximum height. Thus, the twin towers were 450 feet in height for the low and very low OH/D conditions. Similarly, for the medium and high OH/D conditions, the major buildings were set to 80 and 100 percent of their maximum height, respectively. Building

TABLE 4.2.1.3-1. GUIDELINES FOR THE DEVELOPMENT OF OBSTACLE HEIGHT/DENSITY VARIATIONS

Flight corridor	Obstacle height/ Density	Ground Coverage		Max bldg height (%)	Close-in critical obstacles	Perimeter critical obstacles
		Occupied ground space	Open space %			
Valley	Very low (VL)	•40% covered w/ 1 to 3 story bldgs	60	60	•Light poles •Bushes (9 foot)	•Cellular phone tower •Radio tower
	Low (L)	•40% covered w/ 1 to 3 story bldgs •20% covered w/ 4 to 6 story bldgs	40	60	•Helicopter on furthest adjacent pad •Service wires •Ambulance •Large sign •Light poles •Bushes (12 foot)	•Construction crane (boom oriented away from flightpath) •High-tension wires •Tall building
	Medium (M)	•40% covered w/ 1 to 3 story bldgs •20% covered w/ 4 to 6 story bldgs •20% covered w/ 8 to 12 story bldgs	20	80	•Helicopter on closest adjacent pad •Service wires •Ambulance •Fuel truck •Light poles •Trees (15 foot)	•Construction crane (boom oriented into VFR surface) •High tension wire •Tall building •Antenna on tall building
	High (H)	•40% covered w/ 1 to 3 story bldgs •20% covered w/ 4 to 6 story bldgs •20% covered w/ 8 to 12 story bldgs •20% covered w/ 16 to 24 story bldgs	0	100	• Helicopter on run-up spot •Service wires •Ambulance •Fuel truck •Light poles •Pedestrians •Trees (18 foot)	•High tension wire •Cellular phone tower •Two building with VFR protected surface •Antenna on tall building
Metro	Very low (VL)	•40% covered w/ 1 to 3 story bldgs	60	60	•Service wires •Small sign •Bushes (9 foot)	•Smoke stacks
	Low (L)	•40% covered w/ 1 to 3 story bldgs •20% covered w/ 4 to 6 story bldgs	40	60	•Helicopter on furthest adjacent pad •Service wires •Light poles •Ambulance •Hospital wing (close) •Bushes (12 foot)	•Smoke stacks •Wheeled crane •Billboard •Water tower
	Medium (M)	•40% covered w/ 1 to 3 story bldgs •20% covered w/ 4 to 6 story bldgs •20% covered w/ 8 to 12 story bldgs	20	80	•Helicopter on closest adjacent pad •Service wires •Light poles •Ambulance •Hospital wing (Close) •Pedestrians •Trees (15 foot)	•Smoke stacks •Wheeled crane •Billboard •Water tower •Cellular phone tower •Wharf crane
	High (H)	•40% covered w/ 1 to 3 story bldgs •20% covered w/ 4 to 6 story bldgs •20% covered w/ 8 to 12 story bldgs •20% covered w/ 16 to 24 story bldgs	0	100	•Helicopter on run-up spot •Service wires •Light poles •Ambulance •Hospital wing (close) •Ground support equipment •Trees (18 foot)	•Smoke stacks •Wheeled crane •Billboard •Water tower •Cellular phone tower •Wharf crane •1,000 foot antenna 3080-040

heights are expressed as feet MSL to provide a common measure for all obstacle heights in relation to the heliport surface, regardless of the terrain contour surrounding the heliport. The heliport itself was located at an altitude of 100 feet MSL. Building heights are expressed as feet MSL to provide a common measure for all obstacle heights in relation to the heliport surface, regardless of the terrain contour surrounding the heliport. The heliport itself was located a an altitude of 100 feet MSL.

To control the size and number of potential emergency landing sites, the percentage of "open" versus "occupied" ground space was manipulated in the area beneath and adjacent to the VFR protected surfaces. This parameter was expressed as the percentage of city-center surface area that was occupied by buildings or other obstacles exclusive of roads and major buildings described above. The percentage of occupied space grew with increasing OH/D level. For example, in the very low OH/D condition, 40 percent of the selected area was occupied and 60 percent was open. In the low OH/D condition, the percentage of occupied space was increased to 60 percent, leaving 40 percent of the designated area as open space. In the medium and high OH/D conditions, the percentage of occupied space was increased to 80 and 100 percent, respectively.

As the percentage of open versus occupied space was manipulated, changes in obstacle height were also introduced to the visual scene. This was accomplished by using buildings of increasing height to populate the open spaces in the visual scene as obstacle density levels increased. Thus, as the OH/D level increased, not only was the unoccupied space becoming occupied but it was becoming occupied with more menacing obstacles. For example, in the very low OH/D condition, 40 percent of the surface area (exclusive of roads and major buildings) was covered with one to three story buildings, whereas the remaining 60 percent area was open space. In the low OH/D scenario 40 percent of the surface was covered with one to three story buildings, and an additional 20 percent was covered with four to six story buildings.

Similarly, the incremental ground coverage between the low and medium conditions was provided by 8 to 12 story buildings. Finally, the additional ground coverage between the medium and high OH/D conditions consisted of 16 to 24 story buildings.

Finally, critical close-in and perimeter obstacles were manipulated. Close-in obstacles were defined as obstacles on the heliport surface or in the immediate heliport vicinity. Perimeter obstacles were defined as obstacles close enough to influence flight along a flightpath, either by introducing a threat or by providing a positional reference for the pilot. The number, type, size, and location of the obstacles were manipulated. Thus, as the OH/D level increased, not only were more close-in and perimeter obstacles presented, but the obstacles were selected and located to present a greater threat to flight. Obstacles were identified for inclusion based on the inputs of helicopter pilots and operators. Typical close-in obstacles included a fuel truck, a helicopter on the ground with its rotors turning (holding short of the heliport), pedestrians, parked cars, perimeter fencing, light poles, signs, and bushes or trees in the immediate vicinity of the heliport. Perimeter obstacles used in this experiment included a construction crane with variable boom positions, cellular phone towers, a water tower on the top of a building, and reported air traffic in the heliport vicinity.

The location and size of close-in and perimeter obstacles was controlled to increase level of threat as the OH/D level increased. For example, the boom on the construction crane was oriented away from the approach path and located completely outside the VFR protected surface in the medium OH/D condition. In the high OH/D condition, the boom was oriented inward and actually represented a slight incursion into the protected surface. Similarly, the height of bushes and trees included as close-in obstacles grew with increasing levels of OH/D. For the very low and low OH/D conditions, bushes 9 and 12 feet high, respectively, were used as close-in obstacles. For the medium and high OH/D conditions, the bushes were replaced with trees, 15 and 18 feet tall, respectively.

In creating different OH/D levels, the greatest emphasis was placed on manipulation of obstacles within approximately 500 feet of the heliport. To a lesser extent, some manipulation of obstacles between 1,000 feet and the outer limit of the VFR protected surface (4,000 feet) was also performed. With the exception of obstacles located immediately beyond the protected surface, there was little manipulation of obstacles outside the city-center area or beyond the limits of the protected VFR approach surface.

4.2.2 Emergency Conditions

In addition to the 48 normal approach/departure runs, each pilot was presented with eight emergency conditions, four on approach and four on departure. Each emergency occurred under the same conditions for each subject (i.e., for all subjects, an emergency condition was presented on the same flight corridor, under the same TOD/lighting and OH/D conditions). The order of the emergency conditions, and their placement within the experiment scenarios was counterbalanced across subjects. Prior to their participation in the experiment pilots were briefed of the potential for emergencies and the appropriate pilot response to the emergency conditions.

The specific emergency conditions utilized in this experiment, along with the experimental conditions under which they were presented, are listed in table 4.2.2-1. These emergency conditions were selected for inclusion in the experiment based on the urgency of pilot actions required and the fact that they were not catastrophic in nature. Thus, the pilots were forced to react quickly but could maintain control of the aircraft. This provided an objective measure of pilot ability to handle an emergency condition within an ORE.

The introduction of the emergency conditions served two primary objectives. First, the emergency conditions increased the realism of the simulation and helped maintain pilot alertness. Second, pilot responses to the emergency conditions provided a measure of performance under unique or abnormal conditions, potentially providing an indication of the spare capacity or resources that the pilots had during the conduct of the normal scenarios.

Emergency scenarios were conducted identically to the normal scenarios, with the exception of the types of data collected. Data obtained during normal runs were supplemented with additional objective measures and subject matter expert (SME) ratings for the emergency runs. The measures and ratings utilized to judge performance on the emergency scenarios are described in greater detail in section 4.4.5.

TABLE 4.2.2-1. EMERGENCY CONDITIONS

Approach Scenarios

Emergency condition	Flight corridor	Time of day/lighting	Obstacle height/density
Traffic incursion in heliport	Valley	Night-enhanced lighting	High
Dual tachometer failure	Valley	Dusk	Low
Engine oil pressure low	Metro	Day	Medium
Inadvertent IMC due to gradual degradation in visibility	Metro	Night-baseline lighting	Medium

Departure Scenarios

Emergency condition	Flight corridor	Time of day/lighting	Obstacle height/density
Engine oil at high temperatures	Valley	Day	Very low
Inadvertent IMC due to uniform drop in ceiling	Valley	Dusk	High
Transmission chips indication	Metro	Night-baseline lighting	Low
Single engine failure	Metro	Day	Medium

3080-006

4.2.3 Environmental Conditions

Visibility was maintained at two miles and the ceiling was set to 1,000 feet MSL for all approach/departure scenarios. These values are typical of EMS helicopter operations, based on inputs from members of the helicopter operational community. The heliport was located at 100 feet MSL.

During two emergency condition scenarios, the pilot encountered instrument meteorological conditions (IMC). In one approach scenario, the visibility was incrementally reduced to 0.3 miles. In one departure scenario, the ceiling was lowered to 500 feet MSL during climbout. Changes in visibility or ceiling height were not announced to the pilot.

As described earlier in section 3.2, steady winds of 10 knots, gusting to 20 knots (15 knots ± 5 knots), were included in all approach and departure scenarios. Twelve different wind directions, in 30 degree increments relative to the heliport, were used. Wind direction was counterbalanced across experiment conditions and subjects to statistically eliminate the effects of winds on the experiment results. Pilots received wind information upon request from ATC and from a simulated windsock located at the heliport.

4.3 PILOT SELECTION

As described in section 4.2, the ORE experiment was originally designed to include the participation of 12 subject pilots. A total of 14 pilots were brought to the simulation facility and began their participation in the experiment. Of these 14 pilots, only nine completed the entire experiment. The remaining five pilots were removed from the experiment after experiencing simulator sickness during initial simulator familiarization runs, as described in section 5. Eight of

the nine subject pilots completing the experiment were employed by Keystone Helicopters, Inc., of West Chester, PA. The remaining pilot was provided by Corporate Jets, Inc., of West Mifflin, PA. The pilots were paid by their home company for participating in the ORE experiment.

Based on discussions with Keystone and other helicopter operators performing EMS operations, a flight experience range of 3,000 to 4,000 hours (rotary- and fixed-wing combined) was targeted for participation in the ORE experiment. Ultimately, due to the limited number of Keystone pilots who fell within the 3,000 to 4,000 hour range, the target experience range was broadened to 6,500 hours to qualify the required number of subject pilots.

Each pilot completed an information survey as part of their initial briefing (see appendix B). This provided pilot background data and established a profile of the participants. Responses to the pilot information survey provided data on pilot demographics, flight experience (e.g., rotary- versus fixed-wing, single pilot flight versus multiple crew flight time, civilian versus military flight time), instrument flight time, training background, simulator flight time, night flight time, and flight instructor time. Pilots were also asked to provide information concerning their most recent flight experience (i.e., within the sixty days prior to their participation in the ORE experiment). Summary data for the nine pilots who completed the ORE experiment are provided in table 4.3-1.

4.4 PILOT PERFORMANCE ASSESSMENT AND DATA ACQUISITION METHODOLOGY

The objective of the ORE research effort was to provide a comprehensive evaluation of pilot mental workload, flight performance, and pilot perceptions of risk, relating to the effects of obstacle and visibility characteristics during helicopter flight in an ORE. Although there is no universally accepted definition of mental workload, it may be conceptualized as the interaction of several factors, including the capabilities, motivation and state of the human operator; the operator's awareness of the situation; the internal and external environment; and the task demands imposed by the structure of the system-operator interface[15,16,17]. Due to the multifaceted nature of mental workload, researchers and practitioners have generally acknowledged that no single measurement technique provides a valid and reliable measure of all mental workload critical components experienced by the operators of complex systems[17,18,19,20]. Thus, several workload measurement reviews have emphasized the importance of employing a battery of measures to capture the various dimensions of mental workload[15,16,19,20,21,22,23].

Based on these fundamental concepts, a multidimensional battery of measures was applied during the ORE experiment for the evaluation of flight performance, workload, and pilot perceptions. A variation of the methodology used by Boeing Helicopters and the University of Illinois[24] in a previous experiment was employed. Four primary categories of data were obtained during or immediately following each simulation run to assess pilot workload and flight performance. These data categories include:

TABLE 4.3-1. SUMMARY OF PILOT DEMOGRAPHIC DATA COLLECTED FROM PILOT INFORMATION SURVEY

	Summary Average	Range
Total flight time (hours)	4,558	2,700
PIC	3,730	5,650
CFI	295	1,235
Instrument	152	618
Night	1,054	1,035
Simulator	268	974
EMS	620	2,500
Single Pilot	2,737	3,495
Civilian	2249	3,700
Military	2,209	3,903
Helicopter flight time (hours)	*4,122*	*3,400*
PIC	3,344	5,700
CFI	291	1,200
Instrument	118	598
Night	967	1,050
Simulator	265	995
EMS	620	2,500
Single Pilot	2,361	3,450
Civilian	1,814	4,000
Military	2,208	3,900
Airplane flight time (hours)	436	1,600
PIC	386	1,500
CFI	4	35
Instrument	34	150
Night	88	500
Simulator	3	25
EMS	0	0
Single Pilot	376	1,425
Civilian	435	1,598
Military	1	3
Percent time in helicopter (%)		
Total time	90	36
PIC	80	100
CFI	44	100
Instrument	72	63
Night	92	33
Simulator	91	83
EMS	78	100
Single Pilot	85	45
Civilian	63	100
Military	78	100
Flight time last 60 days (hours)		
Helicopter	35	55
Airplane	0	0
Instrument	2	10
Night	11	35

3080-153

1. Primary task measures that consist of flight performance data recorded directly from the simulator.
2. Secondary task measures that consist of embedded tasks during the flight scenario.
3. Subjective ratings of risk, workload, and perception obtained from the pilot.
4. Physiological measures of heart rate and visual blink rate.

The individual categories of data collected during the ORE experiment are presented in figure 4.4-1. A top level depiction of the data collection process is shown in figure 4.4-2. Each of the four primary categories of data are described in the following sections. Specific measures employed in the ORE experiment are also discussed.

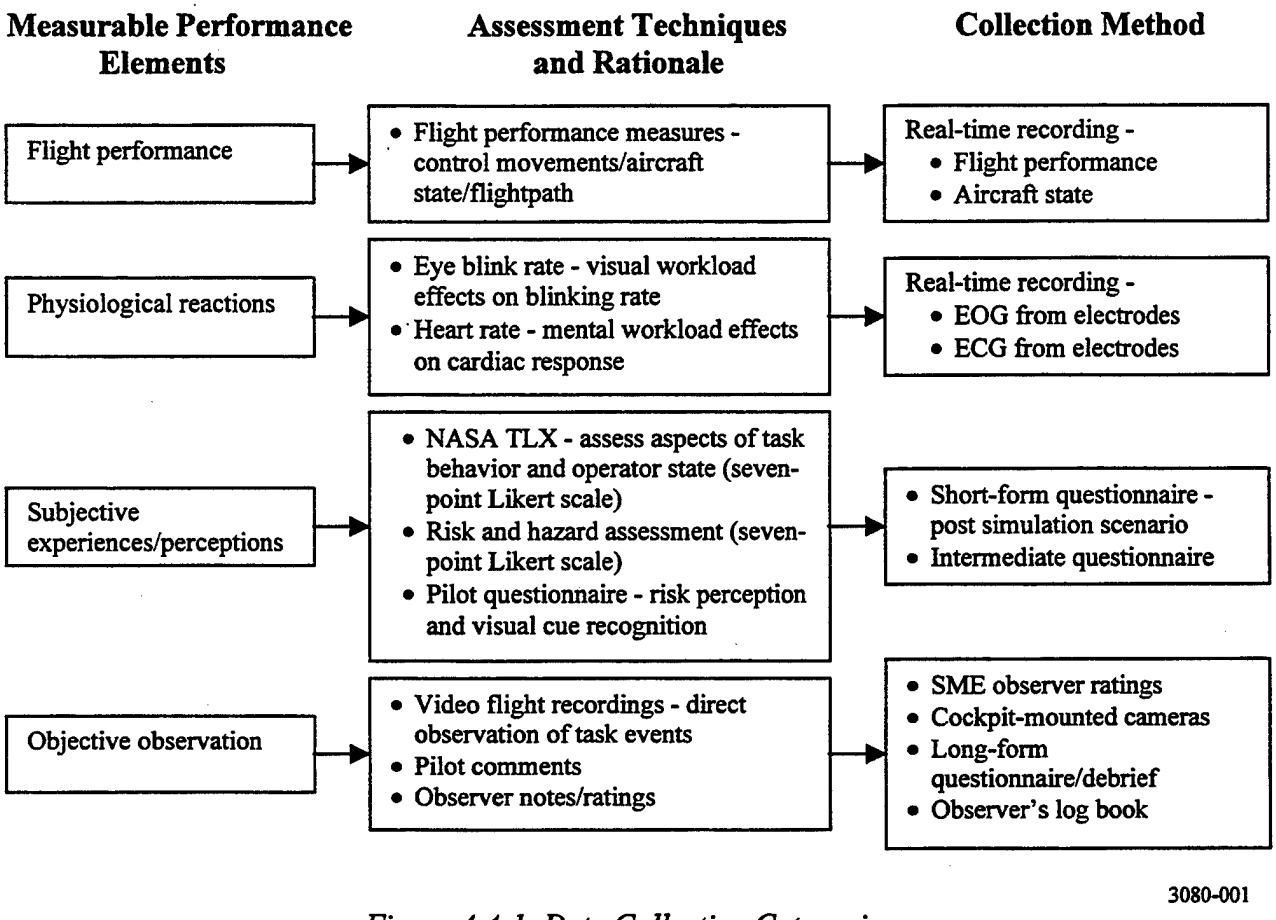

Figure 4.4-1. Data Collection Categories

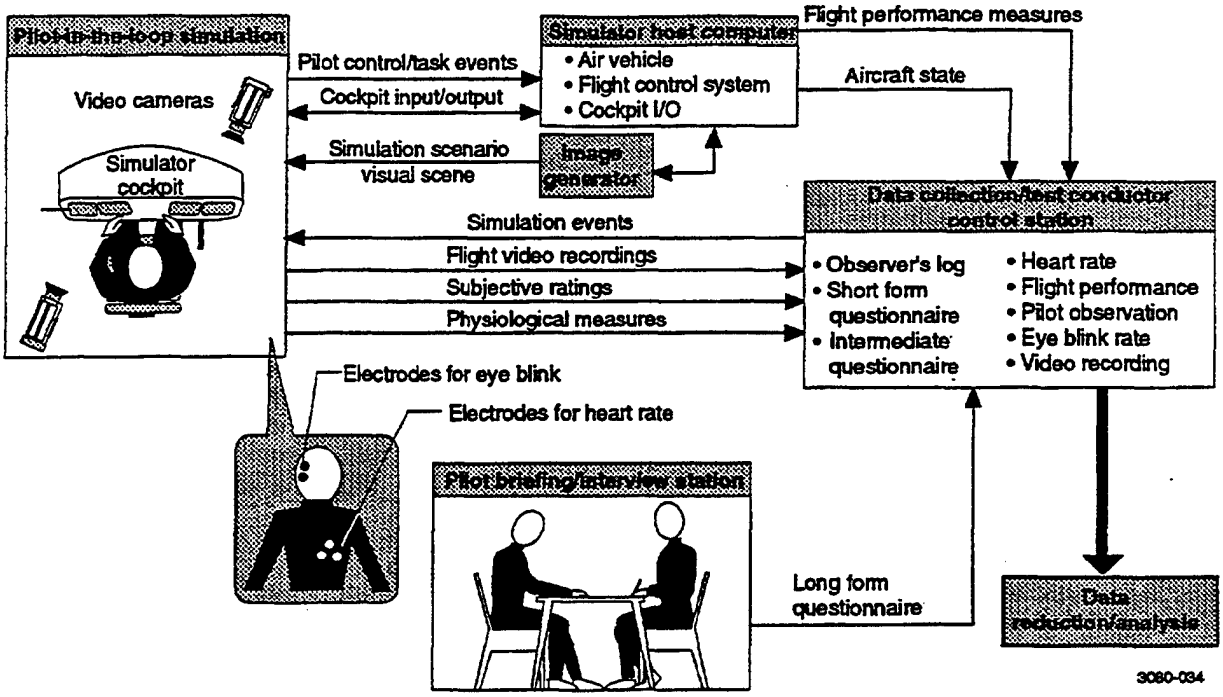

Figure 4.4-2. Data Collection Input/Output

4.4.1 Primary Task Measures

Primary task measures reflect performance on the operator's primary task, or some aspect of the operator's strategy for completing this task (e.g., the number or magnitude of flight control inputs). It is assumed that changes in workload result in corresponding changes in primary task performance. As workload increases, performance on the primary flight performance task decreases. As a result, these measures provide a direct indication of total system performance, accounting for the human in the loop. There are two disadvantages of primary task measures. First, they do not readily transfer to different tasks or scenarios. For example, while RMS tracking error may be a reliable metric of operator performance in a vehicle control task, response time and accuracy are more appropriate for a communications task. Second, they do not adequately assess operator residual capacity. For example, while two individuals may exhibit equivalent performance on a primary task, one may be incapable of meeting additional task demands, while the other may possess spare resources required to meet additional task demands or to perform additional tasks. An analysis limited to primary task performance measures would not distinguish between the level of workload experienced by these two individuals. Similarly, consider an individual who is capable of handling additional task demands without suffering a noticeable degradation in primary task performance. In this case, an analysis limited to primary task measures would fail to identify any change in task demands.

In the ORE experiment, aircraft flight performance was the pilot's primary task. Thus, the primary task measures employed were flight performance measures related to the pilot's ability to control and navigate the aircraft. Examples include adherence to the desired flightpath and recommended airspeeds, landing accuracy, aircraft attitude, and obstacle clearance. In addition,

measures relating to the pilot's underlying technique or strategy for completing the primary task were recorded (e.g., the number and magnitude of control inputs).

The aircraft state and flight performance parameters were sampled at 40 msec intervals. Data was recorded directly from the simulator during simulation runs and electronically transferred to the University of Illinois for further processing to extract task-dependent measures for analysis. Flight information was time-stamped so data could be matched to specific events and synchronized with data from other sources. Table 4.4.1-1 presents a list of the aircraft state and performance measures recorded directly from the simulator.

TABLE 4.4.1-1. AIRCRAFT STATE AND FLIGHT PERFORMANCE DATA RECORDED FROM THE SIMULATOR

1.	Aircraft X, Y coordinates
2.	Aircraft altitude (radar and barometric)
3.	Flight control inputs (collective, cyclic, pedals)
4.	Distance from helipad center
5.	Aircraft pitch (angle and rate)
6.	Aircraft roll (angle and rate)
7.	Aircraft yaw (heading angle and rate)
8.	Aircraft sideslip
9.	Aircraft heading
10.	Distance and heading to helipad
11.	Airspeed
12.	Longitudinal velocity
13.	Lateral velocity
14.	Vertical velocity
15.	Engine/aircraft instrument data
16.	Cockpit switch and indicator status
17.	Elapsed scenario time

3080-108

A limited number of primary flight performance measures were derived from the aircraft state data recorded during the ORE simulation runs. Flight performance measures derived for approach and departure scenarios are listed in table 4.4.1-2. Some measures apply to all flight segments; others do not. For example, touchdown error applies only to the touchdown portion of an approach scenario and has no application to other segments. Similarly, altitude violations are not applicable to the touchdown portion of an approach, but are applied to the in-flight segments. Flight segments are discussed in greater detail in section 6.

4.4.2 Secondary Task Measures

Secondary task techniques require the operator to perform an additional, structured task while simultaneously performing the primary task at hand. Changes in secondary task performance reflect changes in the processing demands of the primary task and indicate divided attention. In general, as the difficulty of the primary task increases, performance of a secondary task declines[25]. In some cases, the operator may fail to complete a secondary task due to the demands imposed by the primary task. Thus, secondary task measures indicate operator residual capacity which may not be easily derived from primary task measures. The main disadvantage of secondary tasks is the potential to artificially interfere with primary task performance.

TABLE 4.4.1-2. PRIMARY FLIGHT PERFORMANCE MEASURES

	Approaches
1.	Segment length
2.	RMS lateral deviation from flightpath
3.	RMS vertical deviation from flightpath
4.	Minimum altitude violations (50 ft below required altitude)
5.	Percentage of time in minimum altitude violations
6.	Maximum altitude violations (50 ft above required altitude)
7.	Percentage of time in maximum altitude violation
8.	Mean airspeed
9.	Cyclic control in puts (magnitude and rate)
10.	Occurrences of excessive bank angle (+/-60°)
11.	Landing touchdown error (feet)
12.	RMS vertical slope error
13.	Occurrences of excessive pitch angle (+/-30°)
14.	Clearance from selected obstacles
	Departures
1.	Segment length
2.	RMS lateral deviation from flightpath
3.	RMS vertical deviation from flightpath
4.	Mean airspeed
5.	Cyclic control inputs (magnitude and rate)
6.	Occurrences of excessive pitch angle (+/-30°)
7.	Clearance from selected obstacles

3080-107

In the ORE experiment, ATC communications and emergency conditions provided secondary tasks on which performance could be measured. Although secondary task data was collected, secondary task performance was not analyzed as part of this research effort. This data is available for analysis in support of future research efforts, although this would require detailed review of videotape data collected during the ORE simulation.

4.4.3 Subjective Measures

Subjective workload measures attempt to capture an individual's experiences, perceptions, and opinions concerning the workload imposed by a specific task or series of tasks. Subjective techniques, particularly in the form of rating scales, have been the most widely used class of workload assessment measure. Some researchers have suggested that by tapping the experiences of the operator, subjective measures offer the most appropriate measures of cognitive workload[26,27]. Subjective techniques offer a number of advantages, including:

- Low cost.
- Ease of implementation.
- Lack of supporting equipment.
- Lack of intrusion on the primary task.
- High degree of subject acceptance.

The primary limitation associated with subjective measures is a high degree of inter-subject variability. Furthermore, although subjective measures generally correspond well with performance data, there have been cases in which subjective data has not correlated well with objective performance data[28, 29, 30]. The potential mismatch between performance and subjective workload measures have led some authors to suggest that neither subjective nor performance measures should be used as the sole basis for assessing operator workload[19]. Finally, a review of recent research also indicates that these measures appear to be more sensitive to intermediate than high levels of workload, and are most reliable when collected immediately after task performance.

In the ORE experiment, subjective measures were used to analyze operator workload and to assess pilot perception of risk. Three different questionnaires were utilized to gather information from the pilots. Each questionnaire is briefly discussed in the following paragraphs.

4.4.3.1 Short-Form Questionnaire

As previously discussed, subjective measures are most reliable when collected immediately following task performance. With this requirement in mind, a questionnaire was developed to be administered to the pilots after each approach/departure scenario. The questionnaire was constructed to fit within the time constraints of the simulation schedule. The NASA Task Load Index (TLX) rating scale was selected to collect subjective ratings of mental workload[31]. The TLX scale, developed at NASA Ames Research Center, has been well validated as a reliable pilot workload assessment instrument. It has been used in civilian and military flight environments, (in simulators and operational aircraft) for both fixed- and rotary-wing aircraft[32, 33] Pilots respond to a standard set of questions related to several different factors using a seven point rating scale with anchored endpoints. In the ORE experiment, the pilots used the TLX scale to rate each approach/departure scenario on the following bipolar scales: mental demand, physical demand, temporal demand, effort, performance, and frustration level.

In addition to the six TLX ratings, each pilot was asked to provide two additional ratings relating to risk perception and overall safety:

1. How safe (in terms of risk) was the last landing or takeoff?
2. To what degree did the obstacles presented create a safety hazard?

Responses to these questions were also provided on a seven point bipolar scale with anchored endpoints.

The short-form questionnaire was administered following each simulated approach or departure, while the pilot remained seated in the simulator cab. The questions were read to the pilot over the intercom system, and pilot responses were recorded by observers in the simulator control room. The pilots had a paper version of the questionnaire for reference in providing their responses. The short-form questionnaire is presented in appendix C.

Originally, the short-form questionnaire also included four open-ended questions. These questions asked for further information pertaining to the factors which contributed to the pilot's

perception of risk, the specific visual cues used by the pilot on approach or departure, obstacle clearance distances, and any additional comments the pilot may have relating to the previous scenario. These questions were removed following the completion of the first two days of simulation. This decision was based on several factors. First, administration of the short-form questionnaire in its original format took longer than expected and made the simulation sessions unacceptably long. Second, extraction of useful information from the responses was beyond the scope of this investigation. These questions formed the basis of the intermediate questionnaire described in section 4.4.3.2.

4.4.3.2 Intermediate Questionnaire

Responses to the four open-ended questions removed from the short-form questionnaire were needed to provide insight into pilot risk perceptions and to determine which visual cues were important to the pilots. These questions were compiled into an intermediate questionnaire administered to the pilots during their simulation break periods. Over the course of the experiment, each pilot provided seven sets of intermediate questionnaire responses, one for each of the seven simulation sessions that they completed. Each session typically encompassed eight simulation scenarios. The intermediate questionnaires, administered in written format were completed by the pilots while waiting for the next session to begin. The Intermediate Questionnaire form is presented in appendix D.

4.4.3.3 Long-Form Questionnaire

The final questionnaire administered to the pilots was termed the long-form questionnaire. This questionnaire was administered at the conclusion of each pilot's final simulation session. This 25-question form enabled the pilots to provide their inputs and perceptions concerning several factors of interest in the ORE research effort. The long-form questionnaire is presented in appendix E.

The long-form questionnaire was divided into four sections:

1. Risk assessment.
2. Visual cues and other features used by the pilots to complete the approach/departure scenarios.
3. Training requirements as they relate to flight in an ORE.
4. The fidelity of the ORE simulation environment.

The first section, "Risk Assessment," was comprised of 13 questions. These questions were used to ascertain the pilots' perceptions of risk associated with specific categories of obstacles. Pilots were asked to identify which obstacles they felt posed the greatest threat to safety during the various segments of flight (takeoff and departure, downwind and base, final approach and touchdown, and hover/taxi), and which of the flight segments they felt were the most dangerous. The pilots also provided rank orderings of several categories of obstacles (from a risk perspective), in relationship to safety of aircraft, occupants, and people on the ground. Questions also examined the impact of limited visibility on the pilots perceptions associated with known and unknown obstacles, the relationship between obstacle density and the pilots' perception of

their ability to cope with an emergency or other in-flight situation, and the pilots' obstacle avoidance priorities.

The second section of the long-form questionnaire, "Simulation Scenarios Just Completed" consisted of five questions. The focus of these questions was on the identification of visual and other internal/external cues the pilots relied on to complete the ORE approach and departure scenarios. Specifically, pilots were asked to describe:

- Visual cues which aided their identification of obstacles and the associated threat to the aircraft.
- Aircraft instruments used to safely complete an approach and landing.
- Additional internal/external cues used to safely complete an approach and landing.
- Features of the landing zone that assisted or detracted from their ability to complete an approach or landing.

The third section of questions on the long-form questionnaire, "Training for ORE Environments" addressed training requirements for preparing a pilot for flight within an ORE. Specifically, the pilots were asked if they felt training was adequate for the approach and departure scenarios they had completed during the ORE experiment, and whether they felt additional checkrides or certification were required for flight in an ORE. The pilots were also asked to recommend specific pilot instruction that could reduce the risk associated with flight within an ORE.

The final section of the long-form questionnaire, "Simulation Fidelity," addressed the pilot's view of the simulated environment in which the ORE experiment was conducted. The pilots were asked to rate the fidelity, or realism, of several components of the simulation, including the helicopter model, lighting conditions, terrain features, manmade features, the cockpit, and scenario realism. The pilots were also asked whether they would have flown any of the approach or departure scenarios differently had they been in an actual aircraft as opposed to being in the simulator.

4.4.4 Physiological Measures

Physiological measures of operator workload involve the quantification of body responses under different levels of task demands. In recent years, a wide variety of physiological measures have been used and validated for the assessment of operator state and mental workload[18]. There are several advantages associated with the use of physiological measures. First, since they do not require overt responses, physiological measures are well suited for tasks that are primarily cognitive in nature. Second, these types of measures may be recorded continuously throughout task performance to provide a dynamic record of operator state. Finally, physiological measures are inherently multidimensional and therefore can be expected to provide a number of views of operator workload. There are also a number of limitations associated with the use of physiological measures, primarily their high cost, the expertise required for successful data collection, analysis and interpretation, and the difficulty in excluding artifacts.

Two physiological measures were recorded during the ORE simulations: electrocardiographic (ECG) activity (heart rate) and electro-oculographic (EOG) activity (eye blink rate). These measures were chosen based on their proven ability to yield consistent and valid results for a broad range of variables. Along with primary task and secondary task measures they provide evidence of changes in pilot mental workload as a function of the manipulation of ORE scenario characteristics. Physiological data was recorded for each run using customized portable collection equipment. This allowed for short turnaround and quick exchange of pilots.

Heart rate measures have been successfully used to provide a continuous and real-time index of pilot mental workload in both simulator[18, 24, 34] and actual flight operations[35]. Since the heart is influenced by the autonomic nervous system, heart rate is related to physical and emotional states. Thus mental load and task demands will affect (and can be observed in) cardiac response. Other normal factors such as the orienting response, stressful and surprising events, can also be observed. ECG activity was recorded from electrodes placed just below and to either side of the heart on each subject. Occurrences of the R-wave (the major positive deflection in the ECG signal) were calculated offline and then analyzed as a simple measure of heart rate.

Measures of blink activity have been employed for over 60 years in the investigation of mental activities[36]. Blink rate, under control of the somatic system, provides a measure directly related to task demands and to task loading. The rate of blinking has generally been found to decrease with increases in the difficulty of visual task processing[37, 38] and when operators transition from auditory to visual tasks[39]. In the present study, measures of blink rate were used to assess changes in operator workload as a function of changes in the ORE variables. Vertical EOG activity was recorded by two electrodes placed above and below the right eye. Blinks were identified offline by first filtering the data (-3 dB at 6.27 Hz; 0 dB at 14.29 Hz) and then identifying voltage deflections which met specified criteria of polarity, amplitude, duration, and velocity. The specific criteria used conform to the morphology of the blinks produced by each individual subject.

4.4.5 Emergency Response Data

As described in section 4.2.2, several objective measures and SME ratings of pilot performance were recorded during the performance of each emergency condition scenario, using the Emergency Response Pilot Score Sheet presented in appendix F. These measures were recorded in addition to the data collected during the baseline experiment. Two time-based objective measures were recorded during the emergency scenarios: the time required for the pilot to recognize the emergency situation and the time to gain control of the situation. Responses were rated from one to five based on the range in which the recorded time fell (e.g., 0-3 sec, 3-10 sec, 10-20 sec, 20-60 sec, or greater than 60 sec for the time to initially recognize the fault).

The SME ratings of pilot response to the emergency conditions were provided by the test conductor, who is an experienced military helicopter pilot familiar with commercial helicopter procedures. In general, the SME ratings related to the pilot's identification and correct recognition of the emergency condition, the appropriateness of the pilot's response to the emergency condition, and the degree to which the pilot was able to maintain control of the

aircraft. The SME ratings were recorded on a five-point bipolar scale (ranging from not very successful to successful).

An in-depth analysis of the emergency response data was not performed as part of this effort for a variety of reasons. First, as previously described, the emergency conditions were introduced primarily as a means to increase the realism of the ORE simulations and to heighten the general state of pilot awareness. Second, the emergency conditions were not systematically presented across all levels of the other experimental variables. For example, the engine oil pressure condition was presented only for an approach on the Metro flight corridor, in daylight, and with medium OH/D. Thus, even with detailed analysis, it would not be possible to assess pilot performance differences in relation to the variables of interest (i.e., TOD/lighting, OH/D). Therefore, detailed analysis of the pilot emergency response data was not attempted. This data is available for further review and detailed analysis.

4.4.6 Video Recording

In addition to the composite set of measures described above, video recordings were made during each of the simulation runs. Four frames were recorded simultaneously. The quadscreen image was also displayed in real-time in the simulation control room, enabling the test conductor to monitor pilot actions.

One panel of the quadscreen display provided a front view of the pilot's head and face from a miniature camera mounted on the side of the glareshield. A second panel presented the cockpit as viewed over the pilot's shoulder by a second camera mounted above and behind the pilot's seat. The third panel displayed the front window view for the scenario directly from the simulator IG. The remaining panel provided a view of the pilot's center console display (see figure 3.3-2). This panel contained information specific to the simulation run being conducted (although this information was blocked from the pilot's view in the cockpit), including the simulation scenario number, wind condition, elapsed simulation run time, date, and TOD. The videotapes also include full audio recording of the experiment.

The videotapes were collected primarily to provide a record of the experiment and a means to explore anomalies that surfaced during analysis of other data. A detailed review and analysis of the videotape data was not conducted. The tapes are available for future review.

4.4.7 Data Collection and Storage

The flight performance, risk assessment and risk perception ratings, and physiological data were written in real-time to a hard disk of a Pentium-based personal computer (PC). This data was backed up on 8-mm computer tapes. Aircraft state and flight performance data were stored by the simulator on disk and later transferred to magnetic tapes. These tapes were resampled offline to extract performance measures related to aircraft state (roll, pitch, sideslip, speed, altitude, and position) and control (collective, stick, and pedal movements).

5.0 EXPERIMENT CONDUCT

This section describes the overall conduct of the ORE simulation evaluations. All of the test subjects were run through the experiment in the same general manner. After the initial test methods are described, test conduct discrepancies and pilot sickness problems are discussed, and solutions are detailed.

5.1 BRIEFING

All of the pilots participating in the experiment were given a briefing immediately after arriving on the first day. In the briefing the pilots were given information on the following subjects:

- Experiment conduct.
- Experiment objectives.
- Simulator characteristics.
- Data collection methods.
- TLX questionnaire instructions.
- Aircraft configuration.
- Mission description.
- Heliport environment.
- Environmental conditions.
- Corridor information.

A briefing packet (appendix G) containing the above information and simulation aircraft technical data was supplied to each of the pilots for reference. Answers to specific questions were provided as needed. Each pilot completed an information survey and signed an informed consent form.

Information on simulator sickness was added to the briefing after the first two pilots completed their evaluations. The remaining pilots were advised of the possibility of simulator sickness, and precautions taken to reduce its likelihood were discussed. Some of the counters measures used to avoid simulator sickness were:

- Blanking the visual screens while entering and exiting the cabin.
- Instructing the pilots to close their eyes prior to each simulation start or stop.
- Blanking the screen during database changes.
- Briefing that symptoms are not abnormal thus reducing anxiety accompanying the development of the sickness.
- Suggesting that the pilots avoid large, rapid head movements and aircraft maneuvers to reduce the potential stimuli for simulator sickness.

5.2 TRAINING

After the physiological data collection devices were affixed, each pilot was given a short training period in order to become familiar with the simulator handling characteristics and flight

environment. The training started in the heliport environment using a condition similar to the ensuing experiment. Initially, training began in hover at a heliport. This was changed when the sparse visual environment of the training heliport and the unfamiliar handling qualities of the simulator caused several pilots to succumb quickly to simulator sickness. The training syllabus was modified after the first set of pilots, in an attempt to reduce the drop-out rate of the test subjects due to simulator sickness.

The modified training syllabus is detailed in table 5.2-1. Starting on a downwind-leg at 110 knots allowed the pilots to familiarize themselves with the aircraft in a stable phase of flight. During this initial run, the pilots were instructed to conduct basic maneuvers. During the second practice run, the pilots were permitted to make the approach to land, but were not confined to a particular landing point or required to hover. Training continued as shown in the table. The training period was designed to get the pilots acquainted with the aircraft and its handling qualities. It was not expected that the short training period would allow for pilot proficiency. The final run included a single-engine failure, to instill a sense of reality and demonstrate that emergency situations were possible.

TABLE 5.2-1. FINAL TRAINING SYLLABUS (POST SIMULATOR CHANGES)

Training runs familiarized pilots with simulated helicopter handing qualities and visual database characteristics			
Start point	**Condition**	**Maneuvers**	**Familiarization goals**
Metro initial condition	Day	• Straight and level flight • Turns left and right • Accelerations and decelerations	• Aircraft handling qualities • Inside/outside environment • Day lighting conditions
Metro initial condition	Day	• Metro approach	• Metro corridor/landmarks • Approach to land techniques • Day lighting conditions
Valley initial condition	Dusk	• Valley approach	• Valley corridor/landmarks • Approach to land techniques • Hover techniques • Dusk lighting conditions • Experiment conduct/protocol
Helipad 5-foot hover	Day	• Valley departure • Hover	• Valley departure course • Hover techniques • Helipad environment • Departure techniques • Experiment conduct/protocol • NASA TLX questionnaire
Helipad 5-foot hover	Night	• Metro departure	• Night lighting conditions • Metro departure course • Emergency conditions • Experiment conduct/protocol • Reality of potential emergency

3080-154

Throughout training, pilots were coached through the runs to assure their recognition of landmarks. The pilots were permitted to accomplish training at their own pace, but training time was limited to approximately 45 minutes. The changes in training, combined with simulator

response time changes (see section 5.5) and countermeasure techniques, reduced the drop-out rate from 50 to 12.5 percent (table 5.2-2).

TABLE 5.2-2. PILOT STATUS SHEET

Pilot number	Status	Status date	Group	Training/ Simulator
Pilot 1*	Excused due to motion sickness	26 Sep 96	1	Unmod
Pilot 2	Completed experiment	27 Sep 96		
Pilot 3	Completed experiment	01 Oct 96	2	Unmod
Pilot 4	Excused due to motion sickness	30 Sep 96		
Pilot 5	Excused due to motion sickness	07 Oct 96	3	Unmod
Pilot 6	Excused due to maintenance problems	07 Oct 96		
Pilot 5a	Completed experiment	10 Oct 96	4	Modified
Pilot 6a	Completed experiment	10 Oct 96		
Pilot 8	Completed experiment	15 Oct 96	5	Modified
Pilot 9	Completed experiment	15 Oct 96		
Pilot 11	Excused due to motion sickness	17 Oct 96	6	Modified
Pilot 12	Completed experiment	18 Oct 96		
Pilot 1a	Completed experiment	22 Oct 96	7	Modified
Pilot 11a	Completed experiment	22 Oct 96		

* Non-sequential numbering to achieve counter balancing from original pilot listing.

3080-018

5.3 TEST CONDUCT

Each pilot participated for two days, completing 56 runs during seven sessions. The experiment design called for two pilots to fly each day with each pilot completing 28 runs each day. Due to variations in training time and simulator problems, pilot run matrices were frequently divided unevenly between the first and second days of simulation. Most pilots finished either three or four sessions each day, alternating to complete seven sessions in two days (figure 5.3-1).

Approximately 45 minutes was needed to complete each eight run session. The run sequence was counterbalanced, resulting in a varied number of approaches versus departures in each session. After each run was completed, the TLX questionnaire was administered verbally and responses were recorded. Between sessions, breaks were given and intermediate questionnaires were administered. Lone pilots (pilots without a partner due to simulation sickness) were allowed 30- to 45-minute breaks between sessions. This break duration was established to replicate the break time these pilots would have received had a second pilot been available.

An audio stamp (for the VCR), and coordination check (to ensure all participants were prepared for the next run) preceded each run. The run was conducted at the pilot's own pace. Radio communications were simulated and are detailed in section 5.4. At the conclusion of each run, the test coordinator called for a simulator stop and the TLX questionnaire was administered. If required, runs were repeated at the conclusion of the pilot's testing period to limit familiarity with that run. The test coordinator recorded any anomalies.

Simulation schedule provided breaks to reduce pilot fatigue; counter-balanced run sequence eliminates training/fatigue effect on data

ORE SIMULATION Daily Schedule		Testing Dates: 14-15 Oct 96
DAY 1		
Time	**Pilot 8**	**Pilot 9**
12:00	Arrive Boeing bldg. 3-10 lobby	Arrive Boeing bldg. 3-10 lobby
12:15 - 13:00	Prebrief/ pilot preparation	Prebrief
13:00 - 13:45	Familiarization runs	Break/pilot preparation
13:45 - 14:30	Break	Familiarization runs
14:30 - 15:15	Session 1	Break
15:15 - 16:00	Intermediate questionnaire/break	Session 1
16:00 - 16:45	**LUNCH**	**LUNCH**
16:45 - 17:30	Session 2	Intermediate questionnaire/break
17:30 - 18:15	Intermediate questionnaire/break	Session 2
18:15 - 19:00	Session 3	Intermediate questionnaire/break
19:00 - 19:45	Intermediate questionnaire/break	Session 3
19:45 - 20:30	Session 4	Intermediate questionnaire/break
20:30 - 21:00	Intermediate questionnaire/debrief	Debrief
DAY 2		
Time	**Pilot 8**	**Pilot 9**
12:15 - 13:00	Arrive Boeing bldg. 3-10 lobby	Arrive/pilot preparation
13:00 - 13:45	Break/pilot preparation	Session 4
13:45 - 14:30	Session 5	Intermediate questionnaire/break
14:30 - 15:15	Intermediate questionnaire/break	Session 5
15:15 - 16:00	Session 6	Intermediate questionnaire/break
16:00 - 16:45	**LUNCH**	**LUNCH**
16:45 - 17:30	Intermediate questionnaire/break	Session 6
17:30 - 18:15	Session 7	Intermediate questionnaire/break
18:15 - 19:00	Intermediate questionnaire/break	Session 7
19:00 - 19:45	Debrief	Intermediate questionnaire/break
19:45 - 20:15		Debrief

SESSION 1					
	Pilot 8			Pilot 9	
Run	Scenario #	Wind	Run	Scenario #	Wind
1	A1	120	**BREAK**		
2	D12	120			
3	A2	090			
4	D11	090			
5	A3	150			
6	D10	150			
7	A25	210			
8	A4	120			
BREAK			1	A15	120
			2	D04	090
			3	A19	090
			4	D08	300
			5	A23	300
			6	D12	210
			7	A25	120
			8	A16	120

Legend: D – Departure A - Approach

3080-009

Figure 5.3-1. Example Pilot Schedule and Log Sheet

Emergency conditions were introduced at various times and an objective assessment was made by the SME after each emergency. The assessment was conducted with the emergency condition score sheet described in section 4.4.5.

5.4 COMMUNICATIONS

ATC communications functions were simulated by the test coordinator. A prerecorded tape of Philadelphia approach control was played during the test rums to simulate additional airborne traffic. The test coordinator used ATC scripting developed by Infinite Computer Technologies, Inc., a contract ATC consultant, to provide a controlled real-time approach simulation. The communications workload was controlled through the use of a consistent series of transmissions. An example of communication contacts is detailed in table 5.4-1 and 5.4-2. Each run required communications on both approach control and common traffic advisory frequency (CTAF) frequencies. Frequencies were selected through a toggle switch on the pilot's collective. Selection of transponder codes was also simulated.

TABLE 5.4-1. TYPICAL ATC SCRIPT - APPROACH

First contact - Initial call to/from approach control - Pilot: "Philadelphia approach control this is LifeFlight 911 over the arboretum inbound requesting the Metro Approach." - ATC: "LifeFlight 911 proceed as requested, traffic is a police helicopter in the vicinity of the stadium. Squawk 3427 and report over Southwind Mall inbound."
Second contact - Secondary call at cell phone tower (Valley) or mall (Metro) - Pilot: "Philadelphia approach control, LifeFlight 911 is over the mall." - ATC: "LifeFlight 911, traffic no longer a factor, Maintain VFR and contact UNICOM over the power plant inbound." Third contact - Switch to UNICOM
Third contact – Switch to UNICOM - Pilot: "St. Erway UNICOM LifeFlight 911 is on final for the Metro Approach." - UNICOM: "Roger LifeFlight 911, traffic reported in the stadium westbound. Winds are 360 at 10 gusts to 15, altimeter two niner niner four."

3080-013

TABLE 5.4-2. TYPICAL ATC SCRIPT – DEPARTURE

First Contact - Departure call - Pilot "St. Erway UNICOM, LifeFlight 911 is departing the helipad for the Valley departure." - UNICOM: "LifeFlight 911 use caution, birds in the vicinity of the twin towers. Contact Philadelphia approach control on 119.7 prior to reaching 600 feet."
Second Contact - Call to departure - Pilot: "Philadelphia approach control, LifeFlight 911 is 600 feet off of St Erway outbound on the Valley approach." - ATC: "Life Flight 911, proceed as requested. Squawk 4335. Traffic is a Bell Jet Ranger in the vicinity of the Capital at 500 feet."

3080-014

5.5 EXPERIMENT MODIFICATIONS

In addition to the training modifications discussed previously, several other adjustments to the experiment were required during execution of the ORE simulation. Changes were made to the ORE simulation after the first six (of fourteen total) candidate pilots flew the simulator. The

changes were made to prevent the remaining subject pilots from experiencing simulator sickness, which caused the dismissal of three of the first six pilots. The primary change to the simulation was an increase in the update rate of the cockpit control inputs to the host computer. This decreased the total system transport delay, which was defined as the time from movement of a cockpit control, to the time when the pilot observes the response in the out-the-window visual display. Transport delay was shown to be a significant cause of simulator sickness symptoms. Previously, data from the cockpit controls were read every third math model time frame. However, a hardware change made to the cab interface computer enabled the cockpit controls to be read into the host computer during every time frame. This substantially decreased the total system response time.

In addition, the aircraft stability augmentation system (SAS) model characteristics were improved by increasing the allowable dead zone in the cockpit controls. This allowed the pilot to make slightly larger control inputs with the SAS still active in that axis. Additionally, the lateral and directional axis attitude hold characteristics were improved.

These changes made the aircraft more stable and easier to control. By decreasing the total system transport delay, the aircraft model responded more like the real aircraft. A Boeing flight test pilot who flew the simulator remarked that it felt "like a heavily loaded light helicopter," which was precisely the intent. The pilot flew the baseline system and then the modified system that he found to be considerably improved. Based on his judgments, the ORE simulation was modified to make these changes permanent.

It is noteworthy that since the simulation was modified, data from the second and third subject pilots may be slightly inconsistent with the remaining data. They may have experienced higher workload requirements and may have made more high frequency inputs to the cockpit controls. In the final analysis, this effect may be insignificant since variability between pilots may overwhelm the simulator differences.

6.0 RESULTS

This section describes the analysis and results of the ORE experiment. The first part of this section focuses on the analysis of flight control measures; that is, measures computed to characterize pilot performance. The second portion of this section analyzes the short-form questionnaire results; in particular, the NASA TLX questionnaire and additional questions administered to the pilots after each approach and departure. In the third section, analyses of the psychophysiological measures (heart rate and blink rate) are presented.

6.1 ANALYSIS OF FLIGHT PERFORMANCE MEASURES

Flight control measures were submitted to repeated measures analysis of variance (ANOVA) to extract reliable relationships to the ORE variables. Results presented below focus on a subset of performance measures showing statistically reliable effects. The significance level (p) is traditionally used to indicate statistically reliable effects. Only measures that differed significantly ($p<.05$) across TOD or OH/D conditions are presented and discussed. To simplify analysis, all altitudes are expressed in feet MSL. The heliport altitude is 100 feet MSL.

6.1.1 Approaches

Figures 6.1.1-1 and 6.1.1-2 present schematic illustrations of the two approaches to the heliport. A representative flight track from one of the nine pilots is plotted on each figure. Figure 6.1.1-1 shows the Valley approach; figure 6.1.1-2 shows the Metro approach. A representative pilot's x/y position for one flight is overplotted on the ground track in the upper portion of the figures; altitude is plotted on the lower portion. These plots also indicate how flights were segmented for statistical analysis. The Valley approach in figure 6.1.1-1 was divided into the following four segments:

1. Modified downwind – from the start point to just west of the microwave tower.
2. Base leg – west of the microwave tower to 1,000 feet south of the drive-in theater.
3. Extended final – 1,000 feet south of the drive-in theater to the twin towers.
4. Short final – twin towers to touchdown.

The Metro approach in figure 6.1.1-2 was divided into the following three segments:

1. Downwind leg – from the start, to a point on the downwind leg abeam the power plant smoke stacks.
2. Base leg – from the end of the downwind leg to the start of descent to the heliport (approximately 3,500 feet south of the heliport and 700 feet MSL).
3. Short final – from the start of the descent to touchdown.

These segments were derived after reviewing all nine pilot's approaches on computer-generated plots, such as those illustrated in figure 6.1.1-1 and 6.1.1-2. The segments correspond to relatively distinct phases of flight. Four different factors were examined for most of the performance and flight control measures: flight corridor (Metro and Valley), TOD (day, dusk,

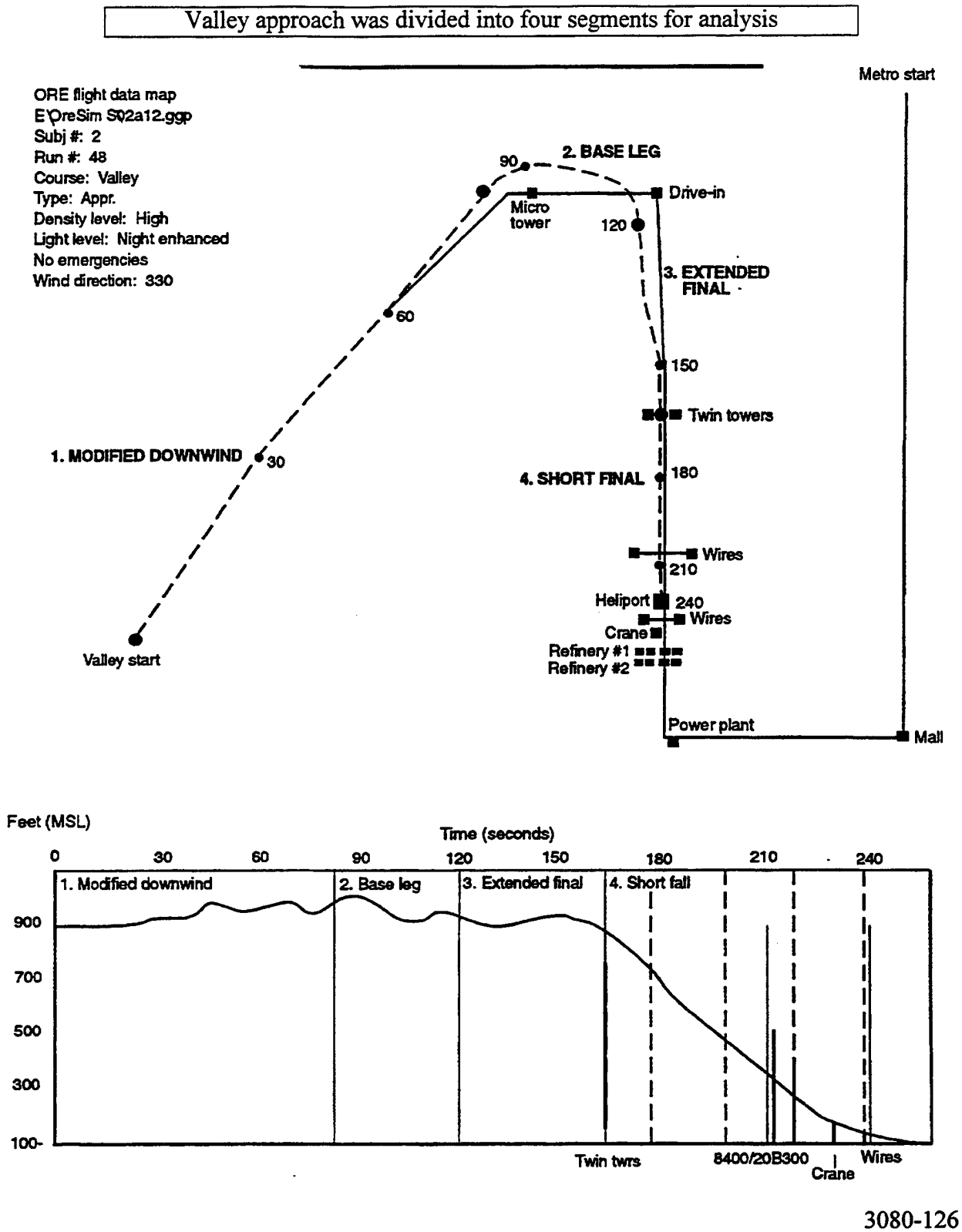

Figure 6.1.1-1. Valley Approach by a Representative Pilot

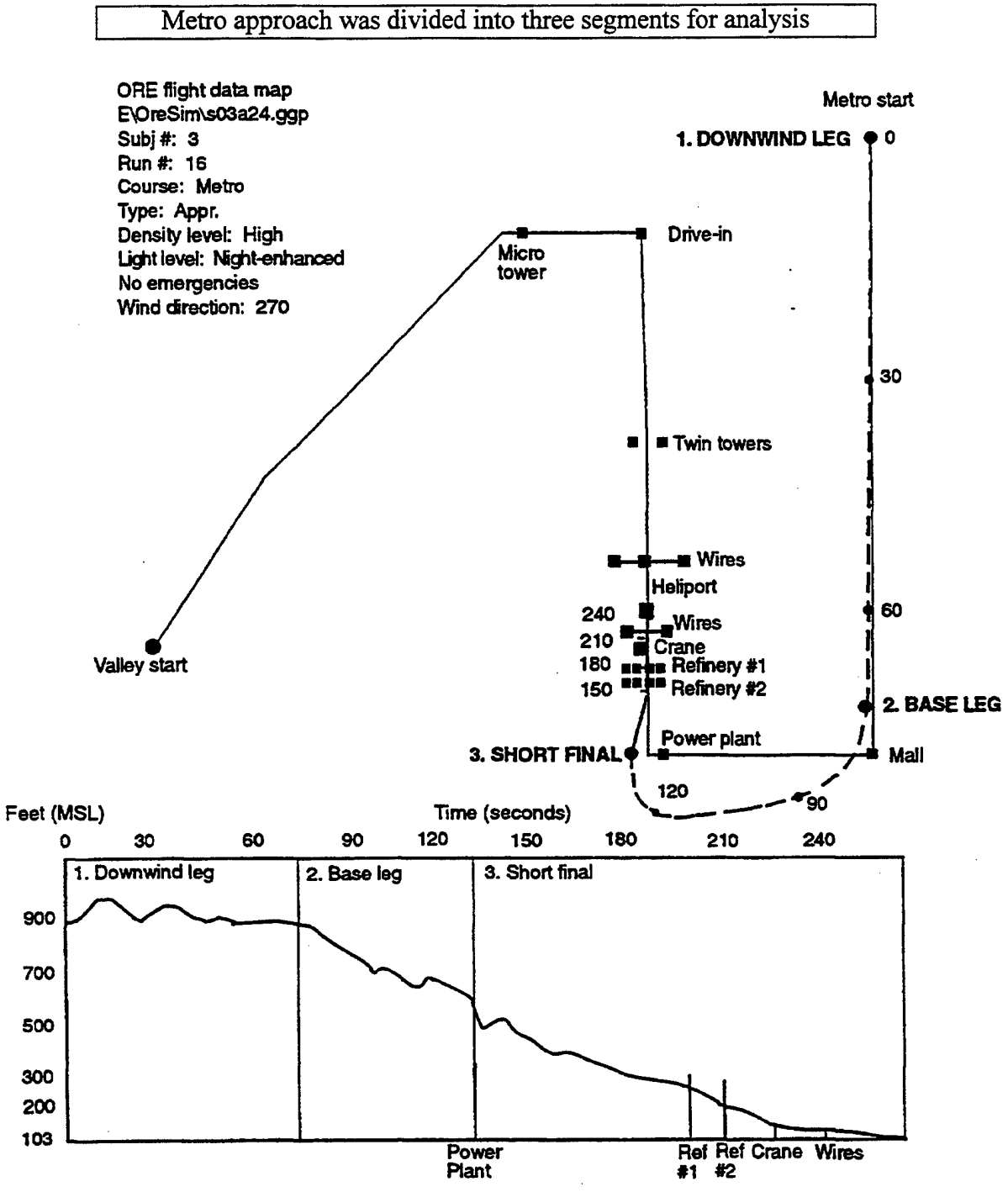

Figure 6.1.1-2. Metro Approach by a Representative Pilot

night baseline, and enhanced night lighting), OH/D (low, intermediate, and high) and flight segment (downwind, base, and final). To balance the design of the analysis, the downwind, base, and short final legs were analyzed in the ANOVAs; the extended final of the Metro approach was not included. All of the analyses reported in the results section are statistically significant at $p<.05$.

6.1.1.1 Segment Times and Speeds

Figure 6.1.1.1-1 presents the variation of mean time required to complete each approach flight segment with TOD. Note the increase in time required to fly the final segment from day, to dusk, to the two night conditions. The time required to fly the downwind segments was unaffected by TOD and the base-leg was just slightly affected. Thus, pilots apparently became more cautious, as visibility decreased from day, to dusk, to night conditions, only when obstacles were close to the flight route, such as on final.

Mean airspeed for final approach decreased as visibility decreased from day, to dusk, to night, but increased when the enhanced lighting system was provided. Mean airspeeds for the final approach segment for day, dusk, night baseline, and night enhanced were 47, 44, 32, and 40 knots, respectively. These data may appear inconsistent with the segment times illustrated for the final segment in figure 6.1.1.1-1, since segment time increased monotonically from the day, to the dusk, to the night baseline, and finally to the enhanced night conditions. This apparent inconsistency is caused by a difference in final segment definition for the airspeed and segment time measures. Because the "Height-Velocity Curve Chart" recommends deceleration at 90 feet above ground level (AGL), mean airspeed calculation was terminated at 90 feet AGL. All other flight performance measures, including segment time, were calculated down to 30 feet AGL, the altitude at which pilots typically leveled off and maneuvered for touchdown.

6.1.1.2 Lateral Flight Path Error

Figure 6.1.1.2-1 presents RMS lateral error for the two flight corridors and the four TOD conditions. Lateral error was larger for the Metro approach than for the Valley approach, probably due to the placement and the nature of the obstacles that provided pilots with visual cues. The downwind on the Valley approach followed a railroad track and ended at a microwave tower signaling the point where a change of course is required for the base leg. At the end of the base leg, a drive-in theater was located almost exactly on the extended centerline, providing pilots with a powerful visual cue that allowed them to line up on the approach centerline long before they could see the heliport. An extended final leg on the Valley approach (segment three left out of the analysis) allowed the pilot to align with the final approach centerline. In addition, the extended final leg passed over a point between two twin high-rise buildings that were less than 200 feet apart at a distance of approximately 5,000 feet from the heliport. All of these visual cues easily allowed the pilots to line up on the approach centerline while they were still a great distance from the heliport. The combination of these various visual cues contributed to reducing lateral tracking error to 108 feet for the Valley downwind and final.

In contrast, the RMS lateral error on downwind and final for the Metro approach was 183 feet. Its downwind began at the arboretum, an area three blocks wide, and continued south to the

Final took longer at dusk and at night

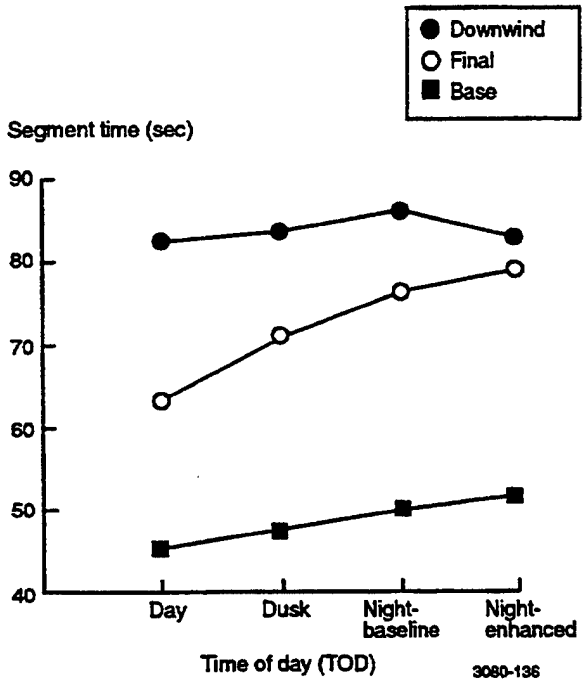

Figure 6.1.1.1-1 Approaches - Segment Time Analyzed Across Valley and Metro Approaches and Across All OH/D Conditions

RMS lateral error was lowest on Valley approach in day and dusk conditions; enhanced lighting reduced lateral error

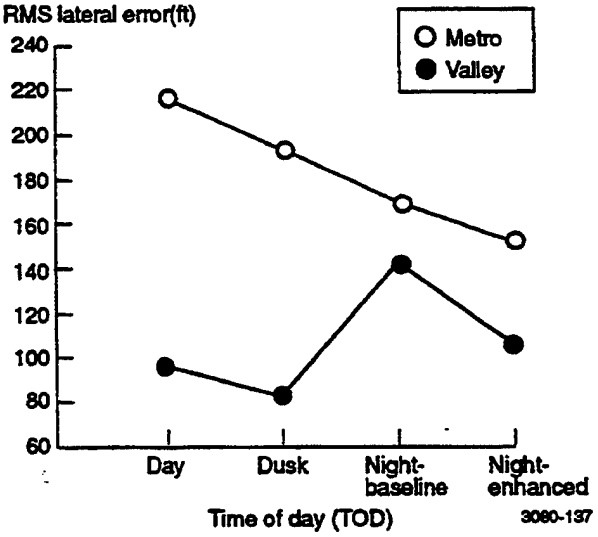

Figure 6.1.1.2-1. Approaches - RMS Lateral Error Analyzed Across All OH/D Conditions and Across Downwind and Final Segments

Shopping Mall (another large area). The final approach segment for the Metro corridor started at the power plant, a landmark that was difficult to see at night according to pilots. Thus, RMS lateral error increased at night for the Metro approach (figure 6.1.1.2-1).

Error decreased as visibility due to TOD decreased, except when TOD affected identification of critical landmarks. Both approach cases show improved night performance with enhanced lighting compared to the basic lighting, indicating that the enhanced heliport lighting and landing direction lights improved spatial orientation.

Across the Valley and the Metro corridors, RMS error decreased from 203 feet on downwind to 87 feet on final. This precise lateral navigation on final was due to the pilots' efforts to complete touchdown at a required landing point (i.e., the heliport).

Base legs for both approach corridors were analyzed separately, across OH/D and TOD conditions. The base leg for the Valley approach started and ended with well-defined point-type landmarks. This contributed to a RMS error of 830 feet for that segment. A much larger error of 2,416 feet was recorded for the Metro base leg. This was due to the differences in landmark characteristics discussed above. Across flight corridors, base leg RMS lateral error also varied as a function of OH/D. Errors were similar for the low and medium OH/D (1,498 and 1,566 feet, respectively); errors were significantly higher in the high OH/D condition (1,777 feet).

6.1.1.3 Vertical Flight Path Error

Final approach vertical RMS errors were measured from a baseline nine-degree approach slope. This reflected the angle of the PAPI. Figure 6.1.1.3-1 presents the RMS vertical error for the four TOD conditions. Vertical errors were largest when visibility was better due to TOD.

RMS vertical error was lowest with the enhanced heliport lighting system. In closing interviews, most pilots reported they did not use the PAPI (which was part of the enhanced lighting system) due to unfamiliarity with or lack of confidence in the PAPI. Other features of the enhanced lighting system may be responsible for the observed improvement.

6.1.1.4 Altitude Violations

Figure 6.1.1.4-1 presents the mean percentage of time below minimum altitude (850 feet MSL) for downwind and base-leg segments at three levels of OH/D. The briefed altitude for the flight corridor was 900 feet MSL. A 650-foot MSL minimum altitude was used on the Metro base-leg to compensate for the step down on that segment. Note that the downwind leg was virtually unaffected by OH/D. However, for flight in low OH/D. the percent of time below minimum altitude was approximately the same on downwind and base leg.

Minimum altitude violations decreased significantly on base leg at higher OH/D. This change may reflect the pilot's increased concern with obstacle clearance, or reluctance to use the Metro approach step down in the higher-density conditions.

RMS vertical error decreased as visibility due to TOD decreased

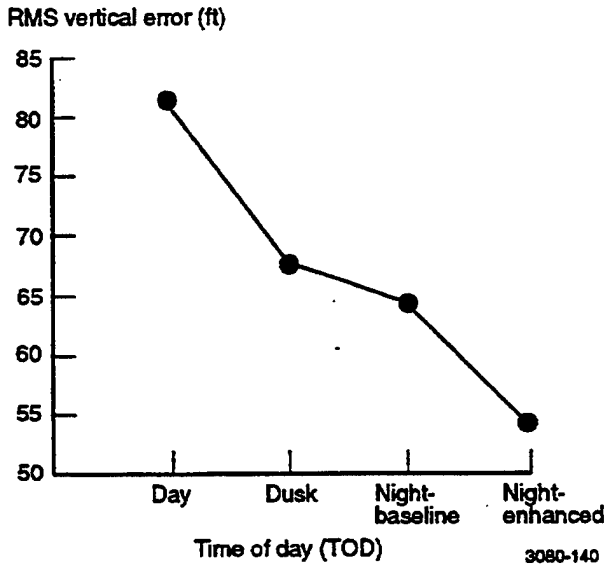

Figure 6.1.1.3-1. Approaches - RMS Vertical Error Analyzed Across Valley and Metro Approaches and Across All OH/D Conditions

Increased OH/D reduced minimum altitude violations on base leg

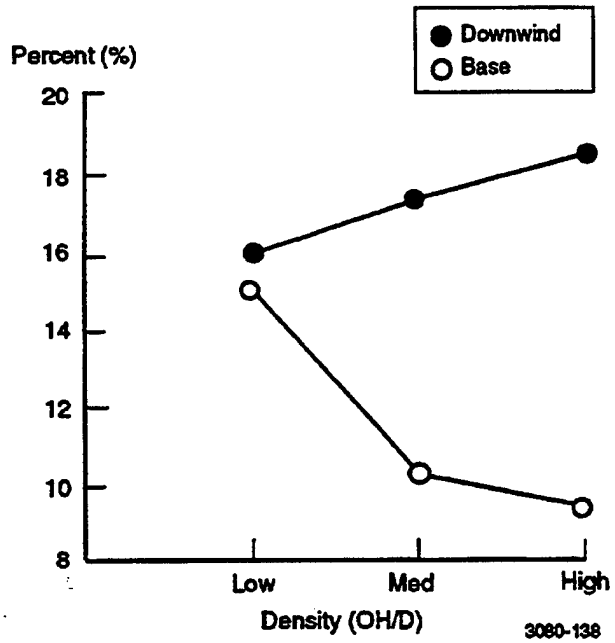

Figure 6.1.1.4-1. Approaches - Percent of Time in Minimum Altitude Violations Analyzed Across Valley and Metro Approaches and Across All TOD Conditions

The percentage of time that pilots violated maximum altitude (1,000 feet MSL) is presented for the two approach corridors and four TOD conditions in figure 6.1.1.4-2. Maximum altitude violations occurred infrequently. The overcast ceiling at 1,000 feet MSL prevented frequent violations. Pilots flew above maximum altitude more often in the Valley's night approaches than under any other approach condition. Sparse lighting and high terrain altitude on the Valley approach, particularly for the downwind leg, may have caused this.

6.1.1.5 Touchdown Error

Touchdown error in the low, medium, and high OH/D conditions was 18, 16, and 26 feet, respectively. This can be attributed to the pilots concerns for other aircraft and pedestrians in the immediate vicinity of the heliport obstacles (present only in higher OH/D conditions).

High terrain on Valley approach caused maximum altitude violation in low light conditions

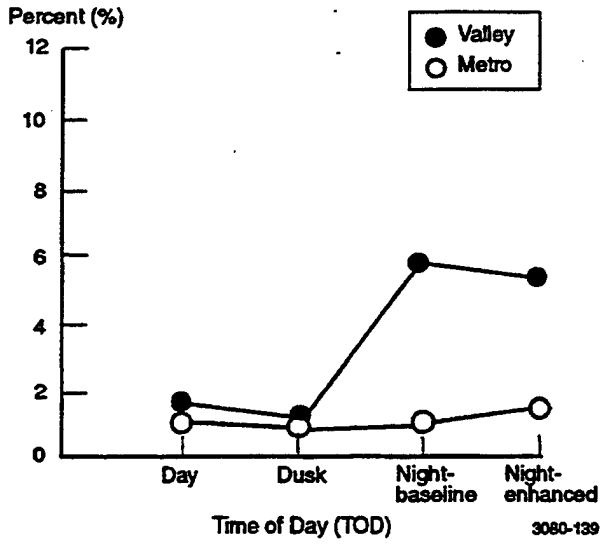

Figure 6.1.1.4-2. Approaches - Percent of Time in Maximum Altitude Violation Analyzed Across All OH/D Conditions

6.1.1.6 Obstacle Clearance On Final

In addition to the flight performance analyses described above, clearances from a number of obstacles in the final segment were calculated. These obstacles were chosen based on information obtained from pilots in the long-form questionnaire and in pilot exit briefings. For the Valley flight corridor these obstacles included:

1. The high power wires extending across the flight course 991 feet north of the heliport, at a height of 215 feet MSL.

2. A building 2,266 feet north of the heliport. The west wall was 226 feet east of the course. The building was 515, 432, and 340 feet MSL in height in the high, medium, and low OH/D conditions, respectively.
3. A building with a construction crane 1,430 feet north of the heliport, whose height was 238 feet MSL.
4. A building 1,725 feet north of the heliport. The east wall was 194 feet west of the course. The building was 415, 352, and 287 feet MSL in height in the high, medium, and low OH/D conditions, respectively.

Clearance from the wires on the Valley approach varied with TOD, decreasing as visibility declined. For the day, dusk, night base and night enhanced lighting conditions, clearance was 161, 121, 93, and 89 feet, respectively. The wires were 77 feet below the glide path centerline. Reduced clearances from day, to dusk, to night flights may be the result of pilot preoccupation with maintaining clearance from more visible obstacles. This hypothesis is consistent with the reduced RMS vertical slope error in the night, as compared to the day and dusk flights illustrated in figure 6.1.1.3-1.

Clearances from the building 2,266 feet north of the heliport varied with the OH/D condition. The variation was related to the height of the building, since building height varied with the density level. The clearances were 404, 303, and 220 feet respectively, in the low, medium, and high OH/D conditions. This pattern of reduced clearances with increased obstacle density indicates that pilots flew over this building at a nearly fixed altitude regardless of the building height. The 100-foot difference between clearances as a function of OH/D mirrored the increase in building height from 340 feet MSL in the low, to 432 feet MSL in the medium, and finally to 515 feet MSL in the high-density condition. No significant variation in clearance across OH/D levels was found for the building with the construction crane.

Finally, clearance from the building 1,725 feet north of the heliport varied with TOD, again decreasing as visibility declined. The clearances for the day, dusk, night baseline, and night with enhanced lighting flights were 364, 311, 211, and 226 feet, respectively. Consistent with the clearances from the wires discussed above, pilots maintained more obstacle clearance when visibility due to TOD is better.

Since the Valley and Metro approaches were different, clearances from different obstacles were computed for the Metro flight corridor. The obstacles on the Metro course for which clearances were computed included:

1. High power wires extending across the flight course 649 feet south of the heliport, at 209 feet MSL.
2. Refinery smoke stacks on a line across the flight course 1,450 feet south of the heliport, ranging in height from 227 to 287 feet MSL.
3. Six smoke stacks on a line across the flight course 1,686 feet south of the heliport, ranging in height from 250 to 320 feet MSL.
4. A crane on wheels 100 feet west of the course and 1,040 feet south of the heliport, at a height of 242 feet MSL.

Clearance from the wires was greatest at high OH/D conditions, increasing from 81 feet in the low OH/D, to 89 feet in the medium OH/D, to 97 feet in the high OH/D flights. The greater clearance maintained in the higher OH/D conditions may have resulted from general concern for maximizing obstacle clearance in these conditions. This hypothesis is consistent with the reduction in minimum altitude violations observed in the medium and high OH/D conditions (figure 6.1.1.4-1).

Clearance from the smoke stacks closest to the heliport in the day, dusk, night baseline, and night with enhanced lighting conditions were 183, 177, 145, and 141 feet, respectively. The clearances from the second line of smokestacks and the crane did not vary as a function of TOD or OH/D.

6.1.2 Departures

The departures were analyzed in much the same way as the approaches, however, the departures contained only a single flight segment. Departure runs were terminated when the pilots left the immediate vicinity of the heliport. Figure 6.1.2-1 shows a typical departure path on the Metro corridor. The upper panel shows the ground track. The lower panel of the figure shows a profile of the departure path.

6.1.2.1 Departure Speeds

Similar to the approach conditions, pilots reduced departure airspeed in low visibility conditions. Mean airspeeds for the day, dusk, and night conditions were 48, 44, and 43 knots, respectively. The decreased airspeed relates to steeper climb used by the pilots in reduced visibility due to TOD (see section 6.1.2.3).

6.1.2.2 Lateral Flight Path Error

RMS lateral error increased from day, to dusk, to night flights (i.e., 110, 128, and 150 feet, respectively). Pilots apparently became more concerned about obstacle clearance as visibility declined. Pilots may have used lateral displacement to achieve obstacle clearance when engine power prevented them from clearing a obstacle vertically. Alternatively, visual navigation cues may have been inadequate to allow the pilots to fly an accurate departure path. This hypothesis could be confirmed through analysis of the quadscreen videos.

6.1.2.3 Vertical Flight Path Error

RMS vertical errors, referenced to a nominal nine-degree departure angle, increased as OH/D increased. The vertical errors for the very low, low, medium, and high OH/D conditions were 175, 178, 208, and 214 feet, respectively. Vertical errors for time day, dusk, and night conditions were 180, 190, and 213 feet, respectively. This data suggests that pilots climbed more steeply under more difficult flight conditions to increase separation between the helicopter and nearby obstacles. Figure 6.1.2-1 shows an example of a vertical climb at the heliport followed by a southbound departure.

One flight segment was used for analysis of departures

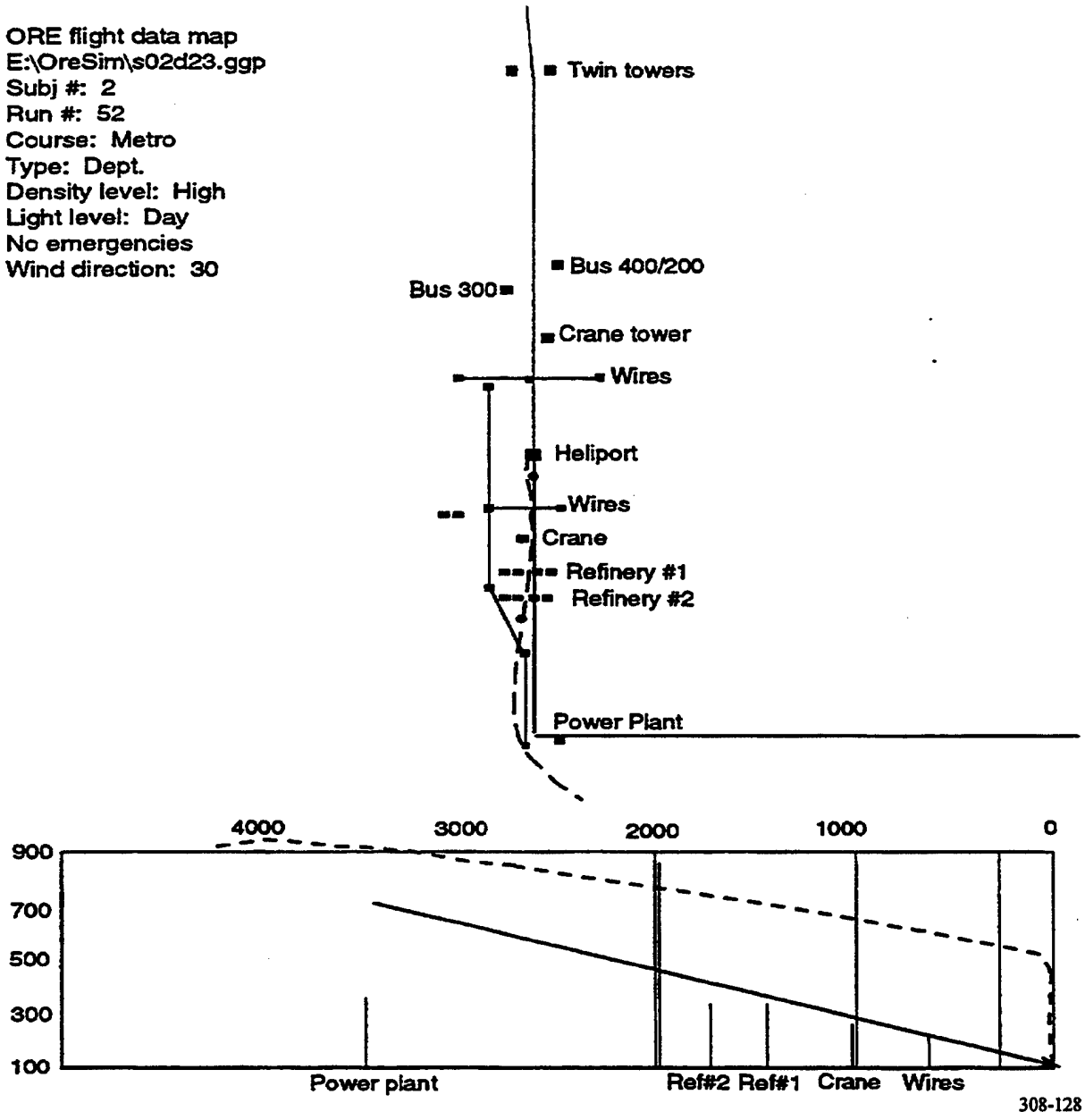

Figure 6.1.2-1. ORE Flight Data Map

6.1.2.4 Obstacle Clearance On Departure

For the departures, clearances were calculated from the same sets of obstacles evaluated for the approaches (see section 6.1.1.6). Clearances from the high power wires on the Valley departure increased from 243 feet in the very low OH/D, to 256 in the low OH/D, to 296 feet in the

medium OH/D, to 309 feet in the high OH/D flights. This data is consistent with the increased RMS vertical errors discussed above.

Clearance from the building 2,266 feet north of the heliport increased as visibility declined (i.e., 369, 411, and 413 feet for the day, dusk, and night flights). Thus, pilots consistently attempted to increase separation from obstacles under reduced lighting condition.

Clearance decreased as OH/D increased (499, 390, 370, and 334 for the very low, low, medium, and high OH/D). Height of this building varied with OH/D as described in section 6.1.1.6. The clearances show that the pilots flew over the building at *765,* 730, 802, and 849 feet MSL as OH/D went from very low to high. Thus, climb angle increased slightly with OH/D. Clearances from the building with the crane increased with OH/D clearances of 340, 392, and 408 feet in the low, medium, and high-density flights, respectively. (The building with the crane was not present in the very-low OH/D condition.) Thus, for obstacles located close to the heliport pilots apparently attempted to maximize obstacle clearance under obstacle-rich conditions.

Clearances from the building 1,725 feet north of the heliport were 419,458, and 511 feet for the day, dusk, and night flights, respectively. These results are consistent with TOD results reported above.

On the Metro departures, clearance from the closest refinery stacks for the day, dusk, and night flights was 305, 311, and 358 feet, respectively, averaged across OH/D levels. Clearances from the more distant refinery stacks produced a similar pattern from the day, dusk, and night flights of 340, 353, and 400 feet, respectively. Thus, in both of these cases pilots increased their distance from obstacles with reduced visibility.

6.2 ANALYSIS OF PILOT QUESTIONNAIRE DATA

Tables 6.2-1 and 6.2-2 present the mean pilot approach and departure ratings for the short-form questionnaires. Higher scores on TLX ratings and hazard/risk assessments indicate higher perceived workload and/or risk. The specific questions that pilots responded to can be found in the "Short-Form Questionnaire" in appendix C.

6.2.1 NASA TLX Measures

Analysis in this section is based on NASA TLX scores. Although analyses were performed on each of the separate subscales (i.e., mental load, physical load, time pressure, rated performance, rated effort, and frustration), this discussion is restricted to the mental workload subscale analysis and composite analysis (i.e., the sum of the scores on the subscales). This approach was found useful by previous researchers, and reduces analysis to a tractable level.

Two effects were statistically reliable for the pilots approach ratings on the mental workload question. Mental workload was rated higher for night flights than for day or dusk flights. The ratings of mental workload for the day, dusk, night baseline, and night with enhanced lighting flights were 4.32, 4.42, 4.83, and 4.75. The enhanced night lighting flights involved slightly less mental workload than the night baseline lighting flights. Although slight, the workload effect is

TABLE 6.2-1. SUMMARY OF SHORT-FORM QUESTIONNAIRE RESPONSES FOR APPROACH

			Mental	Physical	Time	Performance	Effort	Frustration	TLX Summary	Risk	Hazard
Valley Approaches	Low	Day	4.1	3.8	3.7	4.1	3.8	3.6	23.1	2.2	3.1
		Dusk	4.1	4.0	3.3	3.6	3.8	3.1	21.9	2.3	3.6
		Night-baseline	4.8	4.4	4.2	4.7	4.7	4.2	27.0	3.2	3.8
		Night-enhanced	4.1	4.2	3.4	3.2	4.4	3.0	22.3	2.6	3.8
	Medium	Day	4.6	4.4	3.6	3.9	4.7	4.1	25.3	2.9	3.7
		Dusk	4.7	4.4	3.9	3.9	4.8	4.1	25.8	3.2	4.3
		Night-baseline	4.7	4.2	3.3	3.7	4.4	3.9	24.2	2.4	3.5
		Night-enhanced	4.8	4.4	3.7	3.9	4.6	4.2	25.6	3.2	4.8
	High	Day	4.3	4.2	3.3	3.9	4.3	3.8	23.8	3.2	4.3
		Dusk	4.7	4.4	3.7	3.4	4.4	3.8	24.4	2.6	4.1
		Night-baseline	5.0	4.3	3.4	3.9	4.6	4.2	25.4	3.6	4.2
		Night-enhanced	4.9	4.3	4.3	3.8	4.3	3.7	25.3	3.5	4.6
Valley Approaches	Low	Day	4.3	3.8	3.3	3.5	4.0	3.4	22.3	3.0	3.5
		Dusk	4.2	3.8	3.7	3.9	4.1	3.6	23.3	3.1	4.1
		Night-baseline	4.9	4.5	3.6	4.1	4.6	4.0	25.7	3.4	4.6
		Night-enhanced	4.6	4.5	3.6	3.9	4.3	3.9	24.8	3.3	3.9
	Medium	Day	4.2	3.8	3.2	3.4	4.4	3.5	22.5	2.8	4.0
		Dusk	4.3	4.2	3.2	3.6	4.1	3.4	22.8	2.8	3.7
		Night-baseline	4.9	4.3	3.8	3.8	4.5	3.4	24.7	2.7	4.2
		Night-enhanced	5.0	4.7	3.9	4.4	4.5	4.5	27.0	3.6	4.4
	High	Day	4.4	4.4	3.6	3.6	4.4	3.8	24.2	4.1	4.7
		Dusk	4.5	3.8	3.1	3.3	4.3	3.6	22.6	3.0	4.5
		Night-baseline	4.7	4.4	3.8	4.0	4.5	3.8	25.2	3.4	4.9
		Night-enhanced	5.1	4.7	4.1	4.6	4.8	4.1	27.4	3.7	4.7
			Based on Likert rating system								

3080-134

Legend:

Seven-point Likert rating system

Low workload, risk, hazard — High workload, risk, hazard

1 2 3 4 5 6 7

TABLE 6.2-2. SUMMARY OF SHORT FORM QUESTIONNAIRE RESPONSES FOR DEPARTURES

			Mental	Physical	Time	Performance	Effort	Frustration	TLX Summary	Risk	Hazard
Valley Approaches	Very low	Day	3.5	2.9	2.7	3.4	3.2	2.4	18.1	1.7	2.9
		Dusk	3.3	3.2	2.9	3.1	3.0	2.7	18.2	2.1	2.9
		Night-baseline	3.6	3.1	2.8	2.8	3.1	2.9	18.3	2.3	3.3
	Low	Day	4.3	3.7	3.1	3.1	3.8	3.2	21.2	1.8	3.4
		Dusk	3.9	3.3	3.2	3.4	3.6	3.2	20.6	2.7	3.9
		Night-baseline	4.2	3.6	2.9	4.1	3.8	3.1	21.7	2.6	3.3
	Medium	Day	3.2	2.9	2.6	2.9	2.8	2.4	16.8	2.2	3.1
		Dusk	3.8	3.3	3.2	3.6	3.4	2.9	20.2	2.3	4.1
		Night-baseline	4.0	3.7	2.9	3.7	3.5	2.9	20.7	2.2	4.1
	High	Day	3.8	3.3	2.9	2.8	3.3	2.7	18.8	2.4	4.2
		Dusk	3.4	3.2	2.7	3.2	3.4	2.9	18.8	1.9	3.8
		Night-baseline	4.1	3.7	3.8	3.3	4.2	3.3	22.4	2.5	4.2
Valley Approaches	Very low	Day	3.5	3.3	2.6	3.3	3.1	2.9	18.7	1.7	3.0
		Dusk	3.4	2.9	2.7	2.9	3.1	2.6	17.6	1.6	3.2
		Night-baseline	4.2	3.6	3.5	3.6	3.7	3.1	21.7	2.2	3.4
	Low	Day	3.3	3.2	3.1	3.3	3.2	2.8	18.9	1.9	3.9
		Dusk	4.0	3.3	3.2	3.3	3.4	2.9	20.1	2.4	4.2
		Night-baseline	3.7	3.3	2.8	2.9	3.2	2.9	18.8	2.3	3.9
	Medium	Day	3.7	3.3	3.3	3.3	3.5	2.7	19.8	2.8	4.1
		Dusk	3.6	3.2	2.7	3.2	3.2	2.6	18.5	2.4	3.6
		Night-baseline	3.8	3.3	2.9	2.7	2.9	2.8	18.4	2.1	4.0
	High	Day	3.4	3.1	3.1	3.0	3.1	2.7	18.4	2.4	3.5
		Dusk	3.6	3.4	3.3	3.1	3.3	2.8	19.5	2.7	3.8
		Night-baseline	4.2	3.8	3.2	3.2	3.7	3.2	21.3	2.8	3.8
			Based on Likert rating system								

3080-134

Legend:
Seven-point Likert rating system

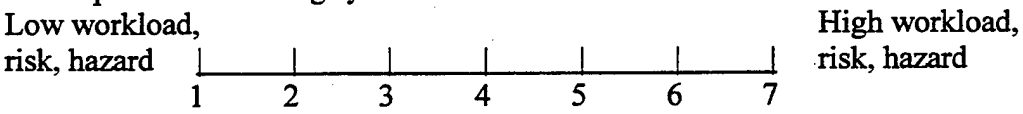

Rating Scale

consistent with several flight performance measures. Ratings of mental workload also increased with OH/D from 4.39 in low OH/D, to 4.65 in medium OH/D, to 4.7 in high OH/D conditions.

The interaction between OH/D and TOD is presented in figure 6.2.1-1. As can be seen in the figure, composite ratings generally increased with density, and were higher for night than for day

Pilot rating of workload increased with OH/D and at night

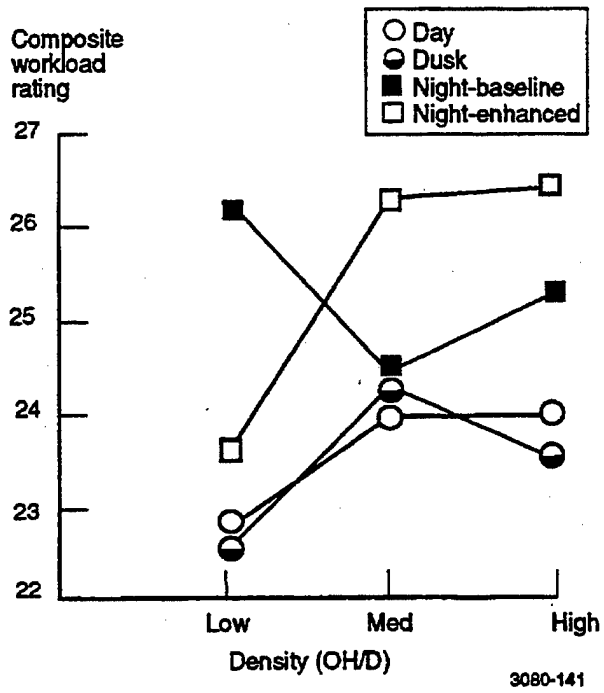

Figure 6.2.1-1. Approach - TLX Composite Data Analyzed Across Valley and Metro Approaches

or dusk flights. Two significant points must be considered when analyzing this data. First, the very high workload rating for the night baseline, low OH/D condition may be due to the relative lack of visual cues for those conditions. This could be confirmed through analysis of quadscreen videos.

Second, the higher perceived composite workload at night with enhanced lighting is likely due to maintaining PAPI centerline guidance. Pilot comments indicated that they considered obstacle clearance to be insufficient while on the PAPI glide path. This was true even though the PAPI was sited in accordance with the FAA Heliport Design advisory circular[3].

Two effects were reliable for departures, one related to mental workload and one related to composite workload. Mean mental workload ratings for the day, dusk, and night flights were 3.59, 3.63, and 3.95, respectively. Figure 6.2.1-2 presents NASA TLX composite TOD ratings. Mental workload ratings increased gradually from day to dusk, then increased significantly for night flights. The greater difficulty in seeing wires at night is most likely the reason for an increase in mental workload.

In summary, the NASA TLX ratings correlated well with the flight-performance measures. Perceived workload increased consistently as visibility declined and as OH/D increased.

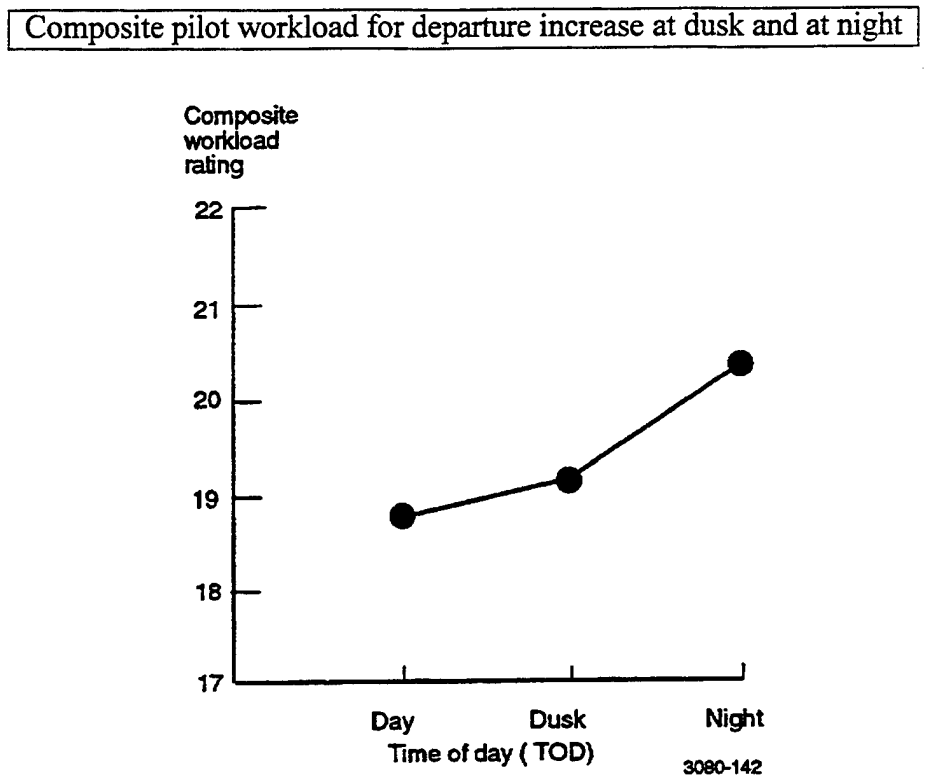

Figure 6.2.1-2. Departure - TLX Composite Analysis Across Valley and Metro Departures and Across All OH/D Conditions

6.2.2 Risk and Hazard Ratings

Risk and hazard ratings were obtained from questions on the short-form questionnaire described in section 4.4.3.1. Approach and departure risk ratings increased with OH/D as illustrated in figures 6.2.2-1 and 6.2.2-2. Metro approaches were rated as more risky than the Valley approaches (3.4 and 2.9, respectively). Hazard ratings also increased with OH/D as indicated in figures 6.2.2-3 and 6.2.2-4. The ratings indicate that pilots were generally sensitive to the increased risk and safety hazards associated with higher OH/D.

The risk rating increase, shown in figure 6.2.2-1, from the medium OH/D to high OH/D can be attributed to the people and helicopters in the immediate vicinity of the heliport. Furthermore, the pilots encountered these conditions immediately prior to rating the risk of the approach. Post-experiment interviews and information volunteered by test subjects indicated that these obstacles were of great concern.

The effect of wires near the heliport is demonstrated in figures 6.2.2-2 and 6.2.2-4. Risk and hazard ratings decreased for the very low OH/D conditions (more so in figure 6.2.2-2). The very low condition is the only condition where the power lines are absent.

Pilot risk rating increased with OH/D

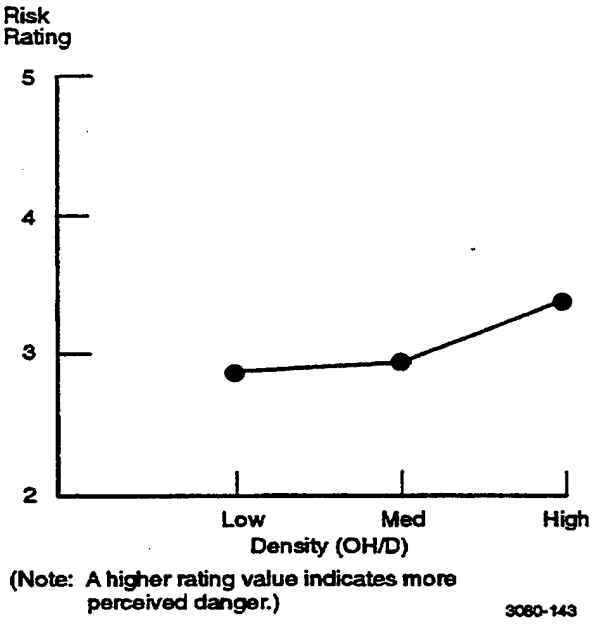

Figure 6.2.2-1. Approach - Risk Factor Analyzed A cross Valley and Metro Approaches and Across All TOD Conditions

Pilot departure risk rating increased with OH/D

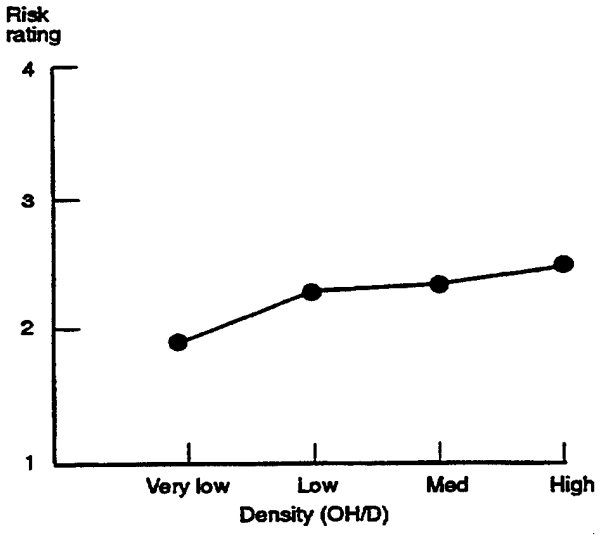

(Note: A higher rating value indicates more perceived danger.)

3080-144

Figure 6.2.2-2. Departure - Risk Factor Analyzed Across Valley and Metro Departure and Across All TOD Conditions

Perceived hazardousness of approach increase at high OH/D

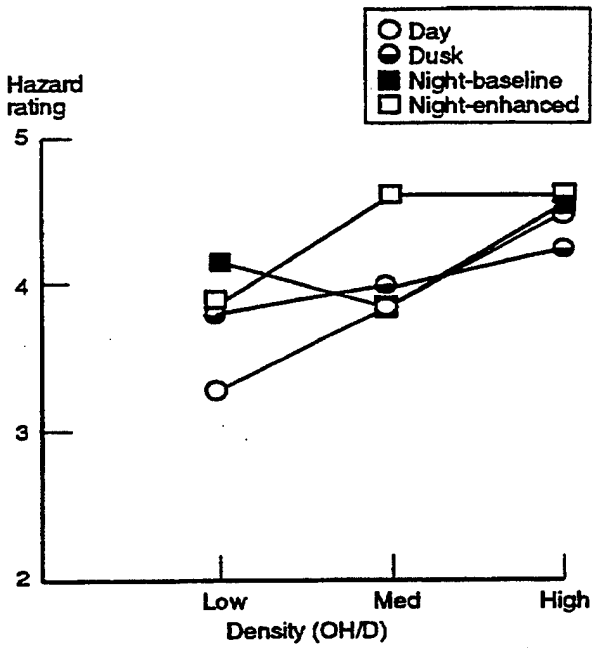

(Note: A higher rating value indicates more perceived safety hazard.)

3080-145

Figure 6.2.2-3. Approach - Hazard Factor Analyzed Across Valley and Metro Approaches

Perceived hazardousness of departure increases at high OH/D

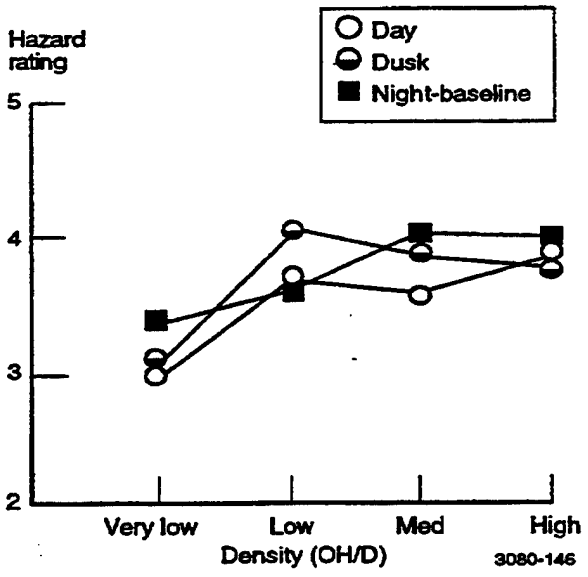

(Note: A higher rating value indicates more perceived safety hazard.)

Figure 6.2.2-4. Departure - Hazard Factor Analyzed Across Valley and Metro Departures

6.3 ANALYSIS OF PHYSIOLOGICAL MEASURES

Two different physiological measures were recorded and analyzed: heart rate and eye blinks. Both measures have previously provided sensitive and reliable indices of pilot mental workload variations during rotorcraft flight[34]. The heart rate and blink rate measures were treated in the same way as the flight performance measures. These measures were averaged within segments, OH/D conditions, corridors, and TOD conditions, and submitted to repeated ANOVA measures.

The statistically reliable effects that were obtained in the ANOVAs are described below. Two interactions were significant for heart rate measures during approach. Heart rate increased throughout the flight for day and dusk conditions (figure 6.3-1). The increase from the downwind to the base segment was also observed for the two night conditions. During night flights, however, heart rate remained approximately the same from the base leg to the final segment Stress may have been reduced during night flights since pilots could not easily see obstacles (pilots were not intimidated by what they could not see).

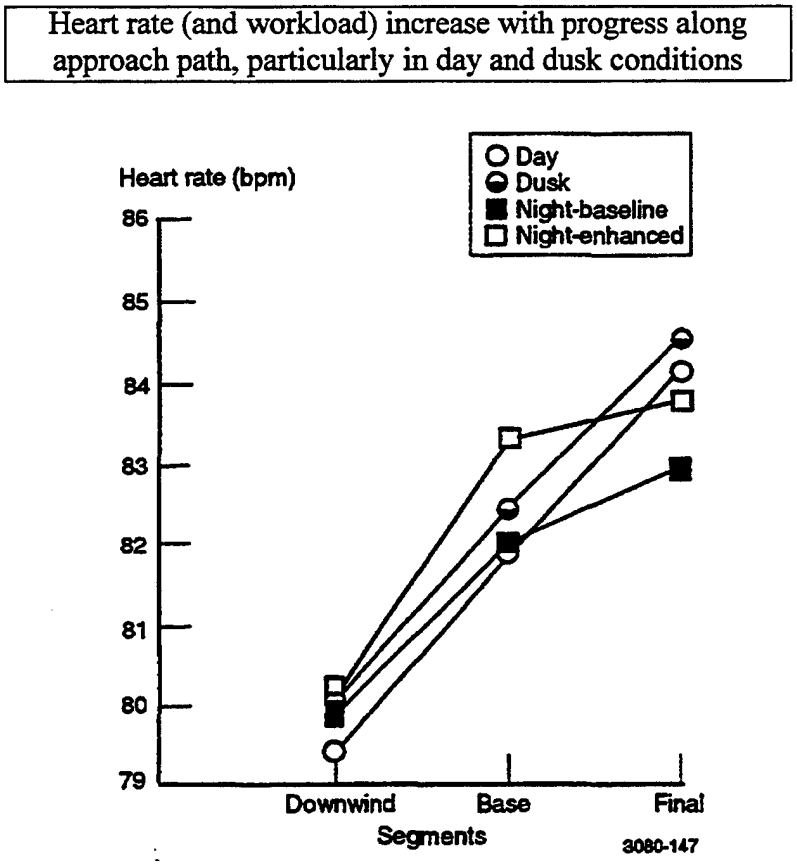

Figure 6.3-1. Approaches - Heart Rate Analyzed Across Valley and Metro Approaches and Across All OH/D Conditions

Heart rate variation with OH/D and TOD conditions is presented in figure 6.3-2. Different heart rate patterns were exhibited across the three OH/D levels. For medium OH/D, heart rate was highest in the day and dusk flights; the lowest heart rates were recorded in the low and high OH/D for these same TOD conditions.

The interaction between corridor and TOD was statistically significant for the departures as shown in figure 6.3-3. For daytime approaches, heart rates were higher for the Valley corridor than for the Metro corridor. Conversely, for night approaches, heart rates were higher on the Metro corridor. No rationale for this difference has been developed.

Analyses were conducted on heart rate measures obtained when pilots were flying in the vicinity of certain obstacles (see the list of obstacles in section 6.1.1.6). Figure 6.3-4 shows heart rate patterns for the obstacle-rich final-flight segment. Heart rate patterns were similar to those found for the overall flightpath (figure 6.3-2).

With the exception of dusk flight, heart rate did not vary with OH/D

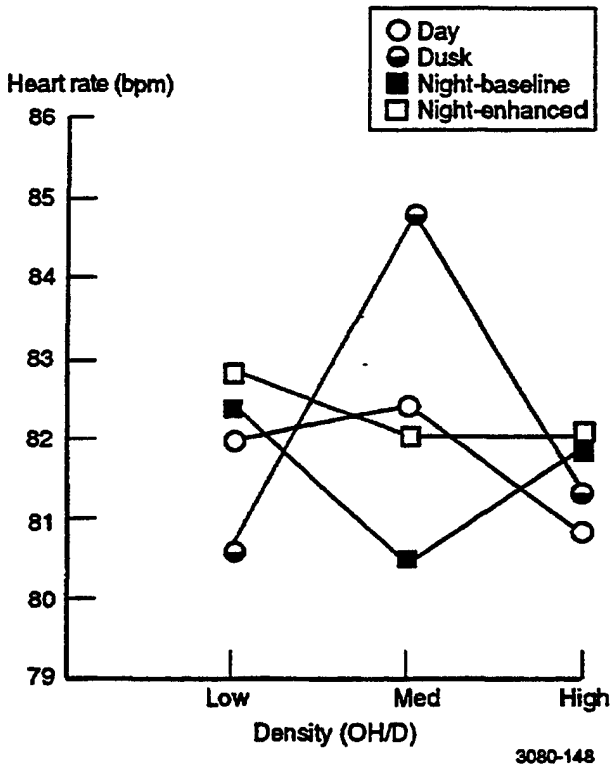

Figure 6.3-2. Approaches - Heart Rate Analyzed Across Valley and Metro Approaches

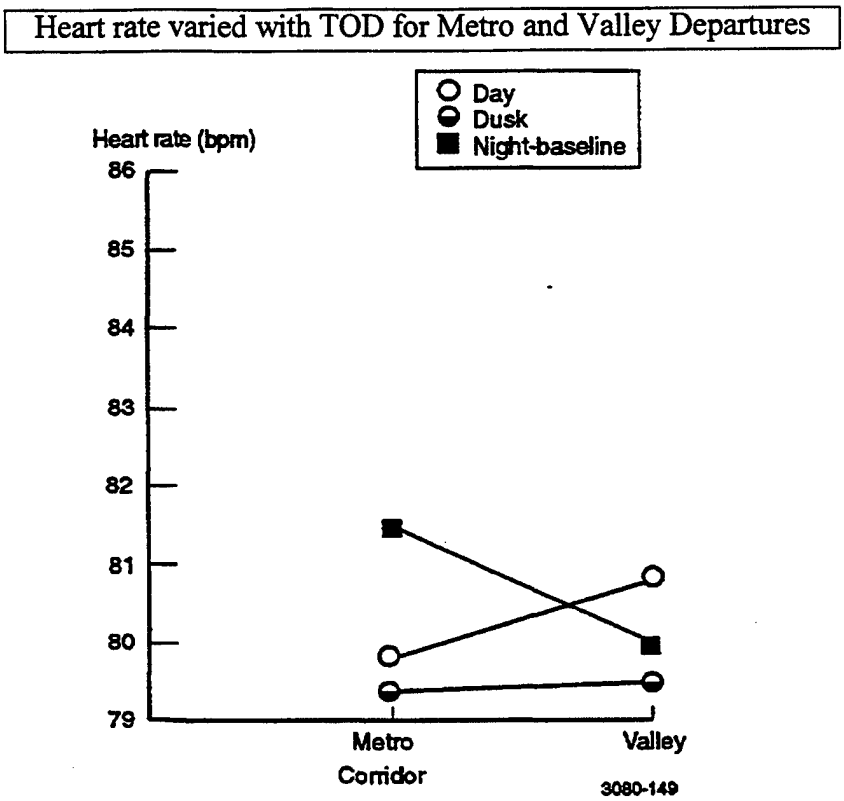

Figure 6.3-3. Departures - Heart Rate Analyzed Across All OH/D Conditions

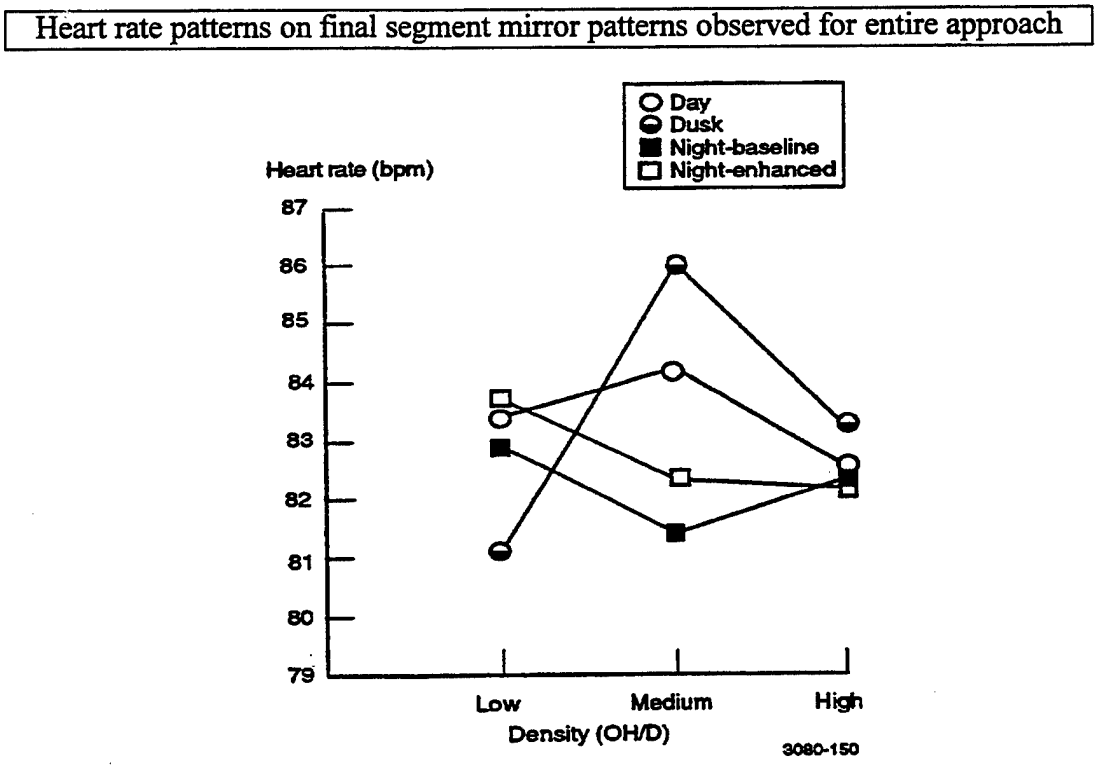

Figure 6.3-4. Approaches (Over Obstacle-Rich Flight Segment) - Heart Rate Analyzed Across Valley and Metro Approaches

In summary, the heart rate measures (while somewhat noisy) indicate changes in pilot mental workload as a function of both flight segment and TOD. As expected, progressively higher heart rates were found later in the approach flights, indicating increasing mental workload as the pilots entered the most obstacle-rich areas and prepared for landing. More interestingly, with respect to TOD, the highest heart rates were found during daytime approaches and nighttime departures. The higher workload on day approaches is attributed to the pilots' ability to see more obstacles than in the lower visibility conditions. In contrast, the effect of visibility was reversed for departures where higher heart rates were observed at night. Two plausible explanations have been developed for this finding. It is possible that inability to see obstacles on departure heightened pilot concerns regarding altitude, airspeed, and power margins. Alternatively, increased heart rate could have been caused by inability to identify suitable emergency landing locations at night.

Figure 6.3-5 shows blink rate for approaches, where reduced blink rates have been traditionally associated with higher workloads[18]. Two effects were significant. Blink rate decreased with progress along the flightpath, from the downwind, to base, to final (13.1, 12.8, and 5.3 blinks per minute, respectively). Blink rate decreased slightly more along the Metro corridor than along the Valley corridor. These measures concur with the flight performance data that showed poorer fight performance on the Metro than on the Valley flights. None of the blink effects were significant during departures.

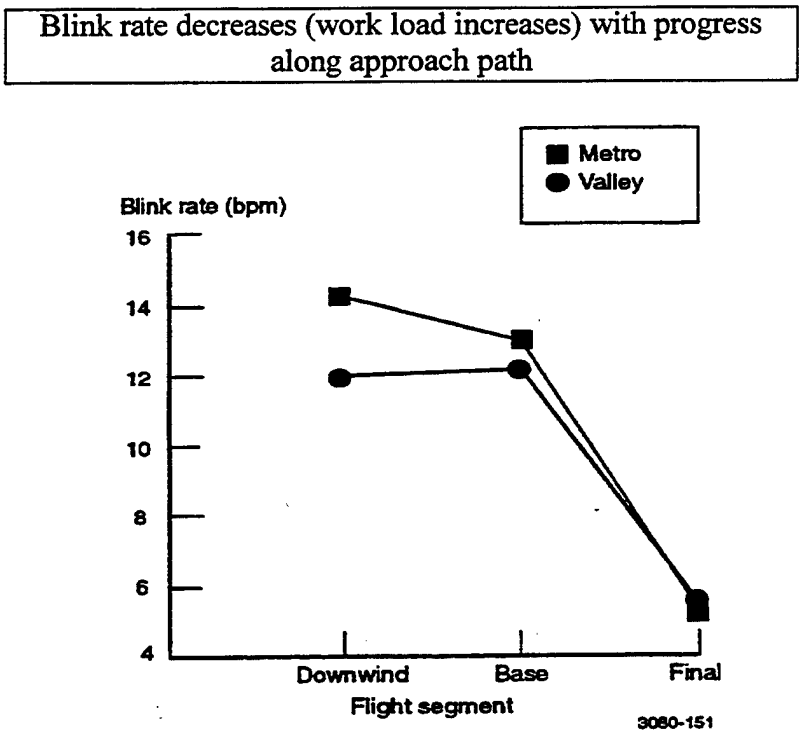

Figure 6.3-5. Approach - Blink Rate Analyzed Across All OH/D and TOD Conditions

6.4 ANALYSIS OF TRACK, ALTITUDE AND HEIGHT-VELOCITY GRAPHICS

Appendix H has been included to support an examination of heliport airspace issues as they relate to the conduct of the ORE simulation experiment. The current airspace dimensions for a heliport are published in Code of Federal Regulations (CFR) 14, Part 77 and are shown in figure 2.1-1 of this report.

The analyses presented to this point in section 6 have identified statistically significant effects of the primary simulation variables, obstacle density and visibility. The plots in appendix H contain various aggregations of all of the data to illustrate any effects of the simulation variables, but do not consider interpretation of their statistical significance, or lack thereof. The following types of plots are presented in this appendix:

- cross track error,
- altitude (Mean Sea Level (MSL)), and
- height-velocity (H-V).

6.4.1 Cross Track Error

These plots illustrate the intended track of the helicopter during the last 4,000 feet of the approach, or first 4,000 feet of the departure, and an analysis of the tracks actually achieved. This analysis includes presentation of the statistical mean of the paths flown, the extremes of the aggregate of paths flown, and a representation of the mean plus and minus two times the standard deviation of the data about the mean, on a point-by-point basis. All data were calculated separately for each point of progress along the intended course line (every fifty feet in the along-track direction). Thus, the "extreme" data does not represent the single flight with the largest overall deviation, but the largest deviation in all of the flights at each fifty-foot increment. In addition, the VFR approach/departure surfaces are also depicted (see figure 2.1-1).

It should be noted that on three of the Metro approaches, the subject pilots flew a short downwind leg and turned onto the final approach at an along-track distance of approximately 3,700 feet from the heliport. Thus for these approaches, there are no data between 4,000 feet and 3,700 feet from the heliport. The flight tracks of the three approaches are presented in figures H.4-1 through H.4-3. These shortened flight tracks caused difficulty in developing statistical measures out to 4,000 feet. This situation was analyzed in two distinct ways:

1. In order to derive statistics out to 4,000 feet, the three approaches were omitted from the statistical database for cross track error. These three approaches were identified as "excepted" data. The remaining data set provides a full range of cross track data from the heliport to 4,000 feet, but it omits the effect of the three shortened flight tracks. These statistical results are presented in Appendix H. The figures that are affected by the omission of the excepted data are:

Figure No.	H.2-5	H.2-13	H.2-17	H.2.21	H.2-29
No. of Approaches Omitted	1	2	3	2	3

2. Clearly the three approaches in question used different airspace than did the remaining approaches. In order to determine the overall effect of the shortened approaches on the approach airspace, two additional statistical graphs were prepared using the excepted data. Comparative statistical data are presented in figures H.4-4 through H.4-7. Figure H.4-4 is a repeat of figure H.2-13 (Night B visibility cases - without excepted data) while figure H.4-5 contains a full data for Night B visibility including the appropriate excepted data. In comparing the two figures, the statistical data are quite dissimilar from a distance of 4,000 feet from the heliport to about 2,500 feet from the heliport. The cross track error statistics go off-scale (greater than 1,000-foot error) at a point about 3,300 feet from the heliport. From the 2,500-foot point to the heliport, the statistical data are quite similar. A very similar pattern is shown in the comparison of figures H.4-6 (without excepted data) and H.4-7 (with excepted data). Again, the cross track error statistics go off-scale at a distance of about 3,300 feet from the heliport. Had there been a "hard-to-see" obstacle in this airspace, would each of these three pilots have hit it?

6.4.2 Altitude

These plots are similar to the cross track plots, except that the altitude dimension is depicted. As before, the statistical mean, extremes and mean plus and minus two times the standard deviation of the data relative to the mean are depicted. The 8:1 sloping "floor" of the VFR approach/ departure surfaces is also shown.

6.4.3 Height –Velocity (H-V)

These plots present a quite different analysis of the flight progress of the helicopter during approach and departure. In these plots the along-track progress is suppressed in favor of a depiction of the direct relationship of altitude above ground level (AGL), versus velocity during the initial stages of departure and the final stages of descent. The data are presented in a manner similar to the above: the mean value of height versus velocity; the extremes of the cases included; and, the mean plus and minus two times the standard deviation of the data about the mean. Also depicted on these plots are the boundaries of height-velocity avoid regions for one engine inoperative (OEI) from the aircraft performance manual. This chart was presented to the subject pilots as a part of the helicopter flight manual given to them during their introductory briefings (see the figures in appendix G). Please note that the data presented are based on ground speed information, while the H-V avoid region definitions are based on airspeed, the difference being winds encountered.

6.4.4 Operational Cases Presented

The experimental data was aggregated and grouped in the following ways. These groupings allow direct comparisons of the Metro corridor versus the Valley corridor, comparisons of low to high obstacle density cases, and comparisons of day to night (and night with enhanced lighting options) cases. The specific cases presented are as follows:

Metro/Valley Arrivals	Metro/Valley Departures
Low Obstacle Density	Low Obstacle Density
Medium Obstacle Density	Medium Obstacle Density
High Obstacle Density	Medium-High Obstacle Density
Day Visibility	High Obstacle Density
Dusk Visibility	Day Visibility
Night-A Visibility	Dusk Visibility
Night-B Visibility (enhanced lighting)	Night-A Visibility
Ensemble	Ensemble

Please note that appendix H also contains additional plots for purposes of depiction of 6-sigma data (mean plus and minus six times the standard deviation of the data about the mean) and also includes depiction of ground speed information. In these plots, only the ensemble cases are included. These plots are included to show the extent of the airspace consumed by these subject pilots during their heliport approaches and departures. Based on extensive research, the FAA has previously concluded that six-sigma data represent a valid measure of protected airspace for VFR operations.

6.4.5 Comparison of the Metro versus the Valley Corridors

The final approach (and initial departure) corridors of the Metro and Valley routes are aligned along the same line (but in opposite directions), as depicted in figure 4.2.1.1-1. However, the visual cues available to the pilots to achieve course alignment in the two cases are considerably different (as intended in the design of the simulation experiment). The cues provided in the final portions of the Metro route (base leg and final) are less obvious than those of the Valley route. Rather than being fly-over points, the cues are located at various points abeam the intended route. For example, an antenna tower is located north of the base leg. A power plant is located just to the east of the final leg. Power lines crossing the river underlie the final, while a sports stadium lies just to the west of the final leg. There is no specific point where the turn to final should be initiated. Likewise, on departure, there is no distinct aim point to guide the outbound segment.

In direct contrast, the Valley route provides positive visual checkpoints defining the latter portions of the arrival: turn to final at the drive-in movie theater; initiate descent after crossing the twin towers. The twin towers (which vary in height depending on the obstacle density case being flown) were located as they were to provide a formidable, although legal, obstacle in the path during arrivals and departures on the Valley route. However, they also provided an excellent visual cue for course alignment similar, in some ways, to a localizer needle.

Examination of the cross track error ensemble (all simulation variable cases included) plots for the Metro Approach case (figure H.2-29) and Valley Approach case (figure H.2-61) shows that the difference in visual cues indeed has a notable effect on the cross track error statistics. A quick review of these plots brings up the first significant difference, which is the mean value (broad black line) in the Metro case shows a "drifting in" from the west, while the mean in the

Valley case is almost dead center on the intended course. Since the Metro approach involves a turn from the westerly base leg onto final, it is apparent that the subject pilots were, on average, slightly overshooting this turn. In the Valley case, no overshoot is possible since the helicopter should already be aligned with the approach course after the turn at the drive-in movie theater (refer to figure 4.2.1.1-1). The Valley approach then crosses a point between twin high-rise buildings that are less than 200 feet apart. In addition, the Valley approach path is parallel to the streets and the associated buildings underneath it. Thus, both day and night, the pilot has many powerful visual cues that help to keep the aircraft on the center of the approach path. One should recognize that this is not typically the case for the vast majority of heliports.

The second significant difference involves the dispersion of the data around the mean. In the Metro case, this dispersion is quite large, as may be seen by examining either the two sigma lines or the data extremes lines. In both cases, these lines do not come within the nominal 500 feet width of the airspace surface until the helicopter is within roughly 1,000 feet of the heliport. In direct contrast, in the Valley case both measures (the two sigma lines and the data extremes lines) are well within the 500 feet boundary over the entire 4,000 feet approach. Also, the two sigma lines are within (roughly) the boundaries of the VFR approach/departure surface as it narrows towards the heliport. During preflight briefings the pilots were educated about the routes and landmarks (and were coached through at least one familiarization flight along each route). However, they were not admonished to strictly adhere closely to the routes, or, for that matter, to alter in any way their normal daily flight procedures, since the objectives of the experiment were to achieve performance as close to normal operations as possible in a simulator experiment. Therefore, it appears that when led by obvious route markers the pilot population almost could not help but adhere closely to the course line, but when given a wide degree of latitude, responded with a wide dispersion in results.

It is also useful to examine the altitude statistics plots for the Metro (figure H.2-30) and Valley (figure H.2-62) approaches. Differences in altitude performance are much less obvious. The mean altitudes at the 4,000 foot point are different for a very good reason: the procedure definitions prescribed different base leg altitudes (Metro: 700 feet; Valley: 900 feet). The two sigma lines are not markedly different between the two cases, although the dispersion in the Metro case is visibly larger. This most likely results from the imposing nature of the twin towers on the Valley approach, even in the low obstacle density case, which would tend to keep the pilot flying consistently higher until the towers are passed. Further inbound, at the 2,000-foot point for example, any difference in dispersions between the two cases is very minor.

A comparison of the cross track error statistics in the departure cases (Metro, figure H.2-93, and Valley, figure H.2-125) reveals a much smaller difference than was apparent in the approach case. This is to be expected since all departures begin on-course (at the heliport). Both mean curves appear to drift off of the course centerline, with the Metro case showing somewhat more drift, as would be expected from the lack of cues. Likewise, the dispersion about the mean is smaller in the Valley case. Note that any data outside of roughly 2,000 feet is not of concern since virtually all cases had exceeded the 500 feet height (above terrain) of the VFR approach/ departure surface.

A comparison of the altitude statistics in the Metro departure case (figure H.2-94) and the Valley departure case (figure H.2-126) shows what appears to be a higher initial rate of climb in the

Metro case. This probably results from the consistent presence of an industrial area and refinery between the heliport and the river, while the Valley case presents few consistent obstructions affecting departure in the immediate vicinity of the heliport. The eventual altitudes (at 4,000 feet) are different due to different cruise altitude assignments.

6.4.5.1 Evaluation of Obstacle Density Effects (Approach)

Comparing the Metro approach Low Density and High Density cross track data (figures H.2-17 and H.2-25) reveals a significant difference in dispersion at the 4,000-foot point, with the High Density case showing greater dispersion. This probably results from the apparent intrusiveness of the broadcast antenna tower located to the north of the base leg, which becomes quite imposing in the high density case. Another influence probably results from the increase in obstacles near the heliport, which may make identifying and intercepting the final approach course more difficult. At 2,000 feet from the heliport that difference becomes minimal.

In the equivalent Valley approach case (figures H.2-49 and H.2-57), dispersions at the 4,000-foot point are roughly equal, due to the influence of the twin towers on course alignment. However, dispersion in the High Density case is slightly higher from 2,000 feet inbound to the heliport due to numerous obstacle differences between the cases along side and in the vicinity of the final parts of the approach.

Regarding the Metro approach Low and High Density altitude data (figures H.2-18 and H.2-26), the mean altitude curves are almost identical, while the dispersions are significantly larger in the High Density case from 2,000 feet inbound to the heliport, showing some impact of obstacle density. In the Valley cases (figures H.2-50 and H.2-58) the mean curve is higher in the high density case. This is primarily due to the influence of the much higher twin towers obstacle which the pilot directly overflies. The dispersion is smaller at 4,000 feet in this case for the same reason. However, as the heliport is approached (2,000 feet inbound) the altitude dispersion in the Valley case becomes much greater in the High Density case versus the Low Density case. This effect is very significant, and illustrates the impact which numerous threatening (though legal) obstacles have on pilot perception during approach.

6.4.5.2 Evaluation of Obstacle Density Effects (Departure)

During the Metro Low and High Density departures (figures H.2-77 and H.2-89), the mean curves illustrate that the pilots had a preference for departing slightly to the right of the nominal course line, which was consistent from the Low to High Density cases. Only the first 1,000 feet to 1500 feet are of interest here since the helicopter is well above 600 feet MSL after that range. The two sigma lines (dispersions) illustrate a very interesting point: they are tighter (closer to the mean) in the immediate vicinity of the heliport, and remain slightly tighter until the helicopter is above 600 feet. This probably results from the influence of looming obstacles on either side of the departure course. A similar, although slightly less pronounced, effect is apparent in the Valley case (figures H.2-109 and H.2-121).

Regarding the altitude data for the Metro Departure (figures H.2-78 and H.2-90) the mean curves show a significantly higher rate of climb in the High Density case, reflecting the pilot's desire to avoid and overfly the obstacles. The altitude dispersions are smaller in the High Density case,

again reflecting the desire to be higher as early as possible. A similar conclusion applies in the Valley Departure case (figures H.2-110 and H.2-122). The mean altitude curve, especially, shows a much higher rate of climb.

6.4.5.3 Evaluation of Visibility Effects (Approach)

The transition from day to dusk to night will be discussed first, followed by a comparison of the Night-B (enhanced lighting aids including landing direction light, a heliport beacon, apron lights, and a PAPI) versus the Night-A case (baseline lighting configuration defined in section 4.1.1). Comparing the Metro Approach Day versus Dusk cases (figures H.2-1 and H.2-5), the mean cross track lines are virtually identical. The dispersions (two sigma lines) are greater in the Dusk case, showing that the pilot has a lower degree of certainty identifying the desired course. This is not surprising, since the desired course seems to be difficult enough to identify even in daylight. The mean altitude curves are virtually identical (figures H.2-2 and H.2-6). Even the altitude dispersions are very similar, indicating that the pilots could identify the heliport (and descend to it normally), even though identifying the course to fly to the heliport was difficult.

The Metro Night-A case provides dramatically different results. The mean cross track curve (figure H.2-9) is precisely on course. The dispersions, while even greater at the outer distances, become smaller once inside 2,000 feet of the heliport, and very significantly smaller inside 1,000 feet. This indicates that even the baseline heliport lighting provides significant cues for course acquisition that are not available during the day. The mean altitudes in the two cases are quite different, as are the altitude dispersions. Overall, in the Night-A case (figure H.2-10), the pilots were flying lower (even at the 4,000-foot point). It is uncertain how much of this is due to the different perspective of night flying, or is due to the trouble the pilots were having identifying the intended course (as indicated by the larger cross track dispersion) resulting in lower altitudes to identify features. In any event, once within 1,000 feet of the heliport, altitude dispersions were even less in the Night-A case, indicating that visual cues from the lights are as good as, or better than, visual cues during daylight.

The Valley approach cross track data (figures H.2-33 and H.2-37), are significantly different than the Metro case. The course acquisition is superior due to the design of the approach and the presence of the twin towers. The data show that pilot performance was better in the Dusk case than the Day case. Both the mean track and the dispersions were better in the Dusk case. The mean altitude curves (figures H.2-34 and H.2-38) start at exactly the same altitude (as influenced by the presence of the twin towers), but descent occurs more rapidly in the Dusk case. Within 2,000 feet of the helipad, the dispersions are also significantly lower in the dusk case. Overall, the Dusk case was more precisely controlled than the Day case. The specific cause is not known, but perhaps the fact that the pilots were well oriented left them with time to concentrate carefully on the mechanics of the procedure when confronted with the lower visibility at dusk.

The cross track data in the Night-A case (figure H.2-41) shows that the flight was also well-controlled, but that a certain amount of wandering occurred in the 3,000 feet to 2,000 feet neighborhood, probably resulting from the different perspective of night operations. In any event, the performance tightened up within 1,000 feet, resulting in a slight improvement over the Dusk case, consistent with the latter stages of the Metro case. The altitude data in the Night-A

case (figure H.2-42) continues the trend from Day to Dusk: The altitudes are lower (after being the same at the 4,000-foot point), and the dispersions within 2,000 feet of the helipad are lower. This indicates that the night cues available from standard helipad lighting provide assistance to the pilot in controlling his descent, which again is consistent with the Metro case.

6.4.5.4 Evaluation of Visibility Effects (Departure)

In this discussion of departure data, the area of interest will be limited to roughly 2,000 feet from the helipad. At that point, most of the flights had exceeded the 600 feet altitude of the VFR approach/departure surface. Also, many of the data runs were terminated early, resulting in "ragged" looking plots.

The cross track data for the Metro Day Departure case (figure H.2-65) shows a significant tendency of the pilot to veer off to the right (by about 7 degrees). This presumably resulted from a tendency to want to avoid obstacles on the left, even though they are legal obstacles. The pilots did not seem to feel bound by the prescribed course in the same way that they were during arrivals. The Dusk data are similar (figure H.2-69). The mean shows slightly less deviation, and the dispersion is also slightly reduced. This trend reverses in the Night-A case (figure H.2-73). While the mean track is closer to the intended course, the dispersion is much, much wider, indicating a severe inability to identify the intended course. As in the approach case on the Metro profile, a lack of obvious visual guideposts results in unpredictable performance. The Altitude data for these three cases are also very revealing. The mean altitude curve reaches 600 feet at 1,500 feet from the heliport (figure H.2-66), while the dusk case (figure H.2-70) reaches that point at 1,400 feet from the heliport. The Night-A case (figure H.2-74) reaches 600 feet in altitude at 1,200 feet from the heliport, indicating that, when uncertain about position, the pilots tended to climb faster to be "above it all" sooner. The altitude dispersion data are not significantly different in the three cases.

In the Valley departure cases for Day, Dusk and Night-A (figures H.2-97, H.2.101, and H.2-105) all show much tighter control over cross track error than the Metro case. Differences in the means and dispersions of these three cases are insignificant, again demonstrating the overwhelming influence of the obvious visual guidepost on performance, regardless of visibility condition. While the altitude data (figures H.2-98, H.2-102, and H.2-106) shows that rate of climb seemed to increase slightly as visibility went from Day to Dusk to Night-A, the effect was rather slight in comparison to the Metro case.

6.4.5.5 Evaluation of Enhanced Lighting Effects (Approach Only)

A comparison of the Metro Night-A versus Night-B cases (figures H.2-9 and H.2-13) reveals a significant influence of enhanced lighting on course identification. This is particularly true of the outer ranges (4,000 feet to 2,000 feet). Once within 2,000 feet, performance is similar. The Altitude data (figures H.2-10 and H.2-14) shows a similar trend; while the means are similar, dispersions are significantly reduced at the outer ranges. Apparently, once within 2,000 feet of the helipad, visual cues have been well identified, and course and final descent control is as good without the enhanced cues.

In the Valley case, as shown in figures H.2-41 and H.2-45, the existence of the enhanced lighting cues tends slightly to improve the cross track dispersions (which were already low). No real improvement was noted in the altitude data (figures H.2-42 and H.2-46). In fact, the Night-B case showed somewhat lower control over altitude dispersions.

6.4.5.6 Evaluation of Height-Velocity Data

It is useful to examine the H-V data in the ensemble cases, since variations with the two simulation variables do not seem to be very significant. In the Metro (figure H.2-32) and Valley (figure H.2-64) Approach cases, the H-V diagrams are very similar. In both cases the mean curves penetrate the avoid region to a significant extent. In the Metro case, even the lowest extreme case touches the curve. This indicates that the pilots were more concerned with establishing and maintaining a stable, consistent final descent profile than they were with the possible risk of operating within the H-V avoid region.

The ensemble departure cases, figures H.2-96 (Metro) and H.2-128 (Valley) show an even greater penetration of the H-V avoid region than was evident in the approach situation. Also, the result is potentially more at risk since significant time is required to reconfigure from full power takeoff to an emergency descent configuration in the event of engine failure. Since the pilots were made aware of the H-V performance of this helicopter in the preflight briefing, it is apparent that they chose to accept whatever risk is associated with operating within the H-V avoid area.

In earlier analyses, helicopter H-V limitations have been extensively studied as a basis for modifying the minimum recommended VFR approach/departure airspace. The analyses of reference 40 examined departure procedures for eight helicopters representing 35 percent of the U.S. helicopter fleet. These departure procedures were deliberately constrained to abstain from flight through the H-V avoid area. Based on these constraints, the authors concluded that "... current FAA minimum recommendations for VFR approach/departure airspace are inadequate to cover the range of helicopters and operational conditions that are routinely encountered." The primary problems are the lack of an acceleration area adjacent to the helipad and the lack of a margin of safety between allowable obstructions and required helicopter performance.

The pilots in this present study were chosen from a population of EMS pilots having between 3,000 and 6,500 flight hours. Their average time as an EMS helicopter pilot was in excess of 600 hours. These pilots chose to fly through the H-V avoid area as a normal procedure both during approach and departure operations. They made this choice even at times when it appeared that they could have avoided it (for example, in departure situations where some acceleration distance was available to them, especially on the "low obstacle density" departure cases). There were no comments recorded that indicate that these pilots were uncomfortable with this choice. The nature of the EMS mission is such that EMS pilots probably have considerably more experience flying in obstacle-rich heliport environments than other helicopters pilots.

7.0 CONCLUSIONS

The conclusions presented in this section are segregated into three major categories, each of which is discussed in a separate subsection:

- Test setup and simulator configuration.
- Experiment conduct and data acquisition.
- Analysis of ORE experiment data.

In general, high-fidelity simulation was found to be a useful tool for conducting this investigation. Simulation provided the flexibility required for successful execution of this phase of the ORE program. The simulator allowed the controlled and repeatable variations of the operational flight environment needed to satisfy the test objectives.

7.1 TEST SETUP AND SIMULATOR CONFIGURATION

The following conclusions relate to the development of specific simulator characteristics for conducting the ORE experiments. Preparing the visual database for these experiments was the single largest simulator development task. A high level of coordination and several iterations were required to develop a visual database that satisfied program objectives.

- Developing a complete visual database to satisfy the requirements of this simulation experiment proved to be an extremely challenging task. The ORE database was extremely complex and detailed, requiring more resources than had been estimated or proposed. This experiment pushed the Boeing simulation visual system to the limit of its capability. Special procedures and configurations were routinely developed to address simulator limitations encountered in generating and displaying the ORE visual database. A more thorough understanding of ORE project database requirements could have averted programmatic difficulties.

- Pilot input is required to develop a satisfactory visual database. The visual scene developed for this simulation drew on the operational experience of both Boeing test pilots and EMS pilots. Their insight and experience led to the development of a realistic and challenging obstacle-rich environment. The program should have included an additional checkpoint that brought in at least two line EMS pilots to assess and evaluate the simulation prior to the actual startup. This might have identified and eliminated a number of problems encountered during the experiment.

- The ORE simulation investigated variations in heliport lighting and demonstrated that different lighting configurations can significantly improve pilot performance under certain visual conditions. Improvements in facility acquisition, lateral tracking, altitude control, and airspeed control were noted.

- The initial program structure provided for two simulation periods, with a data review and test procedure update between the simulation periods. When the program was restructured this

update was eliminated. This proved to be a serious shortfall of the revised program, leading to a number of simulation problems. In retrospect, a detailed pretest review should have been included. This would have avoided and possibly eliminated a number of hurdles that appeared as the simulation experiment proceeded.

7.2 EXPERIMENT CONDUCT AND DATA ACQUISITION

These conclusions are related to the conduct of the experiment and the methods used for data acquisition. Many of the data acquisition techniques have been used in previous experiments and the application of lessons learned in those experiments helped to insure ORE simulation success.

- Real-time recording of questionnaire information into a database format shortened the time required to acquire and analyze the subjective data. Handwritten forms used in previous evaluations were eliminated in favor of electronic recording of subjective data.

- Secondary tasks must be selected to insure that effective workload assessment and quantifiable metrics are provided. In the ORE experiments, pilots were expected to accomplish two secondary tasks while operating the helicopter: radio frequency selection and ATC communication. Many pilots eliminated radio frequency selection as a secondary task by setting frequencies prior to simulator initialization. ATC communications, while well integrated with the flight task, provided little quantifiable workload information.

- The vertical profiles flown by the pilots in most, if not all, of the approaches and departures carried the aircraft through some portion of the height-velocity (H-V) avoid region. (In retrospect, as detailed in section 6.4.3, the only velocity data available to plot these curves was ground speed and not airspeed, on which the H-V diagram is based. Consequently, actual H-V deviations may have occurred in less than 100 percent of the cases.) Such deviations from flight manual recommendations do not represent safe helicopter operating procedures[44]. While pilots may choose to do this during operations at unimproved landing sites where there is a risk of encountering an obstacle, the airspace in the vicinity of a heliport should permit approach and departure operations that do not require helicopters to fly through this region. There is a body of research on airspace requirements that relate to approach and departure operations that eliminate flight through the height/velocity "avoid" region[40,41,42,43]. This research should be used as a basis for establishing heliport airspace criteria. In future simulation testing, questionnaires should be expanded to obtain immediate feedback from pilots when questionable operations occur.

- The use of portable equipment for physiological data acquisition improved the productivity of the simulation sessions. Pilots could be connected and disconnected from the monitoring equipment in a matter of minutes, expediting pilot changes and allowing pilots to move about freely during break periods.

7.3 ANALYSIS OF ORE EXPERIMENT DATA

This section presents conclusions based on analyses of the flight performance data, the physiological measures, and subjective questionnaire data. Other forms of data were collected (video and audio recordings, debriefing questionnaires, and emergency procedure run data) that

were not analyzed due to program constraints. All test subjects were EMS helicopter pilots with an average 4,500 hours helicopter time, of which over 600 hours represent EMS experience. These results may not, therefore, be representative of pilots with significantly less helicopter time or with significantly less experience flying in obstacle-rich heliport environments.

The reader is referred to previously conducted flight test programs[41,42] and analyses[40,41,42,43] that have led the FAA to conclude that the current FAA recommendations for VFR heliport approach and departure airspace are inadequate. The results of the current simulation study support the FAA's previous conclusions in the following areas:

- Pilot comments indicated that they considered obstacle clearance to be insufficient while flying the PAPI glide path. This was true, even though the PAPI was sited in accordance with the FAA Heliport Design advisory circular, reference 3.

- Even thought the test subjects were all experienced EMS pilots flying in what was known to be an obstacle-rich environment, the pilots did not always stay above the 8:1 approach surface during the approaches. Some of the digressions below the approach surface occurred between 2,800 and 4,000 feet from the heliport on the Metro approach. A few digressions occurred within 400 feet of the heliport on the Valley approach. The flight testing cited in reference 41 has shown that flight below the 8:1 approach surface is even more common if the heliport is located in an environment that the pilot believes to be devoid of significant obstacles. This illustrates the need for remedial actions, including greater approach/departure airspace and the marking and lighting of obstacles in close proximity to these airspace boundaries. It is particularly important to mark objects that are difficult to see under normal conditions, such as wires and poles.

- During the Metro approaches and departures, these high-time pilots used considerably more lateral airspace than the current FAA VFR approach/departure surfaces.

- The Valley approach had an unusually large number of visually powerful and well-located visual cues and many of these cues were visible under all visibility conditions simulated. In the approach case, the flight paths stayed within the current VFR approach/departure surfaces. However, the pilots' lateral dispersion exceeded the limits of the current VFR approach/departure surfaces during departures. In the departure flights, the data was biased to the left. The apparent source of the bias, which amounted to seven degrees left of centerline, was apprehension caused by the close proximity of buildings on the right.

- Pilots flew higher on approaches with low visibility, presumably to achieve greater separation from obstacles. While the steeper approaches provided greater obstacle clearance, it meant that the helicopter traveled deeper into the "avoid portion" of the H/V diagram. Had adequate additional airspace been available (below the current 8:1 surface) and had they been assured that this airspace was available, pilots could have flown a shallower approach and it would not have been necessary to fly through the "avoid" portion of the H/V curve.

Obstacles elicit the greatest effect on pilot performance during high visibility conditions (i.e., during day operations), particularly in terms of clearance maintained from prominent obstacles.

Reduced visibility from changes in TOD led to more conservative flight performance and higher perceived workload and risk. The following observations lead to this conclusion:

- Pilots flew higher on approaches with low visibility, presumably to achieve greater separation from obstacles. Thus, pilots selected steeper approach paths as their ability to detect obstacles declined.

- Flight time on the final segment increased with decreasing visibility due to TOD. The largest flight time increase took place between dusk and night flights.

- Pilots flew more variable flight paths on departure with low visibility than with high visibility. This suggests that pilots deviated from the briefed flight paths when unsure about obstacle locations (i.e., when it was difficult to detect obstacles due to low visibility). Directional cues were less precise on departure than on the final segment of the approaches at this heliport. Even though there were many visual cues in the area, pilots appear to have flown in a general direction during departure rather than making full use of the available cues to stay on centerline.

- Overall, pilots' ratings of workload, on both approaches and departures, increased with decreasing visibility. Pilots' ratings of hazardousness also increased slightly with decreased visibility.

- Lower heart rates were recorded for night approaches than for day approaches. This may reflect the inability of pilots to clearly view obstacles under reduced lighting conditions, thereby decreasing their physiological response to the obstacles. On the other hand, when pilots rated the flight workload, their responses suggested that the night-flight conditions caused more workload than the daytime flights. It would appear that heart rate captures an immediate response to flight conditions while the subjective scales reflect consideration of the overall flight.

As OH/D increased, pilots modified their flight paths to maintain additional obstacle clearance. The clearances maintained by the pilots in this experiment indicate that the current VFR approach/departure surfaces do not adequately reflect pilot operating practices in an ORE. OH/D was varied as a single parameter in the simulation study, and the density of relevant obstacles was higher on final than on the downwind or base segments of the flight corridors. The following findings support this conclusion:

- Touchdown error from the center of the heliport grew with increasing OH/D. Close-in obstacles (people and other helicopters, in particular) were of great concern to the pilots in the high OH/D conditions, and pilots deliberately deviated from landing in the center of the heliport.

- Increasing OH/D decreased the percent of time that pilots flew below minimum altitudes on the base-leg segment of the approaches, thus increasing obstacle clearance.

- Vertical error on departure grew with increasing OH/D, particularly in the vicinity of the heliport. This reflects pilot desire to heighten clearance between the helicopter and obstacles

with increasing OH/D, and is consistent with the greater clearances from the power lines observed during higher OH/D conditions.

Increases in workload and perceived risk were observed in high OH/D situations. Except for certain close-in obstacles, these high-time EMS pilots did not consider the operations flown to be unacceptable due to the obstacle density level. Any future testing should include a significant percentage of pilots with less than 1,000 hours of flight experience.

- Heart rate measures indicate higher workload with progress along the approach path, increasing from downwind to final. This increase may be associated with the change in obstacle density and proximity that occurs along the flight path or with the general increase in activity expected as the pilot prepares for landing. No significant heart rate measure variations were observed as OH/D was varied independently of fight segment.

- In a trend similar to the heart rate measures, blink rate decreased from downwind and base-leg segments to the final approach segment, suggesting the need for higher levels of pilot attentiveness in the later segments of an approach. As with the heart rate measures, it is not clear whether this variation is caused by increasing obstacle density or by normal approach workload variations.

- Pilot mental workload ratings, as well as ratings of the riskiness and hazardousness of flights, escalated with increasing obstacle density. These ratings are consistent with the flight performance measures, suggesting increased caution at higher OH/D.

Heliport marking and lighting modifications (that provided visual flight path guidance or improved heliport landing area visibility) enhanced navigation on final approach, albeit with small, but measurable, increased pilot workload. The beneficial effects of enhanced heliport lighting were apparent in pilot flight performance data. Compared to the baseline lighting condition:

- Lateral position error on approach was reduced.

- Pilots were able to fly approaches substantially faster.

- Vertical slope error on approaches was reduced.

Selection and identification of landmarks can increase situational awareness, reduce pilot workload, and improve operational safety by improving navigational accuracy. Linear landmarks (e.g., railroads, roads) along a flight path and point landmarks (e.g., small towers) directly in line with the flight path result in the best navigation accuracy when they are visible. Area landmarks (e.g., parking lots) or landmarks off to the side of the flight path provide less accurate guidance. This is supported by the following findings:

- Lateral flight path error decreased from the downwind to the final approach segment. This general trend indicates that pilots flew with the greatest precision when presented with a navigational target and adequate alignment cues. Alignment cues on final included the

apparent geometry (perspective view) of the heliport and the numerous obstacles surrounding the final approach path.

- Lateral flight path error on downwind was lower on the Valley approach than on the Metro approach. The Valley approach downwind leg followed a railroad track; the Metro approach initiated at an arboretum (an area landmark). At night when unlighted landmarks were not visible, lateral error on both approaches was similar.

Some obstacles generate greater safety concerns than others. Pilots rated the high power wires as the most troublesome obstacle on approaches and departures. Power lines and other wires are often very difficult to see in time to take successful evasive action.

8.0 RECOMMENDATIONS

1. During this program, the vertical profiles flown by the pilots in most, if not all, of the approaches and departures carried the aircraft through some portion of the H/V "avoid" region. Such deviations from flight manual recommendations do not represent safe helicopter operating procedures[44]. While pilots may choose to do this during operations at unimproved landing sites, where there is risk of encountering an unseen obstacle, the airspace in the vicinity of a heliport should permit approach and departure operations that do not require helicopters to fly through this region. There is a body of research on airspace requirements that relate to approach and departure operations that eliminate flight through the H/V "avoid" region[40,41,42,43]. This research should be used by the FAA and the helicopter industry as a basis for establishing heliport airspace criteria.

2. Research should be conducted on lighting configurations to determine which elements contribute to the performance improvements observed in this evaluation. Included in the research should be tests to evaluate whether these lighting configurations enable pilots to stay within the minimum airspace (VFR or IFR visual segment) associated with the configuration's operational use.

3. The ORE evaluations have generated a rich database of pilot performance, workload, and risk perceptions in VFR heliport operations. Data analysis conducted for this phase of the ORE program was limited by a number of constraints. Additional analysis could be conducted on the data obtained from these experiments. If such work is undertaken, the following efforts (with the existing data) could be useful:

a. Review video data to investigate anomalies in other data streams - A number of unexplained trends were observed in the subjective and physiological measures. Review of the audio/video data may provide clues to understand these trends.

b. Compile and review pilot survey information - A cursory review of the pilot survey data was conducted to confirm several of the findings reported here; however, a detailed review of this data is likely to yield additional information on pilot opinion.

c. Interview pilots regarding obstacles of greatest risk - Polling the pilots for opinions on obstacles of greatest risk may help to focus future investigations and provide additional insight into the data already analyzed.

d. Analyze pilot control activity - pilot control positions were recorded during all ORE flights. Significant workload measures could be derived from analysis of pilot control activity across flight segment, TOD, and OH/D conditions.

e. Develop preliminary OQC - through a detailed analysis of approach and departure fight profile data, a preliminary OQC methodology could be developed. This effort would also highlight areas where additional research is required to establish a definitive OQC.

4. The original plan stated in the ORE request for proposals (RFP) included evaluation of other helicopter types and crew combinations. Of particular interest would be evaluations of lower-time pilots and less-capable (single engine) helicopters to generalize the results. Building the visual database was a significant portion of the ORE task. Further use of the database for piloted evaluations could be conducted at considerable lower cost. To better represent the full range of the rotorcraft industry, a significant percentage of future subject pilots should have between 50 and 1,000 hours of flight experience. Consideration should also be given to systematically investigating the effects of different obstacle types within the ORE.

5. Future simulation evaluations of this type should include a "dress rehearsal" simulation session. This session should occur after all simulation development activity is completed, should be conducted with pilots from the same pilot pool used for the actual experiment, and should exercise all facets of the simulation. Adequate time to correct problems that arise in simulation hardware, simulation software, or test methodology must also be scheduled into the experiment.

LIST OF REFERENCES

1. "VFR Heliport Obstacle-Rich Environment (ORE) Request for Proposal (RFP) for Simulation Support Services for Single/Multi-Engine Rotorcraft and Advanced Vertical Flight Aircraft", by Sawyer, B.M., and Richards, B.W., SCTG No. 94RR-12, Science Applications International Corporation (SAIC) for the Federal Aviation Administration, publication date January 1995.

2. "Helicopter Nonprecision Approach Criteria Utilizing the Global Positioning System (GPS)", FAA Order 8260.42, Federal Aviation Administration, publication dated February 1996.

3. "Heliport Design", FAA Advisory Circular 150/5390-2A, publication date 1/10/94.

4. "VFR Heliport Obstacle-Rich Environment: Draft Test Plan", by Sawyer, B.M., Peisen, D.J., and Bolz, E. H., FAA/RD-94/42, Systems Control Technology, Inc. (SCT) October 1991.

5. "VFR Heliport Obstacle-Rich Environment: Test and Evaluation", by Sawyer, B.M., Peisen, D.J., FAA/RD-94/41, Systems Control Technology, Inc. (SCT) July 1991.

6. "VFR Heliport Obstacle-Rich Environment: Simulation Requirements and facilities", by Sawyer, B.M., Peisen, D.J., Bolz, E.H., FAA/RD-94/43, Systems Control Technology, Inc. (SCT) July 1991.

7. "Pilot Briefing Materials", by Sawyer, B.M., SCT No. 93RL-409, Systems Control Technology, Inc (SCT) May 1993.

8. "Flying Qualities of Piloted Airplanes", MIL-F-08785C Military Specification, Air Force Flight Dynamics Laboratory, publication date November 1980.

9. "Helicopter Simulator Qualifications", FAA Advisory Circular 120-63, Federal Aviation Administration, publication date October 1994.

10. "Handling Qualities Requirements for Military Rotorcraft", ADS-33C *Aeronautical Design Standard*, United States Army Aviation Systems Command, Publication date August 1989.

11. "Taxiway Centerline Lighting System", FAA Advisory Circular 150/5340-19, publication date 11/14/68.

12. "Runway and Taxiway Edge Lighting system", FAA Advisory Circular 150/5340-24, publication date 9/3/75.

13. "Specification for Runway and Taxiway Light Fixtures", FAA Advisory Circular 150/5345-46A, publication date 6/7/84.

14. "Precision Approach Path Indicator (PAPI) Systems", FAA Advisory Circular 150/5345-28D., publication date 5/23/85.

15. "Workload – An Examination of the Concept", by Gopher, D. and Donchin, E.; Handbook of Perception and Performance, K. Boff, L. Kaufman, and J. Thomas (Eds.), Wiley 1986.

16. "Mental Workload Since 1979", by Moray, N.; International Reviews of Ergonomics, Vol. 2, pages 123-150, Taylor and Francis 1989.

17. "Engineering Psychology", by Wickens, C.D. and Kramer, A.F.; Annual Review of Psychology, Annual Reviews, Inc. 1985.

18. "Physiological Measures of Mental Workload: A Review of Recent Progress", by Kramer, A.F.; Multiple Task Performance, D. Damos (Ed.), Taylor and Francis 1991.

19. "Operator Workload: Comprehensive Review and Evaluation of Operator Workload Methodologies", by Lysaght, R., Hill, S., Dick, A., Plamondon, B., Linton, P., Wierwille, W., Zaklad, A., Bittner, A., and Wherry, R.; Analytics Technical Report 2075-3, Analytics 1989.

20. 'Workload Assessment Methodology", by O'Donnell, R. and Eggemeier, F.T.; *Handbook of Perception and Human Performance*, K. Boff, L. Kaufman, and J. Thomas (Eds), Wiley 1986.

21. "Factors Determining Workload", by Leplat, J.; Ergonomics, Journal of the Ergonomics Society and the International Ergonomics Association, Vol. 21, pages 143-149, Taylor and Francis 1978.

22. "Measurement of Workload by Secondary Tasks", by Ogden, G., Levine, J., and Eisner, E.; Human Factors, Vol. 21, pages 529-548, Human Factors Society 1979.

23. "Measures of Workload, Stress and Secondary Tasks", by Wickens, C.D.; Mental Workload: It's Theory and Measurement, N. Moray (Ed.), Plenum Press 1979.

24. "Advanced Workload Assessment Techniques for Engineering Flight Simulation", by Grenell J.F., Kramer A.F., Sirevaag, E.J., and Wichens, C.D.; American Helicopter Society (AHS) 1991 Annual Forum, American Helicopter Society May 1991.

25. "Workload Assessment and Prediction", Hart, S. and Wickens, C.; MANPRINT: An Emerging Technology, H. Booher (Ed.), Van Nostrand Reinhold 1990.

26. "Final Report of the Experimental Psychology Group", by Johannsen, G., Moray, N., Pew, R., Rasmussen, J., Sanders, M., and Wickens, C.; Mental Workload: It's Theory and Measurement, N. Moray (Ed.), pages 101-114, Plenum Press 1979.

27. "Mental Workload: What is it? Why bother with it?", by Sheridan, T.; Bulletin of the Human Factors Society, Vol. 23, pages 1-2, Human Factors Society 1980.

28. "The Effect of Intervening Task Performance on Subjective Workload Ratings", by Eggemeier, T., Melville, B., and Crabtree, M.; Proceedings of the Human Factors Society 28th Annual Meeting, pages 954-958, Human Factors Society 1984.

29. "Causes of Dissociation Between Subjective Workload Measures and Performance: Caveats of the Use of Subjective Assessments", by Vidulich, M. and Wickens, C.D.; Applied Ergonomics, Vol. 17, pages 291-296, Elsevier Science, Ltd. 1986.

30. "Dissociation of Performance and Subjective Measures of Workload", by Yeh, Y.Y. and Wickens, C.D.; Human Factors, Vol.30, pages 111-120, Human Factors Society 1988.

31. "Development of the NASA TLX (Task Load Index)", by Hart, S.G. and Staveland, L.E., National Aeronautics and Space Administration, publication date 1987.

32. "Techniques of Subjective Workload Assessment: A Comparison of SWAT and NASA-Bipolar Methods", by Vindulich, M. and Tsang, P.; Ergonomics, Journal of the Ergonomics Society and the International Ergonomics Association, Vol. 29, pages 1385-1398, Taylor and Francis 1986.

33. "Development of the NASA-TLX (Task Load Index): Results of Empirical and Theoretical Research", by Hart, S. and Staveland, L.; *Human Mental Workload,* P. Hancock and N. Meshkati (Eds.), Elsevier 1988.

34. "Assessment of Pilot Performance and Workload in Rotary Wing Helicopters", by Sirevaag, E., Kramer, A., Wickens, C., Reisweber, M., Strayer, D. and Grenell, J.; Ergonomics, Journal of the Ergonomics Society and the International Ergonomics Association, Vol. 9, pages 1121-1140, Taylor and Francis 1993.

35. "Physiological Data Used to Measure Pilot Workload in Actual and Simulated Conditions", by Wilson, G., Purvis, B., Skelly, J., Fullenkamp, P. and Davis, I.; Proceedings of the Human Factors Society 31st Annual Meeting, Human Factors Society 1987.

36. "On the Act of Blinking", by Ponder, E. and Kennedy, W.; Quarterly Journal of Experimental Psychology, Vol. 18, pages 89-110, Taylor and Francis 1927.

37. "A Psycho-physiological Analysis of Multi-Task Processing Demands", by Sirevaag, E., Kramer, A.F., deJong, R., and Mecklinger, A.; Psychophysiology, Vol.. 25,. page 482, Cambridge University Press 1988.

38. "The Eyeblink and Workload Considerations", by Stern, J. and Skelly, J.; Proceedings of the Human Factors Society 8th Annual Meeting, Human Factors Society 1984.

39. "Blink Activity in a Discrimination Task as a Function of Stimulus Modality and Schedule of Presentation", by Goldstein, R., Walrath, L., Stern, J., and Strock, B.; Psychophysiology, Vol. 22, pages 629-635, Cambridge University Press 1985.

40. "Heliport VFR Airspace Design Based on Helicopter Performance", by McConkey, E.D., Anoll, R.K., Hawley, R.J., and Renton, M.B.; FAA/RD-90/4, Systems Control Technology, Inc. (SCT), August 1991.

41. "Heliport Visual Approach and Departure Airspace Tests," FAA/CT-TN87/40, Federal Aviation Administration, Atlantic City NJ, July 1989.

42. "Heliport Visual Approach Surface - High Temperature and High Altitude," FAA/CT-TN89/34, Federal Aviation Administration, Atlantic City NJ, May 1990.

43. "Analysis of Distributions of Visual Meteorological Conditions (VMC) Heliport Data," FAA/CT-TN89/67, Federal Aviation Administration, Atlantic City NJ, March 1990.

44. "Enter At Own Risk " by Keith Engelsman, Flight Safety Foundation: Helicopter Safety, Vol. 16, No. 5, Sep/Oct 1990, Reprint of an article originally published in the Australian CAA's Aviation Safety Digest.

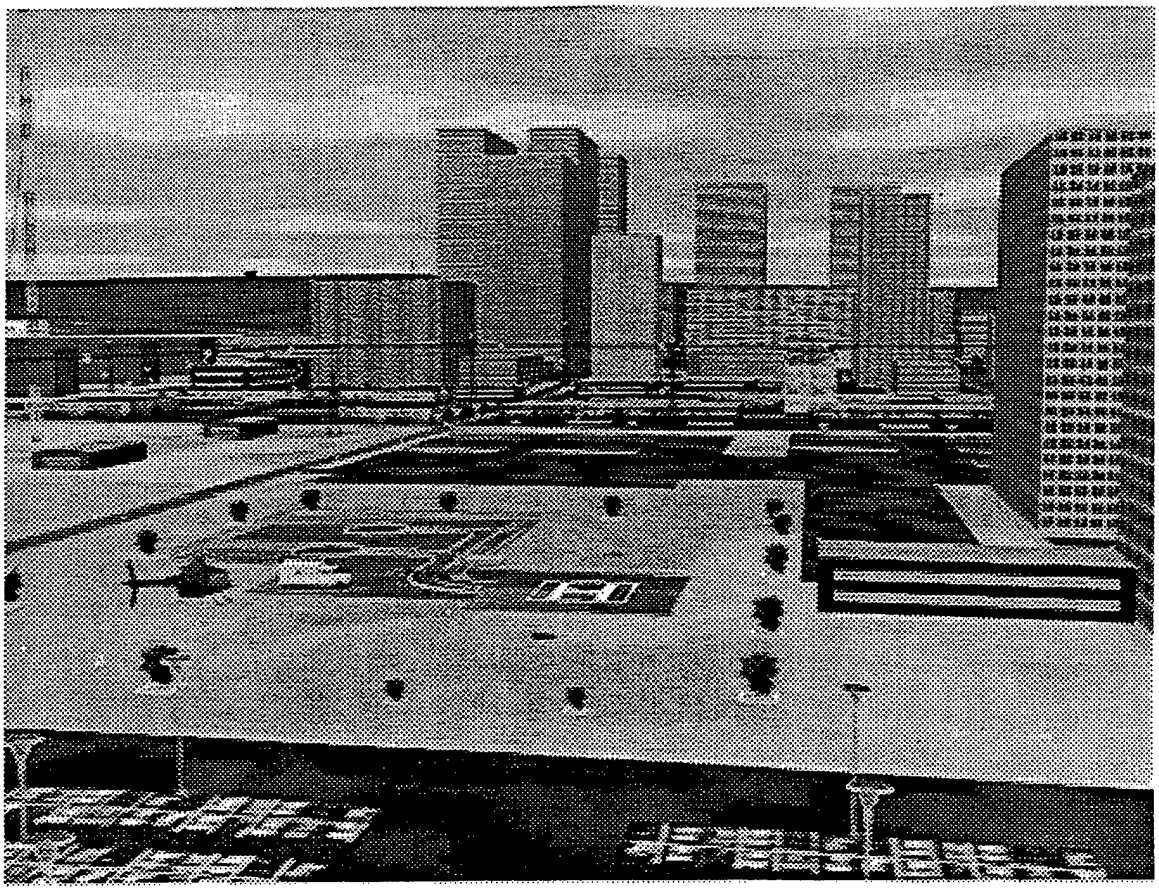

3080-163S

Appendix A

A.1 Overview

The visual database created for the obstacle-rich environment (ORE) experiment is the stimulus of primary interest to researchers. Reactions to obstacles encountered during approaches and departures were measured and analyzed. The visual database was constructed to meet the experimental test matrix requirements for both approach and departure by providing two approach and departure corridors, four lighting variations, and four obstacle density levels. Four variations in obstacle height/density (OH/D), or levels of threat, were created for departure; and three variations in OH/D were created for approach. Parametric variation of obstacle density was achieved by manipulating four distinct scene elements. The four elements were close-in obstacles, perimeter obstacles, occupied space variation, and major building height. Additional variations were incorporated to determine the effects of heliport lighting features.

A.1.1 Flight Corridor

For both the approach and departure cases two flight corridors were created, leading to/from a common heliport in a prototype city-center. Each path offered a unique presentation of terrain and obstacle type. The two flight corridors were designated as the Valley and Metro approach/departure corridors, as depicted in the helicopter route chart shown in Figure A-1.

In general terms, the Valley approach initiated along a ridge line to the north and west of the city-center area, passed over a residential area, and into the prototype city-center. In terms of visual landmarks, the flight corridor followed a set of railroad tracks and then turned east at the microwave tower. Next, the flight corridor turned to the south over the drive-in theater, and proceeded to the city-center heliport. The final approach path passed direct-

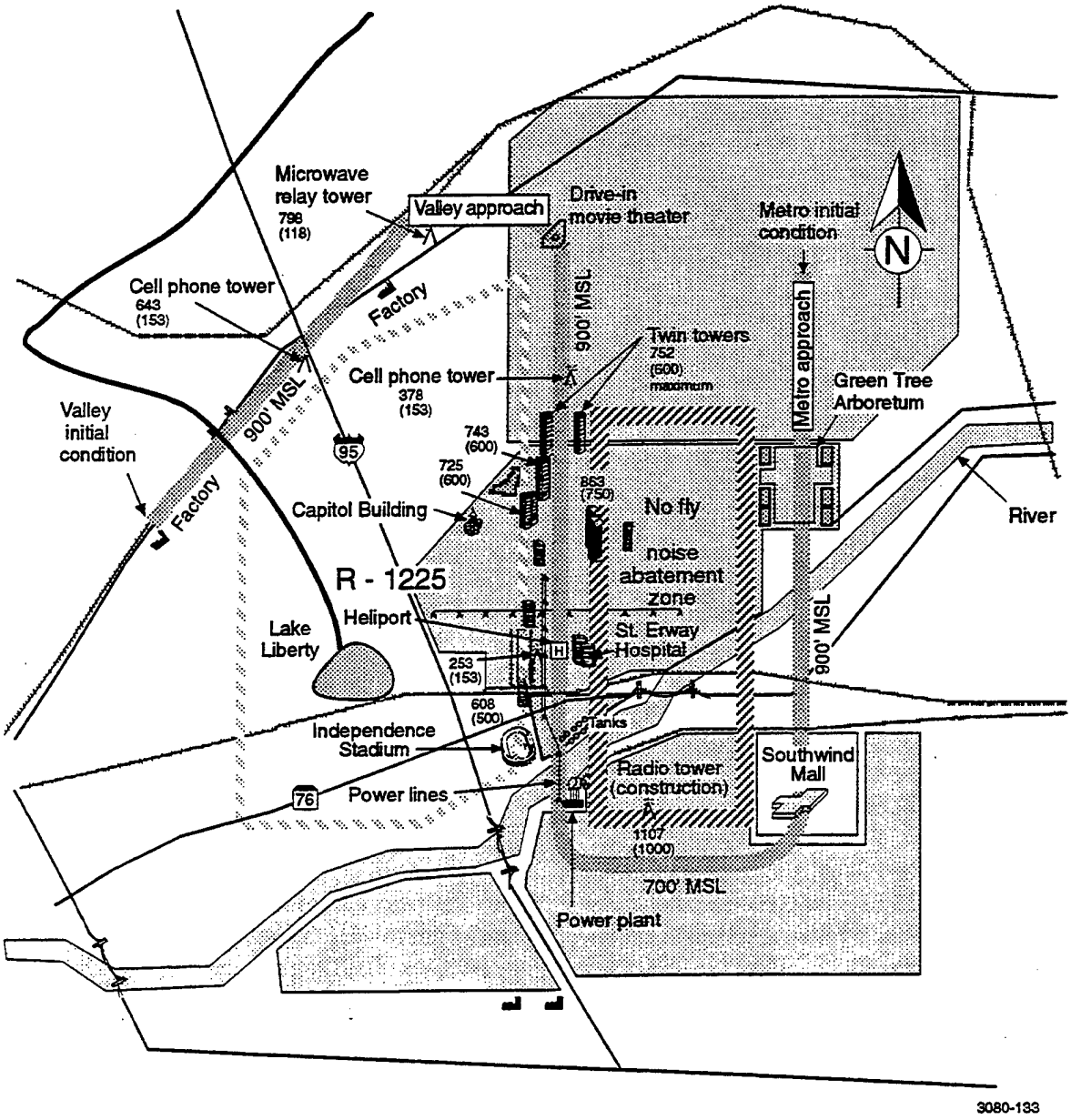

Figure A-1. ORE Helicopter Route Chart

ly over a pair of tall buildings (called the twin towers), the tops of which were located slightly above and beyond the north end of the visual flight rule (VFR) protected surface.

The Metro approach corridor initiated over a residential area, just to the north of the arboretum. The approach corridor passed over the arboretum and a residential area which included a Shopping Mall, turned west over the Shopping Mall, and then turned north to pass over the power lines (west of the power plant) for final approach to the city-center heliport. The Metro approach flightpath also included two passes over a river which cut through the prototype urban area.

Departures from the heliport flew outbound along the same flight corridors used in the approach cases. Departure runs were terminated once the aircraft had sufficiently cleared the obstacle environment of interest (i.e., to save simulation time, the pilot was not required to fly the entire distance to the initialization point of the Valley and Metro approach corridors).

A.1.2 Visibility

Visibility was maintained at two miles and the ceiling was set to 1,000-feet mean sea level (MSL). Heliport elevation was 100-feet MSL. To inject extraordinary conditions into the experiment thereby inducing pilot reaction, each pilot experienced two runs with reduced visibility. A single departure was conducted with the ceiling lowered to 500 feet, and a single approach was conducted during which the visibility was incrementally reduced to 0.3 miles. Changes in visibility were not announced to the pilot.

A.1.3 Time of Day/Lighting Variations

Time of day (TOD) variations are illustrated images taken from three different vantage points. All images show an oblique view of the city environment looking towards the northeast. The first series of images were taken from vantage point A, showing the southern portion of the VFR corridor (with respect to the heliport and VFR protected surface), as shown in Figure A-2. The rendering of day, dusk, and night conditions is shown in Figures A-3, A-4, and A-5, respectively. The next series of images (taken from vantage point B) shows the heliport/hospital area in Figures A-6, A-7, and A-8 in day, dusk, and night conditions, respectively. Likewise Figures A-9, A-10, and A-11 (taken from vantage point C) show day, dusk, and night conditions, respectively, for the northern portion of the VFR corridor. Figures A-5, A-8, and A-11 show the added illumination of the helicopter landing light.

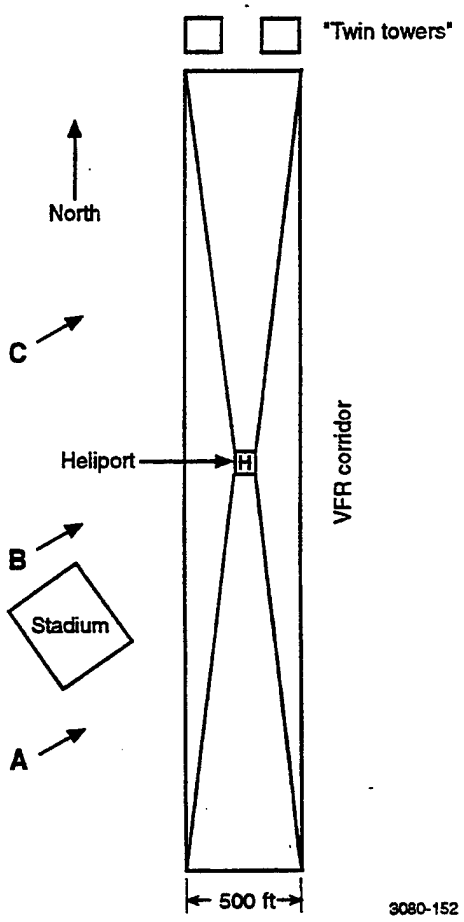

Figure A-2. Vantage Points of Oblique City Images in Relation to VFR Corridor

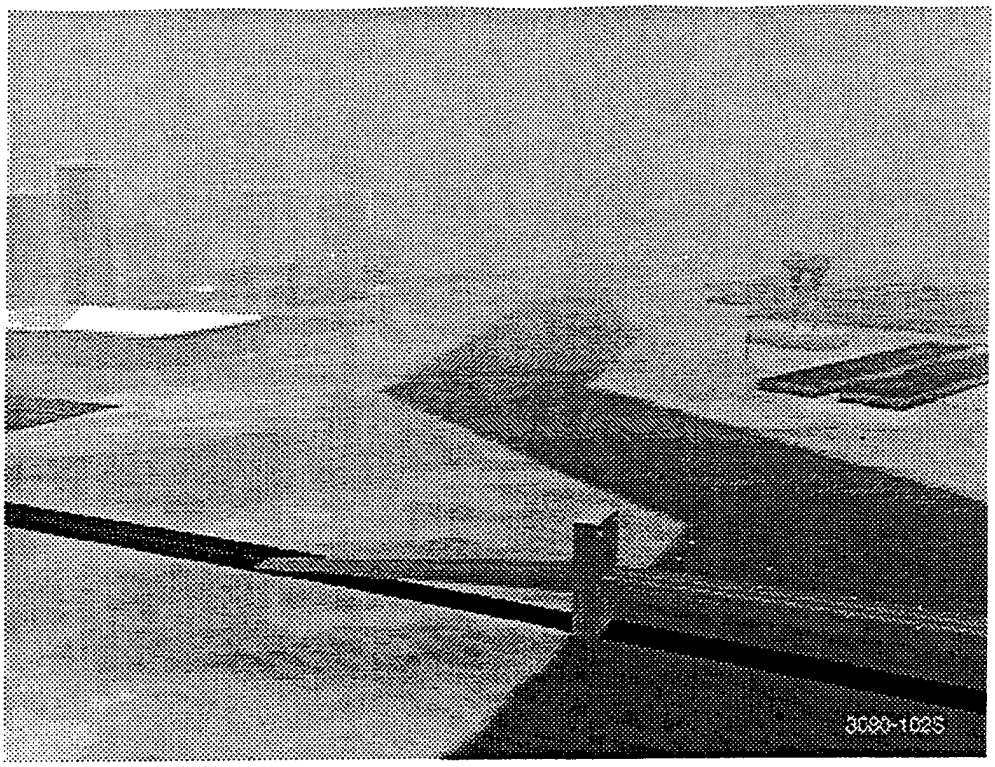

Figure A-3. Area South of Helipad During Day, Viewed Looking Northeast in High Obstacle Density

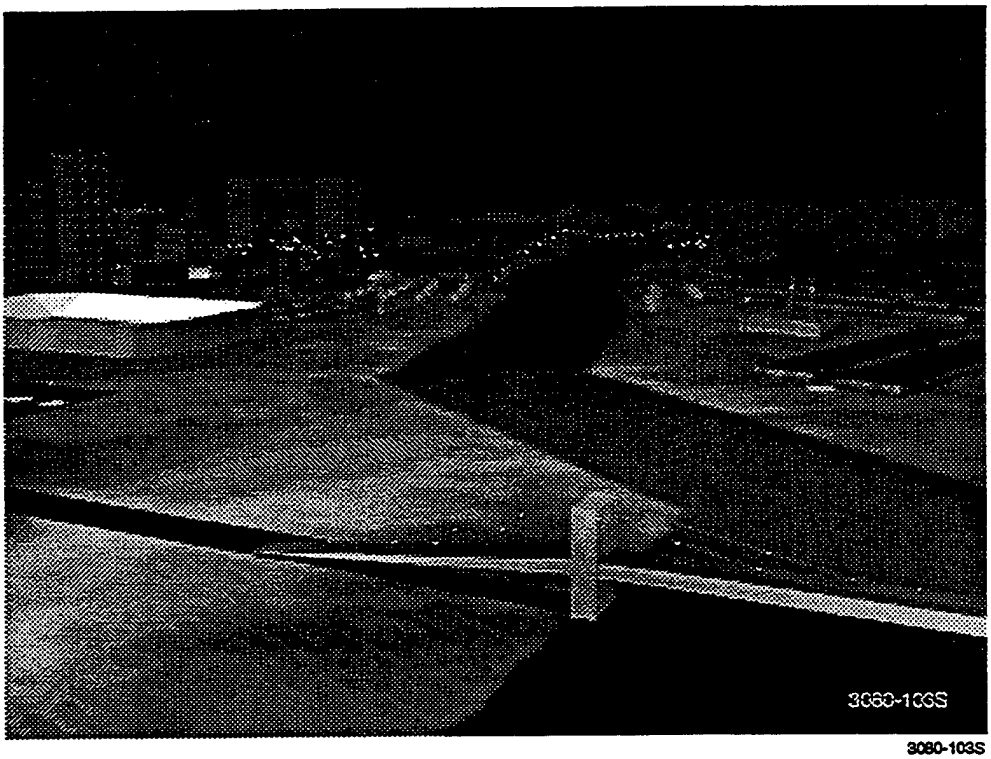

Figure A-4. Area South of Helipad at Dusk, Viewed Looking Northeast in High Obstacle Density

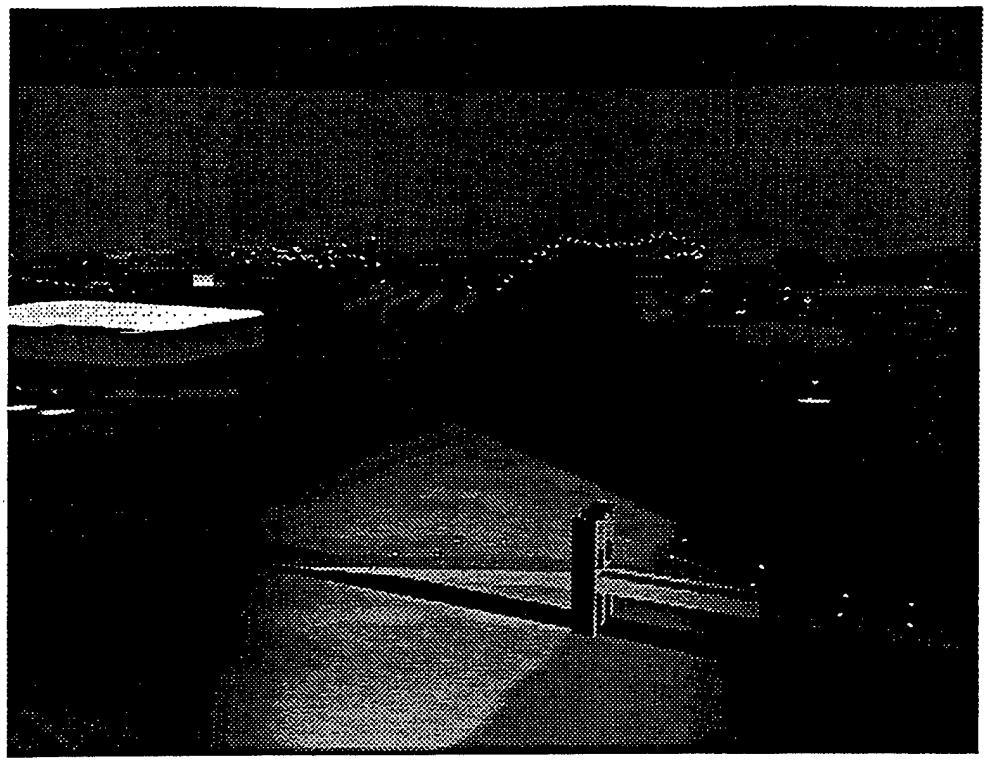

3080-114S

Figure A-5. Area South of Helipad at Night, Viewed Looking Northeast in High Obstacle Density

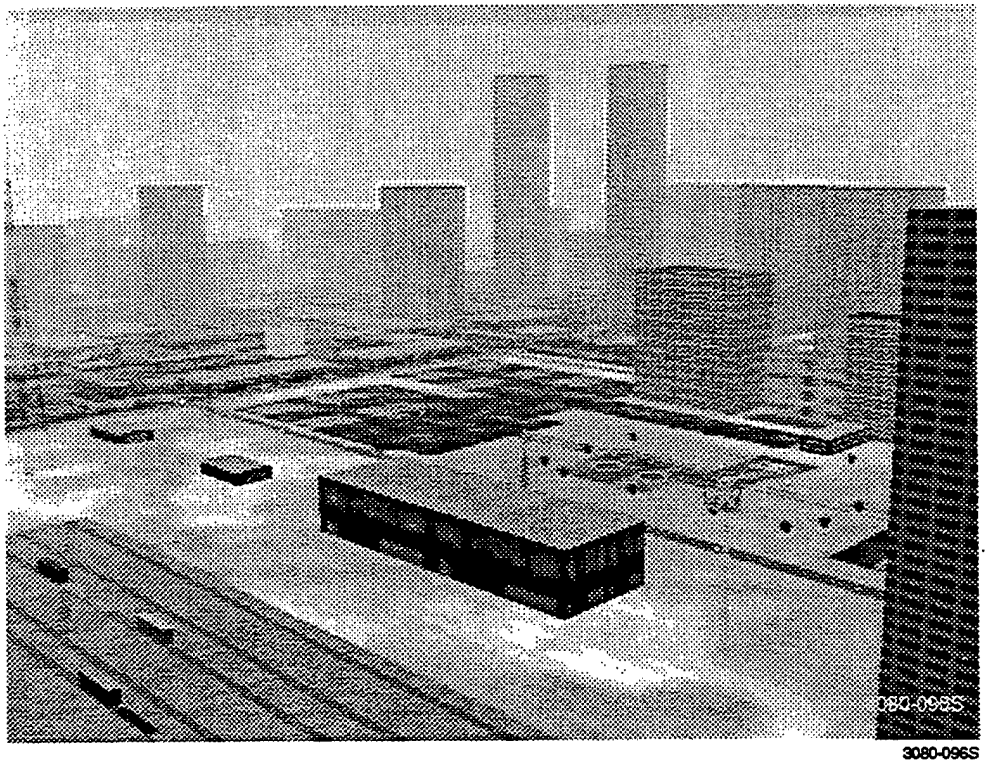

3080-096S

Figure A-6. Helipad Area During Day, Viewed Looking Northeast in High Obstacle Density

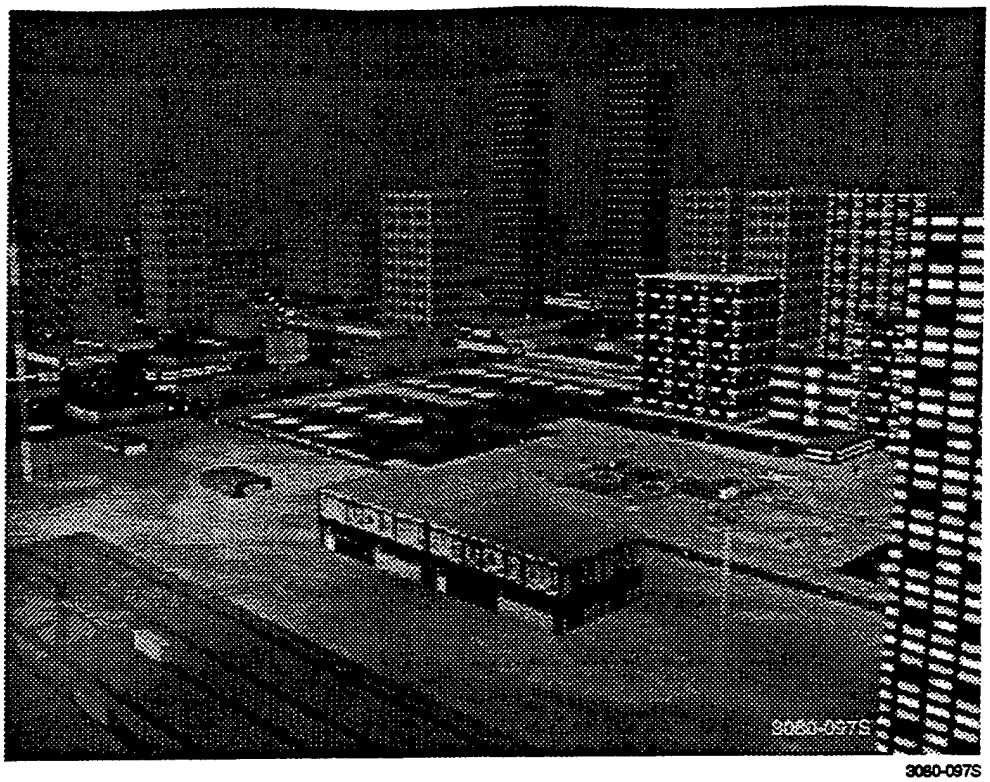

Figure A-7. Helipad Area at Dusk, Viewed Looking Northeast in High Obstacle Density

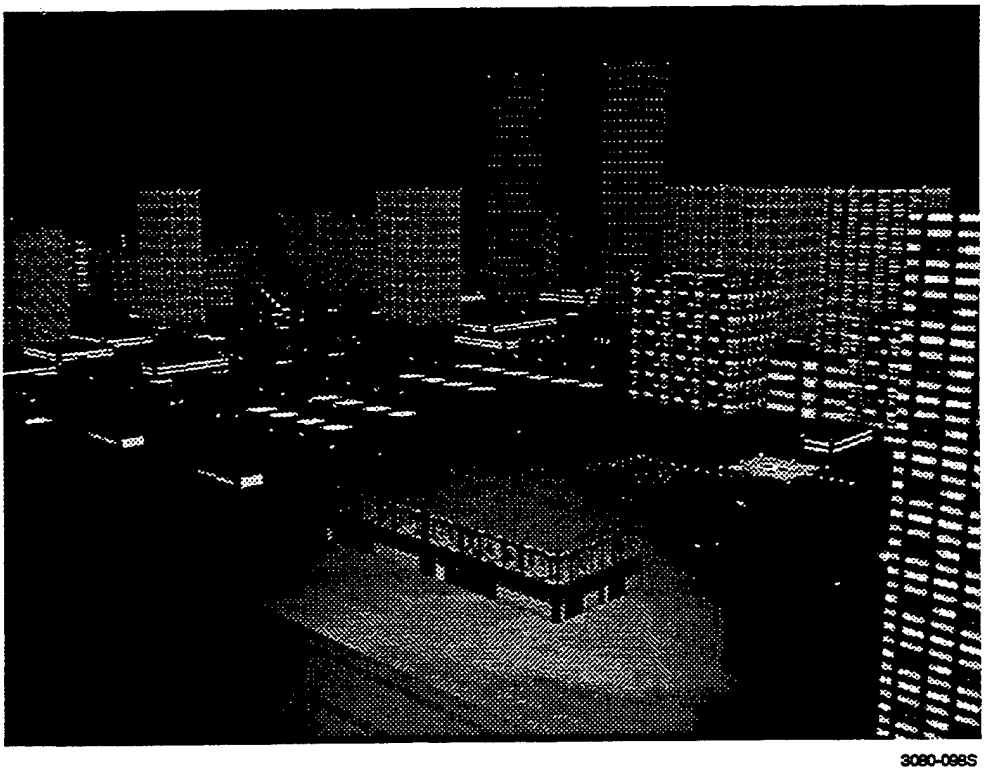

Figure A-8. Helipad Area at Night, Viewed Looking Northeast in High Obstacle Density

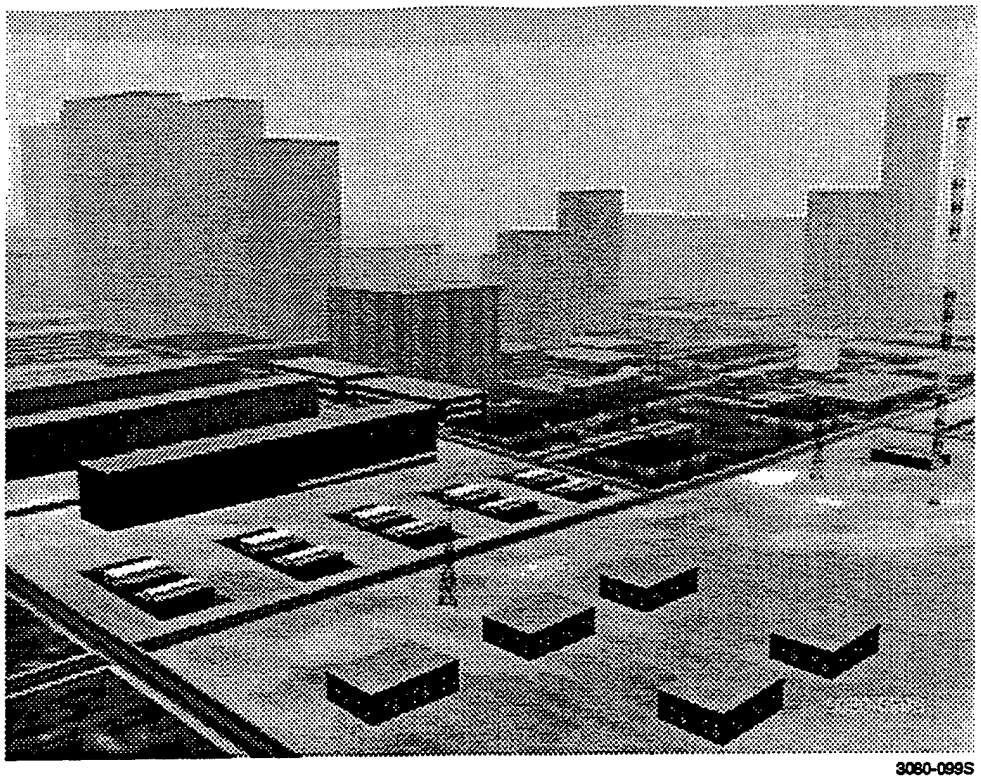

3080-099S

Figure A-9. Area North of Helipad During Day, Viewed Looking Northeast in High Obstacle Density

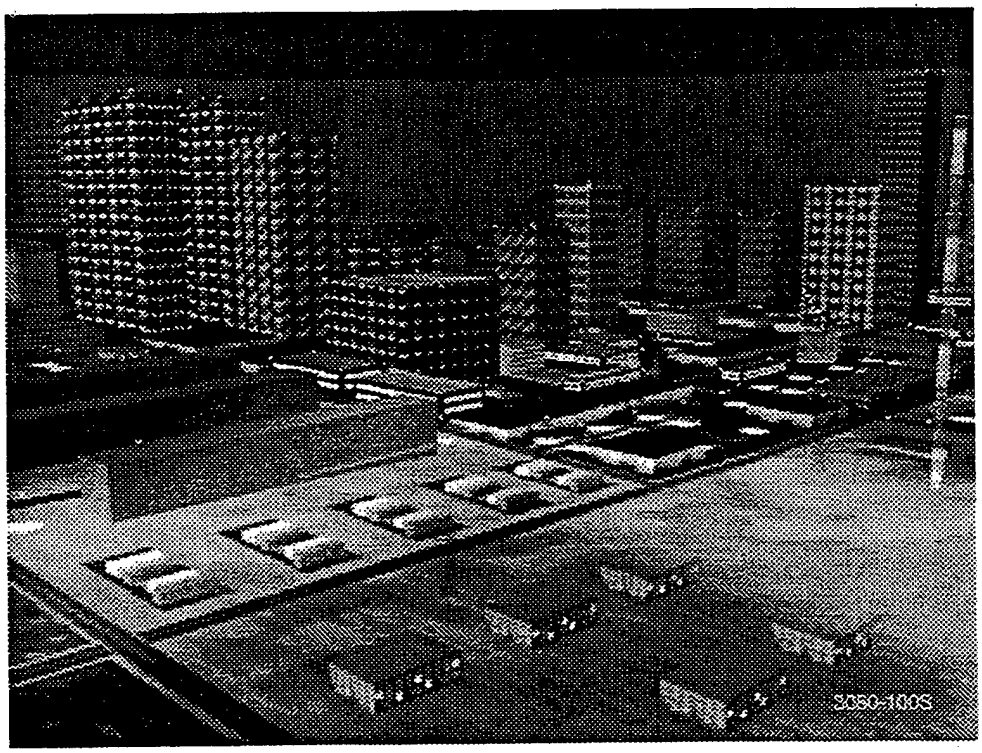

3080-100S

Figure A-10. Area North of Helipad at Dusk, Viewed Looking Northeast in High Obstacle Density

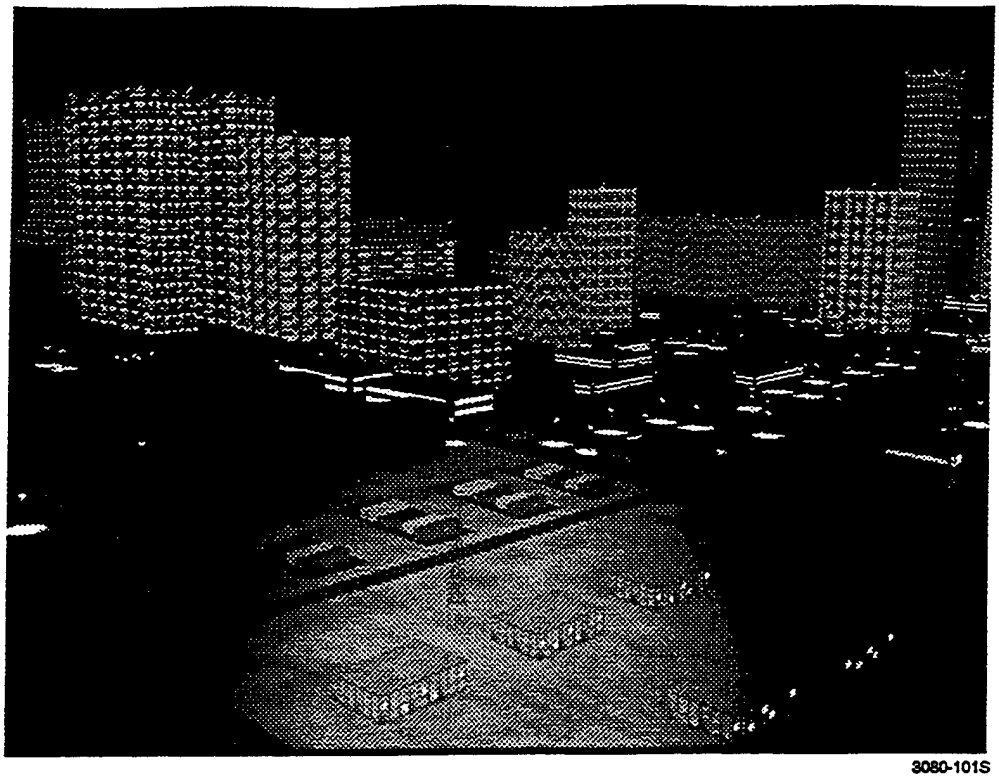

3080-101S

Figure A-11. Area North of Helipad at Night, Viewed Looking Northeast in High Obstacle Density

The approach cases included four variations in TOD and heliport lighting in the ORE experiment:

- Day.
- Dusk.
- Night with baseline heliport lighting.
- Night with an enhanced heliport lighting configuration.

The baseline heliport lighting configuration was defined as a combination of yellow lights that outlined the final approach takeoff area (FATO), an illuminated wind cone, and a taxiway marked with green centerline lights and blue edge lights. The enhanced lighting configuration incorporated the baseline configuration elements and added landing direction lights, a visual glide path indicator, a heliport identification beacon, and illumination of the heliport by means of "floodlights." With the exception of the heliport identification beacon (located atop a nearby building), the lighting variations are illustrated for the heliport scene in a series of images depicted in Figures A-12 through A-15 (these images show the heliport as it would be viewed looking north on the Metro approach path). They show the heliport scene lighting variation for day (Figure A-12), dusk (Figure A-13), night with baseline lighting (Figure A-14), and night with enhanced lighting (Figure A-15). The dusk and night images also show the effect of a helicopter landing light on the ground illumination.

For the departure cases, three variations in TOD and heliport lighting were presented: day, dusk, and night with baseline heliport lighting. The fourth TOD/lighting condition, the (enhanced heliport lighting) configuration was not used for the departure runs since the approach lighting aids were not used for departures.

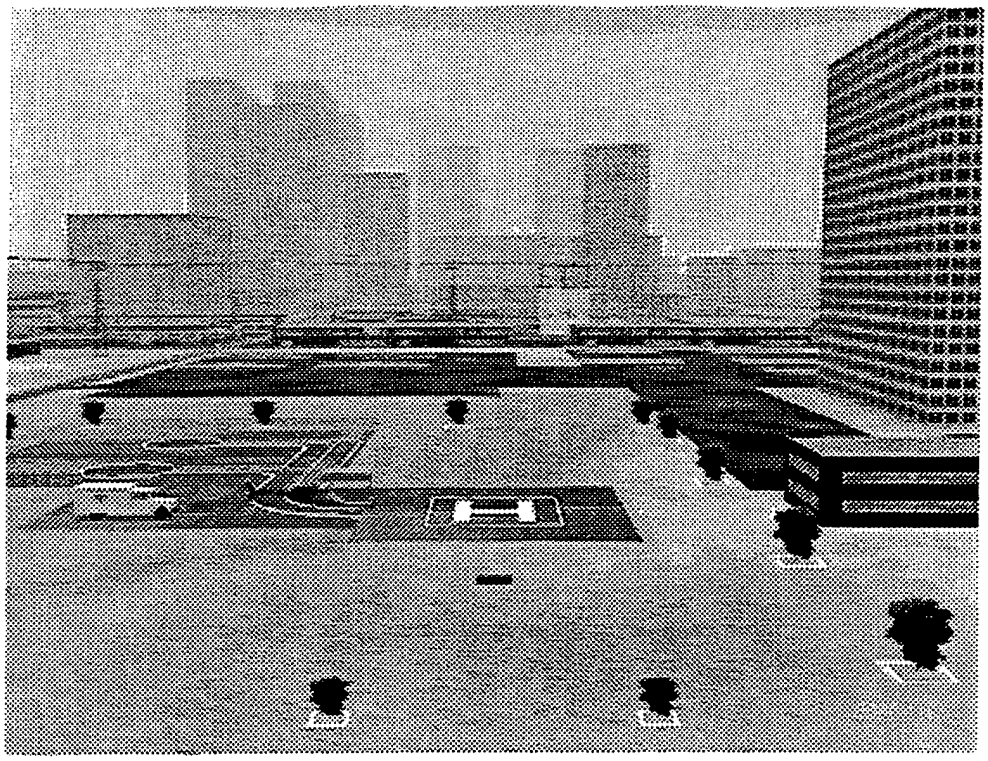

3080-119S

Figure A-12. Helipad During Day, Viewed Looking North in High Obstacle Density

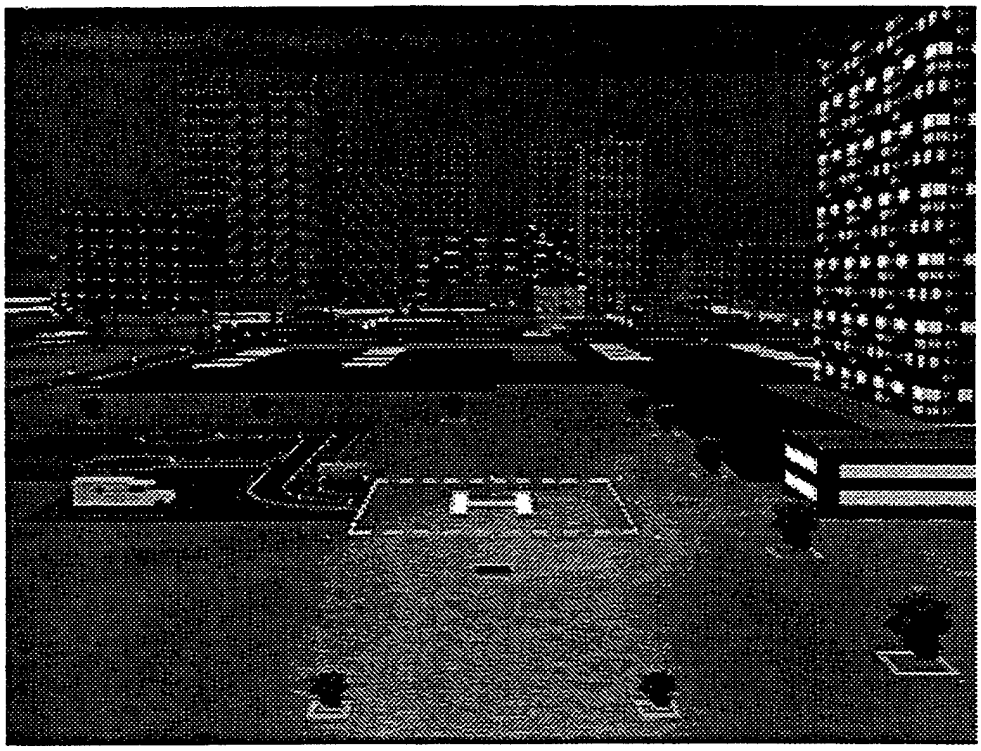

3080-120S

Figure. A-13. Helipad at Dusk, Viewed Looking North in High Obstacle Density

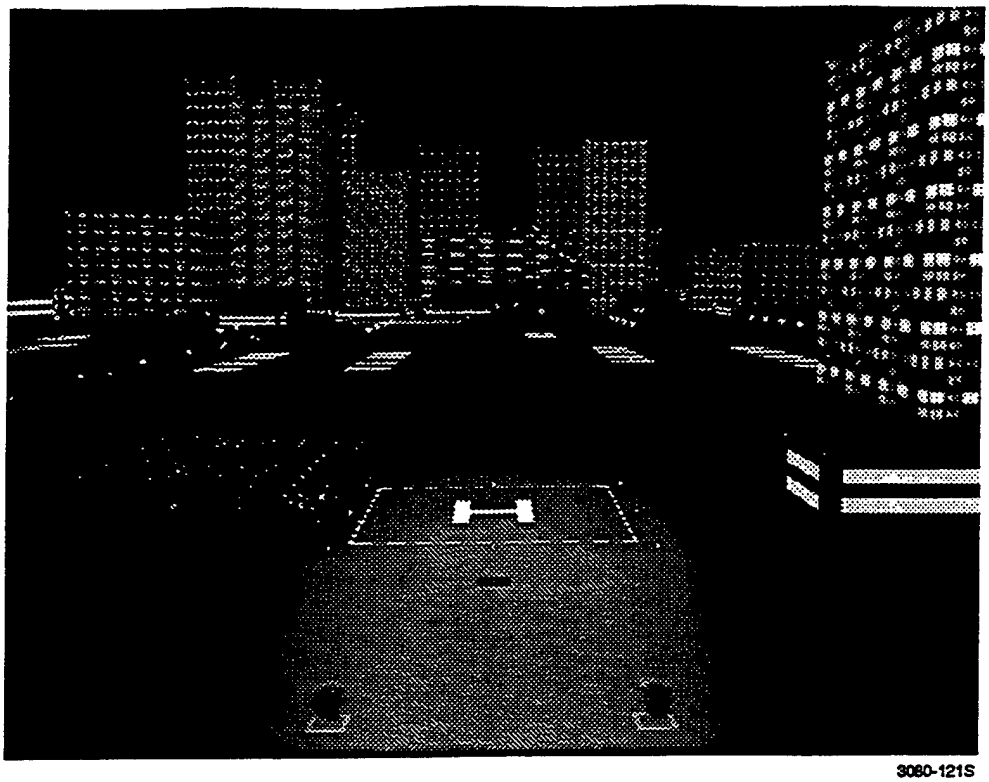

3080-121S

Figure A-14. Helipad at Night, With Baseline Lighting System, Viewed Looking North in High Obstacle Density

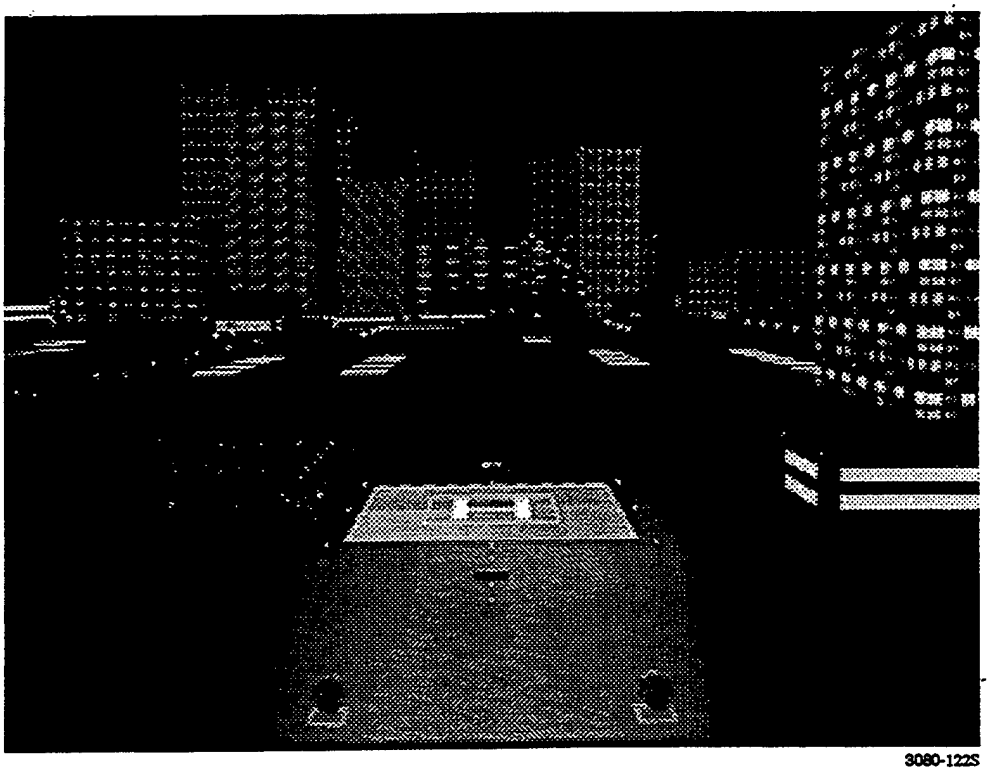

3080-122S

Figure A-15. Helipad at Night, With Enhanced Lighting System, Viewed Looking North in High Obstacle Density

A.1.4 Obstacle Height/Density

In addition to lighting variations, the visual scene OH/D was also varied. Since there was no objective data to quantify OH/D as perceived by the pilot, arbitrary guidelines were developed to define discrete threat levels. These guidelines were then used to develop visual databases corresponding to the different OH/D levels. For the approach cases, three OH/D levels were presented for each approach corridor. The three OH/D levels have been termed as low, medium, and high. For the departure cases, four levels of OH/D were presented for each departure corridor. The four OH/D levels for the departure cases have been termed as very low, low, medium, and high.

Different levels of OH/D were created by varying obstacle height, density, type, and position to discretely change the "level of perceived obstacle threat." This was accomplished by adding or deleting obstacles (i.e. buildings) in the database, as well as by increasing/decreasing the height of selected obstacles near the intended flightpath. Manipulation of obstacles was concentrated in the city-center environment with emphasis on the vicinity of the heliport. Some attention was given to obstacles beyond the boundaries of the VFR protected surface (4,000 feet from heliport). Without knowing what effects these changes would cause, arbitrary variations in scene content could not be assumed to create uniform increments in OH/D between different threat levels.

A.1.4.1 Obstacle Density/Threat Parameterization

OH/D was parameterized by varying four elements of the city-center environment: close-in obstacles, perimeter obstacles, occupied space variation, and height variation of major buildings. Table A-1 presents a summary of the OH/D guidelines for the construction of the visual database.

Close-in obstacles were defined as obstacles on and/or in the immediate heliport vicinity. Perimeter obstacles were defined as obstacles close to the flightpath. During database construction it was anticipated that pilots may perceive these obstacles as either a threat or a positional reference. Obstacles were arbitrarily assigned to these categories to generate a heliport environment that incrementally increased OH/D from the very low to high-density scenario (Table A-1).

Scene content for the different OH/D levels was also modified by variation of the height of thirteen major buildings. As shown in the third column of Table A-1, their height was varied as a percentage of the height in the high-density scenario, which was defined as 100 percent.

The last parameter of OH/D was the variation of occupied space, defined as the percentage of ground area (exclusive of roads and major buildings) that contained some obstacle. Again, this variation was confined to the city-center area of the database. It was anticipated that this variation would have greater effect on pilots during departure, when pilots may be scanning the environment for alternate landing zones.

The best way to view the database is from the pilot's seat of the simulator cab. Without that opportunity, the reader is encouraged to look at the following images illustrating the differences in OH/D. The images were generated by the E&S ESIG 3000 using different ORE databases.

Each series of images presents the OH/D variation for a single location along the intended flightpath. The positions chosen are arbitrary and do not correspond to a particular pilot's flightpath. The view is oriented along the flightpath. It should be noted, however, that several obstacles were clearly visible to the pilot only from the side windows. As such the images shown here do not show the complete variation in obstacles that the pilot experienced. The intent here is to show an aggregate OH/D variation.

The figure title indicates the visual database position from which the image was taken relative to the heliport. All of the following images were generated for day conditions with a two nautical mile visibility and 1,000 foot ceiling. Note that since the heliport was modeled at 100 feet MSL, an image taken 800 feet above the heliport would be at 900 feet MSL, or 100 feet below the cloud ceiling.

TABLE A1. GUIDELINES FOR THE DEVELOPMENT OF OBSTACLE HEIGHT/DENSITY VARIATIONS

Flight corridor	Obstacle height/ density	Ground coverage: Occupied ground space	Ground coverage: Open space %	Max bldg height (%)	Close-in critical obstacles	Perimeter critical obstacles
Valley	Very low (VL)	• 40% covered w/ 1 to 3 story bldgs	60	60	• Light poles • Bushes (9 foot)	•Cellular phone tower •Radio tower
	Low (L)	• 40% covered w/ 1 to 3 story bldgs • 20% covered w/ 4 to 6 story bldgs	40	60	• Helicopter on furthest adjacent pad • Service wires • Ambulance • Large sign •Light poles • Bushes (12 foot)	•Construction crane (boom oriented away from flightpath) •High-tension wires •Tall building
	Medium (M)	• 40% covered w/ 1 to 3 story bldgs • 20% covered w/ 4 to 6 story bldgs • 20% covered w/ 8 to 12 story bldgs	20	80	• Helicopter on closest adjacent pad • Service wires •Ambulance • Fuel truck • Light poles • Trees (15 foot)	•Construction crane (boom oriented into VFR surface) •High-tension wires •Tall building •Antenna on tall building
	High (H)	• 40% covered w/ 1 to 3 story bldgs • 20% covered w/ 4 to 6 story bldgs • 20% covered w/ 8 to 12 story bldgs • 20% covered w/ 16 to 24 story bldgs	0	100	• Helicopter on run-up spot • Service wires • Ambulance • Fuel truck • Light poles • Pedestrians • Trees (18 foot)	•High tension wire •Cellular phone tower •Two buildings within VFR protected surface •Antenna on tall building
Metro	Very low	• 40% covered w/ 1 to 3 story bldgs (VL)	60	60	• Service wires	•Smoke stacks •Small sign Bushes (9 foot)
	Low (L)	• 40% covered w/ 1 to 3 story bldgs • 20% covered w/ 4 to 6 story bldgs	40	60	• Helicopter on furthest adjacent pad • Service wires • Light poles • Ambulance • Hospital wing (close) • Bushes (12 foot)	•Smoke stacks •Wheeled crane •Billboard •Water tower
	Medium (M)	• 40% covered w/ 1 to 3 story bldgs • 20% covered w/ 4 to 6 story bldgs • 20% covered w/ 8 to 12 story bldgs	20	80	• Helicopter on closest adjacent pad • Service wires • Light poles • Ambulance • Hospital wing (close) • Pedestrians • Trees (15 foot)	•Smoke stacks •Wheeled crane •Billboard •Water tower •Cellular phone tower •Wharf crane
	High (H)	• 40% covered w/ 1 to 3 story bldgs • 20% covered w/ 4 to 6 story bldgs • 20% covered w/ 8 to 12 story bldgs • 20% covered w/ 16 to 24 story bldgs	0	100	• Helicopter on run-up spot • Service wires • Light poles • Ambulance • Hospital wing (close) • Ground support equipment • Trees (18 foot)	•Smoke stacks •Wheeled crane •Billboard •Water tower •Cellular phone tower •Wharf crane •1,000 foot antenna

3080-162

A.1.5 Valley Approach

Figures A-16 through A-18 show OH/D variation for the final segment of the Valley approach. This series of images illustrates OH/D variation for a single position north of the twin towers facing south. The height variation of the "Twin Towers" and other buildings can clearly be seen in the OH/D variation. Figures A-19 through A-21 present the view proceeding through the approach as the flight profile crosses the "Twin Towers." Figures A-22 through A-24 show the view after having crossed the VFR corridor threshold where a pilot might be expected to initiate a descent. Figures A-25 through A-27 show a midpoint of the descent. Figures A-28 through A-30 show the view entering the heliport area.

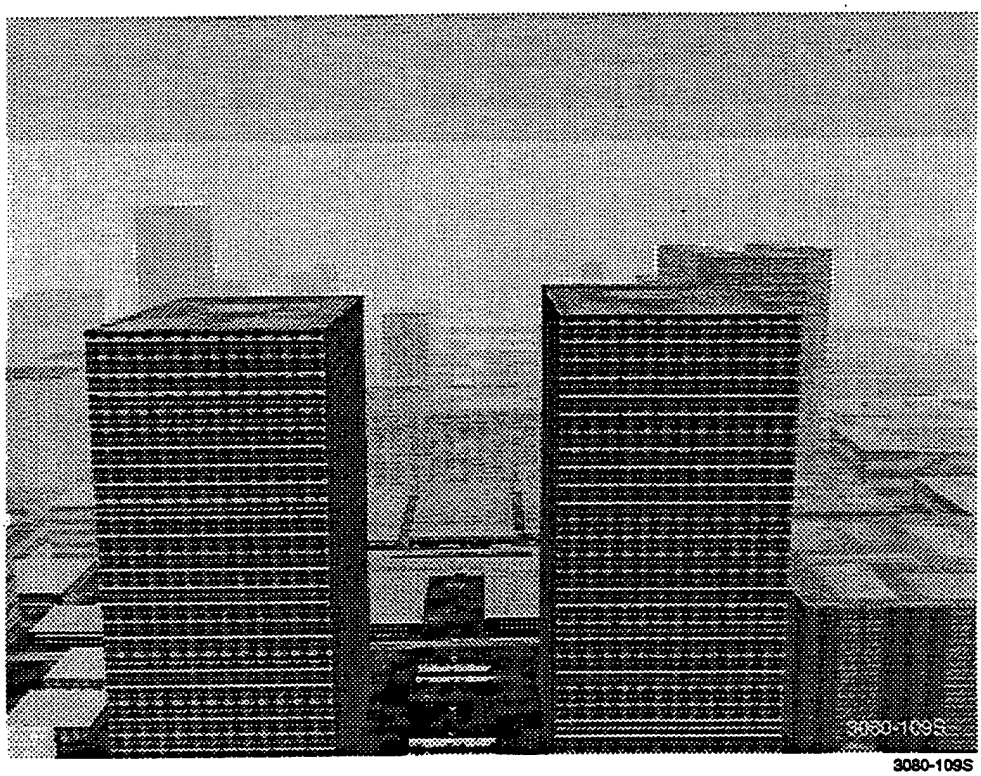

Figure A-16. Arrival From the North, 800' Above Helipad, 6,000' North of Helipad, High Obstacle Density

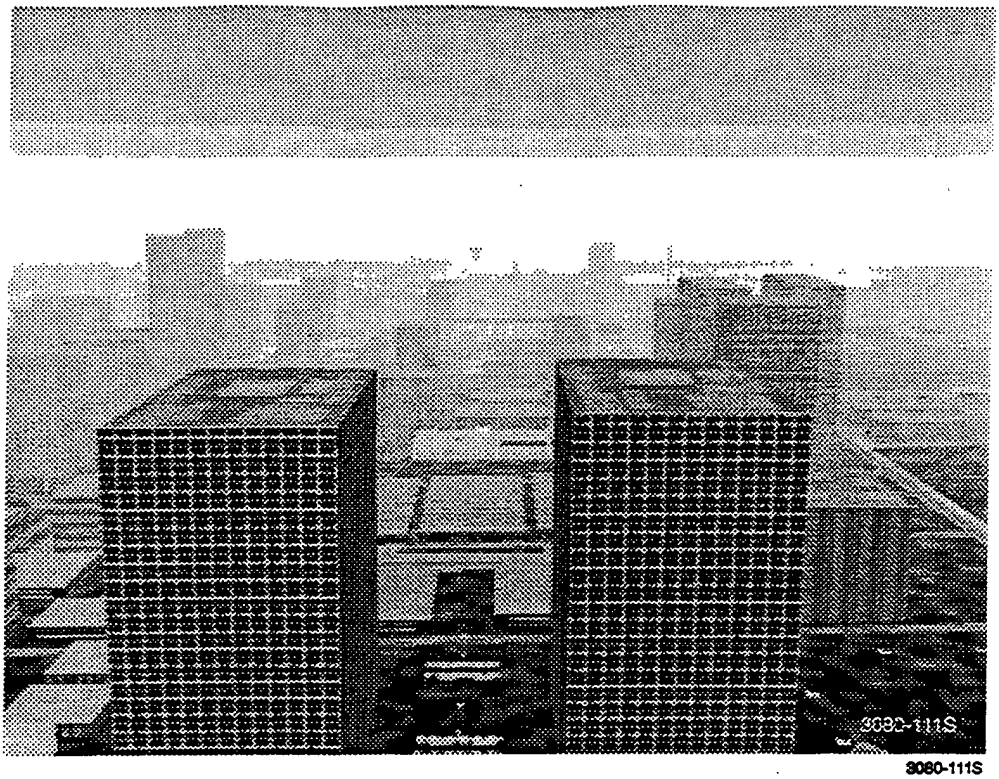

3080-111S

Figure A-17. Arrival From the North, 800' Above Helipad, 6,000' North of Helipad, Medium Obstacle Density

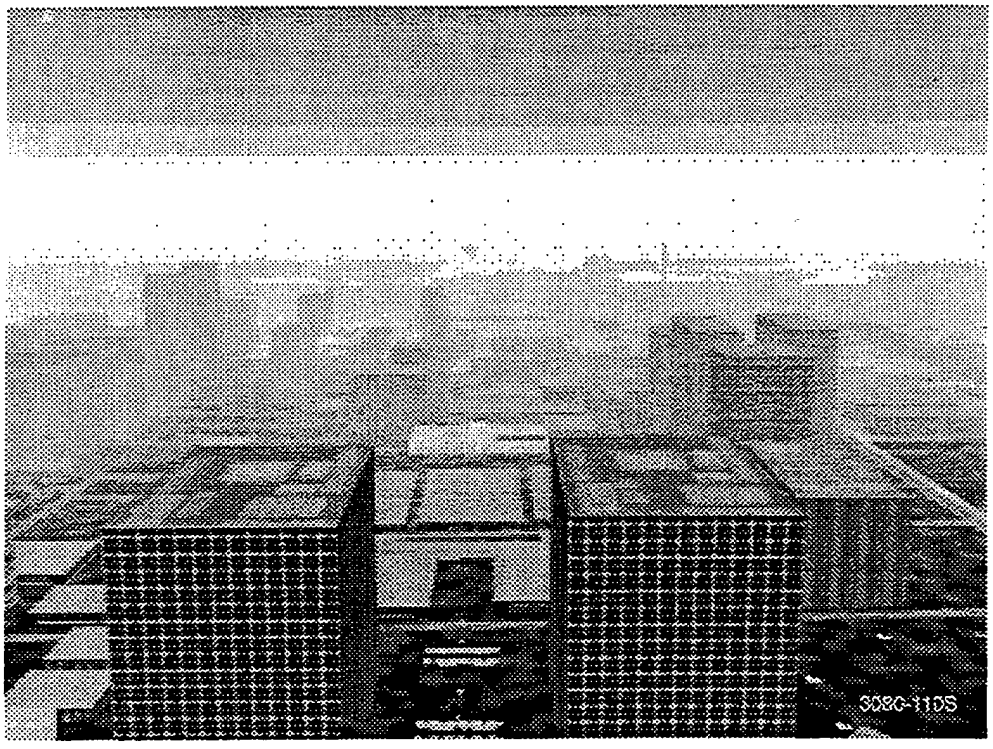

3080-110S

Figure A-18. Arrival From the North, 800' Above Helipad, 6,000' North of Helipad, Low Obstacle Density

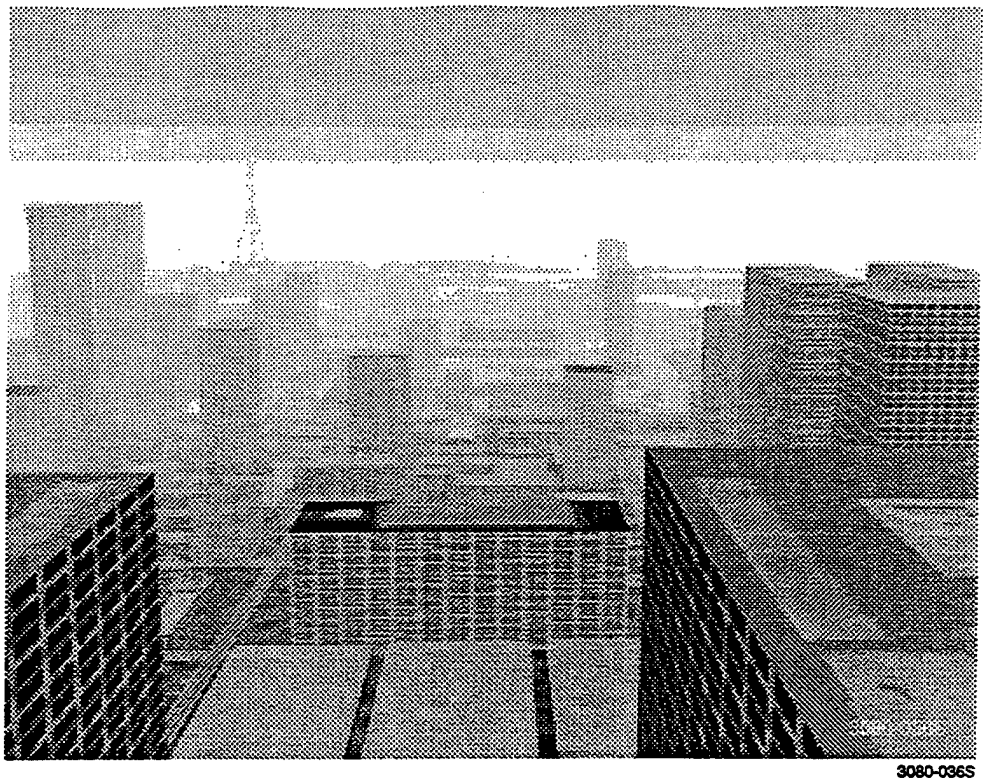

3080-036S

Figure A-19. Arrival From the North, 800' Above Helipad, 5,000' North of Helipad, High Obstacle Density

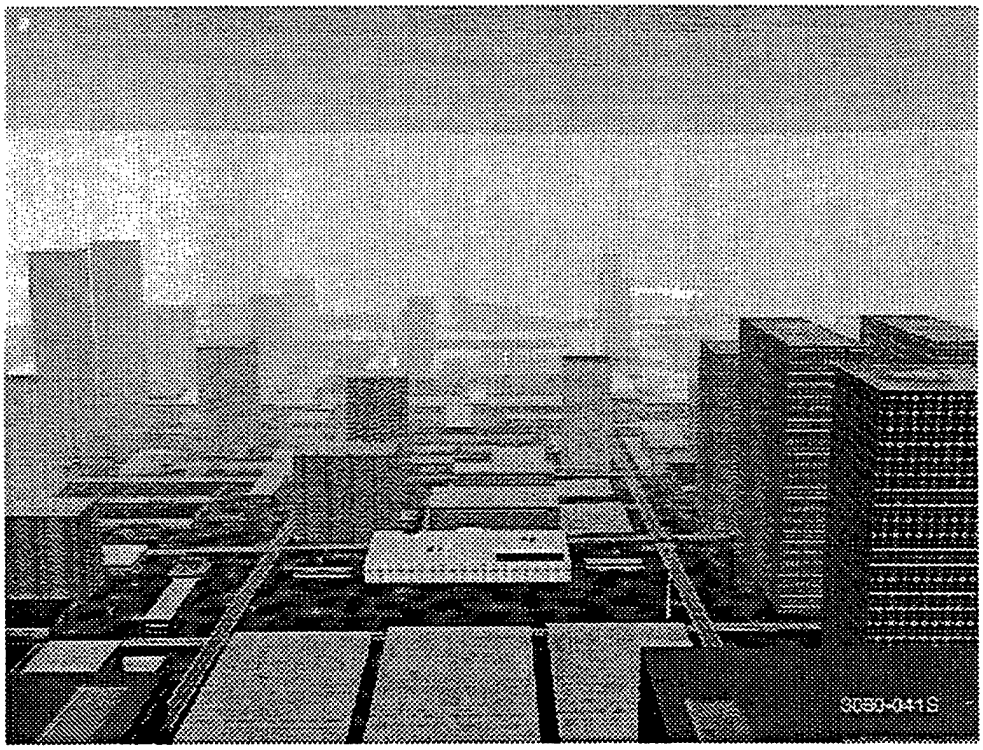

3080-041S

Figure A-20. Arrival From the North, 800' Above Helipad, 5,000' North of Helipad, Medium Obstacle Density

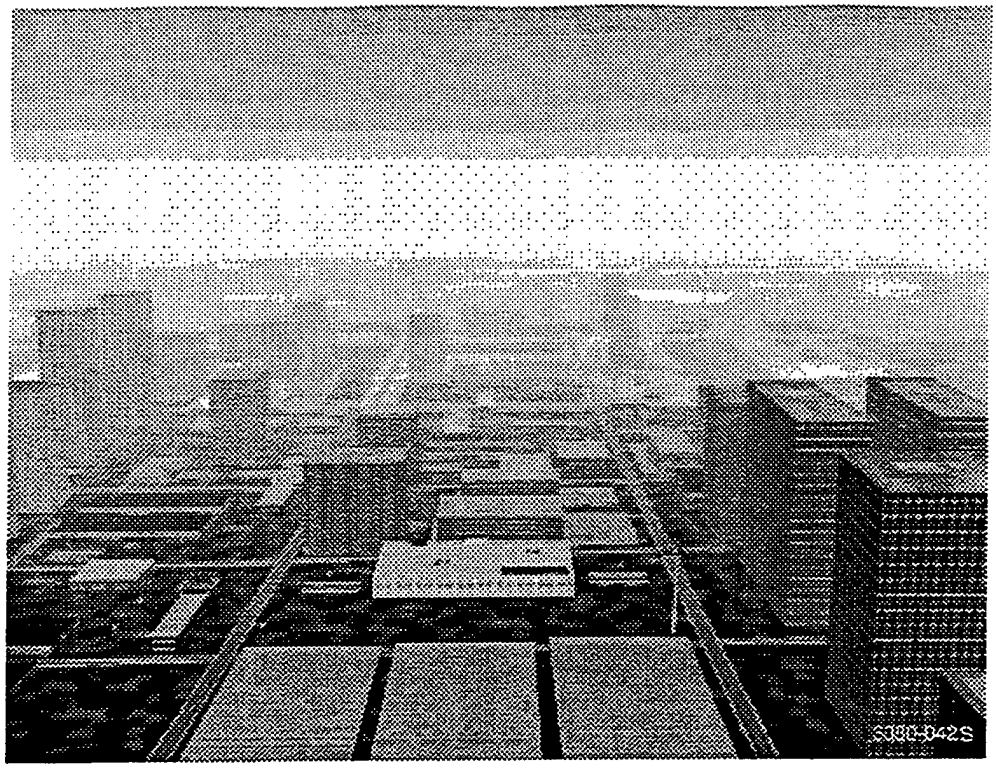

3080-042S

Figure A-21. Arrival From the North, 800' Above Helipad, 5,000' North of Helipad, Low Obstacle Density

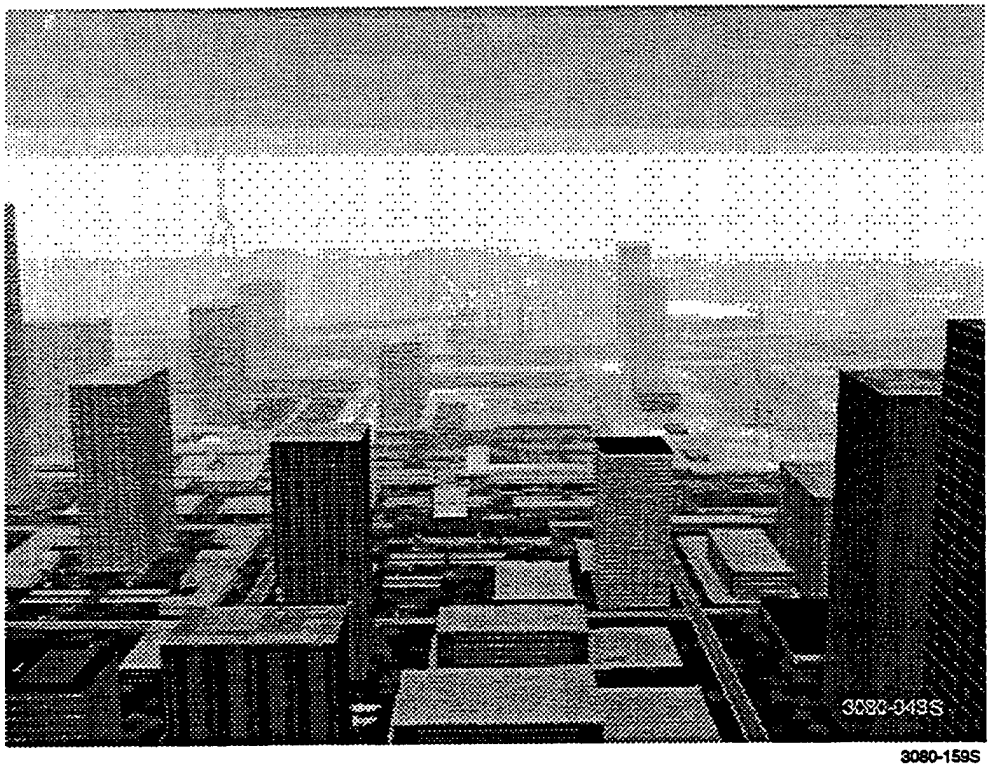

3080-159S

Figure A-22. Arrival From the North, 800' Above Helipad, 4,000' North of Helipad, High Obstacle Density (Valley Approach)

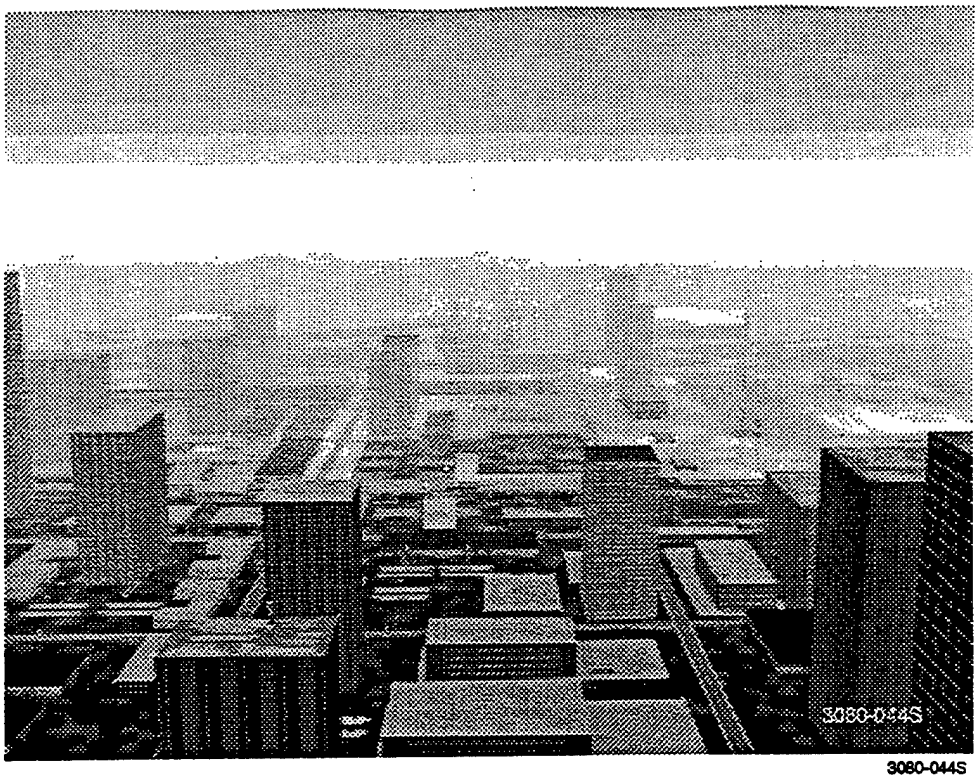

3080-044S

Figure A-23. Arrival From the North, 800' Above Helipad, 4,000' North of Helipad, Medium Obstacle Density

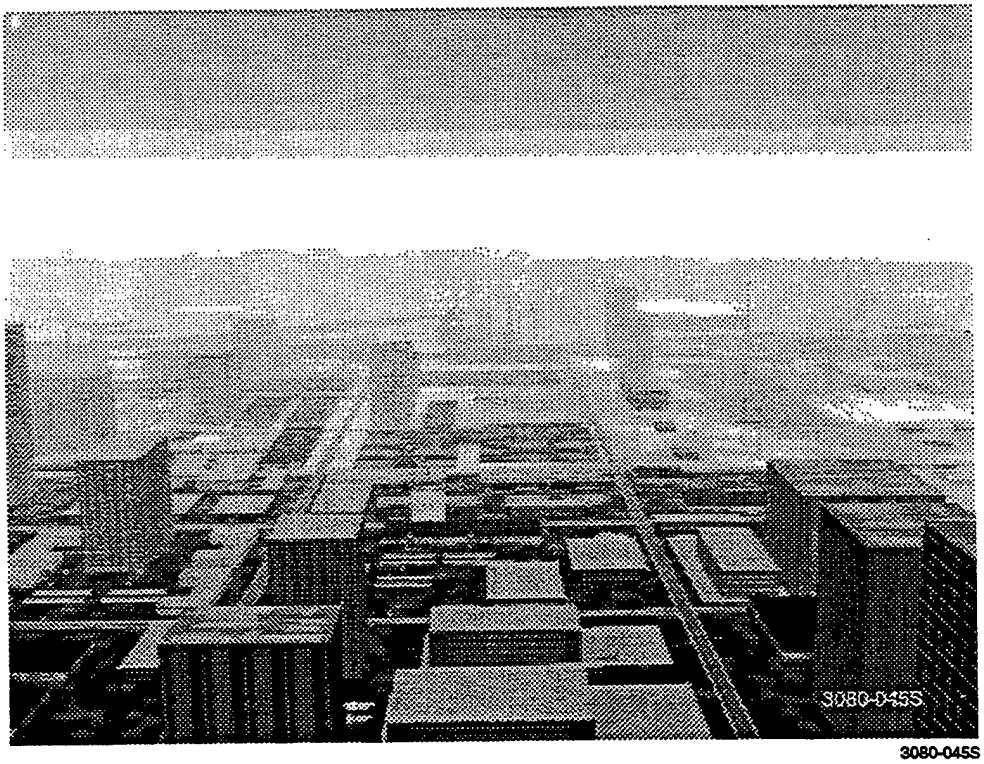

3080-045S

Figure A-24. Arrival From the North, 800' Above Helipad, 4,000' North of Helipad, Low Obstacle Density

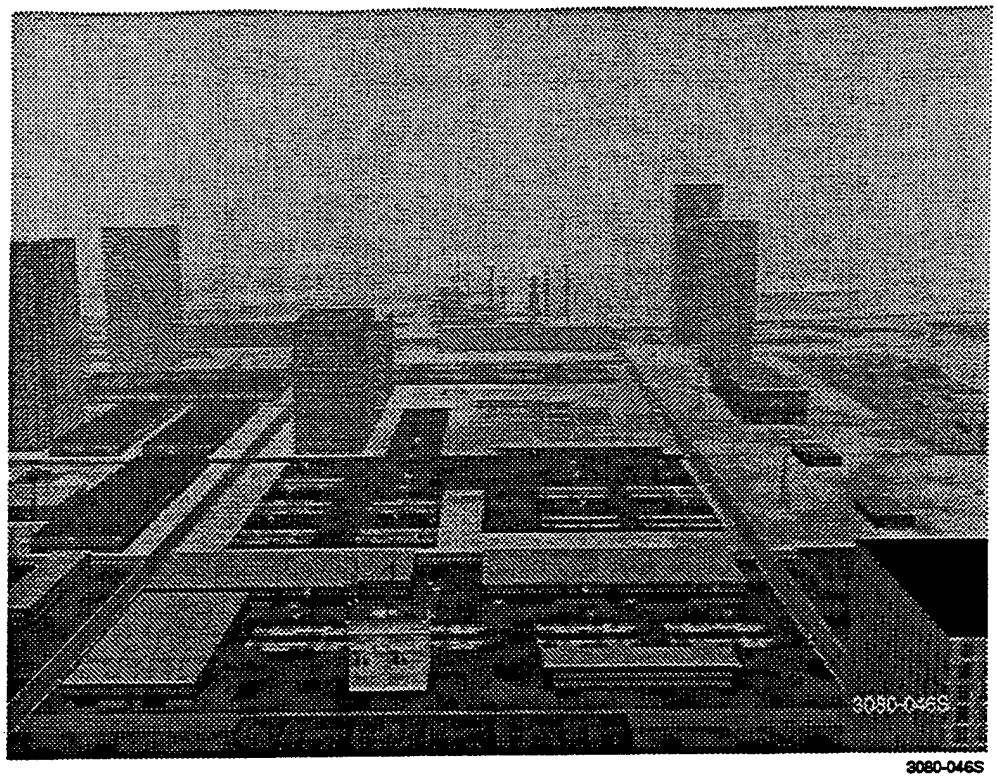

3080-046S

Figure A-25. Arrival From the North, 500' Above Helipad, 2,500' North of Helipad, High Obstacle Density

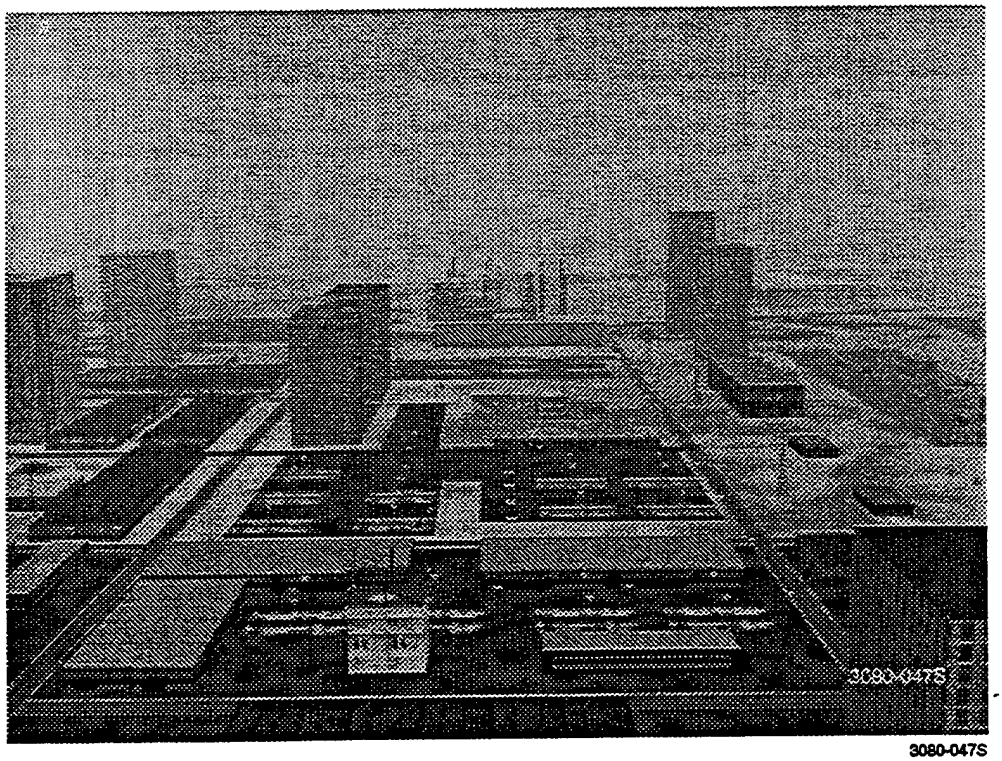

3080-047S

Figure A-26. Arrival From the North, 500' Above Helipad, 2,500' North of Helipad, Medium Obstacle Density

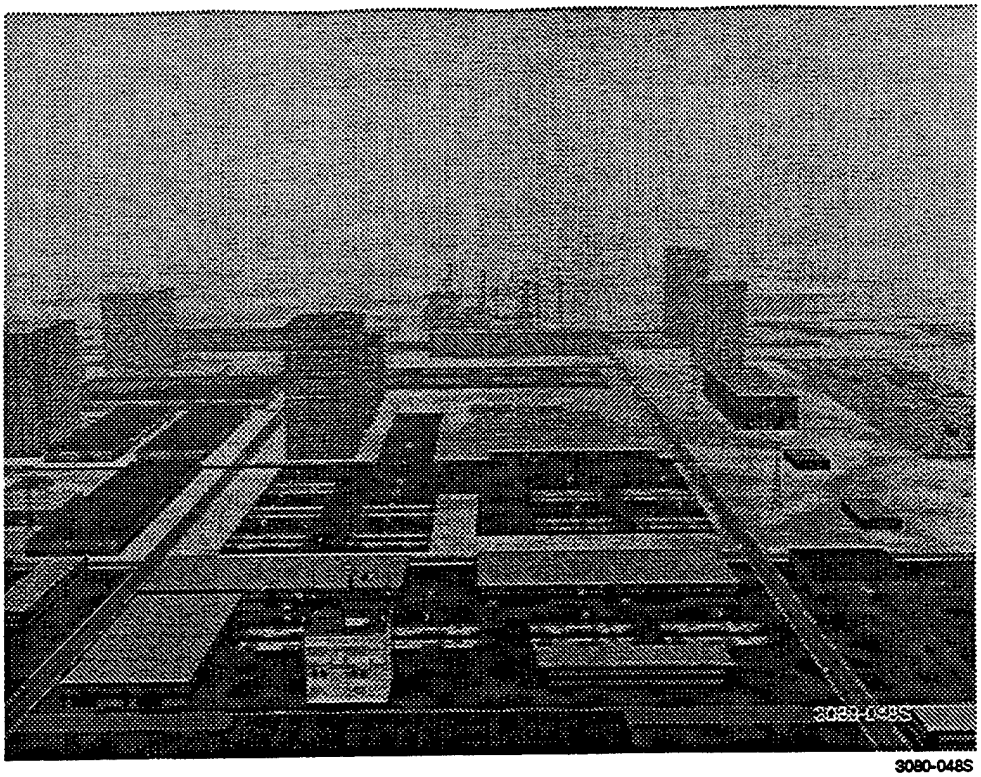

3080-048S

Figure A-27. Arrival From the North, 500' Above Helipad, 2,500' North of Helipad, Low Obstacle Density

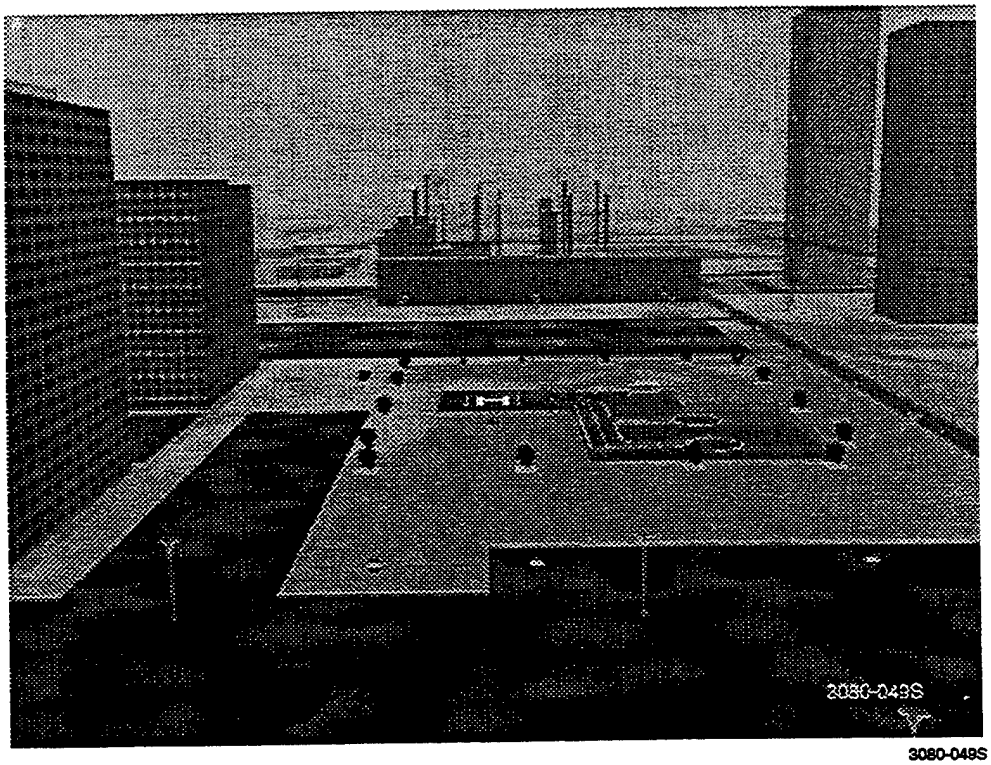

3080-049S

Figure A-28. Arrival From the North, 200' North of Helipad, 1,000' North of Helipad, High Obstacle Density

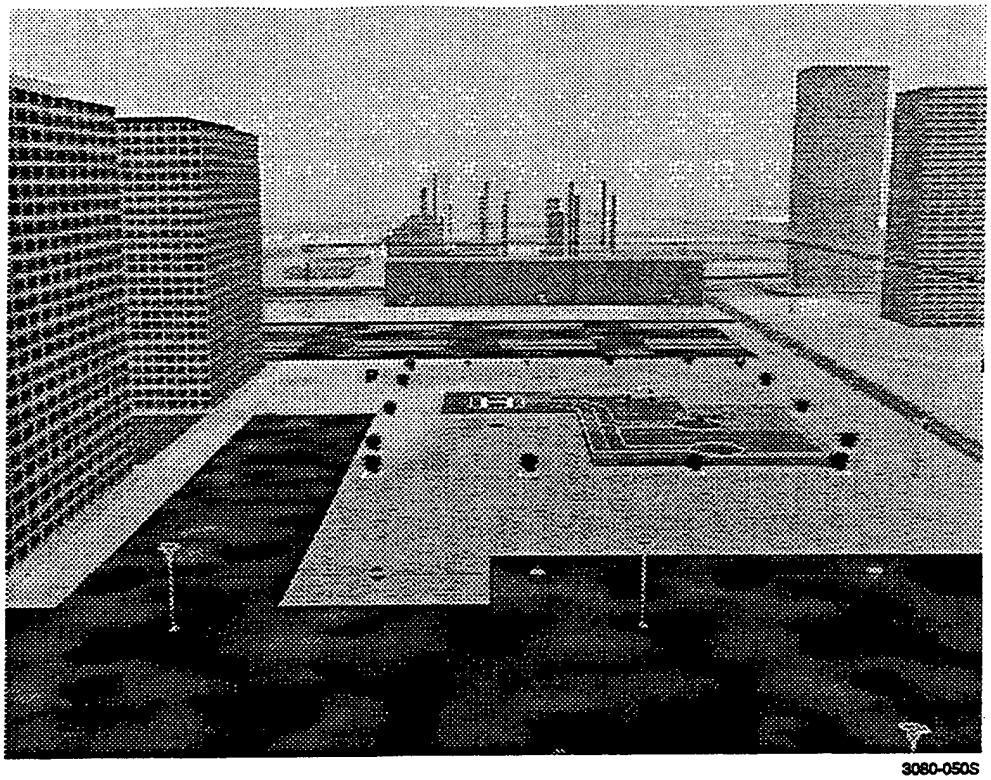

3080-050S

Figure A-29. Arrival From the North, 200' above helipad, 1000'North of Helipad, Medium Obstacle Density

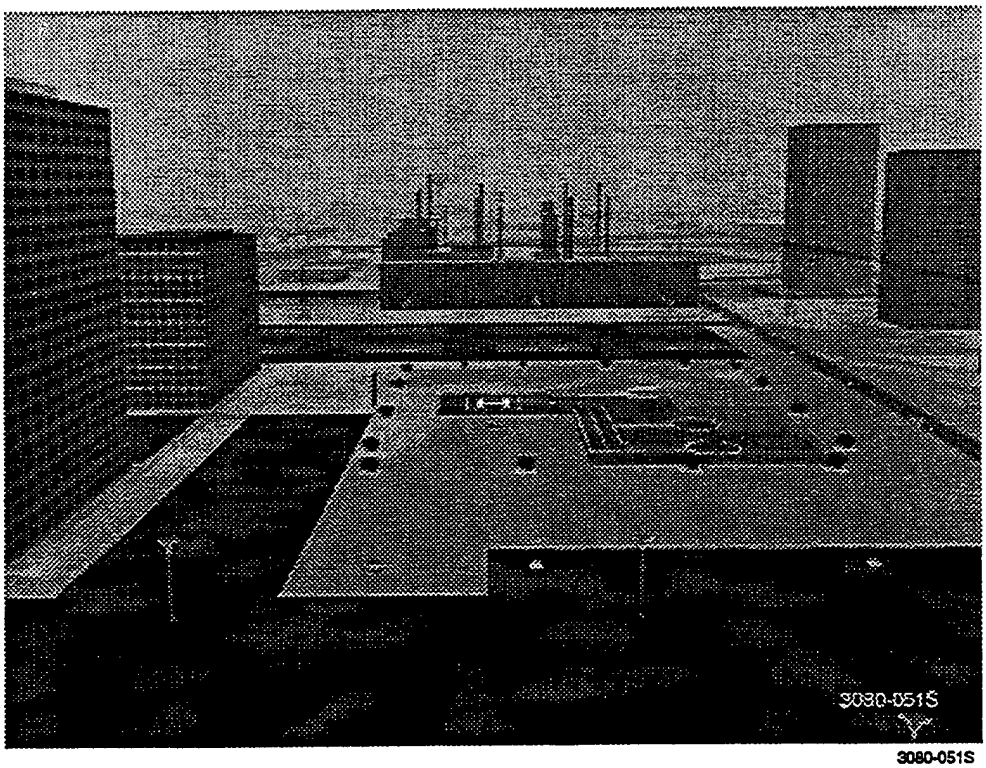

3080-051S

Figure A-30. Arrival From the North, 200' Above Helipad, 1,000' North of Helipad, Low Obstacle Density

A.1.6 Metro Approach

Figures A-31 through A-33 show OH/D variation for the final segment of the Metro approach. They illustrate OH/D variation for a single location south of the heliport facing north . Figures A-34 through A-36 present the view proceeding through the approach after having crossed the VFR corridor threshold. Figures A-37 through A-39 show a mid-point of the descent. Figures A-40 through A-42 show the view entering the heliport area.

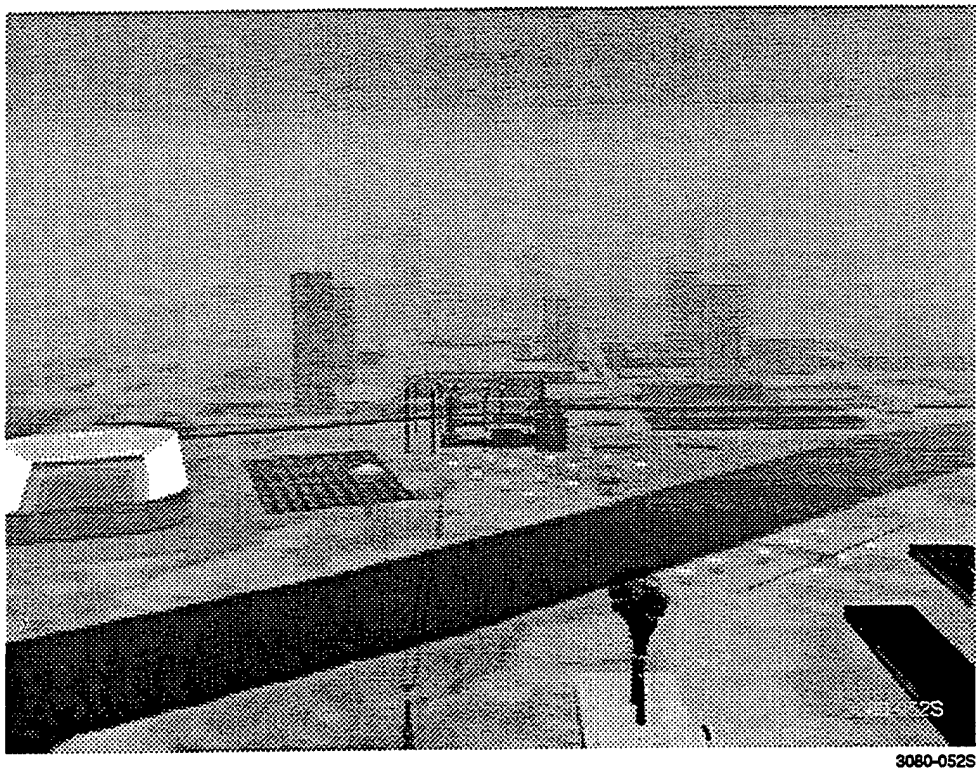

3080-052S

Figure A-31. Arrival From the South, 800' Above Helipad, 6,000' South of Helipad, High Obstacle Density

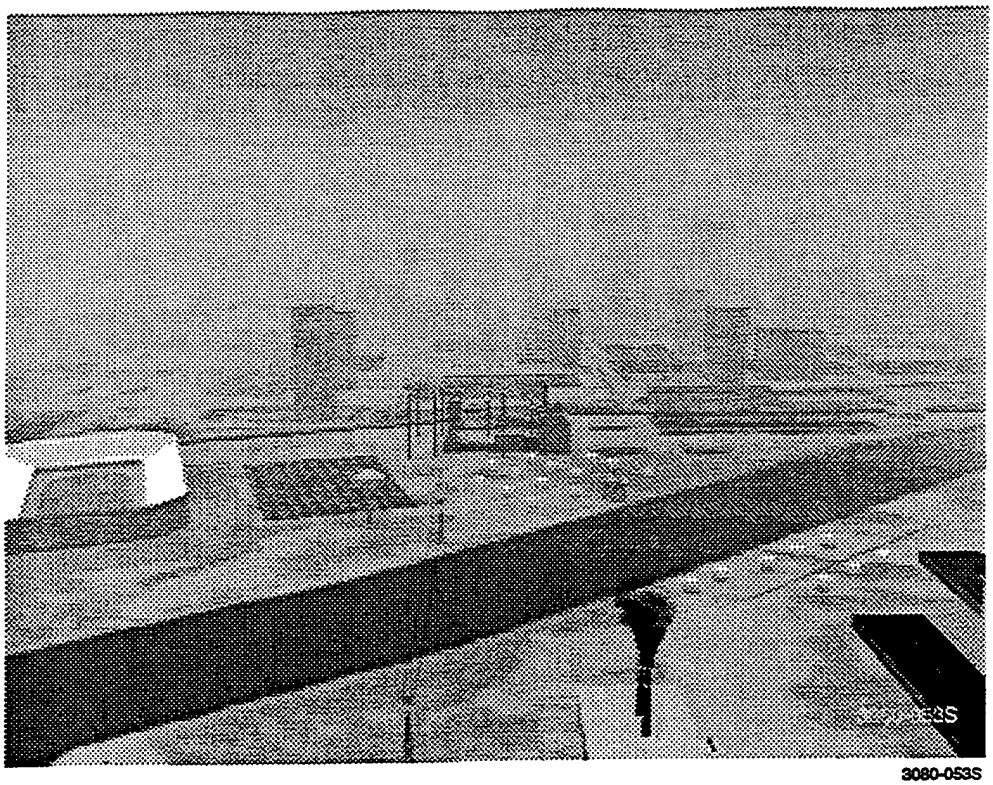

3080-053S

Figure A-32. Arrival From the South, 800' Above Helipad, 6,000' South of Helipad, Medium Obstacle Density

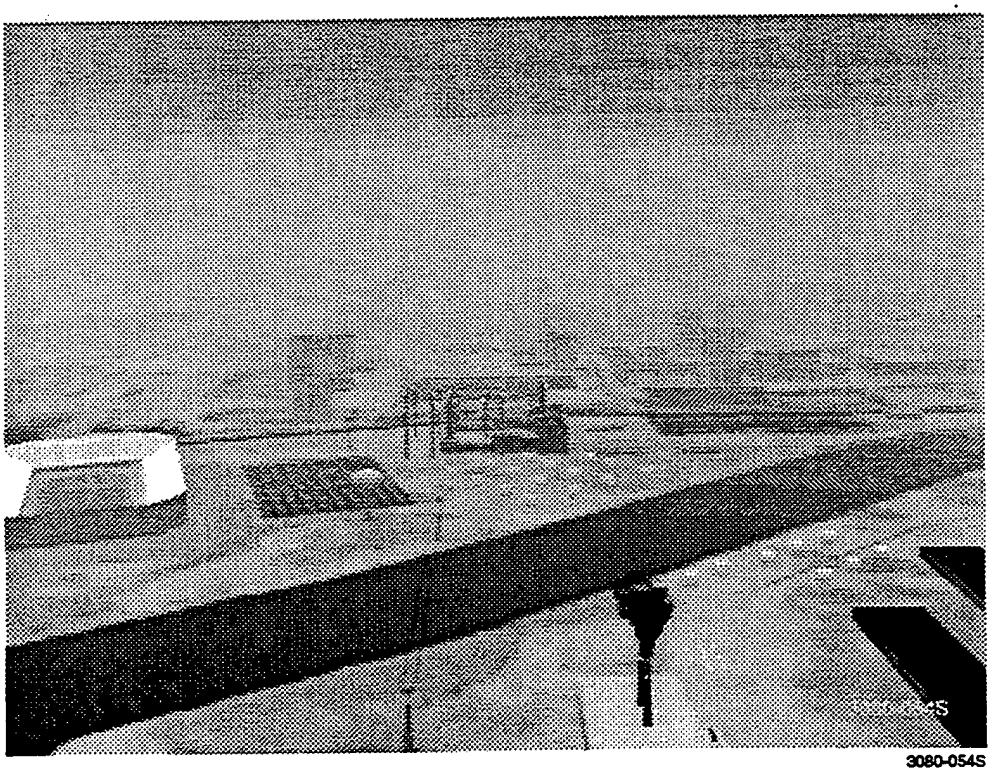

3080-054S

Figure A-33. Arrival From the South, 800' Above Helipad, 6,000' South of Helipad, Low Obstacle Density

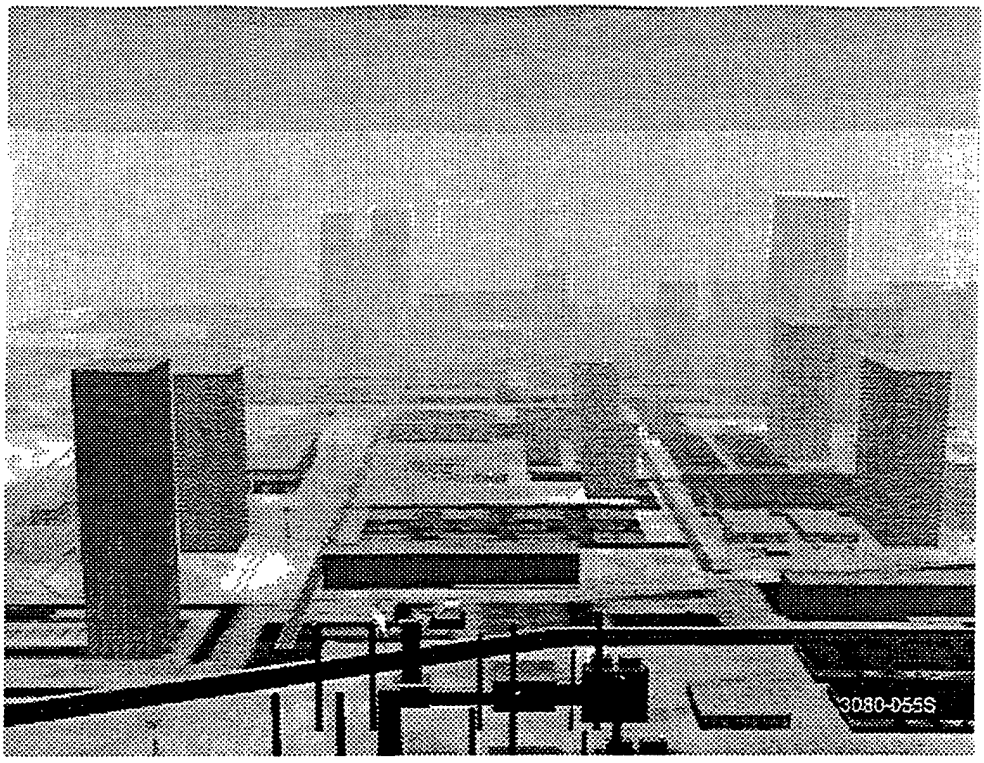

3080-055S

Figure A-34. Arrival From the South, 800' Above Helipad, 4,000' South of Helipad, High Obstacle Density

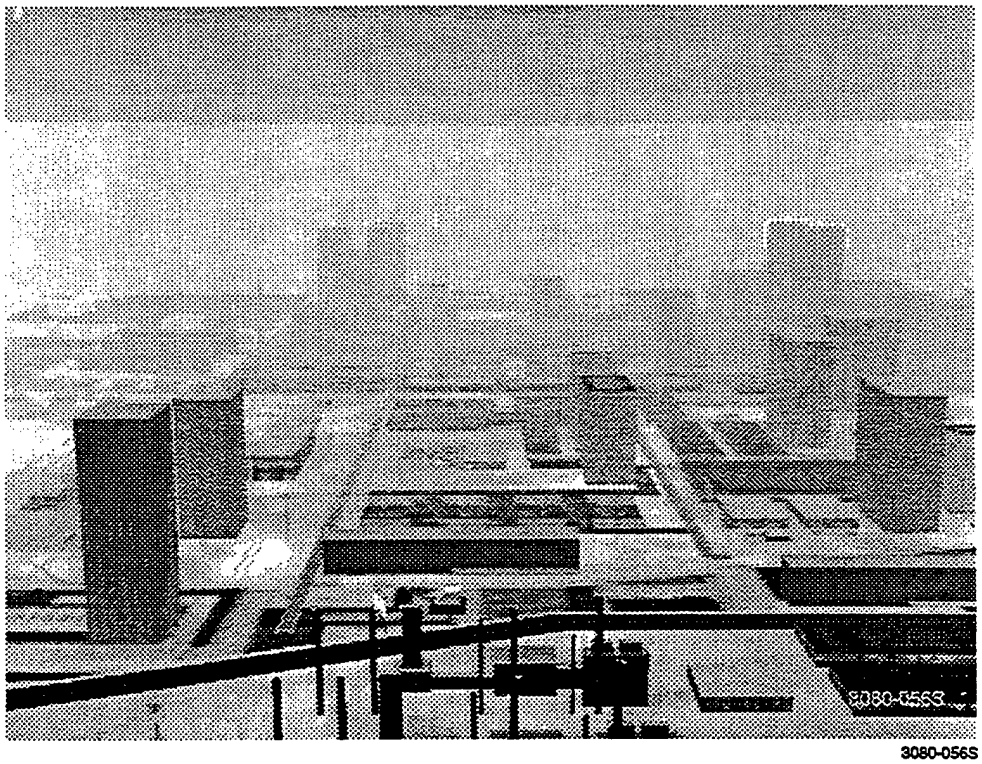

3080-056S

Figure A-35. Arrival From the South, 800' Above Helipad, 4,000' South of Helipad, Medium Obstacle Density

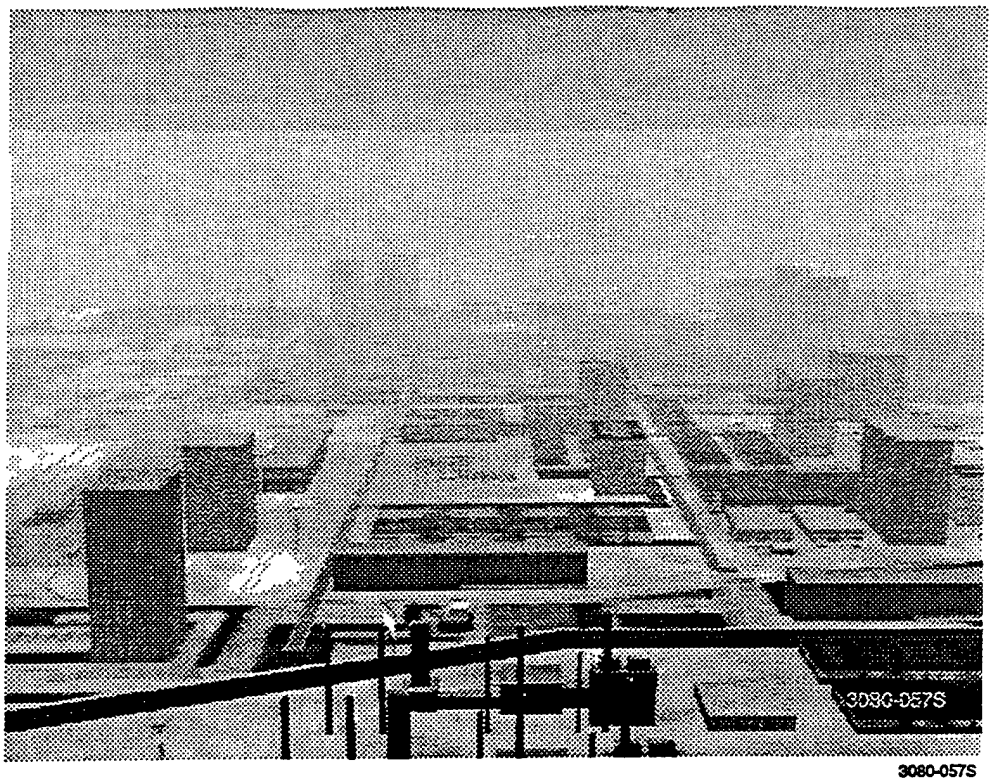

3080-057S

Figure A-36. Arrival From the South, 800' Above Helipad, 4,000' South of Helipad, Low Obstacle Density

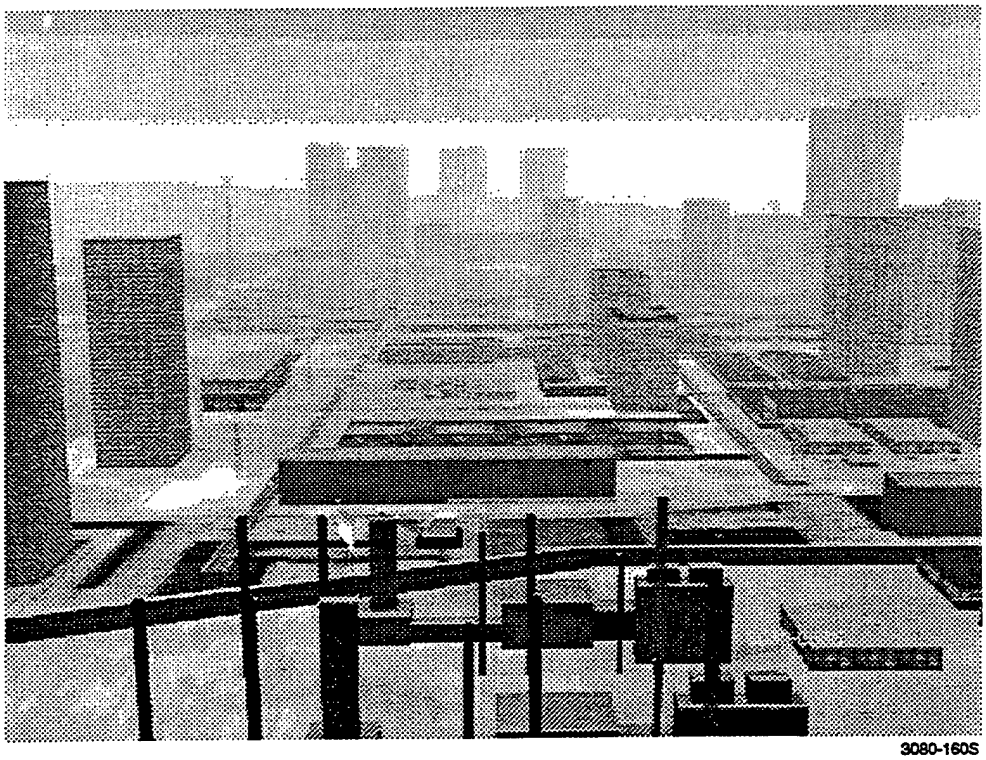

3080-160S

Figure A-37. Arrival From the South, 500' Above Helipad, 2,500' South of Helipad, High Obstacle Density (Metro Approach)

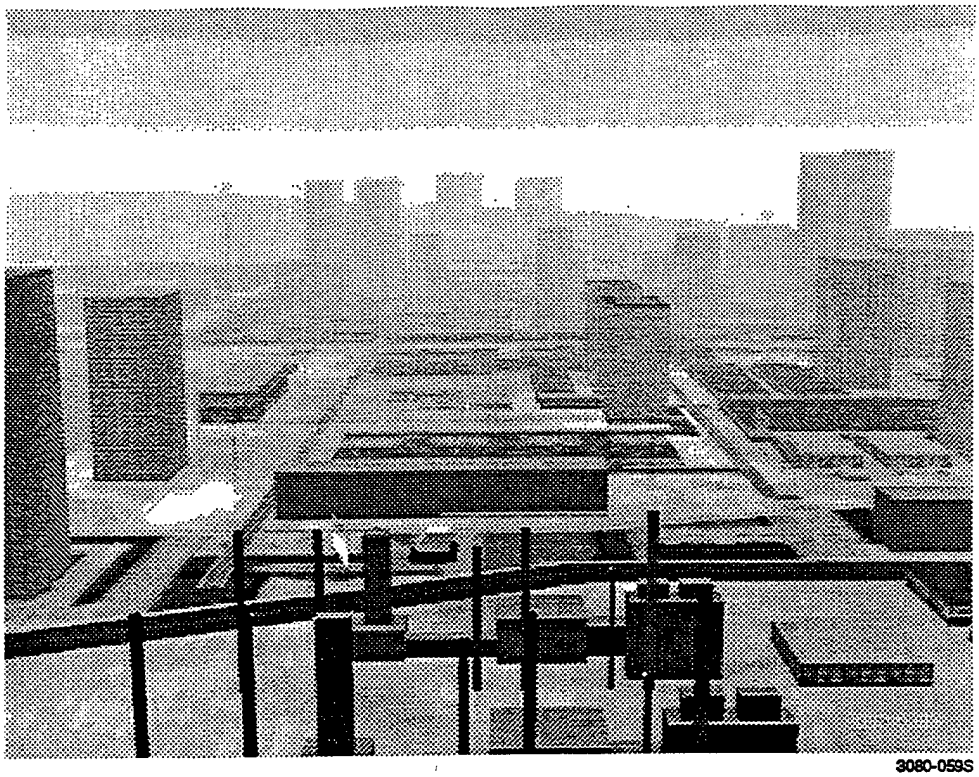

3080-059S

Figure A-38. Arrival From the South, 500' Above Helipad, 2,500' South of Helipad, Medium Obstacle Density

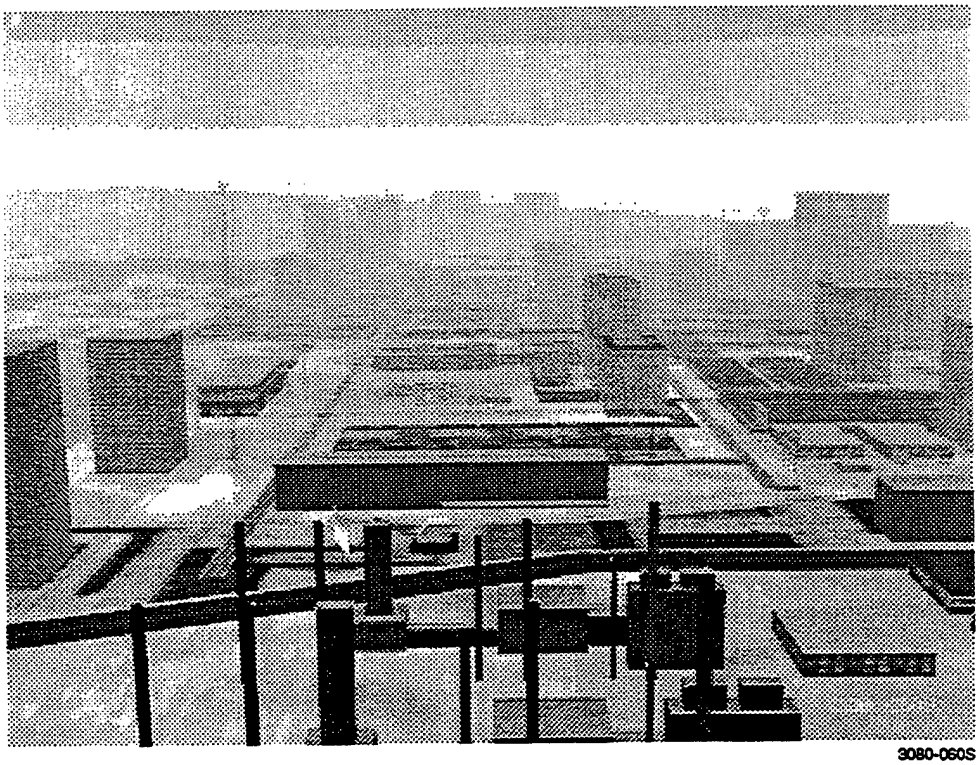

3080-060S

Figure A-39. Arrival From the South, 500' Above Helipad, 2,500' South of Helipad, Low Obstacle Density

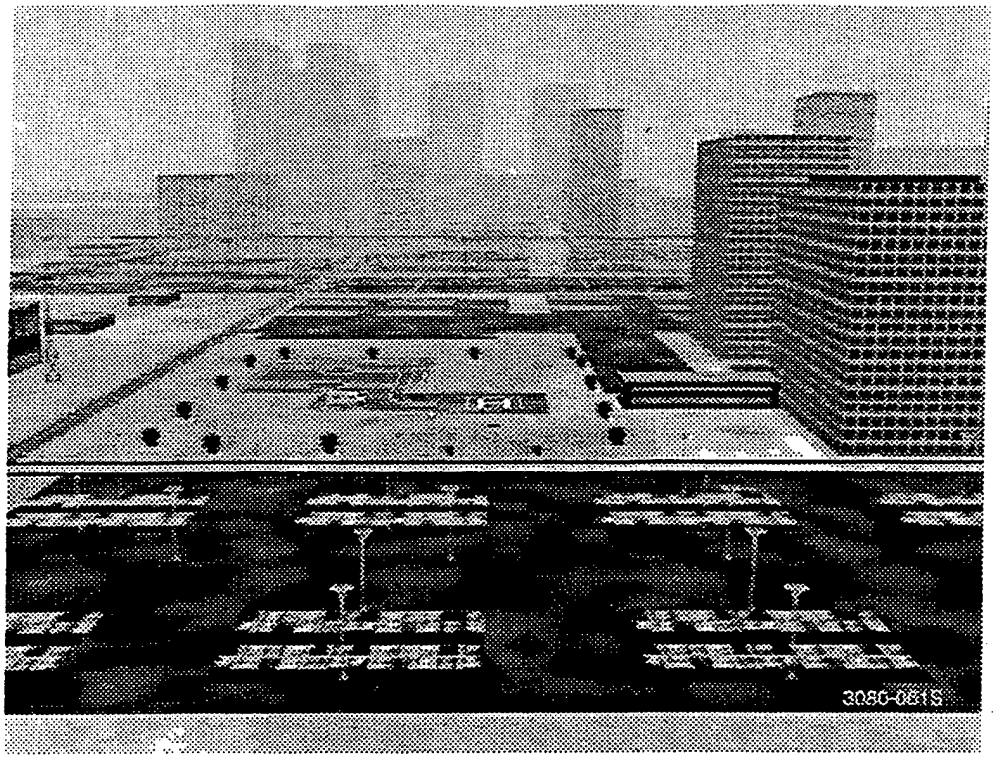

3080-061S

Figure A-40. Arrival From the South, 200' Above Helipad, 1,000' South of Helipad, High Obstacle Density

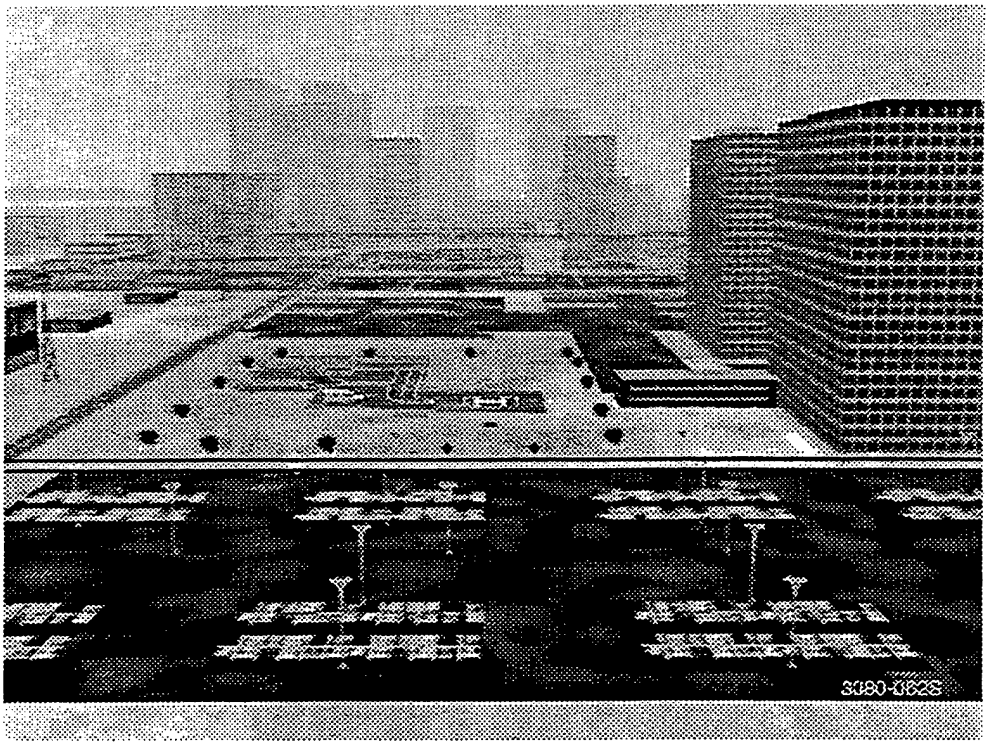

3080-062S

Figure A-41. Arrival From the South, 200' Above Helipad, 1,000' South of Helipad, Medium Obstacle Density

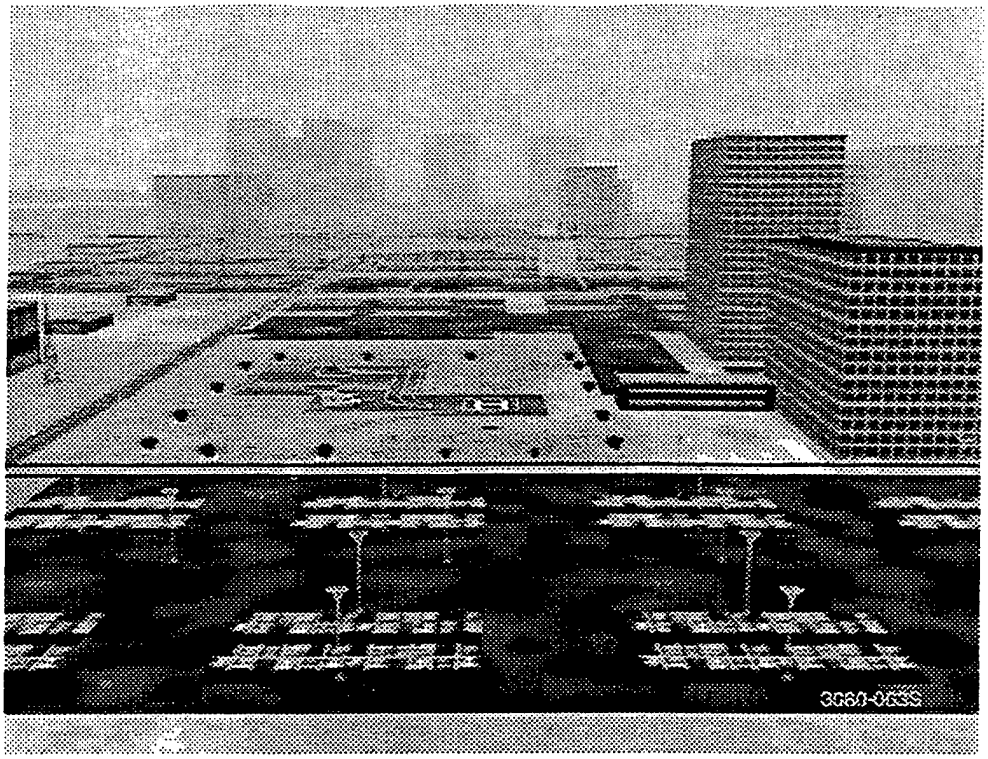

3080-063S

Figure A-42. Arrival From the South, 200' Above Helipad, 1,000' South of Helipad, Low Obstacle Density

A.1.7 Valley Departure

Figures A-43 through A-46 illustrate OH/D variation for the Valley departure as seen from the heliport looking north. Several pilots, rather than gaining forward speed after liftoff, simply made a vertical climb from the heliport to avoid the obstacle environment. The pilot's front window view is illustrated in Figures A-47 through A-50. Figures A-51 through A-54 show a midpoint of the climbout. Figures A-55 through A-58 show the view at the climbout end.

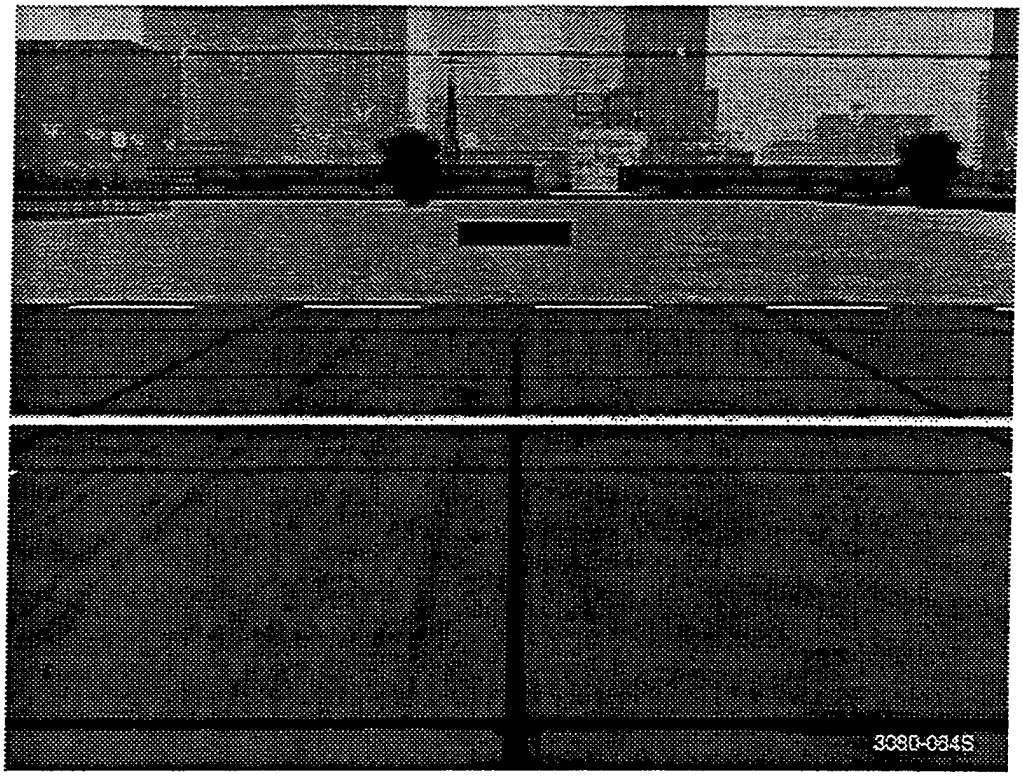

Figure A-43. Departure to the North, at Liftoff, High Obstacle Density

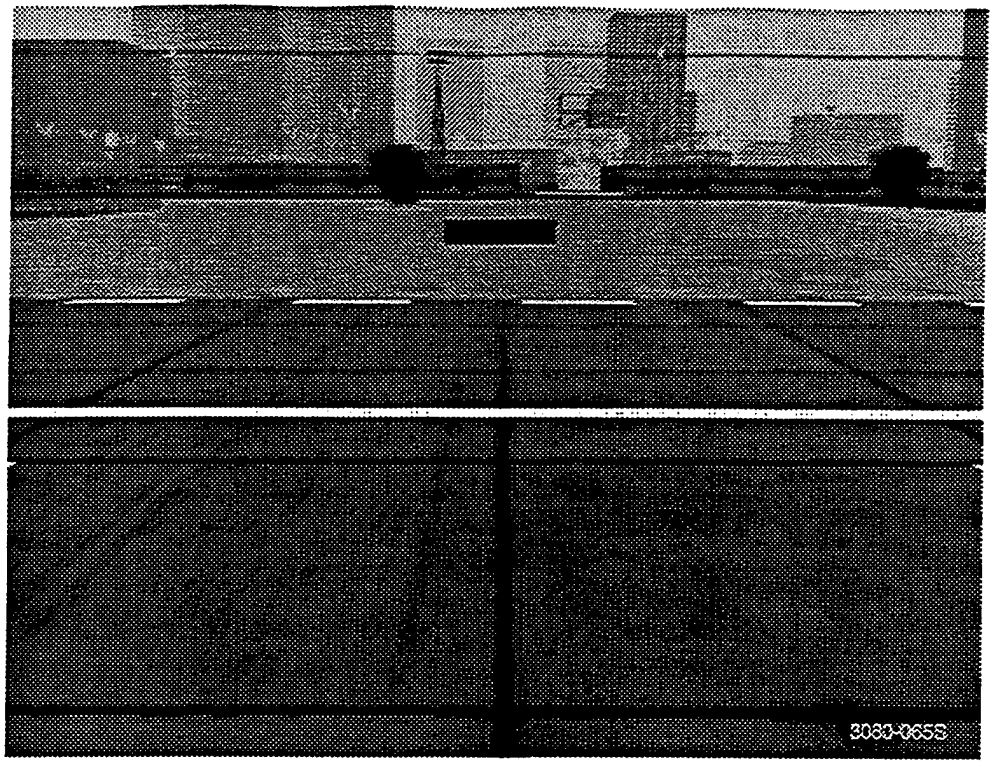

3080-065S

Figure A-44. Departure to the North, at Liftoff, Medium Obstacle Density

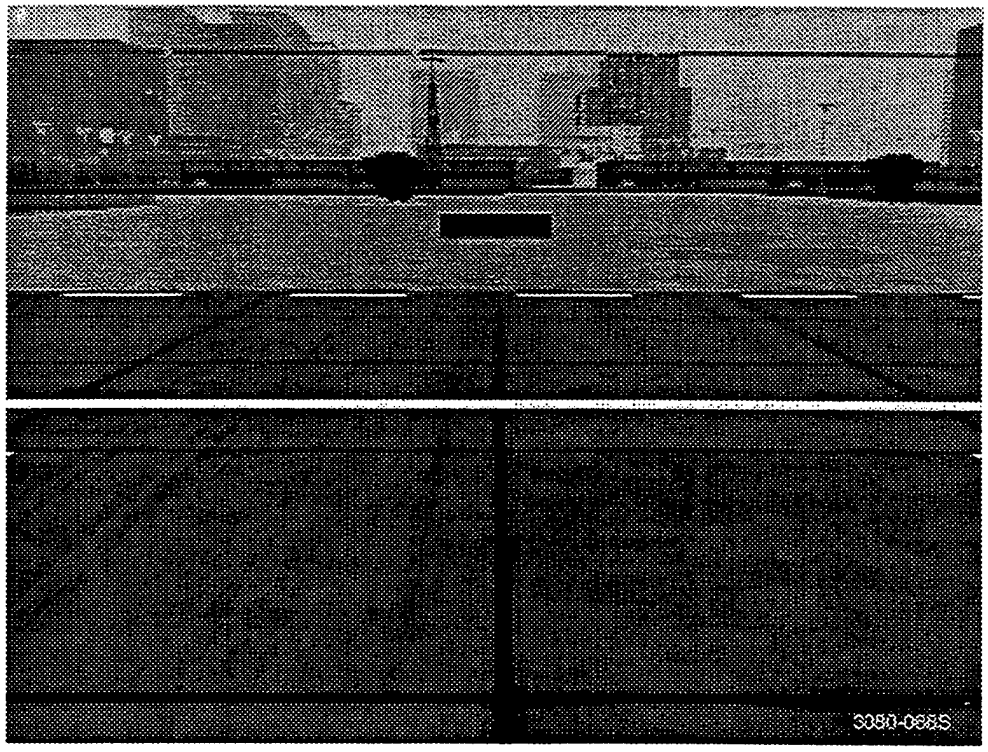

3080-066S

Figure A-45. Departure to the North, at Liftoff, Low Obstacle Density

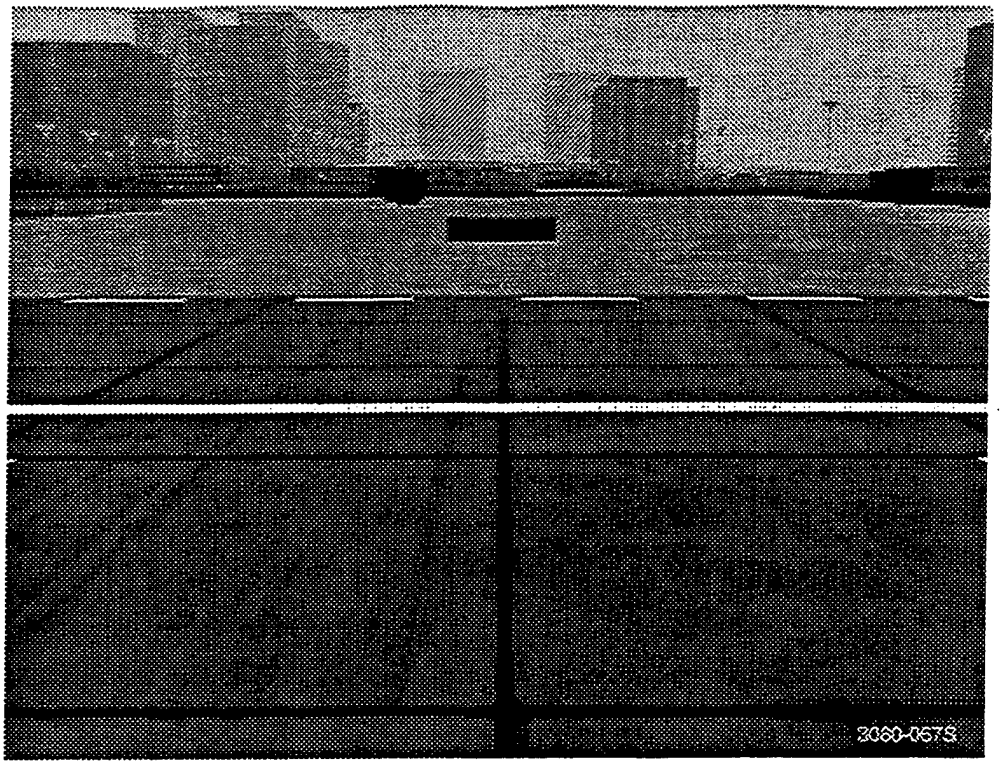

3080-067S

Figure A-46. Departure to the North, at Liftoff, Very Low Obstacle Density

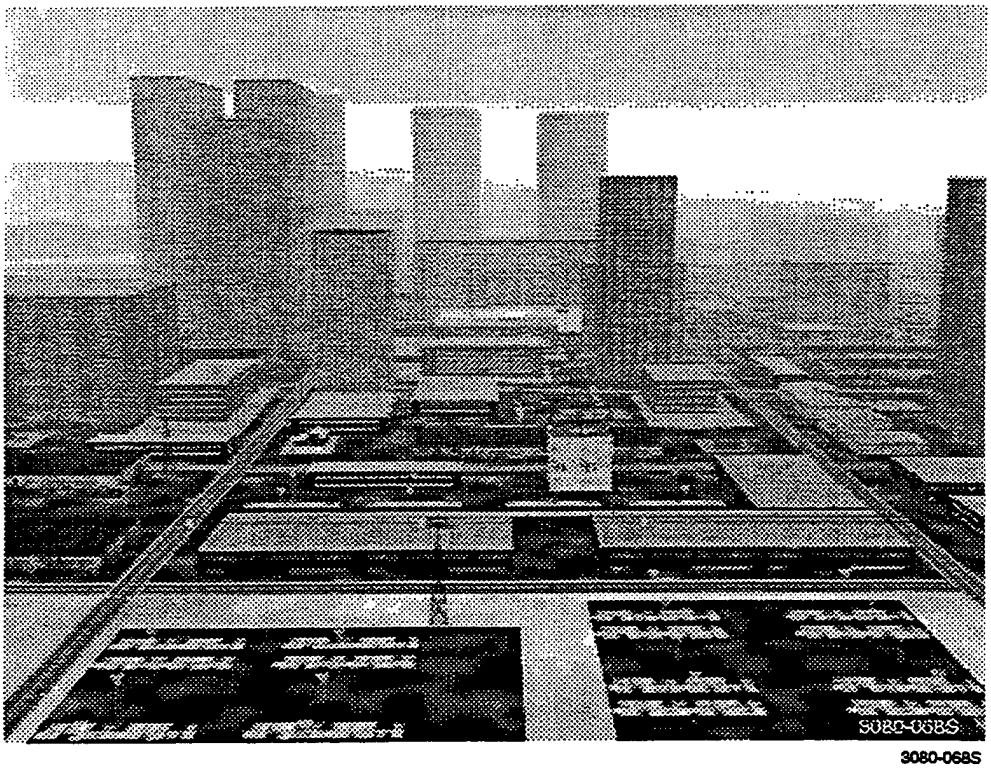

3080-068S

Figure A-47. Departure to the North, 400' Directly Above Helipad, High Obstacle Density

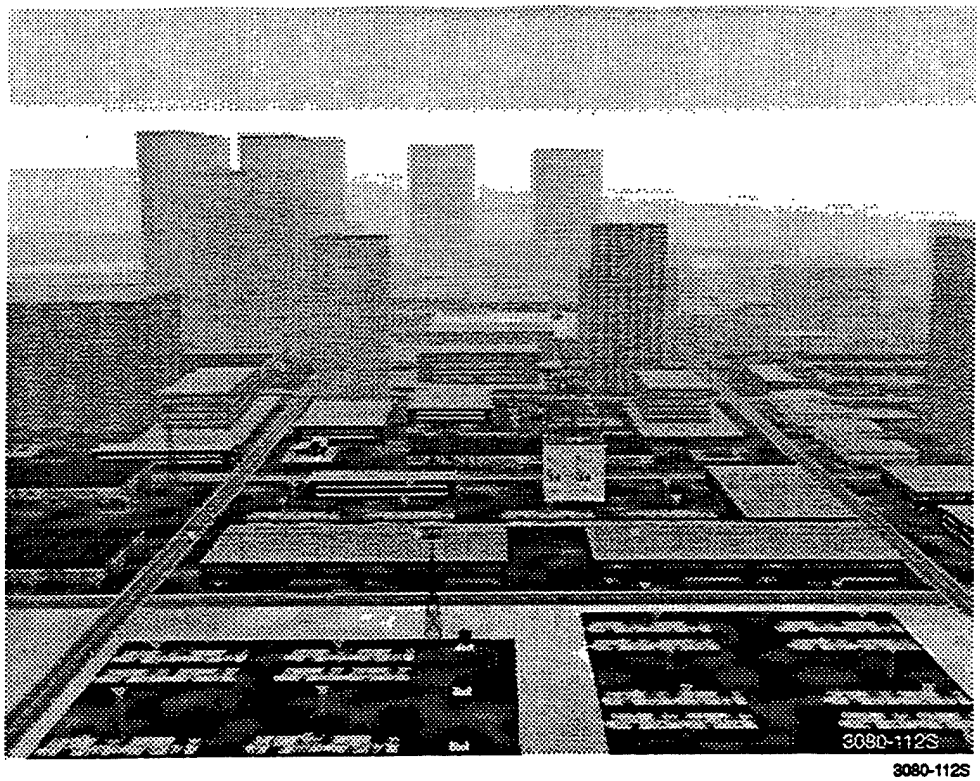

3080-112S

Figure A-48. Departure to the North, 400' Directly Above Helipad, Medium Obstacle Density

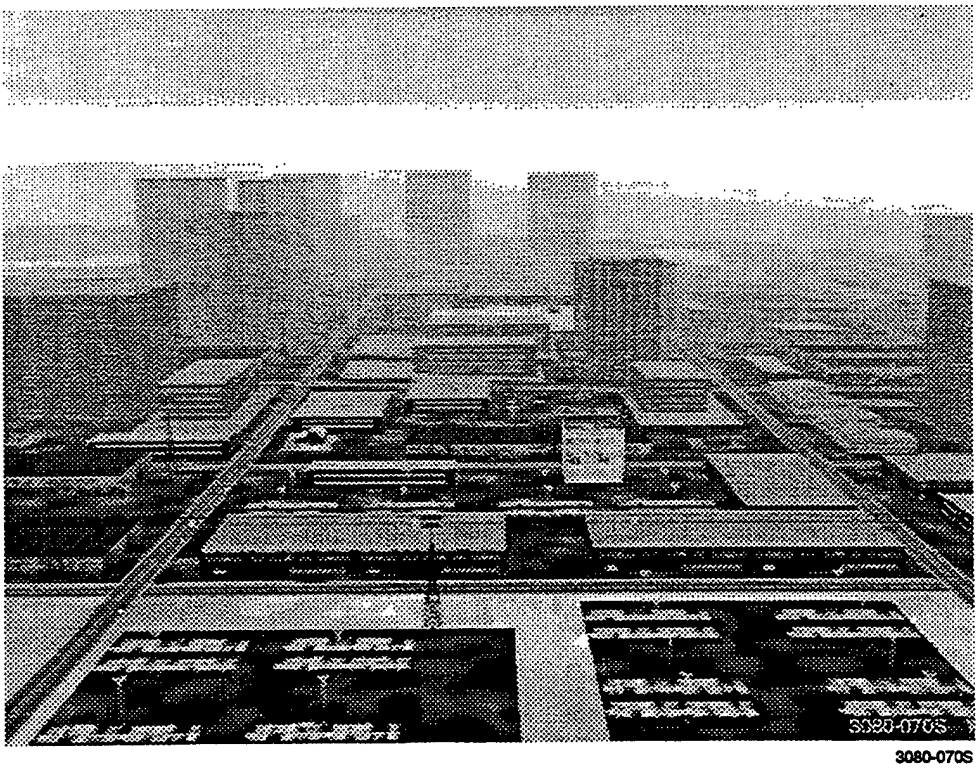

3080-070S

Figure A-49. Departure to the North, 400' Directly Above Helipad, Low Obstacle Density

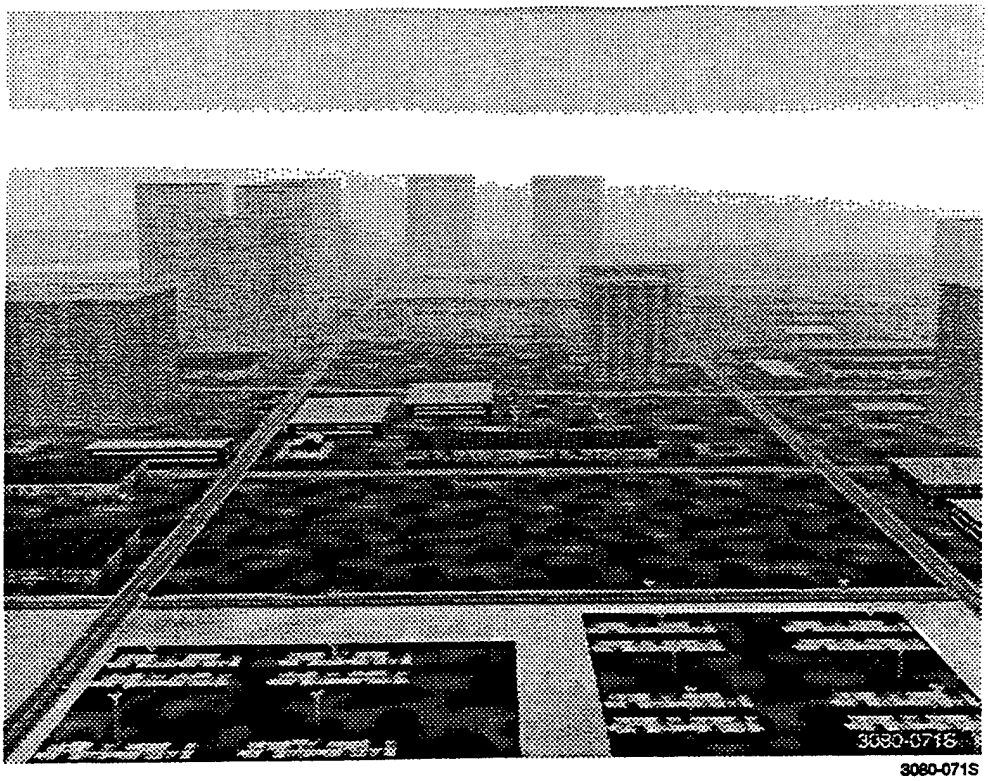

Figure A-50. Departure to the North, 400' Directly Above Helipad, Very Low Obstacle Density

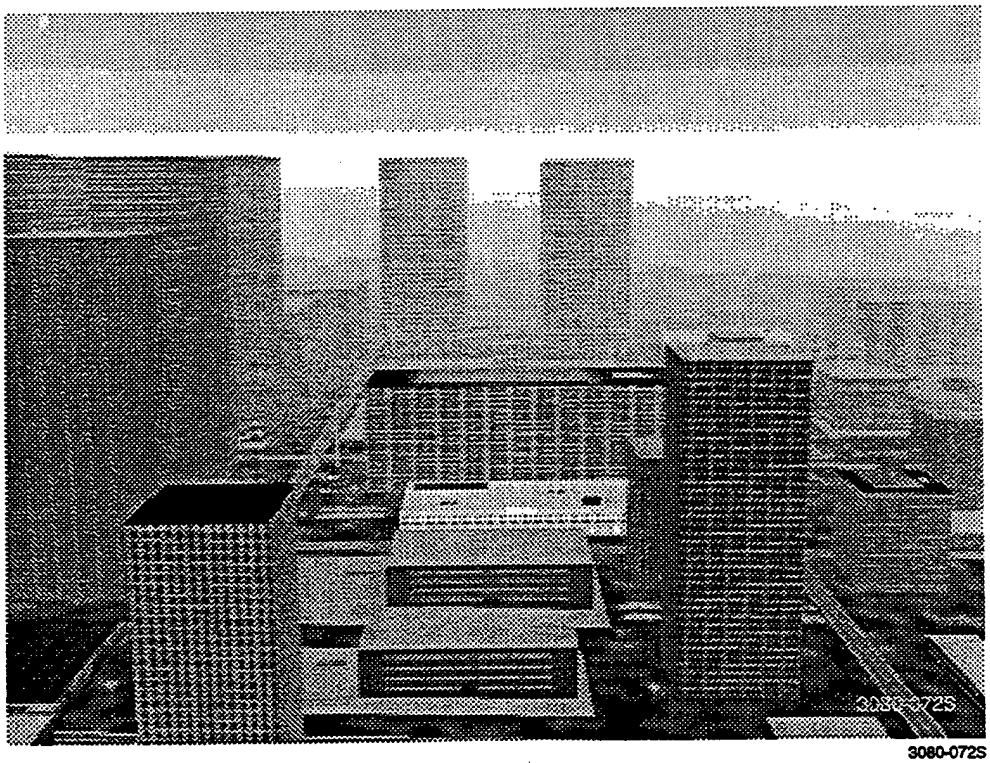

Figure A-51. Departure to the North, 600' Above Helipad, 1,000' North of Helipad, High Obstacle Density

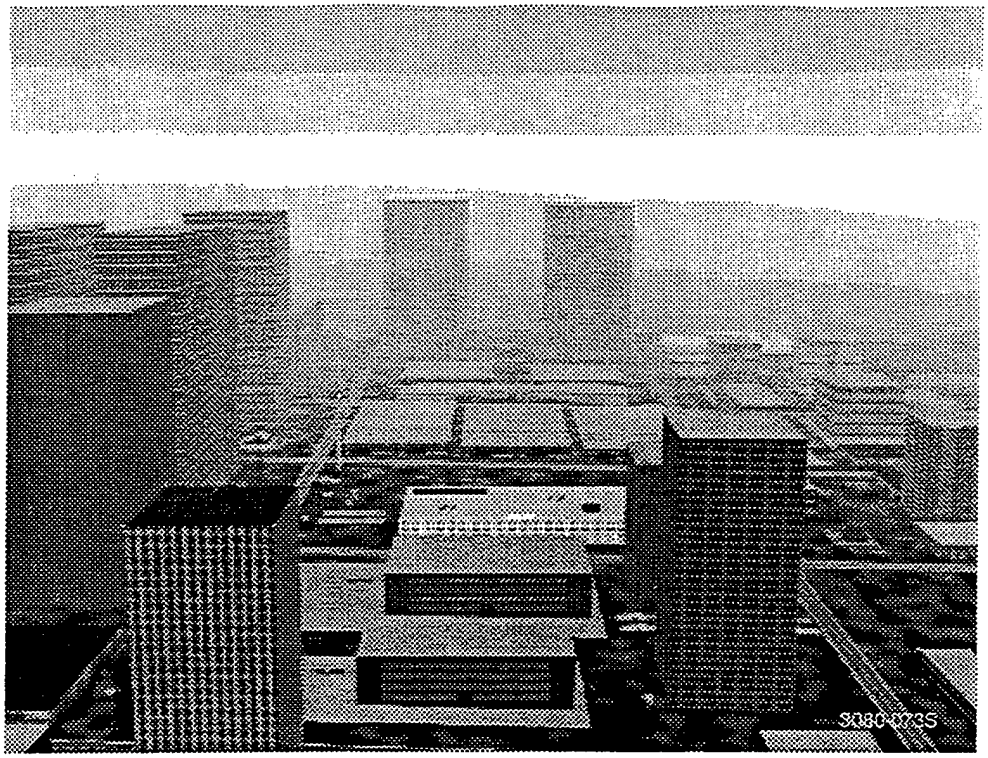

3080-073S

Figure A-52. Departure to the North, 600' Above Helipad, 1,000 North of Helipad, Medium Obstacle Density

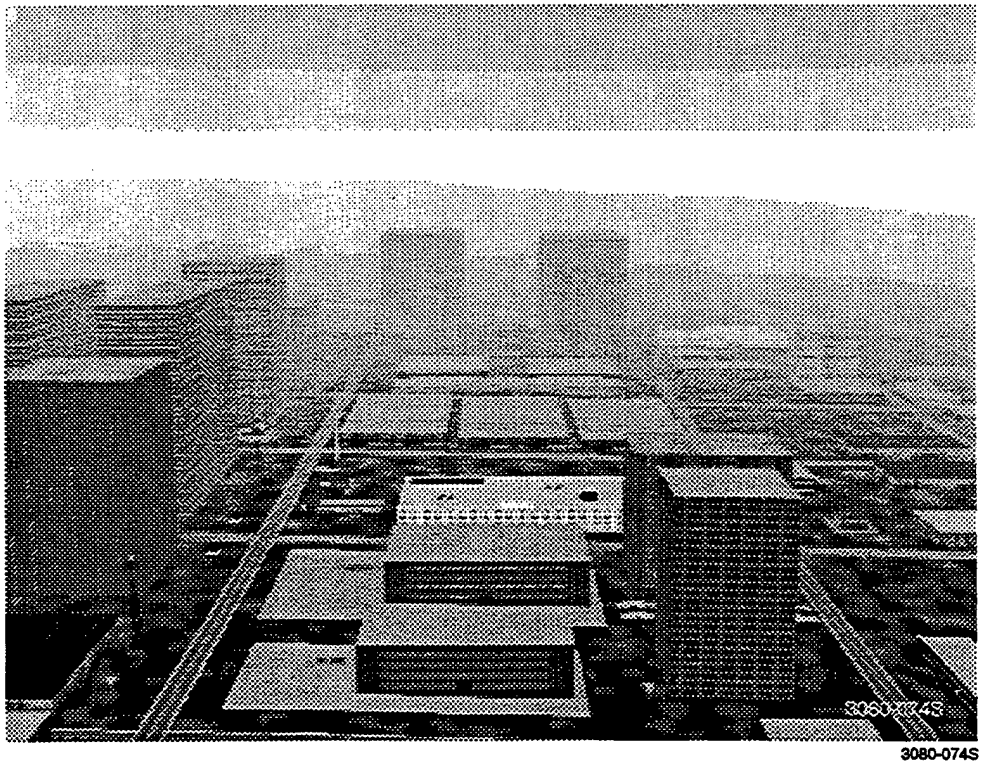

3080-074S

Figure A-53. Departure to the North, 600' Above Helipad, 1,000 North of Helipad, Low Obstacle Density

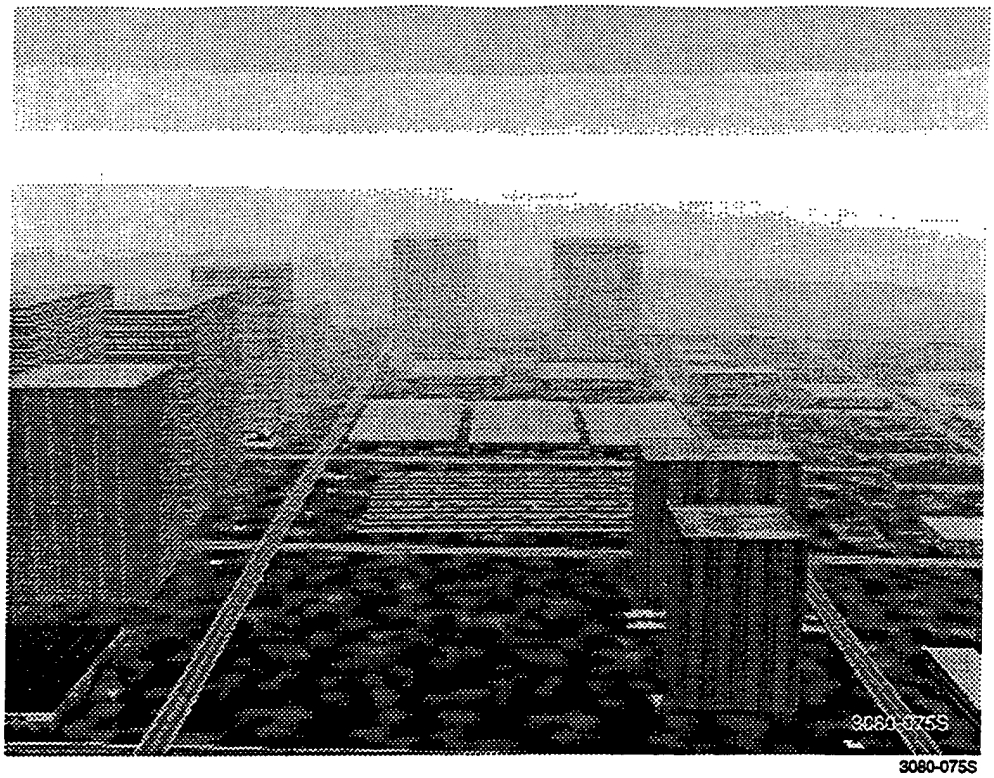

3080-075S

Figure A-54. Departure to the North, 600' Above Helipad, 1,000 North of Helipad, Very Low Obstacle Density

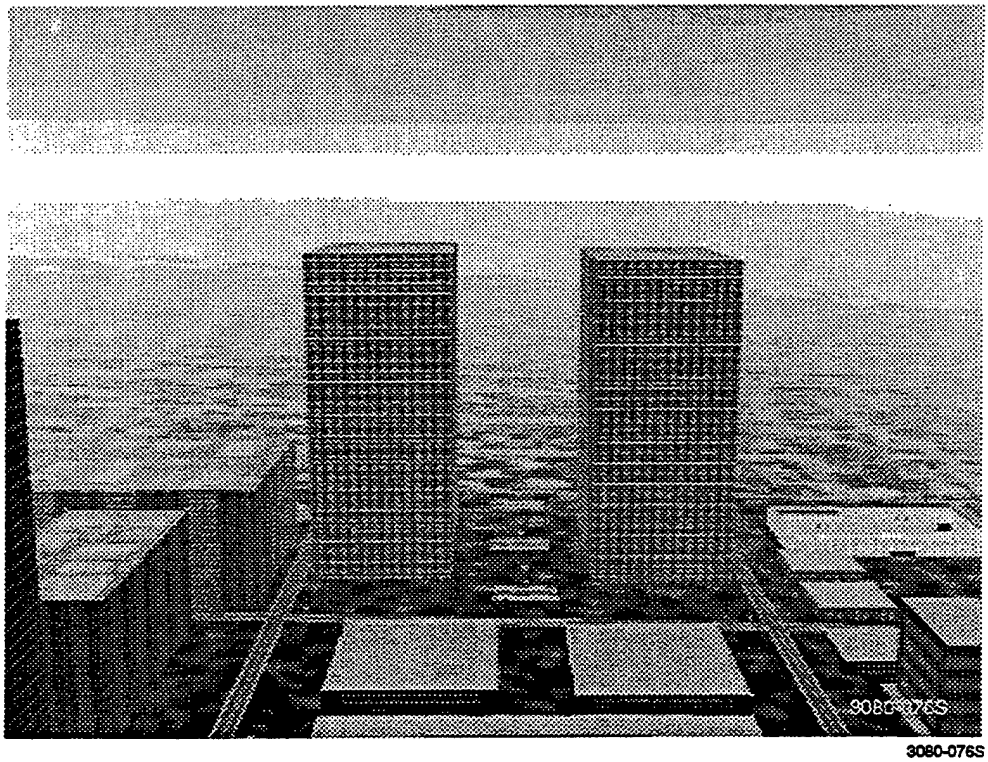

3080-076S

Figure A-55. Departure to the North, 800' Above Helipad, 2,500 North of Helipad, High Obstacle Density

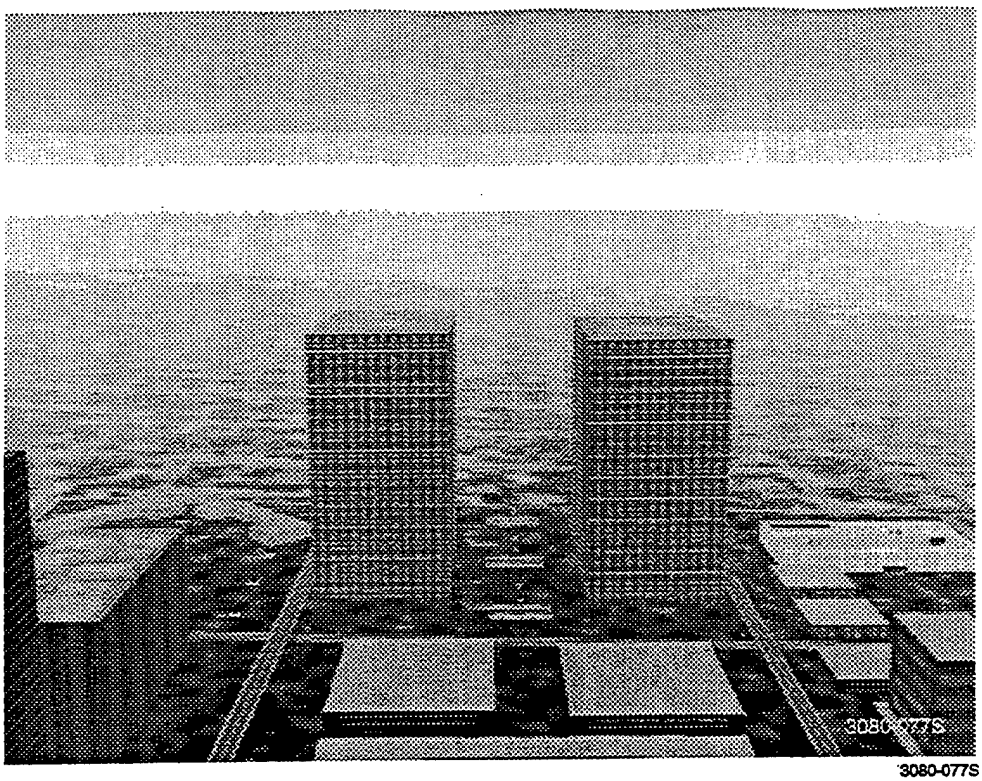

3080-077S

Figure A-56. Departure to the North, 800' Above Helipad, 2,500 North of Helipad, Medium Obstacle Density

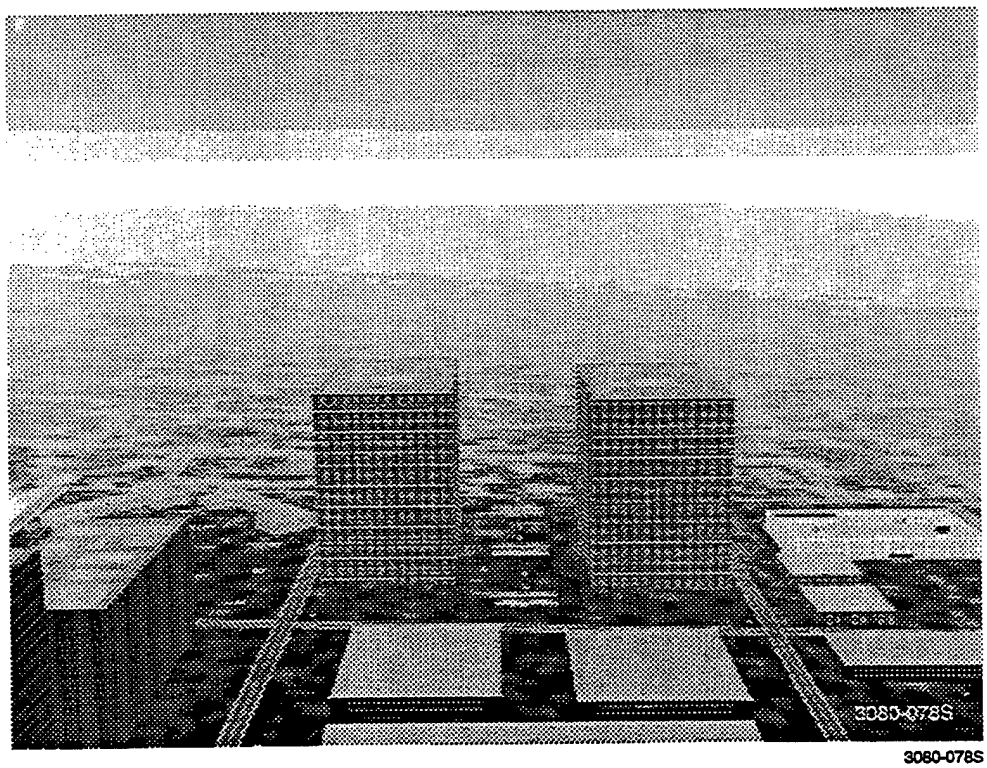

3080-078S

Figure A-57. Departure to the North, 800' Above Helipad, 2,500 North of Helipad, Low Obstacle Density

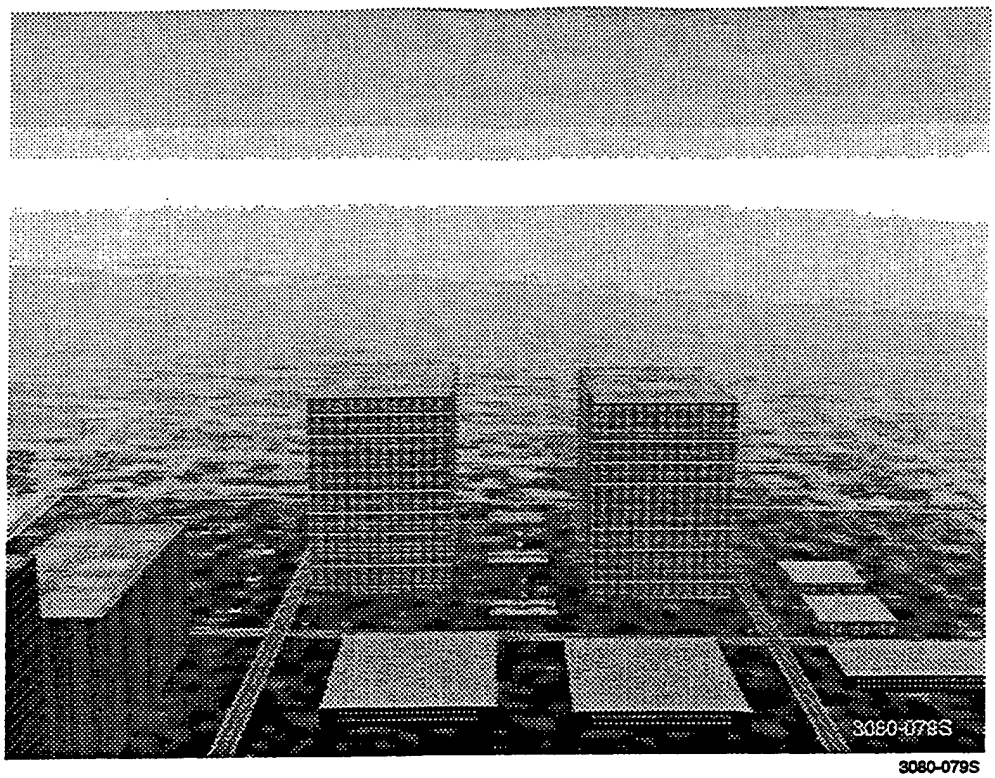

Figure A-58. Departure to the North, 800' Above Helipad, 2,500 North of Helipad, Very Low Obstacle Density

A.1.8 Metro Departure

Figures A-59 through A-62 illustrate OH/D variation on the Metro departure as seen from the heliport looking south. As on the Valley departure, several pilots made a vertical climb from the heliport to avoid the obstacle environment, rather than gaining forward speed after liftoff. The front window view seen by these pilots is illustrated in Figures A-63 through A-66. Figures A-67 through A-70 show a climbout midpoint. Figures A-71 through A-74 show the view at the climbout end.

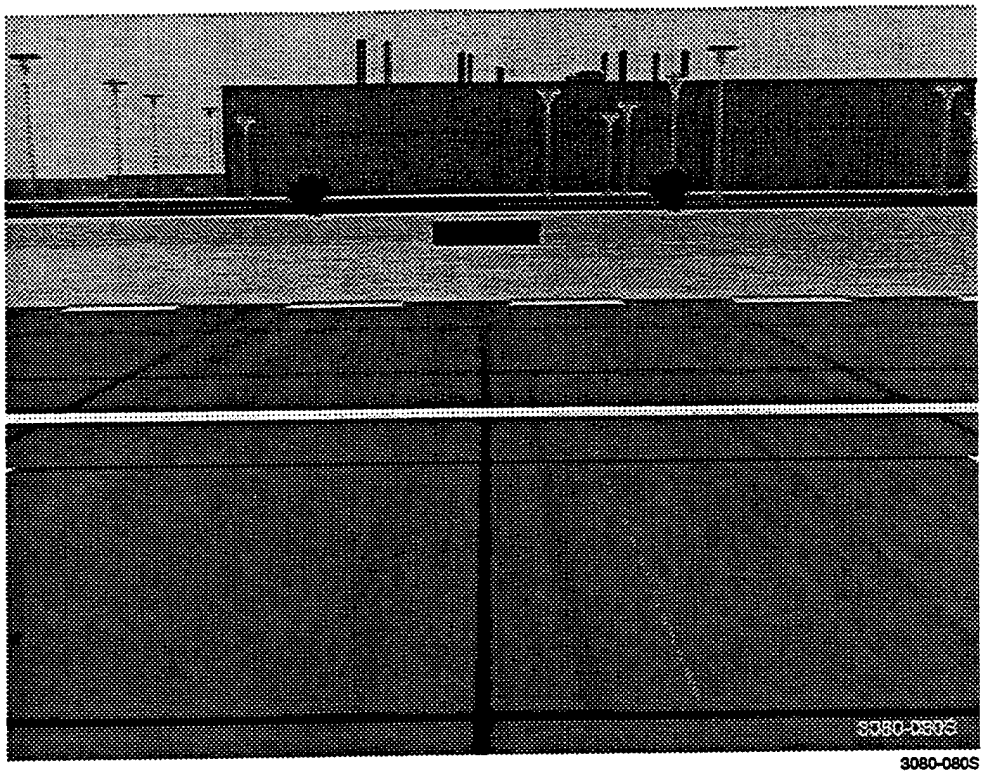

Figure A-59. Departure to the South, at Liftoff, High Obstacle Density

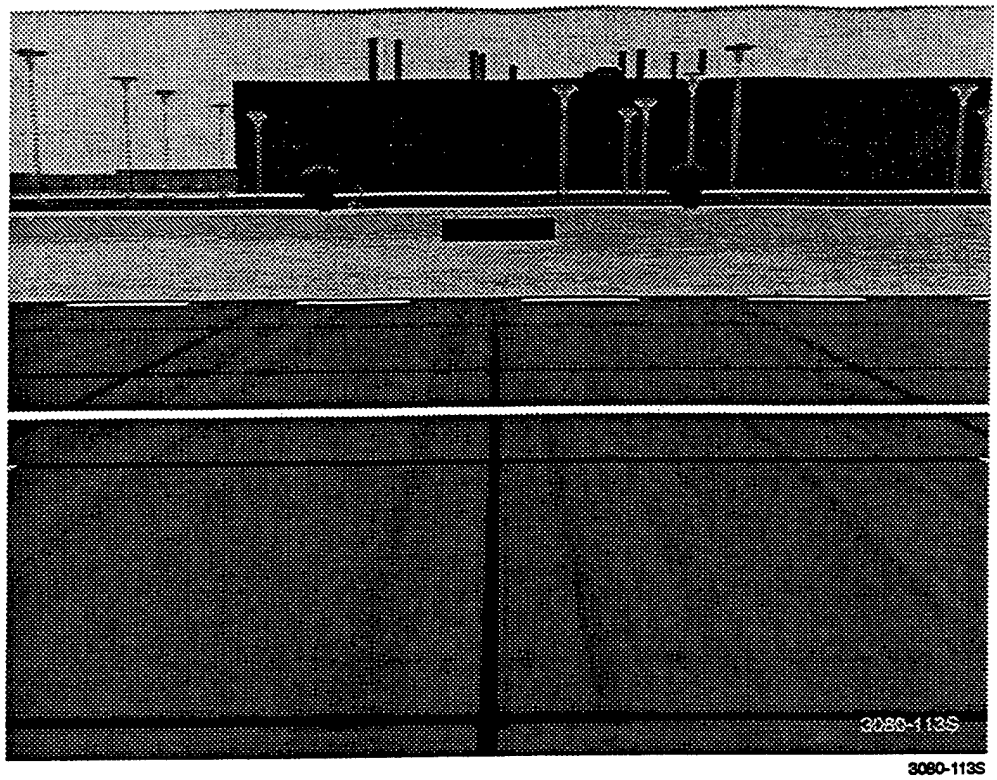

3080-113S

Figure A-60. Departure to the South, at Liftoff, Medium Obstacle Density

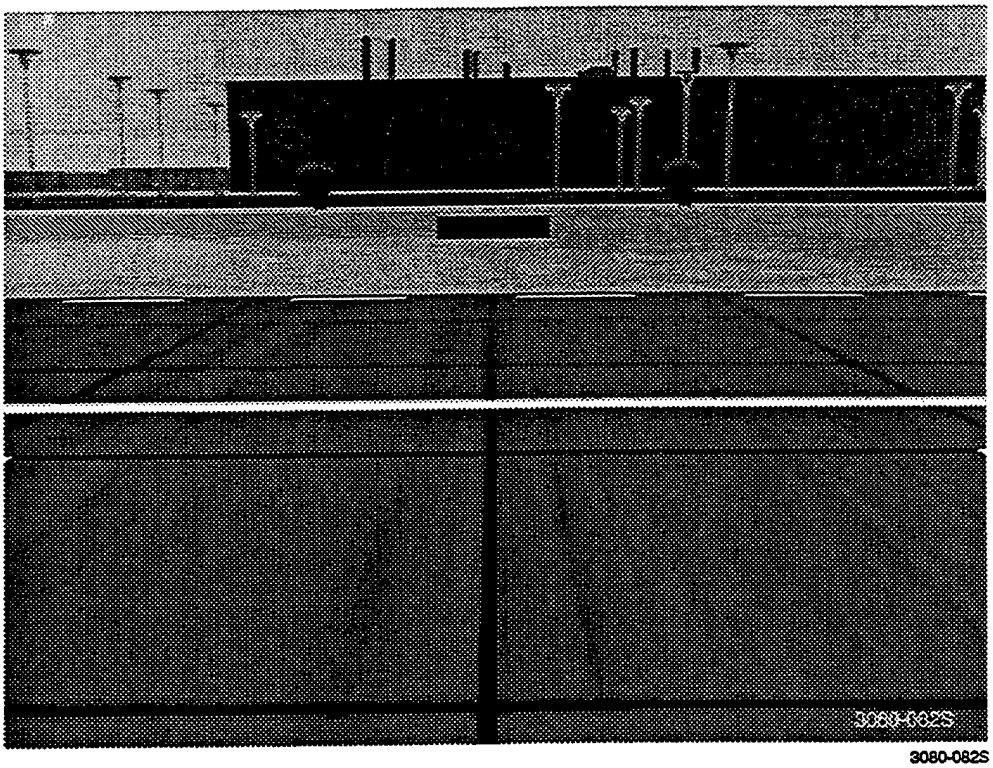

3080-082S

Figure A-61. Departure to the South, At Liftoff, Low Obstacle Density

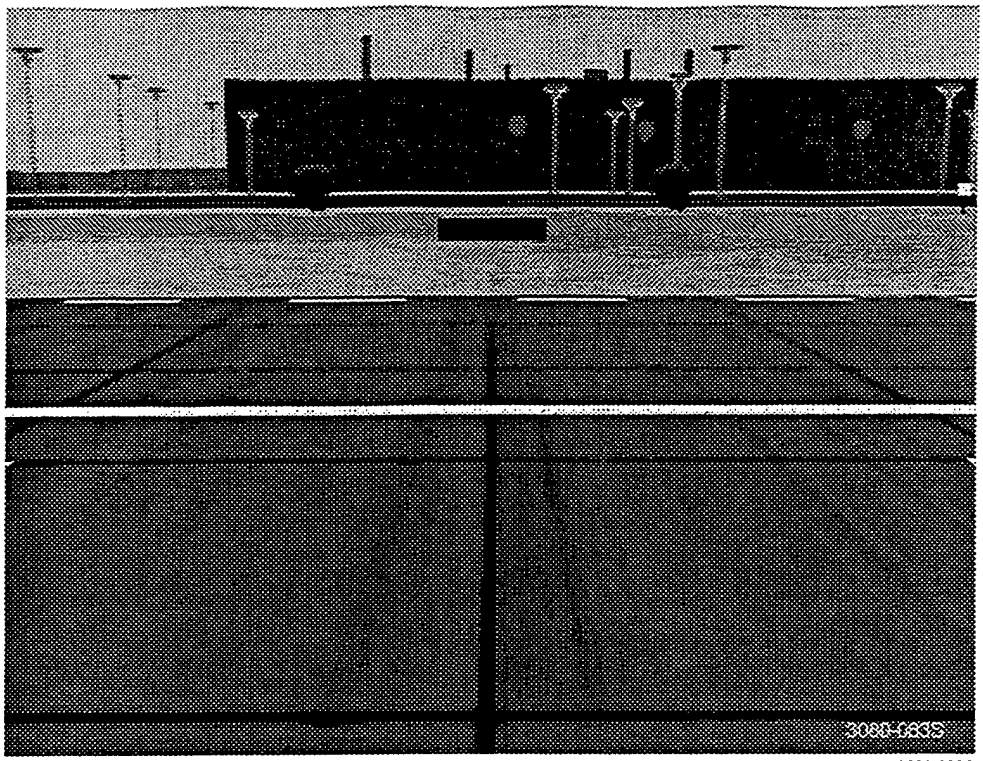

Figure A-62. Departure to the South, At Liftoff, Very Low Obstacle Density

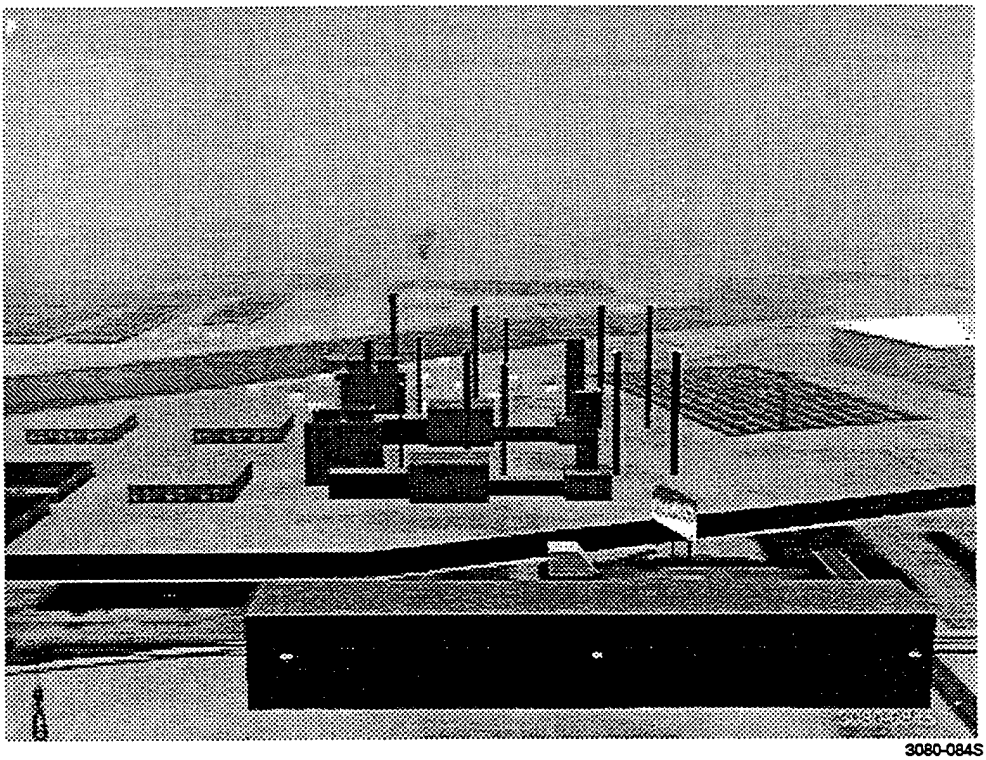

Figure A-63. Departure to the South, 400' Directly Above Helipad, High Obstacle Density

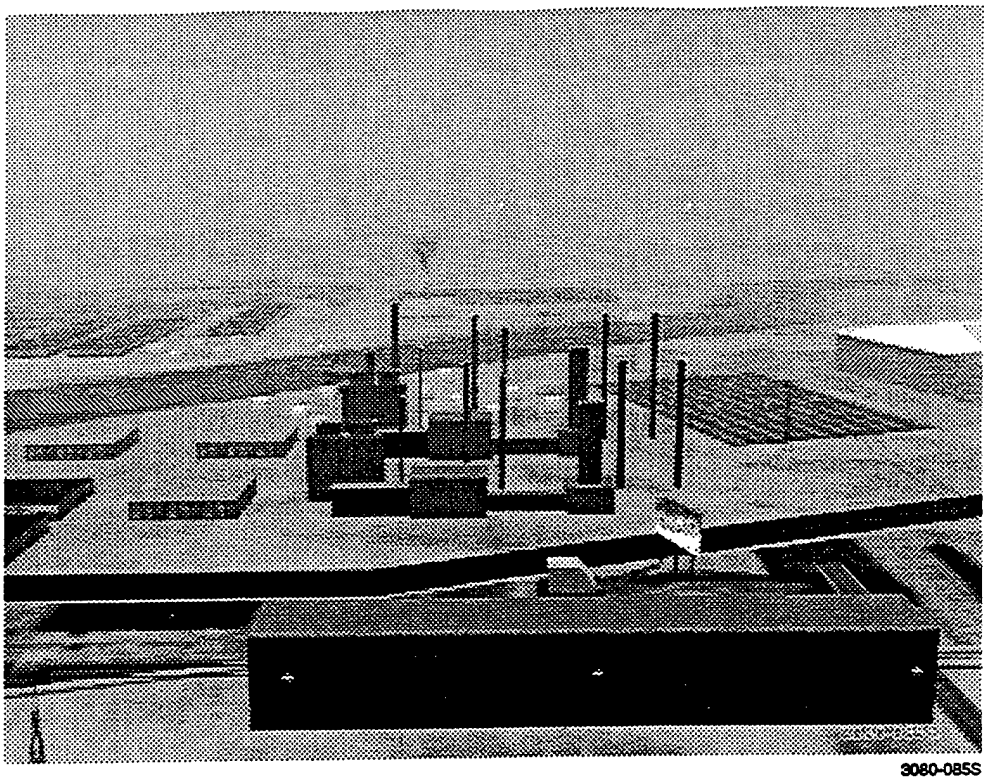

3080-085S

Figure A-64. Departure to the South, 400' Directly Above Helipad, Medium Obstacle Density

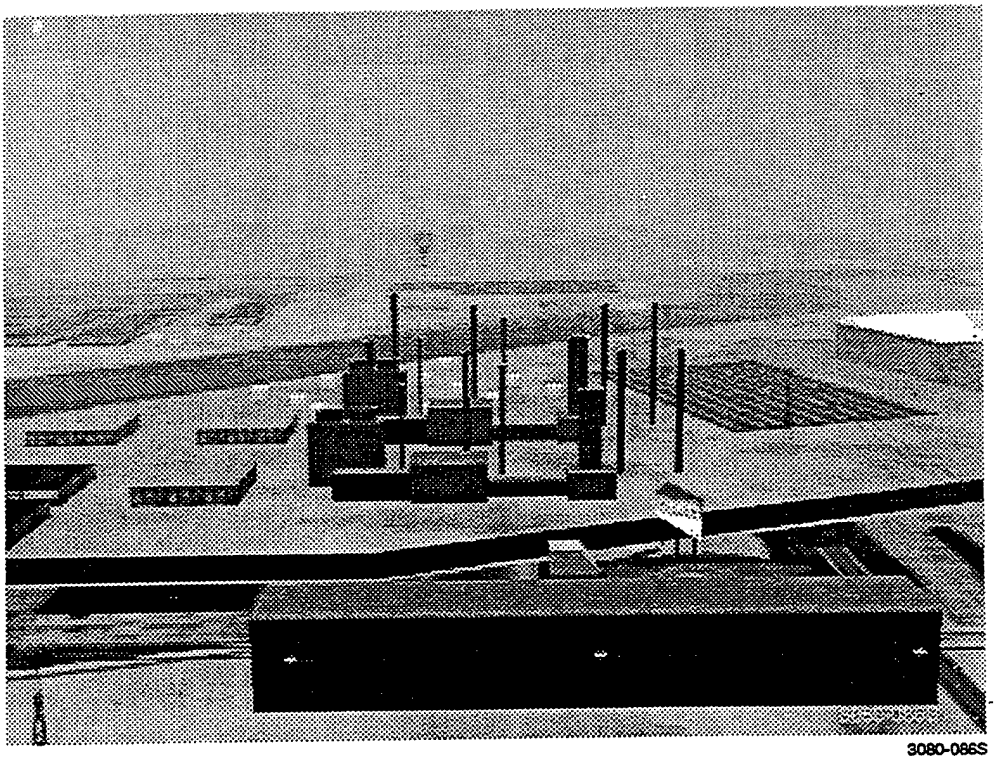

3080-086S

Figure A-65. Departure to the South, 400' Directly Above Helipad, Low Obstacle Density

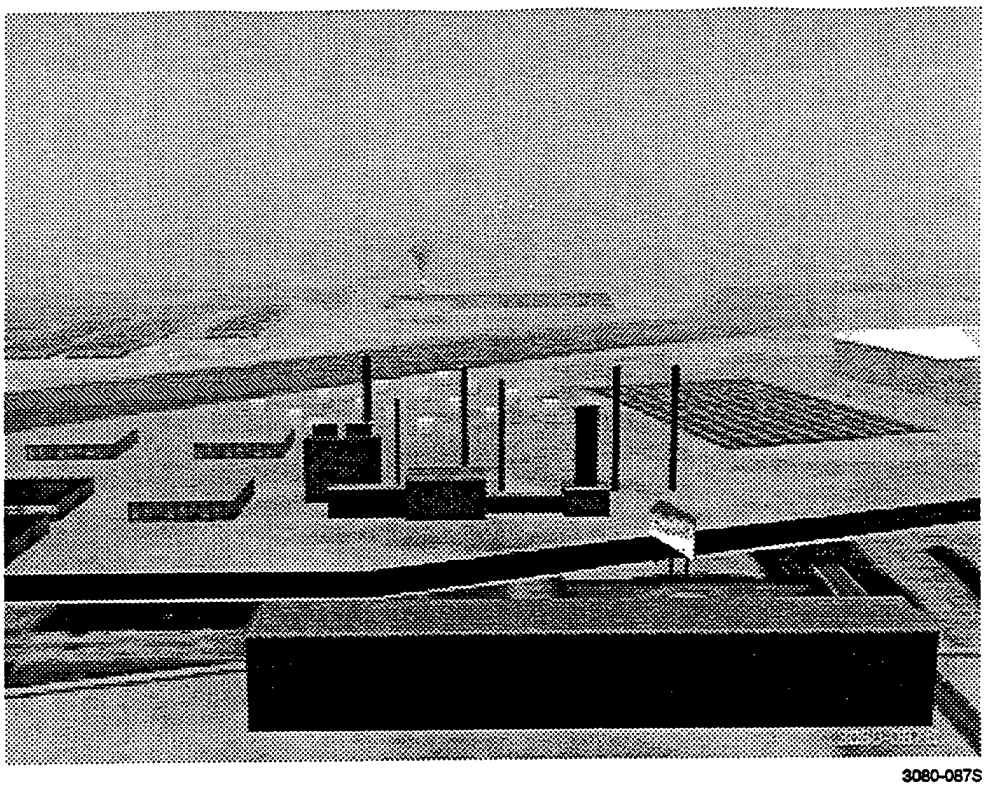

3080-087S

Figure A-66. Departure to the South, 400' Directly Above Helipad, Very Low Obstacle Density

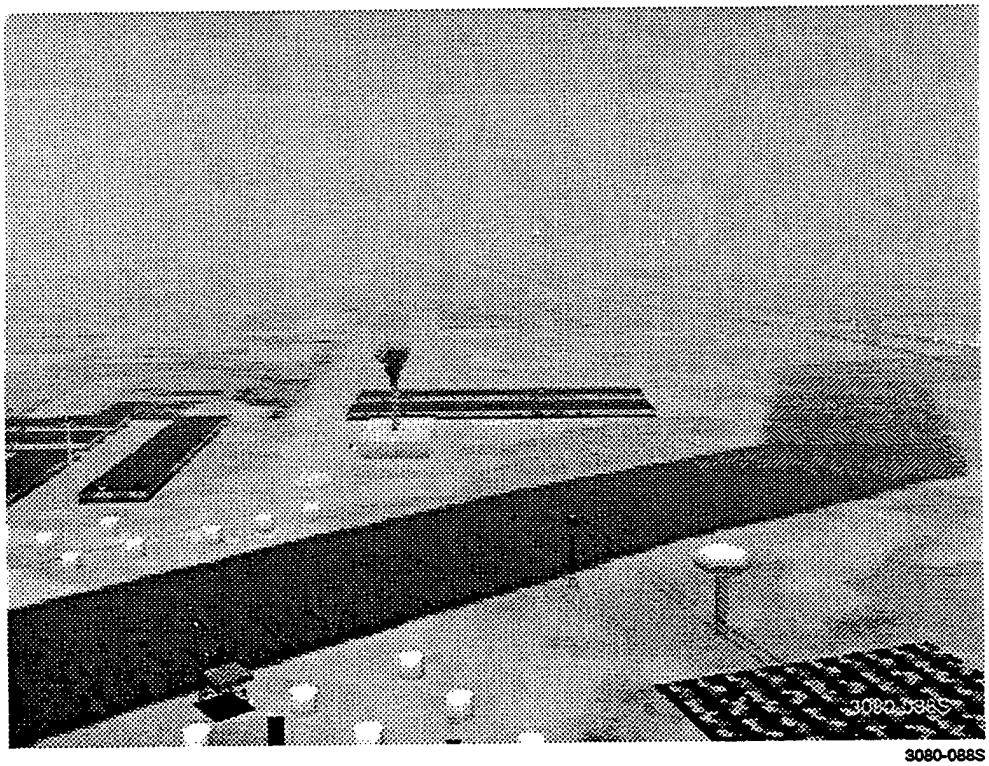

3080-088S

Figure A-67. Departure to the South, 600' Above Helipad, 1000' South of Helipad, High Obstacle Density

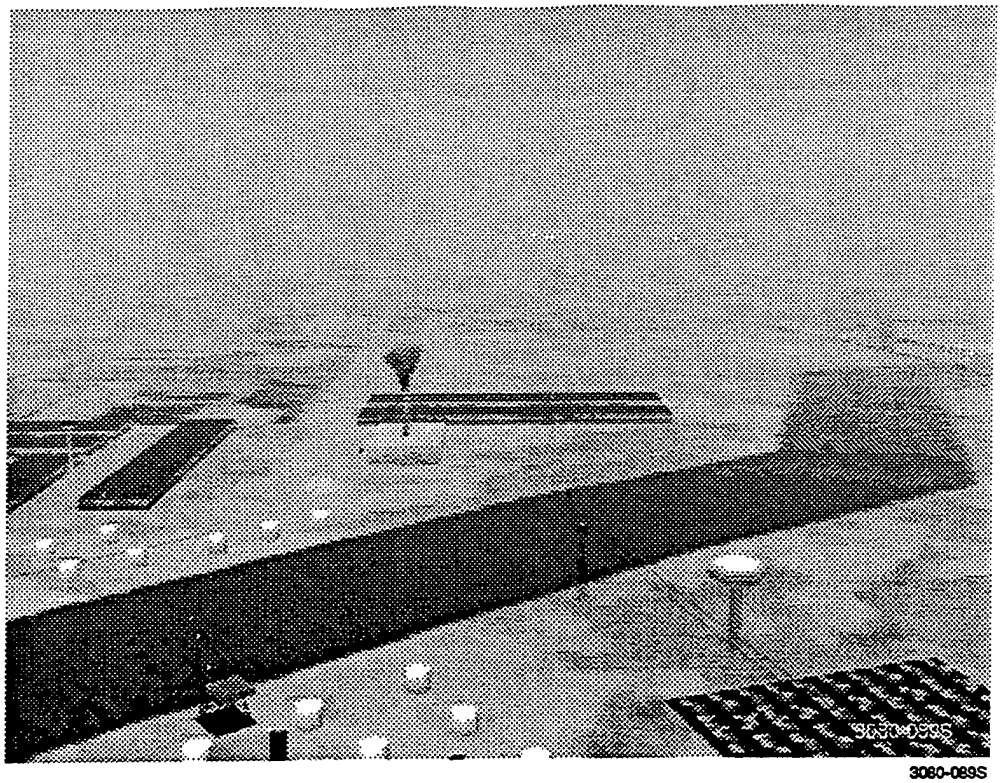

3080-089S

Figure A-68. Departure to the South, 600' Above Helipad, 1000' South of Helipad, Medium Obstacle Density

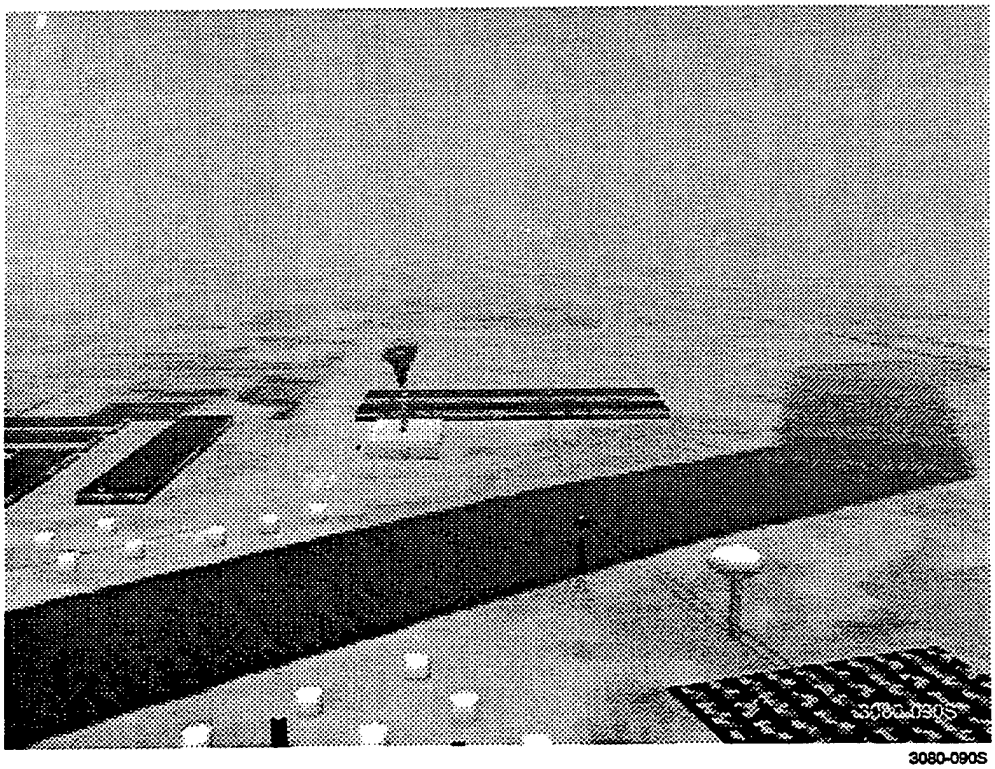

3080-090S

Figure A-69. Departure to the South, 600' Above Helipad, 1,000 South of Helipad, Low Obstacle Density

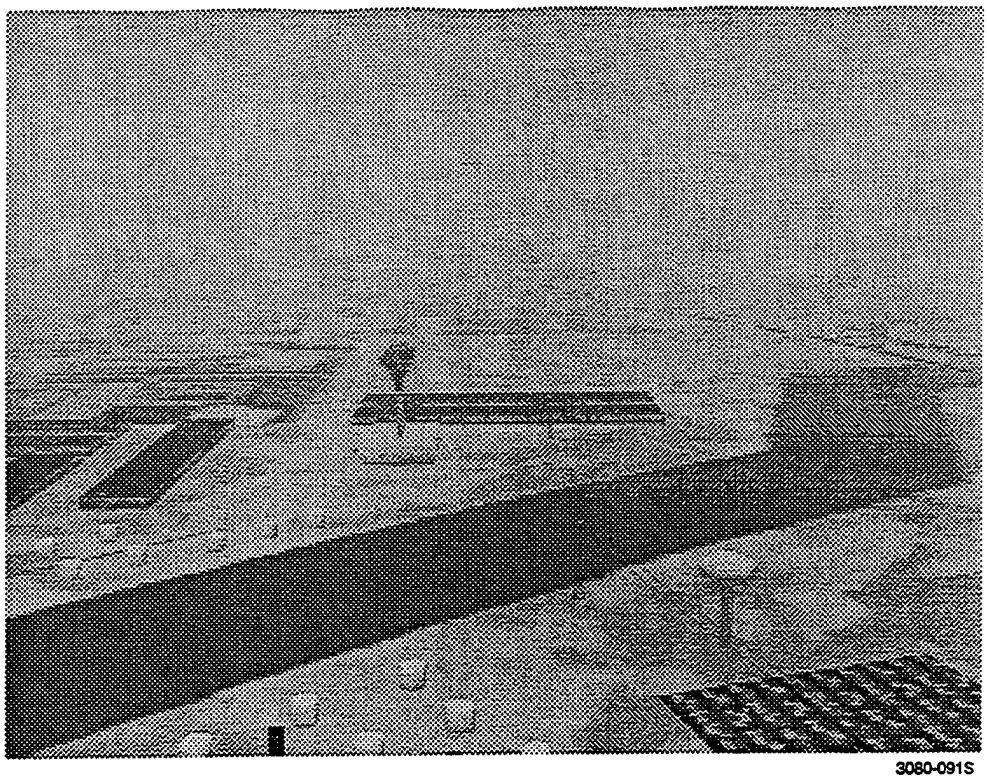

3080-091S

Figure A-70. Departure to the South, 600' Above Helipad, 1000' South of Helipad, Very Low Obstacle Density

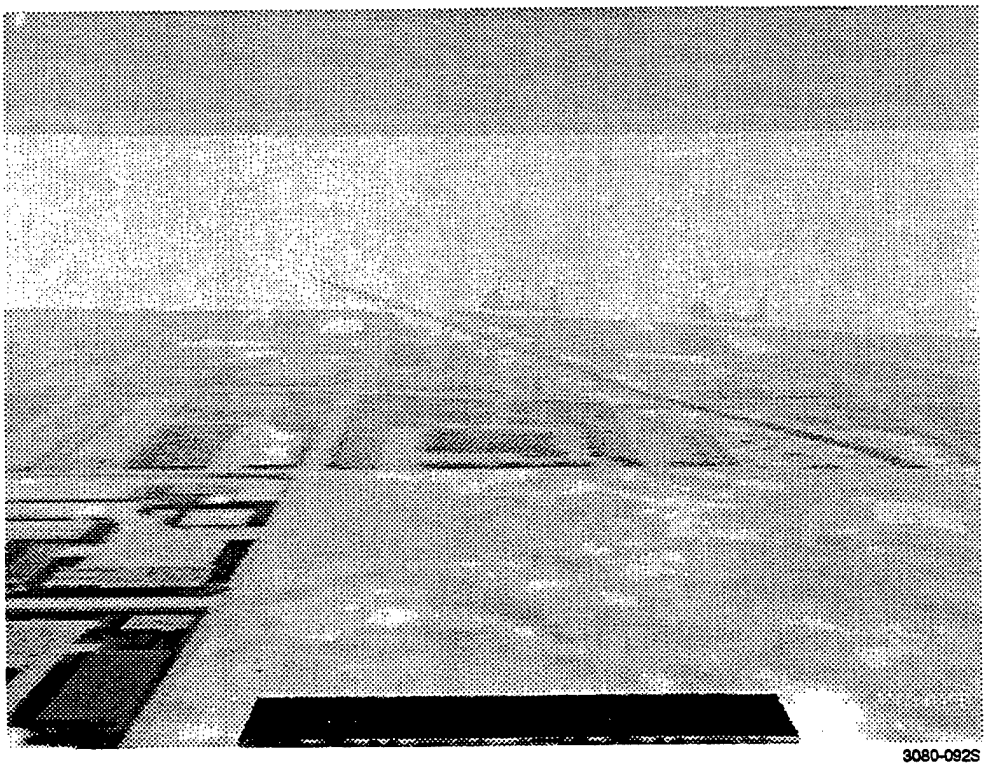

3080-092S

Figure A-71. Departure to the South, 800' Above Helipad, 2,500' South of Helipad, High Obstacle Density

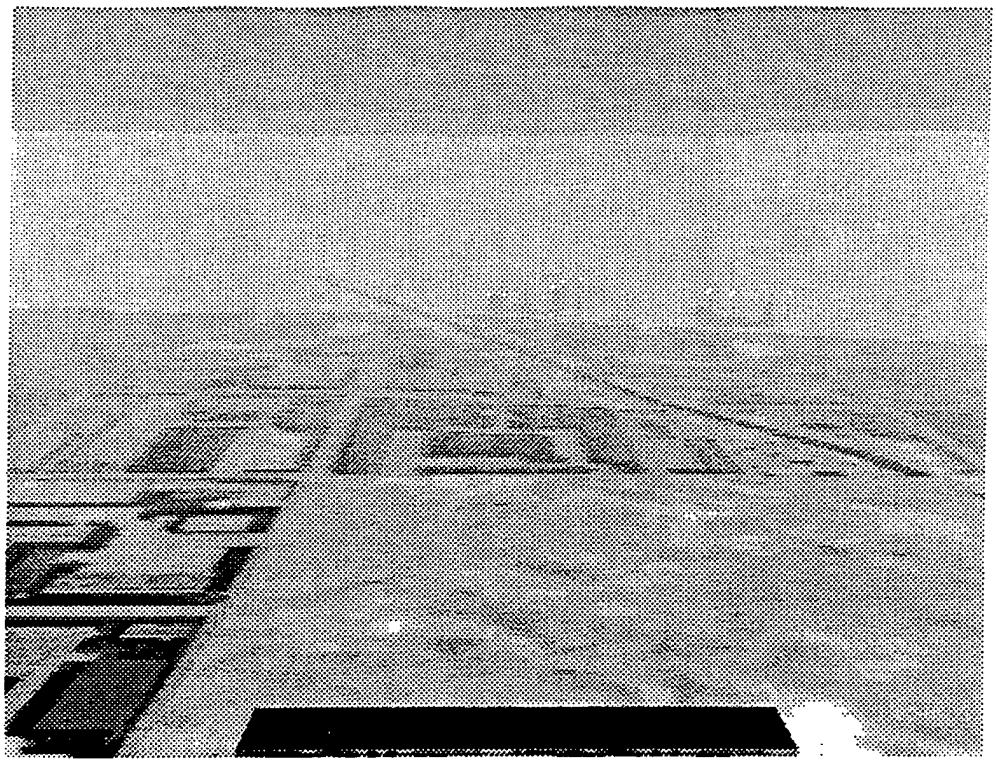

3080-093S

Figure A-72. Departure to the South, 800' Above Helipad, 2,500' South of Helipad, Medium Obstacle Density

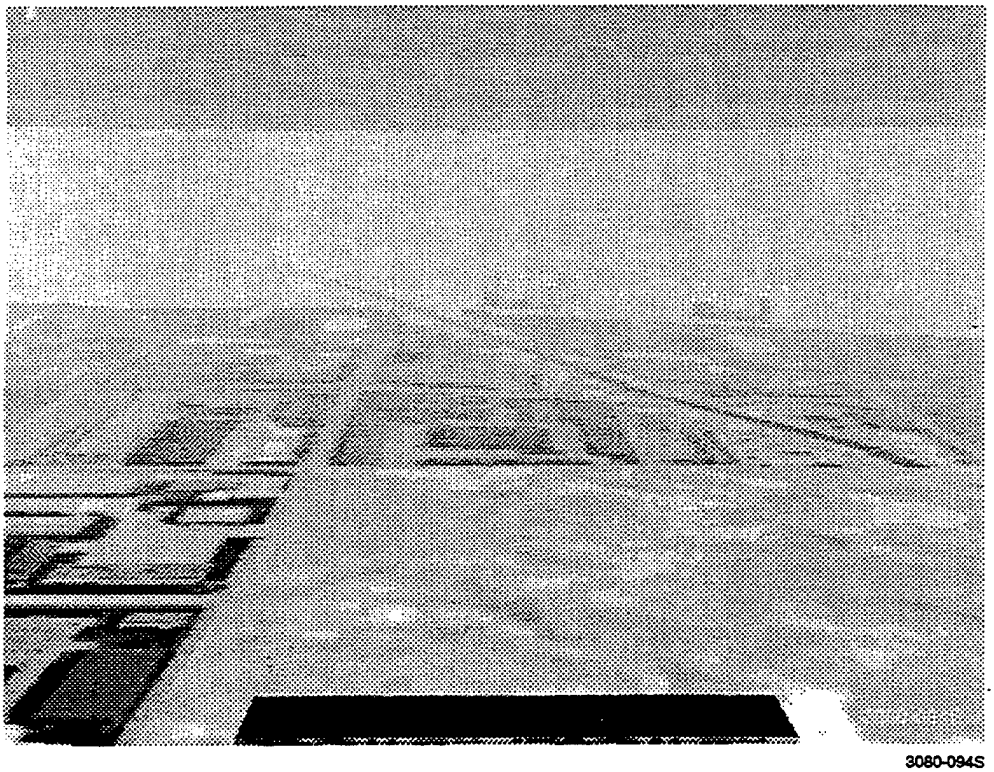

3080-094S

Figure A-73. Departure to the South, 800' Above Helipad, 2,500' South of Helipad, Low Obstacle Density

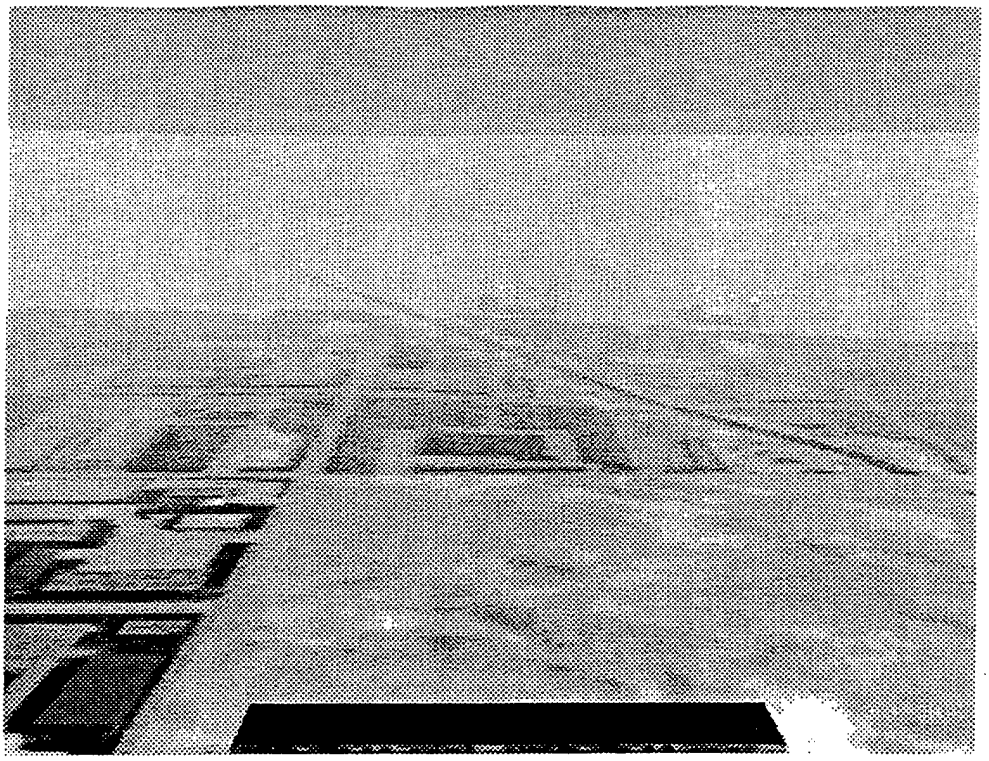

3080-095S

Figure A-74. Departure to the South, 800' Above Helipad, 2,500 South of Helipad, Very Low Obstacle Density

Appendix B. Pilot Information Survey

PILOT INFORMATION SUMMARY

The following information is requested to assist in the collection of data and assessment of results for the study of Obstacle Rich Environments. Your participation and honest answers are very important to the safe operation in and development of future heliport environments. Your answers and performance will remain confidential.

Name:_____ Date:_____

Class Medical Held:_____ Date of last Medical: _____

Certificates held and year of issue:_____

_____

Type ratings held, year of issue, and time in type:_____

_____

Total Time:_____	**Helicopter:**_____	**Airplane:** _____
PIC:_____	PIC:_____	PIC:_____
CFI:_____	CFI: _____	CFI: _____
Instrument:_____	Instrument:_____	Instrument:_____
Night:_____	Night:_____	Night:_____
Simulator:_____	Simulator:_____	Simulator:_____
EMS:_____	EMS:_____	EMS:_____
Single-pilot :_____	Single-pilot :_____	Single-pilot :_____
Civilian:_____	Civilian:_____	Civilian:_____
Military:_____	Military:_____	Military:_____

Flight time last 60 days: Helicopter: _____ Airplane: _____

Instrument: _____ Night: _____Types and number of hrs. _____

_____

Briefly describe your experience with and the approximate hours of operation in obstacle rich environments (environments with large densities of objects potentially hazardous to flight). _____

_____

_____

Have you ever had an incident or an accident due to an obstacle? (If so, please describe briefly.) _____

_____

_____

Present employer? _____ Responsibilities: _____

_____

Previous employer? _____ Responsibilities: _____

_____

Briefly describe your training background. (specifically military and/or civilian training):

_____

_____

Military service history (if applicable): _____

_____

Associations and professional activities: _____

_____

Appendix C. Short-Form Questionnaire

ORE WORKLOAD RATING SCALES
(Complete after each mission)

1. How much mental and perceptual activity (e.g. thinking, deciding, calculating, remembering, looking, searching, etc.) was required during the last landing or takeoff?

1	2	3	4	5	6	7
low activity						high activity

2. How much physical activity (e.g. pushing, pulling, turning, controlling, activating, etc.) was required during the last landing or takeoff?

1	2	3	4	5	6	7
low activity						high activity

3. How much time pressure did you feel due to the rate of pace at which the flight tasks occurred during the last landing or takeoff?

1	2	3	4	5	6	7
low time pressure						high time pressure

4. How successful did you think you were in performing your last landing or takeoff?

1	2	3	4	5	6	7
excellent performance						poor performance

5. How hard did you have to work (mentally and physically) to perform your last landing?

1	2	3	4	5	6	7
low effort						high effort

6. How insecure, discouraged, irritated, stressed, and annoyed, verses secure, gratified, content, relaxed ,and complacent did you feel during your last landing or takeoff.

1	2	3	4	5	6	7
low frustration						high frustration

7. How safe (in terms of risk) was the last landing or takeoff?

1	2	3	4	5	6	7
very safe						not at all safe

8. To what degree did the obstacles presented create a safety hazard?

1	2	3	4	5	6	7
not at all hazardous						very hazardous

Appendix D. Intermediate Questionnaire

Intermediate Questionnaire

(To be filled out during breaks between sessions)

Pilot #: _____

Date: _____

Time: _____

Run numbers covered: _____

Session Number:_____

1. What factors were responsible for your perceived level of risk during the last session of landings or takeoffs?

2. What outside visual cues were useful to you for the successful completion of the last session of landings or takeoffs?

3. Please indicate the aircraft's clearance to the closest obstacle on the preceding runs, and specify the obstacles.

4. Are there any additional comments that you wish to add concerning the last session of landings or takeoffs?

Appendix E. Long-Form Questionnaire

PILOT QUESTIONNAIRE

(To be completed at the conclusion of experiment)

Risk Assessment

1. What obstacles pose the greatest threat to safety in the, Downwind, and Base segment of flight?

2. What obstacles pose the greatest threat to safety in the Departure segment of flight?

3. What obstacles pose the greatest threat to safety in the Final segment of flight?

4. What obstacles pose the greatest threat to safety in the Hover and Taxi segment of flight?

5. What is the most dangerous segment of flight?

   With obstacles?

   Without obstacles?

6. Does limited visibility increase stress more for known or unknown obstacles?

7. Did your ability to cope with in-flight situations (e.g., system failures, traffic avoidance, aircraft emergencies) change with higher densities of obstacles? If so, how?

The following four questions refer to potential obstacles during take-offs and landings:

8. Rank the following obstacles in relationship to aircraft or occupant safety. (1 = over-flight most dangerous; 10 = least dangerous)

_____ Antenna	_____ Railroad Yard
_____ Skyscraper	_____ Smoke Stack
_____ Road	_____ Poles & Wires
_____ Full Stadium	_____ School
_____ Dense Woods	_____ Housing Development

9. Rank the following obstacles in relationship to safety of persons on the ground. (1 = over-flight most dangerous; 10 = least dangerous)

_____ Antenna	_____ Railroad Yard
_____ Skyscraper	_____ Smoke Stack
_____ Road	_____ Poles & Wires
_____ Full Stadium	_____ School
_____ Dense Woods	_____ Housing Development

10. Rank the following in terms of avoidance priorities. (1= most important to avoid; 8 = least important)

_____ Required noise avoidance areas
_____ Densely populated areas (Schools, full Stadiums, etc.)
_____ Potential obstacle areas
_____ Fly friendly noise avoidance areas
_____ Obstacles that would be a hazard in the event of an engine failure
_____ Populated areas (housing communities)
_____ ATC required avoidance areas
_____ Obstacles that create a known hazard to flight
_____ No fly area
_____ Restricted areas
_____ Uncontrolled airports

11. Are there any other things that you would classify as an "obstacle" that are not listed above?

12. What percentage of your normal flight operations are performed within, what you would consider, an obstacle rich environment (ORE)?

13. Please list some of the high risk areas for an ORE that you have experienced and why you consider them to be high risk.

Simulation scenarios just completed

14. What were the visual cues that helped you identify the obstacles and their potential threat to the aircraft?

15. What instruments did you rely upon during the approaches to ensure a successful approach and landing?

16. What other items did you rely upon during the approaches to ensure a successful approach and landing? (Consider internal and external cues and factors.)

17. What features of the landing zone assisted or detracted from the departures?

18. What features of the landing zone assisted or detracted from the approaches?

Training for ORE Environments

19. Did you feel the official certified training that you received in the past for your ratings has adequately prepared you for the flights you just completed?

20. Do you feel additional training would reduce the risks of operation within an ORE?

21. Is there additional instruction that you would recommend for operations within an ORE and should this additional training or specialized training be required to operate within an ORE?

22. Do you feel a "checkride" is required for operation into or for lower minimums in an ORE environment?

Simulation Fidelity

23. On a scale of one to seven please rate each of the following for achievement of realistic conditions: (1 = simulation achieved realistic conditions; 7 = simulation failed to achieve realistic conditions)

____ Ambient light conditions day
____ Ambient light conditions night
____ Visibility
____ Motion of out-the-widow display
____ Terrain features
____ Man-made features
____ Aircraft response
____ Scenario realism
____ Communications
____ Cockpit
____ Wind

24. Overall, was the simulation a realistic portrayal of flight conditions? Comments?

25. How would you have flown any of the approaches or departures differently if you had flown them in a helicopter rather than a helicopter simulator? (Include as an option avoiding the approach or departure entirely.)

The ORE investigation team and the FAA thank you for participating in our study. There is additional room at the end of this sheet and on the back of this questionnaire for additional comments. Please feel free to comment on general observations concerning the different scenarios, heliport lighting options, fidelity of the simulation, concerns about generalization of the results, and suggestions for improvements to the simulation. Please help us to obtain true results by not discussing your experiences with pilots who have not yet taken part in our experiment.

Appendix F. Emergency Response Pilot Score Sheet

Pilot Score Sheet

Response Time:

Initial recognition of fault:

# & type of E.P.	0-3 sec	3-10 sec	10-20 sec	20-60 sec	60+ sec
1 - _____	5	4	3	2	1
2 - _____	5	4	3	2	1
3 - _____	5	4	3	2	1
4 - _____	5	4	3	2	1
5 - _____	5	4	3	2	1
6 - _____	5	4	3	2	1
7 - _____	5	4	3	2	1
8 - _____	5	4	3	2	1

Time to regain control of situation:

# of E.P.'s	0-15 sec	15-30 sec	30-45 sec	45-60 sec	60+ sec
1	5	4	3	2	1
2	5	4	3	2	1
3	5	4	3	2	1
4	5	4	3	2	1
5	5	4	3	2	1
6	5	4	3	2	1
7	5	4	3	2	1
8	5	4	3	2	1

Response Actions:

not very successful.....very successful

- Assesses all factors affecting situation:

1 1.....2.....3.....4.....5

2 1.....2.....3.....4.....5

3 1.....2.....3.....4.....5

4 1.....2.....3.....4.....5

5 1.....2.....3.....4.....5

6 1.....2.....3.....4.....5

7 1.....2.....3.....4.....5

8 1.....2.....3.....4.....5

not very successful.....very successful

- Evaluate situation with respect to published emergency procedure:

1	1.....2.....3.....4.....5
2	1.....2.....3.....4.....5
3	1.....2.....3.....4.....5
4	1.....2.....3.....4.....5
5	1.....2.....3.....4.....5
6	1.....2.....3.....4.....5
7	1.....2.....3.....4.....5
8	1.....2.....3.....4.....5

- Correctly identifies extraordinary condition:

1	1.....2.....3.....4.....5
2	1.....2.....3.....4.....5
3	1.....2.....3.....4.....5
4	1.....2.....3.....4.....5
5	1.....2.....3.....4.....5
6	1.....2.....3.....4.....5
7	1.....2.....3.....4.....5
8	1.....2.....3.....4.....5

- Maintains aircraft control out of potentially dangerous attitude or position:

1	1.....2.....3.....4.....5
2	1.....2.....3.....4.....5
3	1.....2.....3.....4.....5
4	1.....2.....3.....4.....5
5	1.....2.....3.....4.....5
6	1.....2.....3.....4.....5
7	1.....2.....3.....4.....5
8	1.....2.....3.....4.....5

	not very successful.....very successful

- Maintains aircraft within recommended aircraft limitations:

1	1.....2.....3.....4.....5
2	1.....2.....3.....4.....5
3	1.....2.....3.....4.....5
4	1.....2.....3.....4.....5

5	1.....2.....3.....4.....5
6	1.....2.....3.....4.....5
7	1.....2.....3.....4.....5
8	1.....2.....3.....4.....5

- Provides satisfactory level of safety throughout extraordinary condition:

1	1.....2.....3.....4.....5
2	1.....2.....3.....4.....5
3	1.....2.....3.....4.....5
4	1.....2.....3.....4.....5
5	1.....2.....3.....4.....5
6	1.....2.....3.....4.....5
7	1.....2.....3.....4.....5
8	1.....2.....3.....4.....5

Comments:

Appendix G. Pilot Briefing Packet

ORE TEST PROTOCOL INSTRUCTIONS

Good morning/afternoon. My name is _____, and I am a member of the Boeing Research Team for this study.

Thank you for taking the time to participate in the obstacle rich environment simulation study. You were given a pre-flight packet that explained today's activities. Right now I will review some additional material with you.

The goal of this project is to support the Federal Aviation Administration to determine the effect of obstacle rich environments on pilot workload and flight safety. The obstacle rich environment simulator presents a high fidelity representation of an operational heliport that allows variation of obstacle densities and heights. The results of this study will help determine solutions for enhancing operational benefits of vertical flight aircraft subject to heliport airspace regulations.

The simulator is a generic multi-engine helicopter with fixed gear. The cockpit is similar to most helicopters but it contains only the instrumentation and gauges to satisfy experiment requirements. I will explain the simulator in more detail in just a few minutes.

You will be the only pilot in the simulator. Your total time will extend across two days, requiring approximately 8 hours each day. Your time in the simulator each day will consist of four 1 hour segments. Each segment will consist of four approach and departure missions, 8 missions total. During each flight we will be collecting physiological data including heart rate, breathing rate, and blink rate. This will require fixing non-intrusive electrodes to your face and chest. We will explain the physiological data collection methods in detail during the familiarization trial.

After each mission you will asked to assess the workload you experienced. At the end of each session you will be asked to fill out an intermediate questionnaire form that will ask you perceptions of the last series of runs. A description of workload is also included in this packet. Upon completing all missions on the simulator, a researcher will debrief and interview you concerning the study. The debriefer will also have you fill out a biographical information questionnaire for background purposes.

Again, the purpose of this study is to gain information that will be used to establish heliport airspace regulations. In no way is the study an evaluation of your professional performance. The flight segments will also be videotaped to allow further detailed review and to ensure the data we record are complete and correct.

For purposes of the experiment, your test data will be identified by a number. Your name will not be associated with your data. All data we collect from you, the video tapes, and the debrief data will be held in confidence and used for research purposes only. You will not be identified in any reports that are written as a result of this study.

A test administrator will describe the testing procedures in detail to you the day of your scheduled flights. If you have any questions, please ask the test administrator prior to beginning the study.

Once again, thank you for your participation.

BOEING HELICOPTER SIMULATION TEST

OBSTACLE RICH ENVIRONMENTS

PRE-FLIGHT PACKET

Thank you for taking the time to participate in the obstacle rich environment study. Please review this entire packet and complete all necessary information prior to arriving at the Boeing facility.

Your packet should include the following items:

1. INTRODUCTION
2. LIFEFLIGHT 911 HELICOPTER OPERATIONS FLIGHT MANUAL
3. WORKLOAD RATING SCALES
4. DAILY SCHEDULE
5. PILOT INFORMATION SUMMARY

BOEING HELICOPTER SIMULATION TEST

OBSTACLE RICH ENVIRONMENTS

INTRODUCTION

The goal of this project is to support the Federal Aviation Administration (FAA) to determine the effect of obstacle rich environments on pilot workload and flight safety and pilot perceptions of workload and flight safety. An obstacle rich environment is an area of airspace with a high density of obstacles that are potentially hazardous to flight yet still comply with Federal Aviation Administration guidelines regarding obstacles. The obstacle rich environment simulator presents a high fidelity representation of an operational heliport that allows variation of obstacle densities and heights. The results of this study will help determine solutions for enhancing the operational benefits of vertical flight subject to heliport airspace regulations.

The simulator is configured to represent a generic multi-engine helicopter with fixed gear. The cockpit is similar to most helicopters but it contains only the instrumentation and gauges to satisfy experiment requirements. A more detailed description of the helicopter configuration modeled in the simulator is included in this packet.

You will be the only pilot in the simulator. Your total time will extend across two days, requiring approximately 8 hours each day. Your time in the simulator each day will consist of four 1 hour segments. Each segment will consist of four approach and departure missions, 8 missions total. Please review the LifeFlight 911 Helicopter Operations Flight Manual before arriving at the test. The manual provides necessary instructions, maps, and emergency procedures required to fly your missions.

During each flight we will be collecting physiological data including heart rate, breathing rate, and blink rate. We will explain the physiological data collection methods in detail during the initial briefing and familiarization trial. Your performance will be assessed as a function of workload. Your performance will be determined from deviations from specified route corridors, proper use of radio communications, and procedures used when dealing with emergency procedures. After each mission you will asked to assess the workload you experienced. A description of workload is also included in this packet. At the end of each session you will be asked to fill out an intermediate questionnaire form that will ask you perceptions of the last series of runs. Upon completing all missions on the simulator, a researcher will debrief and interview you concerning the study. The debriefer will also have you fill out a post-experiment questionnaire that will help assess the safety and fidelity of the simulator.

Again, the purpose of this study is to gain information that will be used to establish heliport airspace regulations. In no way is the study an evaluation of your personal performance. The flight segments will also be videotaped to allow us to review it in detail at a future date, to ensure the data we record are complete and correct.

For purposes of the experiment, your test data will be identified by a number. Your name will not be associated with your data. All data we collect from you, the video tapes, and the debrief

data will be held in confidence and used for research purposes only. You will not be identified in any reports that are written as a result of this study.

A test administrator will describe the testing procedures in detail to you the day of your scheduled flights. A meal of cold sandwiches will be provided. However, if this does not suite your needs please make arrangements to bring your own meals. If you have any questions, please ask the test administrator prior to beginning the study. Once again, thank you for your participation.

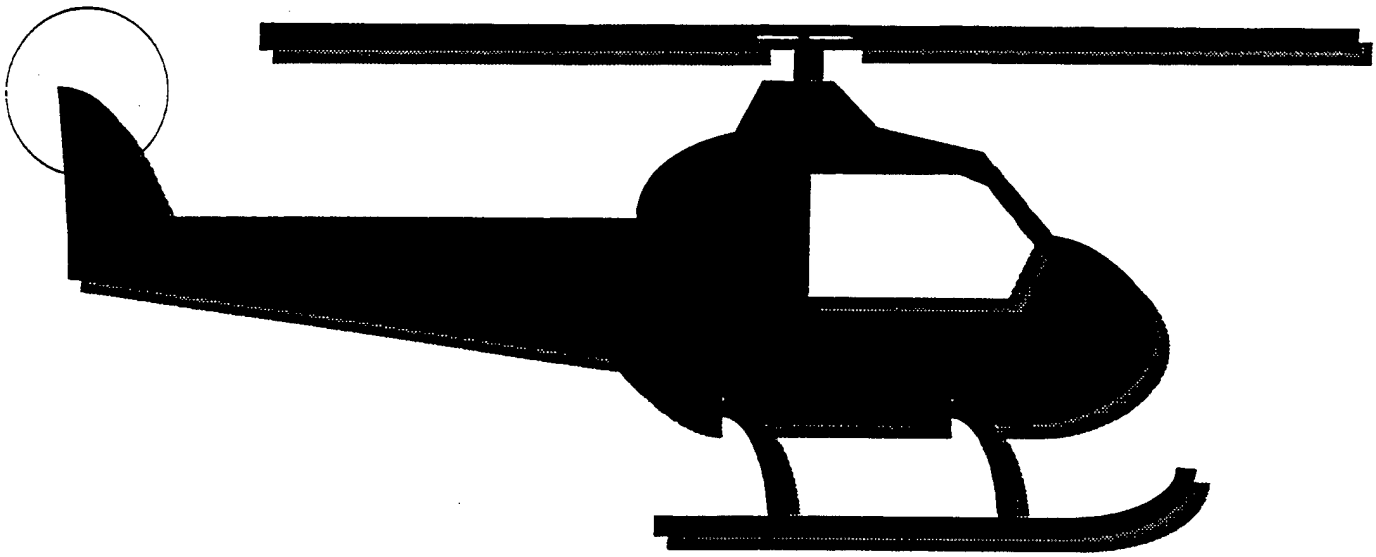

OR-E0
Helicopter

OPERATORS FLIGHT MANUAL

AIRCRAFT SIMULATOR DESCRIPTION

The simulation helicopter is a generic multi-engine helicopter with fixed gear. The aircraft is equipped with full VFR flight instruments, but avionics and gauges are limited to only those which will satisfy the experimental conditions. Requirements for cockpit checks and switch positions will be satisfied by verbally stating normal procedures. The use of the transponder with squawk codes will be performed verbally. Emergency procedures will be scored by reference to the emergency procedures provided, use of best judgment, and safety of aircraft occupants. The helicopter is equipped with a 4-axis stability augmentation system and cyclic and yaw beep trim and trim switch. Position of switches will be detailed in the cab orientation. The aircraft is at max gross weight and limitations are per the LifeFlight 911 helicopter flight manual.

Approach control, UNICOM, and company radio calls will be required and counted in overall performance evaluations. Your call sign will be "LifeFlight 911". The radio calls will be made via the VHF radio with selected and stand-by frequencies. Selection and swap of frequencies is accomplished with use of the cooley hat on the collective. The cyclic has a trigger switch that must be depressed upward for radio transmissions and administrative communications. A cockpit voice recorder will record "hot-mike" and ATC transmissions.

The simulator used for this study is an engineering research simulator. It is not an operational training simulator, as not all of the features of the simulator are entirely realistic. During the course of the experiment, if you experience a phenomenon that you feel is not realistic, please react as if it were. You will have an opportunity later to comment on the fidelity of the simulator.

For instance, the simulation helicopter is a generic multi-engine helicopter with fixed gear. The landing gear, however, do not react quite like skids, although you are asked to execute the mission as if they were. For this reason the approach and landing simulation task is considered to end at touchdown. At that point you may press the stop button on the cyclic to terminate the run.

The simulator is fixed-base, meaning that no acceleration cues are simulated at the cockpit. Motion cueing is provided by the out-the-window imagery. You may sense a mismatch because you do not feel the accelerations in the motion you can see. If you feel ill due to this perceived mismatch, you are asked to alert on of the researchers. This is not a reflection on pilot skill, but rather a recognition of the mismatch of motion cues.

Mission Description

Your mission is the transportation of a severely burned child, his mother, and your crew to (and from) St. Erway Hospital. The boy's condition is critical and the doctors have advised that any delays may impact on the chances of survival. The mission time is planned to be approximately 45 minutes. You have sufficient fuel for the mission and to any alternates if required.

Environment

The heliport is a joint use public and hospital heliport located just inside of Philadelphia airspace. Routing is severely limited due to a restricted area and several "no fly" areas that are extremely sensitive to noise and helicopter activity. Be aware that local police helicopters have been granted permission to fly in those areas. You will fly the approach and departure routes for both the valley and metro corridors under three lighting conditions (day light, dusk, night). An additional night condition is added to the approaches to evaluate the use of enhanced lighting conditions at night. Additionally, the flight scenarios are designed so that the ground based obstacles will vary in density and height. Each of the scenarios will require communication with Philadelphia approach control (119.7 or 124.5). The heliport is within a class B airspace with it's own UNICOM frequency of 123.0. The airspace becomes very crowded at times and all position reports for uncontrolled airports advised by the AIM are required. A discrete company frequency of 120.4 is available as required. Each approach will begin with a call to Philadelphia approach control. Your aircraft has been cleared into Class B airspace but radar contact has not yet been established. Departure routes begin with calls to UNICOM traffic and contact with Philadelphia approach control is required prior to reaching 600 ft. MSL.

In order to avoid the restricted area and the no-fly areas, helicopter routes have been established and must be strictly adhered to. The route that is initiated at the beginning of each run is required. Alternate routes cannot be requested or initiated. The routes you will be flying are as follows:

Corridor Approach Brief

METRO APPROACH:

I.C.- (Initial Condition)
Airspeed - 110 kts.
Heading - 180 deg
Altitude - 900 ft. MSL

From the I.C. proceed south tracking 180°. The Arboretum will soon come into view. Continue tracking 180° through the center of the Arboretum then directly over the Southwind Mall maintaining 900' MSL. After passing over the Mall turn west. Establish a base leg tracking west and no lower than 700 ft. MSL. You will see the bridge to your front and the stadium off to the right front. The alignment on final approach course is obtained by turning right and flying directly over and parallel with the power lines that cross over the river. The power lines are west of the power plant but, east of the stadium. If you pass the bridge or the stadium you have gone to far. Approach the pad by continuing to track 360° to the pad.

METRO DEPARTURE:

I.C.- (Initial Condition)
Hover Height - 5 ft.
Airspeed - 0 kts.
Heading - 180 deg

From the helipad depart south tracking 180°. Contact Philadelphia approach prior to reaching 600 ft. MSL. Continue climb to 700 ft. msl. After passing over the power plant turn left to 090°. The experiment run will terminate after the turn to the east.

VALLEY APPROACH:

I.C.-
Airspeed - 110 kts.
Heading - 030 deg
Altitude - 900 ft. MSL

The I.C. is a position over a factory adjacent to the railroad tracks. From I.C. proceed north-east above the railroad tracks. After flying over the factory next to the railroad tracks the lighted bridge will come in to view. The leg will continue along the railroad tracks past the cell phone towers and over another factory. The terrain rises in the area to the north so altitude discipline is critical. As soon as the microwave tower comes into to view depart the railroad tracks and turn toward the microwave tower. Enter the base leg by turning 090° after passing North of the tower. The base leg is flown at 900 ft MSL on a 090° track from the microwave tower until reaching the drive-in movie theater when a turn to the right is made. The alignment on final approach course is obtained by flying south directly between the twin towers at a minimum of 900 ft MSL. The descent is begun after passing over the twin towers. Continue tracking 180° to the pad.

VALLEY DEPARTURE:

I.C.- (Initial Condition)
Hover Height - 5 ft.
Airspeed - 0 kts.
Heading - 360 deg

From the helipad proceed north tracking 360°. Contact Philadelphia approach prior to reaching 600 ft. MSL. Continue climb to 900 ft. msl. After passing over and between the twin towers turn left to 270°. The experiment run will terminate after the turn to the west.

PLEASE NOTE

Navigation in the areas outside city center may be difficult especially at night. Please maintain vigilance to landmarks during practice sessions. Due to the requirement to counterbalance the runs between test subjects a night scenario may be initiated as a first run.

Emergency Conditions and Extraordinary Events

A series of emergency conditions and "extraordinary events" will be introduced at varied intervals. Your performance will be judged by your actions following the event. Compliance with published emergency procedures, reaction to potential obstacles, and judgment will be some of the items evaluated during emergency conditions and "extraordinary events".

Familiarization Training

You will be provided with approximately 30 minutes to become familiarized with the simulator. Provided below is the familiarization syllabus that will be completed prior to beginning the test.

OUTBOARD MFD

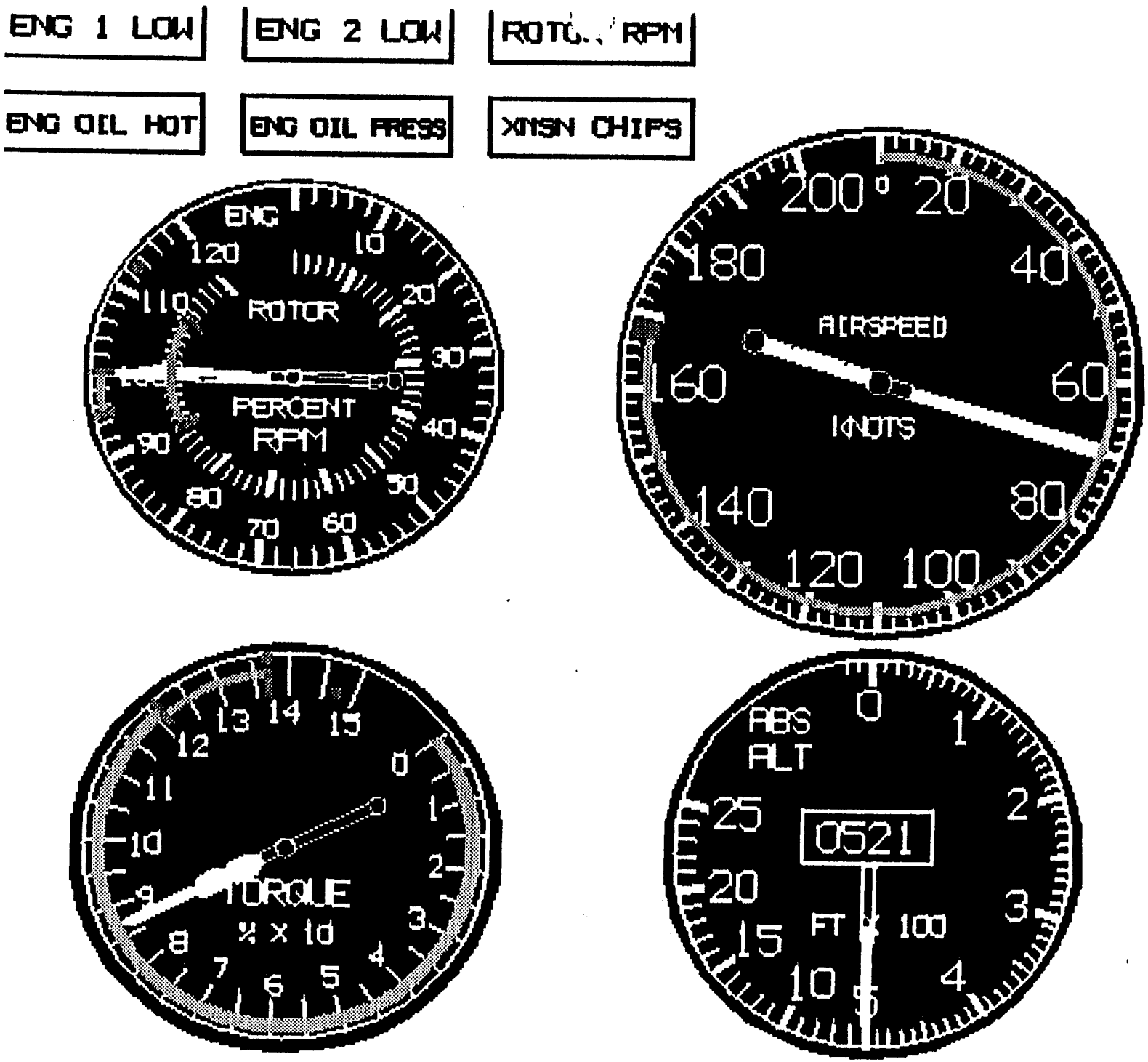

INBOARD MFD

G-12

SELECTED FREQUENCY	121.5
	TRANSMIT
STANDBY FREQUENCY	119.1
AIRSPEED	70 KIAS
ALTITUDE	798 FT
DISTANCE TO HELIPORT	1.7 NM

SCENARIO: 13
PILOT: 8 WIND: 3
ELAPSED TIME: 01:24
SEPTEMBER 24 1996 16:42

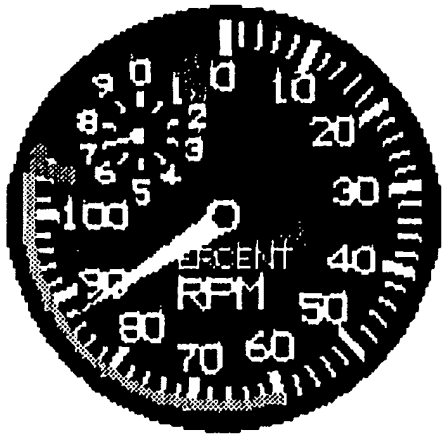

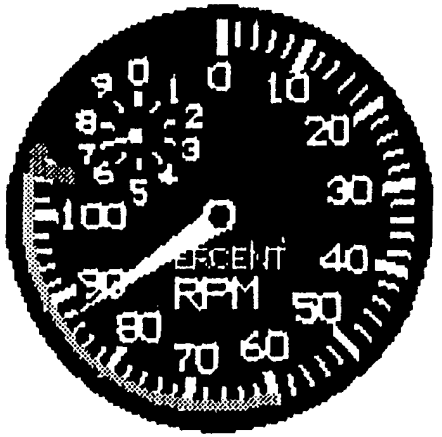

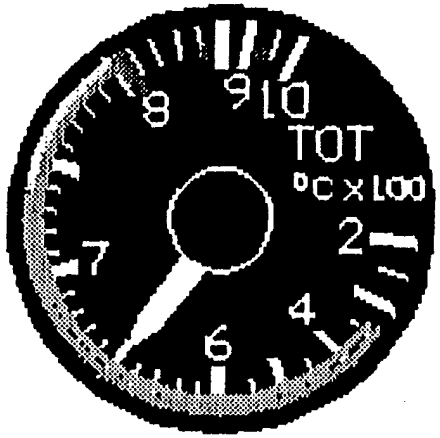

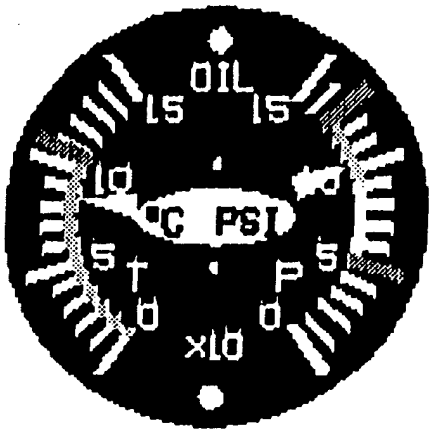

CENTER CONSOLE
G-13

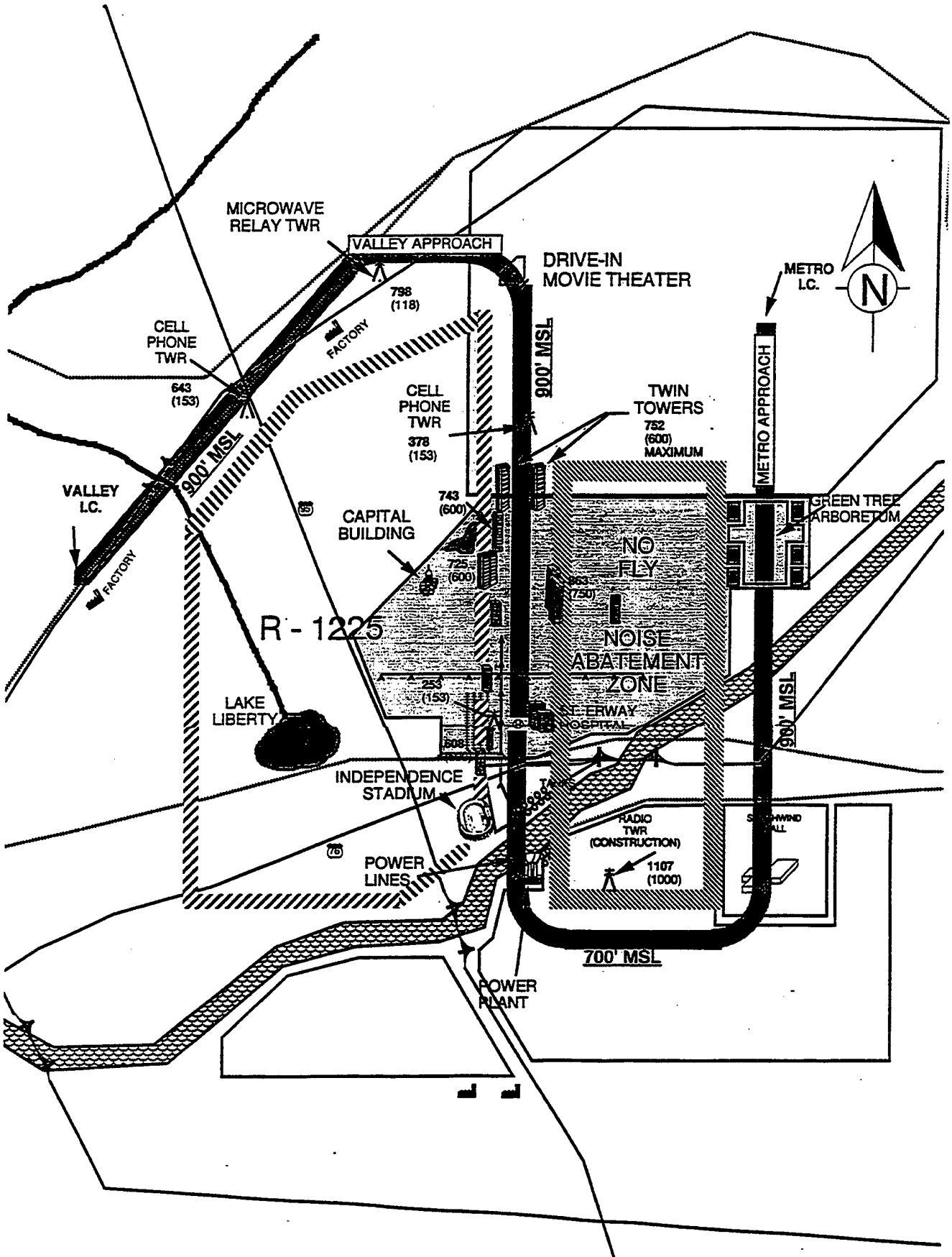

ORE HELICOPTER ROUTE CHART

TURBINE OUTLET TEMPERATURE (T.O.T.)

ALL ENGINES

(OUTER MARKING)

- 330 to 738°C Continuous
- 738 to 810°C Take off range
- 810°C Max. take off (5 min.)

ONE ENGINE INOPERATIVE (OEI)

(INNER MARKING)

- 330 to 810° C Continuous
- 810° C Maximum
- 843° C Transient (6 sec.)
- 927° C Starting

  Momentary peak (1 sec.)

  Not to exceed 10 sec. above 810°C

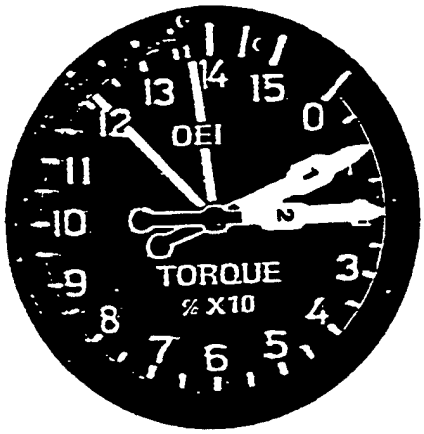

TORQUE

ALL ENGINES

(OUTER MARKING)

- 0 to 121% Continuous
- 121% Maximum
- 137% Transient (6 seconds)

ONE ENGINE INOPERATIVE (OEI)

(INNER MARKING)

- 0 to 137% Continuous
- 137% Maximum
- 147% Transient (10 seconds)

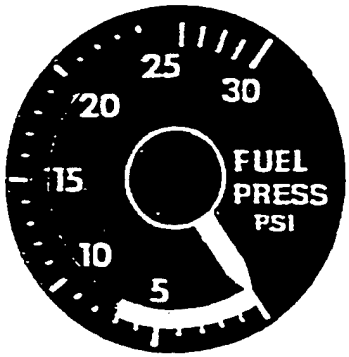

FUEL PRESSURE

- 0 to 7 PSI Cautionary
- 7 to 25 PSI Continuous
- 25 PSI Maximum

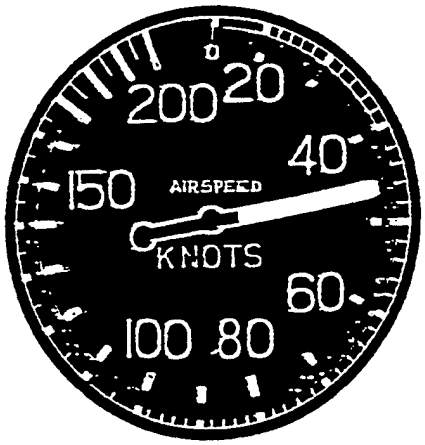

AIRSPEED

- 0 to 168 Kts IAS
- 168 Kts IAS Maximum

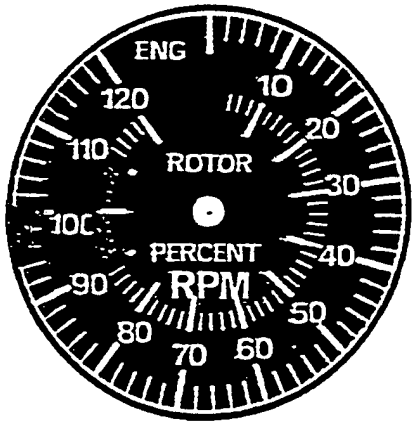

ENGINE & ROTOR RPM
POWER TURBINE (N2)

- 95% Minimum
- 95 to 100% Continuous
- 100% Maximum
- ● 113% Transient (15 seconds)

ROTOR

- 90% Minimum
- 90 to 110% Continuous
- 110% Maximum

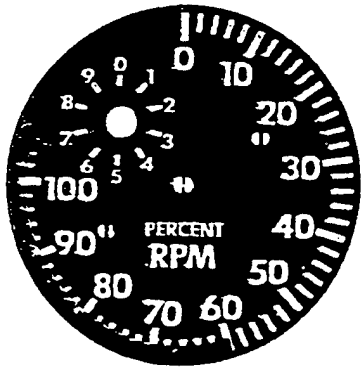

GAS PRODUCER

- 60 to 105% Continuous
- 105% Maximum
- ● 106% Transient (15 seconds)

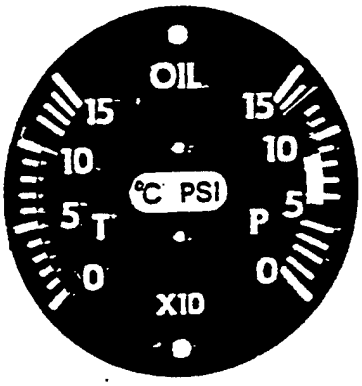

OIL PRESSURE (ENGINES)

- 50 PSI Minimum
- 50 to 90 PSI Cautionary
- 90 to 130 PSI Continuous
- 130 PSI Maximum

OIL TEMPERATURES (ENGINES)

- 0 to 107° C Continuous
- 107° C Maximum

OIL PRESSURE(TRANSMISSION)

- 30 PSI Minimum
- 30 to 50 PSI Continuous
- 50 to 70 PSI Cautionary
- 70 PSI Maximum

OIL TEMPERATURE (TRANSMISSION)

- 0 to 115° C Continuous
- 115° C Maximum

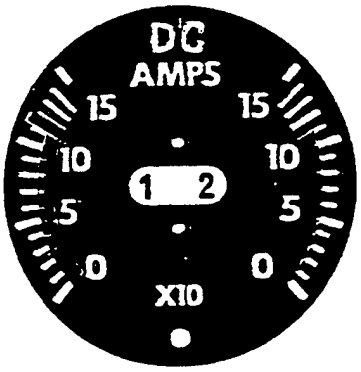

AMMETER

- 0 to 115 Amp Continuous
- 115 Amp Maximum
- 150 Amp Transient (20 sec.)

RATE OF CLIMB
SINGLE–ENGINE

MAXIMUM CONTINUOUS POWER
ROTOR RPM 100%
ANTI ICE OFF
ELECTRICAL LOAD – 115 AMPS TOTAL

BEST R/C AIRSPEED (SEE PERTINENT DIAGRAM)

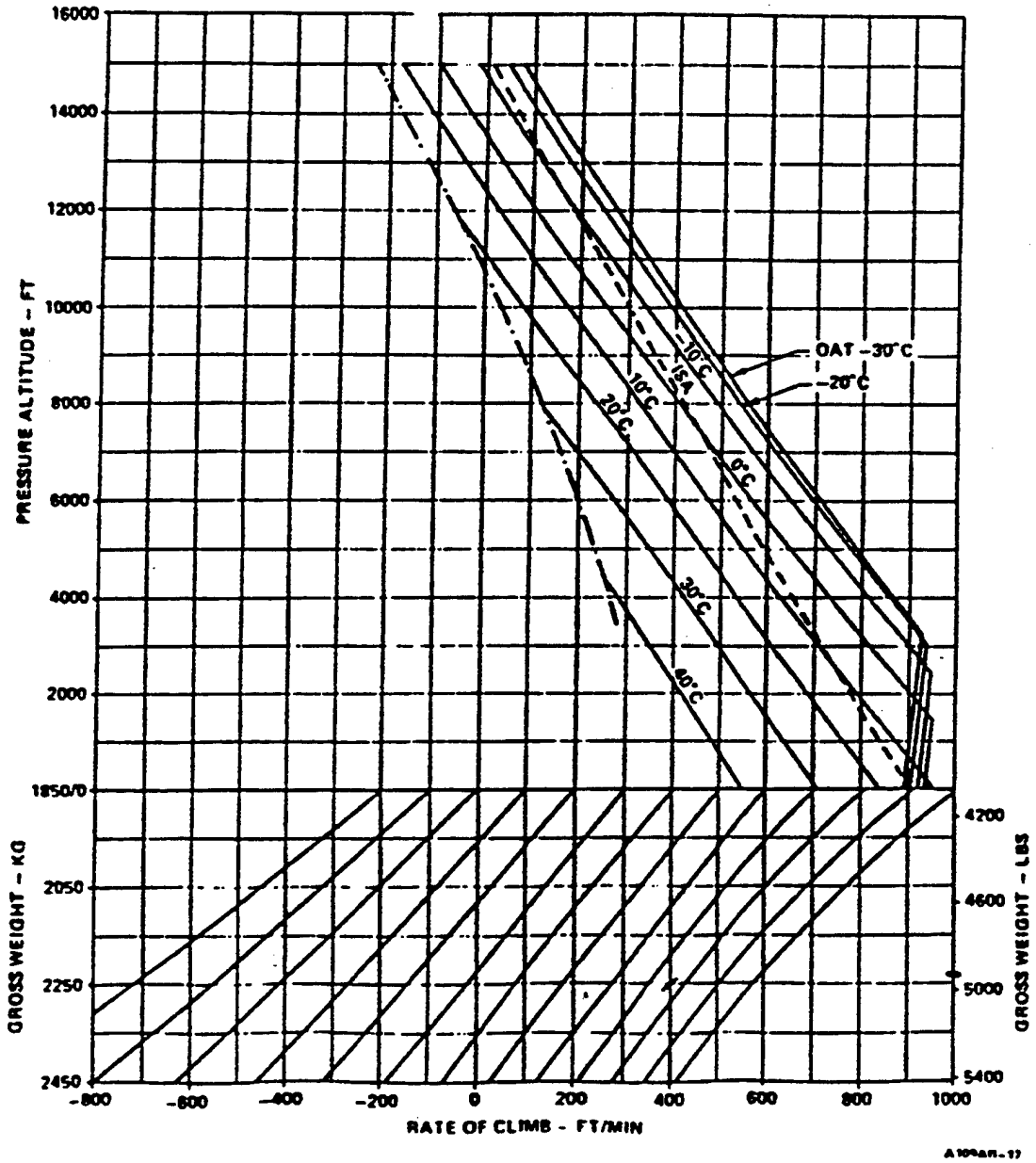

BEST RATE OF CLIMB AIRSPEED
SINGLE–ENGINE

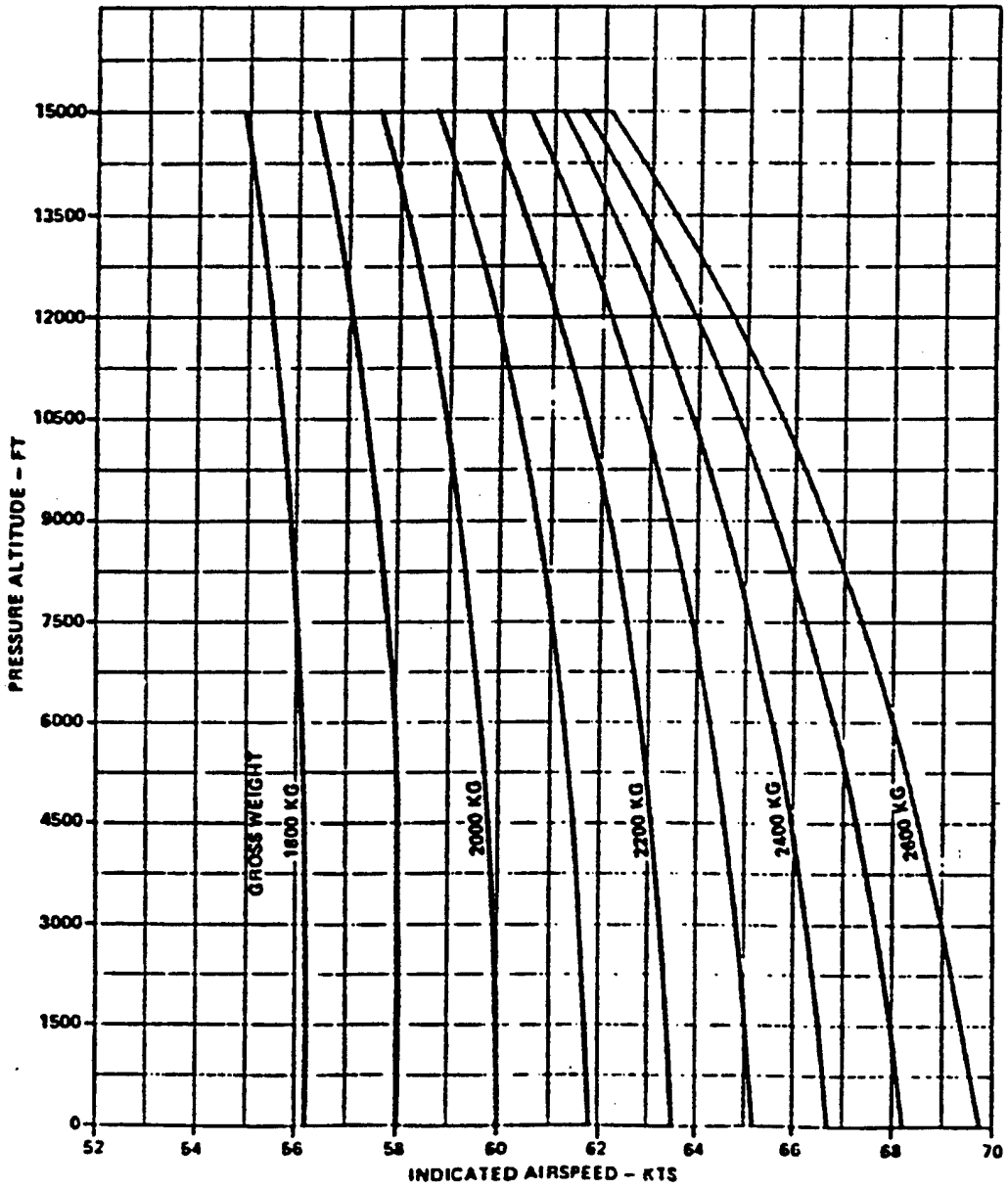

RATE OF CLIMB
ALL–ENGINES

TAKE OFF POWER — 60 KTS IAS
ROTOR RPM 100%
ANTI ICE OFF
ELECTRICAL LOAD - 115 AMPS TOTAL

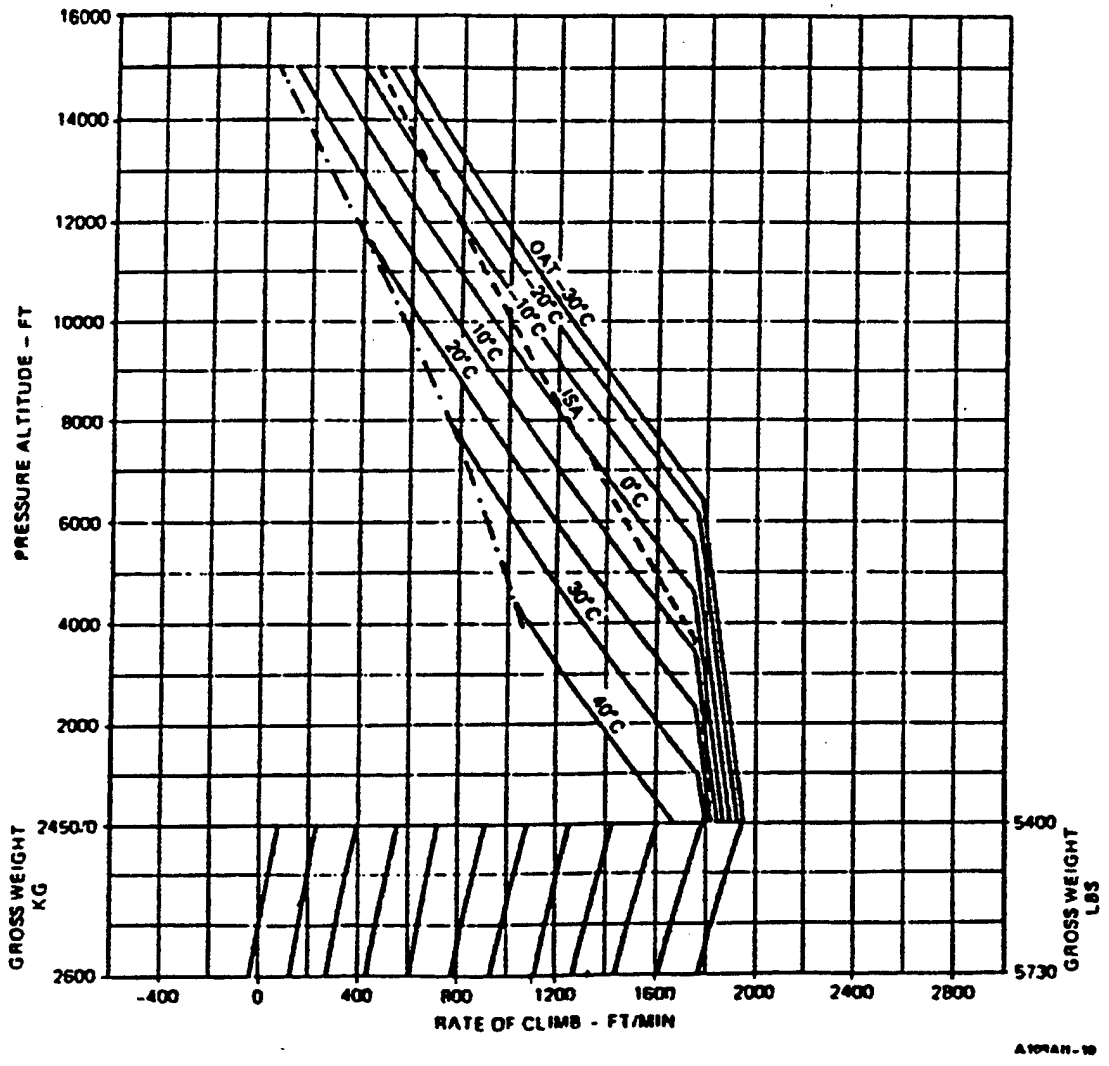

HEIGHT – VELOCITY DIAGRAM
(ONE ENGINE INOPERATIVE)

GROSS WEIGHT 2600 KG (5730 LBS)
APPLICABLE FOR LEVEL SOD OR HARD SURFACE
LANDING GEAR DOWN
AVOID OPERATION IN SHADED AREAS

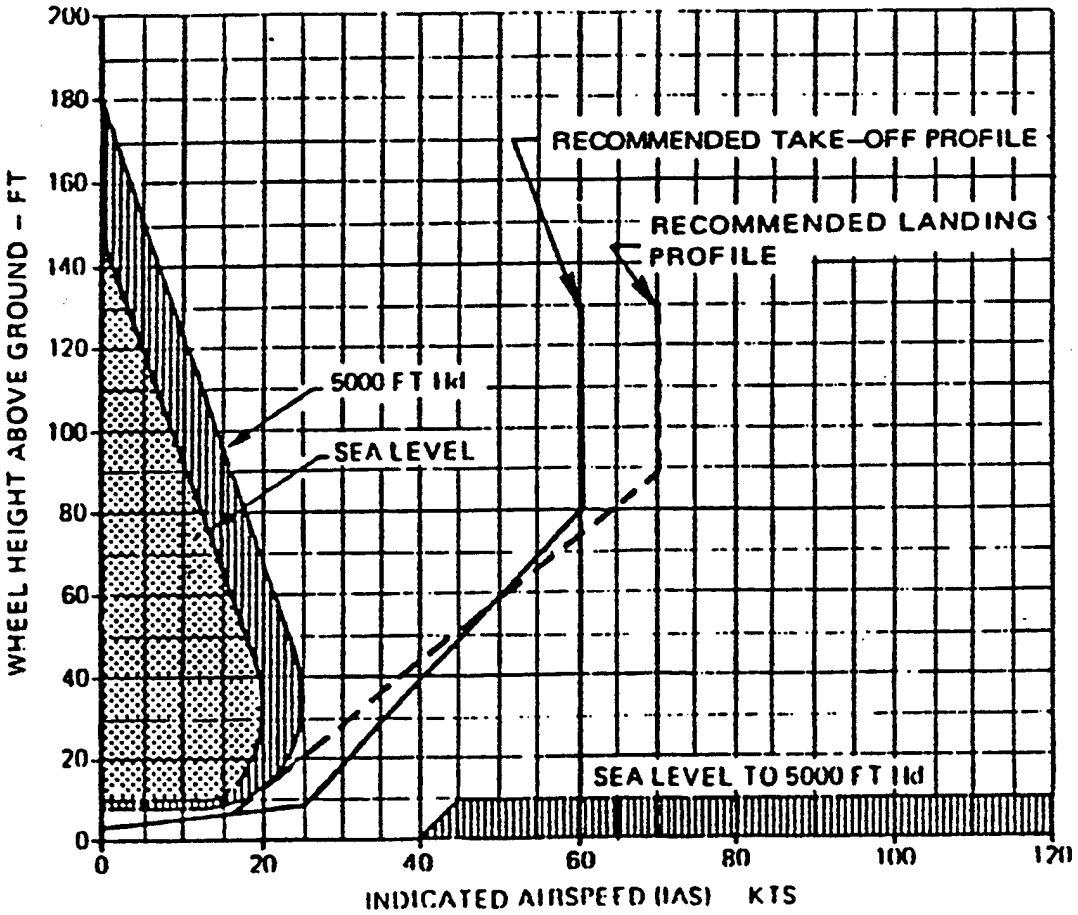

EMERGENCY PROCEDURES

ENGINE FIRE:

ENG1 (2) FIRE light will illuminate if an engine fire exists. The affected engine should be shut down then land as soon as possible.

1. **Engine Control Lever** (affected engine) - OFF

2. **Land as soon as possible.**

SINGLE ENGINE FAILURE:

Illumination of the ENG 1(2) LOW light accompanied with an aural beep are indications of a probable engine failure. The collective should be lowered to maintain the rotor within limits. The affected engine should be shut down and proceed to a suitable landing site.

CAUTION:
Do not shut down engine before verifying engine failure with other indications.

1. **Collective and beep trim** - adjust to maintain rotor RPM at 100%, engine torque, and TOT within limits.

2. **Engine Control Lever** - pull to IDLE for several seconds to check that proper engine was selected, then ECL OFF.

3. **Proceed to suitable landing site.**

NOTE
The engine warning light (and aural beep) is activated when at least one of the following exist.

A. A gas producer N1 (RPM) unbalance of 20% or more.
B. The gas producer N1 (RPM) on the low engine is below idle.

DUAL ENGINE FAILURE:

Indications for engine failure are the same as for single engine failure. The collective must be reduced to maintain rotor RPM within limits. An autorotative descent with air speed 70 to 75 kts should be established. At approximately 70 to 100 ft above the ground, initiate a flare to reduce helicopter to a near level attitude. As the helicopter settles, apply collective at approximately 4 feet to cushion the touch down.

1. **Collective decrease** - to maintain rotor RPM.

2. **Cyclic adjust** - to attain 70 - 75 KIAS Autorotative descent.

3. **Engine Control Levers** - OFF

4. **Make autorotative landing.**

TAILROTOR MALFUNCTION - CRUISE:

The result of the tail rotor failing will be a rapid right yaw. Severity depending on the airspeed at the time of failure. The vertical stabilizer produces an anti-torque component which is a function of forward speed. A 100 kts. the vertical stabilizer supplies all anti-torque for zero sideslip; however the landing should be made with the control levers set to OFF.

1. **Collective reduce** - as necessary to eliminate yaw to the right.

2. **Airspeed / Control adjust** - as necessary to reach a suitable landing area.

- Upon reaching the intended point of landing.

3. **Engine Control Levers retract** - to OFF position.

4. **Collective adjust** - for autorotative descent.

5. **Make autorotative landing.**

#1 (#2) OIL PRESS LIGHT ON:

Engine oil pressure below minimum is indicated by illumination of the #1 (#2) OIL PRESS light. Confirm oil pressure with gage before shutting down engine.

1. **Oil pressure** - check below minimum limits.
2. **Engine Control Lever** (affected engine) - OFF
3. **Refer to single engine failure emergency procedure.**

#1 (#2) OIL HOT LIGHT ON:

The illumination of the #1 (#2) OIL HOT light normally is an indication of engine oil temperature above maximum limits. Confirm engine oil temperature above maximum limits by checking gauge. If above limits shut down engine.

1. **Oil temperature** - check above maximum limits.
2. **Engine Control Lever** (affected engine) - OFF
3. **Refer to single engine failure emergency procedure.**

XMSN OIL PRESS LIGHT ON:

Transmission oil pressure below minimum is indicated by illumination of the XMSN OIL PRESS light. A power reduction is required to reduce strain loads on the transmission and a landing should be made as soon as possible.

1. **Torque** - reduce
2. **Land as soon as possible**

XMSN CHIPS LIGHT ON:

Illumination of the XMSN CHIPS light is an indication of the presence of metal particles in the transmission oil. A reduction in power is required to reduce transmission loads. A landing should be made as soon as possible.

1. **Torque** - reduce

2. **Land as soon as possible**

Weather Brief

Standard Day:

Temperature: 59° F / 15° C

PA: 100 ft.

Ceiling: 1000 ft.

Visibility: 2 NM

Wind: Variable at 5 to 15 kts.

ADDITIONS TO PRE-BRIEF INSTRUCTIONS

• Enhanced Lighting - One half of the night lighting conditions will contain enhanced lighting. The enhanced lighting will consist of a rotating beacon, approach lighting and a PAPI (Precision Approach Path Indicator).

• Terrain - The terrain is bowl shaped so that the city is at the bottom of the bowl and the elevation in the center is 100 ft. MSL. The terrain gradually slopes up to approximately 800 ft. MSL in the far outlying areas.

• Protocol Commands - We will use standard commands to enhance safety and efficiency. They are as follows:

Sim. control: "Clear for I.C." - Simulator will trim for initial condition. CAUTION: Pilots must clear flight controls!
Pilot: (After clear of controls) "Clear"

Sim Control: "_____ Ready" - Query ORE participants if ready to begin run.
ORE Participant: (After ready) "Ready"

Sim Control: "Flying" - Starts simulation run

Anyone: "Sim Stop" - (Stops simulation) Pilot should depress the sim stop switch

NASA-TLX SUBJECT INSTRUCTIONS

Right now I will describe the technique that will be used to assess workload you experience during each mission. Workload is a difficult concept to define precisely, but a simple one to understand generally. The factors that influence your workload may come from the task itself, your feelings about your performance, how much effort you put in it, or the stress and frustration you felt. The workload contributed by different task elements may change as you get more familiar with a task, perform easier or harder versions of it, or move from one task to another. Physical components of workload are relatively easy to conceptualize and evaluate. However, the mental components of workload may be more difficult to measure.

Since workload is something that is experienced individually by each person, there are no effective metrics that can be used to estimate the workload of different activities. One way to find out about workload is to ask people to describe the feelings they experienced during a specific task. Because workload may be caused by many different factors, we would like you to evaluate several of them individually rather than lumping them into a single global evaluation of overall workload. NASA developed a set of six workload rating scales of which you will use to evaluate the workload you experienced during the different missions. A description of those scales was provided to you in your pre-briefing packet. Please take some time now to review the scale descriptions again. If you have questions about any of the scales in the table, please ask a member of the research team about it. It is extremely important that they be clear to you. You may keep the definitions with you for reference during the experiment.

After performing each mission, a test administrator will ask you to verbally rate each workload dimension individually. The administrator will record your ratings on the rating scale while you remain in the simulator. Please consider your responses carefully for each mission. *Your ratings will play an important role in the evaluation being conducted, thus, your active participation is essential to the success of this experiment and is greatly appreciated!*

WORKLOAD RATING SCALES

We are not only interested in assessing your performance but also the experiences you had during each mission. Right now we are going to describe the technique that will be used to examine your experiences. In the most general sense we are examining the "workload" you experienced. Workload is a difficult concept to define precisely, but a simple one to understand generally. The factors that influence your experience of workload may come from the task itself, your feelings about your own performance, how much effort you put in, or the stress and frustration you felt. The workload contributed by different task elements may change as you get more familiar with a task, perform easier or harder versions of it, or move from one task to another. Physical components of workload are relatively easy to conceptualize and evaluate. However, the mental components of workload may be more difficult to measure.

Since workload is something that is experienced individually by each person, there are no effective metrics that can be used to estimate workload of different activities. One way to find out about workload is to ask people to describe the feelings they experienced. Because workload may be caused by many different factors, we would like you to evaluate several of them individually rather than lumping them into a single global evaluation of overall workload. This set of six rating scales was developed for you to use in evaluating your experiences during different tasks. *Please read the descriptions of the scales carefully.* If you have a question about any of the scales in the table, please ask a test administrator about it before you begin the test. It is extremely important that they be clear to you. You may keep the scales and descriptions with you for reference during the experiment.

After performing each of the missions, you will be asked to provide a verbal rating of workload using a 7 point scale. Each rating scale has two endpoint descriptors of which you will base your ratings. A test administrator will explain each scale to you and record you ratings. Please consider you responses carefully in distinguishing among the different missions. Your ratings will play an important role in the evaluation being conducted, thus, your active participation is essential to the success of this experiment and is greatly appreciated by all of us.

Please review the attached definitions of workload dimensions. If you are unsure of the definitions, please ask a test administrator to explain them to you.

In addition to the workload ratings, you will be asked to verbally respond to a number of open-ended questions. These questions are presented after the workload rating scales.

ORE SIMULATION
Daily Schedule

Pilot Numbers:
Testing Dates:

Day 1		
TIME	**SERIES A**	**SERIES B**
12:00	Arrive Boeing Bldg. 3-10 lobby	Arrive Boeing Bldg. 3-10 lobby
12:15 - 13:00	Pre-brief / Pilot Preparation	Pre-brief
13:00 - 13:45	Familiarization Runs	Break / Pilot Preparation
13:45 - 14:30	Break	Familiarization Runs
14:30 - 15:15	Session 1	Break
15:15 - 16:00	Intermediate Questionnaire / Break	Session 1
16:00 - 16:45	LUNCH	LUNCH
16:45 - 17:30	Session 2	Intermediate Questionnaire / Break
17:30 - 18:15	Intermediate Questionnaire / Break	Session 2
18:15 - 19:00	Session 3	Intermediate Questionnaire / Break
19:00 - 19:45	Intermediate Questionnaire / Break	Session 3
19:45 - 20:30	Session 4	Intermediate Questionnaire / Break
20:30 - 21:00	Intermediate Questionnaire/ De-brief	De-brief

DAY 2		
TIME	**SERIES A**	**SERIES B**
12:15 - 13:00	Arrive Boeing Bldg. 3-10 lobby	Arrive / Pilot Preparation
13:00 - 13:45	Break / Pilot Preparation	Session 4
13:45 - 14:30	Session 5	Intermediate Questionnaire / Break
14:30 - 15:15	Intermediate Questionnaire / Break	Session 5
15:15 - 16:00	Session 6	Intermediate Questionnaire / Break
16:00 - 16:45	LUNCH	LUNCH
16:45 - 17:30	Intermediate Questionnaire / Break	Session 6
17:30 - 18:15	Session 7	Intermediate Questionnaire / Break
18:15 - 19:00	Intermediate Questionnaire / Break	Session 7
19:00 - 19:45	De-brief	Intermediate Questionnaire / Break
19:45 - 20:15		De-brief

INFORMED CONSENT FORM

I, _____, have been briefed by a test administrator as to the purpose of the study in which I have been asked to participate. I fully understand the purpose of the study and what my participation will entail, and I have been provided with the opportunity to ask questions of the test administrator.

The test administrator informed me that the study will require me to complete a biographical information questionnaire, participate in flying mission scenarios in the Boeing helicopter simulator, allow for physiological data and performance data to be collected, and be debriefed regarding the details of the mission after completing the simulator flight. Approximately 8 hours of flight time over two days will be required to complete these activities.

I am aware that the physiological data collection will require fixing electrodes to my face and chest and that I will experience no pain or discomfort. Also, I understand that this study will impose very little stress. The mission scenarios in which I will participate are segments of routine simulator training. My participation in this study will assist the Federal Aviation Administration in determining the effect of obstacle rich environments on pilot workload and safety.

As part of the data analysis, my data will be combined with that of other individuals, and I no longer will be identifiable as a participant. I have been informed that my name and all experimental data associated with me will be held in confidence. I have been informed that I have the right to withdraw from this study at any time, and that the test administrators may terminate my participation in the interest of safety and the study.

I have been informed that if I want additional details concerning the study I can contact any of the test administrators in the simulator facility during the study, or contact Mr. Brian Sawyer, SAIC, (703) 414-7024; Mr. Jim Grenell, Boeing, (610) 591-6906; or Dr. Arthur F. Kramer, University of Illinois, (217) 244-1933, upon completion of the study.

Signed: _____

Date: _____/_____/_____

Witness: _____

Date: _____/_____/_____

Appendix H. Flight Data Plots

H.1 Introduction

This appendix contains helicopter data plots for the following four variables:

1. Cross Track Error – lateral distance of the helicopter from the heliport approach course (feet)
2. Altitude – MSL elevation of the helicopter, where heliport elevation is 100 feet
3. Ground Speed – in knots
4. Height/Velocity Plot – AGL elevation (feet) versus ground speed (knots)

On the cross track error plots, the boundaries of the approach/departure surfaces are marked using light lines labeled "Airspace." On the altitude plots, the floor of the approach/departure surface is depicted as the "8:1 Slope." The ground speed plot does not depict any airspace or operational limits. The H/V plots depict the boundaries of the "avoid" regions from the "Height-Velocity Diagram OEI" included with the helicopter performance data in Appendix G. Appendix H contains three sections of plots as outlined below.

H.2 Visibility and Obstacle Density

The simulation results are grouped and aggregated to illustrate the effects of the two primary simulation variables, Visibility and Obstacle Height/Density. Four basic cases are shown: Metro Approach (figures H.2-1 through H.2-32), Valley Approach (H.2-33 through H.2-64), Metro Departure (H.2-65 through H.2-96), and Valley Departure (H.2-97 through H.2-128). In each group the plots illustrate the effects of visibility levels, then obstacle height/density levels, followed lastly by ensemble plots (including all data). Data mean, mean ± two standard deviations, and extremes are shown in each case.

H.3 Six-Sigma Data

This section contains eight figures (H.3-1 through H.3-8): Cross Track Error and Altitude for each of the four basic cases. They are similar to the ensemble plots in H.2 except that mean ± six standard deviations are shown, and the scales are adjusted accordingly.

H.4 Excepted Data

There are three cases in the Metro Approach environment where the helicopter only reached a distance of approximately 3,700 ft from the heliport on the base leg prior to turning onto the final approach course. For these three flights, data is unavailable beyond this distance. In order to address this problem, the data were analyzed by two different methods. In the first method, the three flights were simply omitted from the data analysis and the three flights were identified as "excepted" data. These data are presented in figures H.2-1 through H.2-128 and H.3-1 through H.3-8. In the second method, the excepted data are included in the data analysis to demonstrate their impact upon the statistical results. These flight tracks are illustrated in figures H.4-1 through H.4-3 in order to show the extent of the problem and the eventual normality of the flight tracks as the heliport is neared. The effect of these cases in the statistics is illustrated in figures H.4-4 through H.4-7. Figures H.4-4 and H.4.6 represent statistical plots based on omitting the excepted data. Figures H.4-5 and H.4-7 represent statistical plots from full data sets. Figures H.4-4 and H.4-5 represent the Night B visibility case where two of the excepted runs occurred. Figures H.4-6 and H.4-7 illustrate the effect on ensemble statistics where there were three excepted flights.

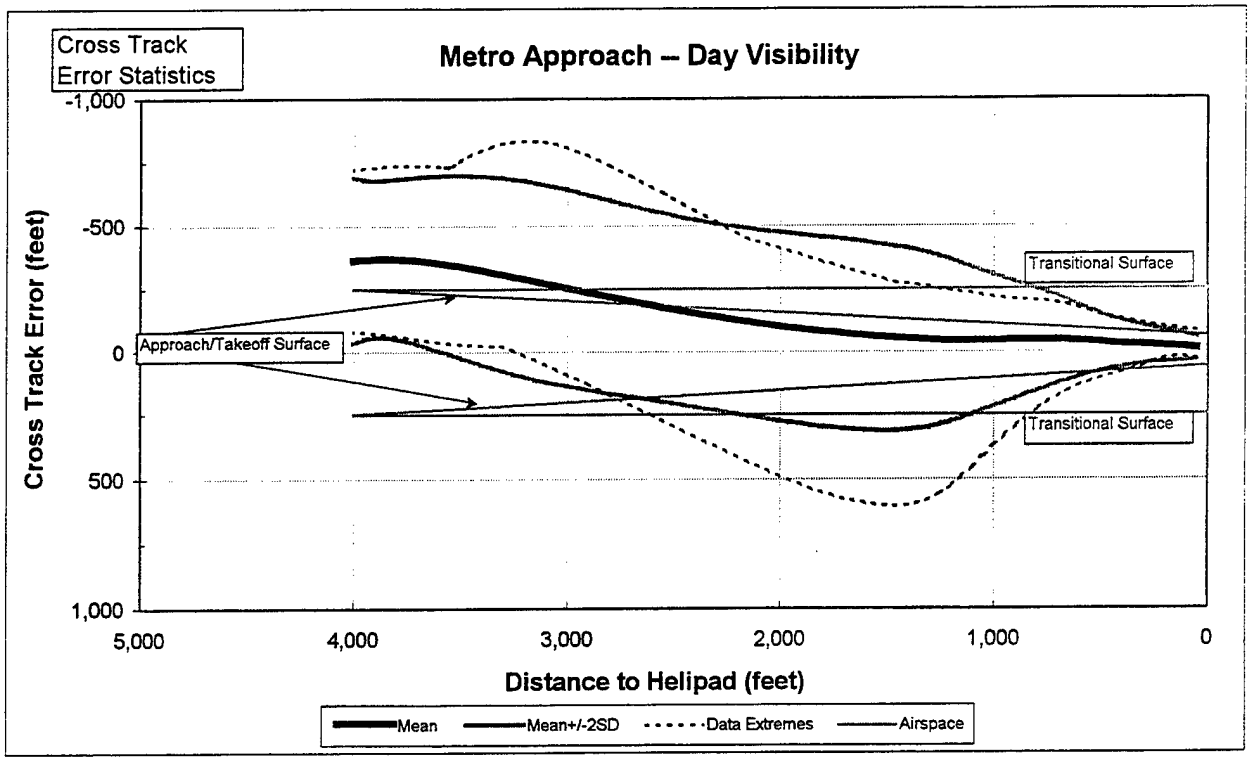

Figure H.2-1 Metro Approach Day Visibility Cross Track Data

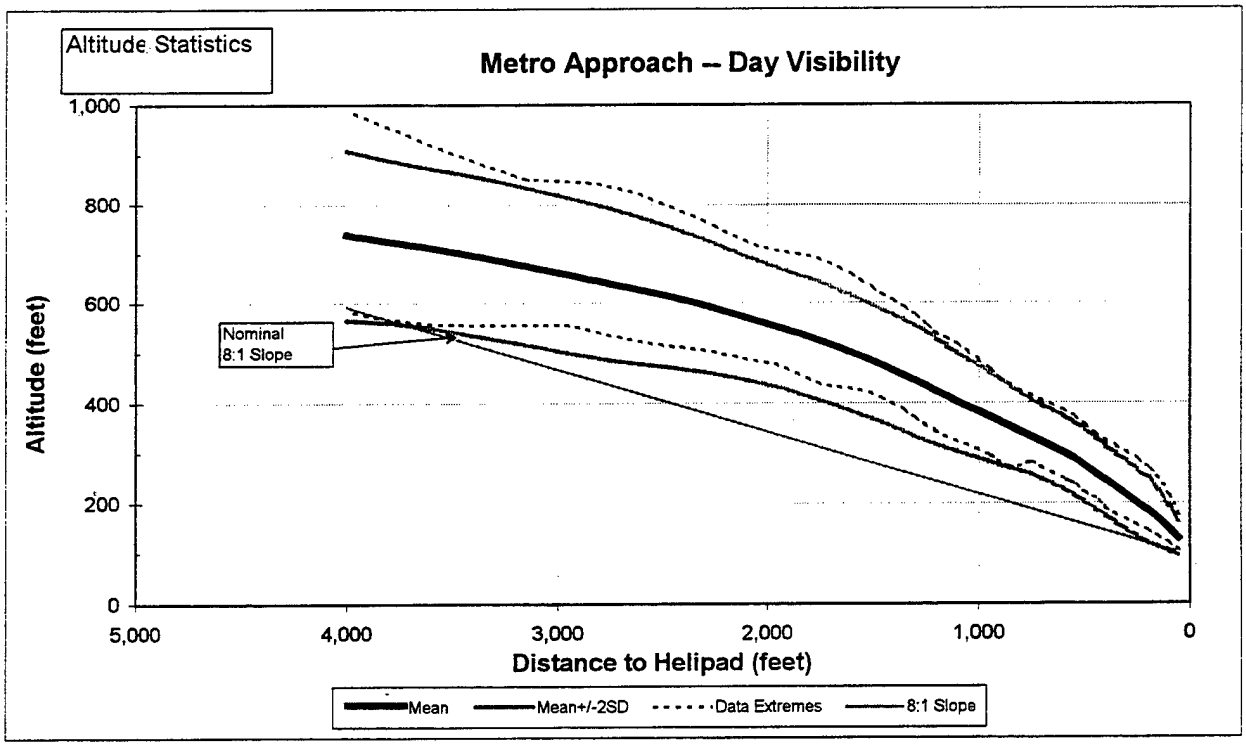

Figure H.2-2 Metro Approach Day Visibility Altitude Data

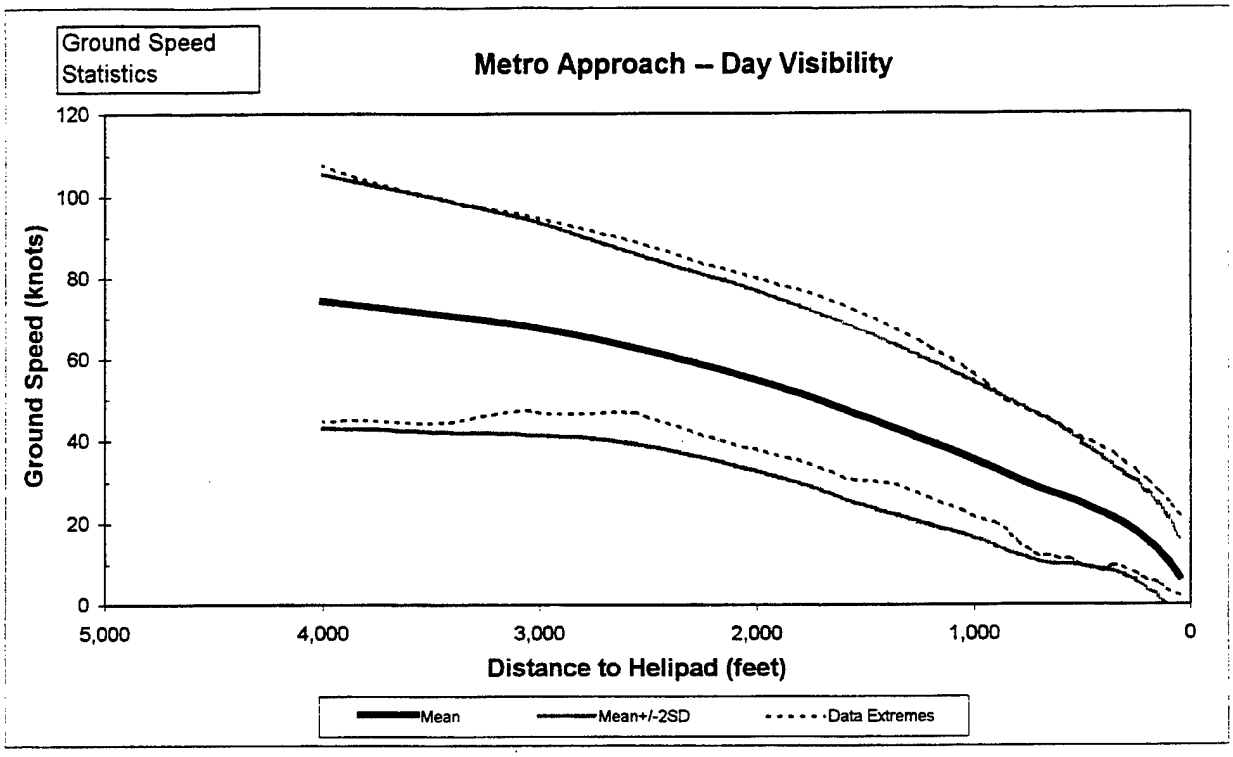

Figure H.2-3 Metro Approach Day Visibility Ground Speed Data

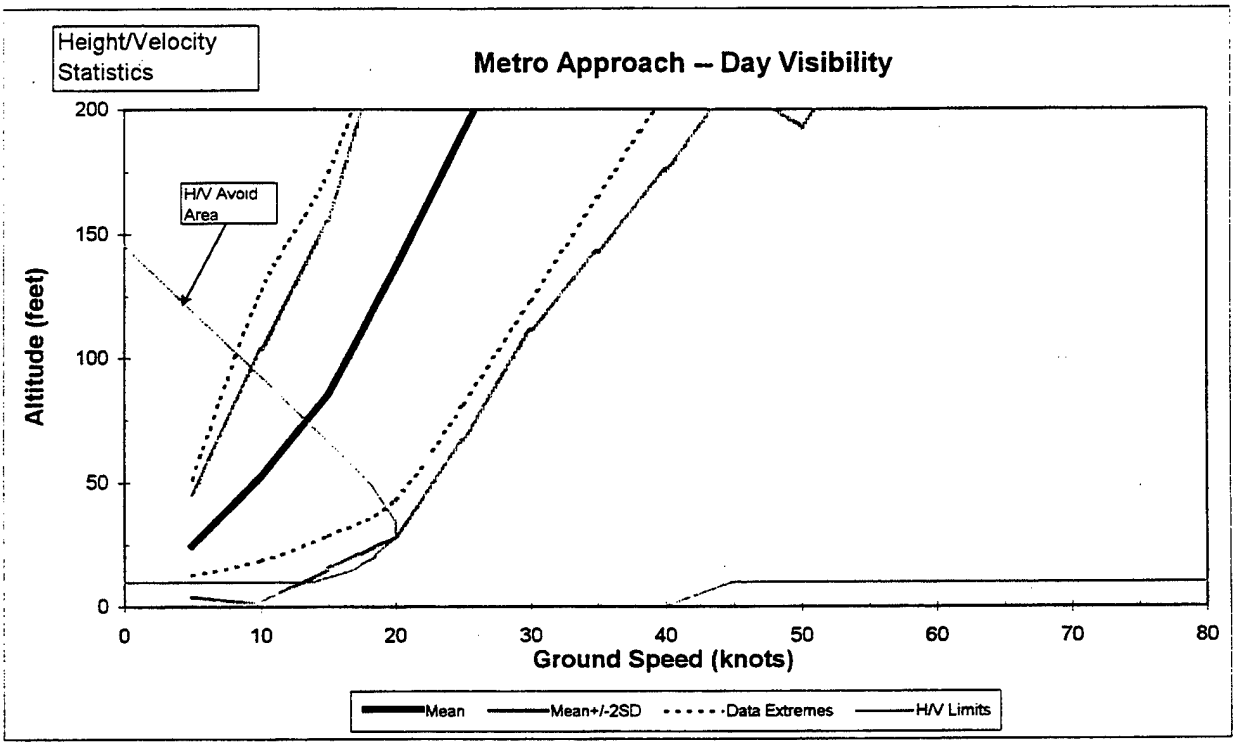

Figure H.2-4 Metro Approach Day Visibility Height/Velocity Data

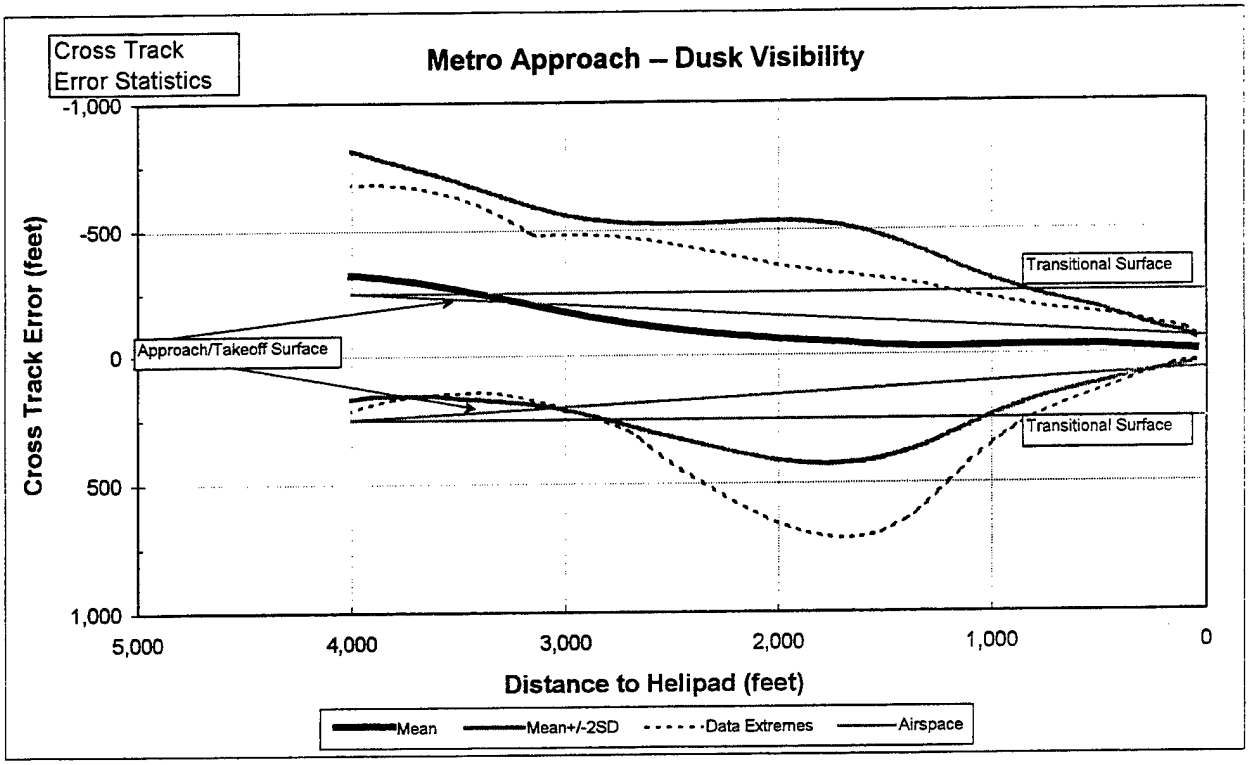

Figure H.2-5 Metro Approach Dusk Visibility Cross Track Data

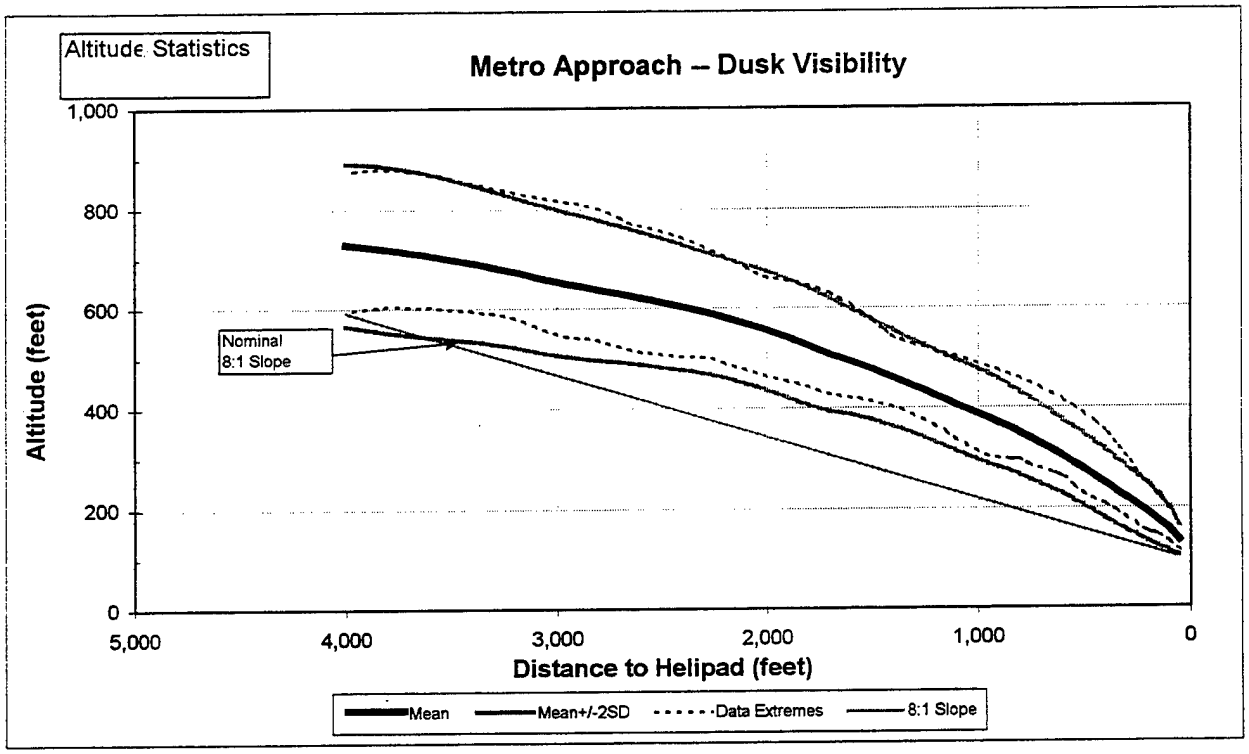

Figure H.2-6 Metro Approach Dusk Visibility Altitude Data

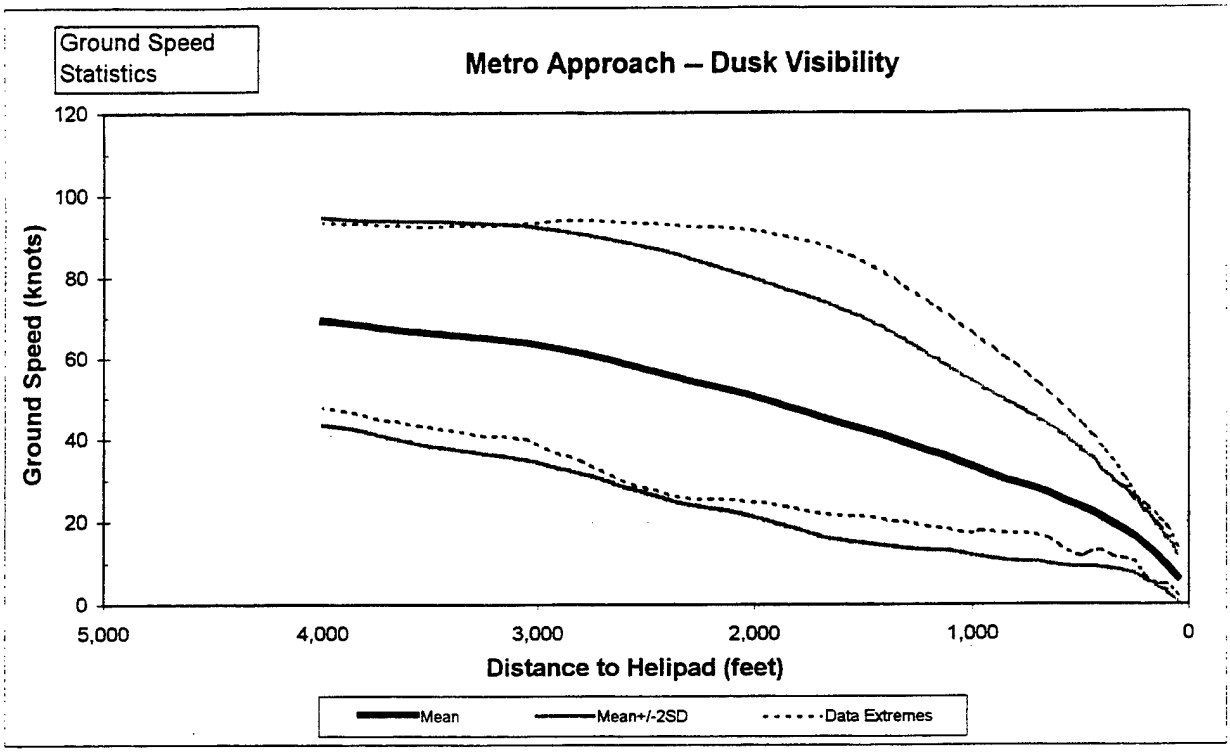

Figure H.2-7 Metro Approach Dusk Visibility Ground Speed Data

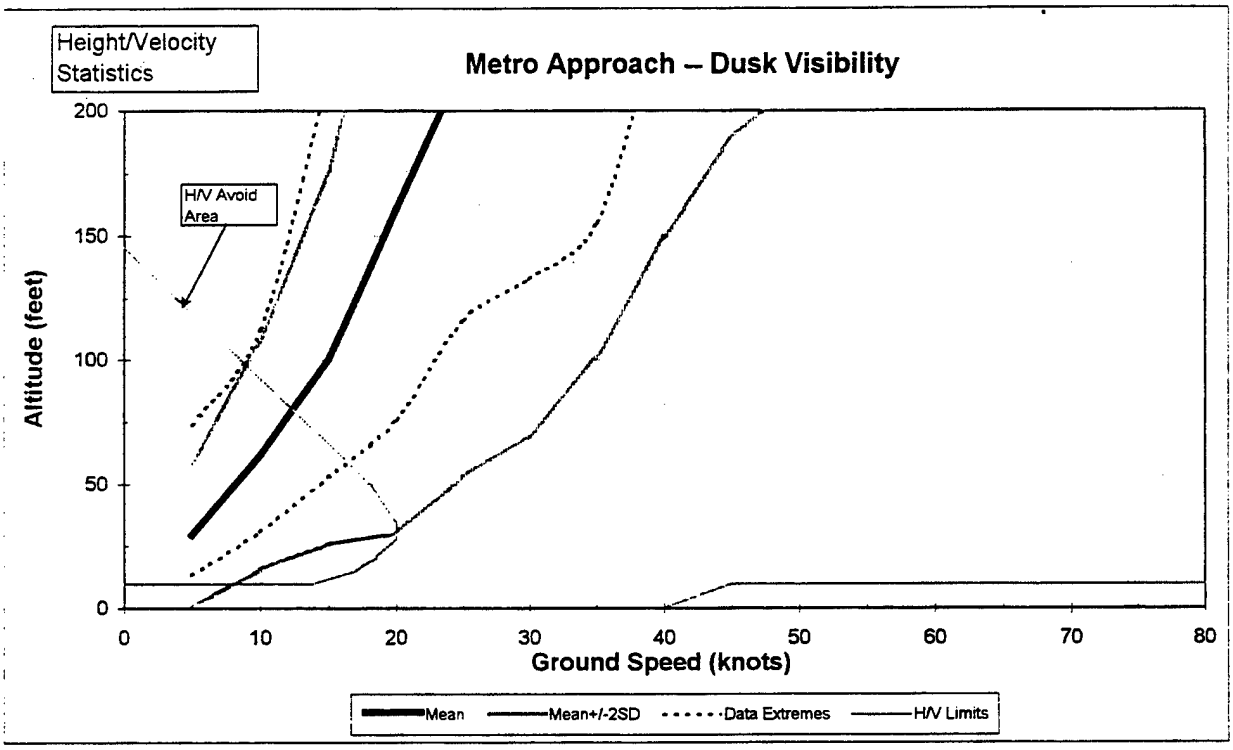

Figure H.2-8 Metro Approach Dusk Visibility Height/Velocity Data

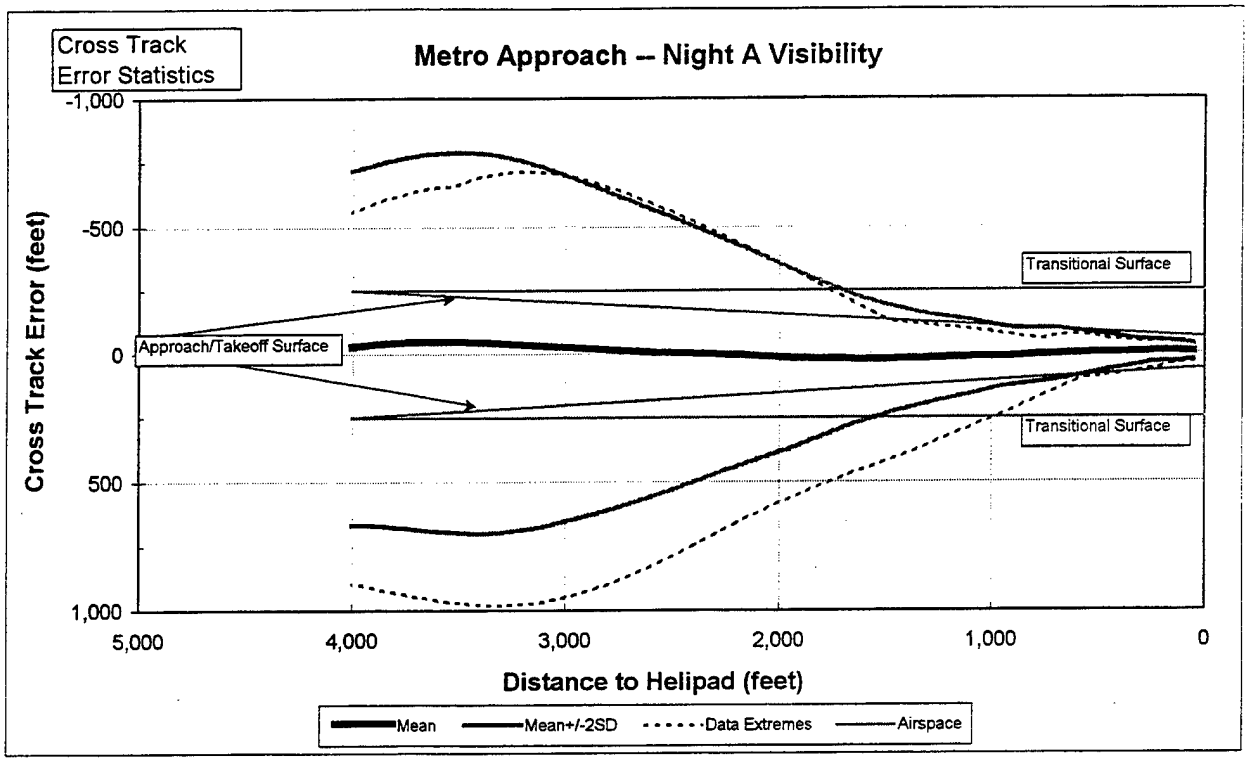

Figure H.2-9 Metro Approach Night A Visibility Cross Track Data

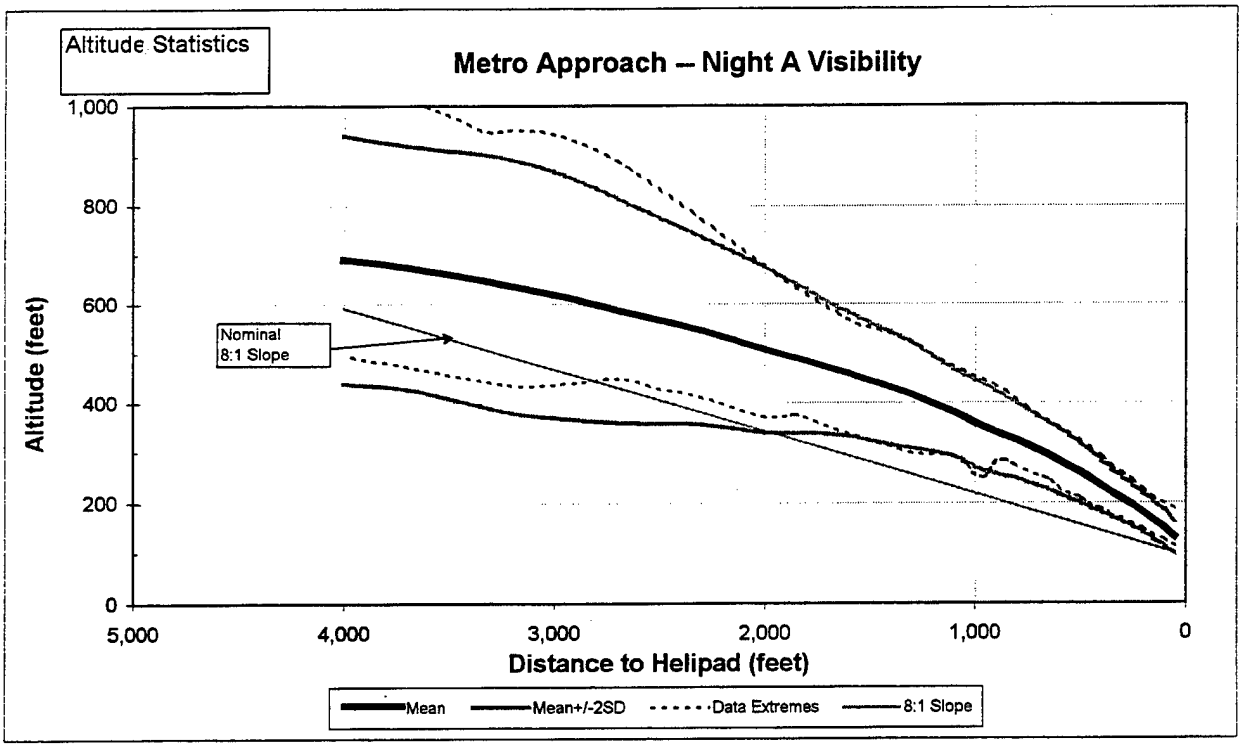

Figure H.2-10 Metro Approach Night A Visibility Altitude Data

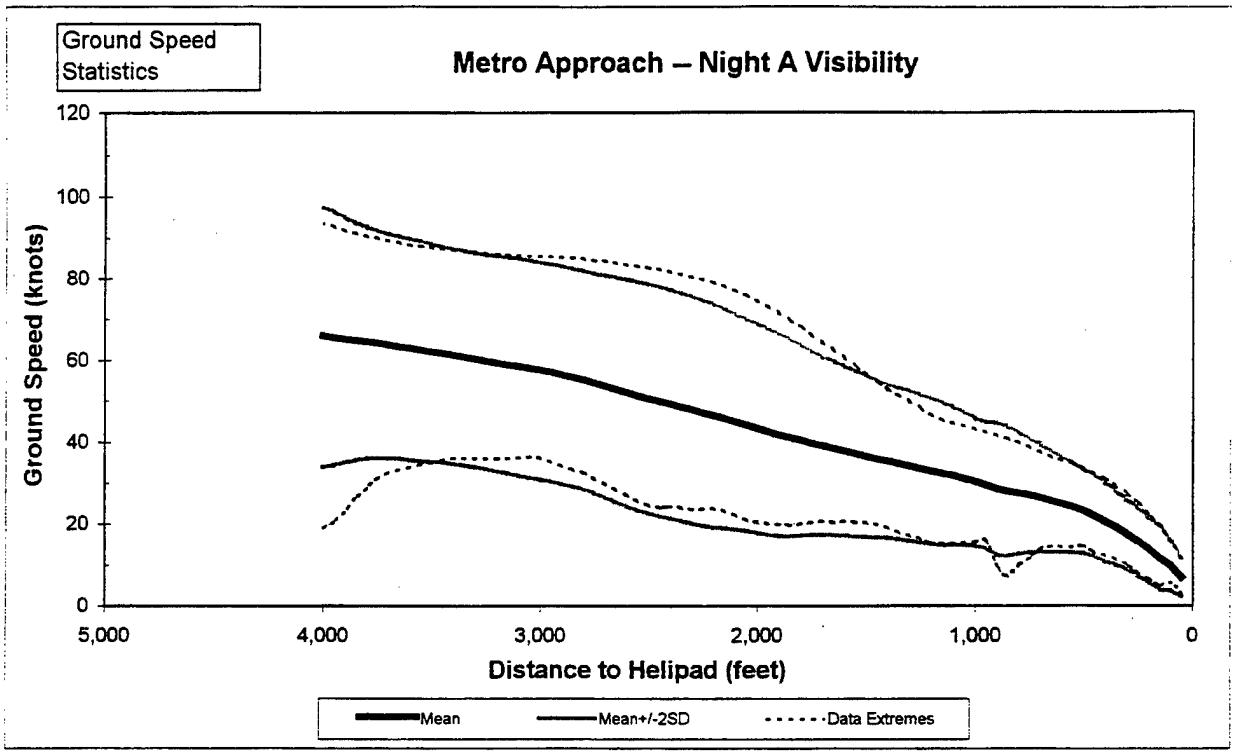

Figure H.2-11 Metro Approach Night A Visibility Ground Speed Data

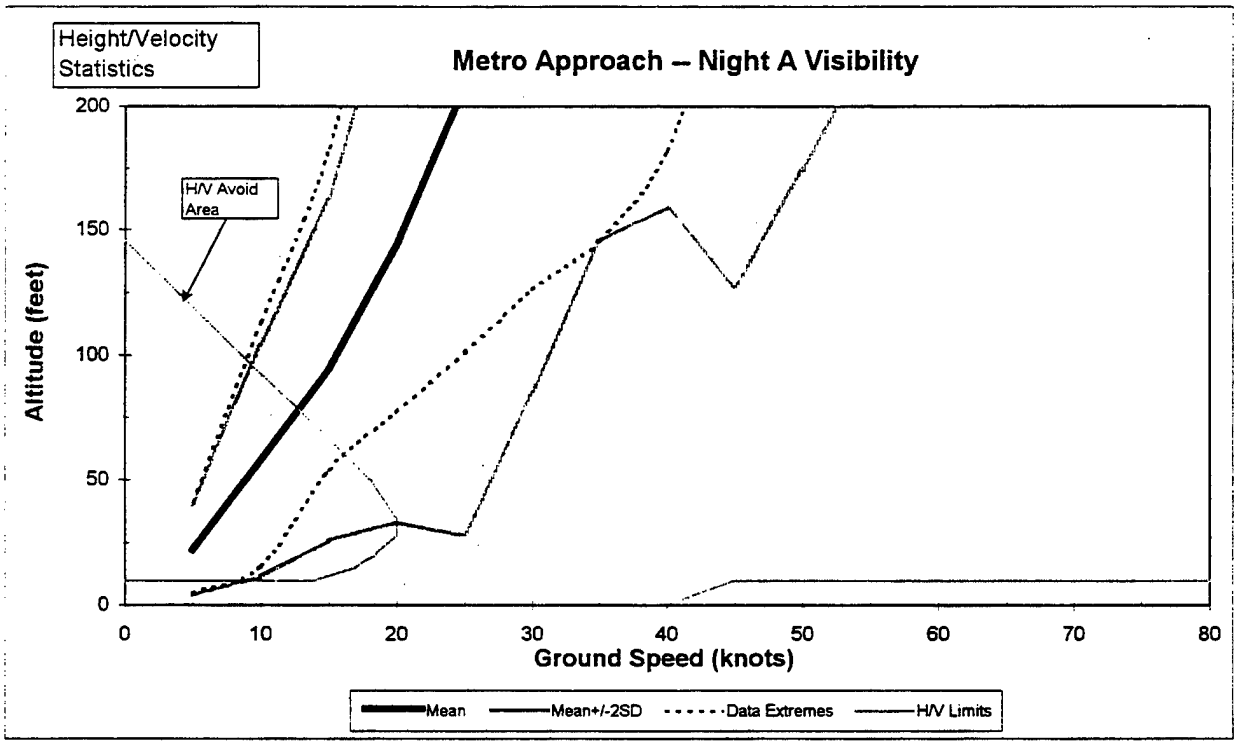

Figure H.2-12 Metro Approach Night A Visibility Height/Velocity Data

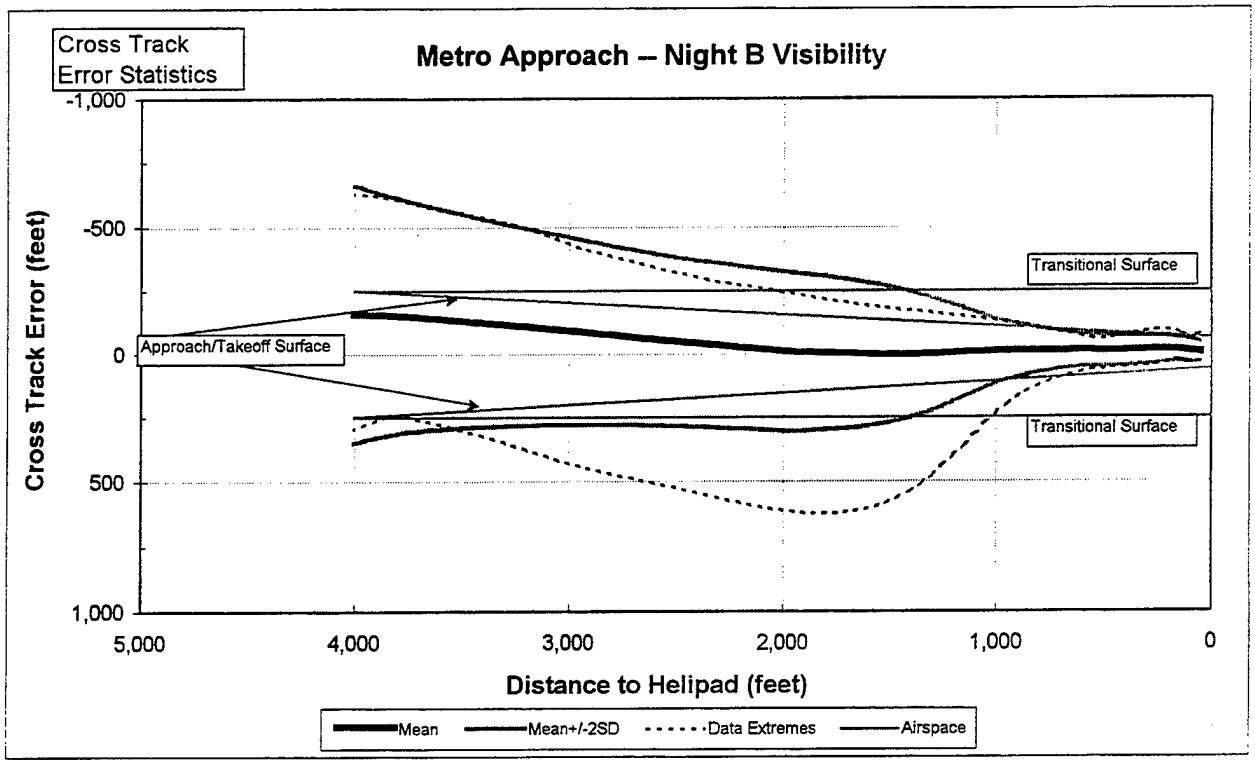

Figure H.2-13 Metro Approach Night B Visibility Cross Track Data

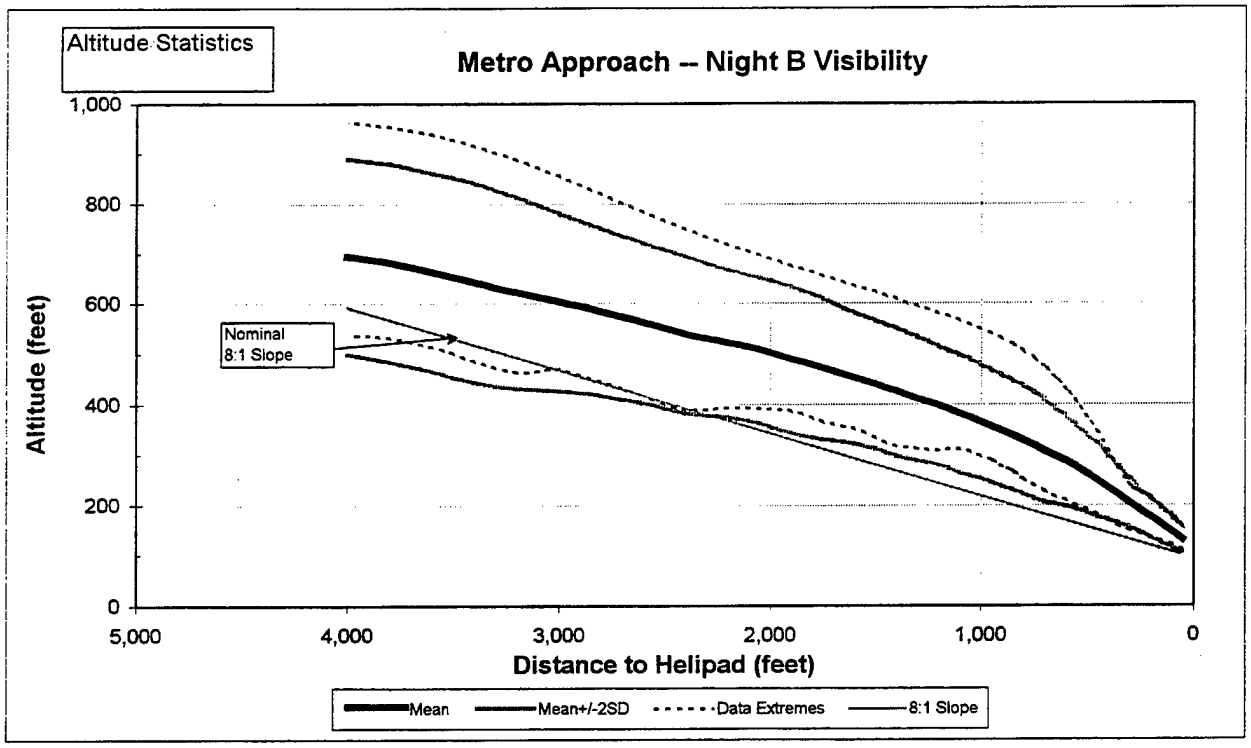

Figure H.2-14 Metro Approach Night B Visibility Altitude Data

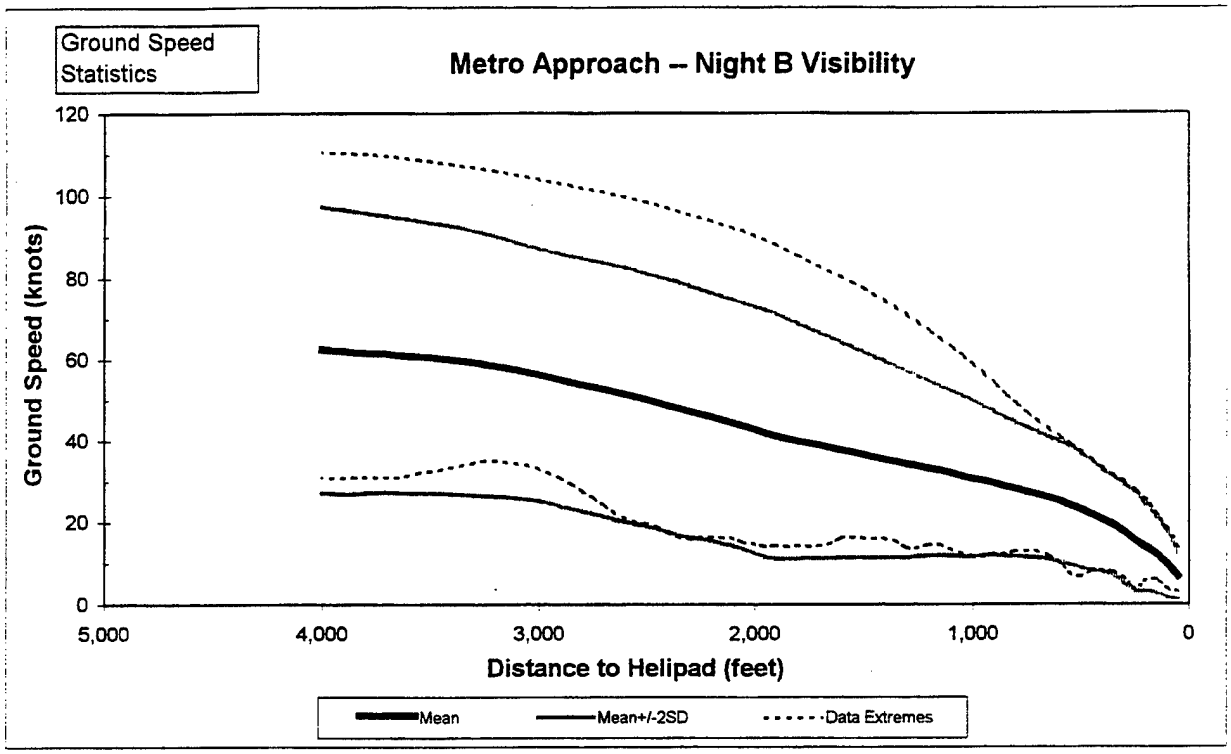

Figure H.2-15 Metro Approach Night B Visibility Ground Speed Data

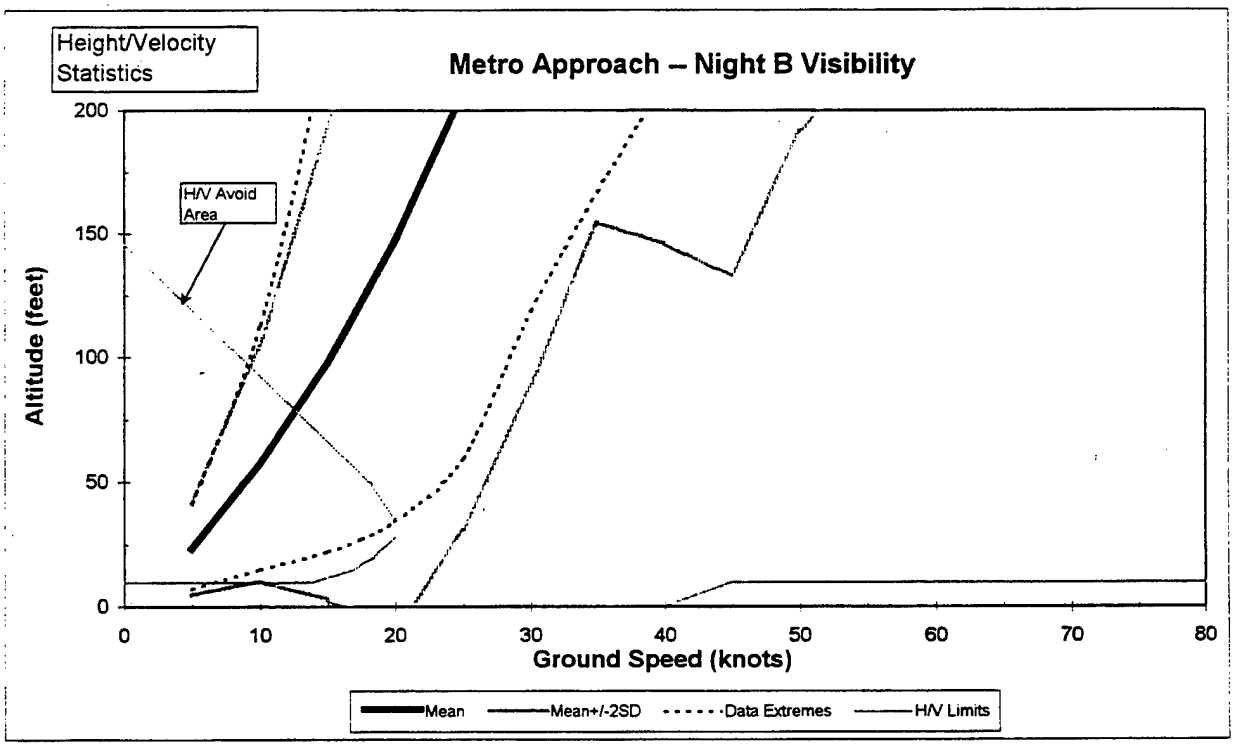

Figure H.2-16 Metro Approach Night B Visibility Height/Velocity Data

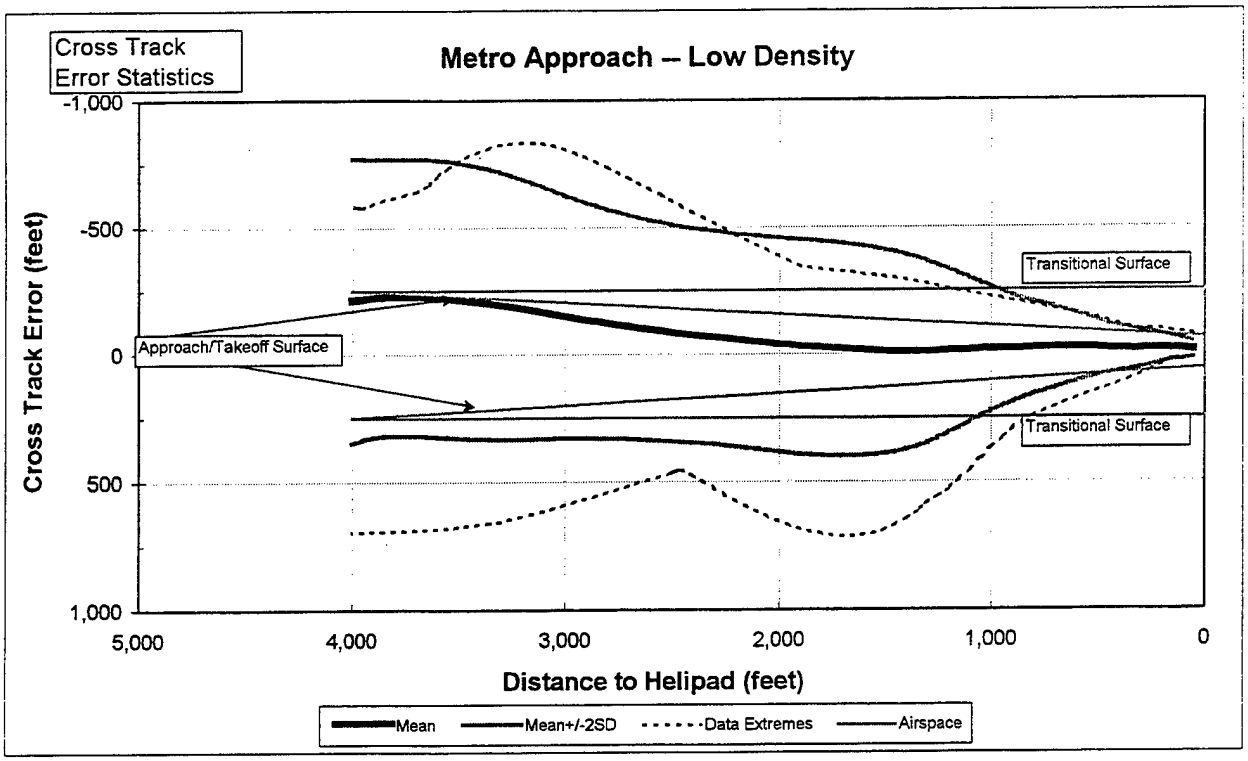

Figure H.2-17 Metro Approach Low Density Cross Track Data

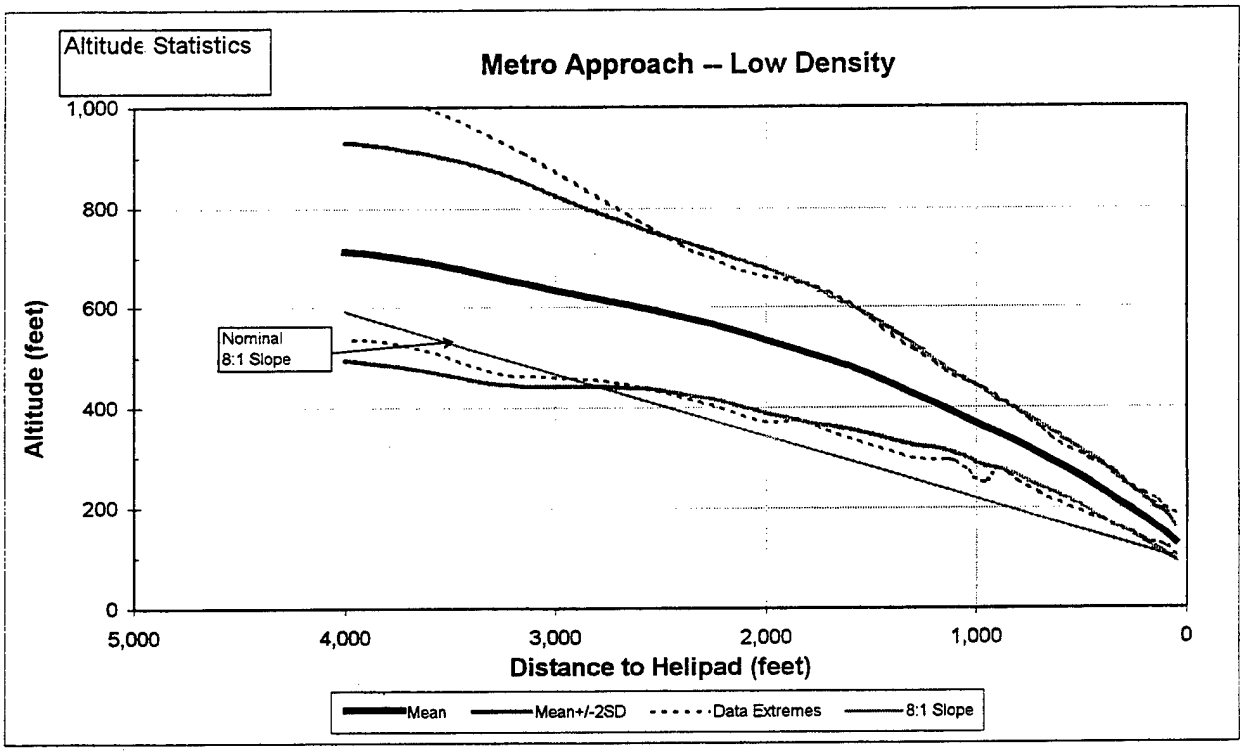

Figure H.2-18 Metro Approach Low Density Altitude Data

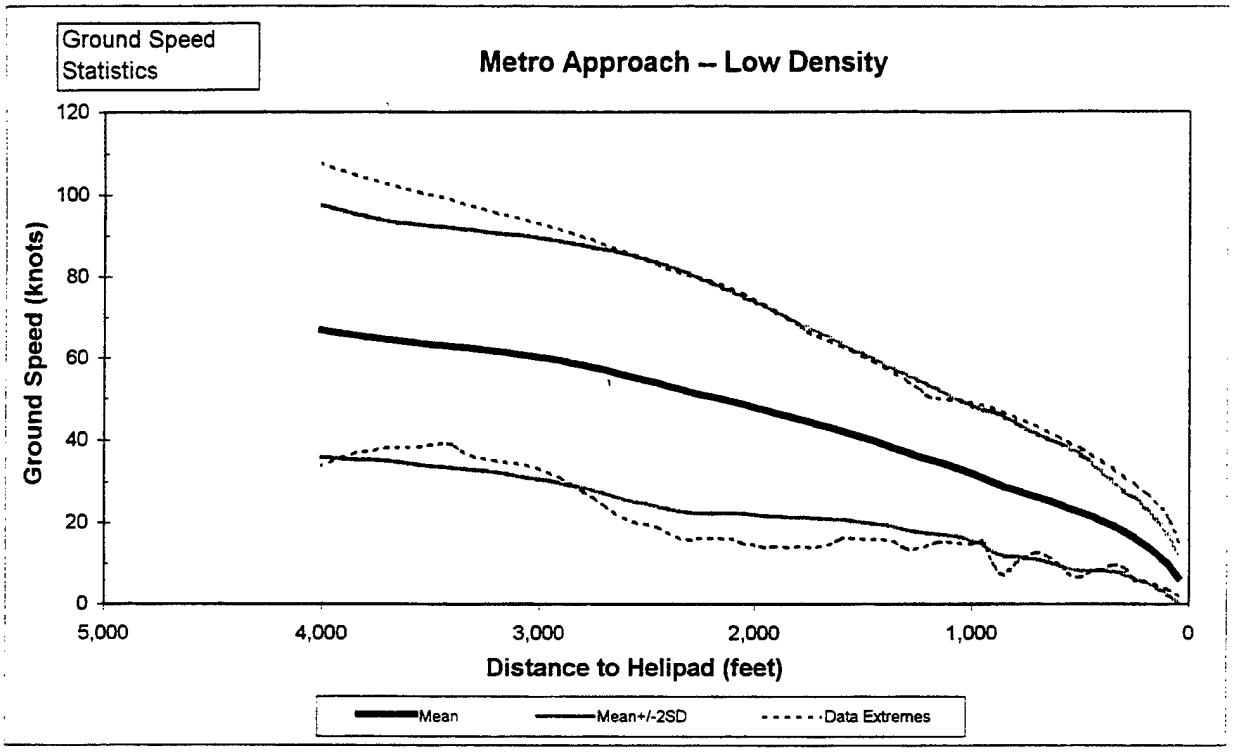

Figure H.2-19 Metro Approach Low Density Ground Speed Data

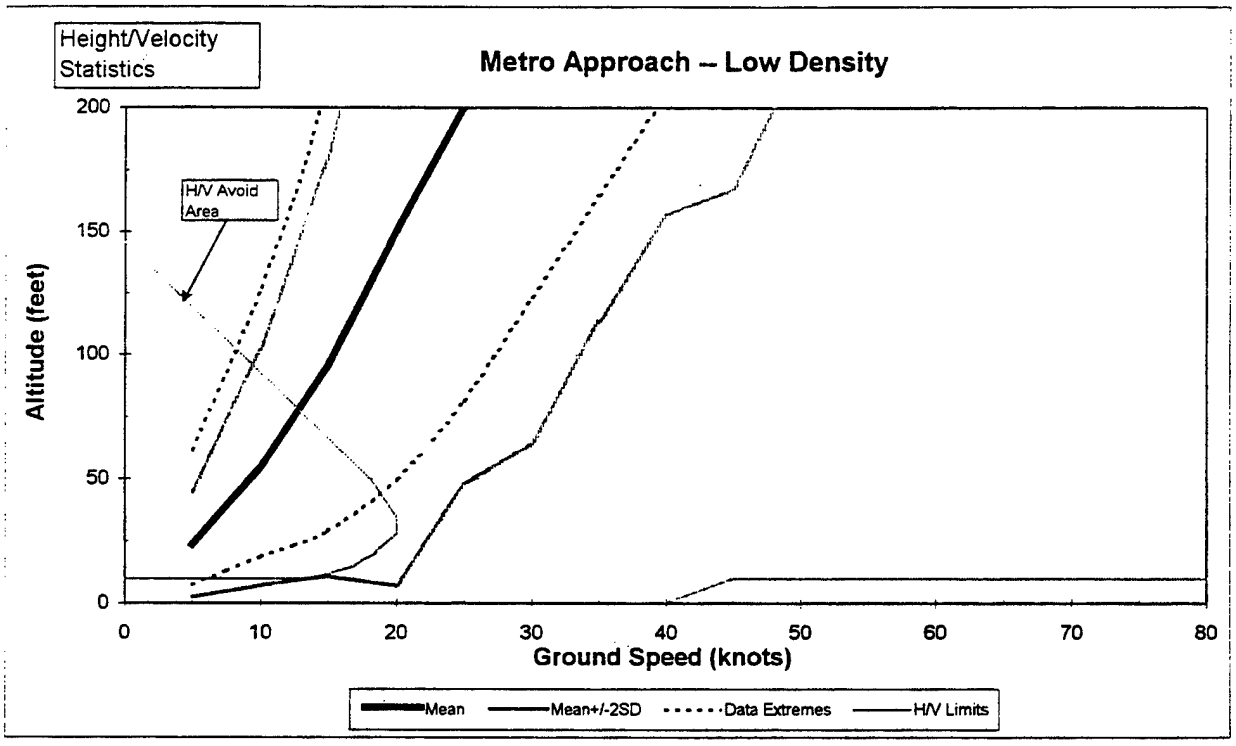

Figure H.2-20 Metro Approach Low Density Height/Velocity Data

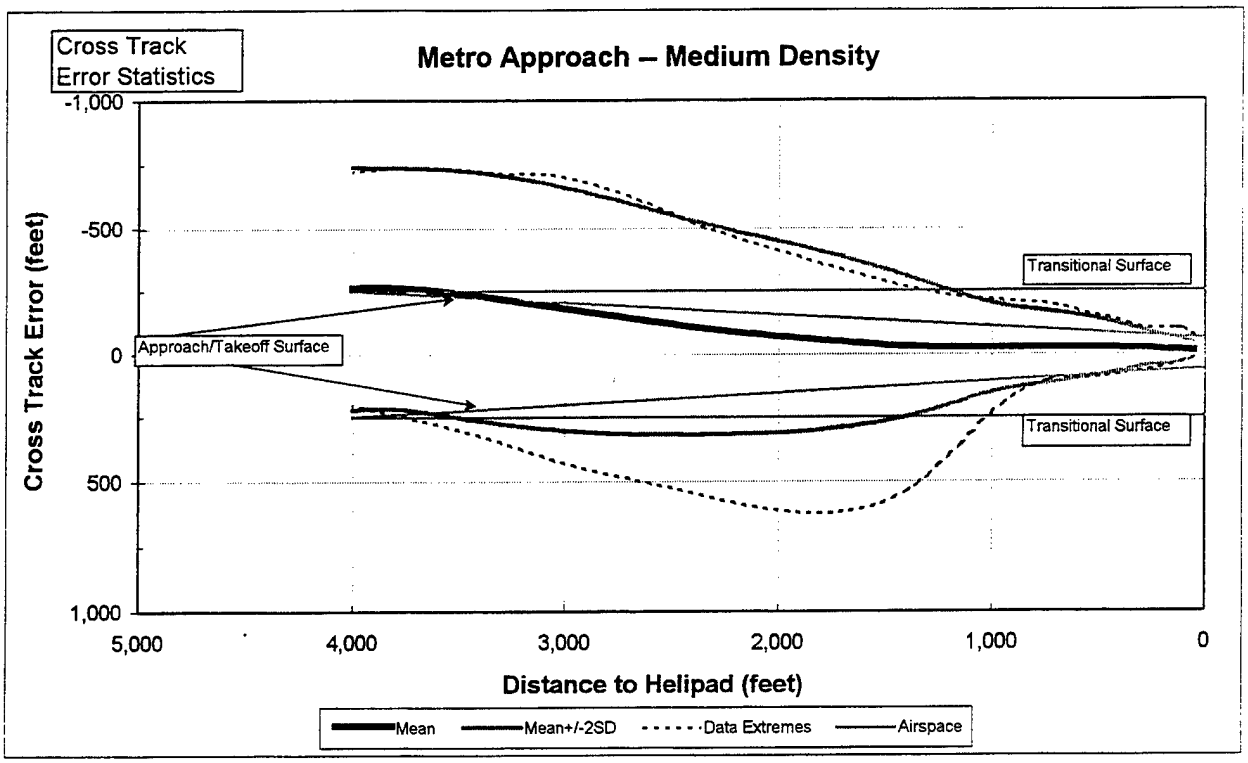

Figure H.2-21 Metro Approach Medium Density Cross Track Data

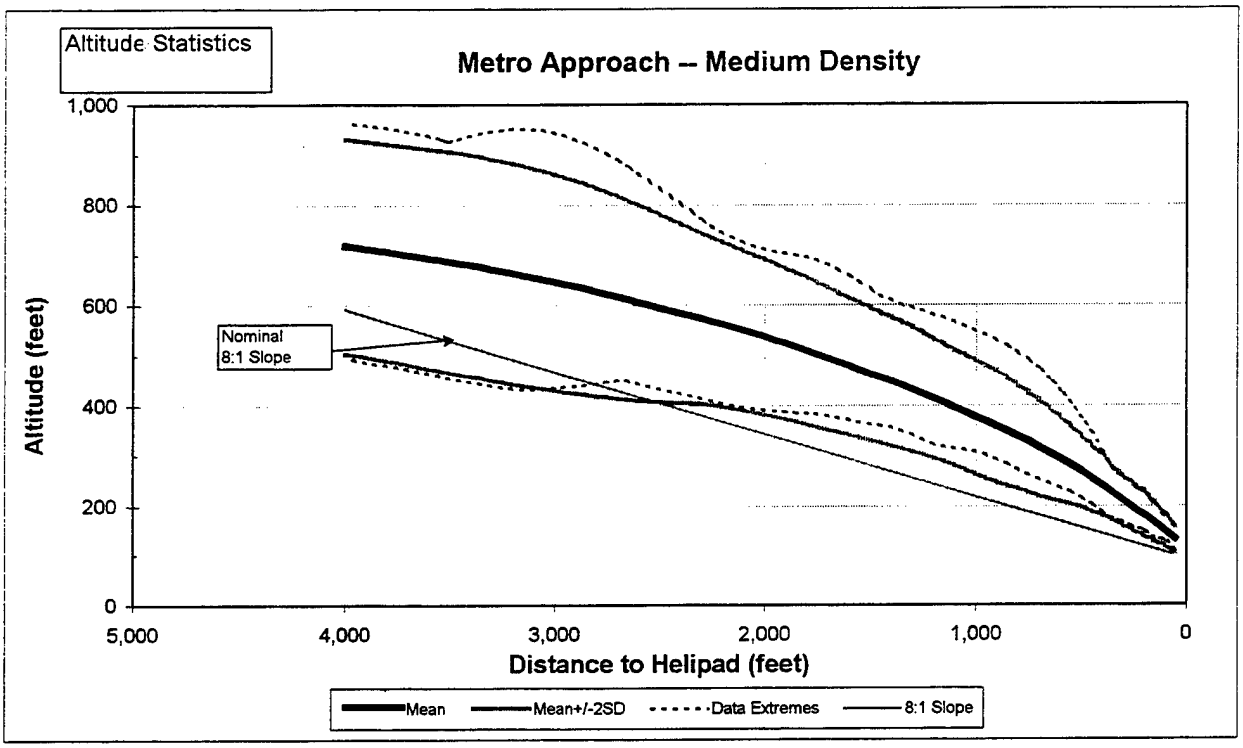

Figure H.2-22 Metro Approach Medium Density Altitude Data

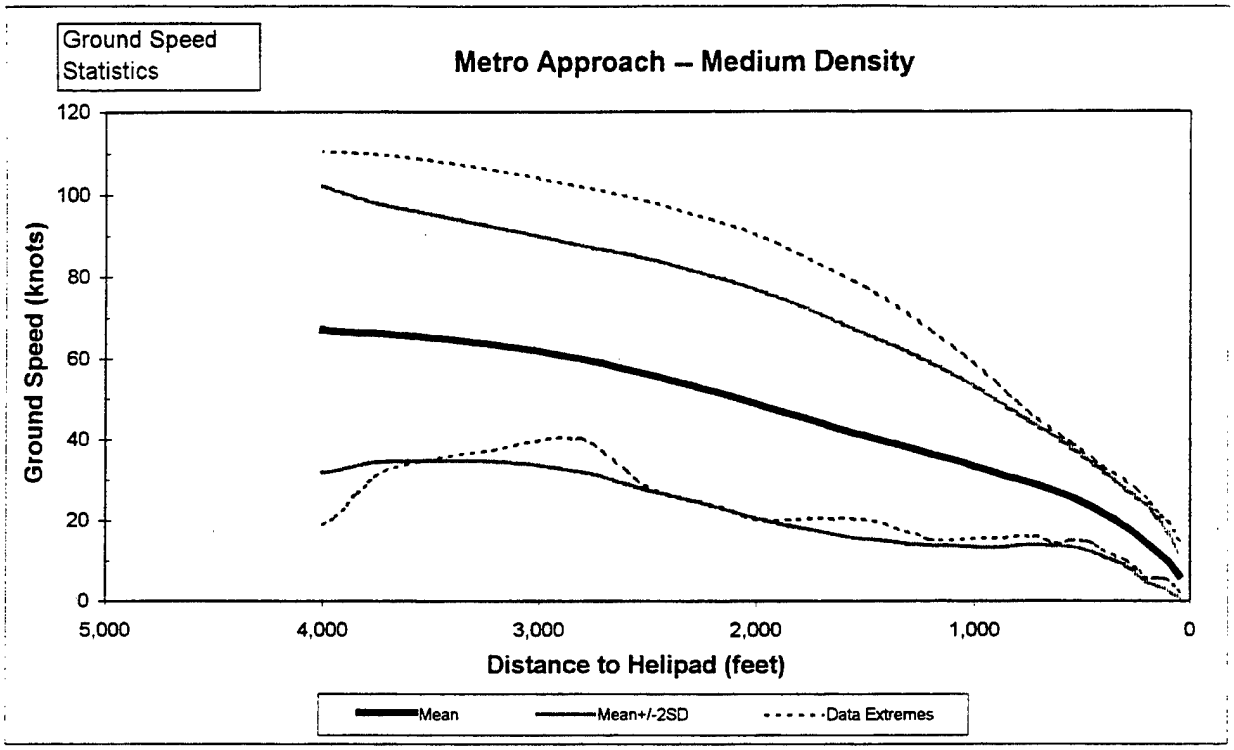

Figure H.2-23 Metro Approach Medium Density Ground Speed Data

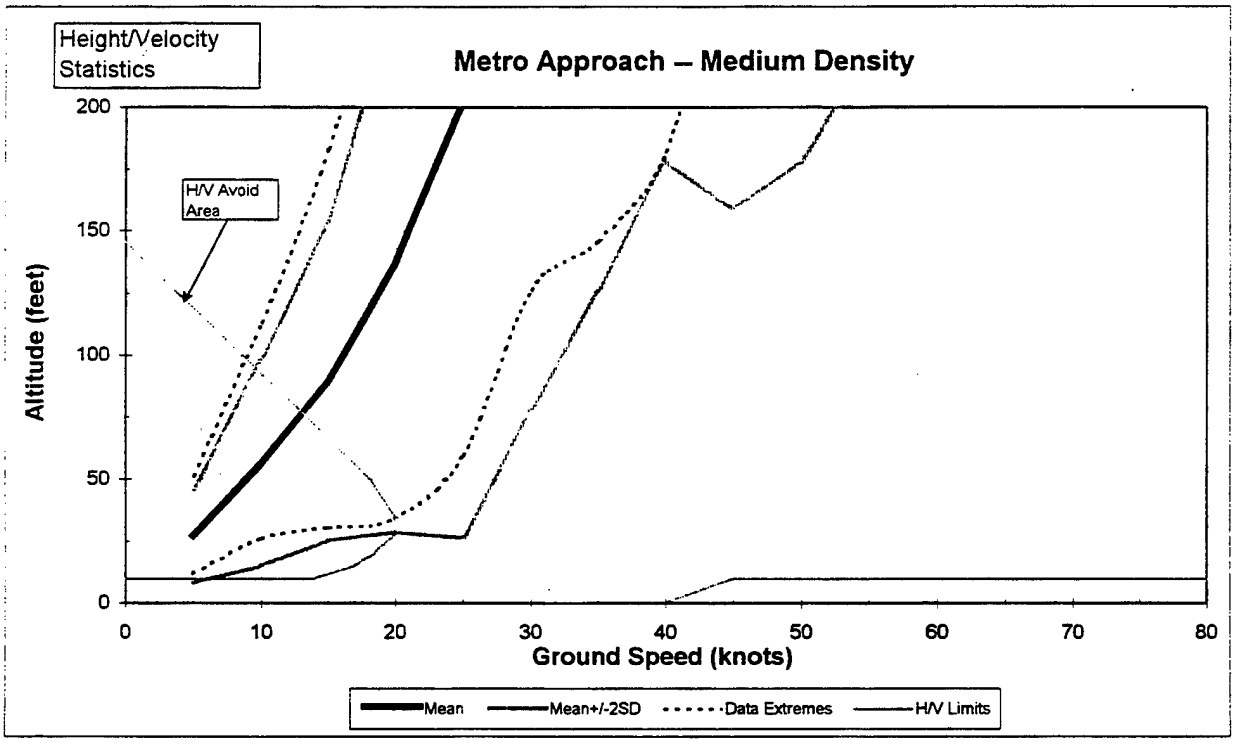

Figure H.2-24 Metro Approach Medium Density Height/Velocity Data

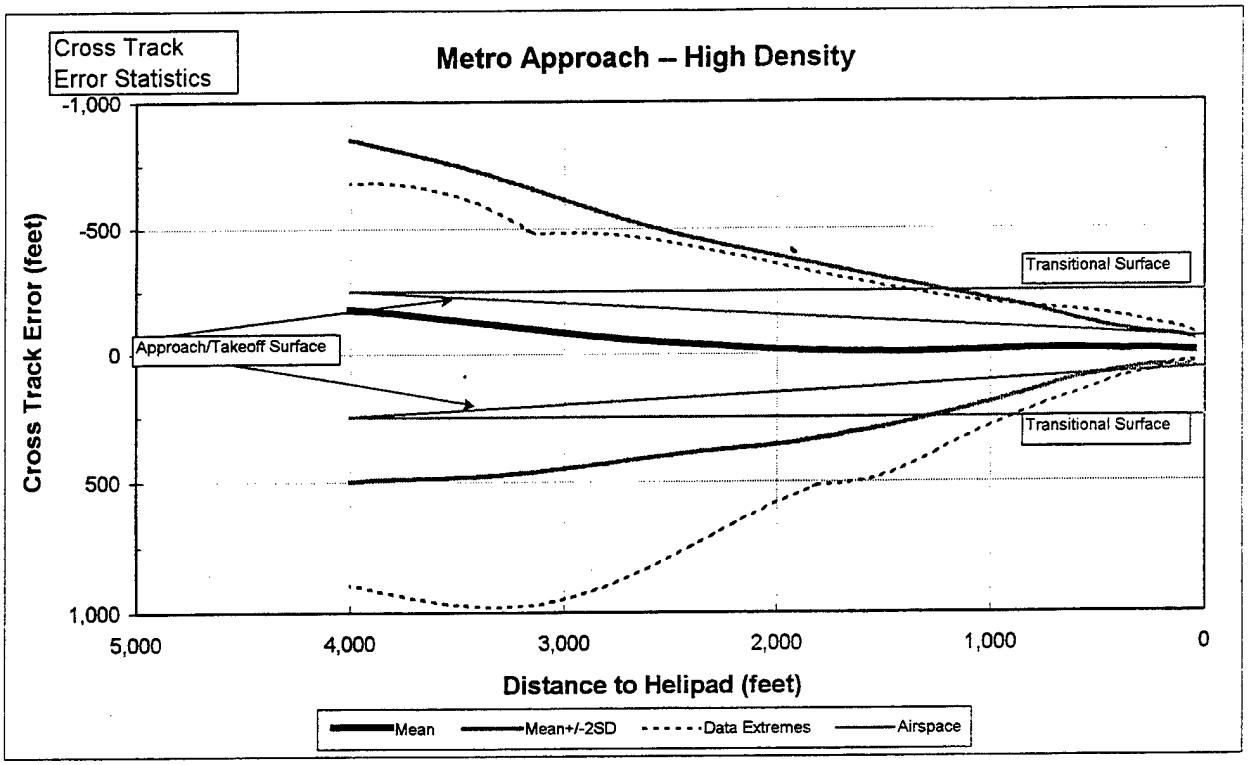

Figure H.2-25 Metro Approach High Density Cross Track Data

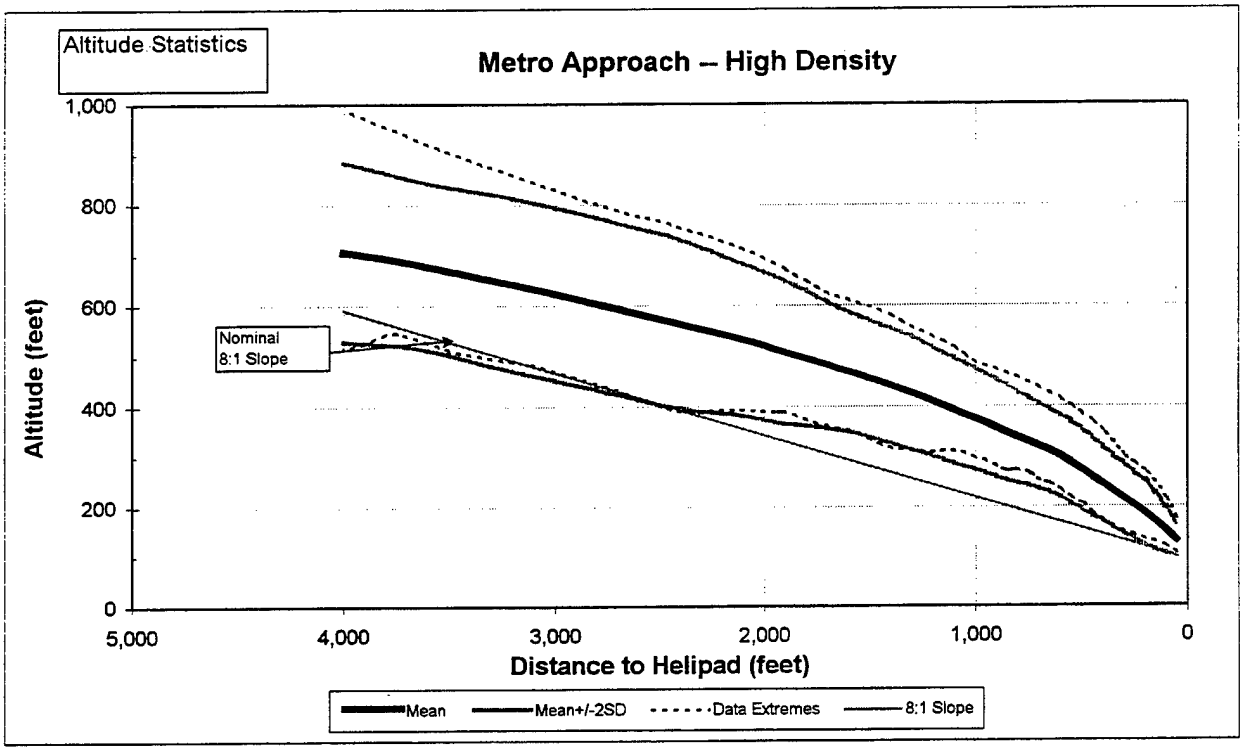

Figure H.2-26 Metro Approach High Density Altitude Data

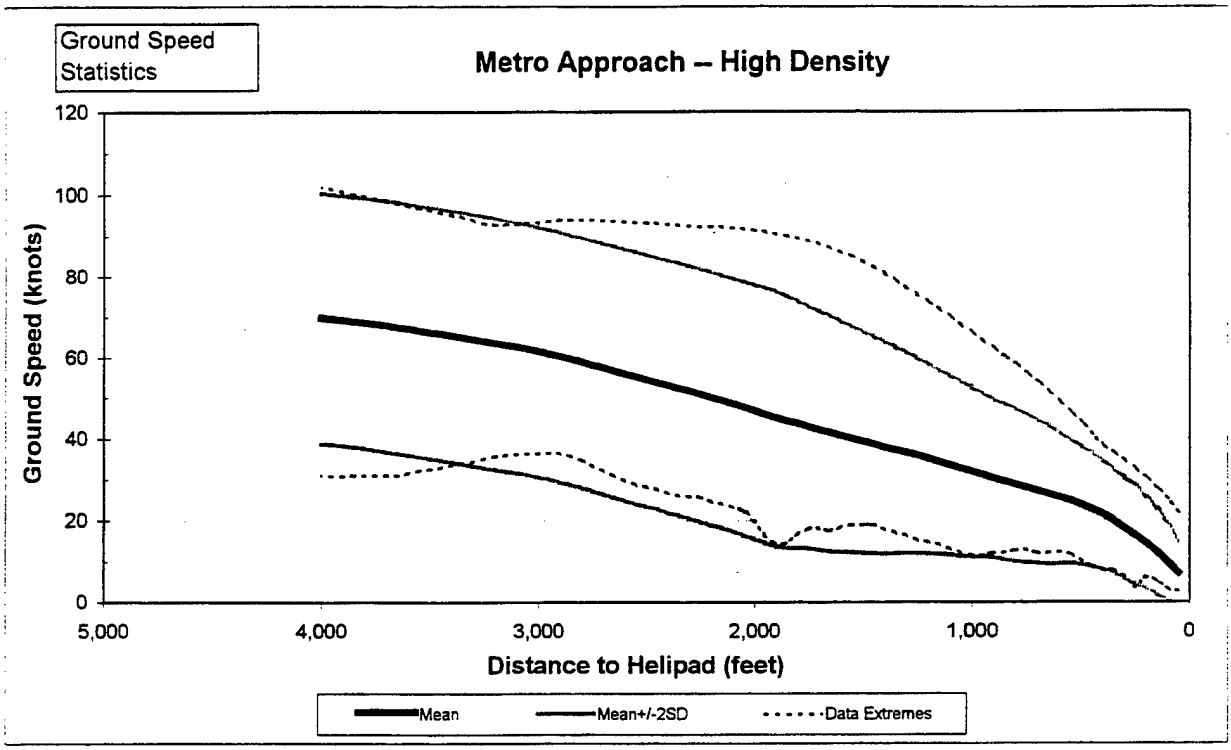

Figure H.2-27 Metro Approach High Density Ground Speed Data

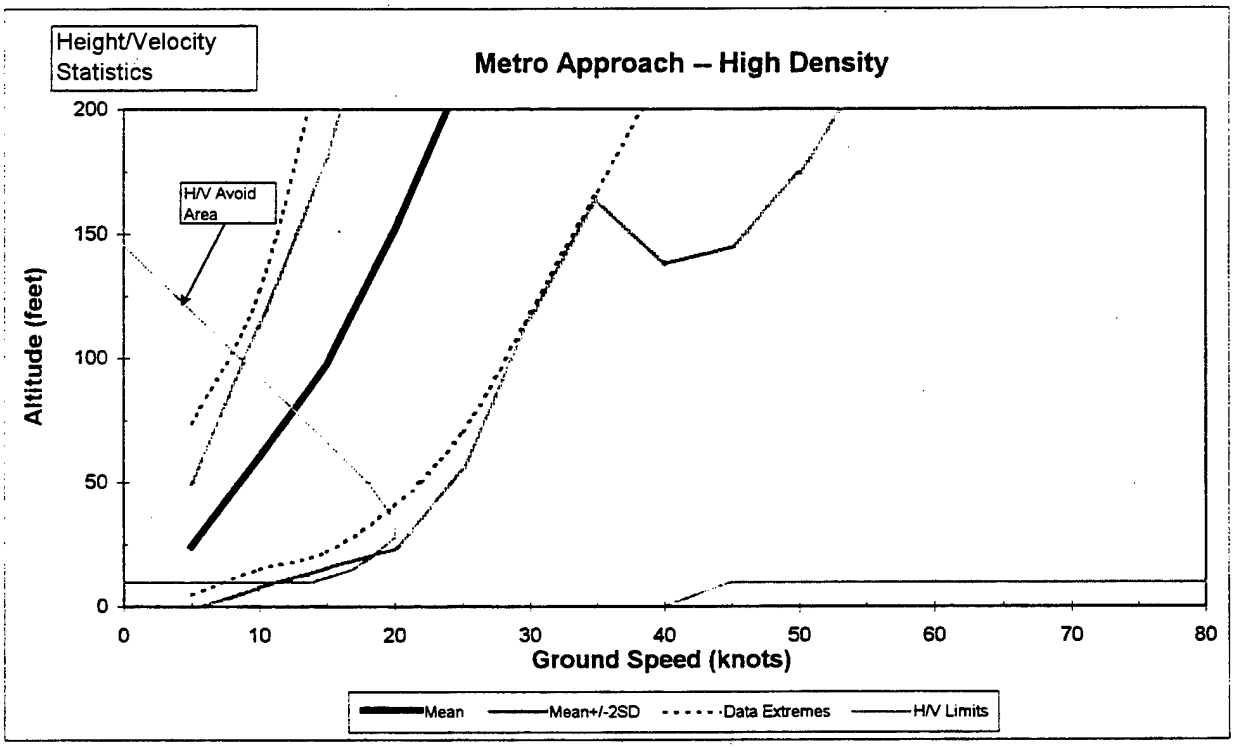

Figure H.2-28 Metro Approach High Density Height/Velocity Data

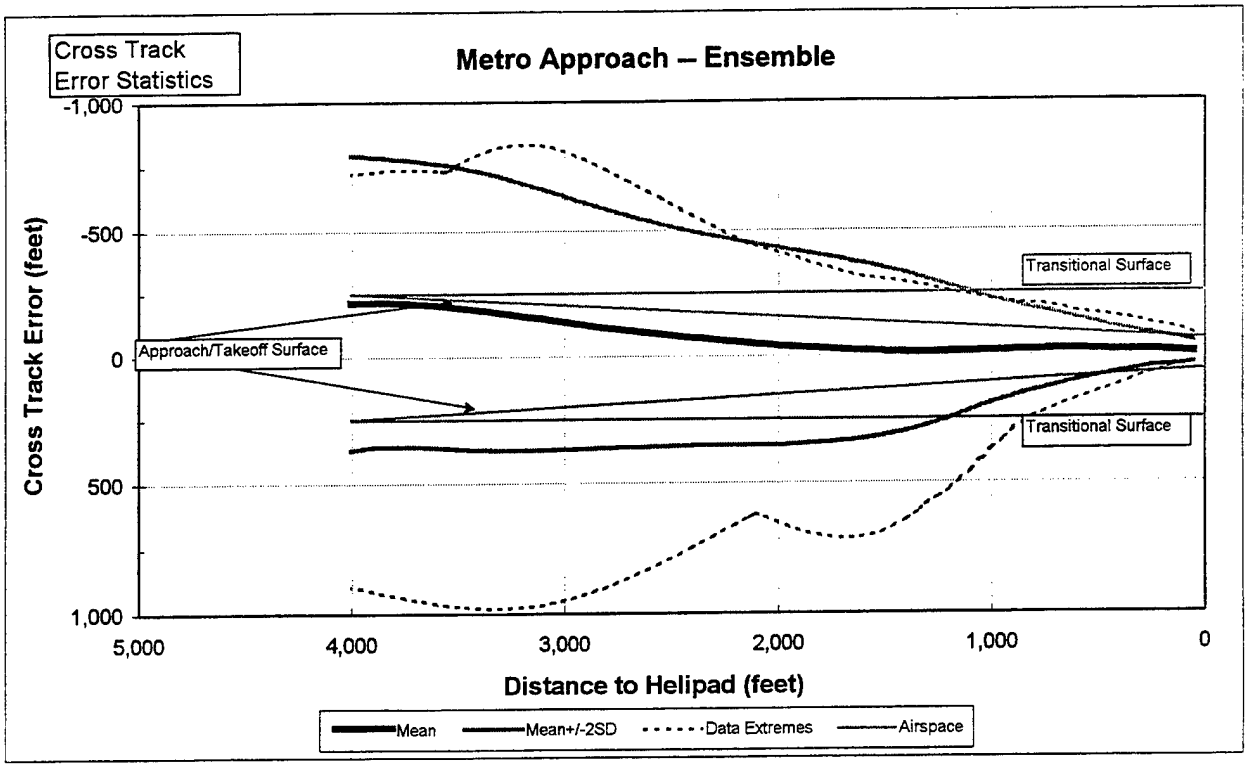

Figure H.2-29 Metro Approach Ensemble Cross Track Data

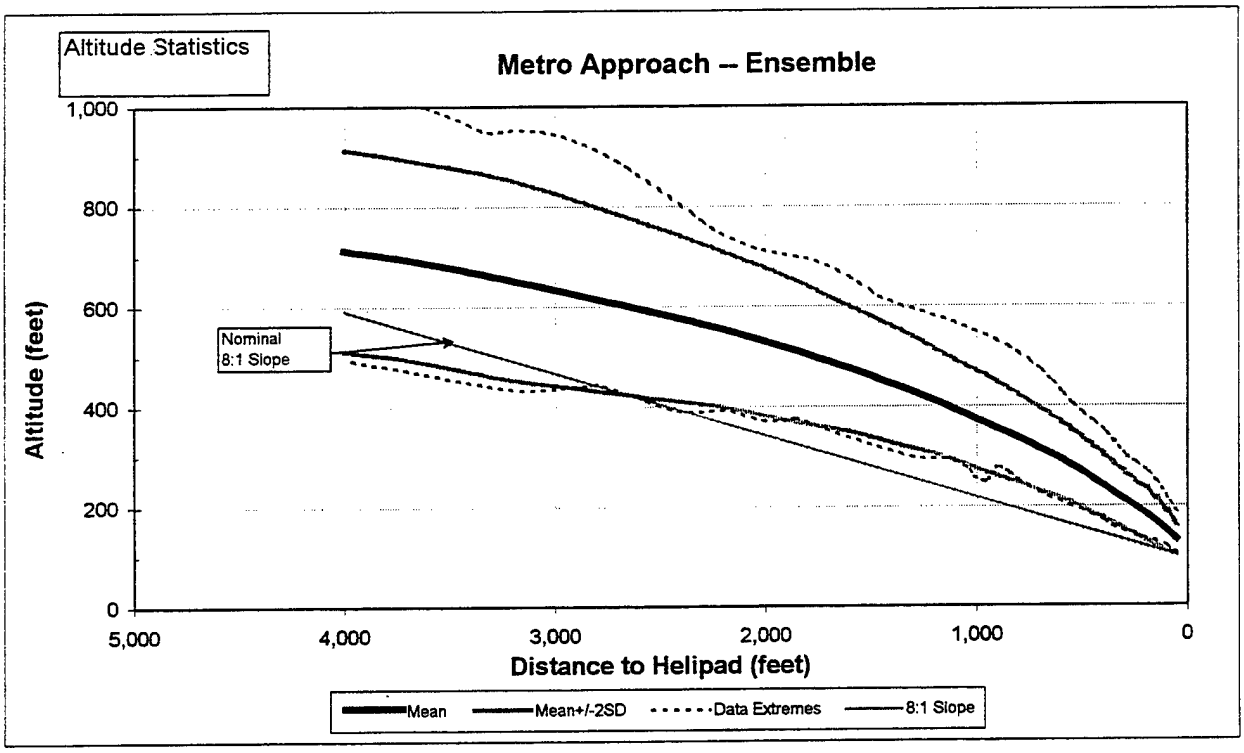

Figure H.2-30 Metro Approach Ensemble Altitude Data

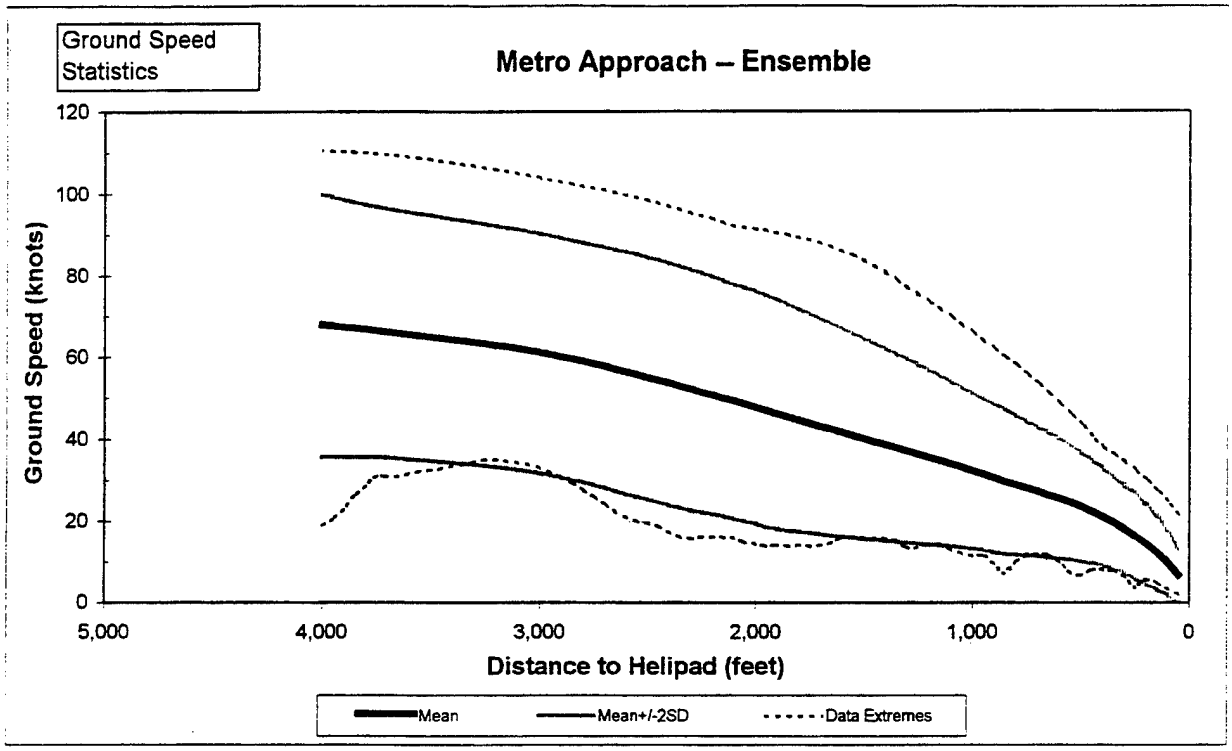

Figure H.2-31 Metro Approach Ensemble Ground Speed Data

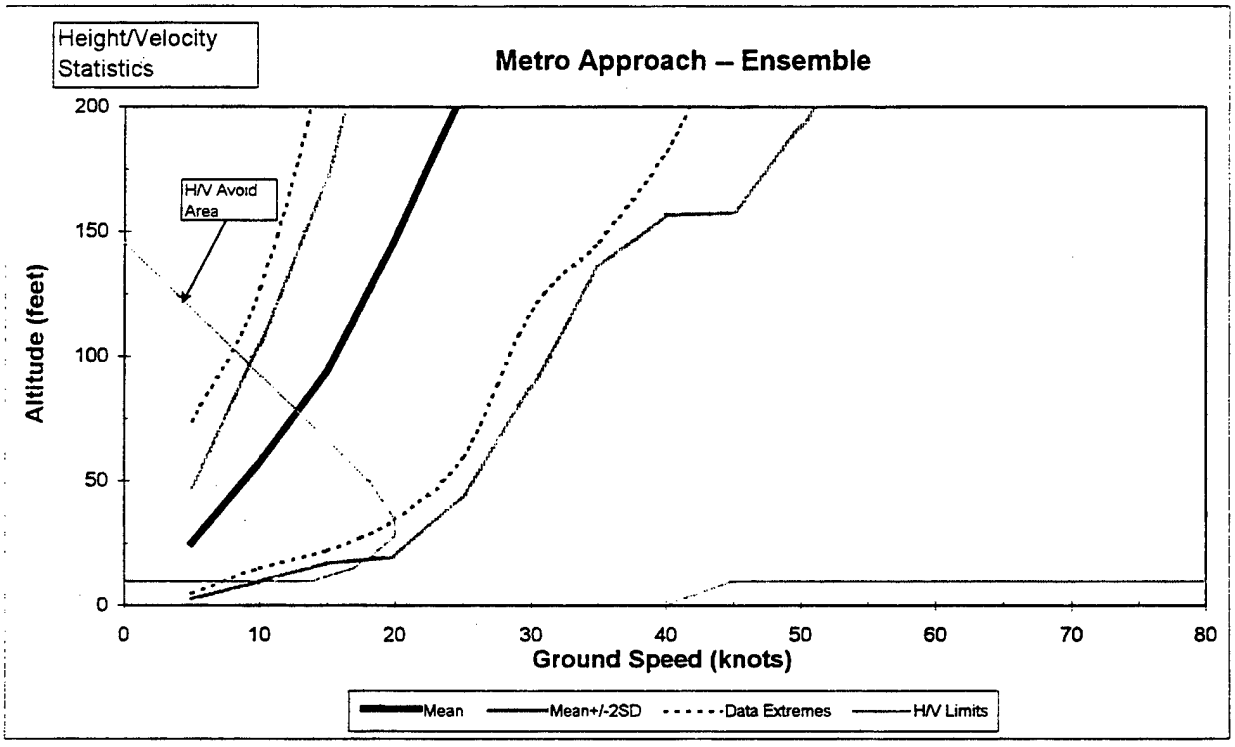

Figure H.2-32 Metro Approach Ensemble Height/Velocity Data

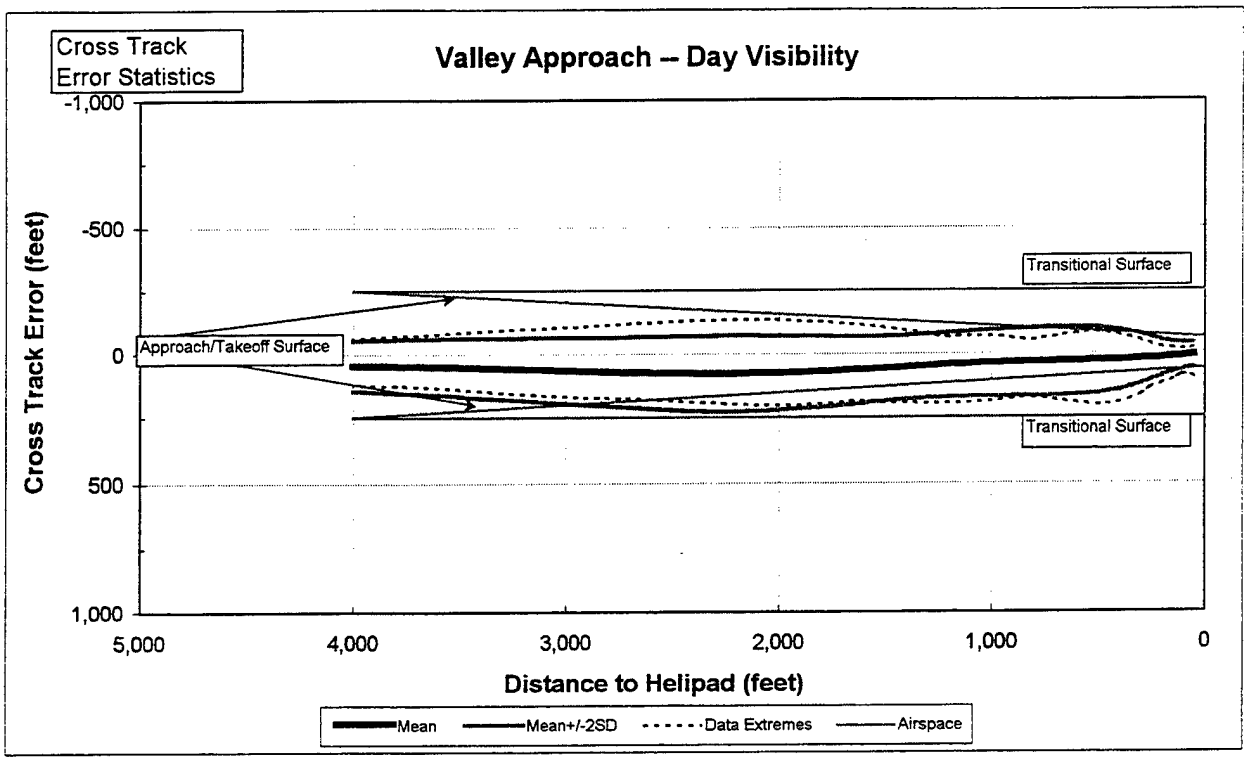

Figure H.2-33 Valley Approach Day Visibility Cross Track Data

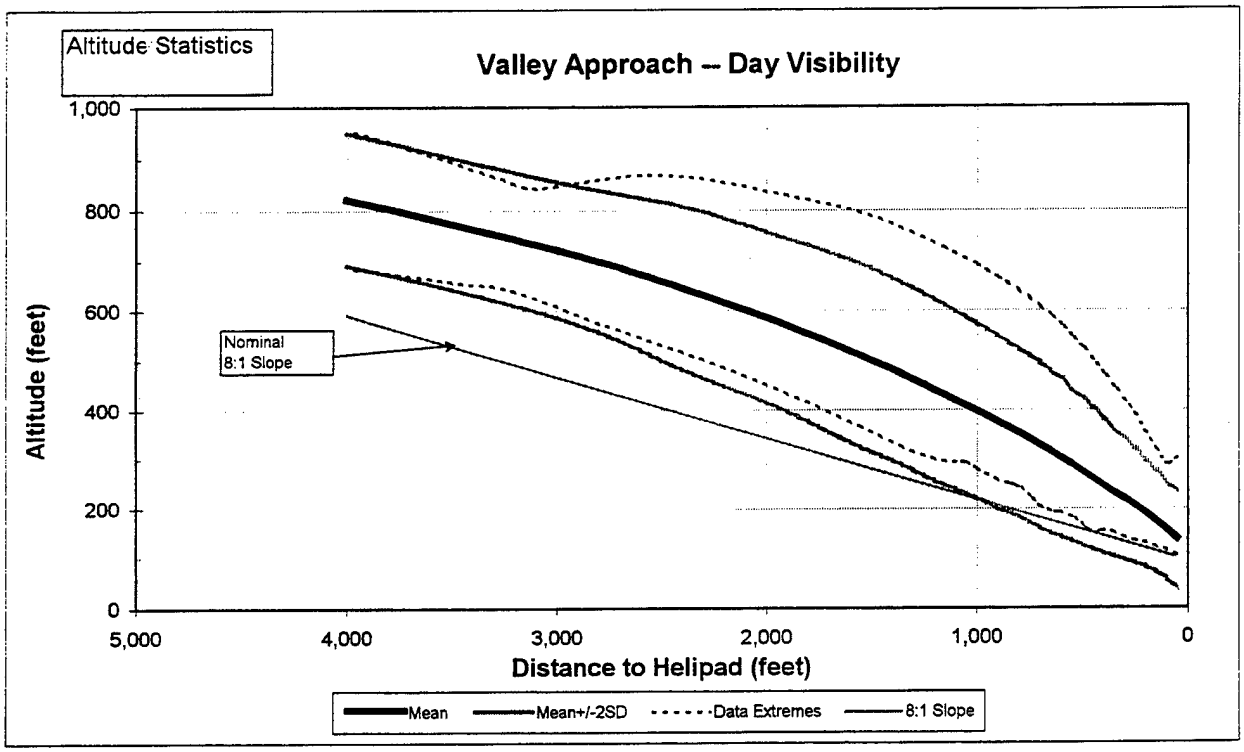

Figure H.2-34 Valley Approach Day Visibility Altitude Data

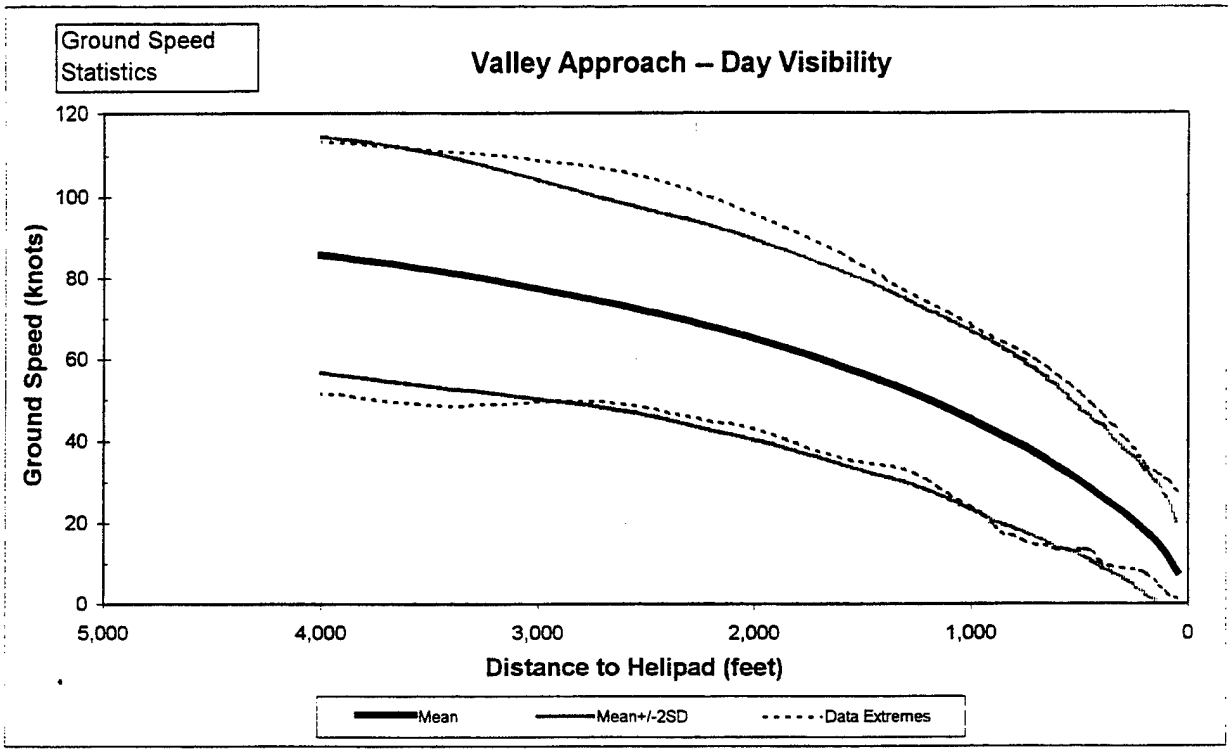

Figure H.2-35 Valley Approach Day Visibility Ground Speed Data

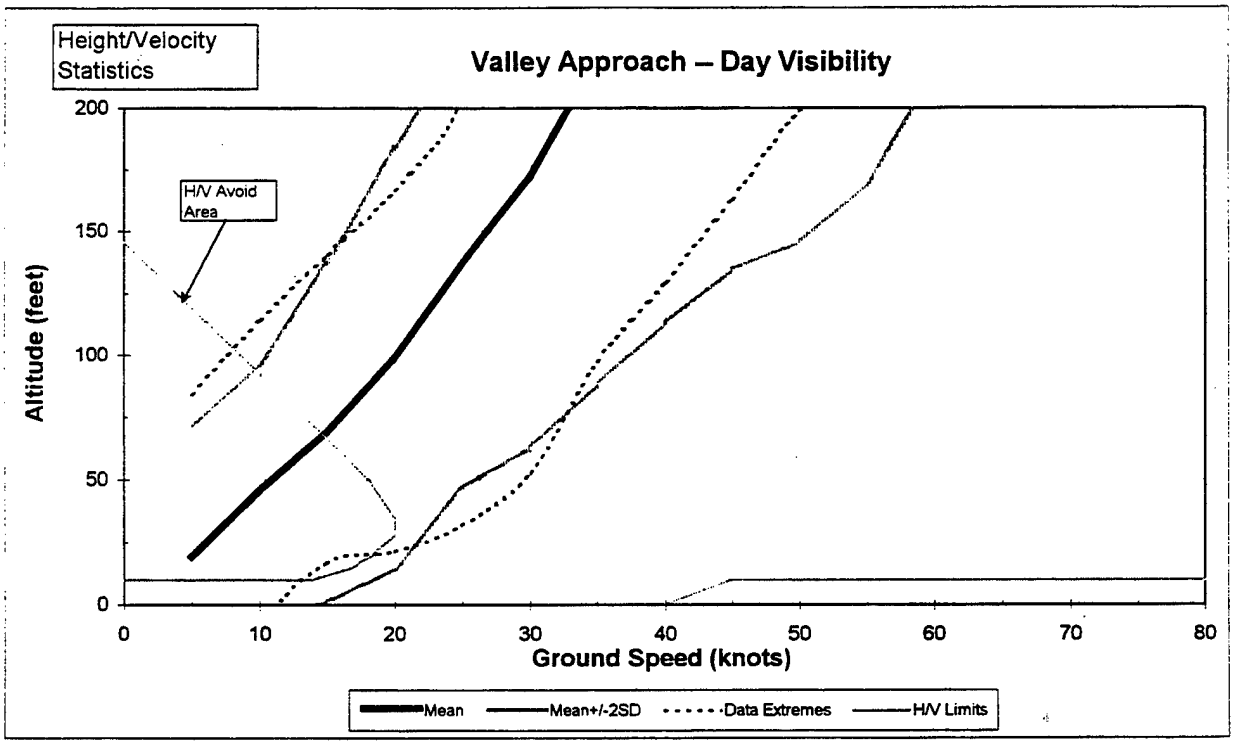

Figure H.2-36 Valley Approach Day Visibility Height/Velocity Data

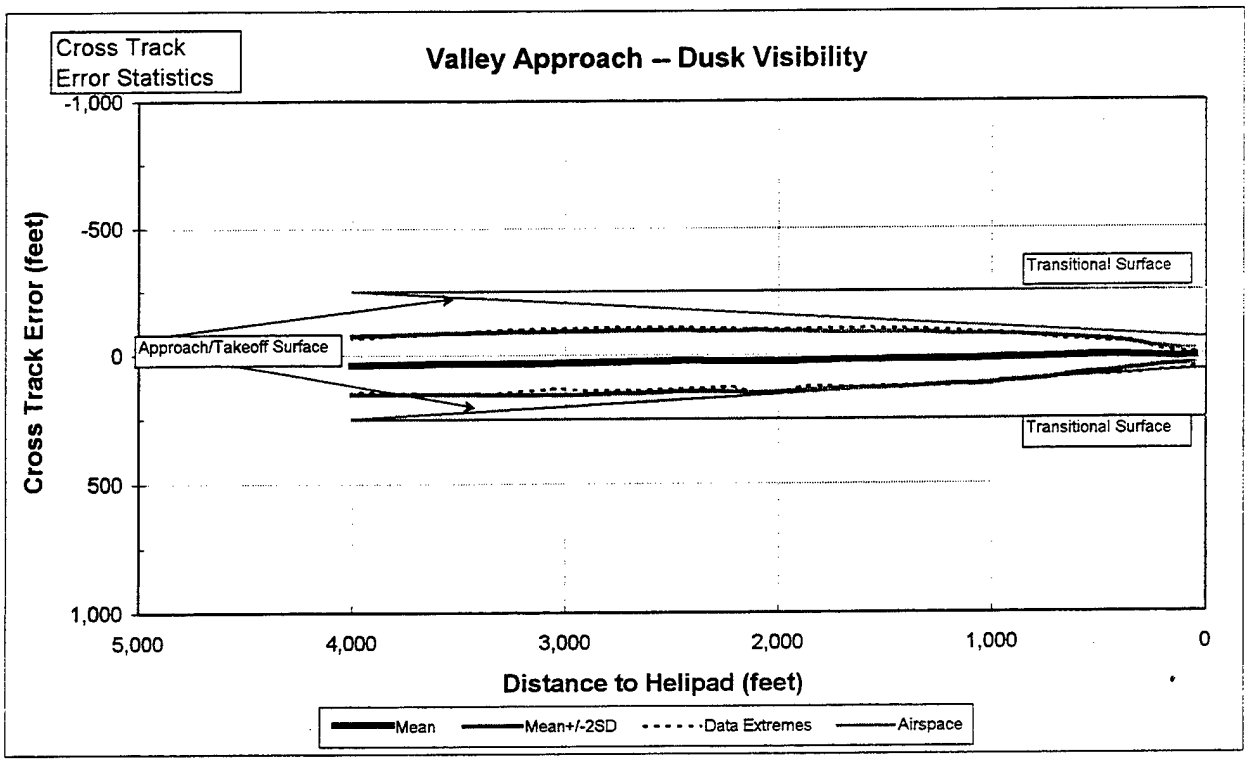

Figure H.2-37 Valley Approach Dusk Visibility Cross Track Data

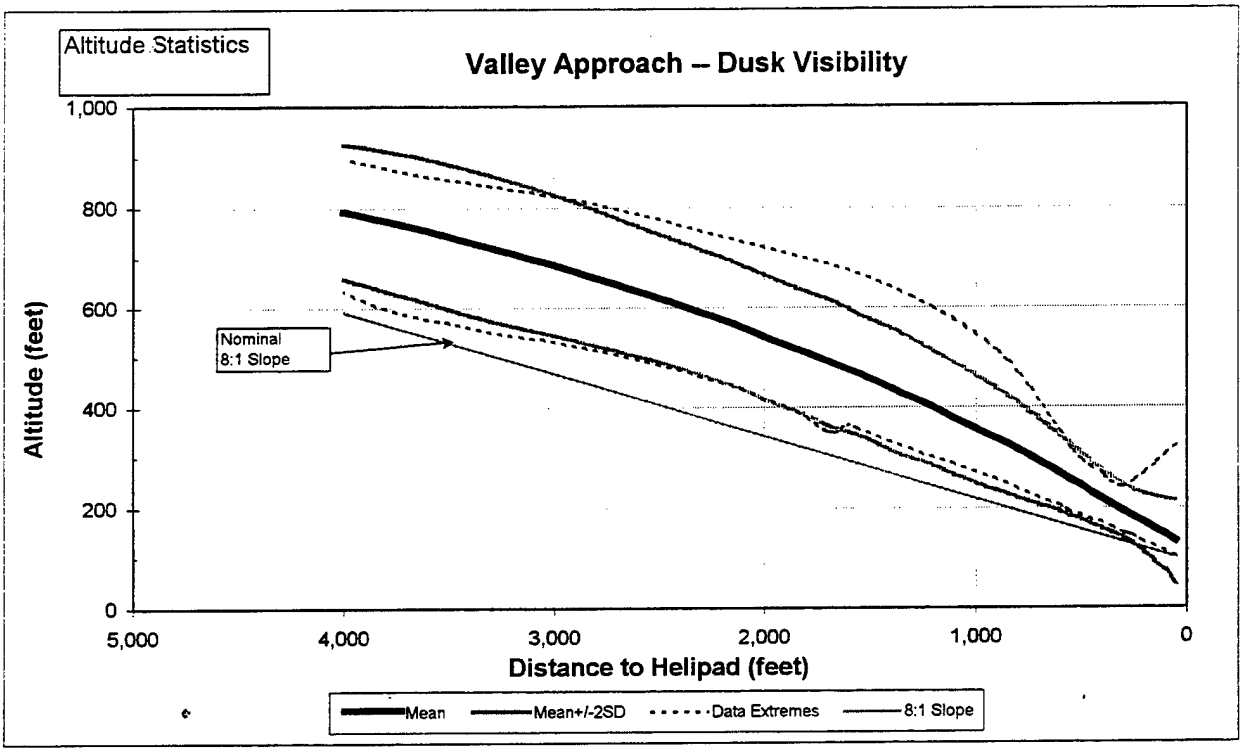

Figure H.2-38 Valley Approach Dusk Visibility Altitude Data

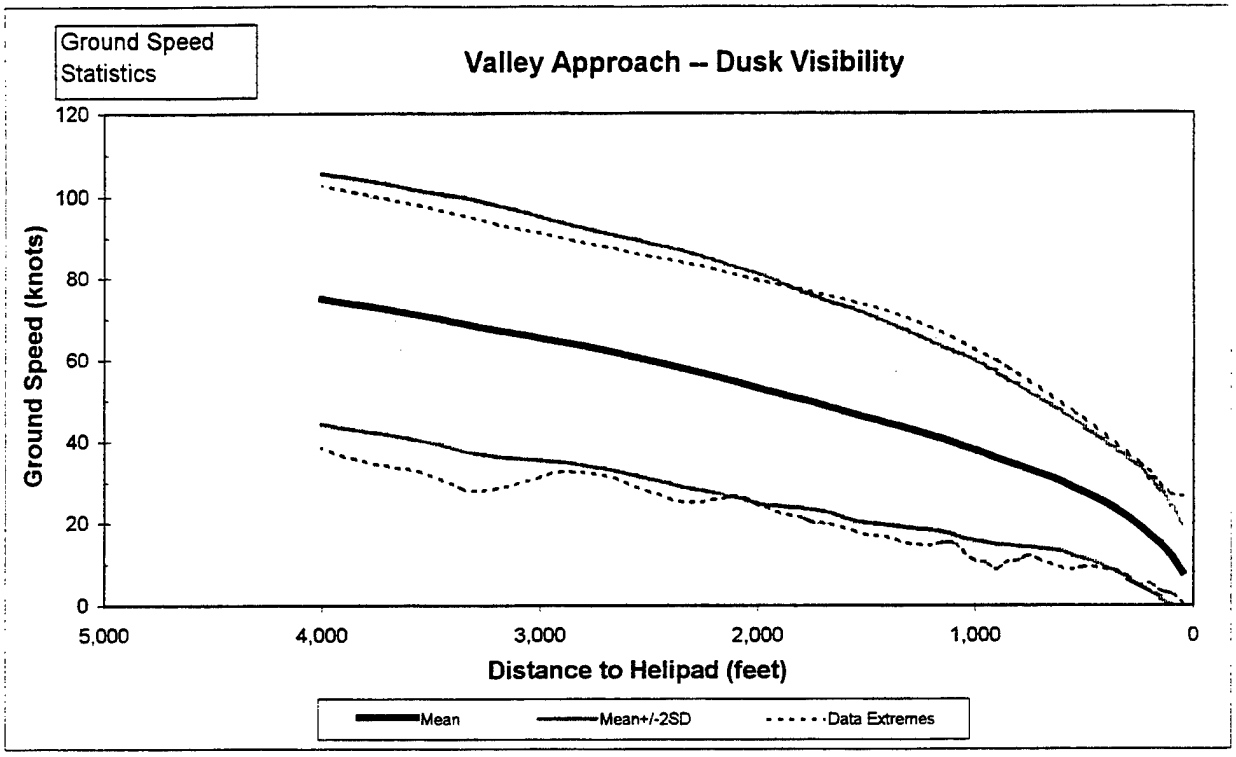

Figure H.2-39 Valley Approach Dusk Visibility Ground Speed Data

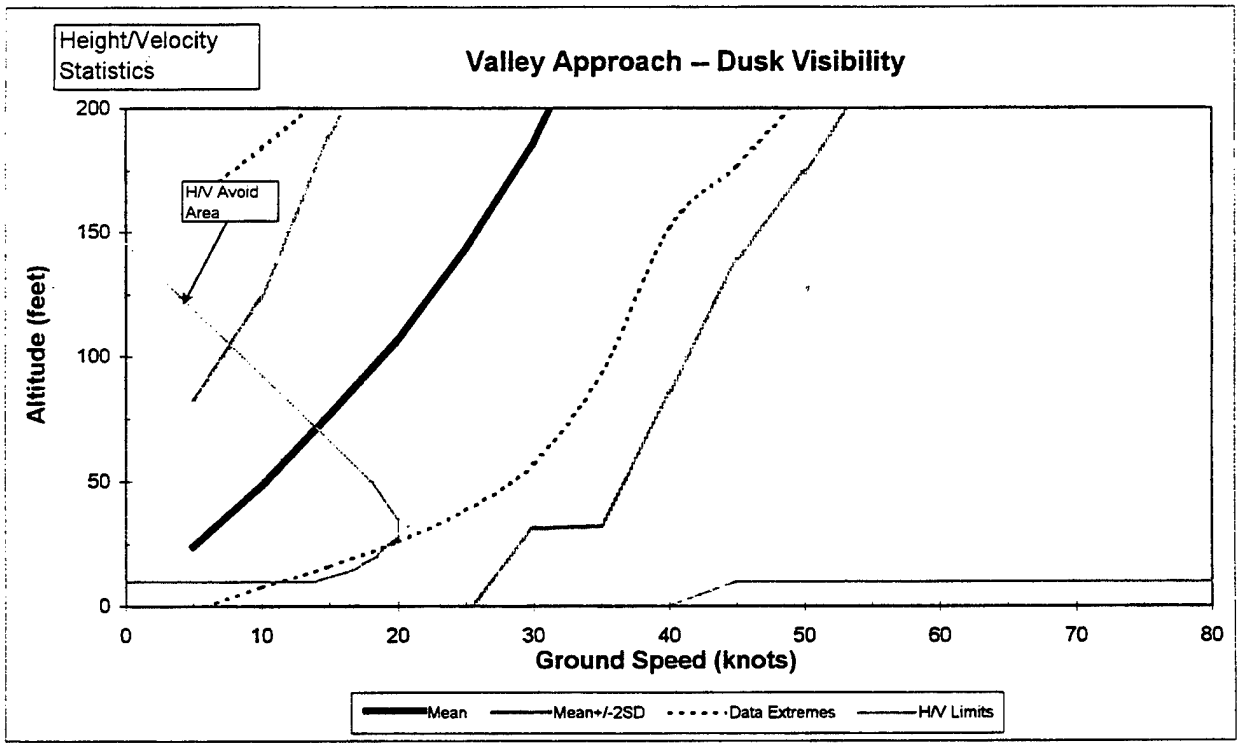

Figure H.2-40 Valley Approach Dusk Visibility Height/Velocity Data

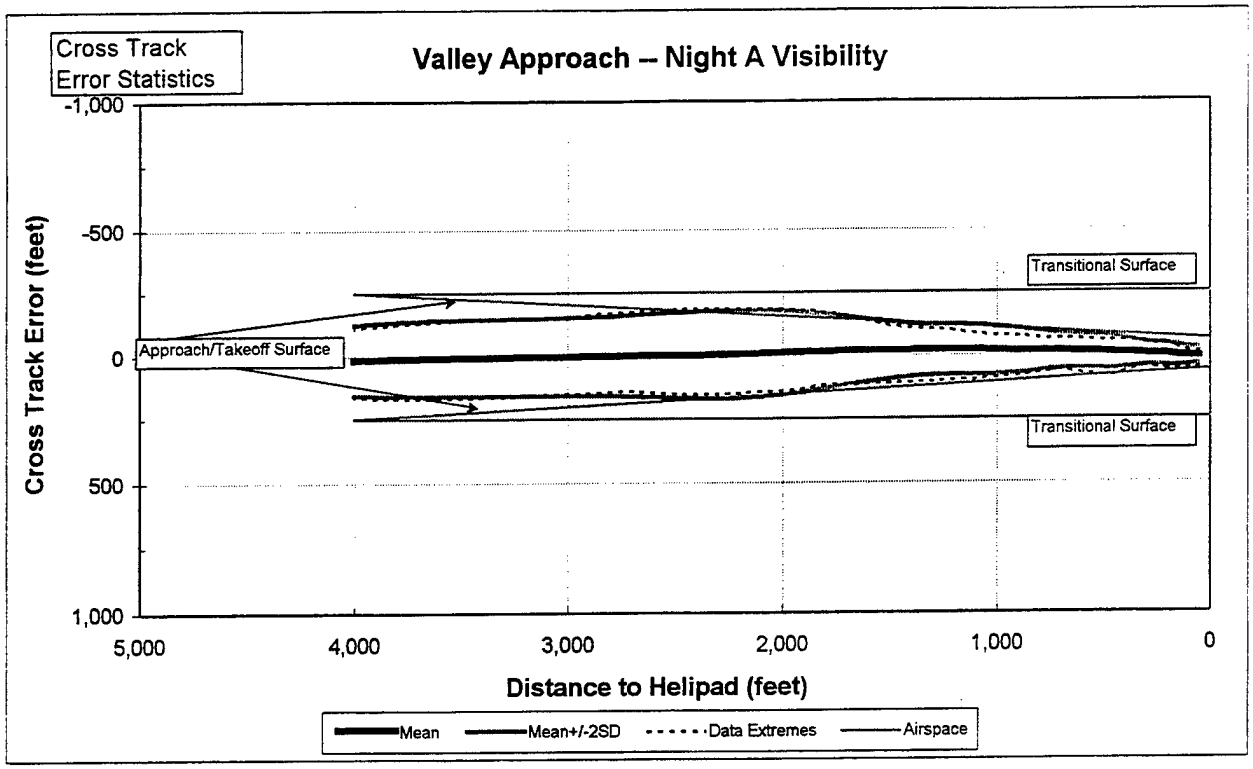

Figure H.2-41 Valley Approach Night A Visibility Cross Track Data

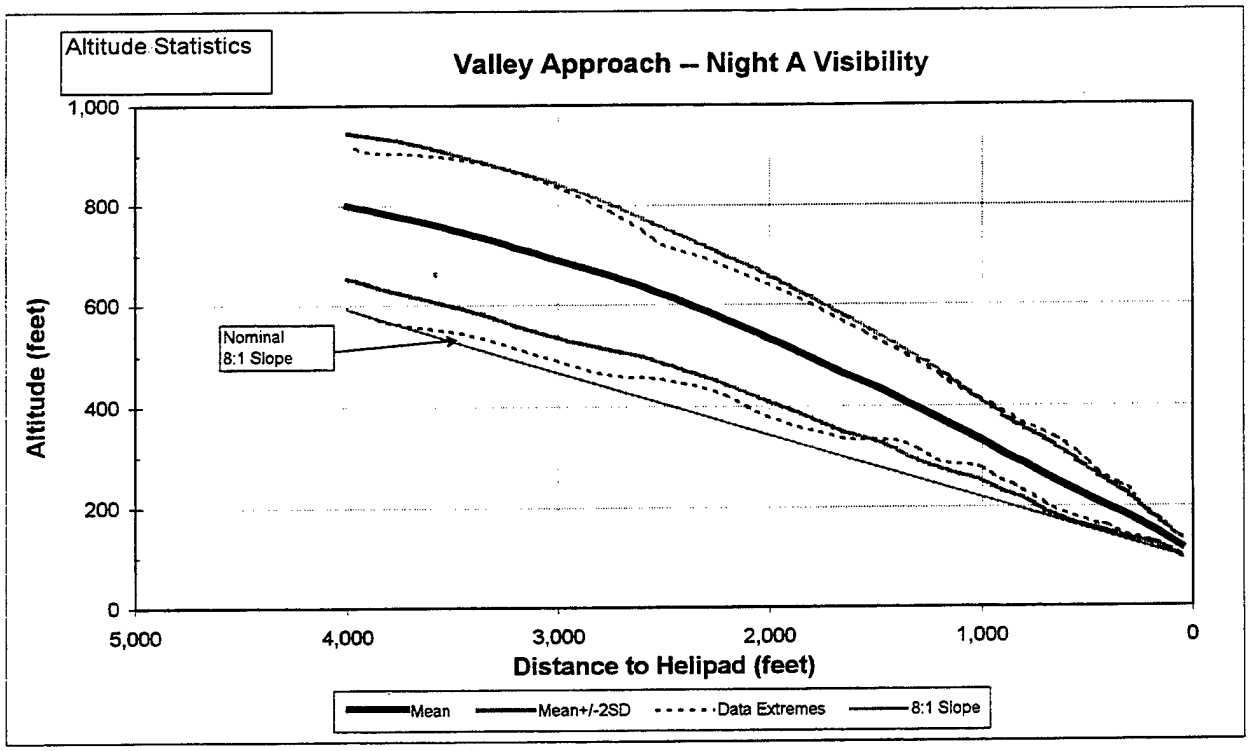

Figure H.2-42 Valley Approach Night A Visibility Altitude Data

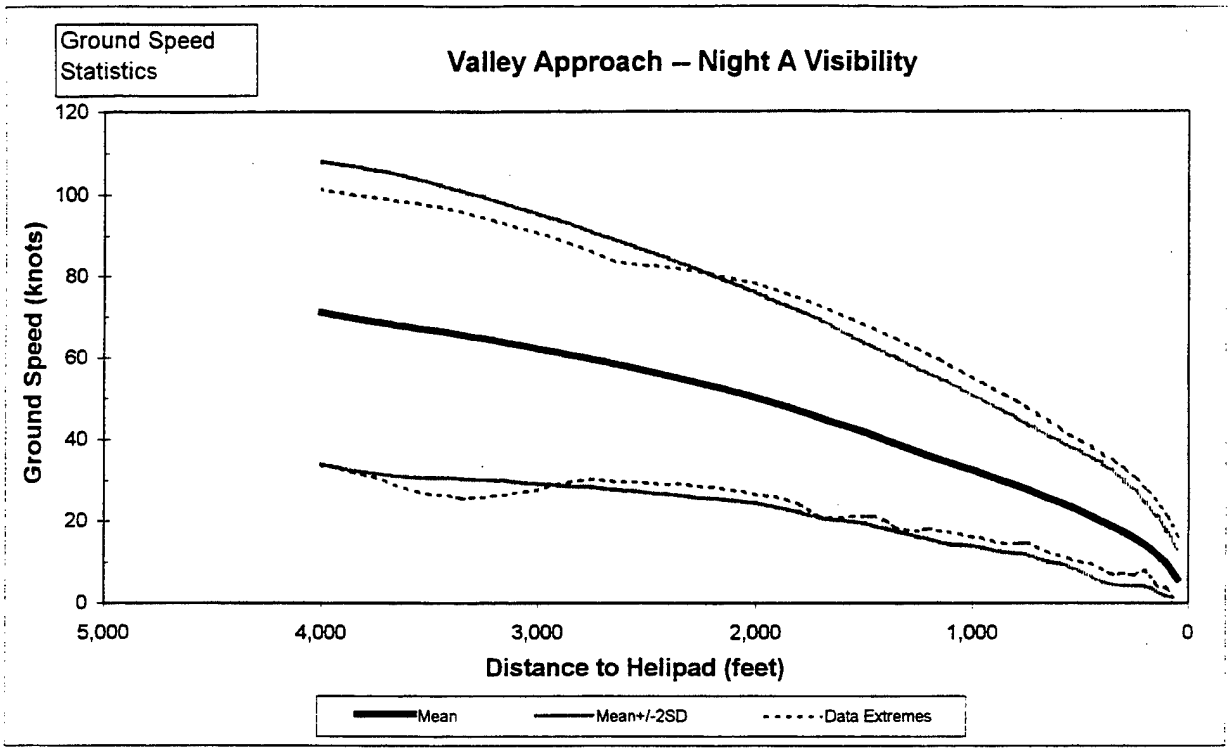

Figure H.2-43 Valley Approach Night A Visibility Ground Speed Data

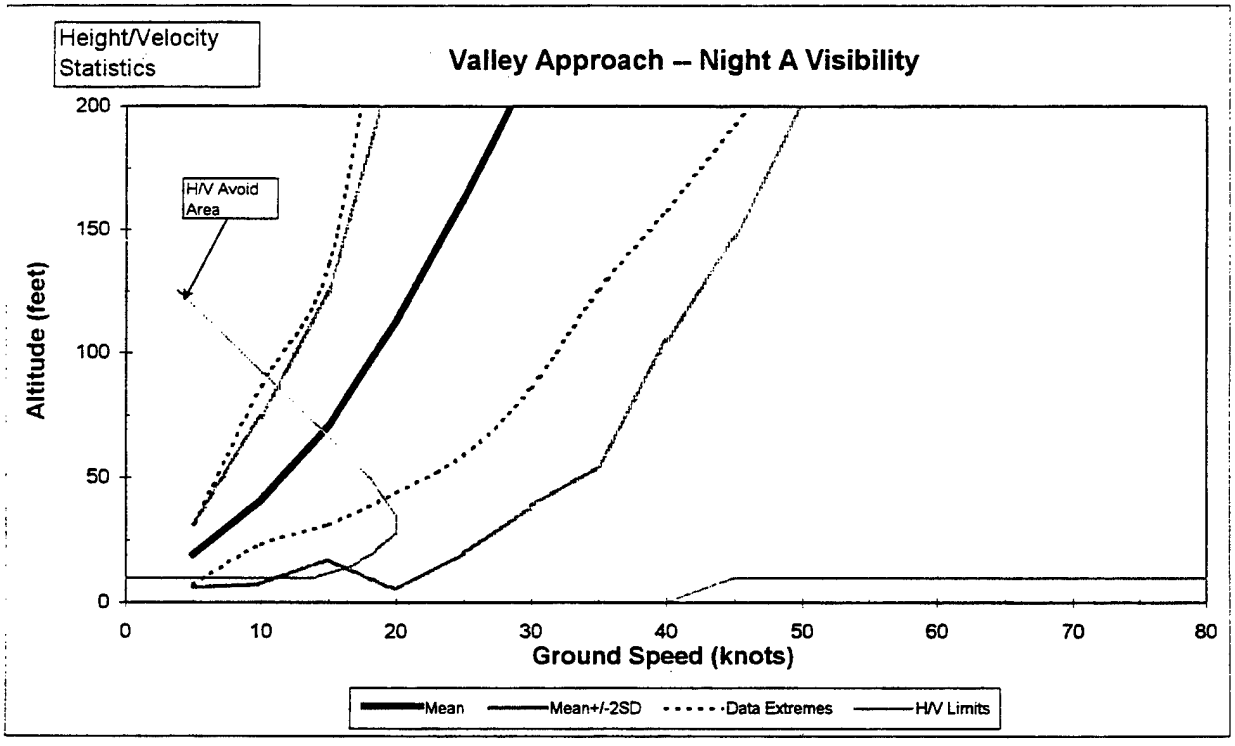

Figure H.2-44 Valley Approach Night A Visibility Height/Velocity Data

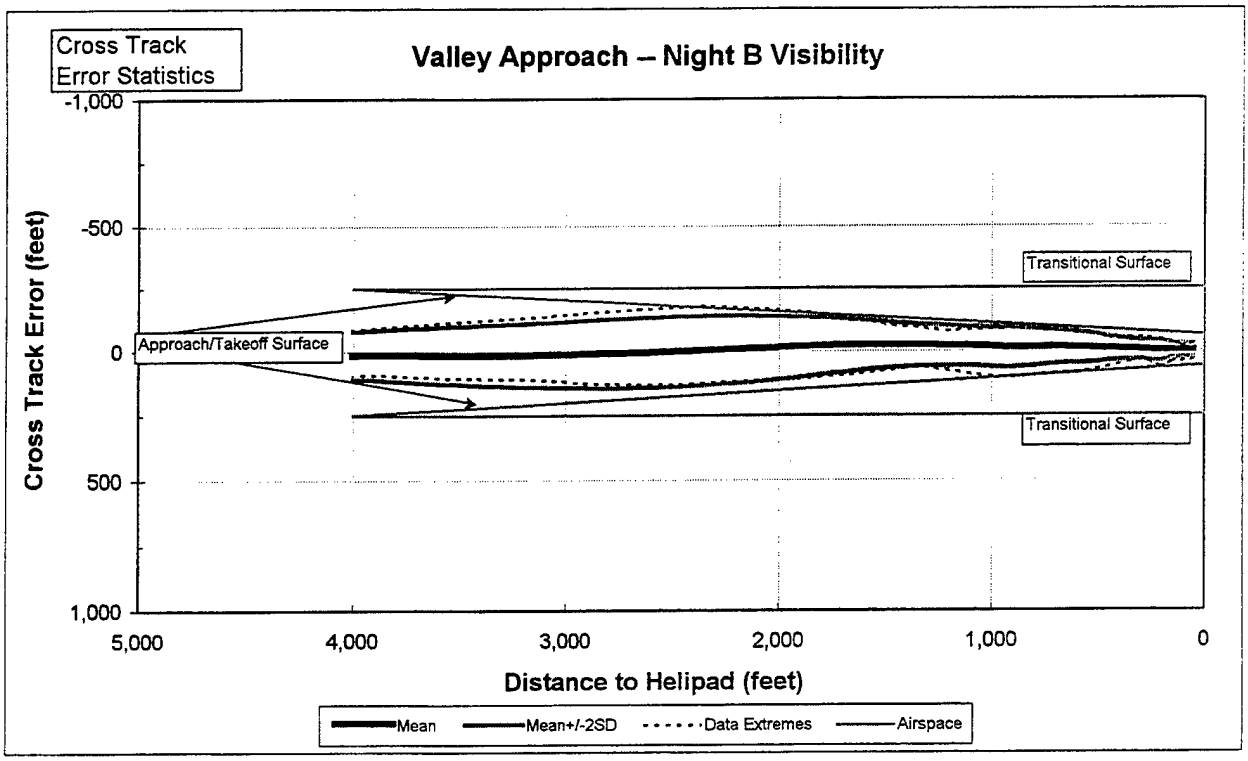

Figure H.2-45 Valley Approach Night B Visibility Cross Track Data

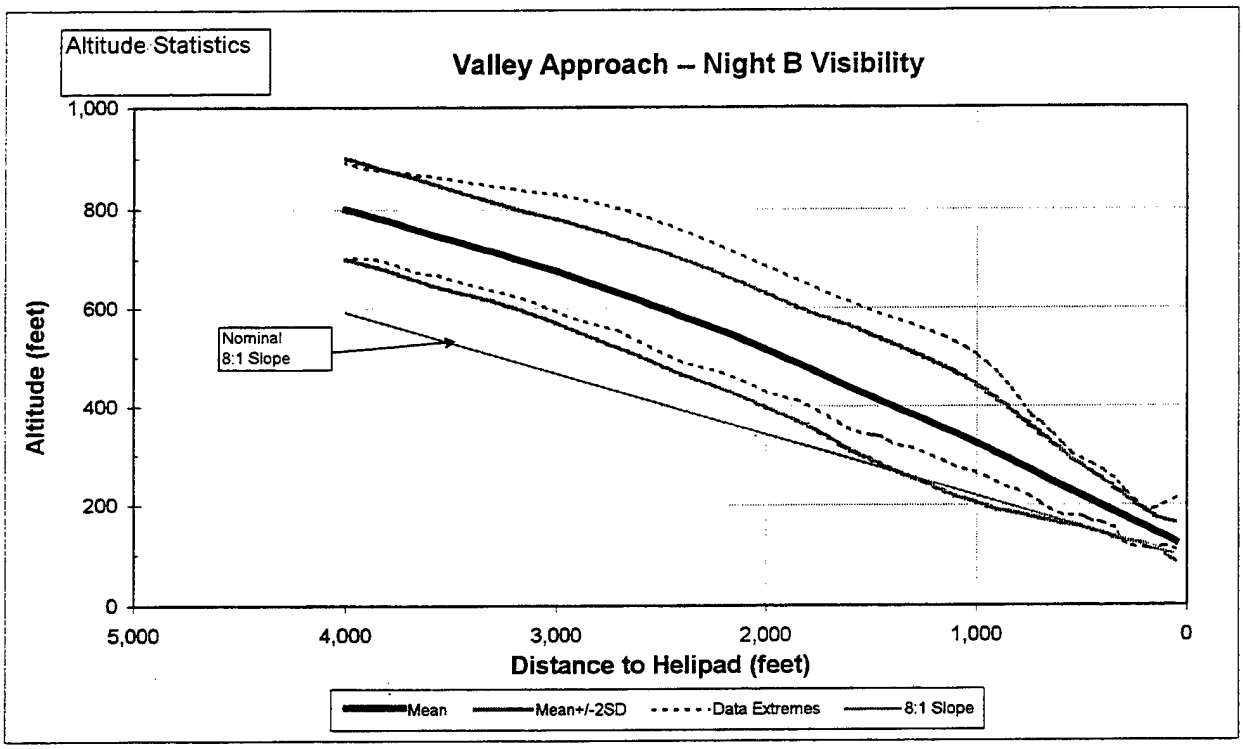

Figure H.2-46 Valley Approach Night B Visibility Altitude Data

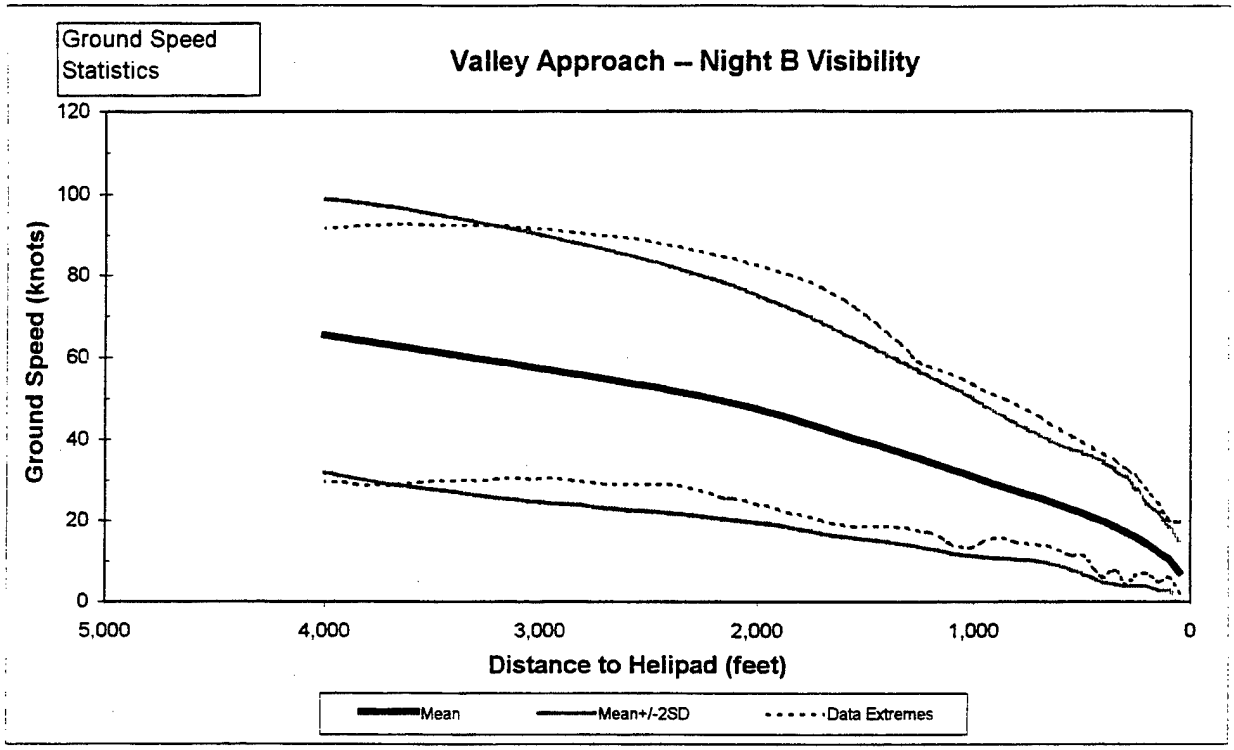

Figure H.2-47 Valley Approach Night B Visibility Ground Speed Data

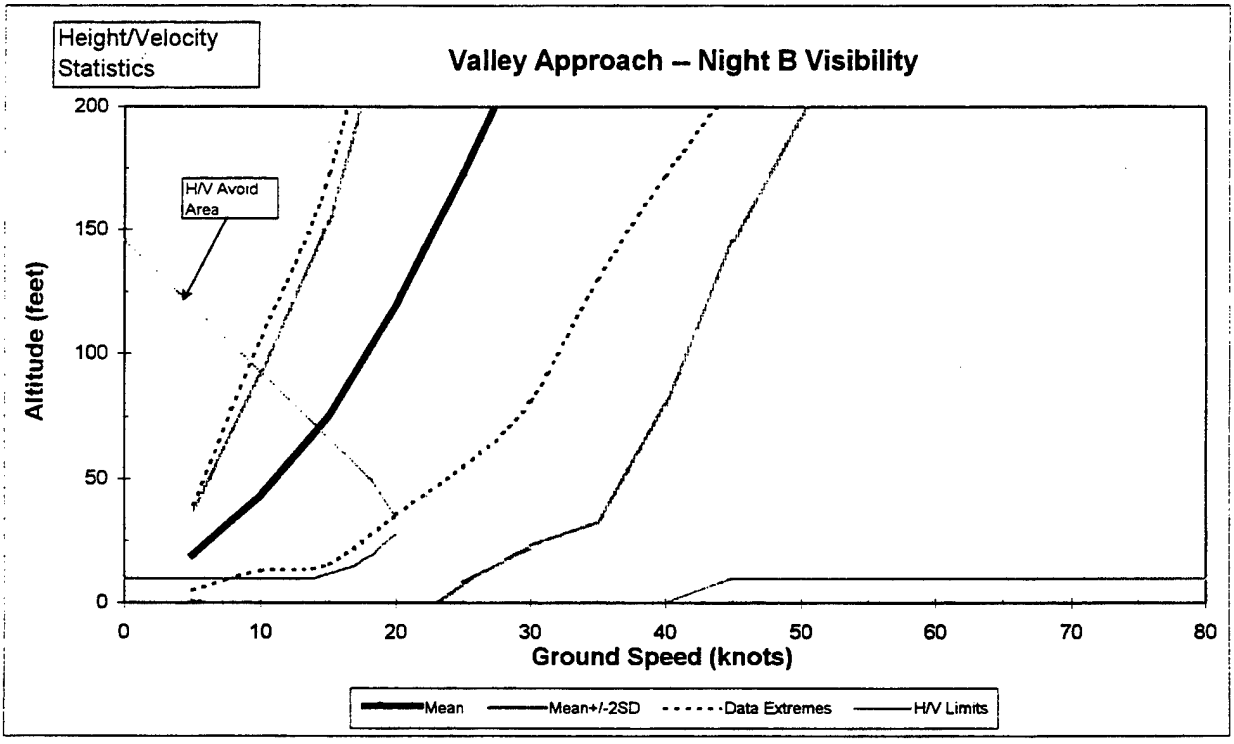

Figure H.2-48 Valley Approach Night B Visibility Height/Velocity Data

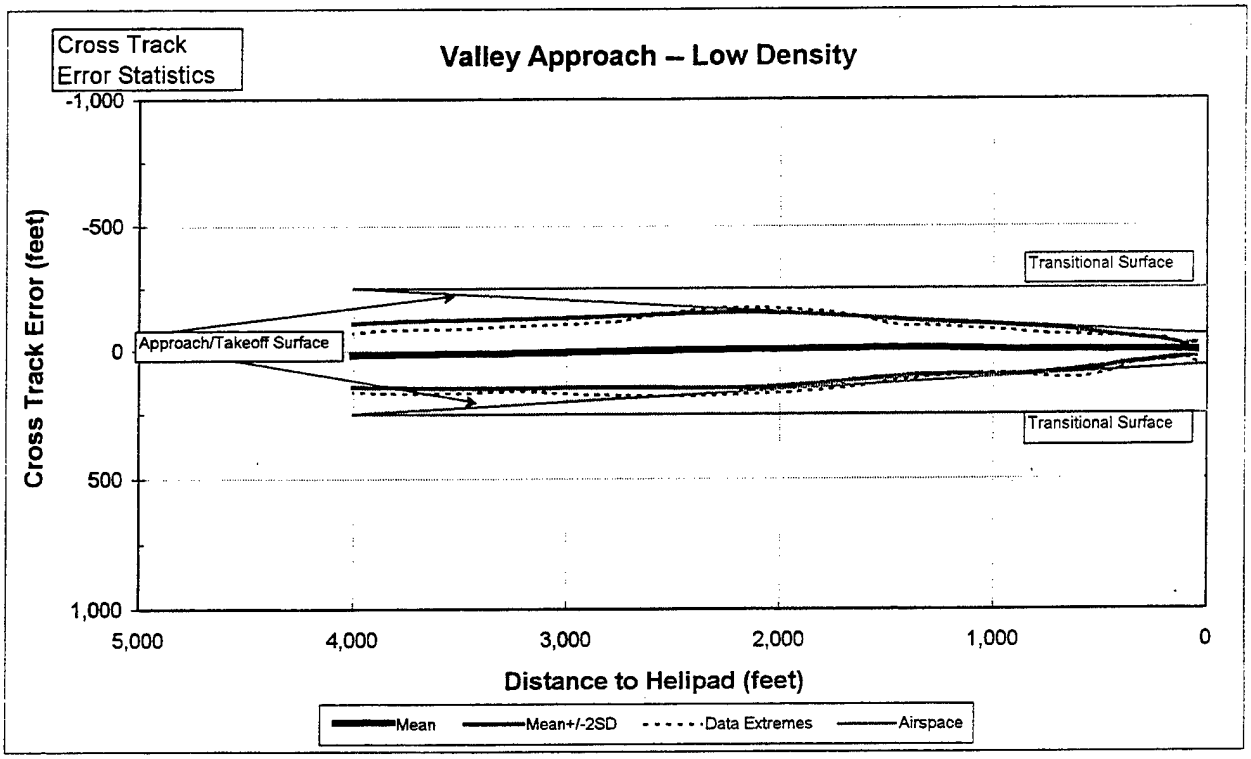

Figure H.2-49 Valley Approach Low Density Cross Track Data

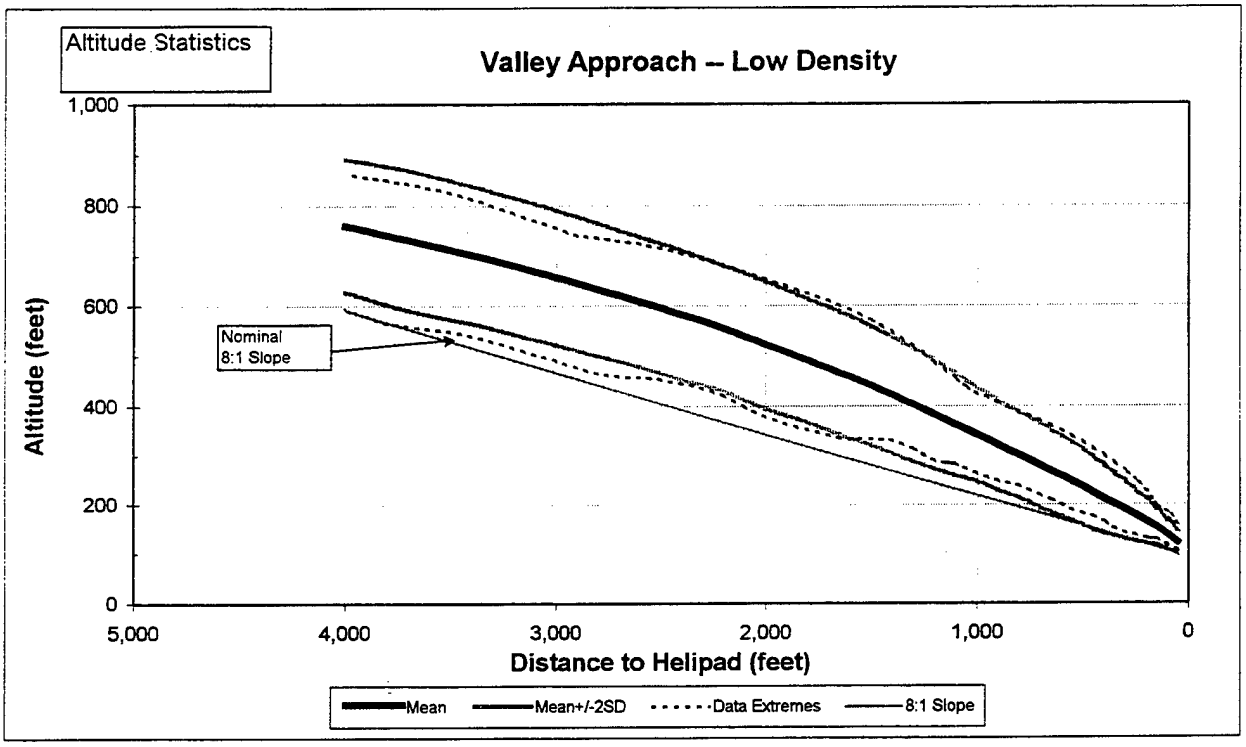

Figure H.2-50 Valley Approach Low Density Altitude Data

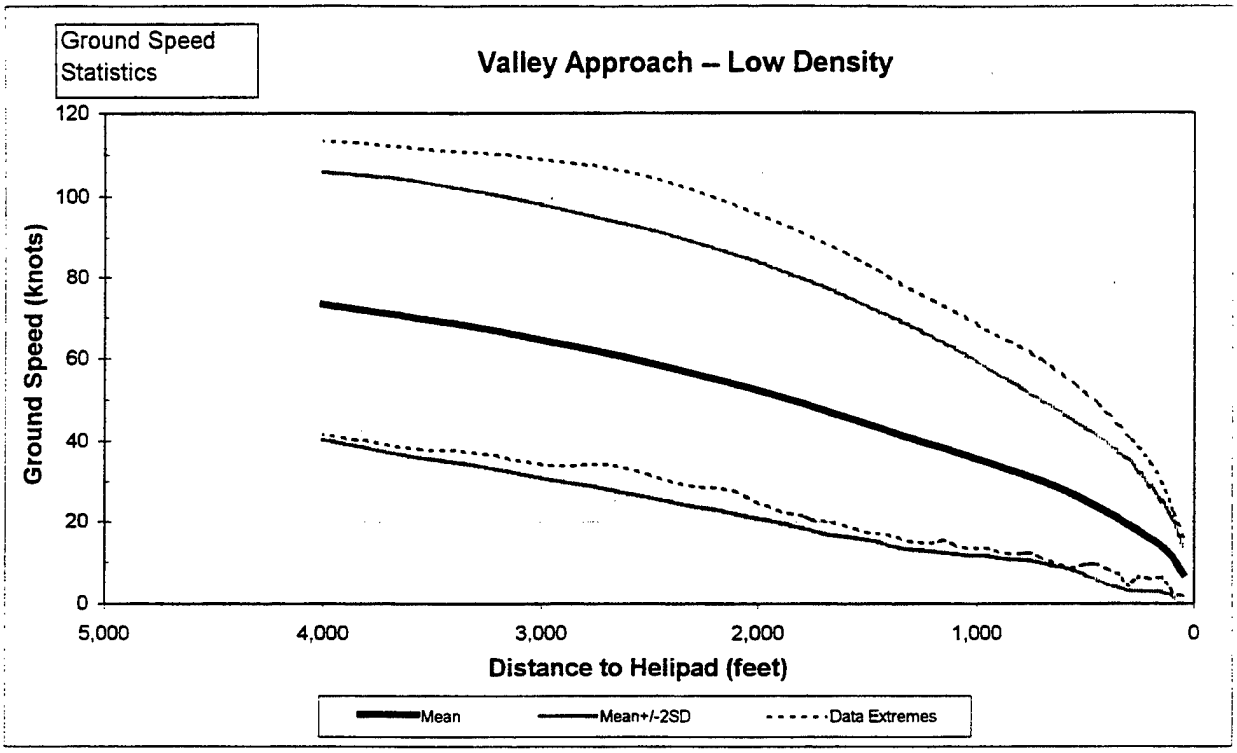

Figure H.2-51 Valley Approach Low Density Ground Speed Data

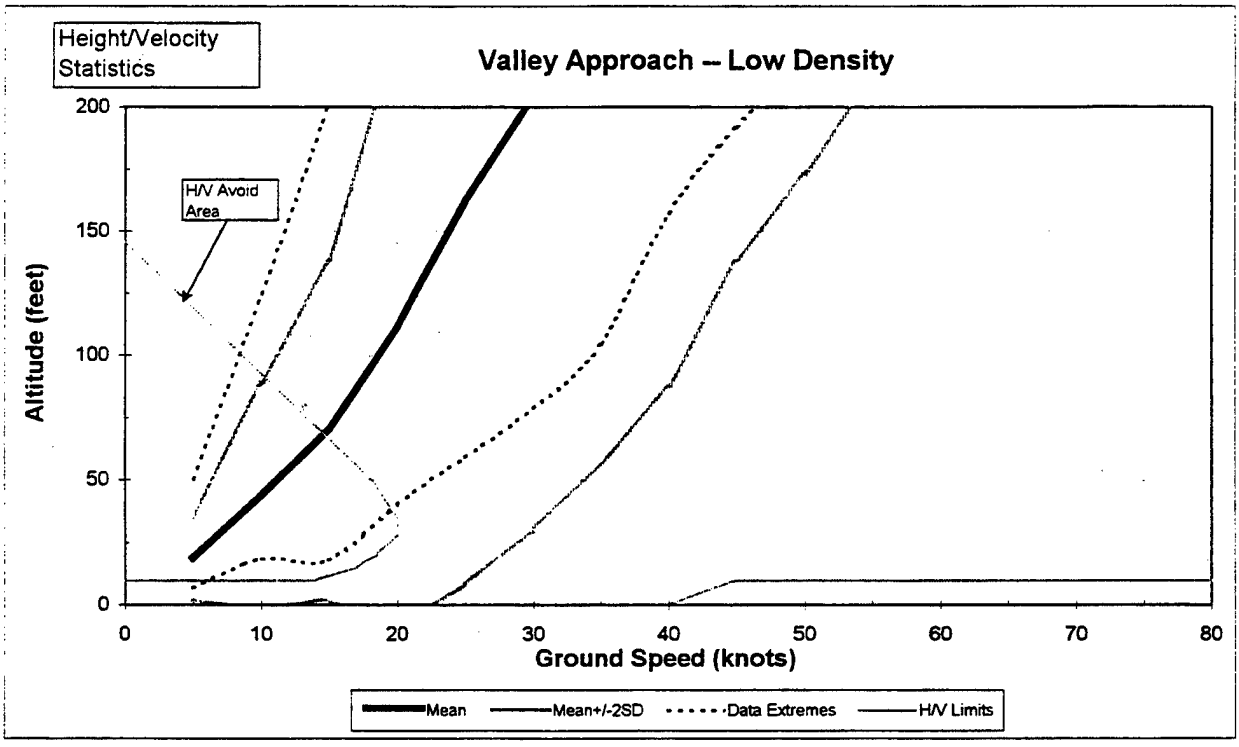

Figure H.2-52 Valley Approach Low Density Height/Velocity Data

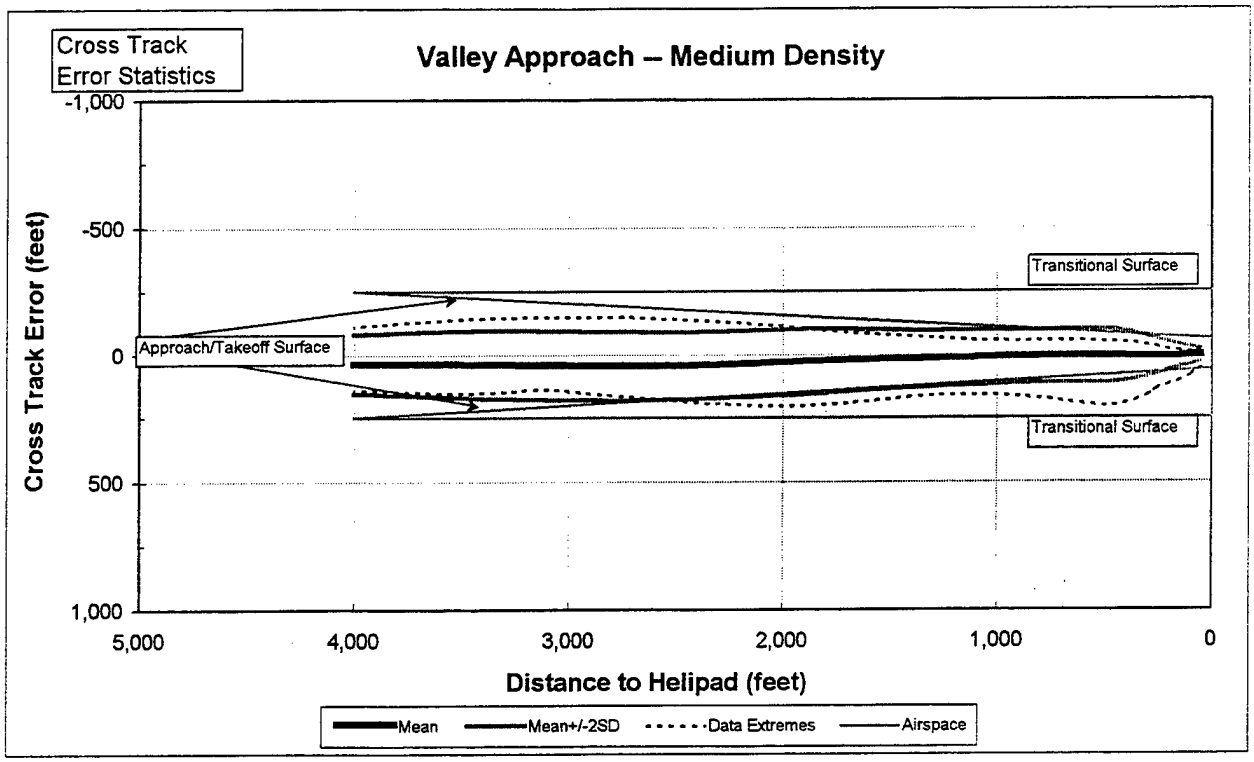

Figure H.2-53 Valley Approach Medium Density Cross Track Data

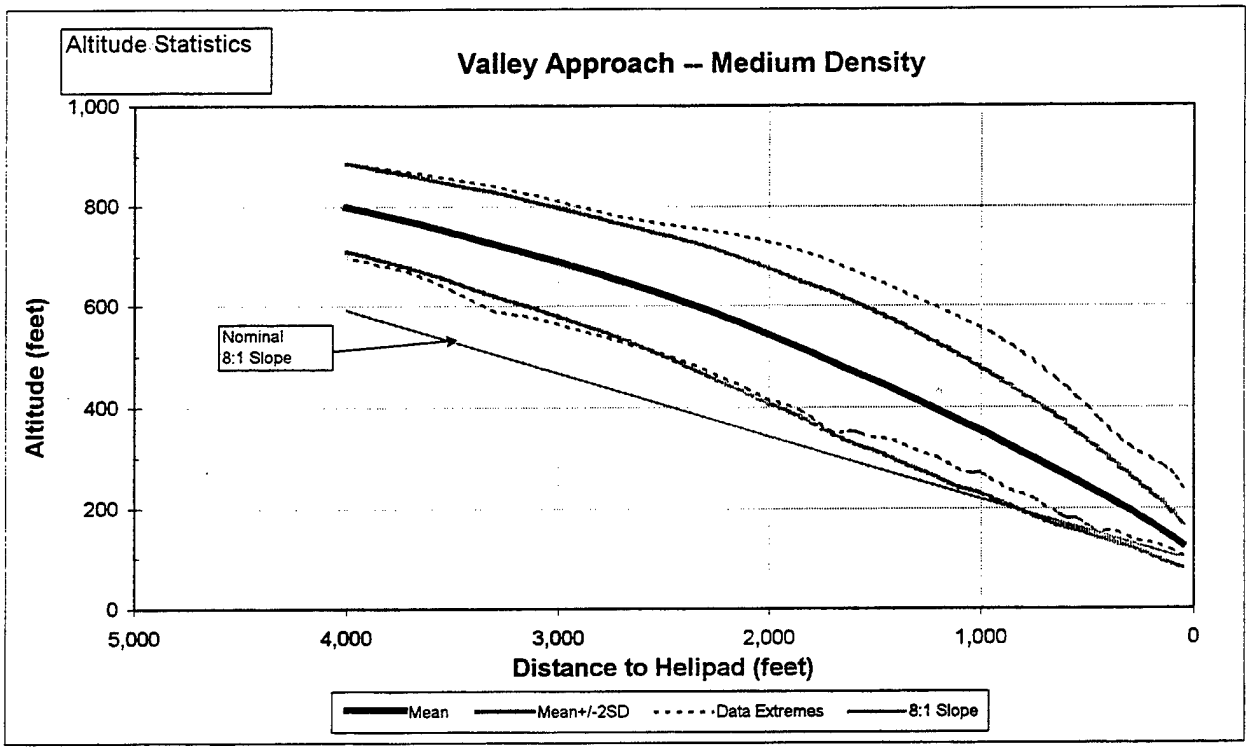

Figure H.2-54 Valley Approach Medium Density Altitude Data

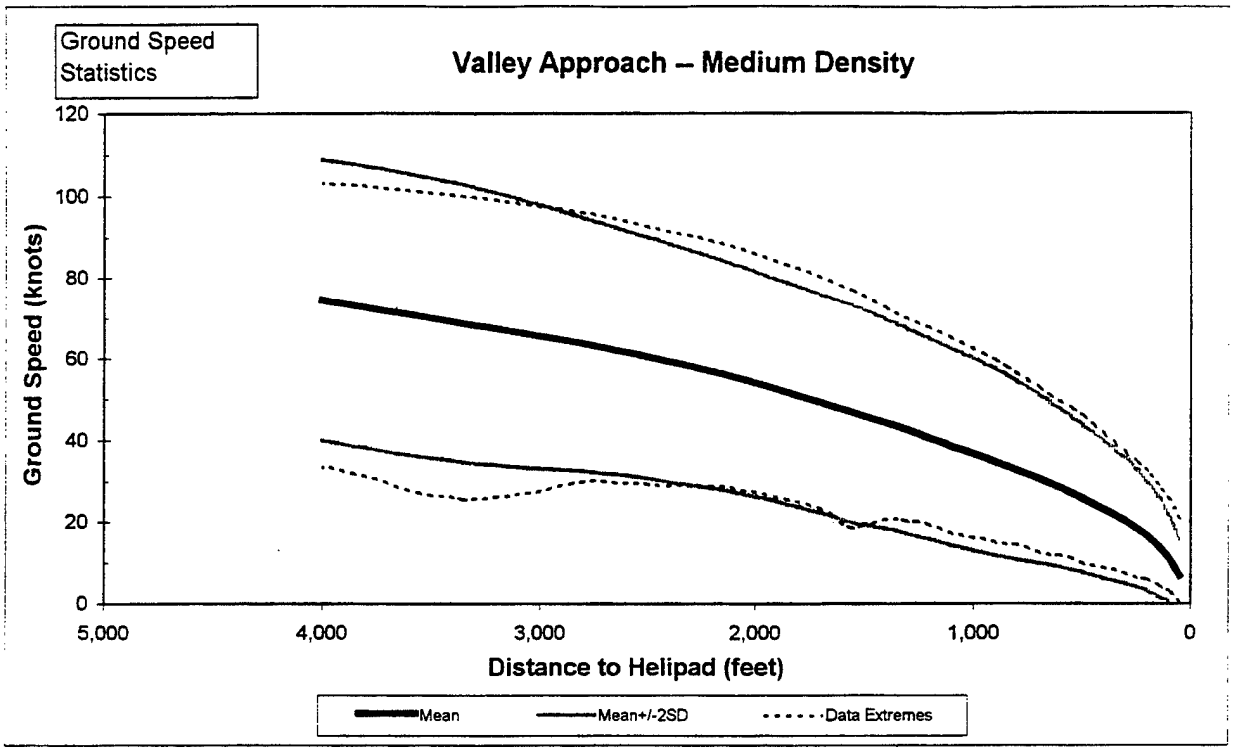

Figure H.2-55 Valley Approach Medium Density Ground Speed Data

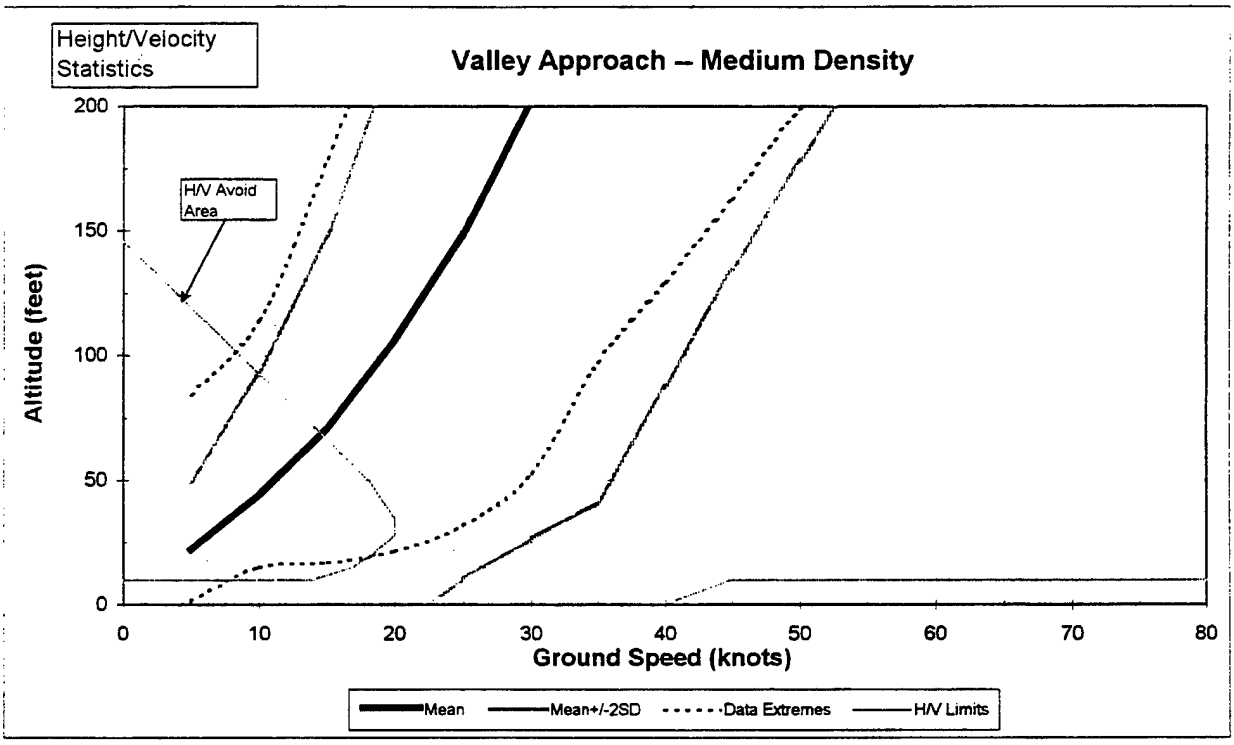

Figure H.2-56 Valley Approach Medium Density Height/Velocity Data

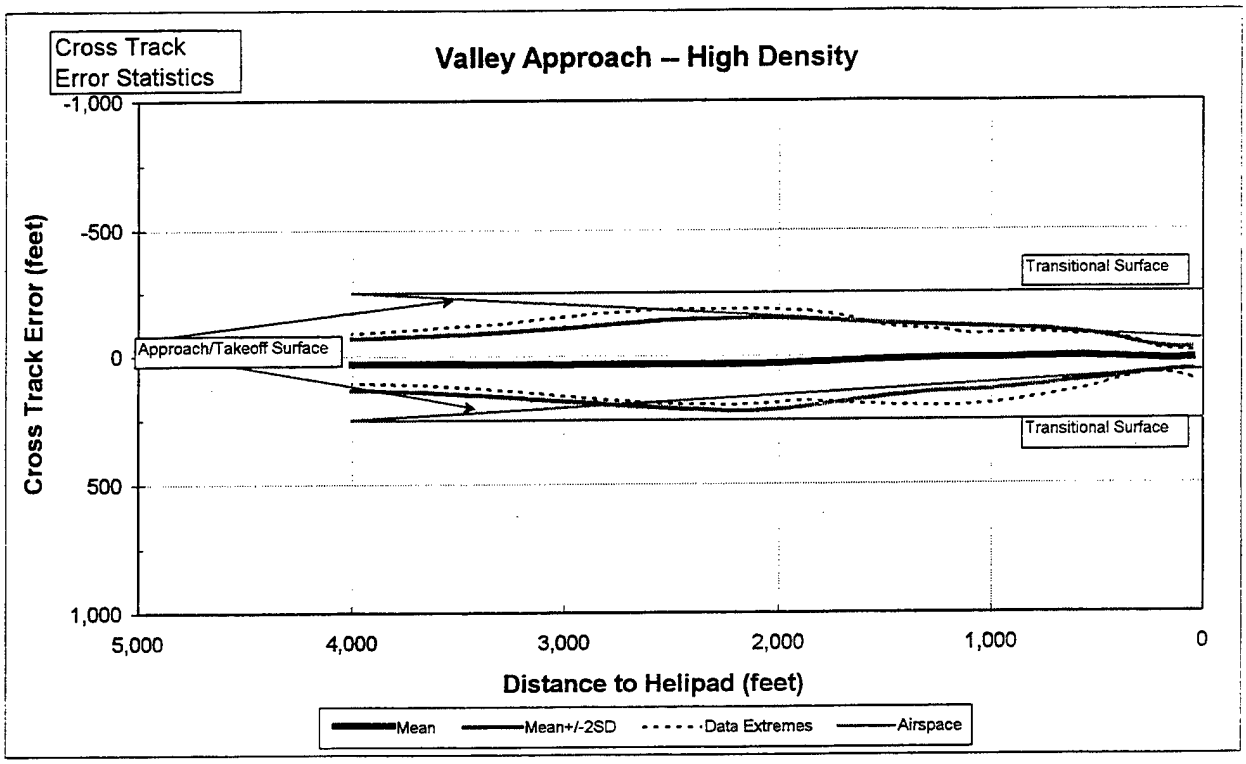

Figure H.2-57 Valley Approach High Density Cross Track Data

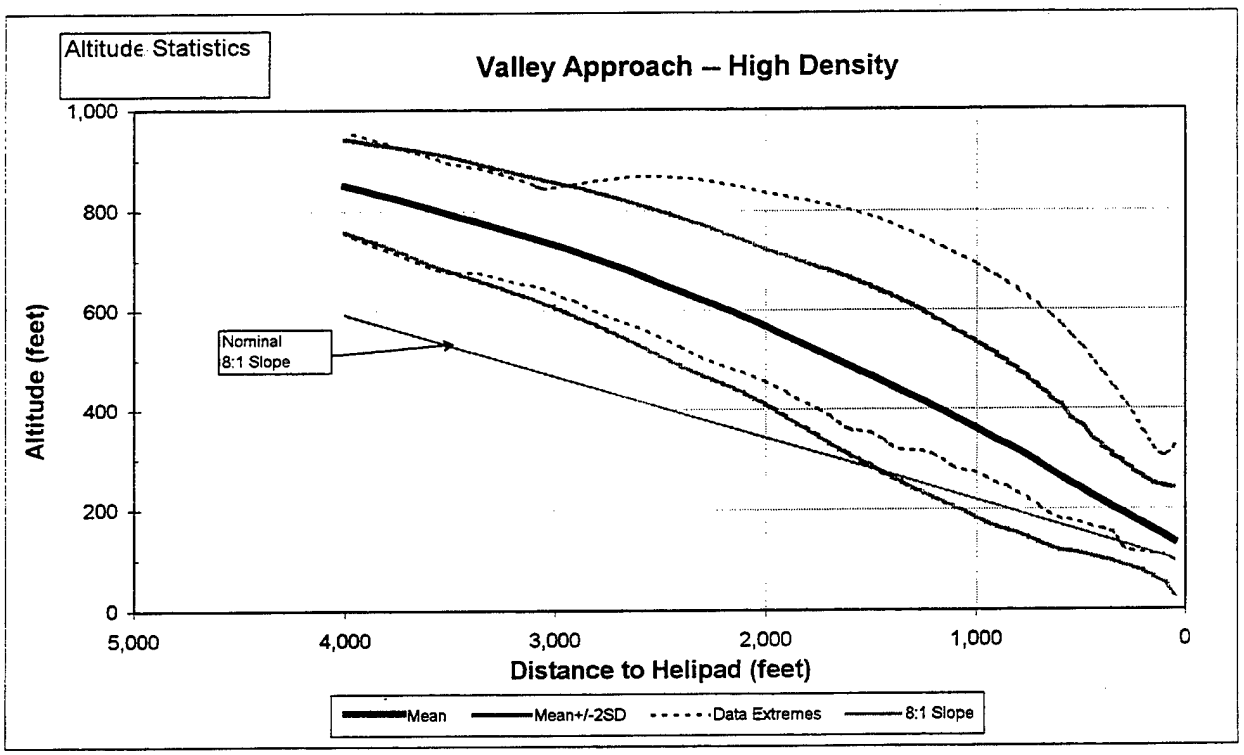

Figure H.2-58 Valley Approach High Density Altitude Data

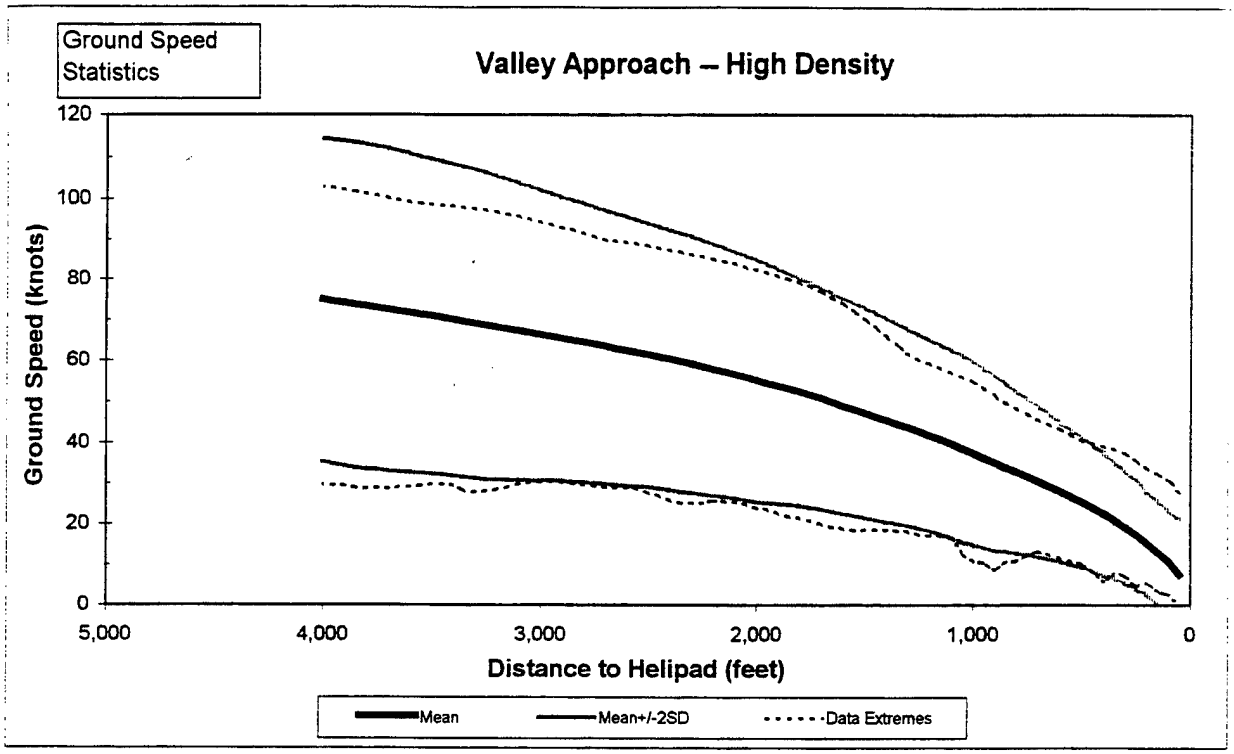

Figure H.2-59 Valley Approach High Density Ground Speed Data

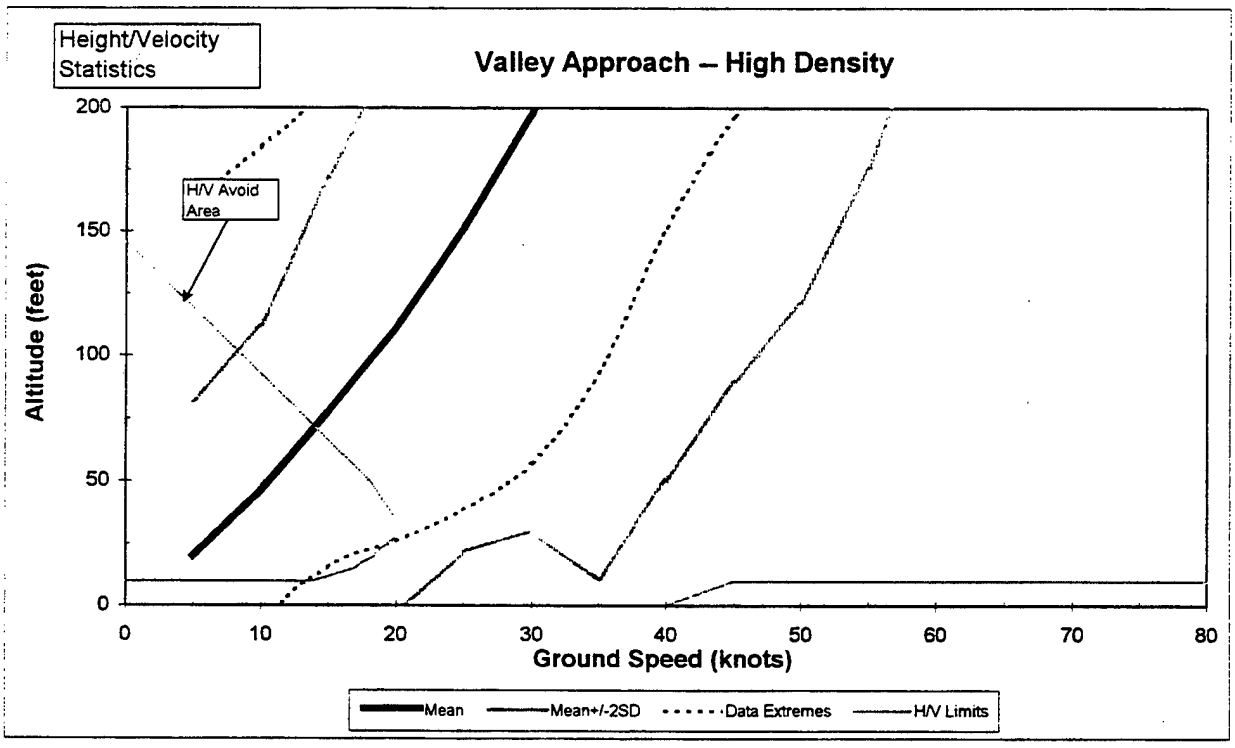

Figure H.2-60 Valley Approach High Density Height/Velocity Data

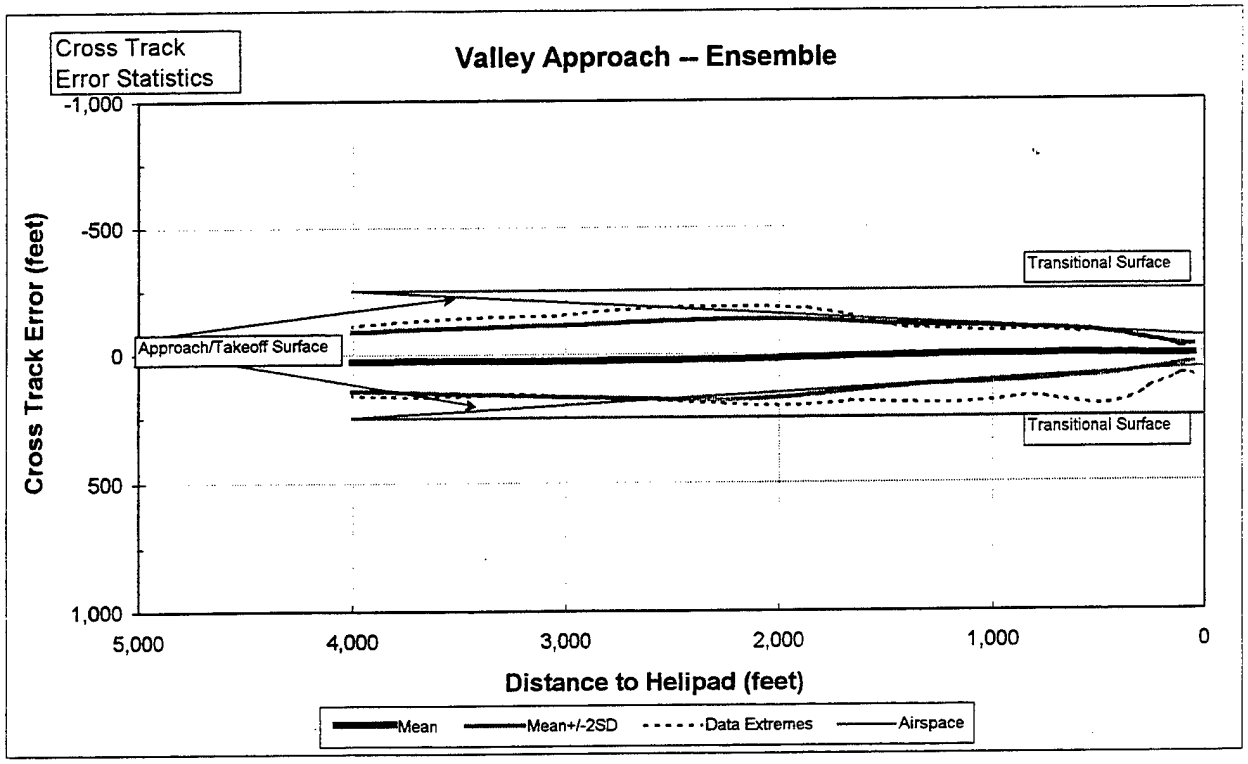

Figure H.2-61 Valley Approach Ensemble Cross Track Data

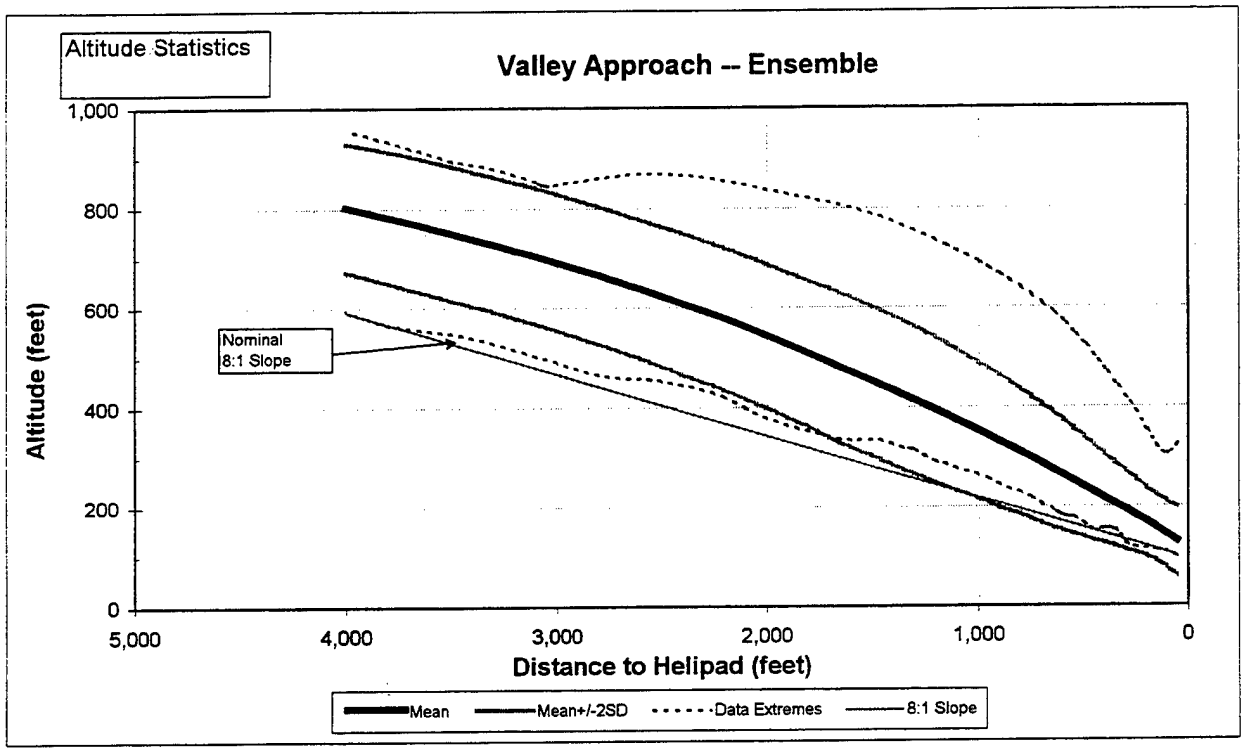

Figure H.2-62 Valley Approach Ensemble Altitude Data

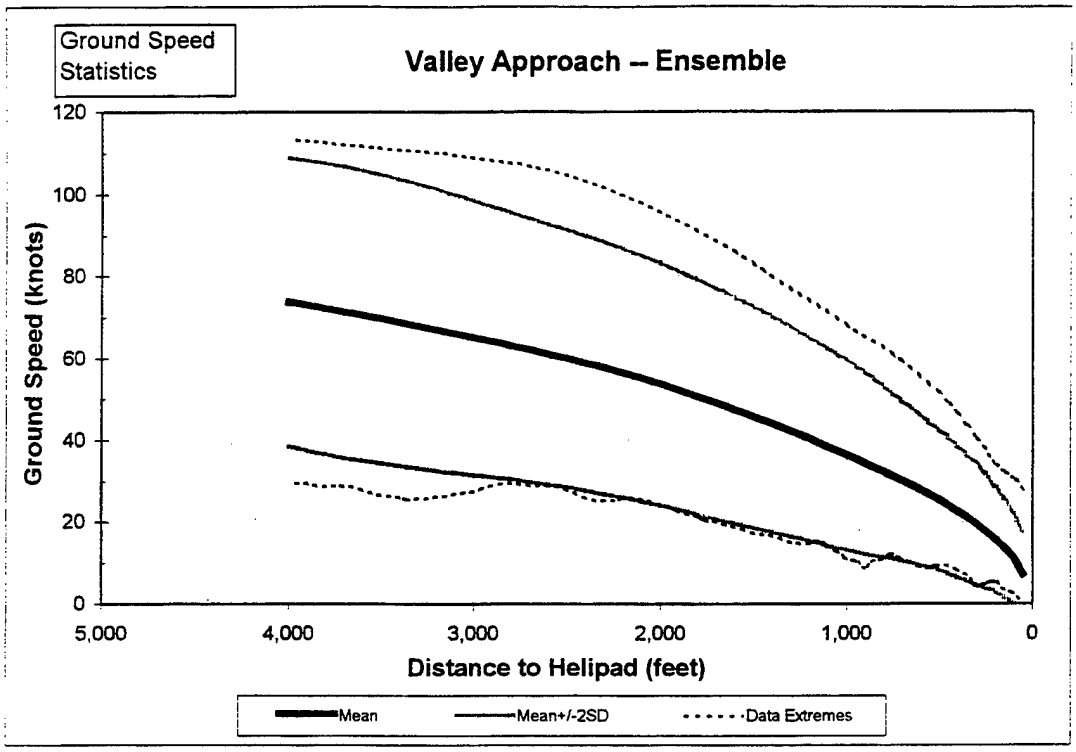

Figure H.2-63 Valley Approach Ensemble Ground Speed Data

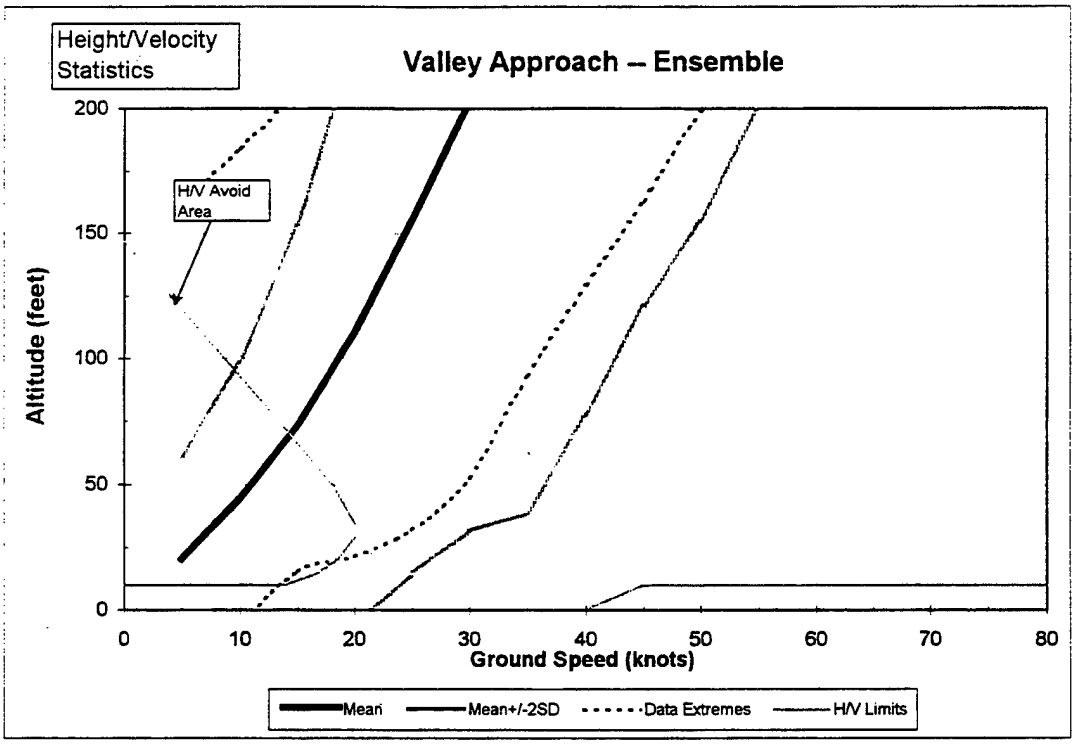

Figure H.2-64 Valley Approach Ensemble Height/Velocity Data

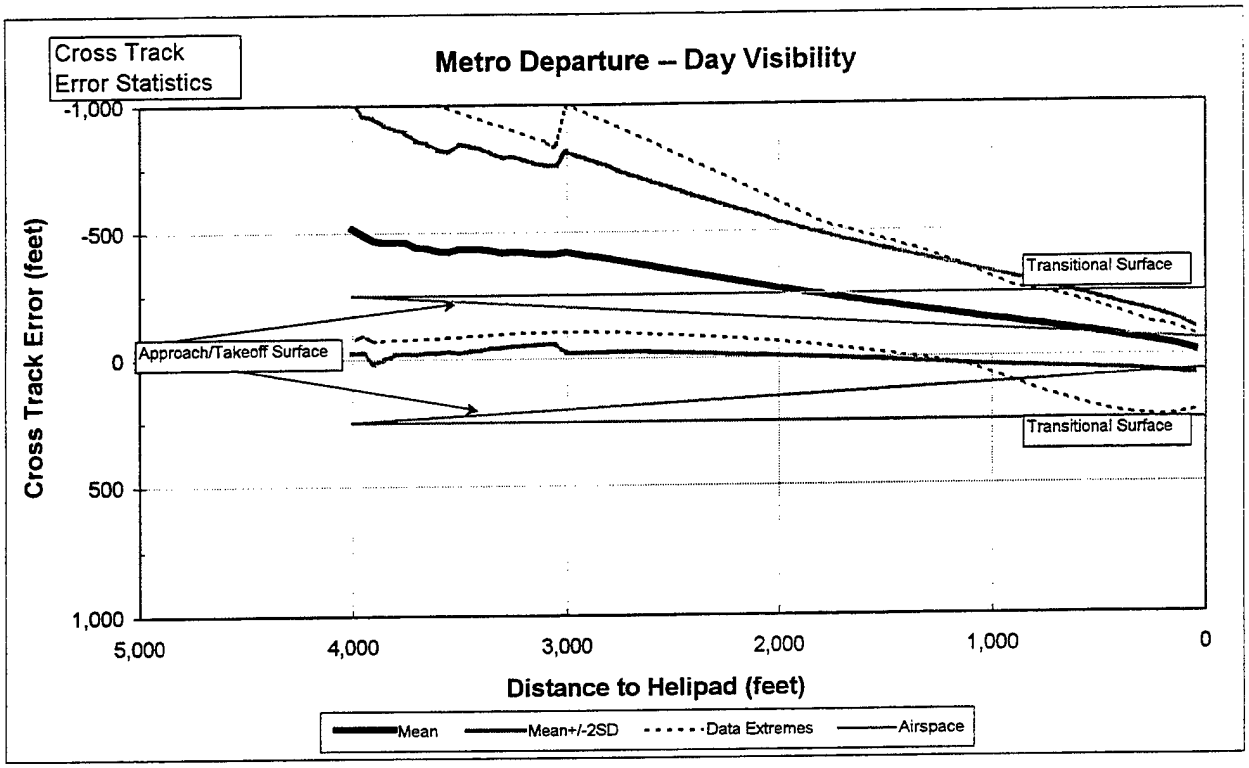

Figure H.2-65 Metro Departure Day Visibility Cross Track Data

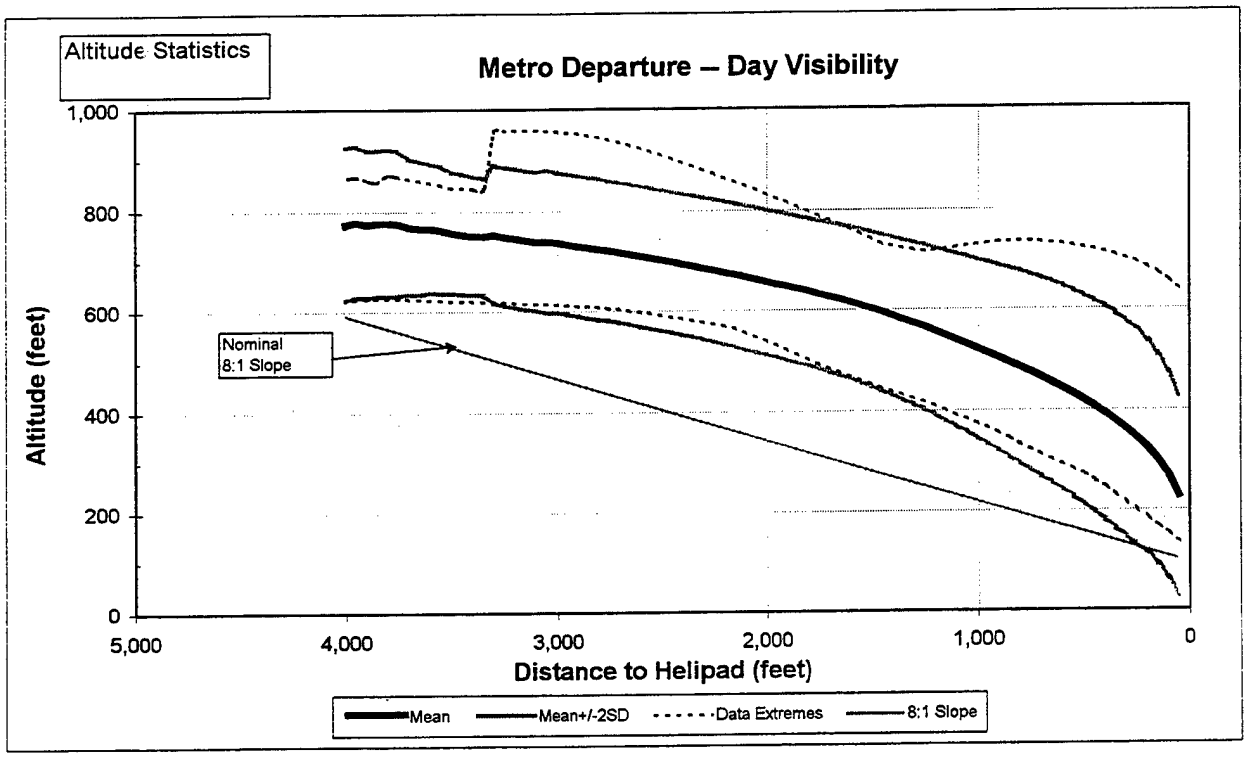

Figure H.2-66 Metro Departure Day Visibility Altitude Data

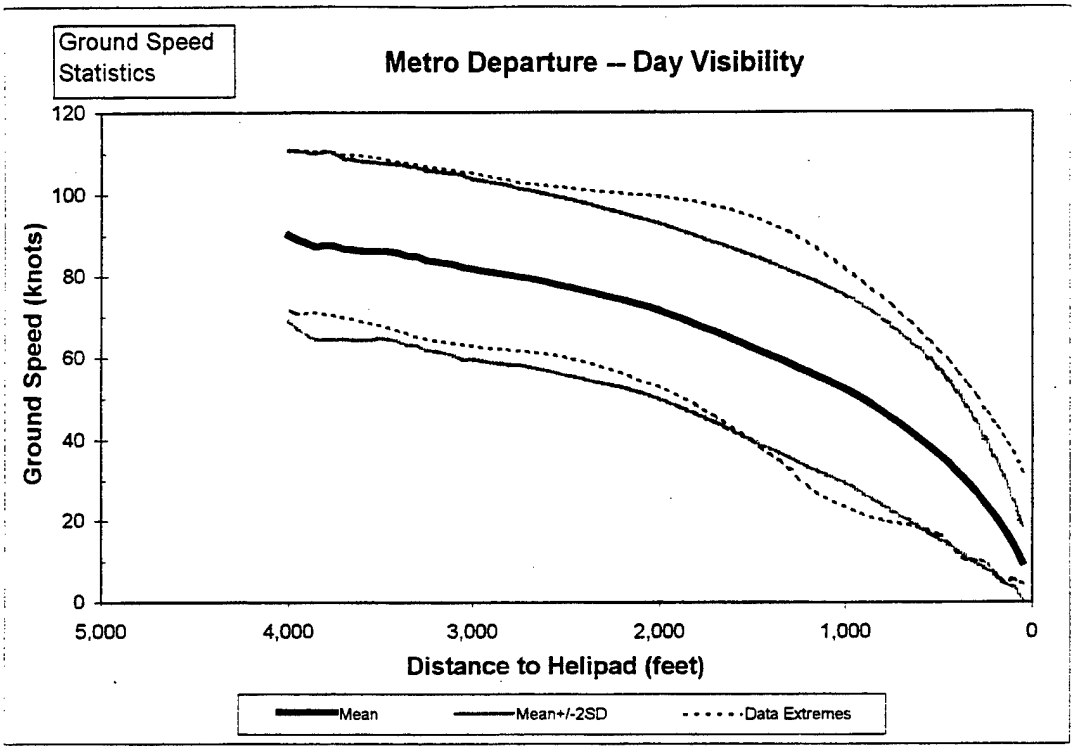

Figure H.2-67 Metro Departure Day Visibility Ground Speed Data

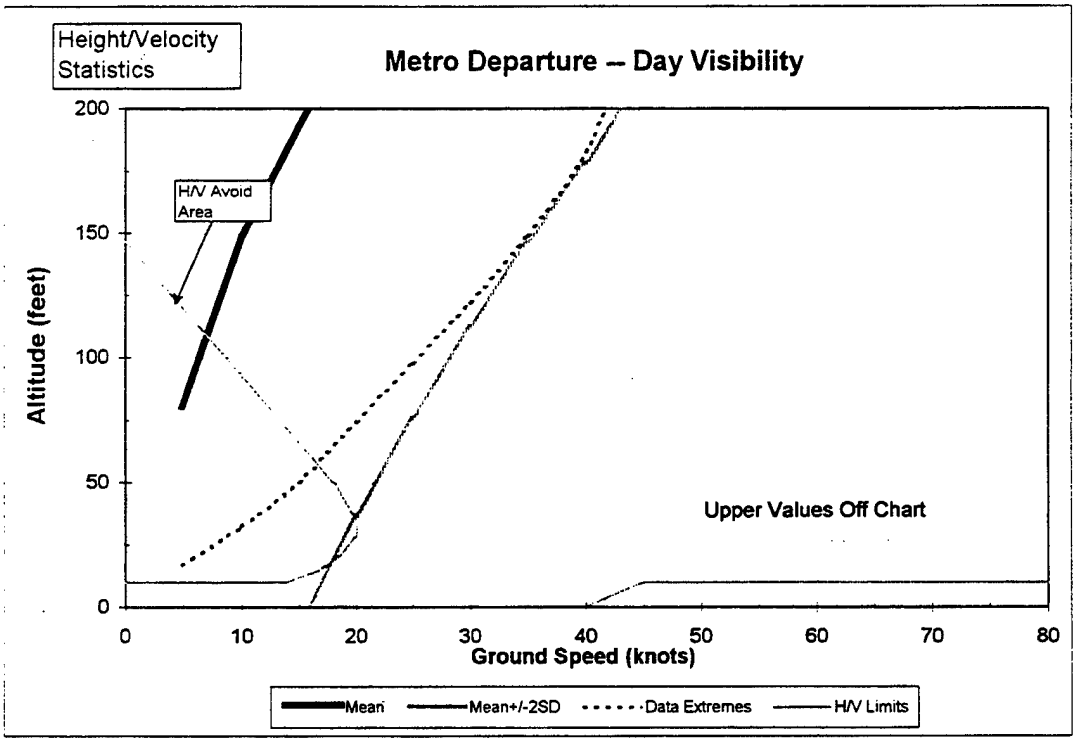

Figure H.2-68 Metro Departure Day Visibility Height/Velocity Data

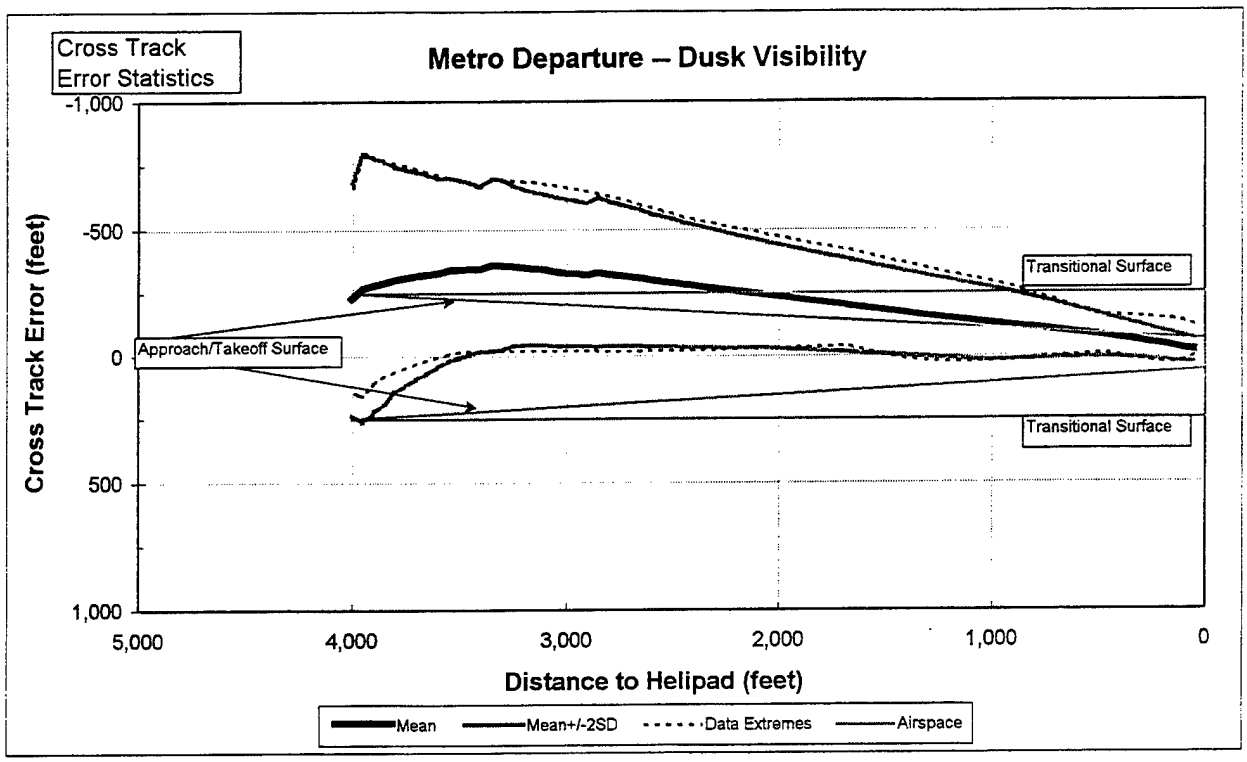

Figure H.2-69 Metro Departure Dusk Visibility Cross Track Data

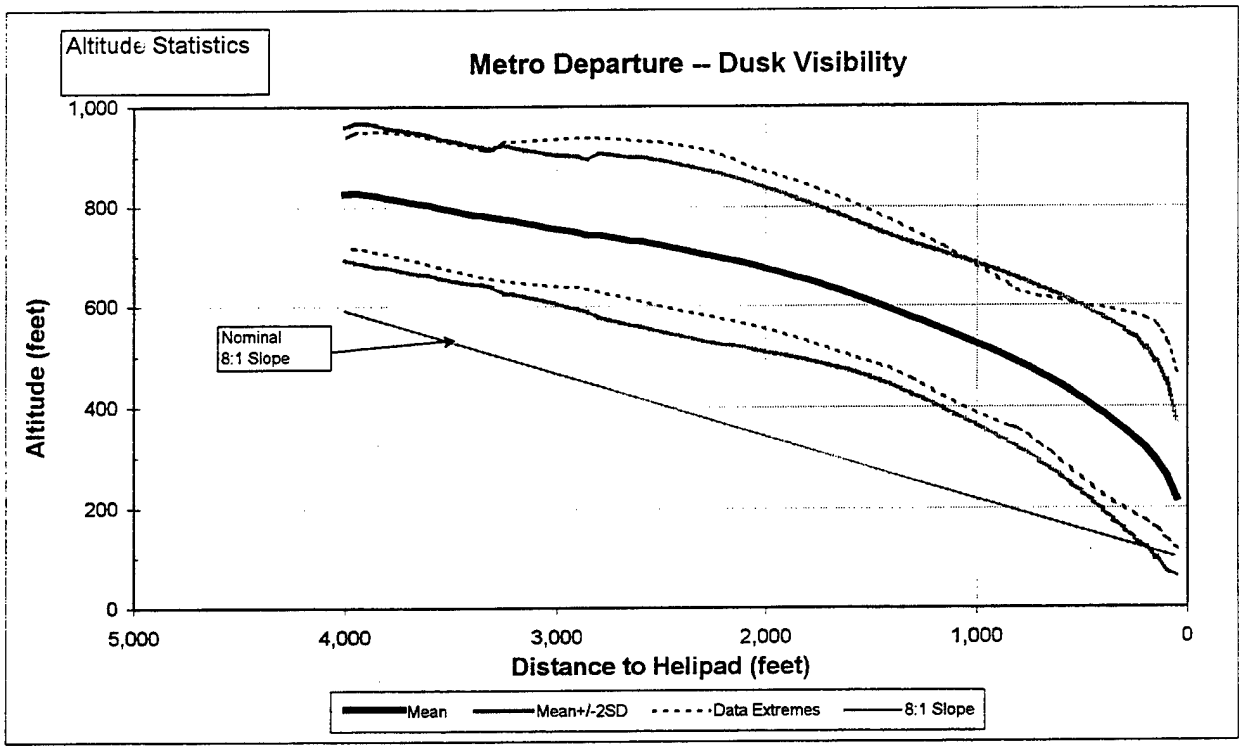

Figure H.2-70 Metro Departure Dusk Visibility Altitude Data

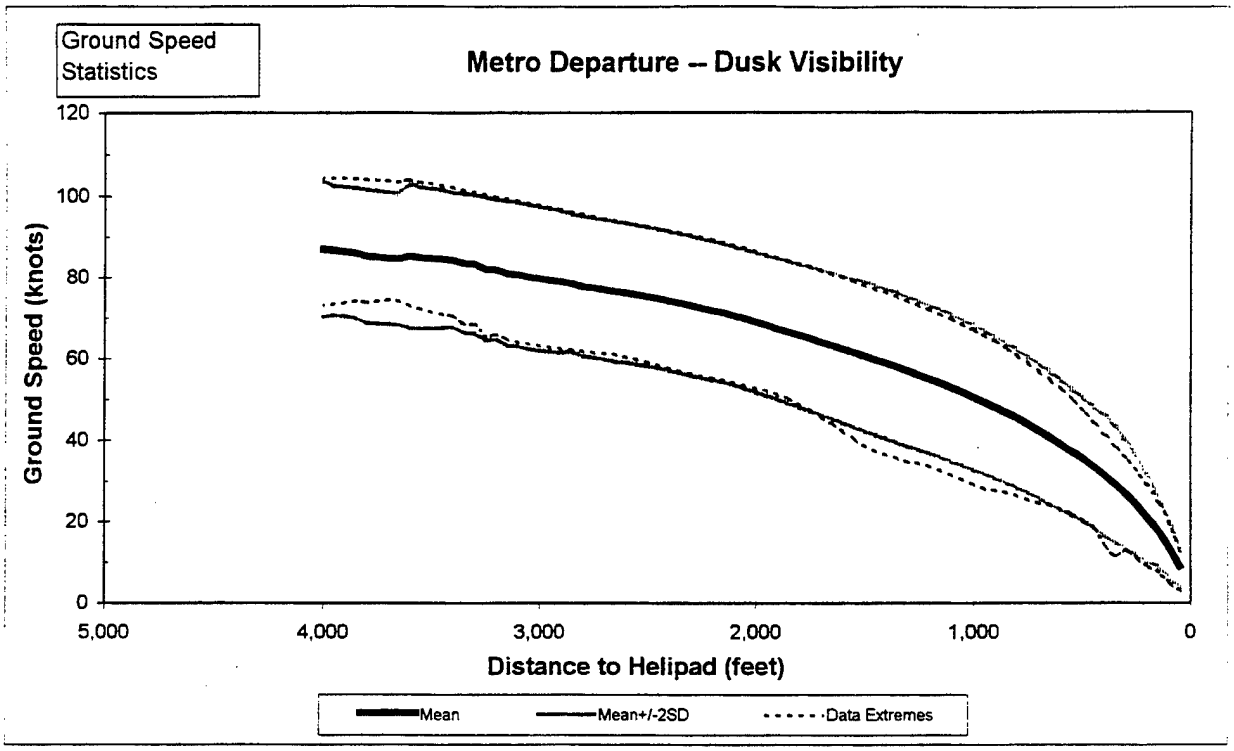

Figure H.2-71 Metro Departure Dusk Visibility Ground Speed Data

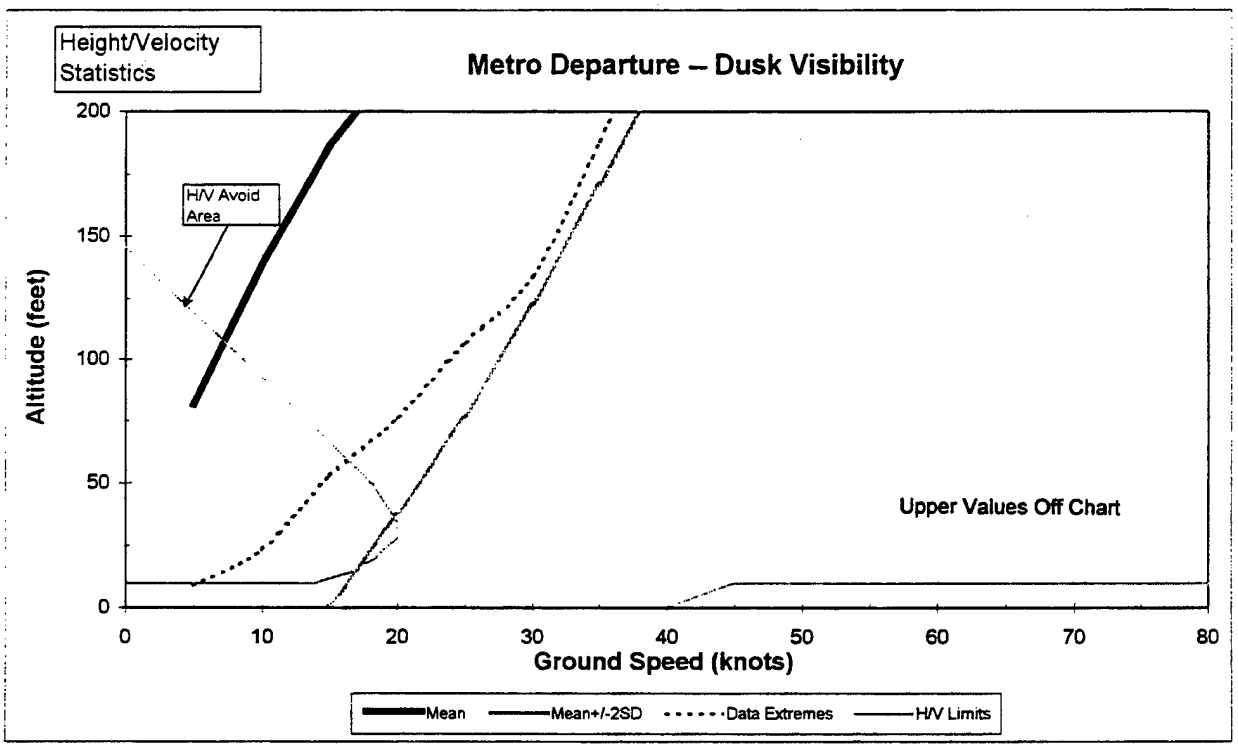

Figure H.2-72 Metro Departure Dusk Visibility Height/Velocity Data

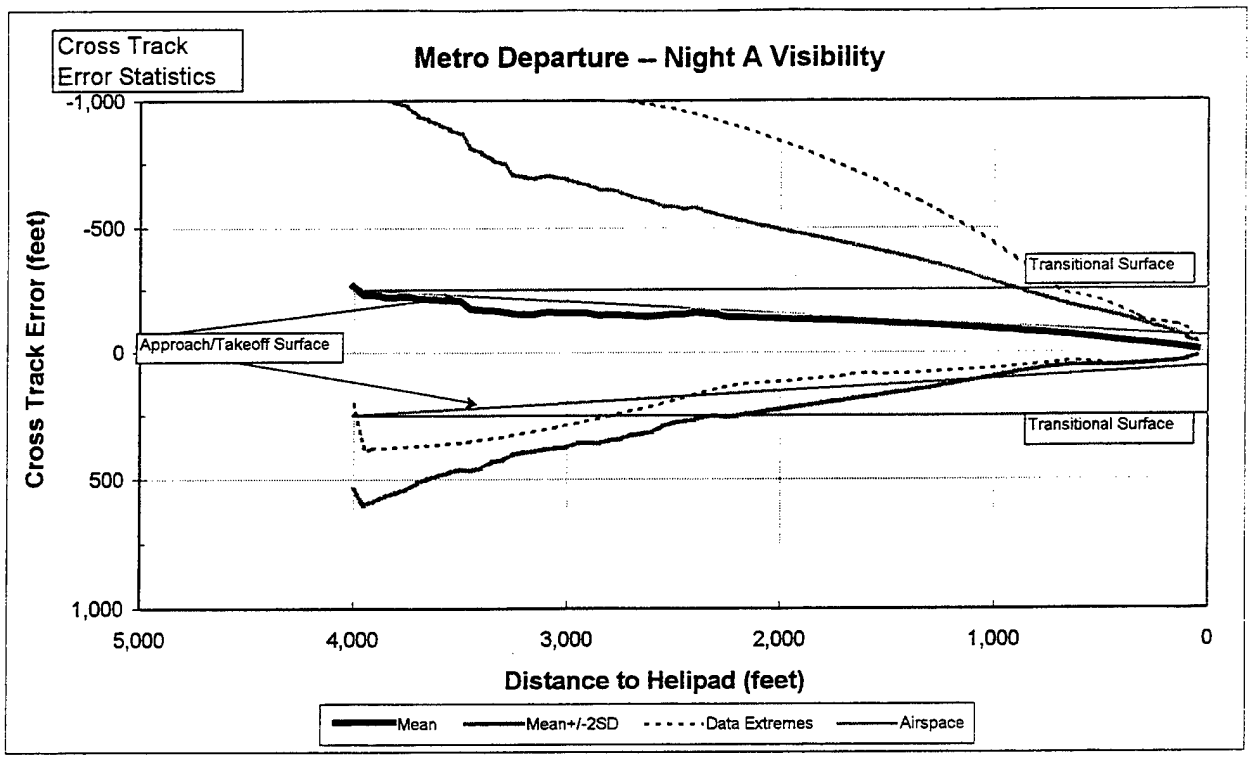

Figure H.2-73 Metro Departure Night A Visibility Cross Track Data

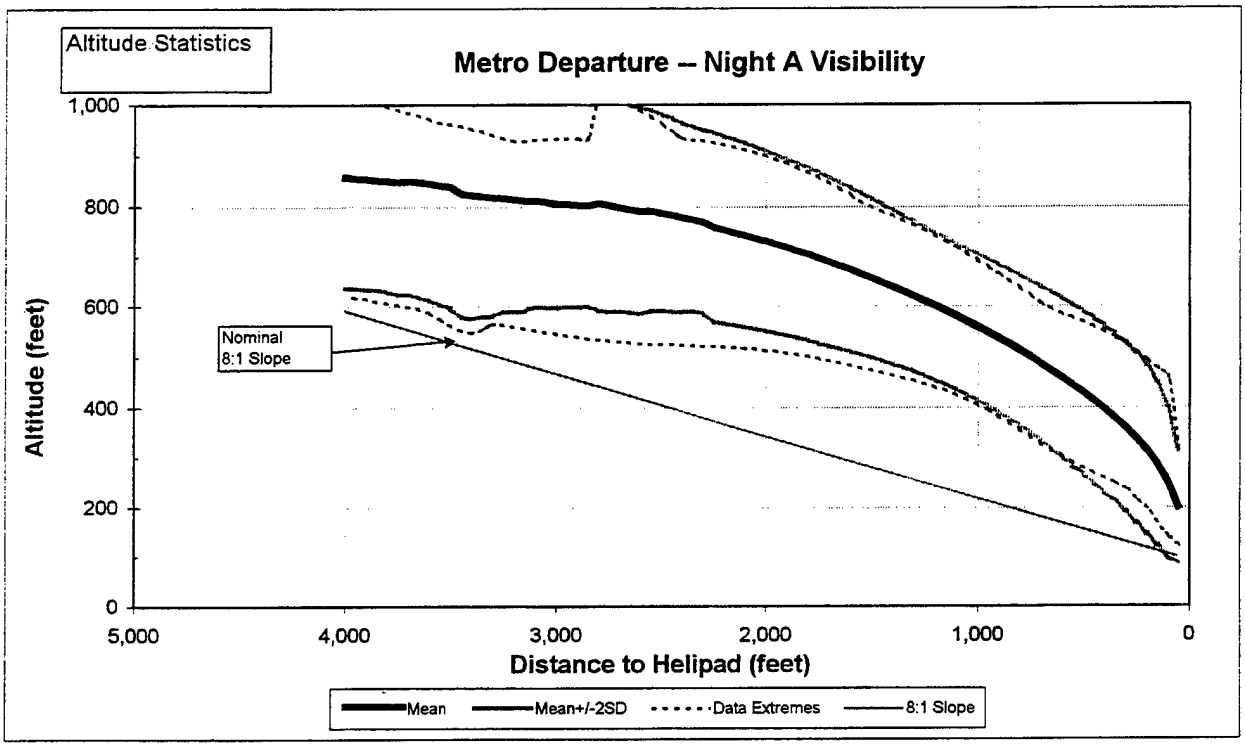

Figure H.2-74 Metro Departure Night A Visibility Altitude Data

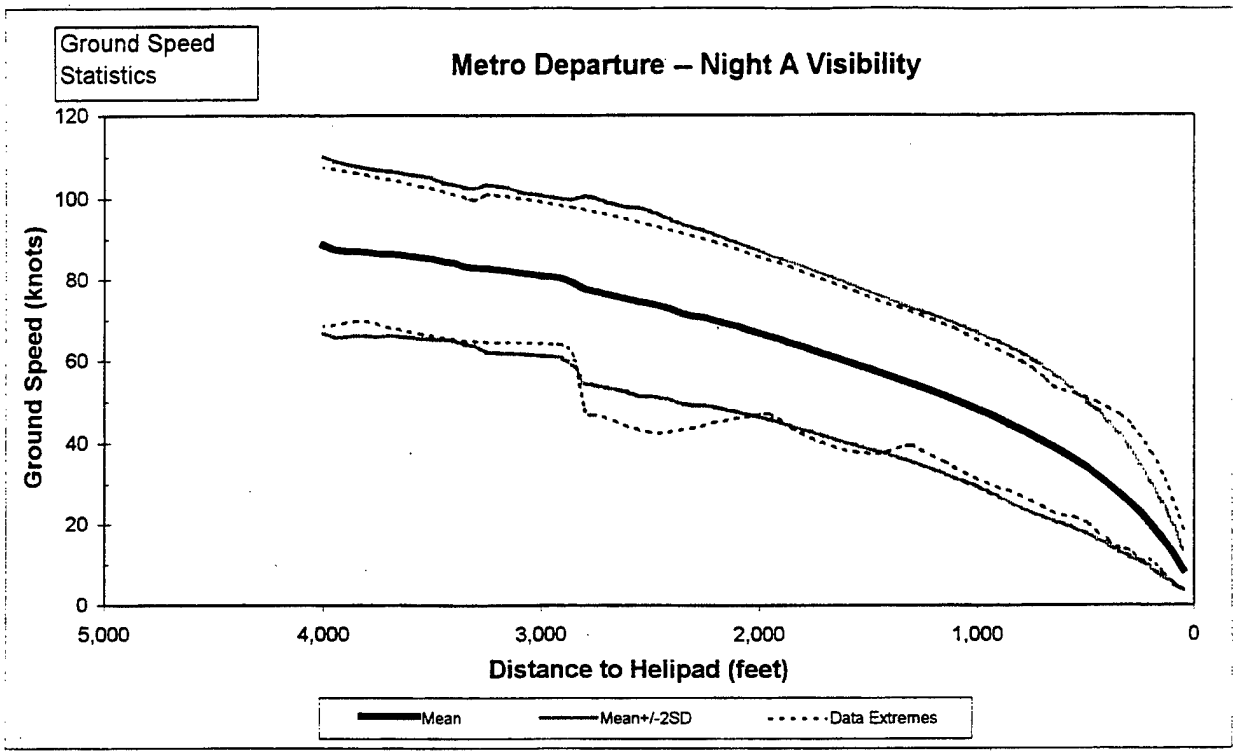

Figure H.2-75 Metro Departure Night A Visibility Ground Speed Data

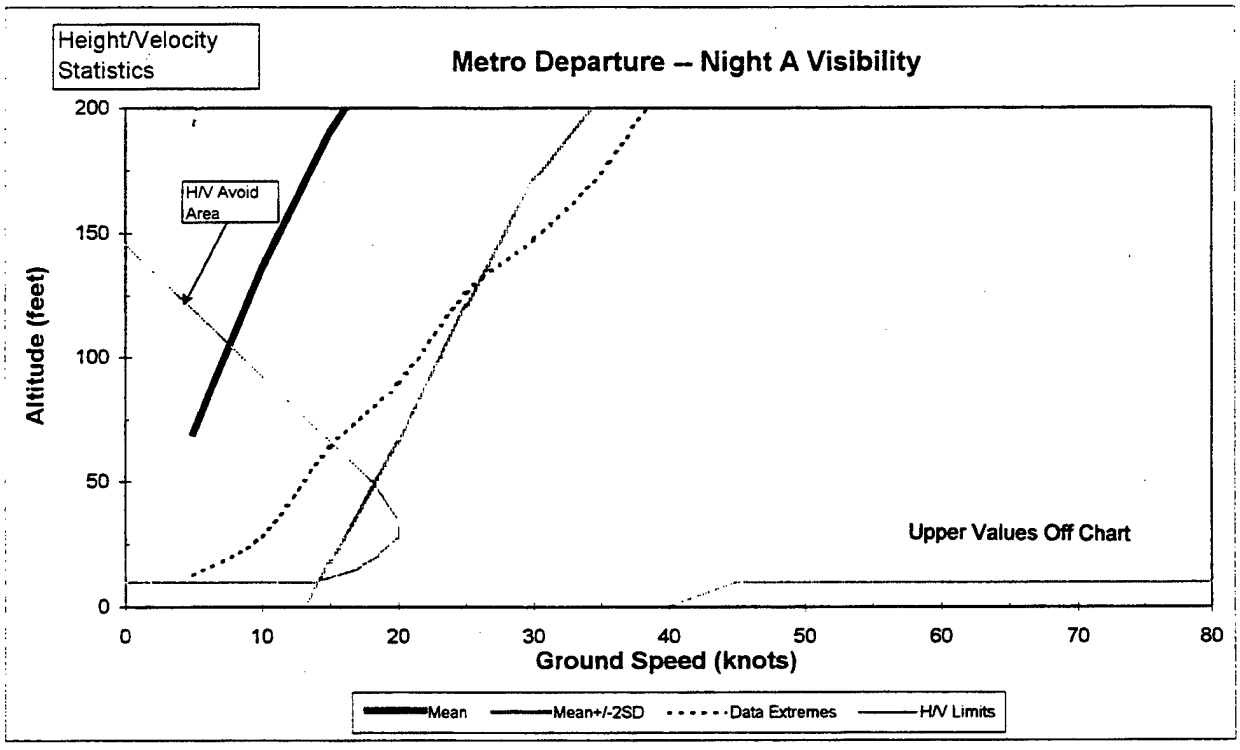

Figure H.2-76 Metro Departure Night A Visibility Height/Velocity Data

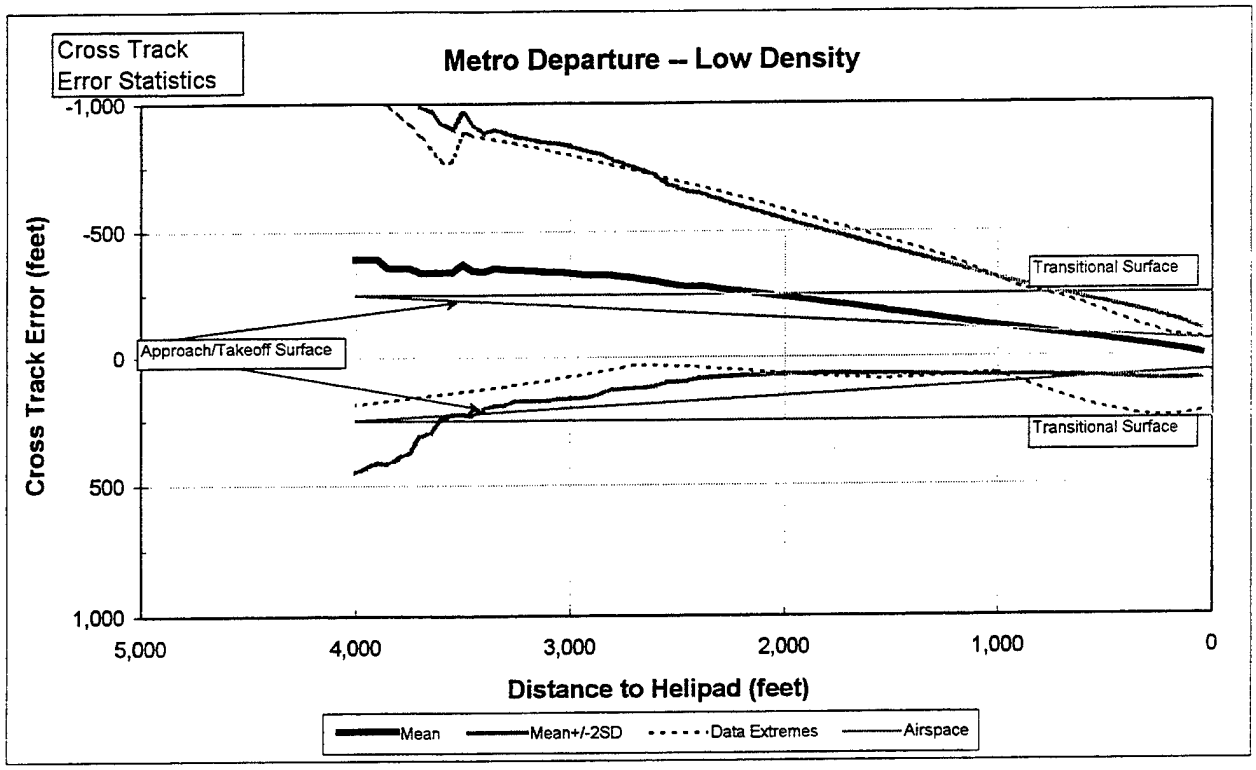

Figure H.2-77 Metro Departure Low Density Cross Track Data

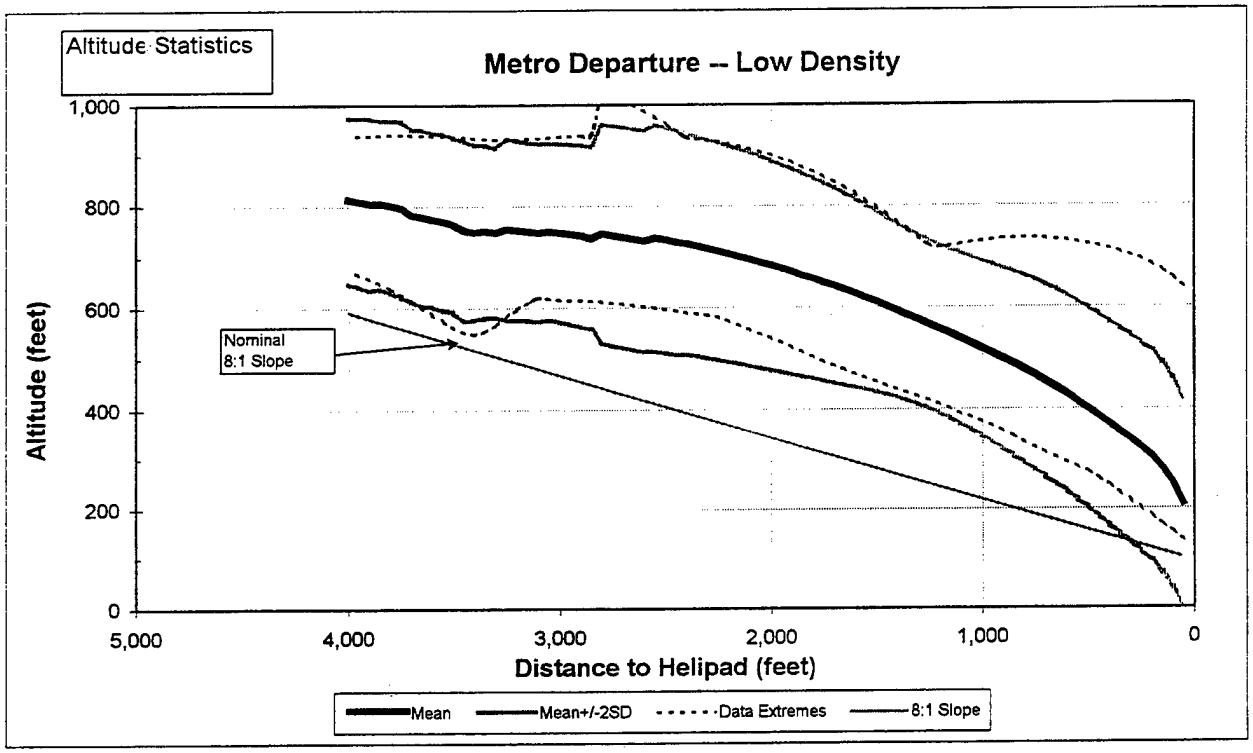

Figure H.2-78 Metro Departure Low Density Altitude Data

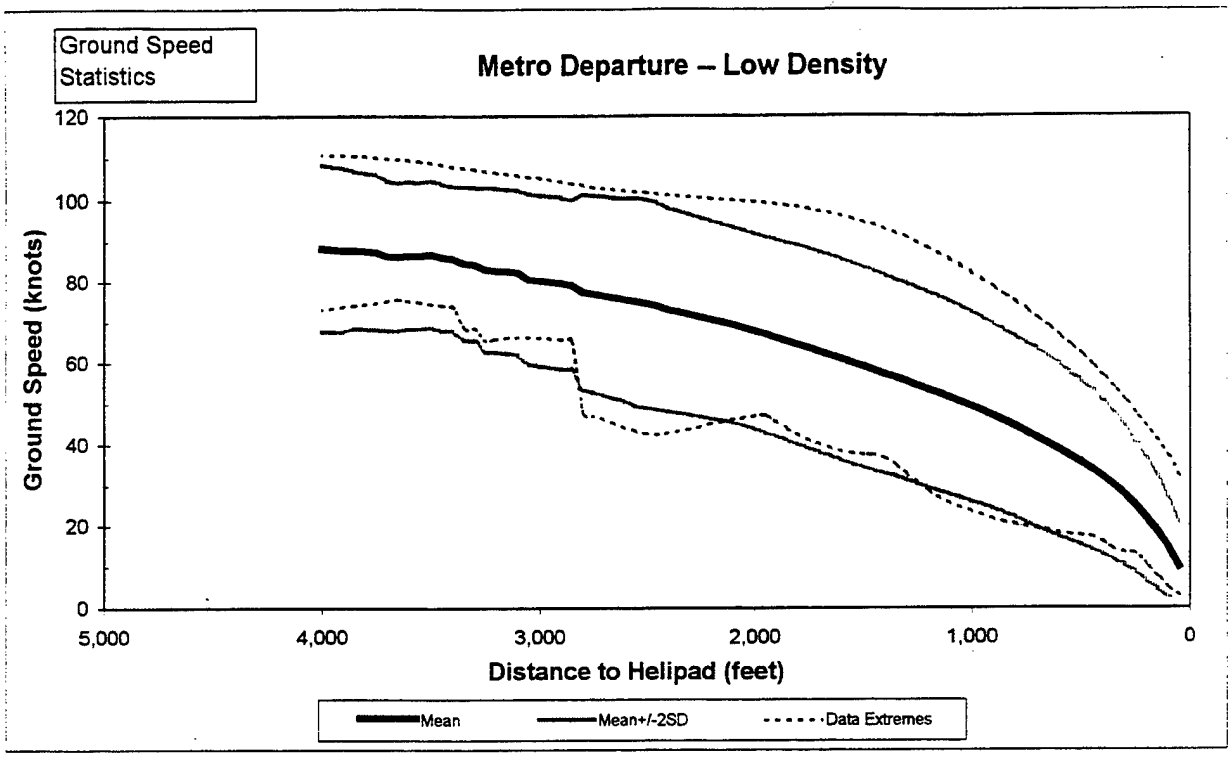

Figure H.2-79 Metro Departure Low Density Ground Speed Data

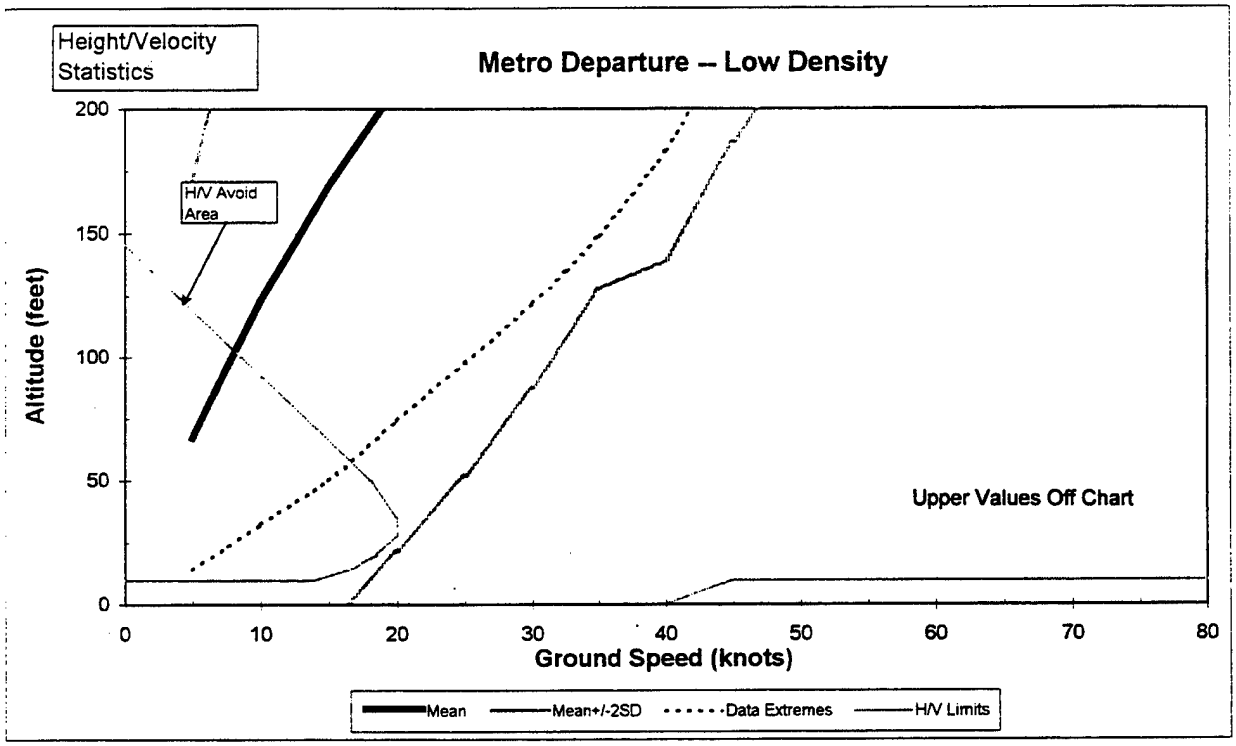

Figure H.2-80 Metro Departure Low Density Height/Velocity Data

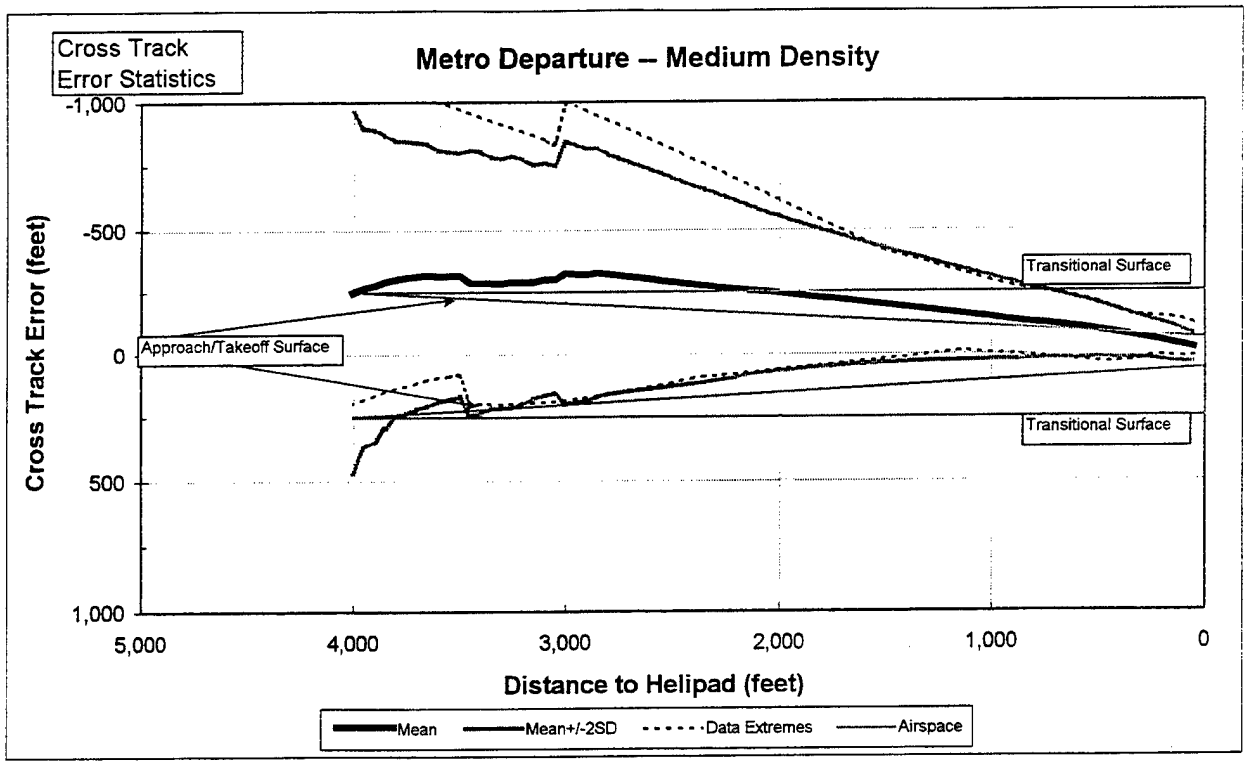

Figure H.2-81 Metro Departure Medium Density Cross Track Data

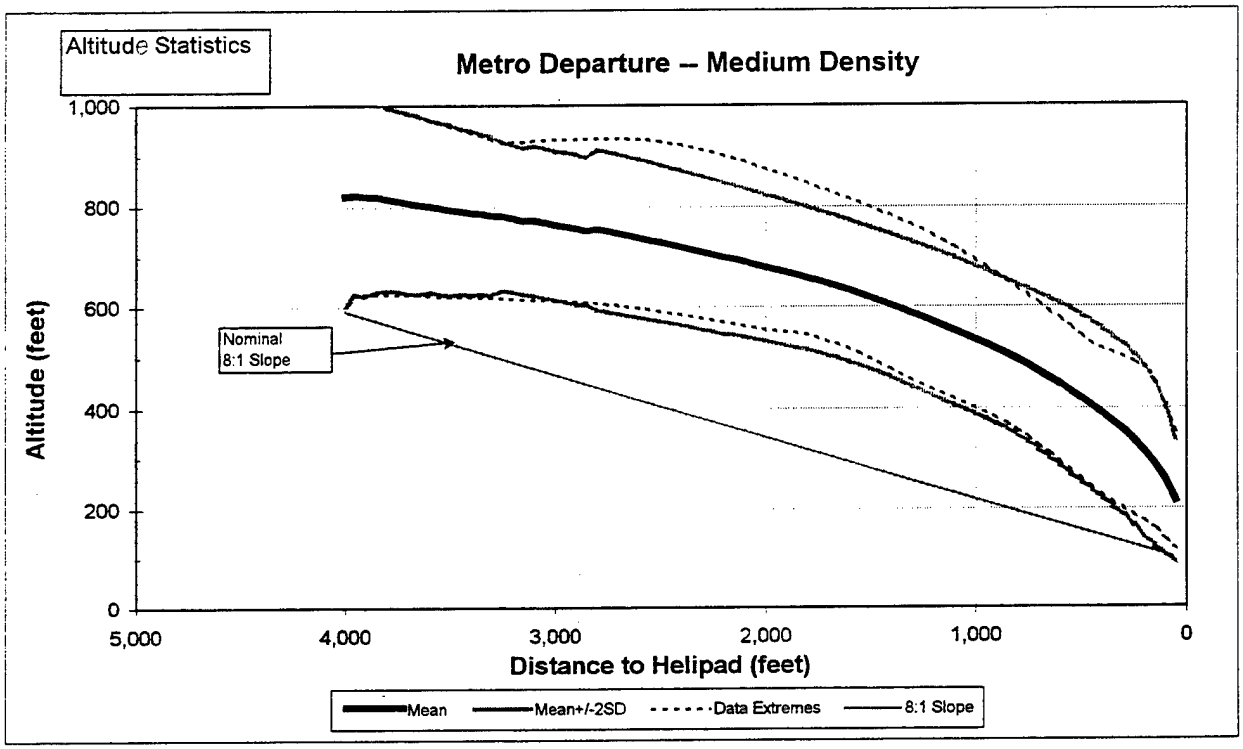

Figure H.2-82 Metro Departure Medium Density Altitude Data

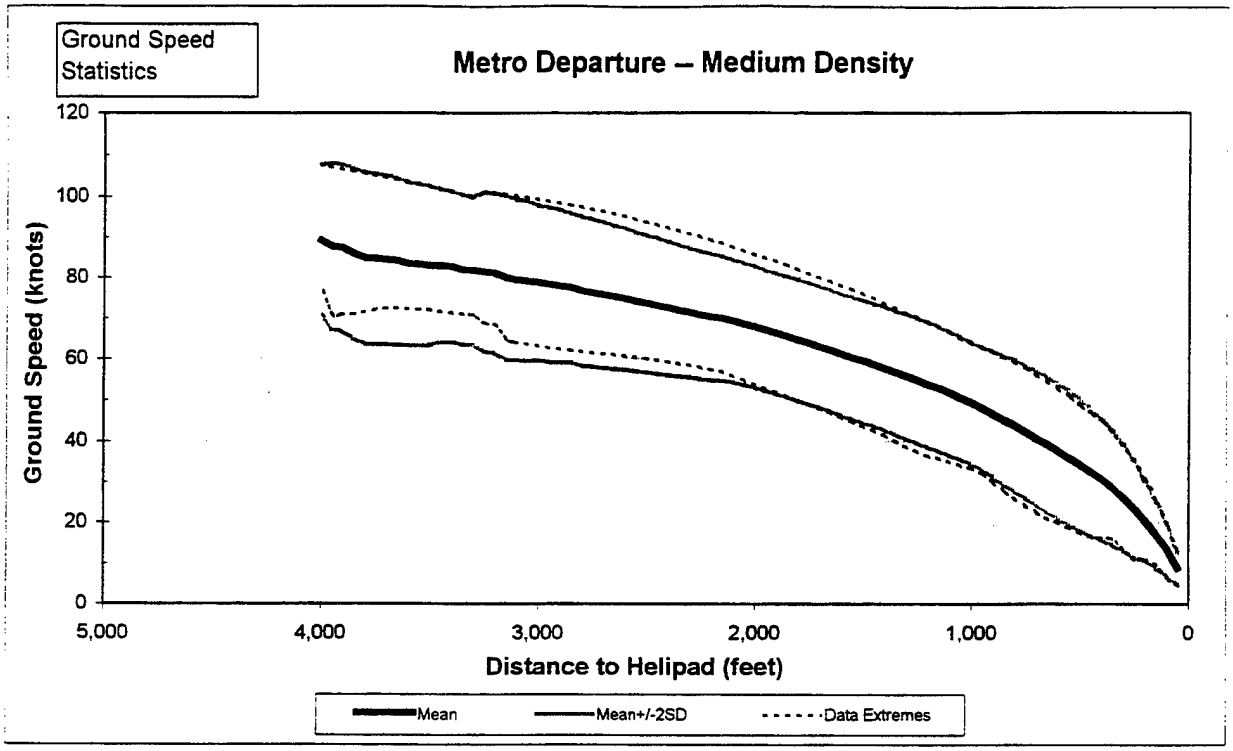

Figure H.2-83 Metro Departure Medium Density Ground Speed Data

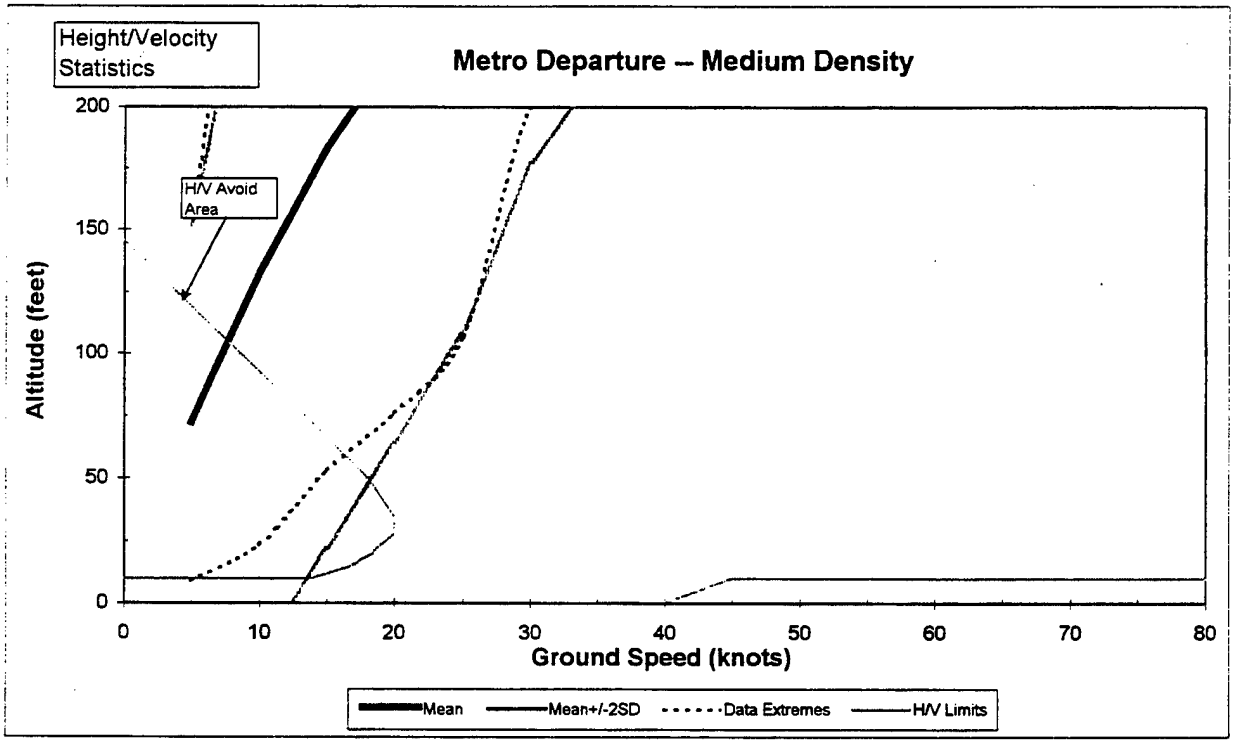

Figure H.2-84 Metro Departure Medium Density Height/Velocity Data

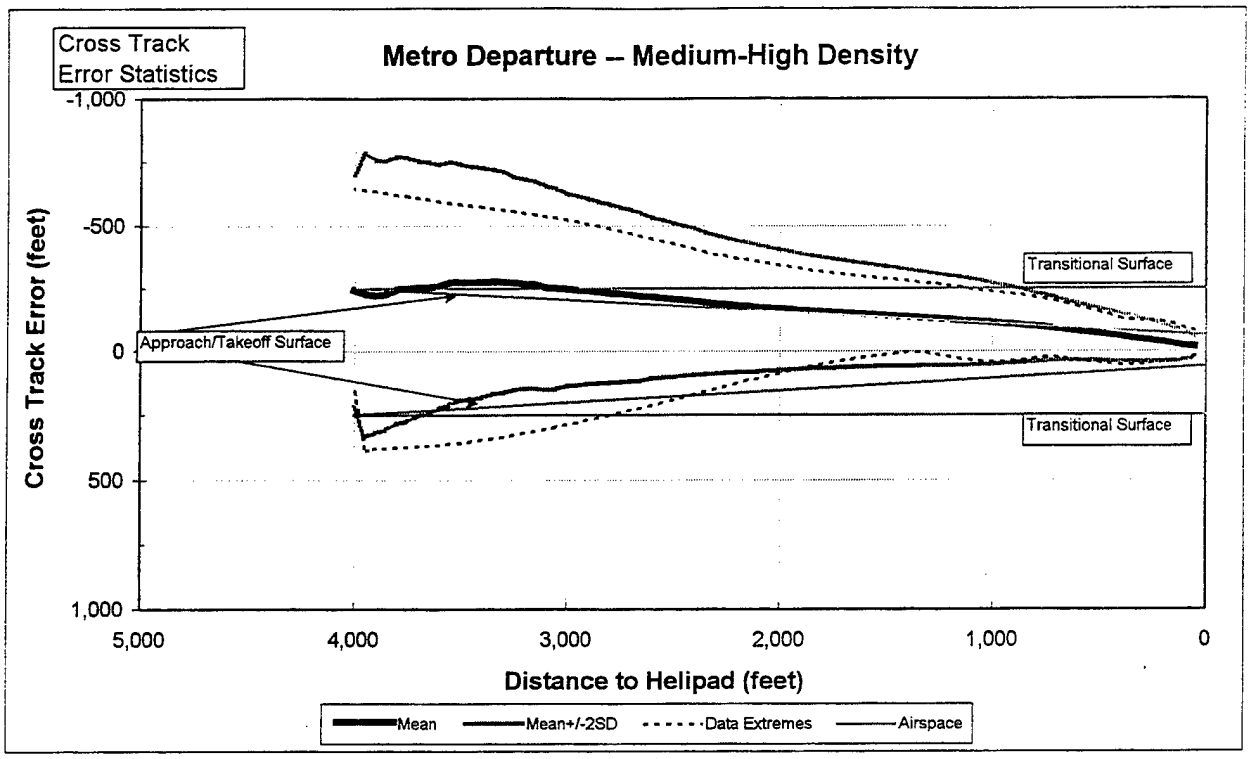

Figure H.2-85 Metro Departure Medium-High Density Cross Track Data

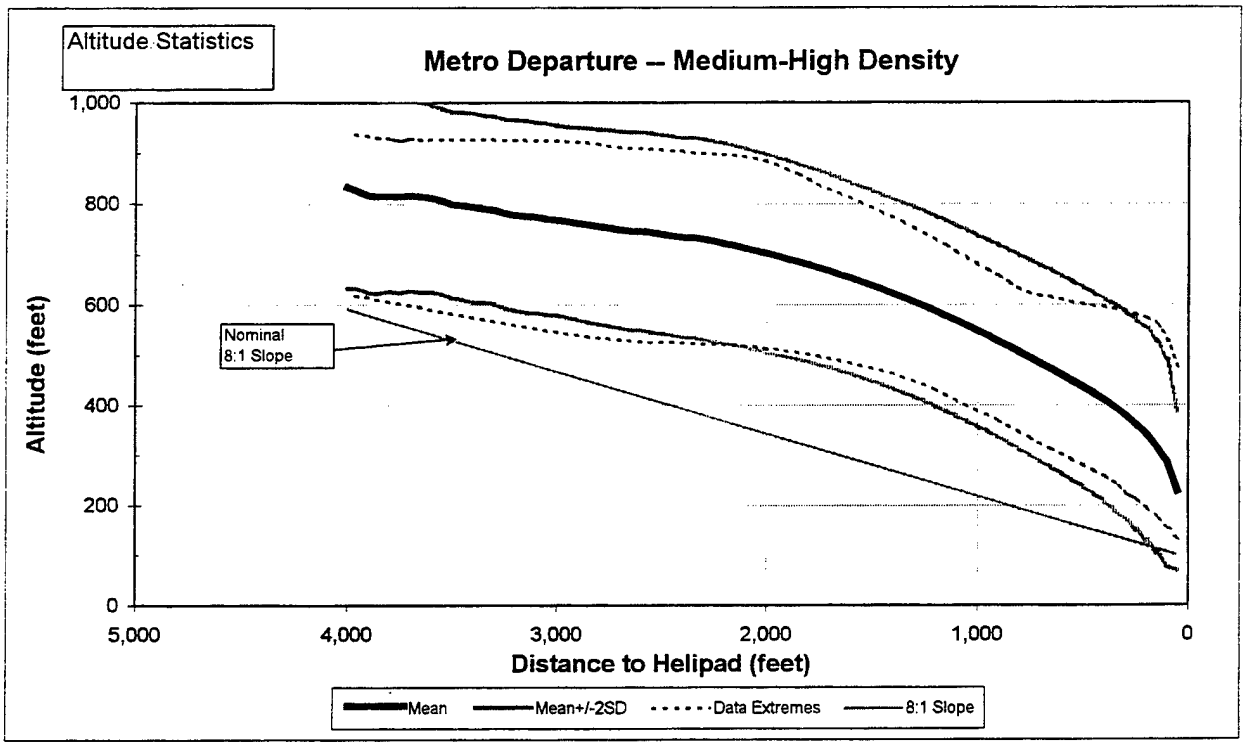

Figure H.2-86 Metro Departure Medium-High Density Altitude Data

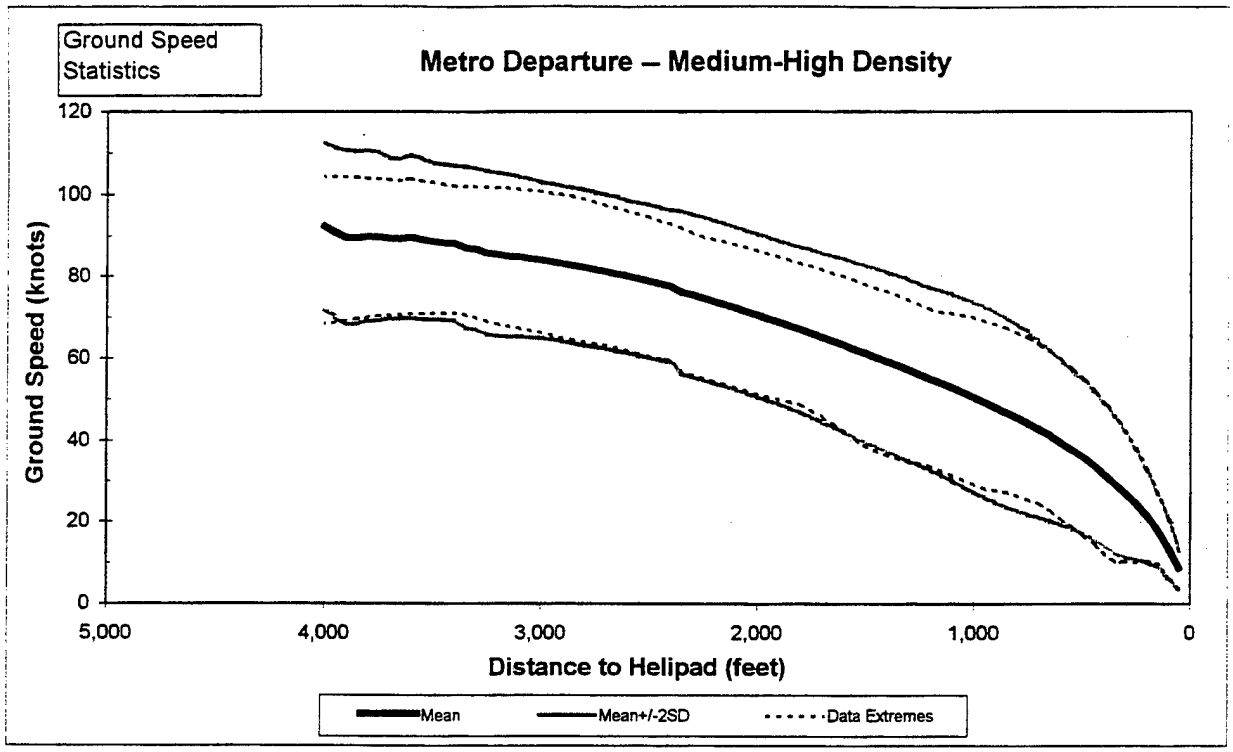

Figure H.2-87 Metro Departure Medium-High Density Ground Speed Data

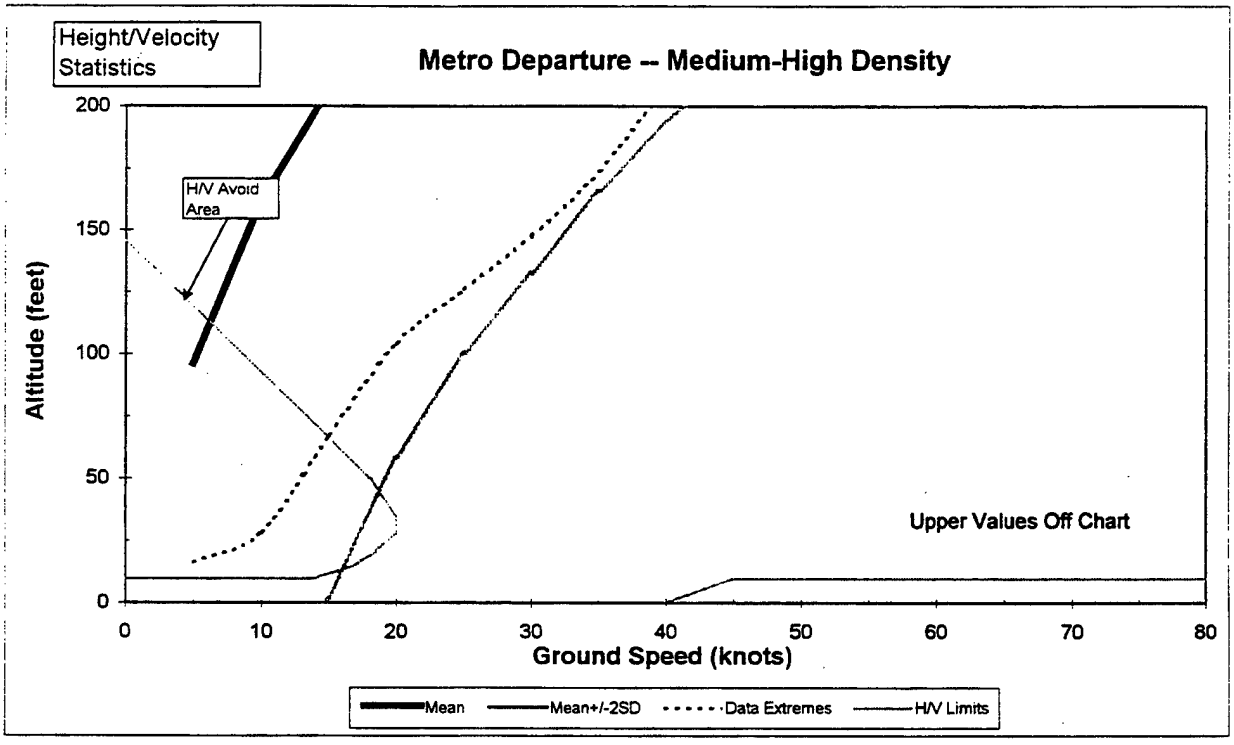

Figure H.2-88 Metro Departure Medium-High Density Height/Velocity Data

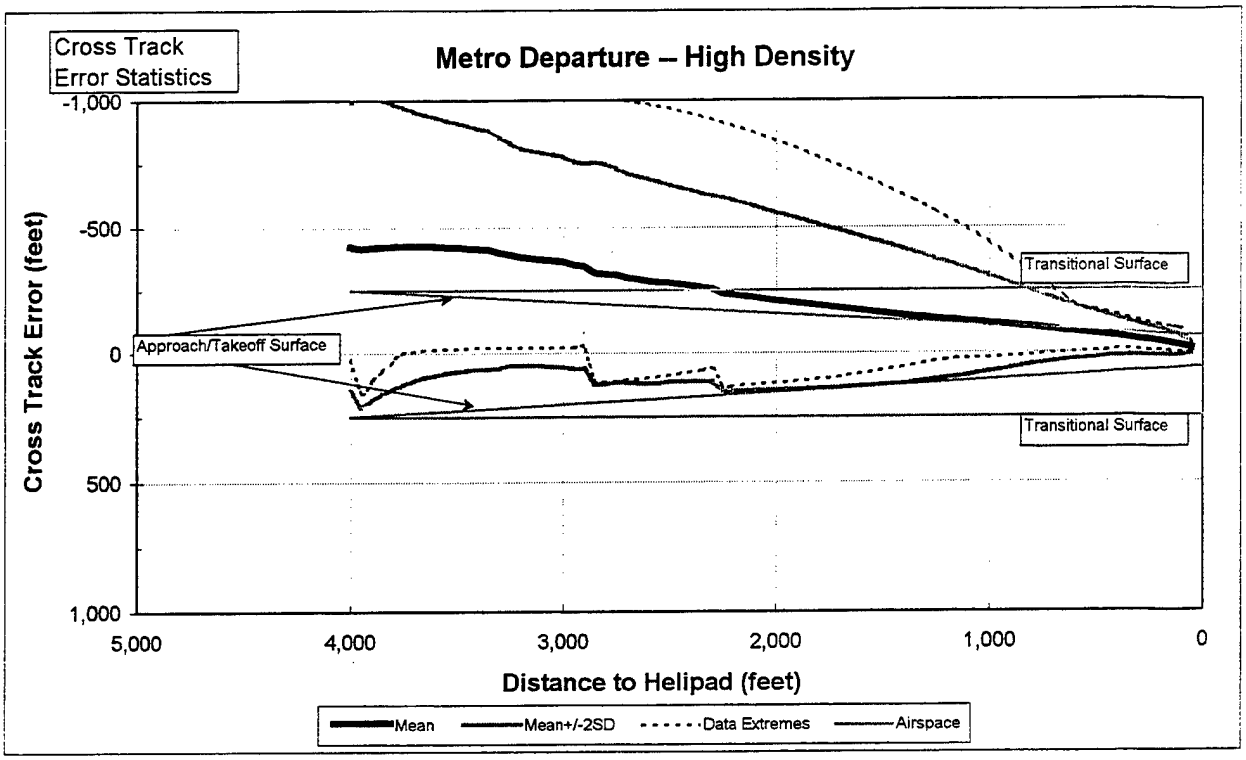

Figure H.2-89 Metro Departure High Density Cross Track Data

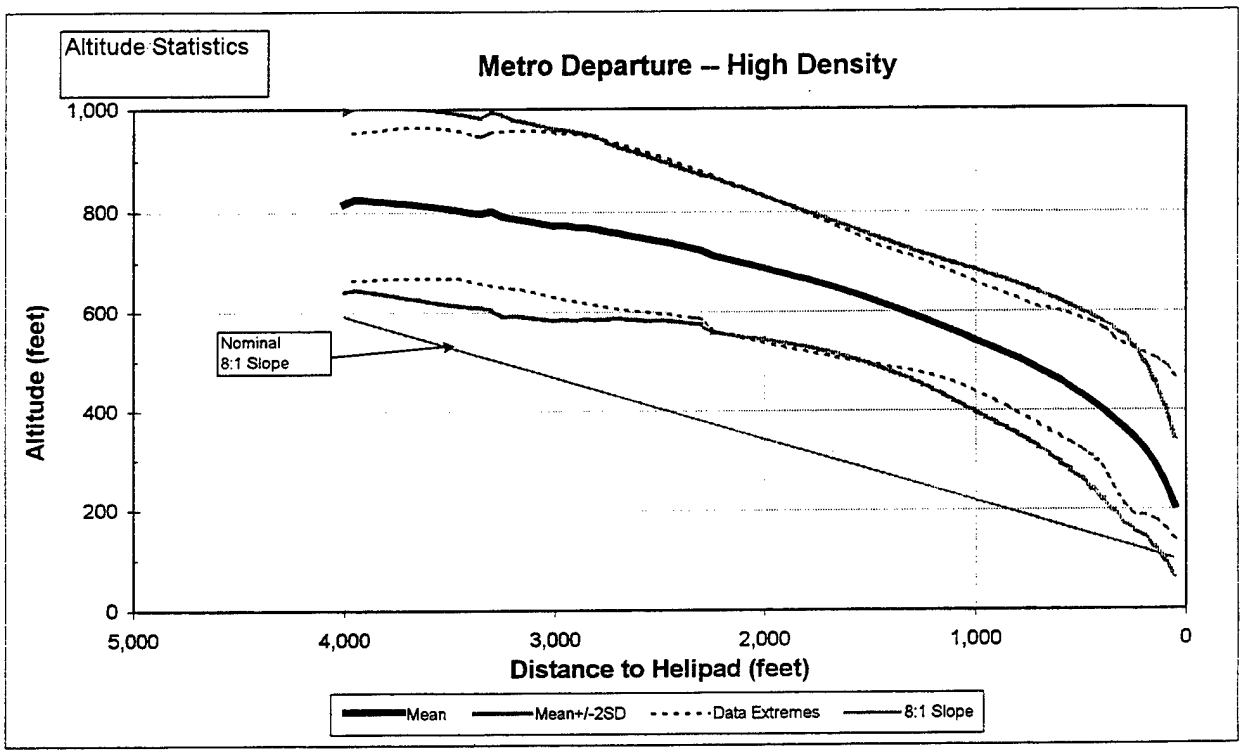

Figure H.2-90 Metro Departure High Density Altitude Data

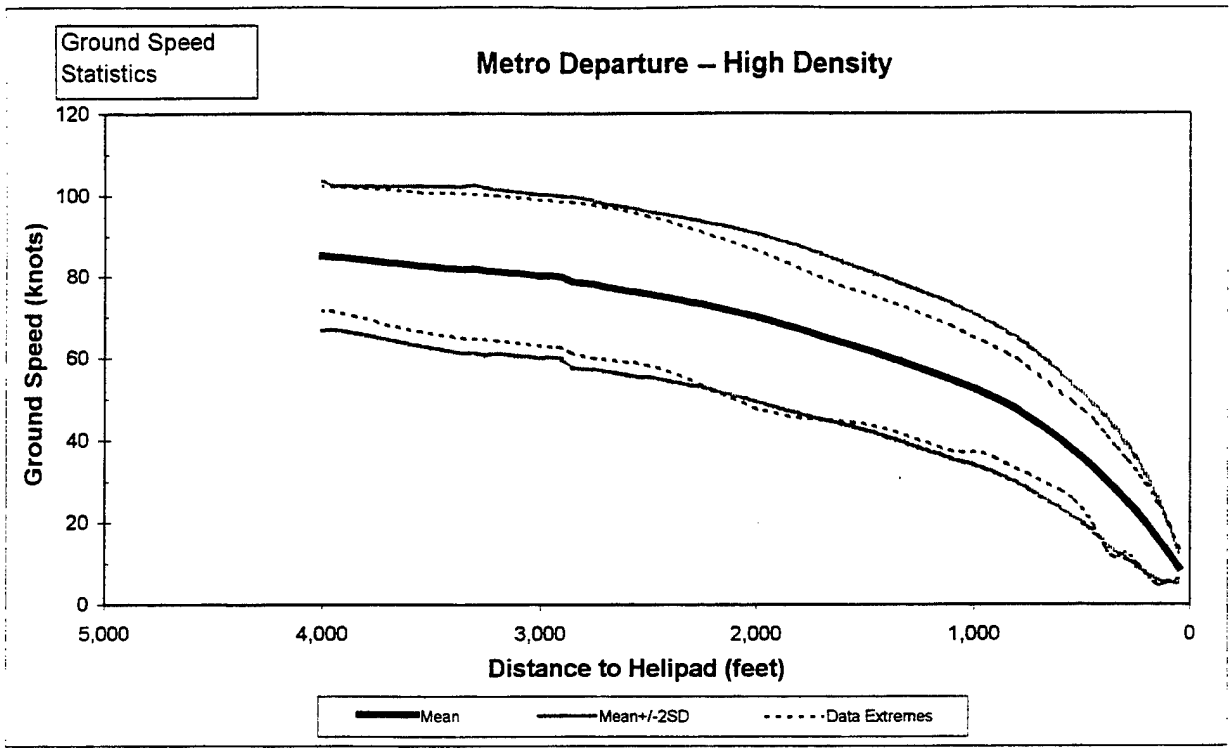

Figure H.2-91 Metro Departure High Density Ground Speed Data

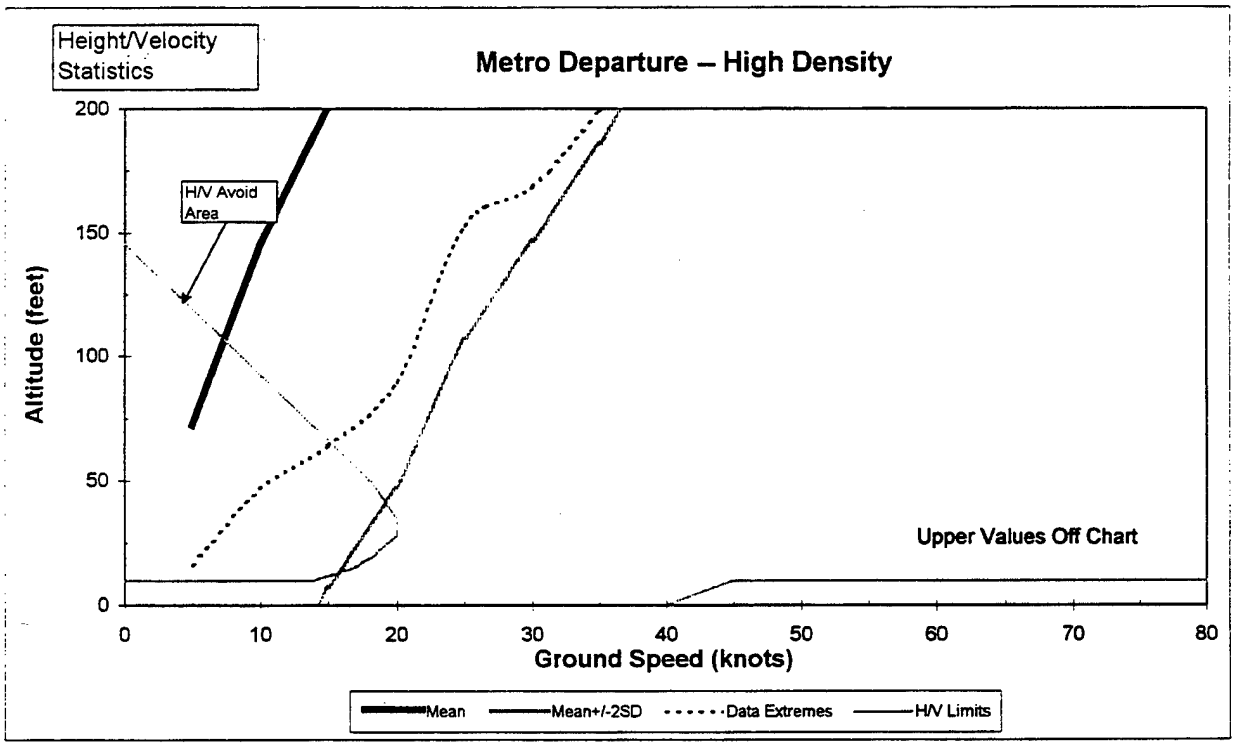

Figure H.2-92 Metro Departure High Density Height/Velocity Data

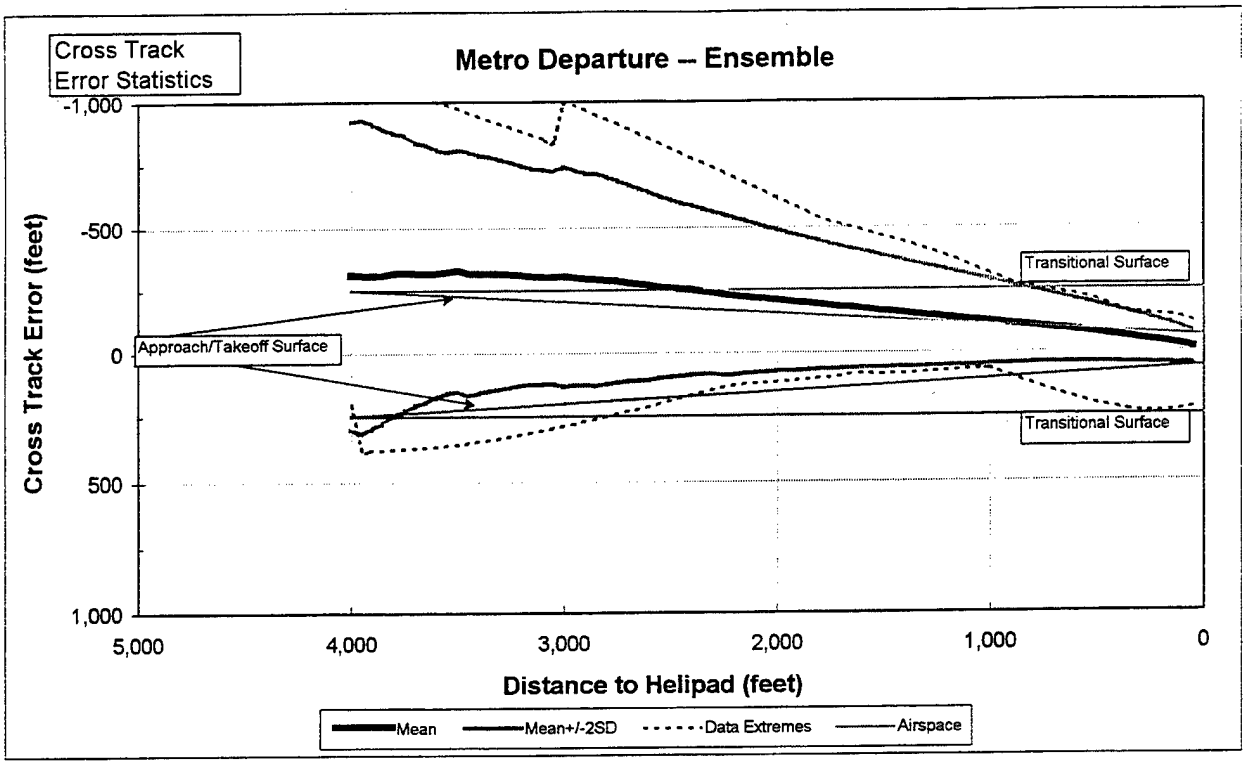

Figure H.2-93 Metro Departure Ensemble Cross Track Data

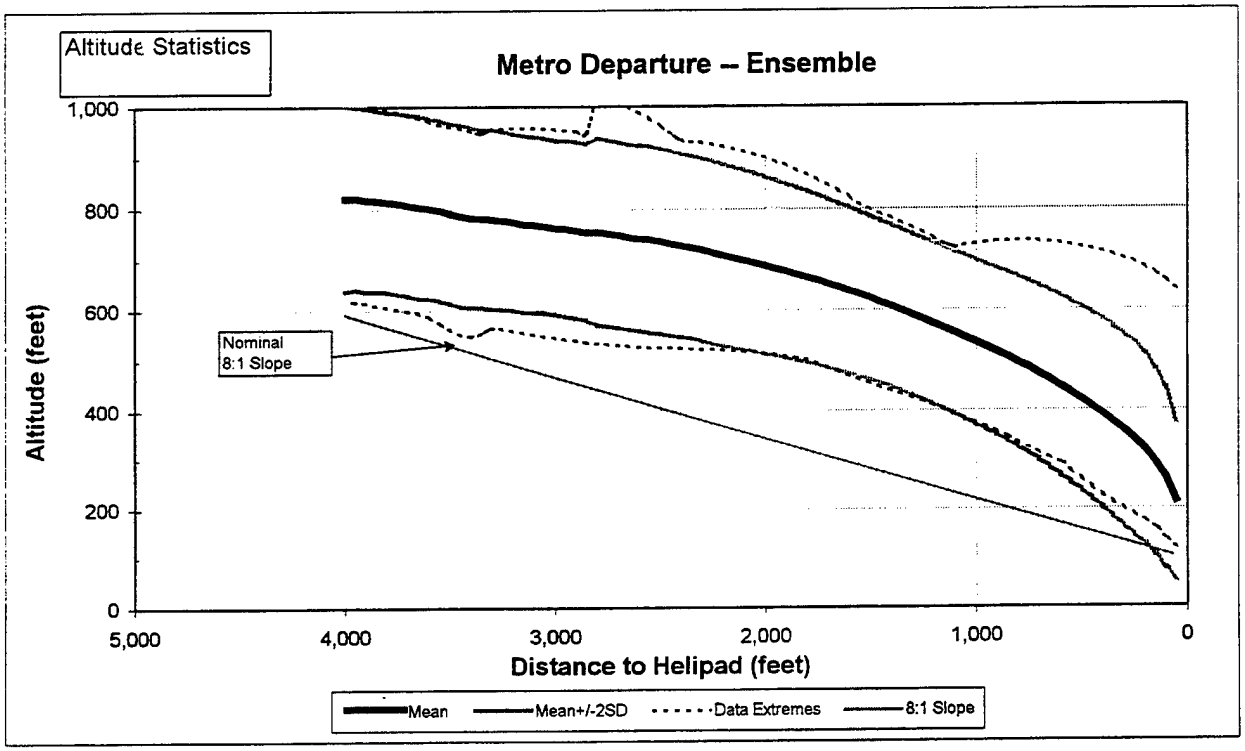

Figure H.2-94 Metro Departure Ensemble Altitude Data

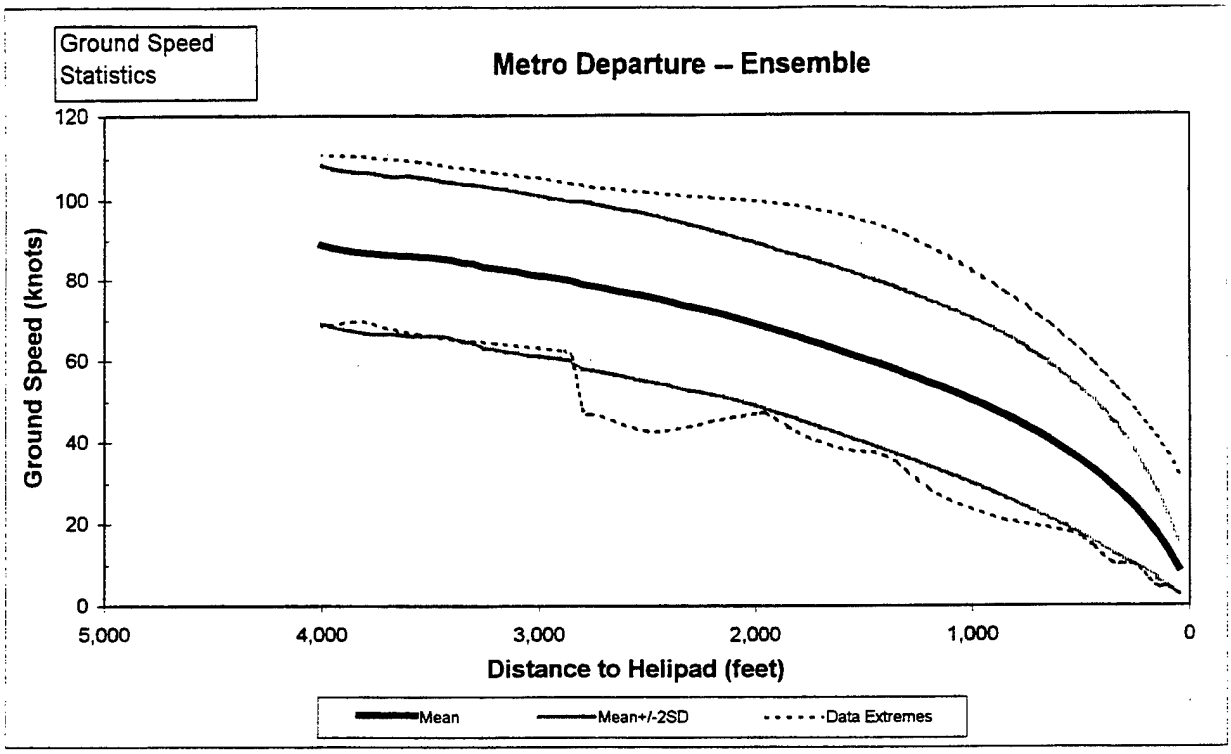

Figure H.2-95 Metro Departure Ensemble Ground Speed Data

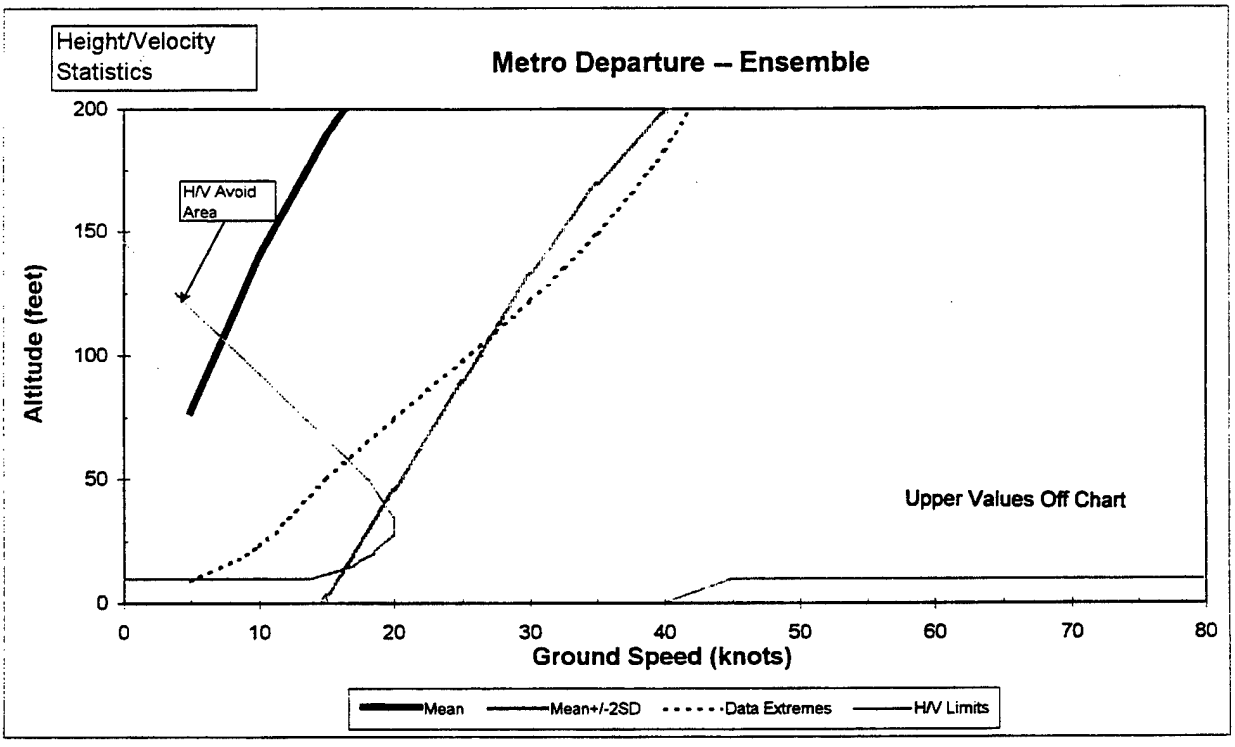

Figure H.2-96 Metro Departure Ensemble Height/Velocity Data

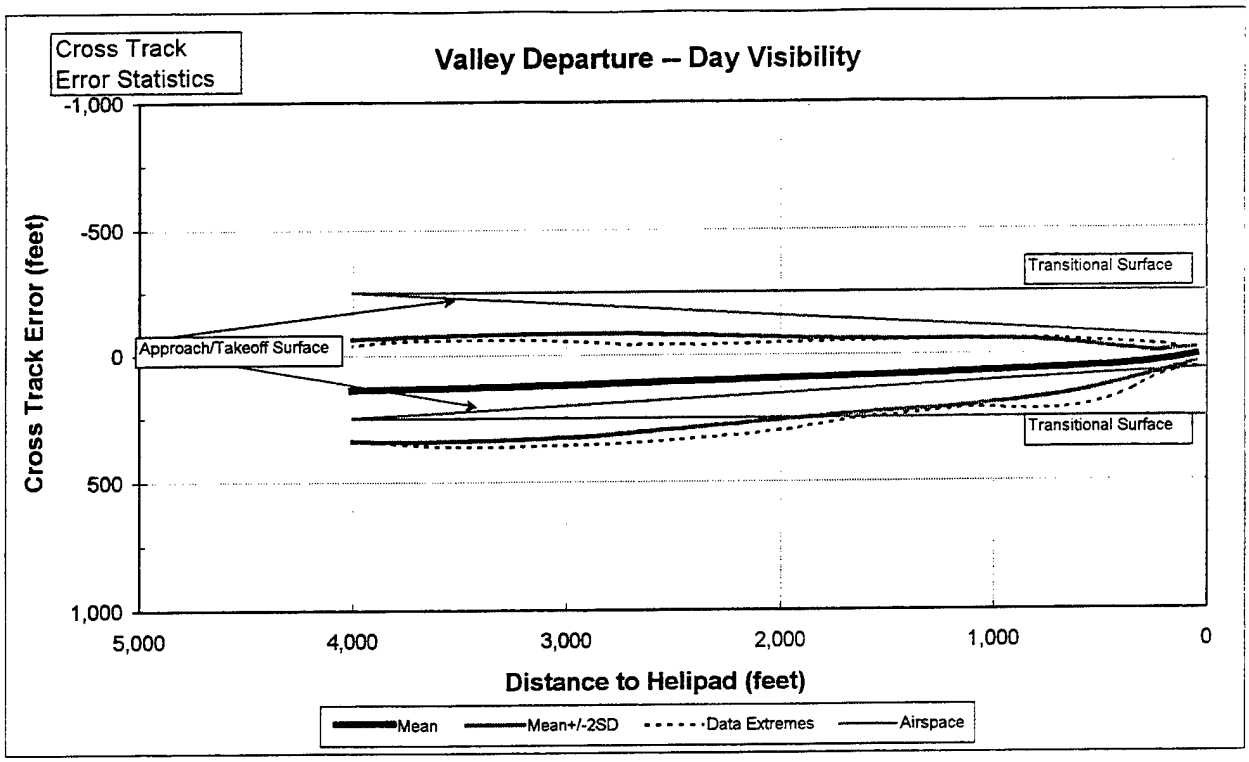

Figure H.2-97 Valley Departure Day Visibility Cross Track Data

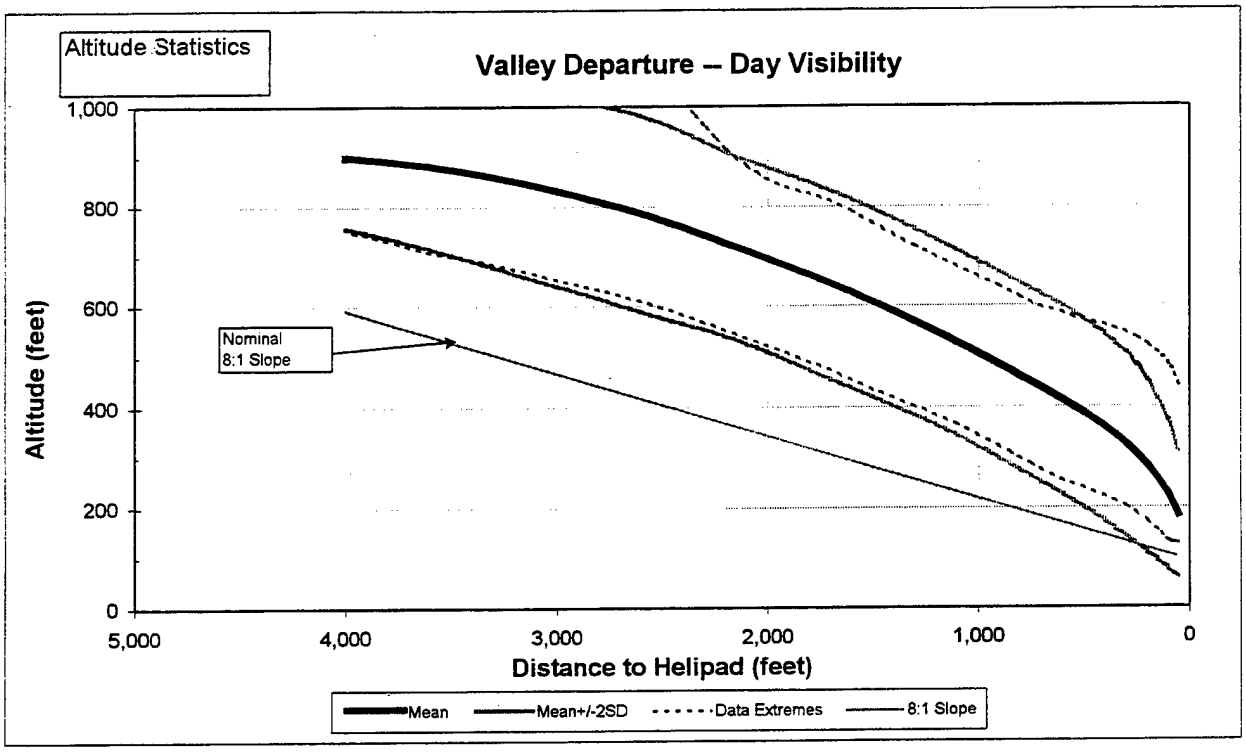

Figure H.2-98 Valley Departure Day Visibility Altitude Data

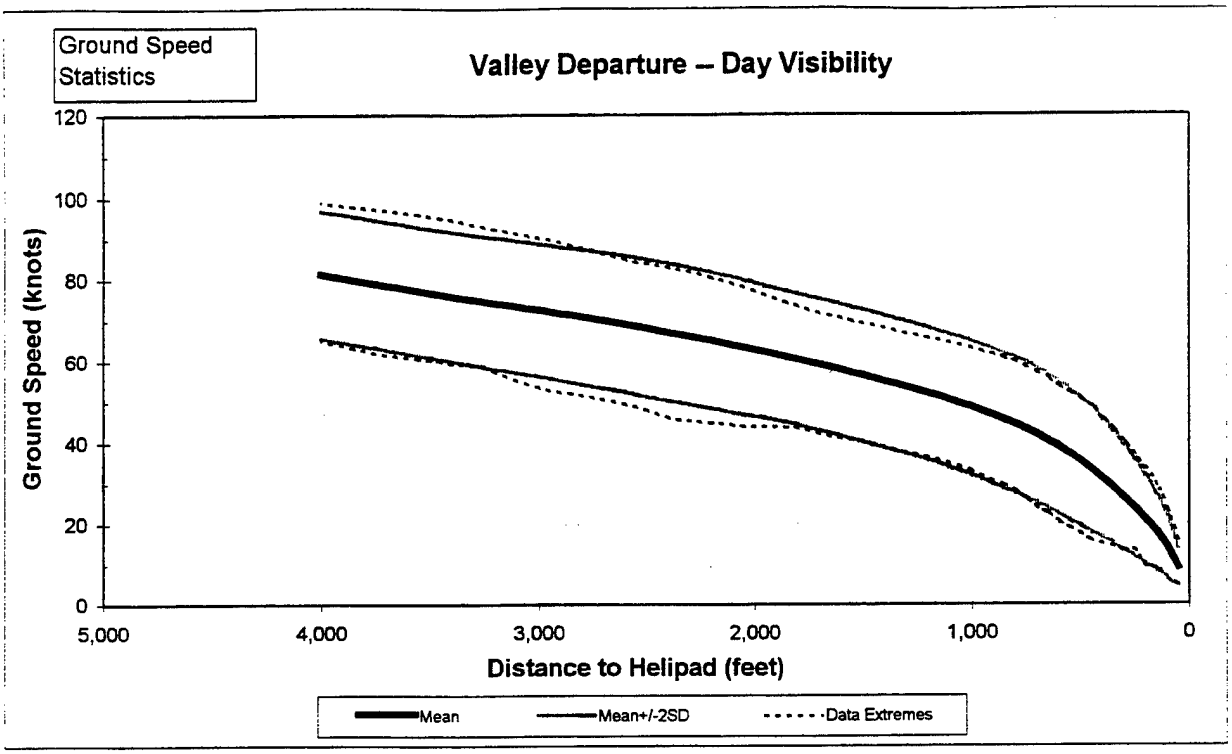

Figure H.2-99 Valley Departure Day Visibility Ground Speed Data

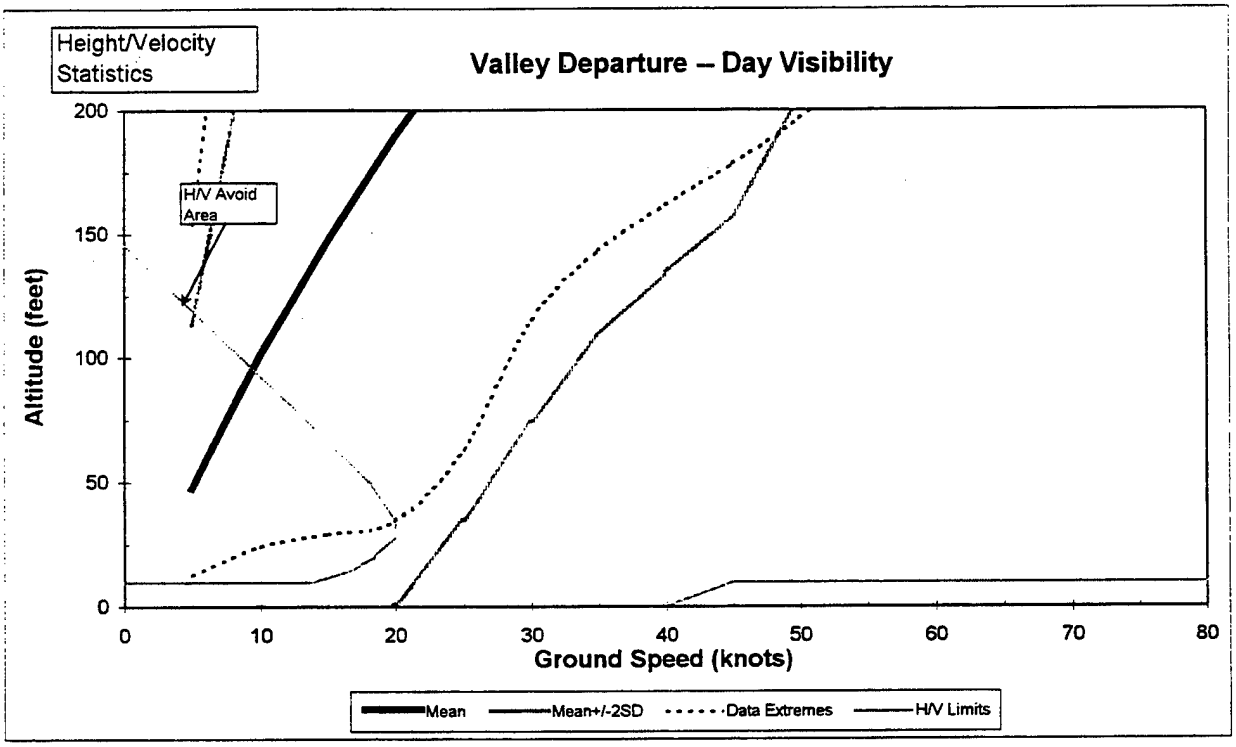

Figure H.2-100 Valley Departure Day Visibility Height/Velocity Data

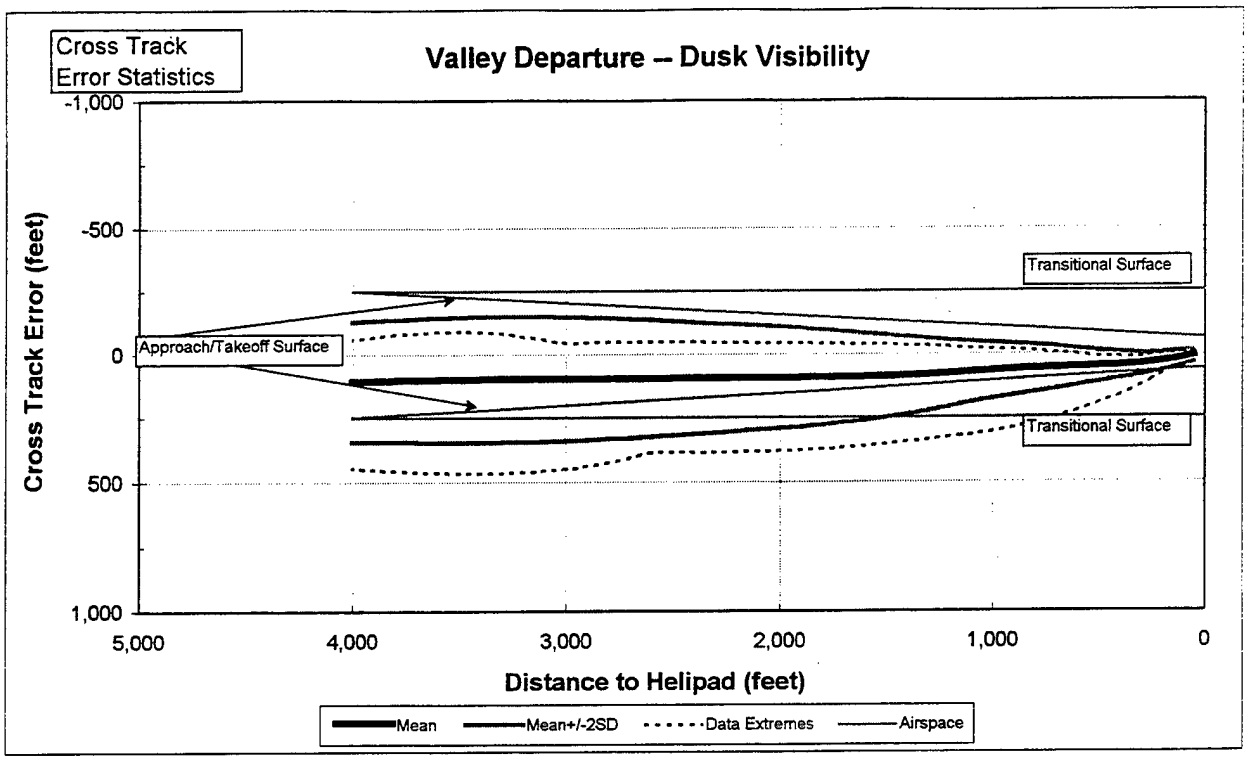

Figure H.2-101 Valley Departure Dusk Visibility Cross Track Data

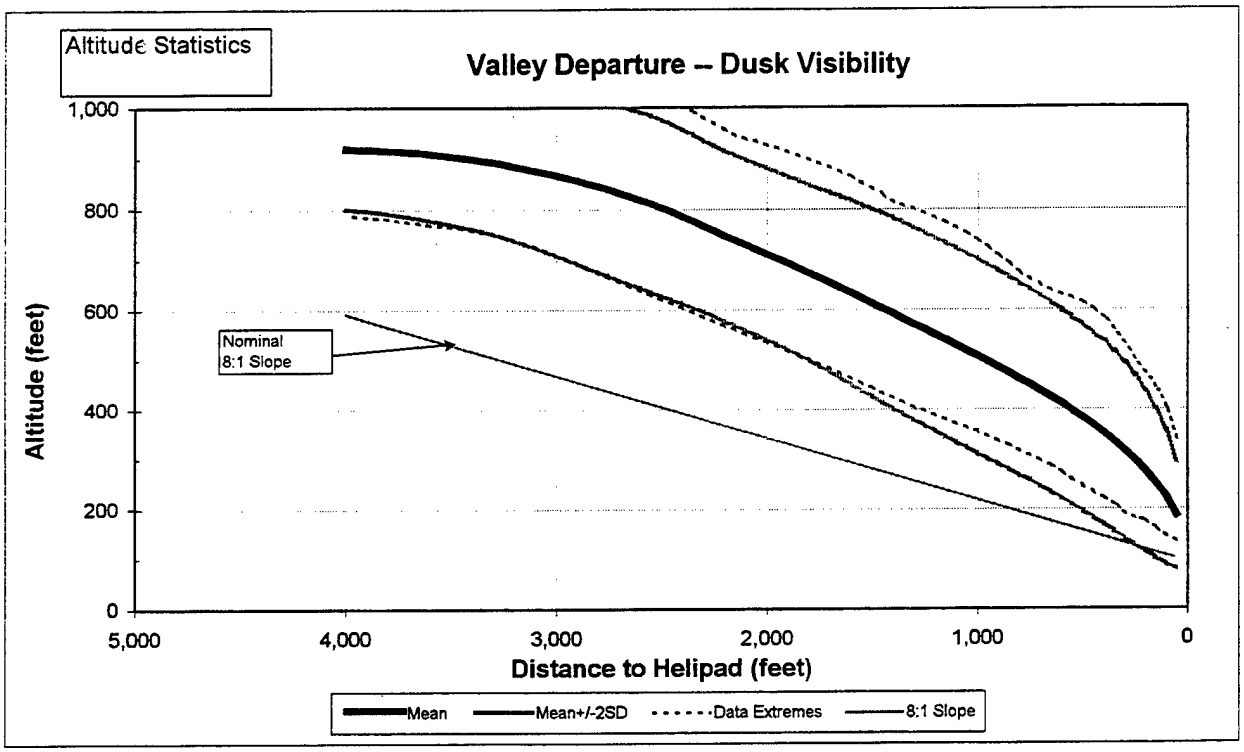

Figure H.2-102 Valley Departure Dusk Visibility Altitude Data

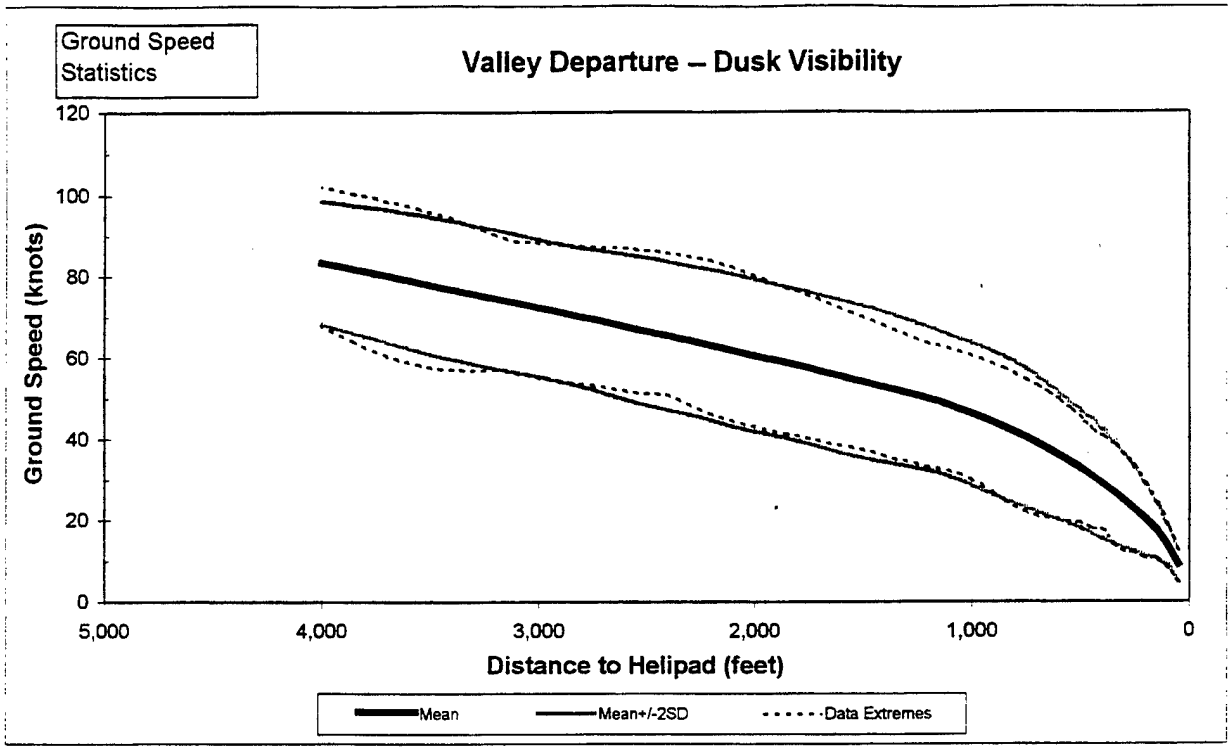

Figure H.2-103 Valley Departure Dusk Visibility Ground Speed Data

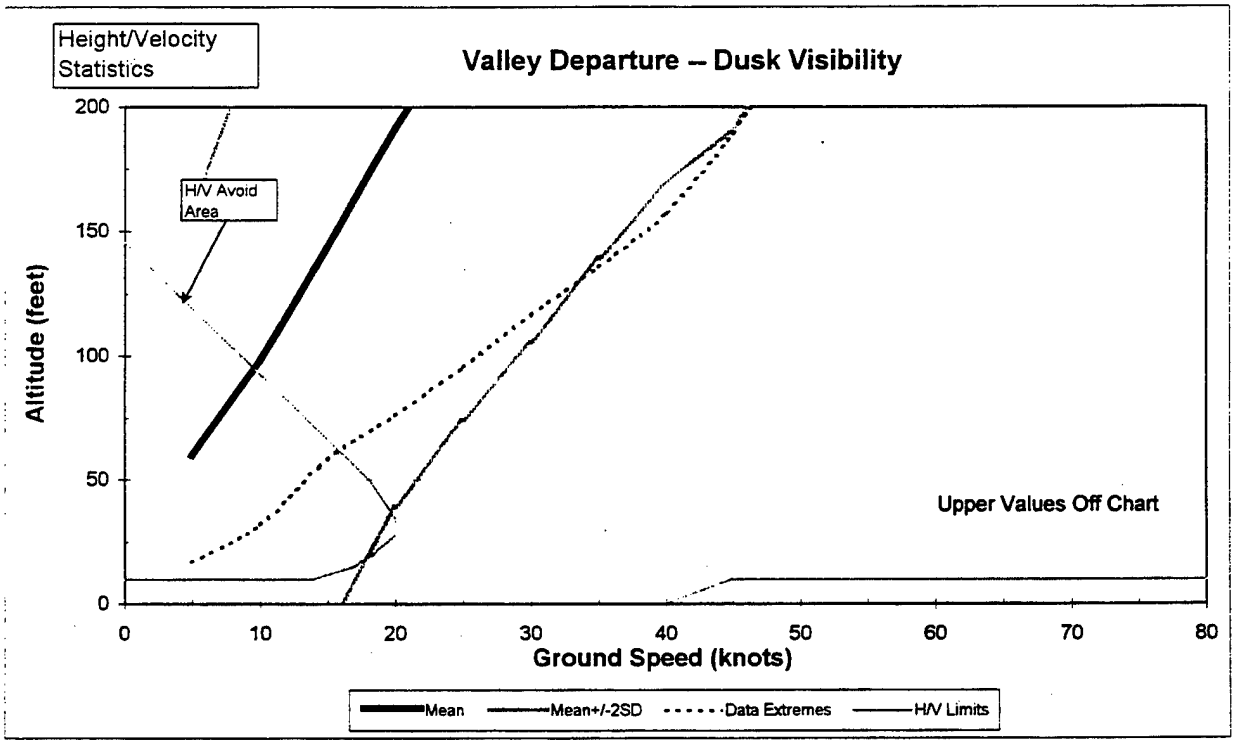

Figure H.2-104 Valley Departure Dusk Visibility Height/Velocity Data

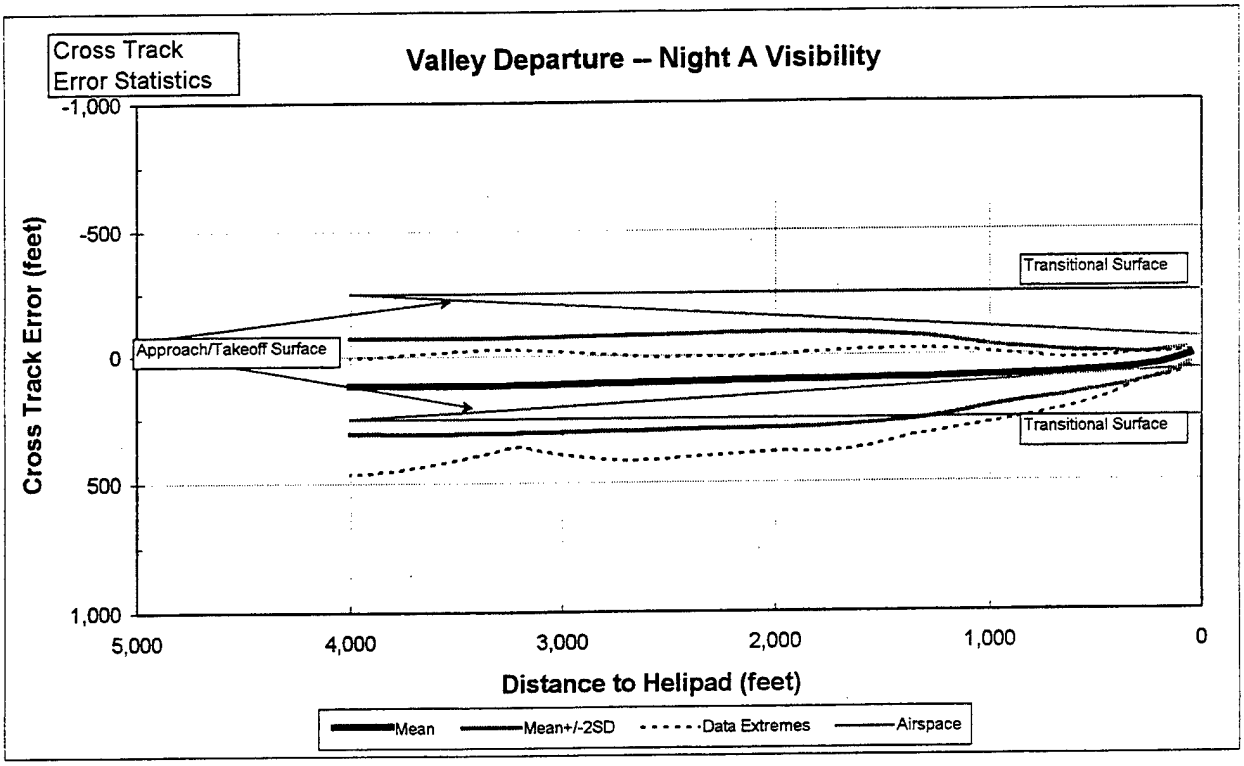

Figure H.2-105 Valley Departure Night A Visibility Cross Track Data

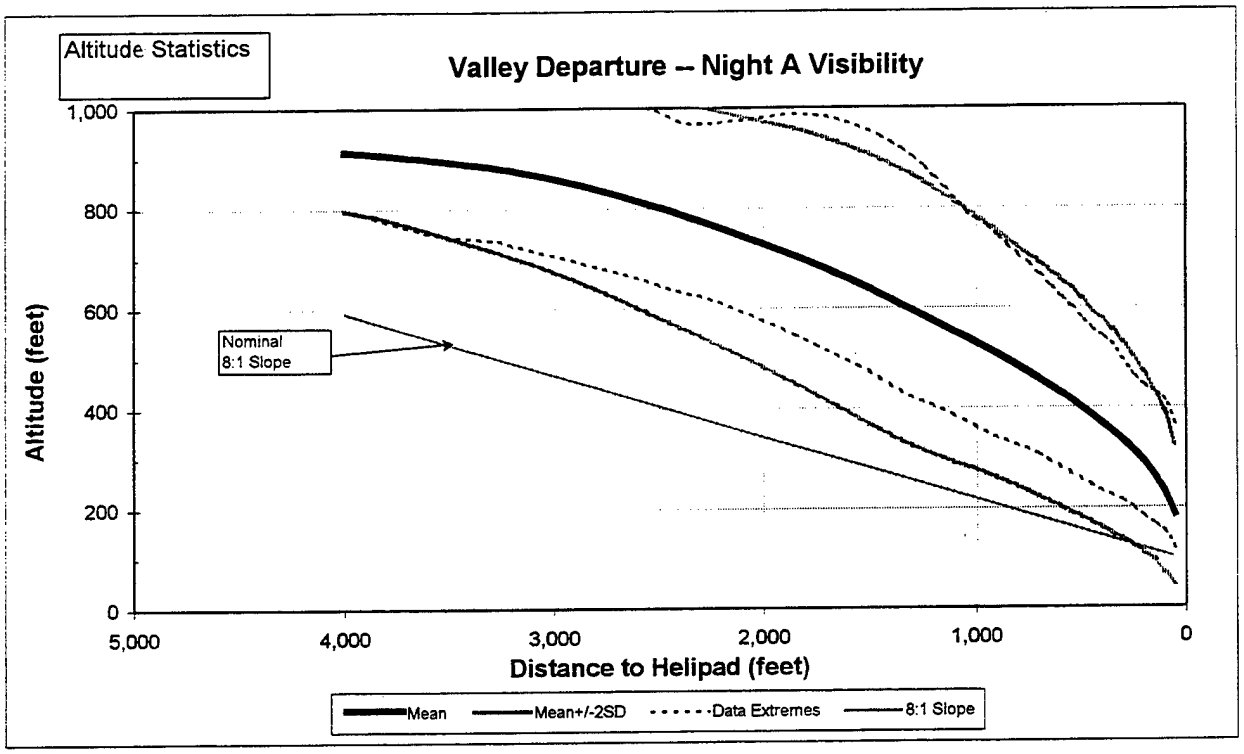

Figure H.2-106 Valley Departure Night A Visibility Altitude Data

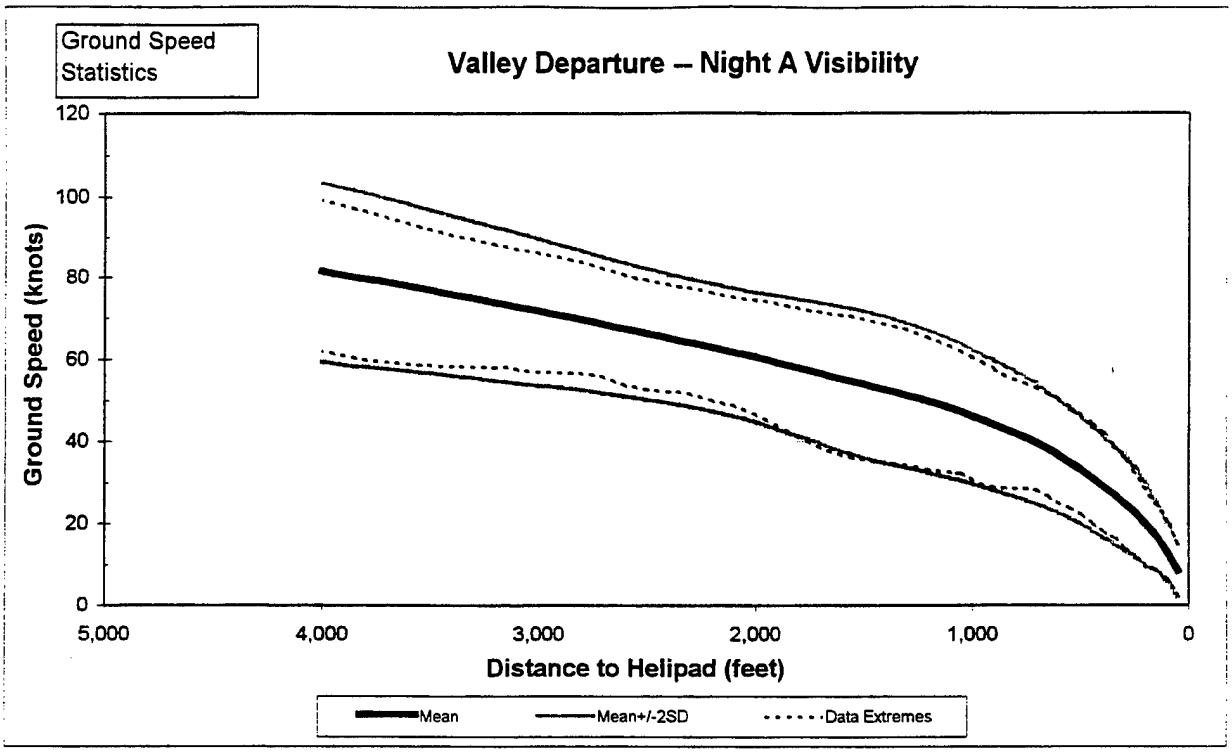

Figure H.2-107 Valley Departure Night A Visibility Ground Speed Data

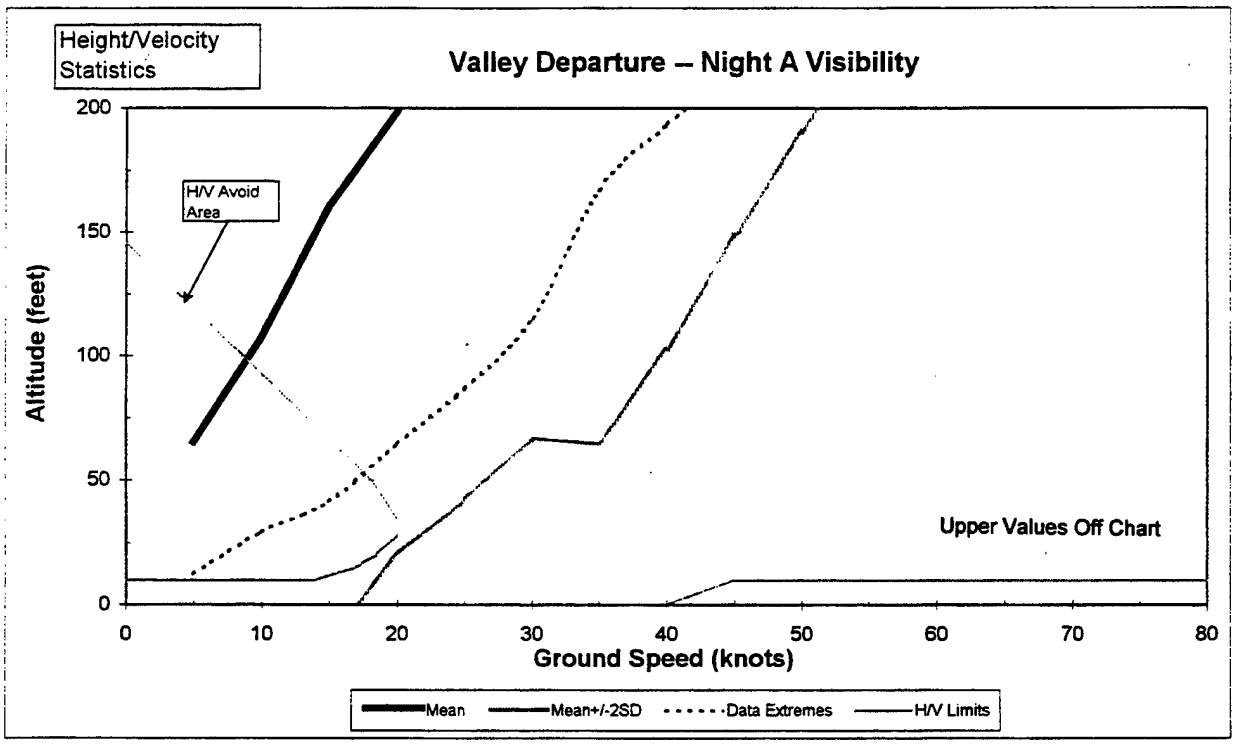

Figure H.2-108 Valley Departure Night A Visibility Height/Velocity Data

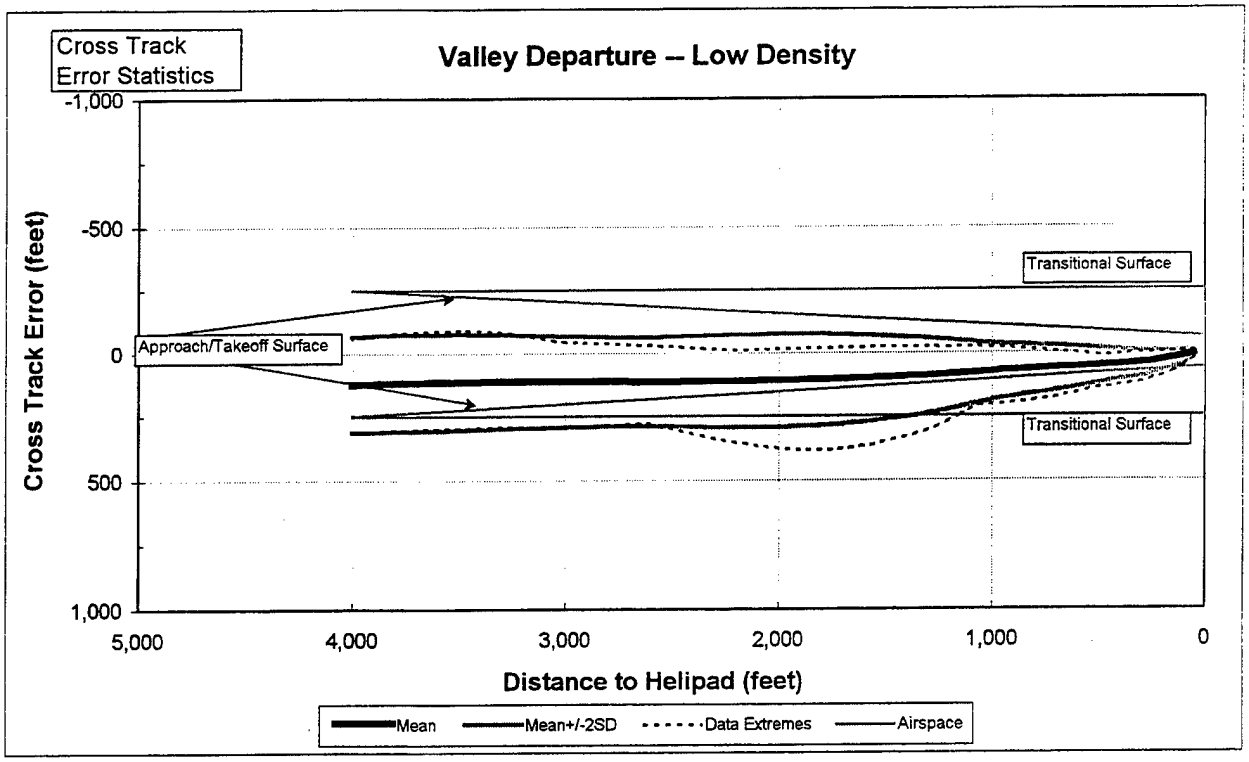

Figure H.2-109 Valley Departure Low Density Cross Track Data

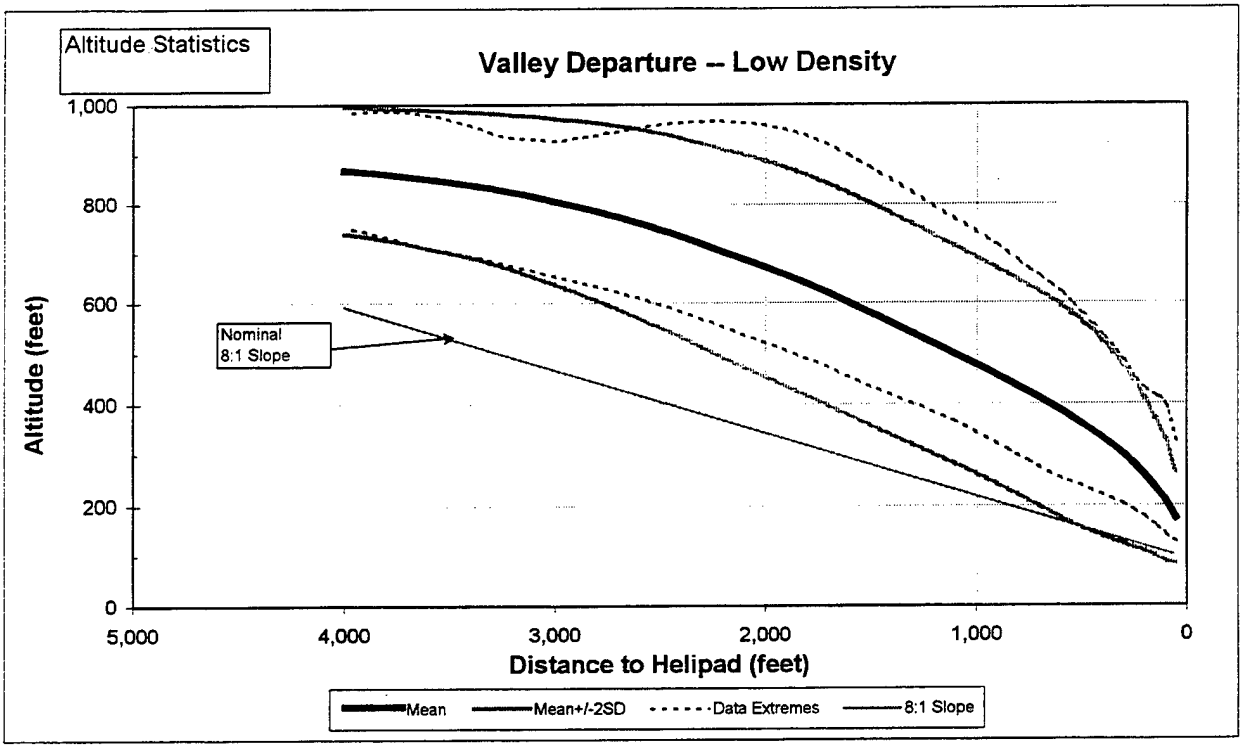

Figure H.2-110 Valley Departure Low Density Altitude Data

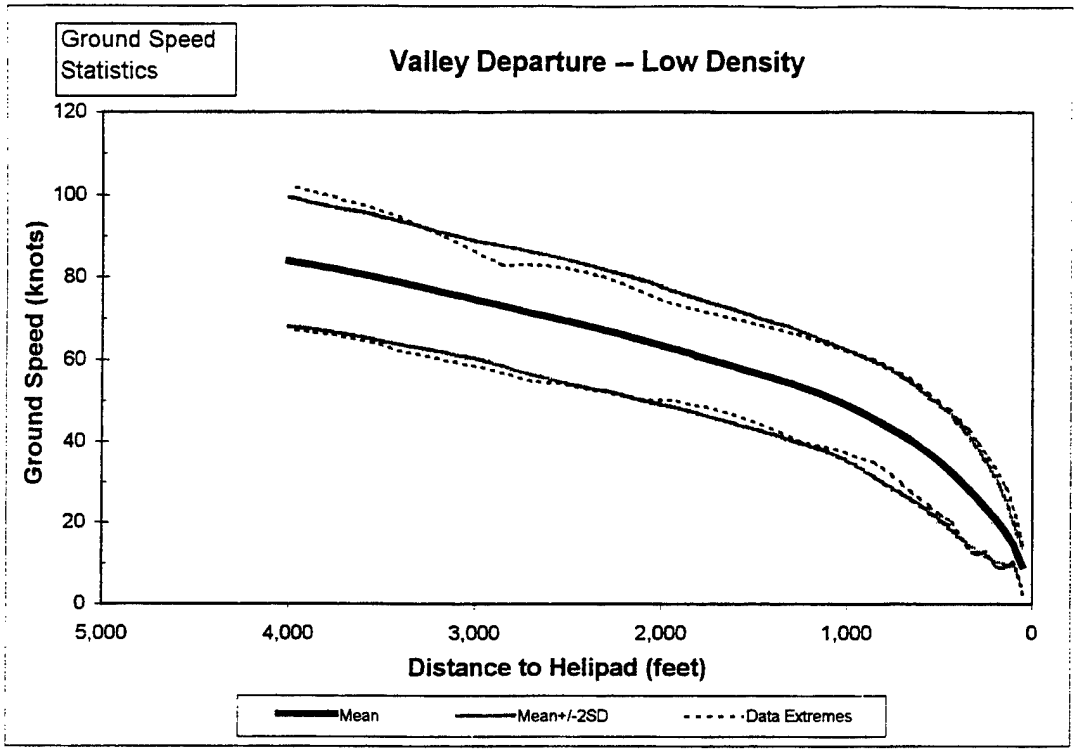

Figure H.2-111 Valley Departure Low Density Ground Speed Data

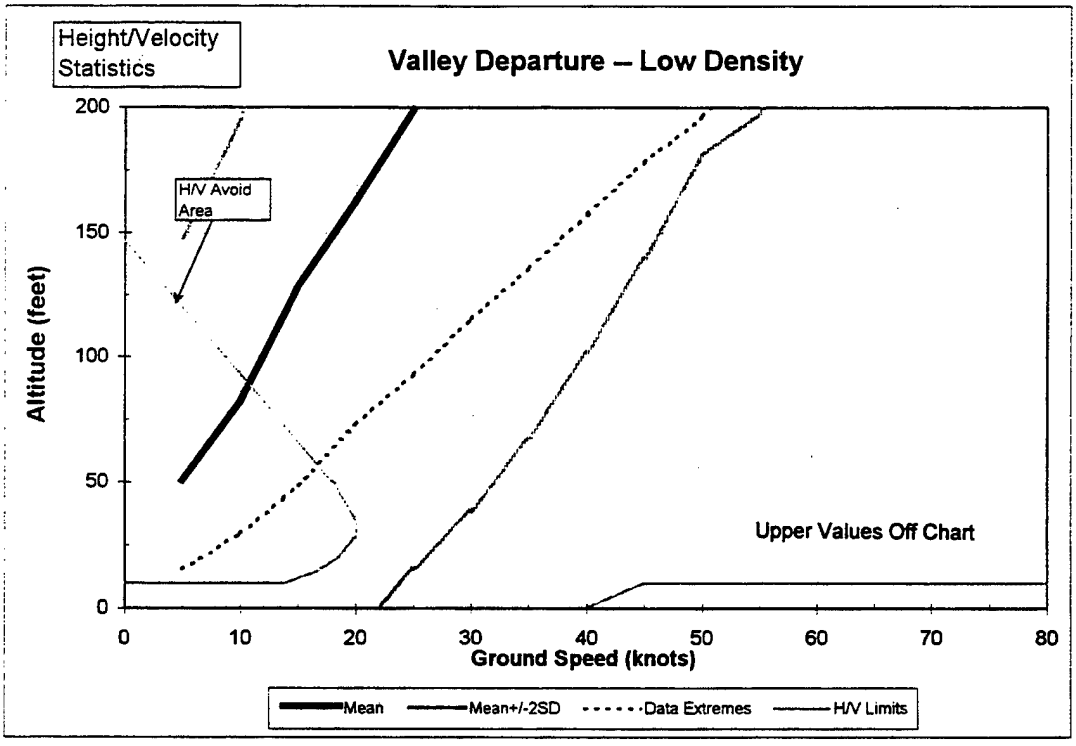

Figure H.2-112 Valley Departure Low Density Height/Velocity Data

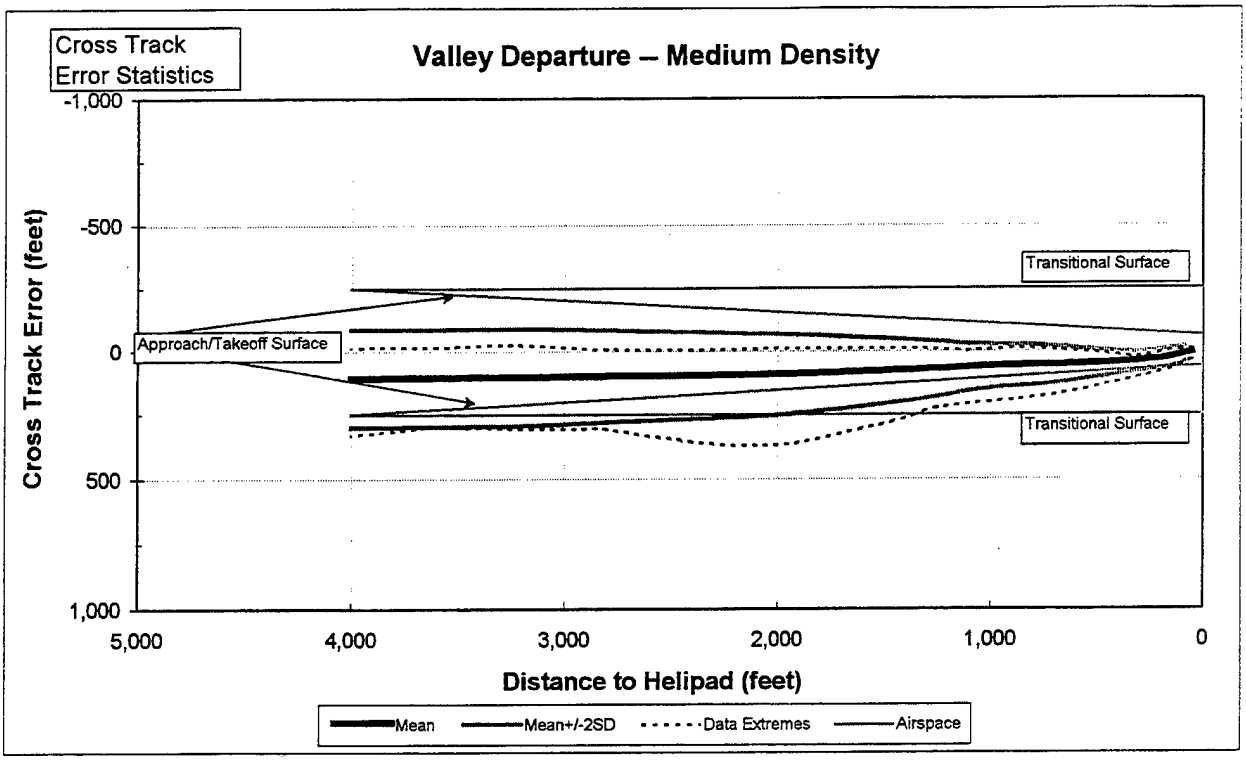

Figure H.2-113 Valley Departure Medium Density Cross Track Data

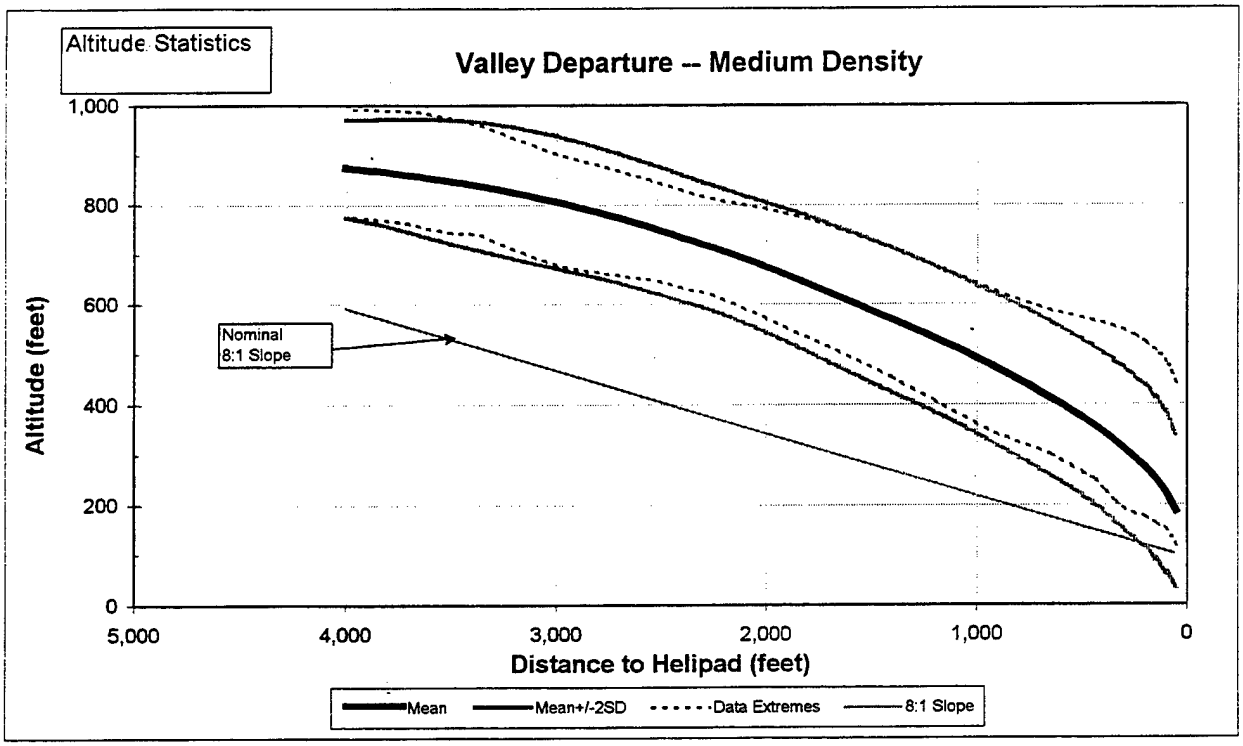

Figure H.2-114 Valley Departure Medium Density Altitude Data

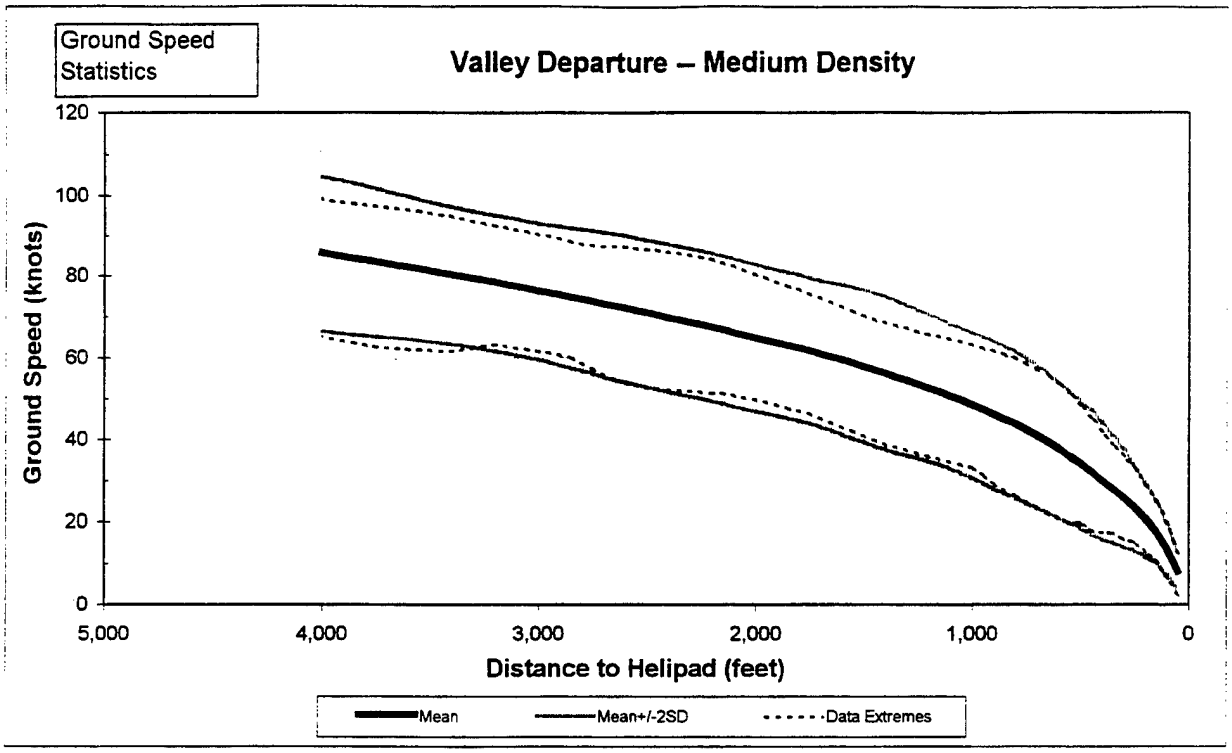

Figure H.2-115 Valley Departure Medium Density Ground Speed Data

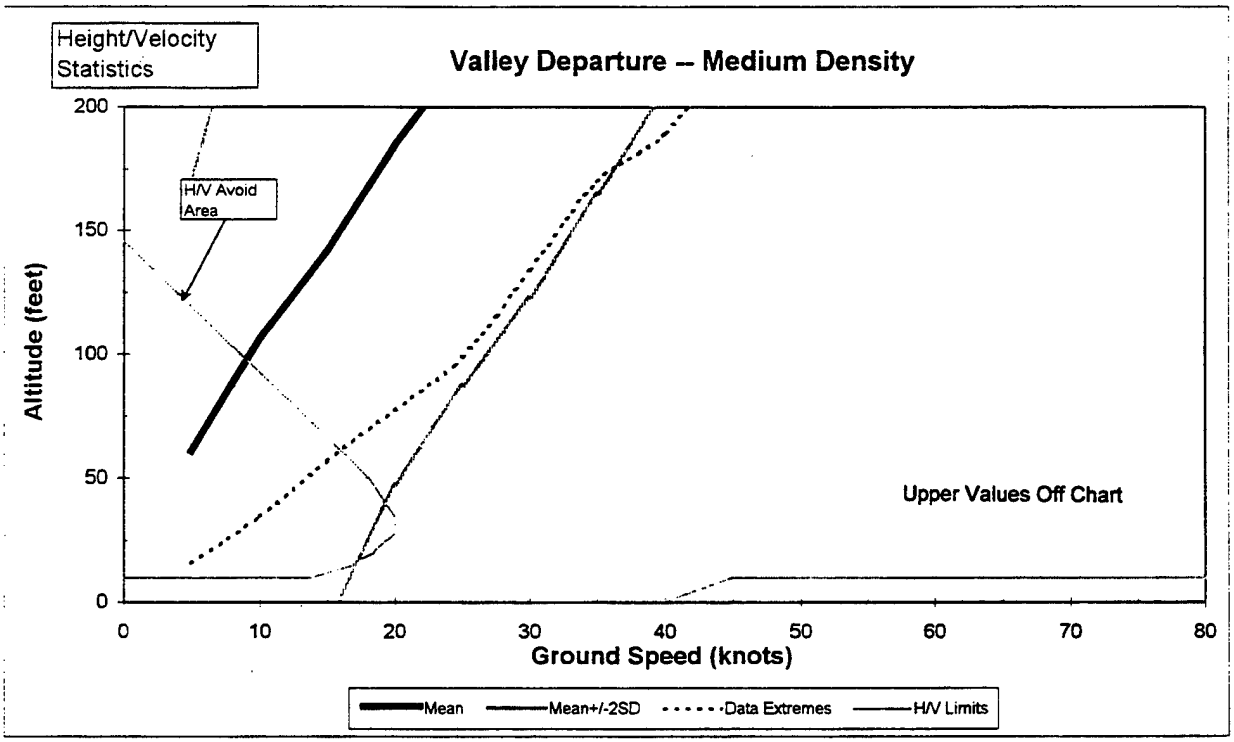

Figure H.2-116 Valley Departure Medium Density Height/Velocity Data

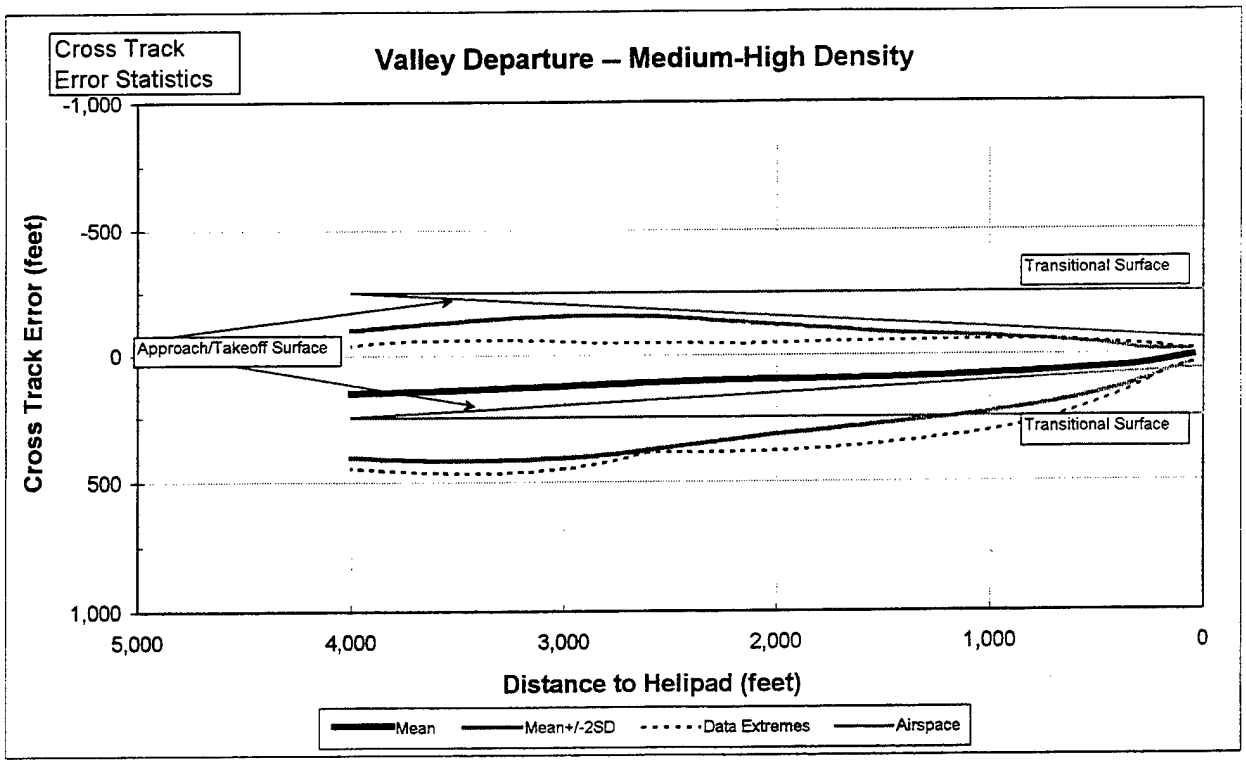

Figure H.2-117 Valley Departure Medium-High Density Cross Track Data

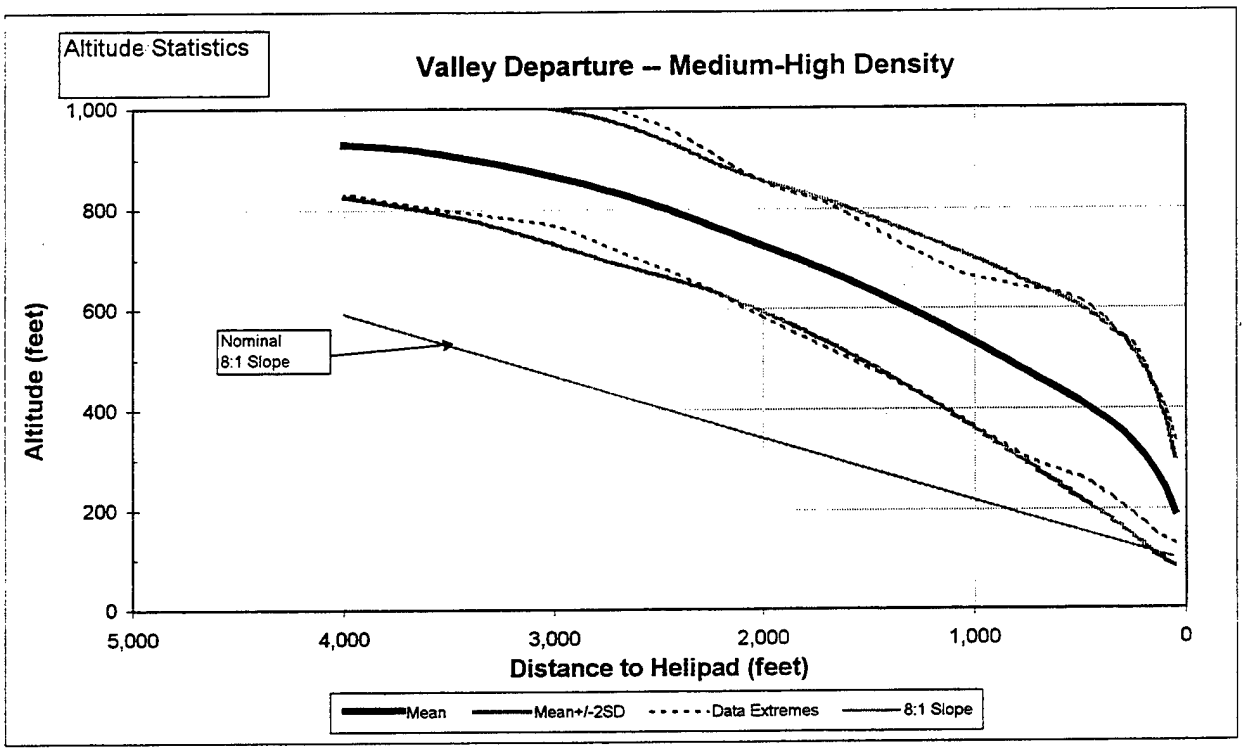

Figure H.2-118 Valley Departure Medium-High Density Altitude Data

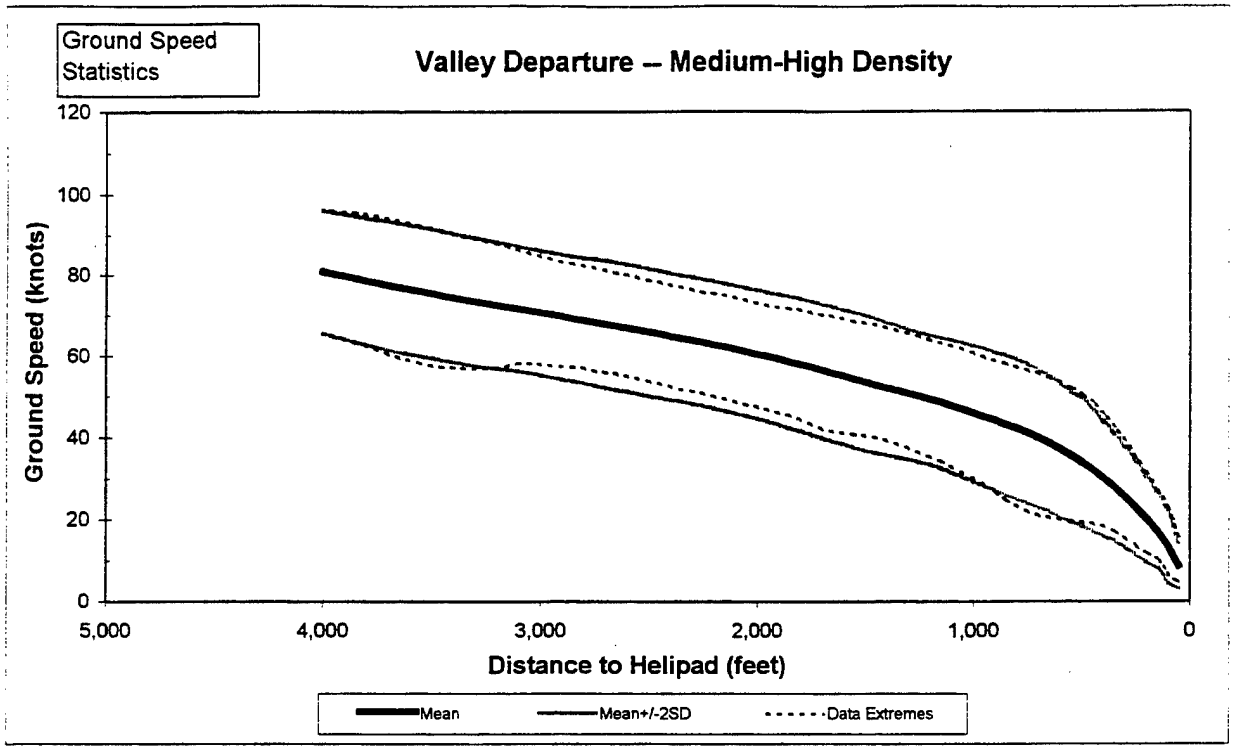

Figure H.2-119 Valley Departure Medium-High Density Ground Speed Data

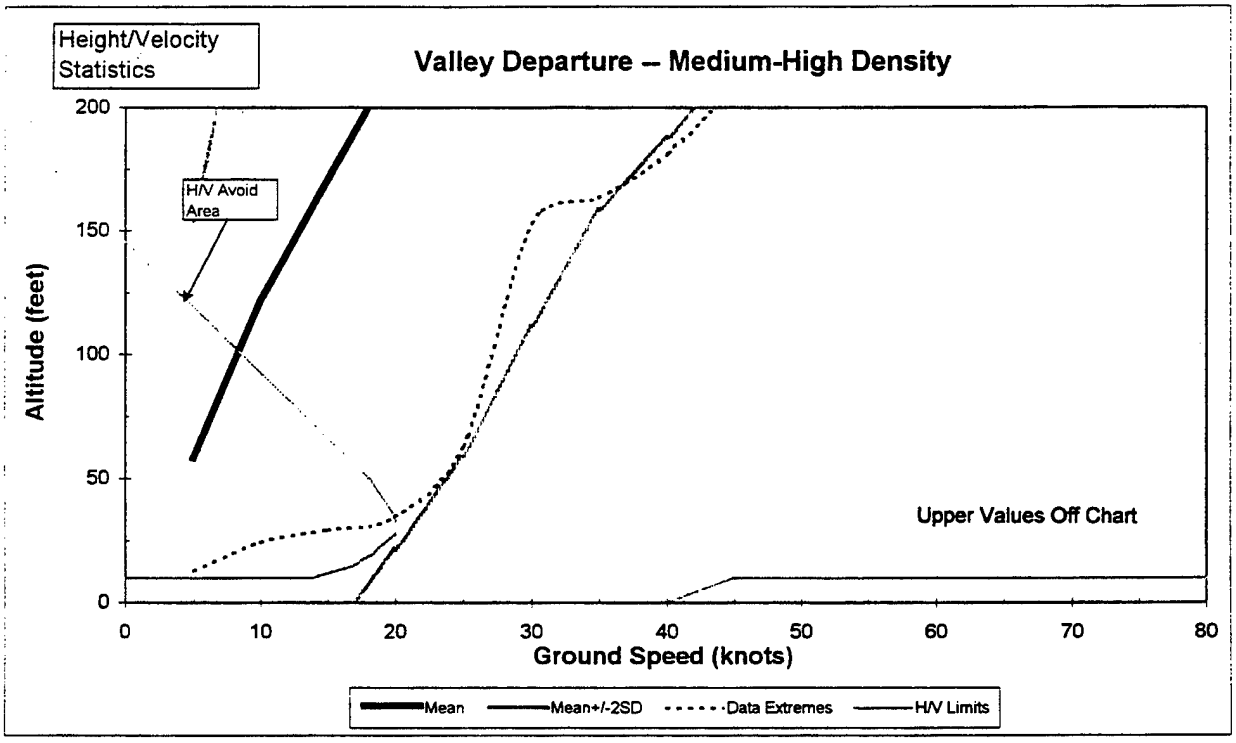

Figure H.2-120 Valley Departure Medium-High Density Height/Velocity Data

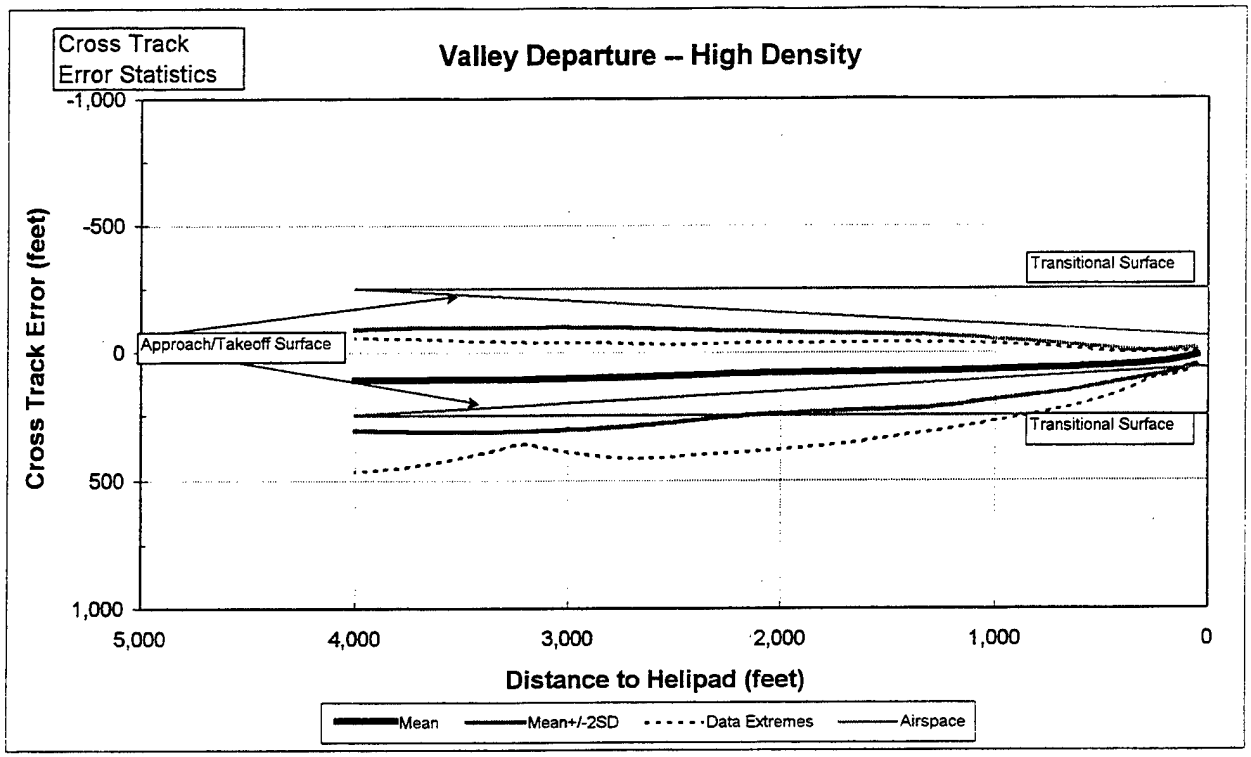

Figure H.2-121 Valley Departure High Density Cross Track Data

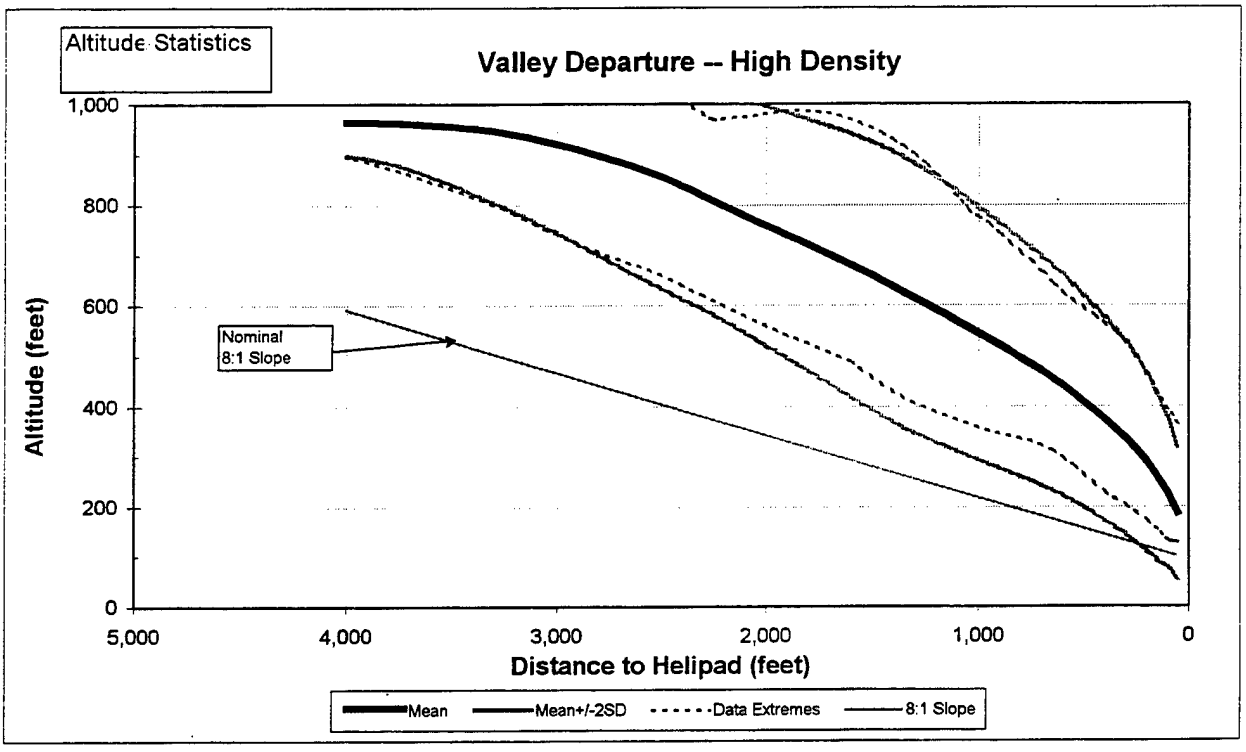

Figure H.2-122 Valley Departure High Density Altitude Data

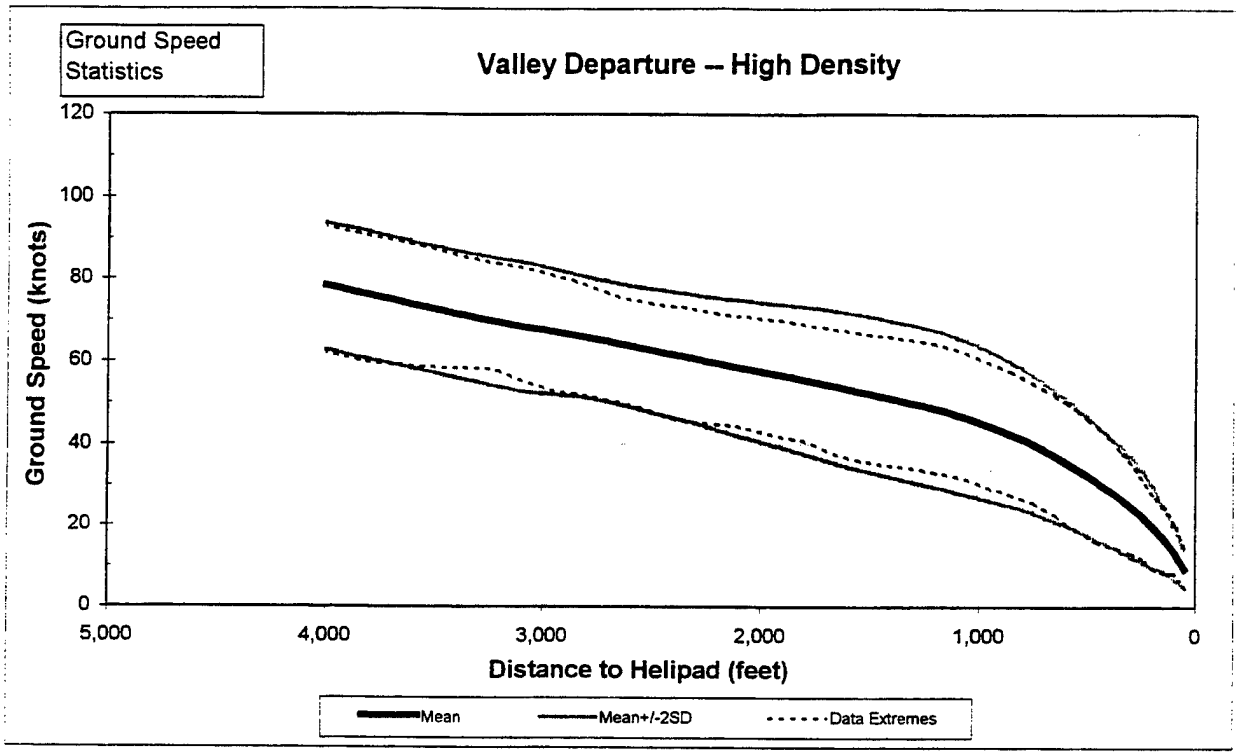

Figure H.2-123 Valley Departure High Density Ground Speed Data

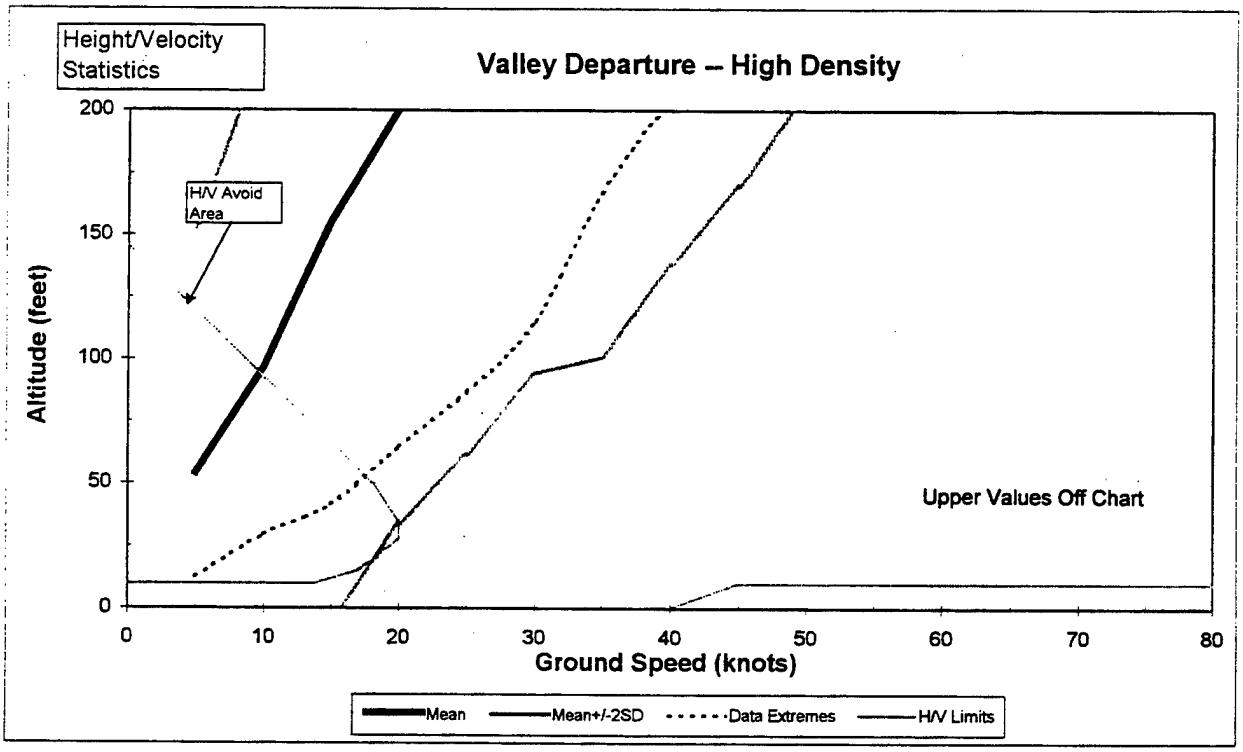

Figure H.2-124 Valley Departure High Density Height/Velocity Data

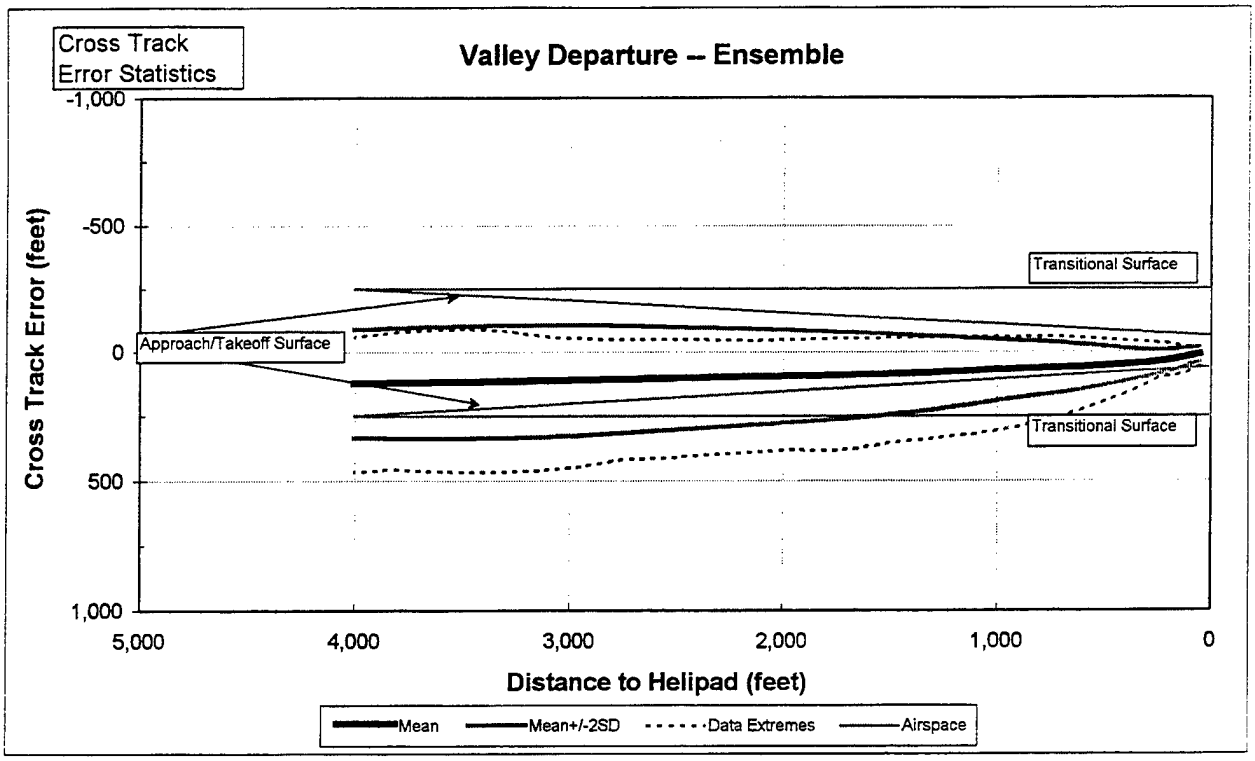

Figure H.2-125 Valley Departure Ensemble Cross Track Data

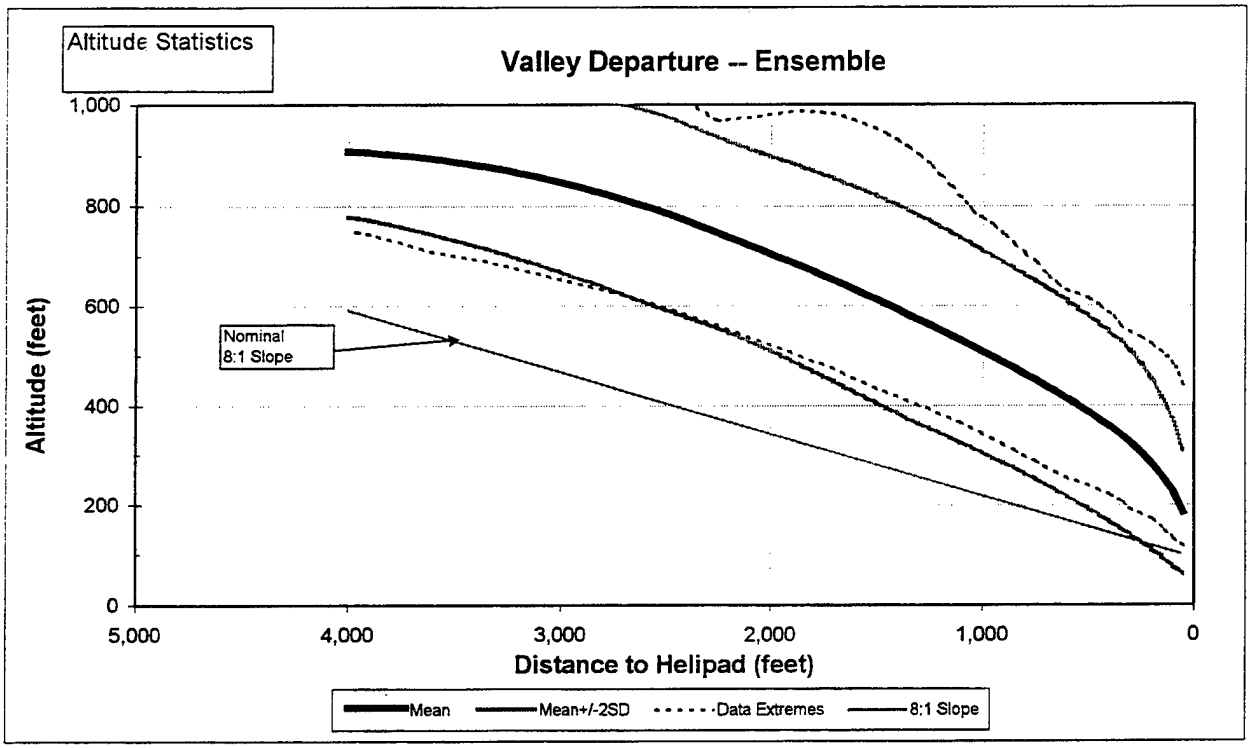

Figure H.2-126 Valley Departure Ensemble Altitude Data

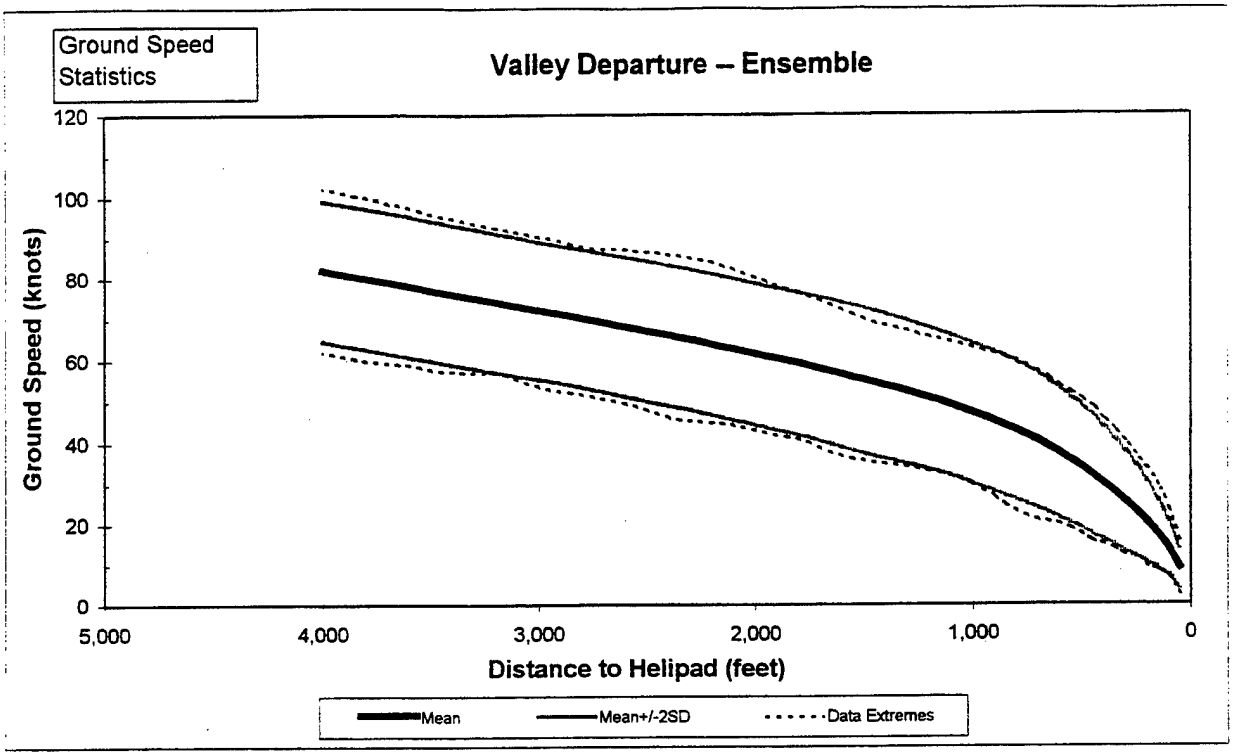

Figure H.2-127 Valley Departure Ensemble Ground Speed Data

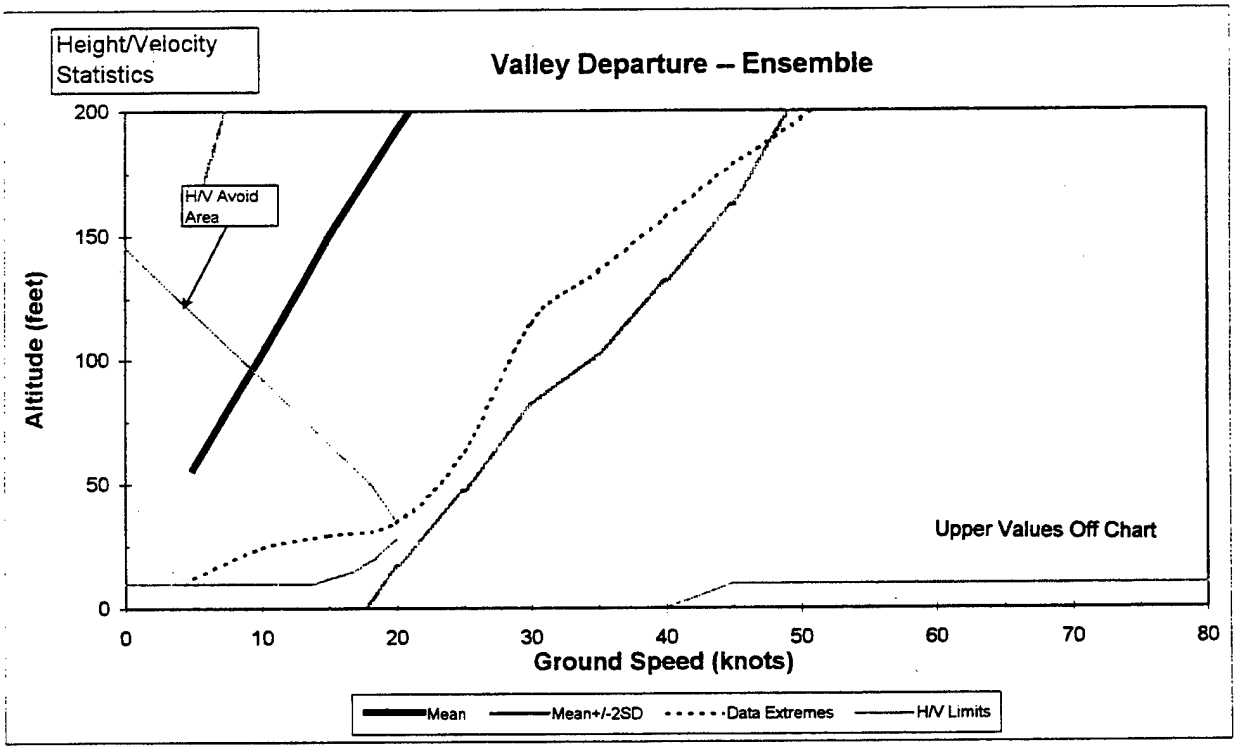

Figure H.2-128 Valley Departure Ensemble Height/Velocity Data

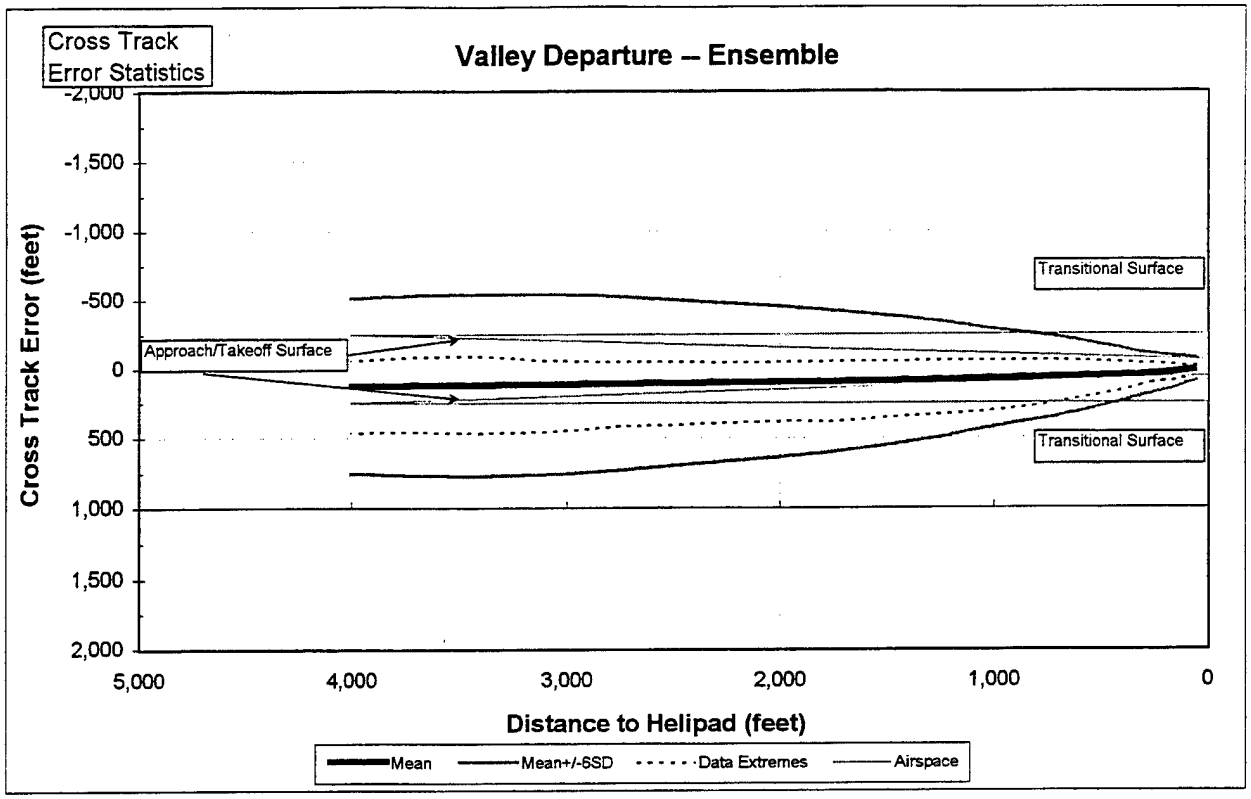

Figure H.3-1 Metro Approach Ensemble 6-Sigma Cross Track Data

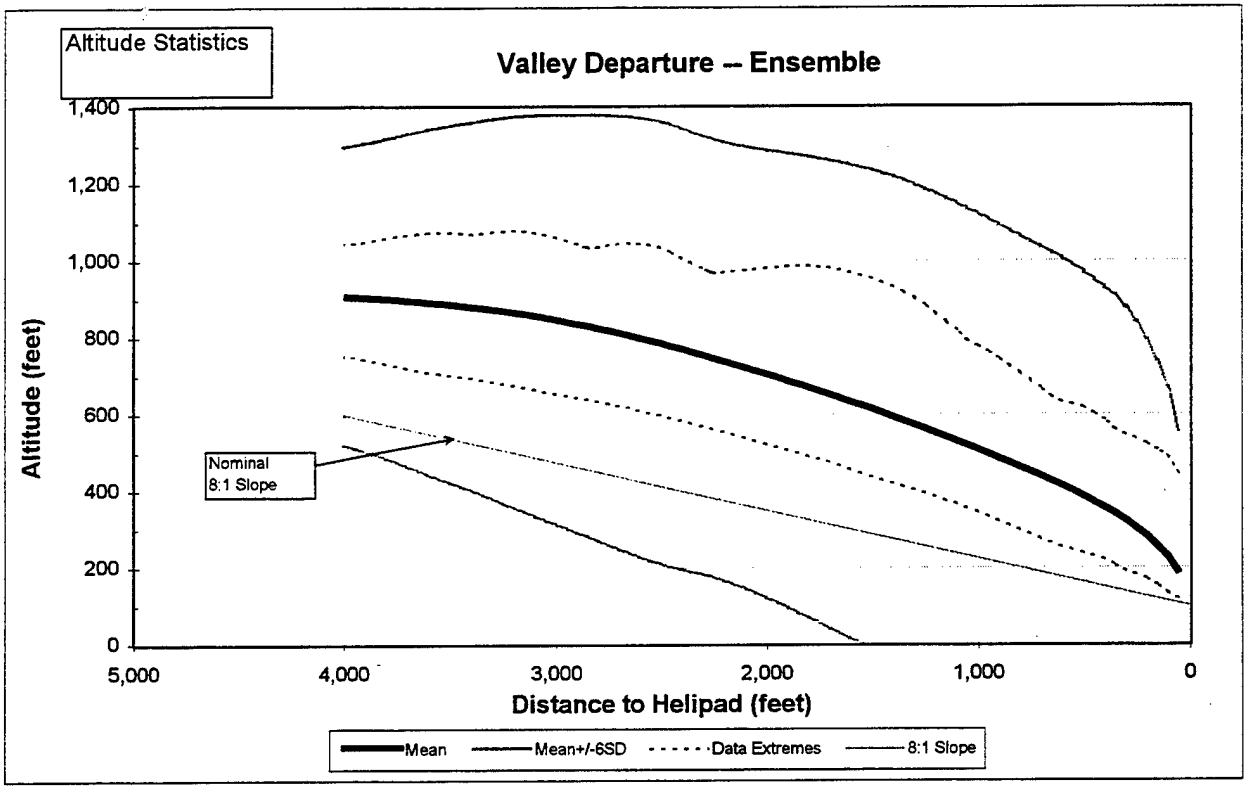

Figure H.3-2 Metro Approach Ensemble 6-Sigma Altitude Data

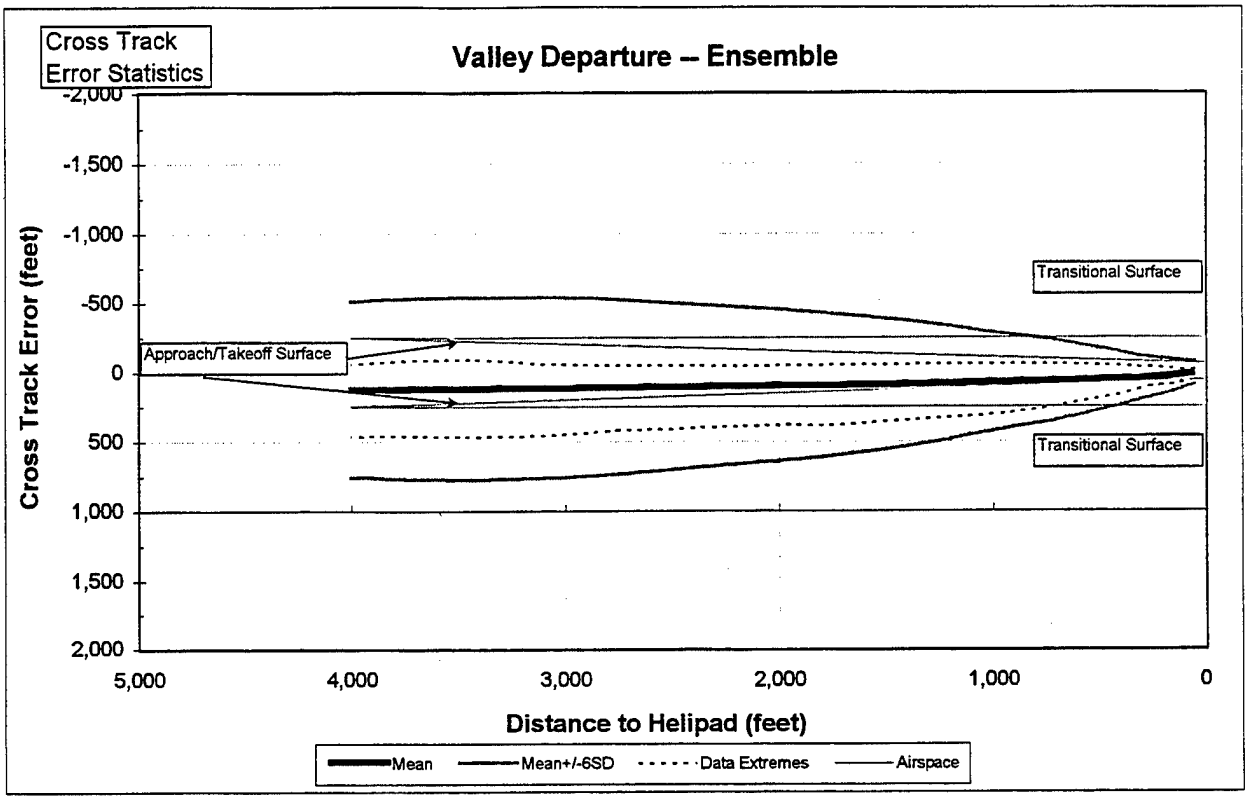

Figure H.3-3 Valley Approach Ensemble 6-Sigma Cross Track Data

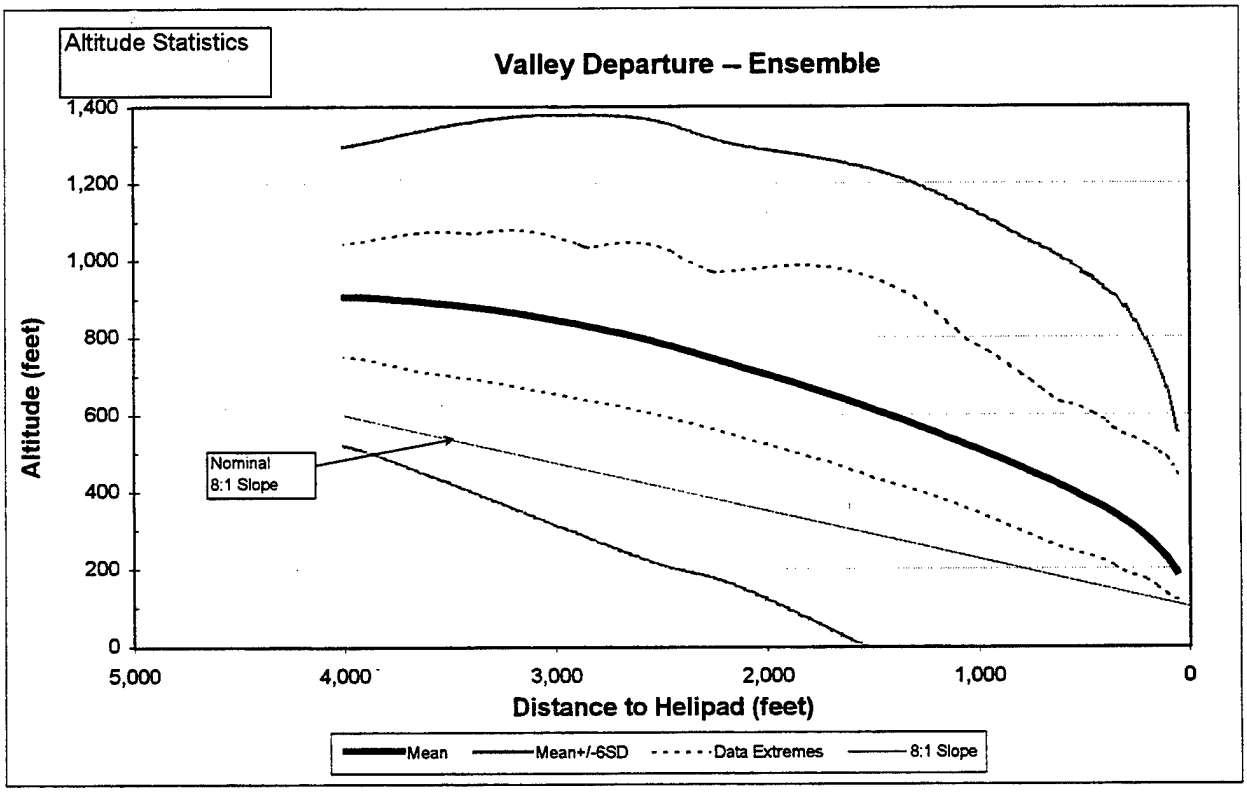

Figure H.3-4 Valley Approach Ensemble 6-Sigma Altitude Data

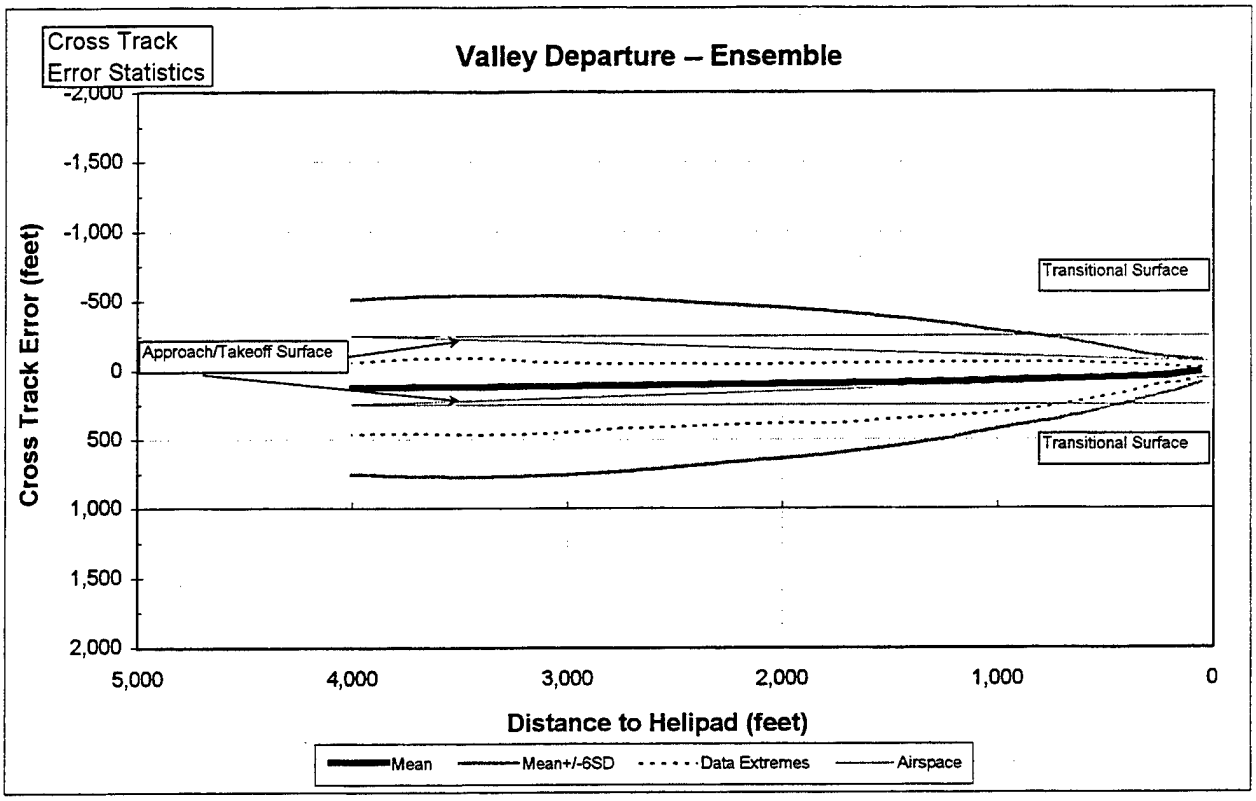

Figure H.3-5 Metro Departure Ensemble 6-Sigma Cross Track Data

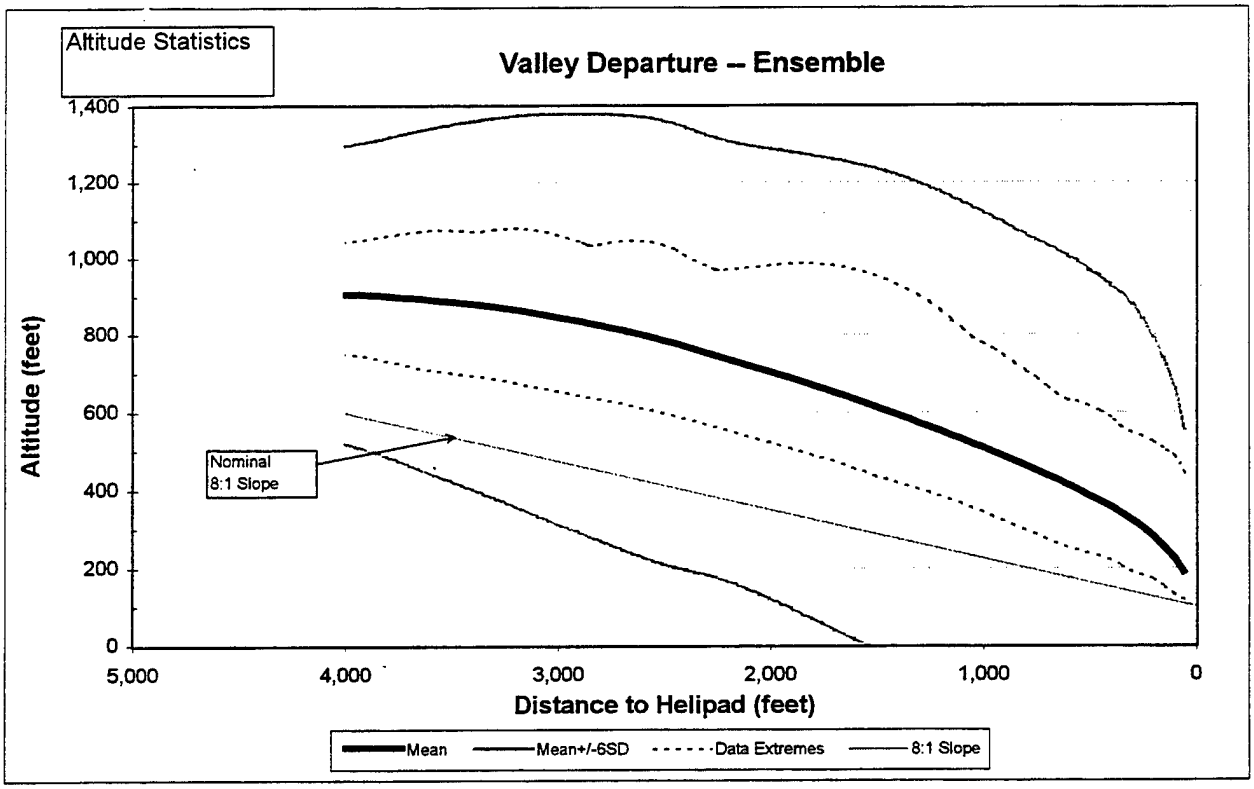

Figure H.3-6 Metro Departure Ensemble 6-Sigma Altitude Data

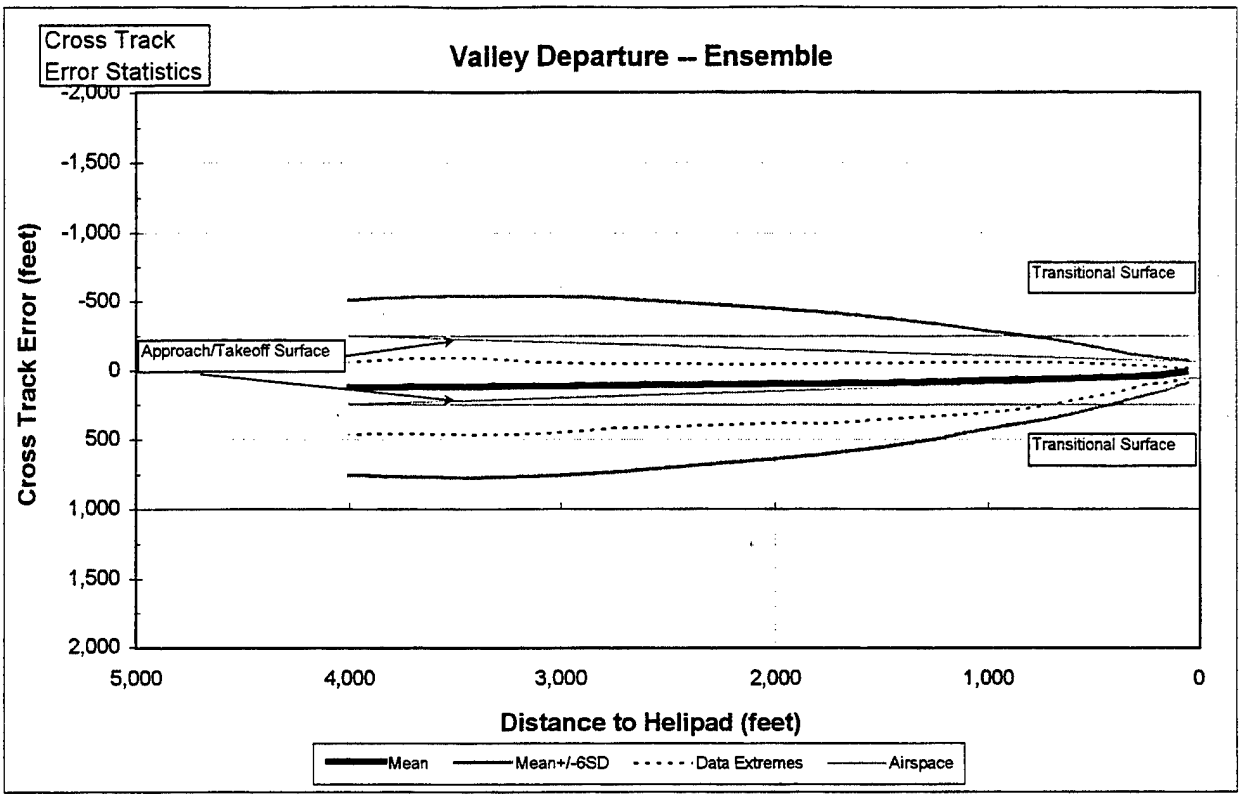

Figure H.3-7 Valley Departure Ensemble 6-Sigma Cross Track Data

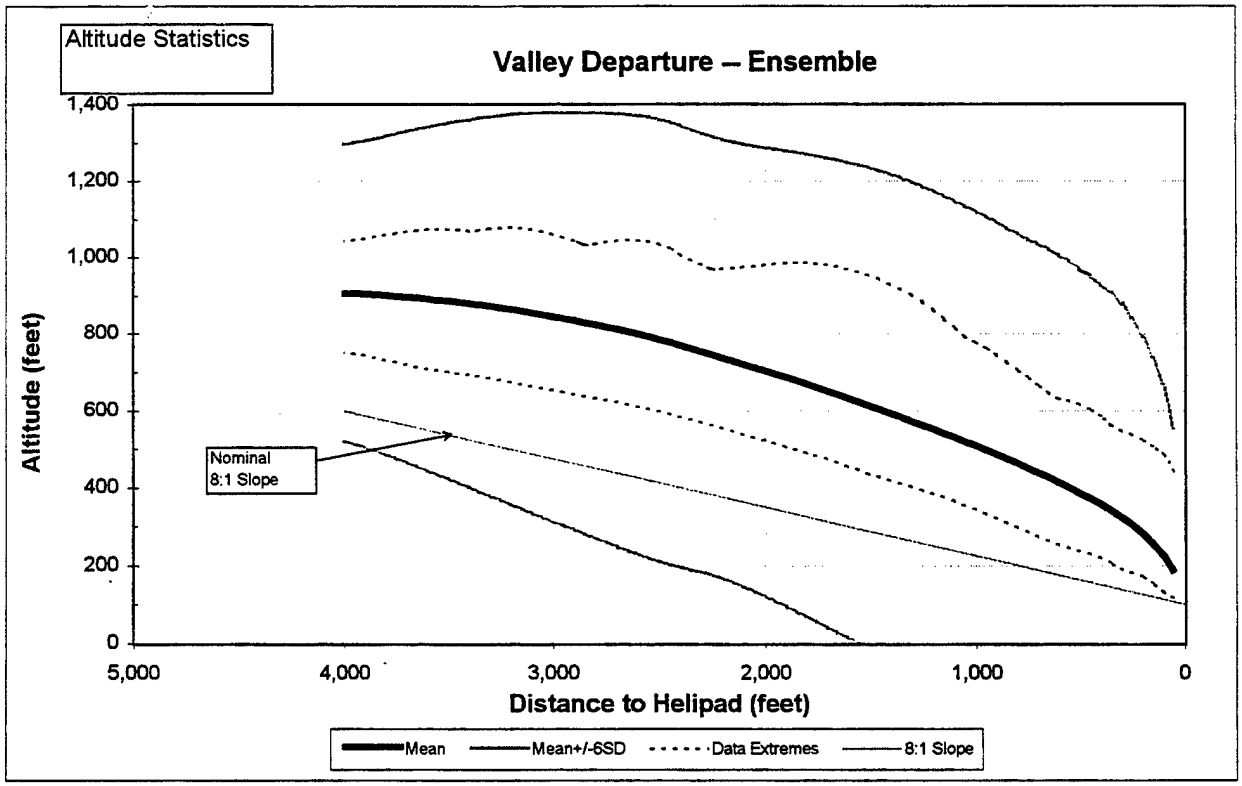

Figure H.3-8 Valley Departure Ensemble 6-Sigma Altitude Data

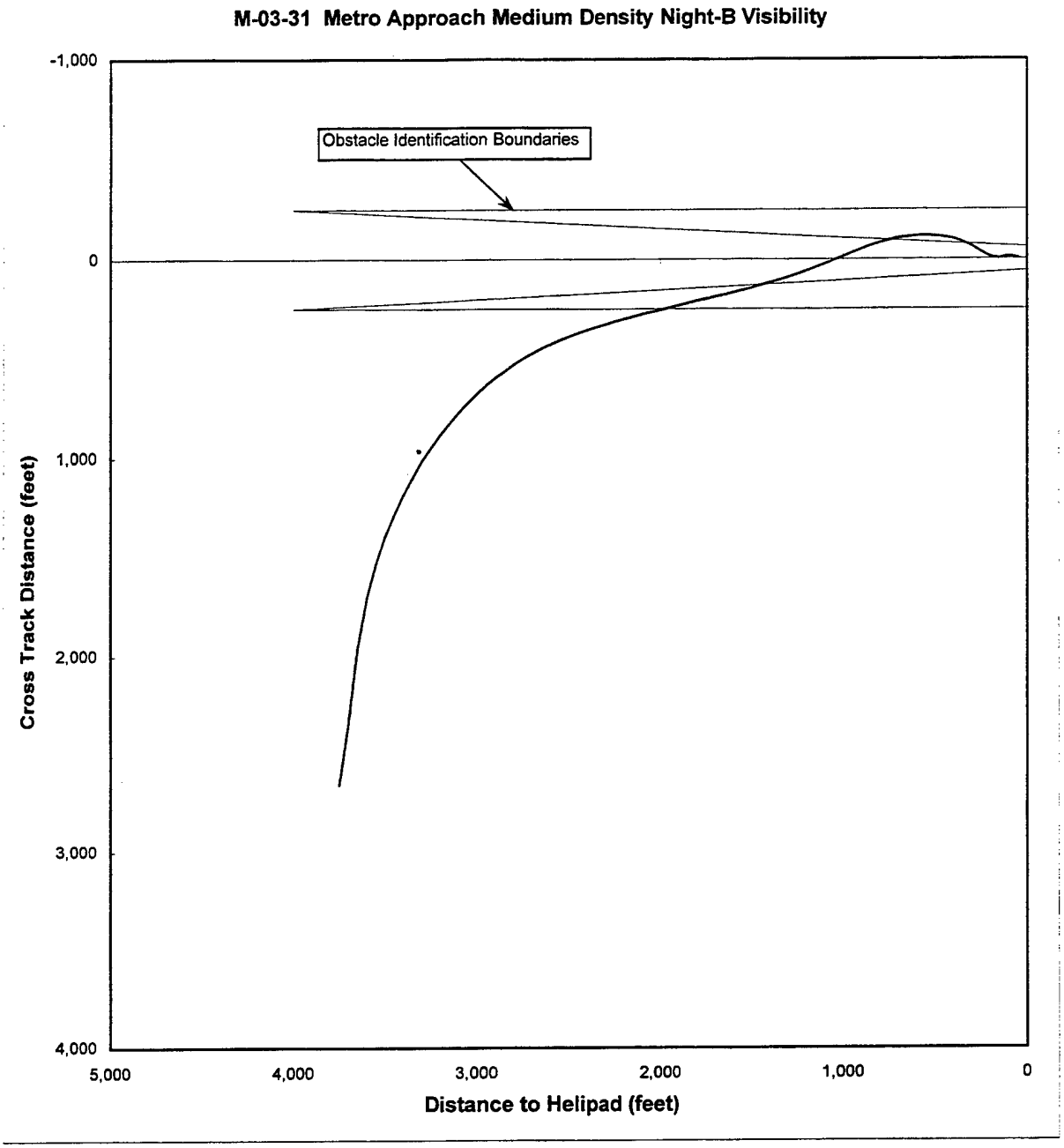

Figure H.4-1 Excepted Data -- M-03-31

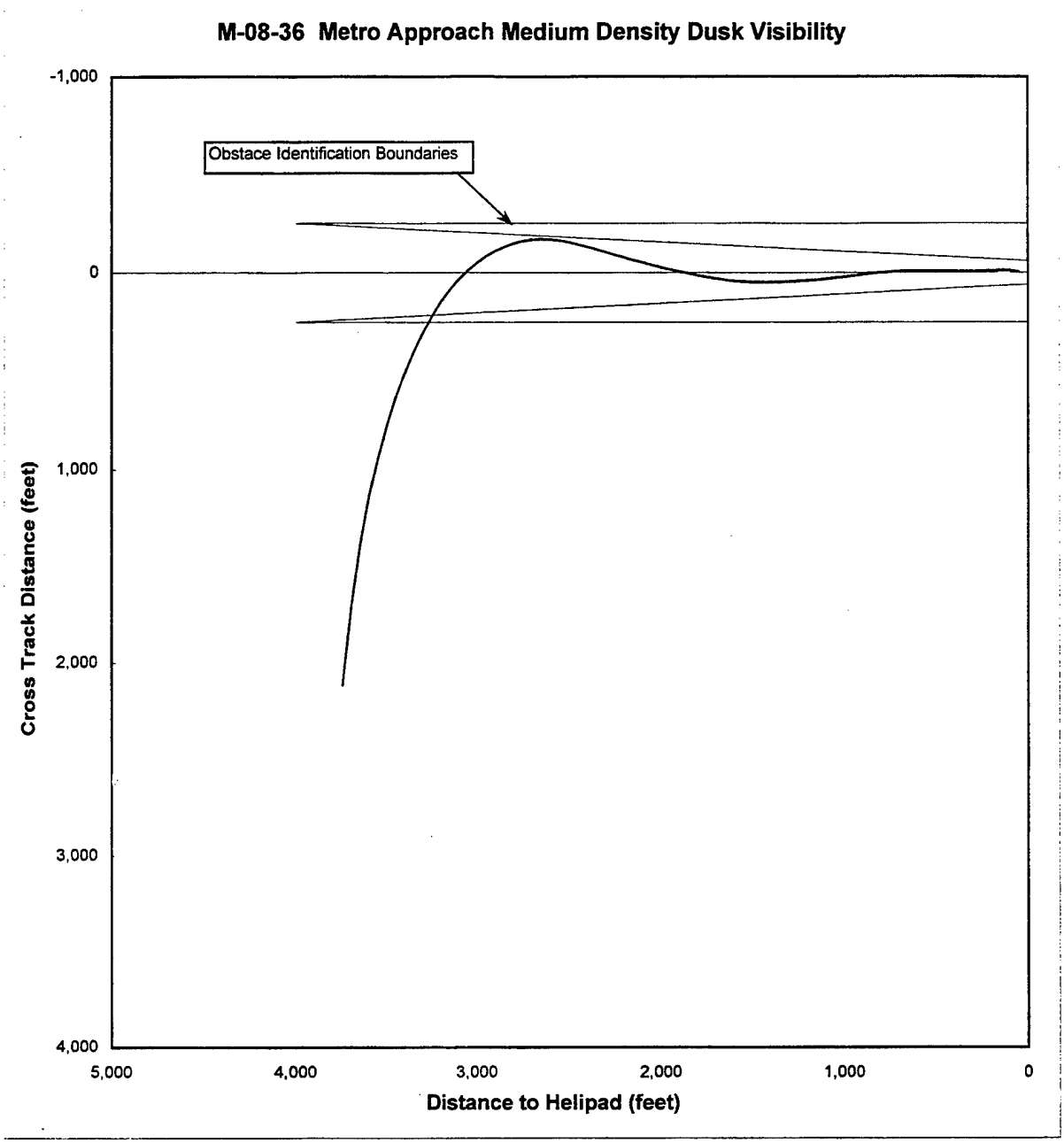

Figure H.4-2 Excepted Data -- M-08-36

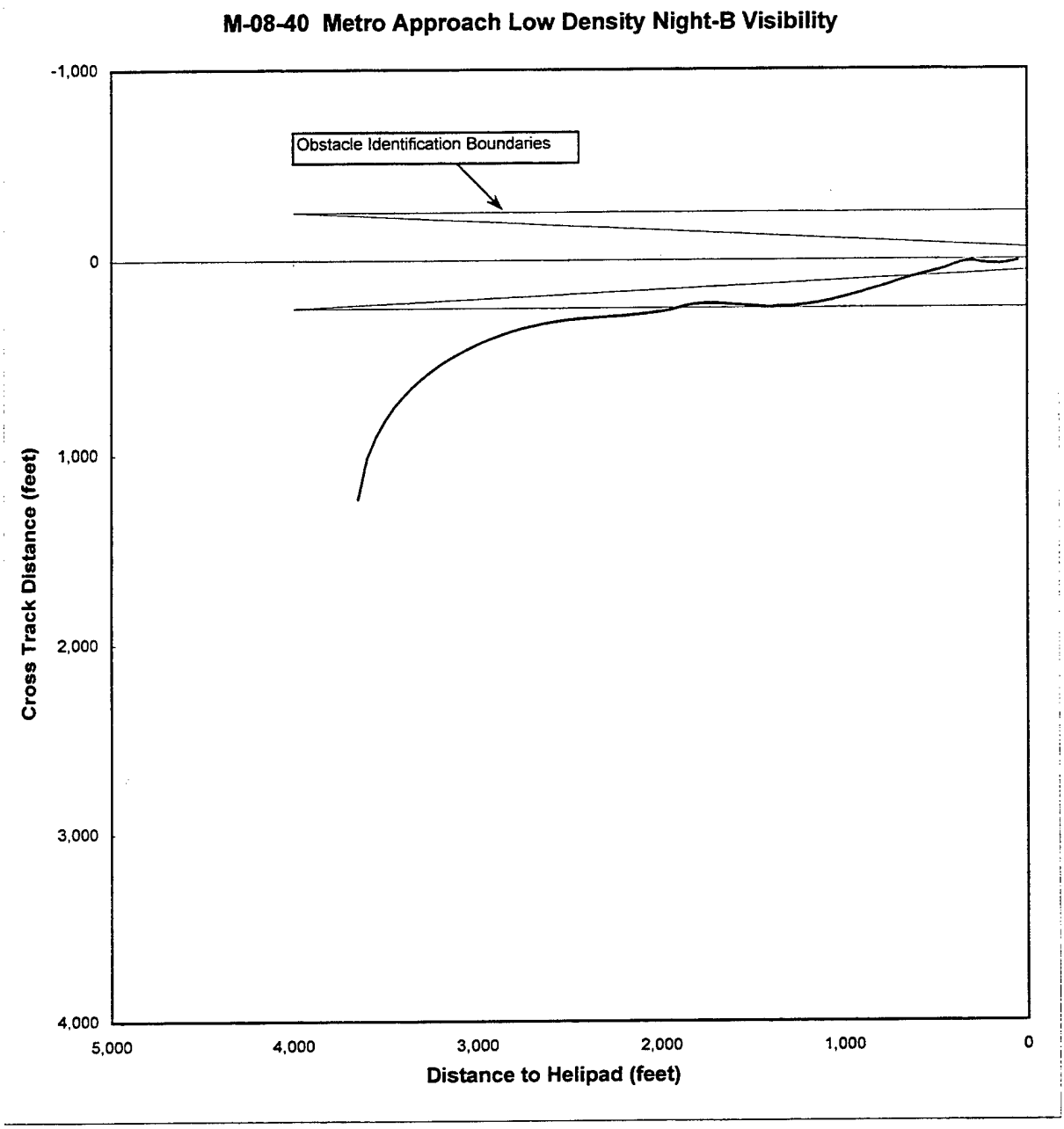

Figure H.4-3 Excepted Data -- M-08-40

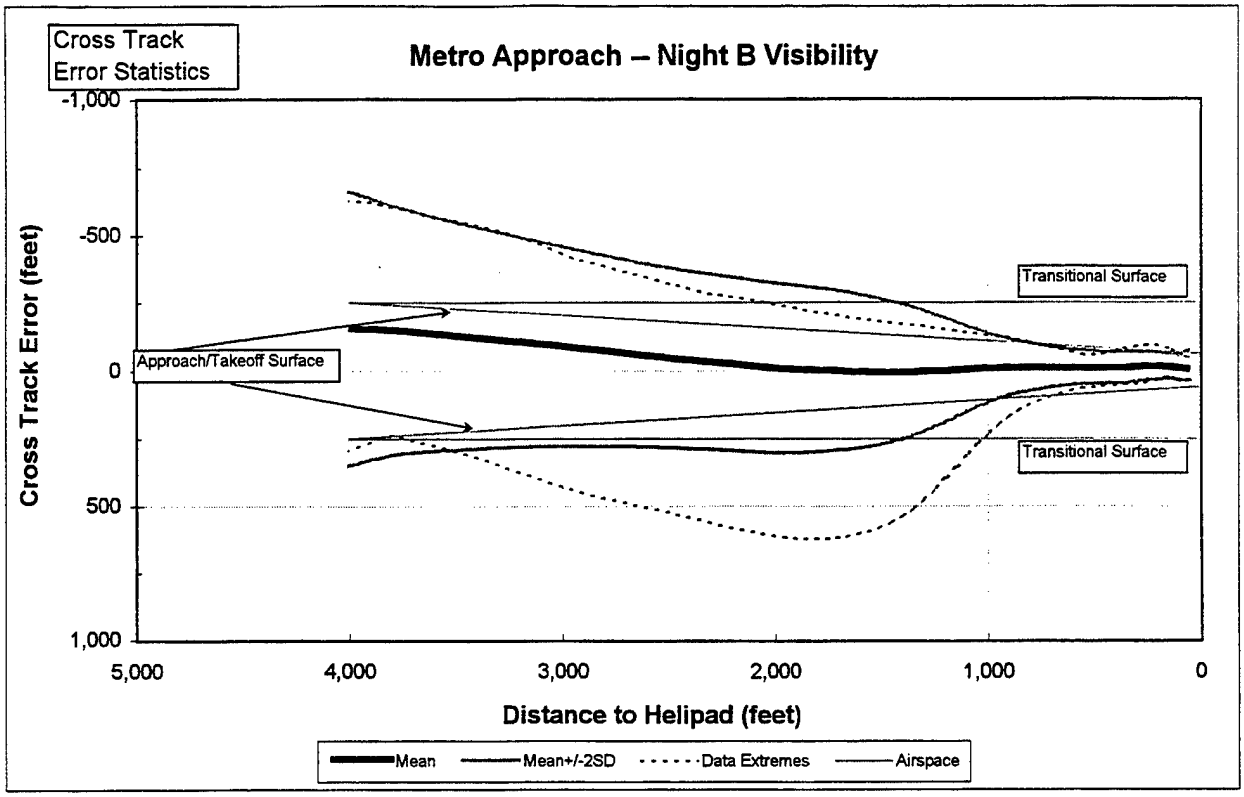

Figure H.4-4 Figure H.2-13 Repeated

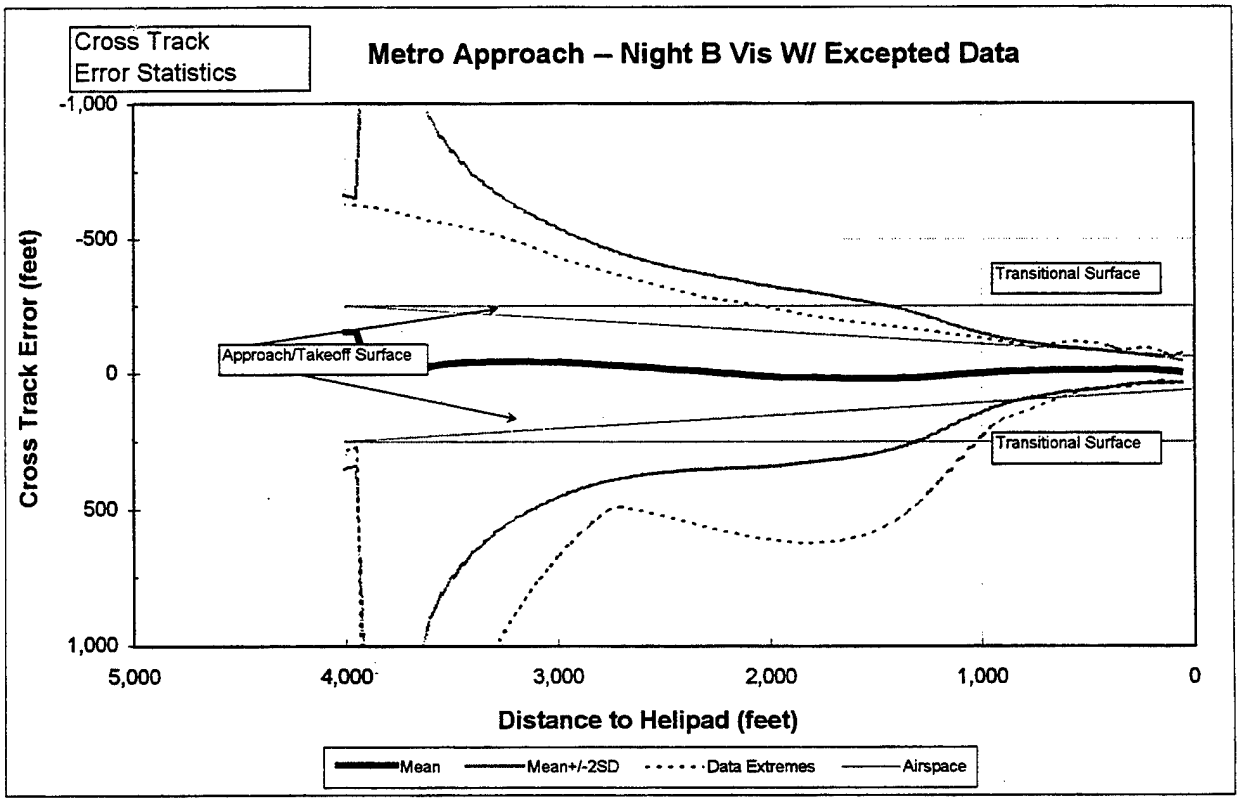

Figure H.4-5 Figure H.2-13 with Two Excepted Simulation Runs Included

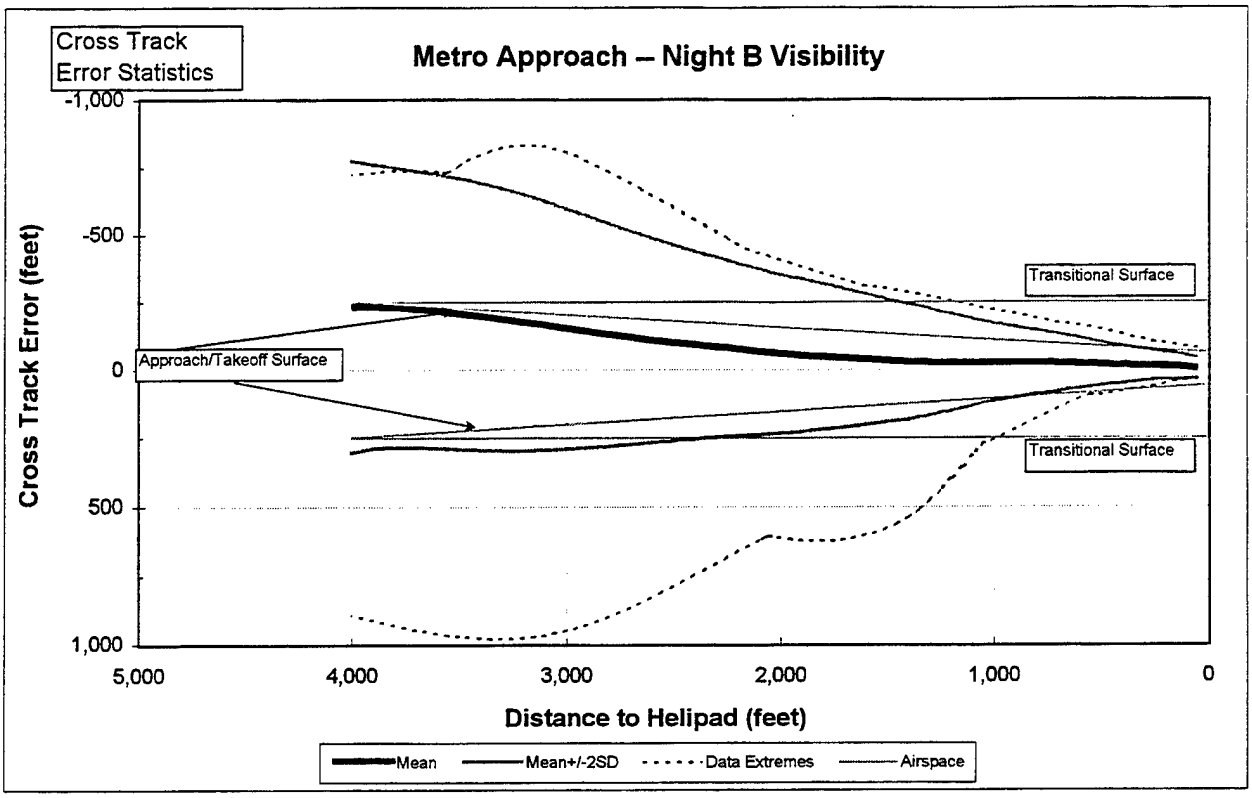

Figure H.4-6 Figure H.2-29 Repeated

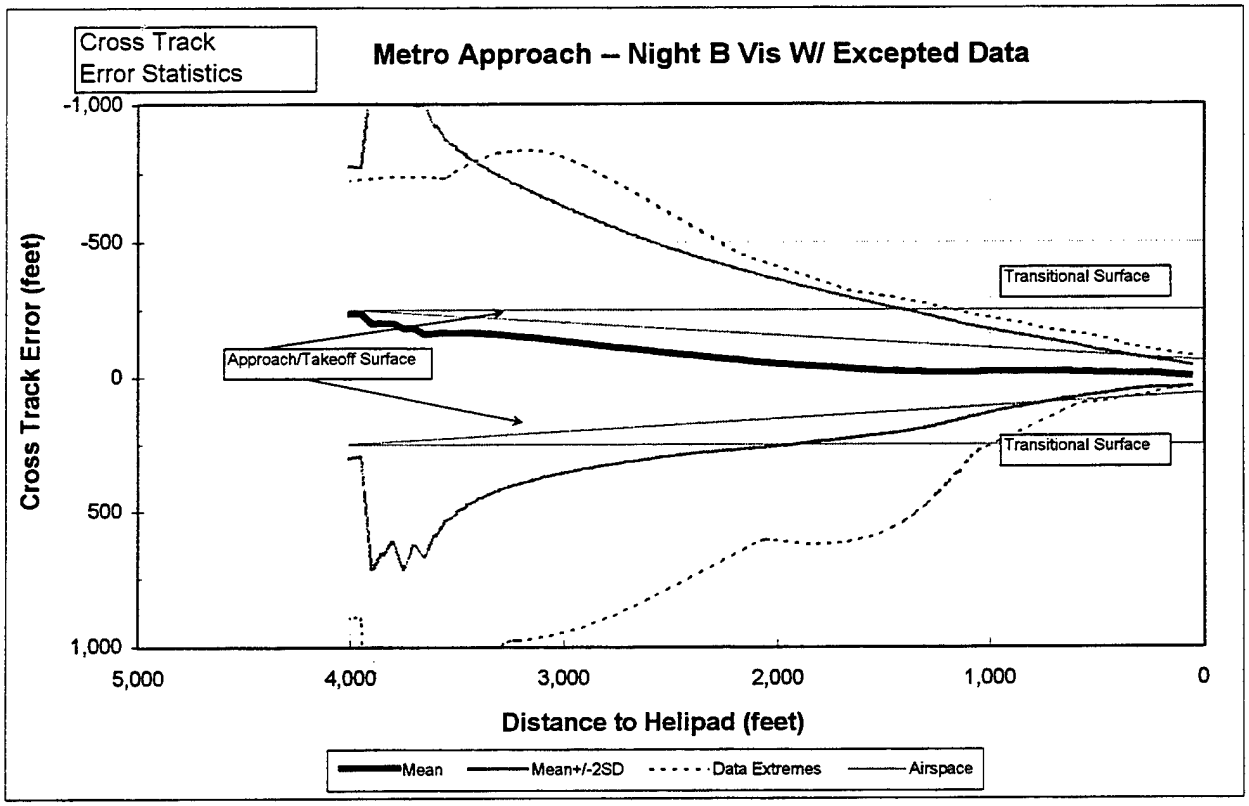

Figure H.4-7 Figure H.2-29 with Three Excepted Simulation Runs Included

Appendix I. Acronyms

AC	Advisory Circular
AGL	Above Ground Level
ANOVA	Analysis of Variance
ATC	Air Traffic Control
ATSO	Air Transportation Systems Operation
AVF	Advanced Vertical Flight
CFI	Certified Flight Instructor
CFR	Code of Federal Regulations
CRT	Cathode Ray Tube
CTAF	Common Traffic Advisory Frequency
ECG	Electocardiographic
EMS	Emergency Medical Services
EOG	Electro-Oculographic
FAA	Federal Aviation Administration
FATO	Final Approach Takeoff Area
FOV	Field of View
GPS	Global Positioning System
H-V	Height-Velocity
IFR	Instrument Flight Rules
I/O	Input/Output
IG	Image Generator
IMC	Instrument Meteorological Conditions
MEH	Multi-Engine Helicopter
MFD	Multifunction Display
msec	Millisecond
MSL	Mean Sea Level
NASA	National Aeronautics and Space Administration
OEI	One Engine Inoperable
OH/D	Obstacle Height/Density
OQC	Obstacle Qualification Criteria
ORE	Obstacle-Rich Environment
PAPI	Precision Approach Path Indicator
PC	Personal Computer
PIC	Pilot in Command
R&D	Research & Development
RFP	Request for Proposal
RMS	Root Mean Square
SAIC	Science Applications International Corporation
SAS	Stability Augmentation System
SCT	Systems Control Technology, Inc.
SEH	Single-Engine Helicopter
SGI	Silicon Graphics Iris
SME	Subject Matter Expert

SP	Single Pilot
TERPS	Terminal Instrument Procedures
TLX	Task Load Index
TOD	Time of Day
UCE	Usable Cue Environment
UNICOM	Aeronautical Advisory Station (Universal Communication)
VCR	Video Cassette Recorder
VFR	Visual Flight Rule
VGSI	Visual Glide Slope Indicator
XMSN	Transmission